Monitoring and modelling suspended sediment flux in British upland catchments

Armstrong, Alona

Monitoring and modelling suspended sediment flux in British upland catchments

Alona Armstrong
Department of Geography
2005

One volume

Submitted for the degree of Doctor of Philosophy to the University of Durham.

Monitoring and modelling suspended sediment flux in British upland catchments

Alona Armstrong

Despite the acknowledged importance of fine sediment in upland river systems, and the associated downstream impacts, there is limited understanding of suspended sediment processes in such environments. This thesis examines the dynamics and delivery of suspended sediment in six upland catchments in Northern England (Burnhope, Candleseaves, Langtae, Rough Sike, Swinhope and Trout Beck) and assesses the impact of different rating curve models on sediment load estimates.

To assess the impact of model choice on suspended sediment load estimates a suite of rating curve models were developed using linear regression and generalised linear models. Best estimates of specific suspended sediment yields from the six study sites ranged from 11.2 to 38.3 t km^{-2} yr^{-1} (comparable to existing estimates from similar British upland catchments). Linear regression corrected by smearing was established as the most applicable general model. However, according to model choice variability in load estimates for each site ranged from 14% to 271% (coefficient of variation). Several indicators of model fit were assessed and led to the conclusion that no single indicator could be used to identify the most appropriate model.

The sediment dynamics of the systems are highly responsive, especially those with continuous peat cover. Catchment area, maximum relief, total channel length, stream order and mean discharge all correlated with suspended sediment load; load is an almost linear power function of catchment area. Clock-wise (class 2) hysteresis dominated in all catchments (66% on average) and was attributed to exhaustion of within-channel and local hillslope sediment sources. Analysis of the spatial variation in suspended sediment concentration also indicated the catchments were supply-limited. The spatial variation in suspended sediment concentration, bed sediment storage, organic matter content and geochemistry of suspended sediment in the Rough Sike and Trout Beck catchments demonstrated that sediment quantity and character vary spatially. More sediment is supplied by the lower order catchments and soil type exerts weak control over sediment quantity and character. Given the relative dominance of organic and mineral sediment between catchments it was suggested that volumetric yield should be calculated when assessing landscape change.

This study has substantially increased the existing uplands suspended sediment database and has given insight into sediment dynamics and temporal and spatial controls on sediment delivery. Analysis of multiple catchments has highlighted key methodological issues including the fundamental importance of model choice in rating curve development.

Acknowledgements

I would like to thank the following people for their help and contributions to this thesis:

...Jeff Warburton and Nick Cox for their supervision, invaluable enthusiasm, approachability, and taking the time to teach me numerous things along the way.

...Dave Higgitt who was my supervisor before his appointment in Singapore.

...The Department of Geography for funding my Ph.D.

...The Lake District National Park Authority for support of studies at Candleseaves and Iron Crag.

...Mr Dent for allowing access to Swinhope.

...Martin Evans for allowing me to incorporate the Rough Sike data and Vicky Holliday for allowing me to incorporate the Burnhope and Langtae data.

...The Environmental Change Network for the Moor House and Upper Teesdale NNR data.

...The Environment Agency for the Trout Beck discharge data.

...Sarah Clement, Duncan Wishart, Rich Johnson and Jeff Warburton for help, enthusiasm and fun in the field.

...Brian Priestly, Eddie Million, Derek Coates, Frank Davies, Neil Tunstall, Ian Dennison and Amanda Smith who made my time spent in the lab more enjoyable and helped with analyses and field kit. Also, thanks to Eddie, Derek and Neil for helping out in the field.

...The other support staff, especially Derek Hudspeth, Christine Bones, Stella Henderson and the IT team.

...Rob Ferguson & Graham Leeks for taking the time to examine me.

...And finally, family and friends, within and outside the department, for support, help, advice, good times, and understanding throughout my stay in Durham.

Contents

List of Figures

Chapter 8: Suspended sediment rating curve development

List of Tables

Declaration

This thesis, or material contained within it, has not been previously submitted for a degree in this or any other university. Where relevant, all material which is the work of others has been acknowledged.

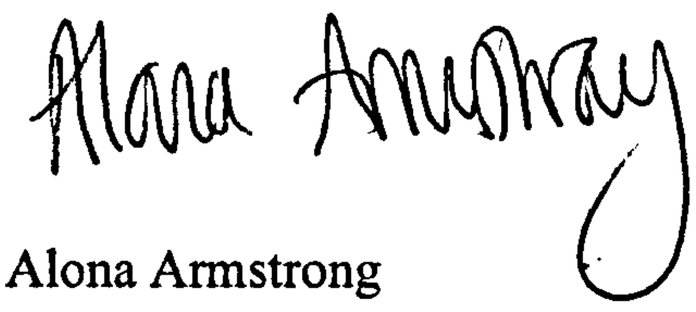

Alona Armstrong

Chapter One: INTRODUCTION

1.1 Overview

The purpose of this chapter is to outline the rationale for this study; to state the aim and specific objectives which it seeks to fulfil; and summarise the contents of the thesis.

1.2 Rationale

Suspended sediment is the proportion of solids transported by rivers in the water column. It is commonly separated from dissolved components by 1.2 μm. The size of the largest particles varies according to material available and transport capacity of the river. The suspended sediment concentration (SSC) is the weight of sediment per volume of water, commonly expressed as mg l^{-1}. Multiplying SSC by the water discharge (Q) gives the instantaneous flux, or load, of suspended sediment being transported down the river. Both SSC and Q vary considerably over time. In principle the annual suspended sediment load can be obtained by integrating the product of SSC and Q over time. In practice this 'true' load can normally only be estimated, because SSC is normally measured much more infrequently than Q. The interpolation or prediction of SSC at intervening times introduces uncertainty to the estimate of annual load. The annual load is often divided by the catchment area to give the specific suspended sediment yield in t km^{-2} yr^{-1}. Very few studies report actual loads or yields given the SSC data demands.

Suspended sediment fluxes and character are highly variable, both temporally and spatially. The temporal variability occurs from an intra-storm to an inter-annual scale and the spatial variability from channel cross-section to global scale. The variability results from the complex interplay of internal and external factors, namely climate, hydrological regime, lithology and the history of the catchment, which affect sediment supply (Figure 1.1).

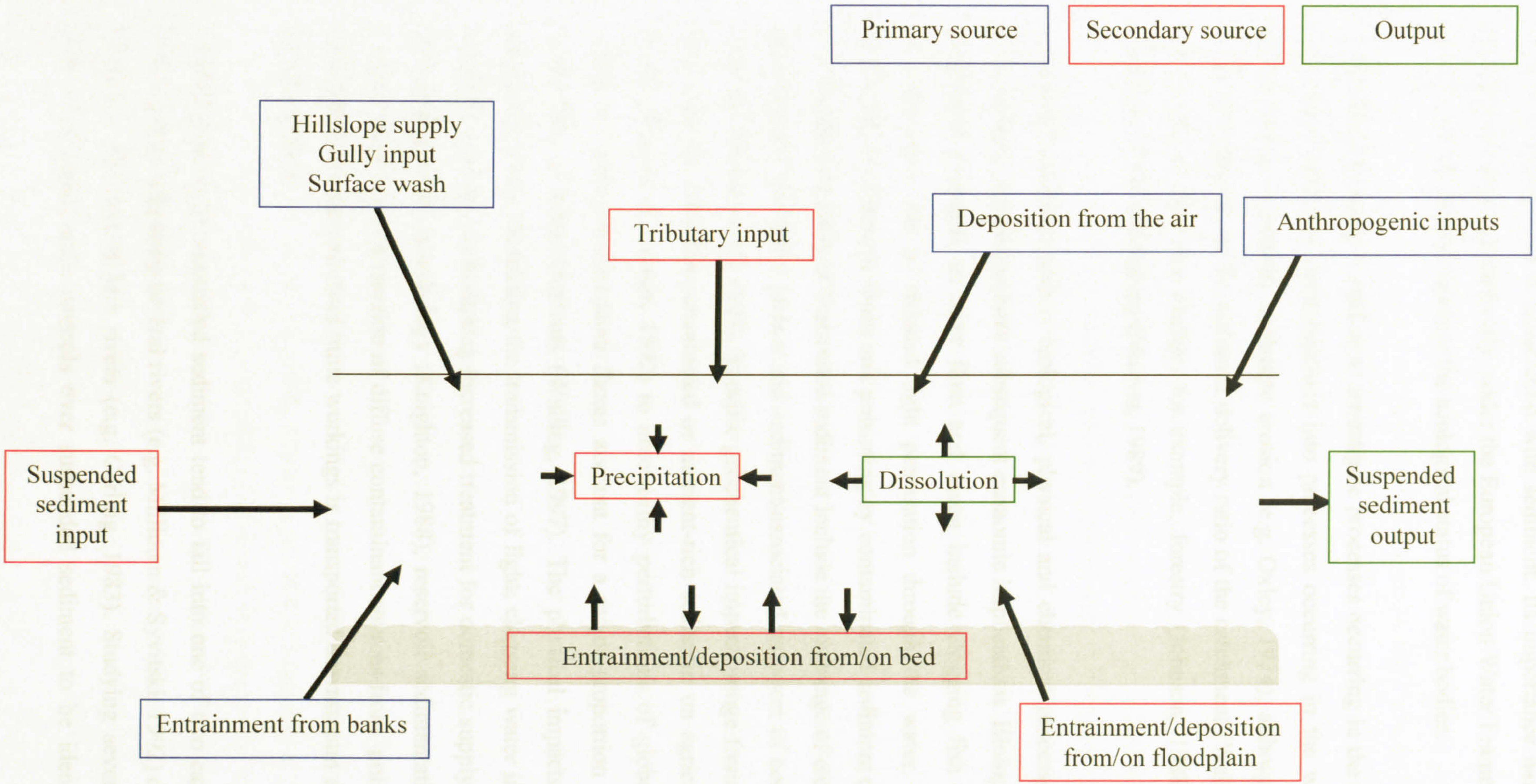

Figure 1.1. Generalised conceptual model of SSC within a river.

Suspended sediment is one of the most important river water quality properties as many toxins are transported in association with sediment. Its importance has been recently highlighted, although indirectly, under the European Union Water Framework Directive (WFD), which aims to increase the ecological status of water bodies.

Suspended sediment is studied to investigate processes occurring in the river system or the wider landscape. Investigations into processes occurring in the wider landscape include those examining landscape erosion (e.g. Oxley, 1974), although the value of such data depends on the sediment delivery ratio of the catchment (Walling, 1999) and the impact of land use change, for example, forestry (Johnson, 1988), urbanisation (Walling, 1974) and mining (Marron, 1989).

Suspended sediment affects biological, physical and chemical processes operating in river systems, which can have subsequent economic implications. Biological impacts of suspended sediment on river flora and fauna include clogging fish gills, reducing photosynthesis due to reduced light penetration through the water, increasing the likelihood of disease in fauna and poisoning by contaminated sediment (Ritchie, 1972). The chemical impacts of suspended sediment include the exchange of elements between the sediment and water phases and sediment-associated transport of contaminants and nutrients (House *et al.*, 1997). Specific geochemical impacts range from the deposition of a layer of infertile/contaminated or nutrient-rich sediment on agricultural land by floods (Braune & Looser, 1992) to noteworthy perturbations of global geochemical cycles, as sediment-associated fluxes account for a major proportion of the land to ocean flux of many elements (Walling, 1997). The physical impacts of suspended sediment include decreasing the transmission of light; clogging water intakes of water abstraction works; necessitating increased treatment for domestic supply (Jones, 1997); changing channel morphology (Knighton, 1988), reservoir sedimentation (Braune & Looser, 1989); and production of diffuse contaminant sources from point sources (e.g. contaminated sediment from mine workings is transported downstream and redeposited in floodplains).

Existing studies of suspended sediment tend to fall into one of two categories: larger scale studies comparing several rivers (e.g. Milliman & Syvitski, 1992) or smaller scale studies of just one or two rivers (e.g. Carling, 1983). Studying several large rivers allows the larger scale controls over suspended sediment to be identified, such as

precipitation, topography and geology. However, with many of these studies the data are compiled from various sources and therefore different monitoring and modelling techniques were used. Smaller scale studies generally do not compare enough catchments to allow inferences to be made regarding larger scale controls such as topography and geology. Instead they tend to focus on the form of the relationship between suspended sediment concentration and discharge. Given the generally smaller catchment sizes these studies allow consideration of sediment preparation and delivery processes which operate at a smaller scale, e.g. freeze-thaw of river banks, a particularly intense storm, activation of certain sediment sources etc. The signals of such factors are harder to detect in larger catchments given the greater number of influential factors and more variable sediment sources. Very few studies examine multiple smaller catchments, although several studies examine nested or paired catchments (e.g. Johnson, 1988; Oxley, 1974; Francis & Taylor, 1989), in an attempt to attribute sediment fluxes to both smaller scale processes and larger scale controls. Gurnell (1987) characterises spatial aspects of suspended sediment delivery but for proglacial streams.

In comparison with other environments, studies of suspended sediment dynamics in the British uplands are scarce. The lack of upland studies is likely to be a result of the logistics of working in such areas and the perceived limited influence of suspended sediment in British upland environments on humans. However, upland areas are of key importance for several reasons:

(1) Uplands cover approximately one-third of Britain's land surface (Fielding & Haworth, 1999).

(2) There is concern regarding erosion in upland Britain (DoE, 1995; Evans, 1997; Tallis *et al.*, 1997).

(3) The headwaters of a drainage basin (which are generally in the uplands), can be argued to be the most important part of a drainage basin in terms of erosion and transport of sediment (Beschta, 1987). For example over 80% of the sediment load of the Amazon is derived from the Andes which consists of only 10% of the catchment area (Gibbs, 1965; Meade *et al.*, 1985). Milliman & Syvitski (1992) established that with the exception of mountain streams, upland streams have the highest suspended sediment load and specific sediment yields (Figure 1.2).

(4) There are generally fewer controls over suspended sediment dynamics in smaller catchments (Jansson, 1988) and therefore it is easier to isolate the influence of

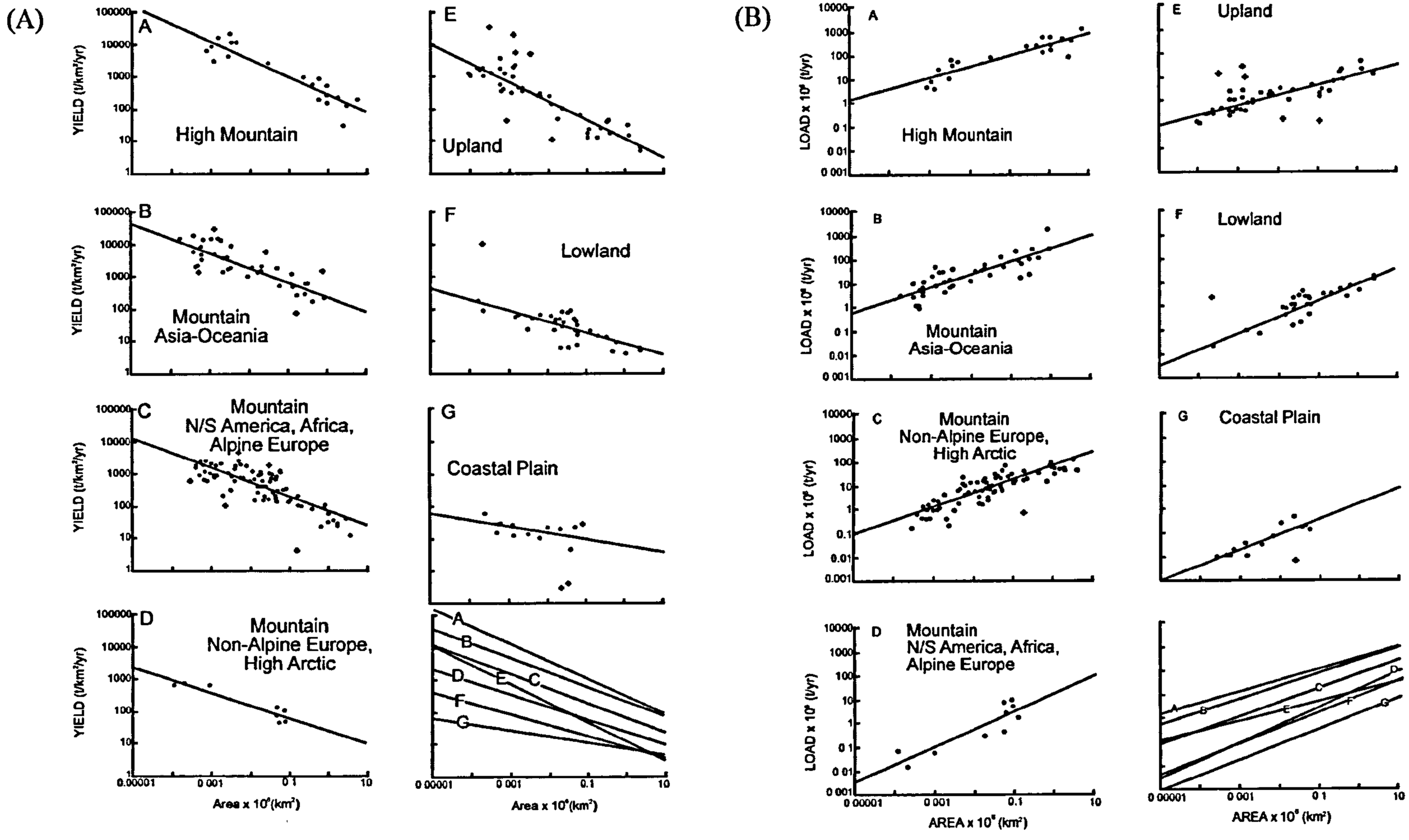

Figure 1.2. Scatter plots, categorised by the altitudinal setting of the catchments, of (A) yield as a function of catchment area and (B) load as function of catchment area. Source: Milliman & Syvitski, 1992.

individual factors. Consequently studying smaller catchments may help elucidate controls in larger catchments.

(5) Two-thirds of surface water storage reservoirs in Britain are in the uplands of the west and north (Stott *et al.*, 1986) and management regimes require knowledge of suspended sediment fluxes.

(6) Large-scale mining was undertaken in many upland areas and mining relicts are often in close proximity to the river channel. Coupled with limited vegetation (due to the high toxicities), such areas are easily eroded and so are a dominant source of contaminants within many river systems (Lewin & Macklin, 1987).

(7) Peat is the largest terrestrial carbon store (greater than biomass) and upland areas often include large peat deposits. Erosion and transfer of peat is of concern as it is composed of 50% organic carbon (Ball, 1964). Furthermore, fluvial transport of organic carbon is the major carbon pathway from the land to the ocean (Prentice, 2001) but is relatively under-studied and poorly quantified within Britain (Hope *et al.*, 1994, 1997a, 1997b; Tipping *et al.*, 1997; Worrall *et al.*, 2003b). Despite the low suspended sediment loads, and hence low organic carbon loads, of British rivers in the global context (Jansson, 1988), quantification is important at a national scale, especially with regard to movement towards carbon neutrality.

Despite the importance of suspended sediment in a British management context there is no British standard suspended sediment monitoring and modelling framework. In developing an appropriate framework four main aspects, which may introduce bias into quantifications of suspended sediment fluxes, need to be considered: (1) sampling method; (2) sampling regime; (3) modelling method if a quasi-continuous suspended sediment series needs to be established; and (4) load estimation technique. Studies have examined these sources of bias and have shown their effect can be considerable. For example, Phillips *et al.* (1999) investigated the effect of different load estimation techniques on the accuracy and precision of load estimates; Olive & Rieger (1988) and Walling *et al.* (1992) examined the effect of different sampling regime on load estimations; and Edwards & Glysson (1999) outlined the disadvantages of suspended sediment samplers. The effect of model choice has been investigated by some authors (e.g. Fenn, 1989 and Asselman, 2000), although usually the effect of different model types on the suspended sediment load of one catchment.

In summary, there are few studies which investigate suspended sediment dynamics in British upland catchments, despite their importance. Those studies which have been undertaken used different monitoring, modelling and load estimation techniques, as there is no standard British protocol. The different monitoring, modelling and load estimation techniques introduce bias to load estimates, and therefore prevent direct comparison between catchments (unless part of a paired or nested catchment study). There is also limited knowledge of the relative importance of large- and small-scale controls over suspended sediment delivery.

1.3 Aim

The aim of this thesis is to monitor and model suspended sediment flux in six British upland catchments at event and annual time-scales in an attempt to elucidate both catchment-specific and larger scale controls over suspended sediment dynamics. Investigating numerous catchments using the same methods allows comparisons to be made, generalisations to be derived, and differences explained.

1.4 Objectives

To fulfil the aim of this investigation the following specific objectives are examined:

1. Establish appropriate techniques for monitoring suspended sediment flux in British upland streams (given available records and technology).
    a. Monitor suspended sediment in a range of catchments representative of the British uplands and produce a database of suspended sediment loads.
    b. Examine the spatial variation in suspended sediment dynamics and properties at the between and within catchment spatial scales.
    c. Examine the temporal variation in suspended sediment dynamics at storm to sub-annual time-scales.
    d. Infer sources of suspended sediment and controls over the delivery of sediment from those sources.
2. Establish appropriate techniques and identify the optimum technique for modelling suspended sediment flux in British upland streams.

1.5 Thesis framework

The format of this thesis is as follows:

Chapter 2 is a review of suspended sediment in terms of its nature, sources and sinks, the factors affecting its delivery, temporal variability from inter-event to intra-annual

time-scales, the importance of the magnitude and frequency of storm events, and finally outlines existing suspended sediment studies in British upland catchments.

Chapter 3 is a review of monitoring methodologies applicable to suspended sediment studies. It presents the various monitoring equipment and sampling regimes and outlines the uses, advantages, and disadvantages of each.

Chapter 4 is a review of suspended sediment modelling methodologies. It gives a general introduction to modelling and then describes the various techniques used to model suspended sediment, with reference to examples.

Chapter 5 describes the study catchments including location, catchment characteristics and justification for choice.

Chapter 6 outlines the selected field and laboratory methods adopted in this study and illustrates how they link together.

Chapter 7 presents the results of investigation into the spatial controls over suspended sediment delivery within Moor House National Nature Reserve. The variation in suspended sediment concentration at eight spatially distributed sampling locations, during storm events, and at two nested gauging sites, at fixed-intervals, are investigated and related to catchment characteristics. The spatial variability in bed sediment storage at eight locations in the channel network is examined and related to local flow speeds, the grain size distribution of the channel bed and the amount of periphyton. The varying organic-mineral balance of suspended sediment throughout the channel network is demonstrated and related to catchment characteristics. The temporal variation in the organic-mineral balance is also discussed. Finally, the results of some exploratory data analysis, using principal components analysis of suspended and source sediment geochemistry are given.

Chapter 8 focuses on the development of sediment rating curves and load estimates, using a range of models and a range of data sub-sets, for each of the study sites. The models are assessed with regard to the correlation coefficient, root mean square error, graphical analysis of the rating curve position in relation to the data points, a range of

model diagnostic plots and the percentage difference between the actual and estimated sampled period load estimate.

Chapter 9 discusses the results of chapter 8 with reference to methodological concerns, comparison of the rating curves developed across all sites, and analysis of catchment sediment dynamics based on the load estimates obtained from the optimal model for each site. The load and yield estimates are then compared to those of other British upland catchments.

Chapter 10 examines the inter-storm variation in the discharge-suspended sediment concentration relationship and infers sediment sources. This is achieved using hysteresis plots and quantified indicators of antecedent catchment conditions and storm characteristics for each storm in each catchment. These results are combined and generalisations made regarding sources of suspended sediment throughout all the study sites and the importance of antecedent catchment conditions and storm characteristics.

Chapter 11 gives the main conclusions of the thesis, provides a synthesis of the outcomes of chapters 7, 8 and 9; recommends the optimal monitoring and modelling methods for British upland catchments; outlines limitations and suggests future research; and gives examples of the application and importance of the outcomes of this study to other investigations.

Chapter Two: BACKGROUND TO SUSPENDED SEDIMENT

2.1 Overview

This chapter provides an overview of suspended sediment. It begins with a definition of suspended sediment, outlines factors affecting its transport and places the contribution of suspended sediment to total river load in context. The differences between hydraulic- and hydrological-based studies are outlined. The nature of suspended sediment is discussed, with specific reference to grain size, organic-mineral balance and geochemistry. The effects of such characteristics on the relationship between suspended sediment concentration and discharge are described. The chapter moves on to outline the various sources and sinks of suspended sediment within river catchments. Factors affecting suspended sediment dynamics are then discussed with examination of large- and small-scale controls and the inter-play between them. Spatial variation in suspended sediment, at a range of scales, is discussed in this section. Temporal variability in suspended sediment dynamics is then considered at intra-event to inter-annual scales. Following this, examples of magnitude-frequency relations are given. A brief overview of suspended sediment studies in Britain is provided and this is followed by a detailed discussion of existing British upland studies.

2.2 Sediment transport phases

Sediment is transported in different phases within river channels. The detailed definition of these phases varies within fluvial literature. Graf (1998), among others, outlines three phases of sediment transport: bed load, suspended load and wash load. Bed load is defined as larger particles which remain in close contact with the channel bed and move downstream by gliding, rolling or short jumps (Figure 2.1). Wash load is defined as the finest particles which are very rarely in contact with the bed (Figure 2.1). Last,

suspended load is defined as particles which are occasionally in contact with the channel bed and move by large jumps through the water column in accordance with local hydraulic conditions (Figure 2.1). Alternatively, Knighton (1998) defines two phases of sediment transport: bed load, which remains in close contact with the bed, and suspended load, which consists of particles which have limited contact with the bed (i.e. the sum of Graf's (1998) wash and suspended load). Beschta (1987) categorises sediment transport into suspended load, consisting of clay and silt particles and bed load, consisting of gravel, cobbles and boulders with a transition phase consisting of sand-sized particles. Also, some authors refer to suspended sediment as all suspended material, including Evans & Warburton (in press), while others use suspended sediment to define just the mineral fraction (e.g. Flemming & Poodle, 1970).

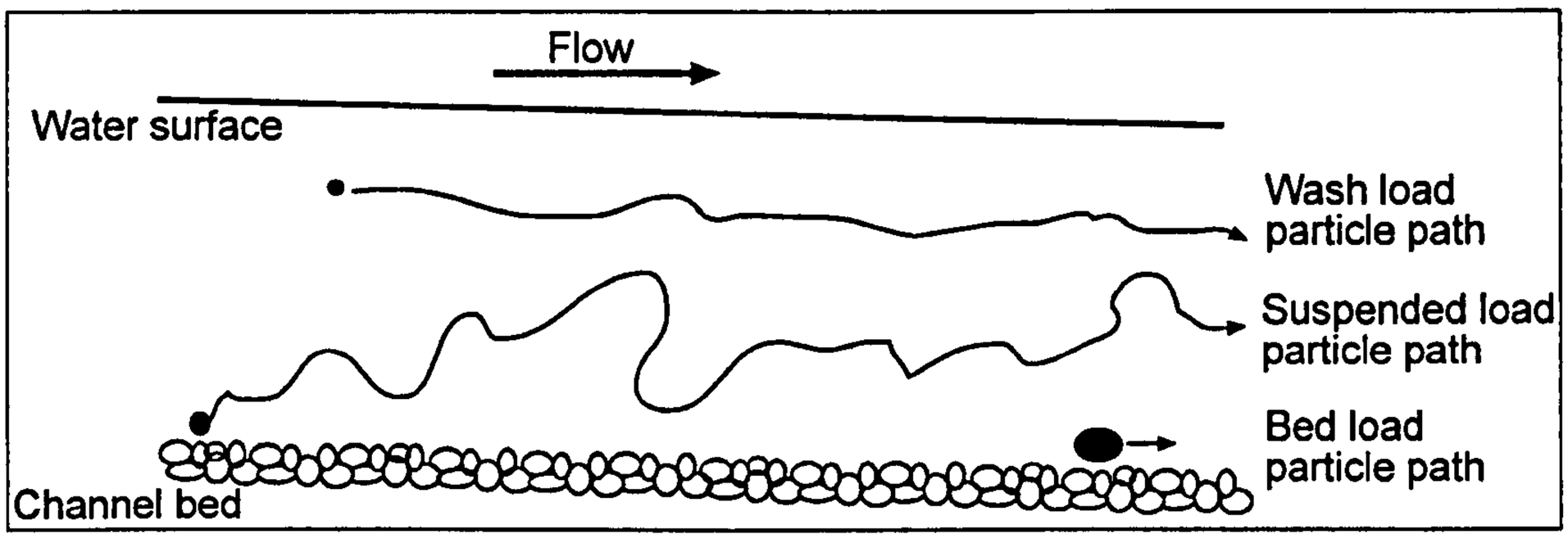

Figure 2.1. The three modes of sediment transport within channels.

The definitions used throughout this investigation are:

- Sediment will refer to both inorganic and organic fractions.
- Suspended load: particles which are in limited contact with the bed (i.e. the sum of the wash load and true suspended load) on the basis that the monitoring techniques used do not separate wash load and true suspended load components.
- Bed load: particles which remain in close contact with the bed.

Although the monitoring techniques do not separate the wash load, particles which are rarely in contact with the bed, and suspended bed load, particles which are occasionally in contact with the bed, these terms will be used when it is necessary to discuss them separately given the different controlling factors.

Suspended load is commonly the dominant form of sediment transport from the land to the oceans but the exact proportions vary from river to river. For example, Leeks (1992)

found that for three catchments in Plynlimon, Mid-Wales (Hore, Tanllwyth and Cyff) over four years 62.9% and 37.1% (on average) of sediment was transported as suspended and bed load respectively. The maximum amount of sediment transported in suspension was 94.3% and the minimum 39.9% for these catchments. Johnson (1995) reported that between 94.0% and 99.9% of sediment was transported in the suspended phase in Monachyle and Kirkton, West Scotland. Bed load in mountain streams generally accounts for a larger proportion of sediment transported due to the higher channel gradients (Wohl, 2000; Schick & Lekach, 1993).

The concentration of suspended sediment at any given moment is a function of erosion, entrainment, transport and deposition at that location and upstream from that location. These processes are dependent on various physical laws including hydraulic parameters and particle characteristics, but are also influenced by conditions within the channel. The strength of bonds between cohesive particles is often more important than the physical characteristics in terms of the ability of the stream to entrain the particles (Knighton, 1998), which complicates any physical rules regarding particle characteristics and movement thresholds. In addition to specific particle characteristics, changes in the amount of sediment transported by a stream and the relative importance of each phase of transport are controlled by changes in the supply of solids, changes in the supply of liquid (i.e. stream discharge) and change in bed elevation downstream (Graf, 1998). The proportion of sediment in each transport phase can be obtained by hydraulic formulae, field measurements or physical models (with varying degrees of success). Hydraulic formulae generally compute the transport capacity of the stream, i.e. the amount of sediment the stream is capable of transporting given various properties (e.g. viscosity, velocity, shear stress etc.).

2.3 Hydraulic and hydrological approaches

Suspended sediment dynamics can be studied from hydraulic or hydrological perspectives. Simons & Sentürk (1992, pp872-873) defined hydraulics as 'the applied science concerned with the behaviour and flow of liquids' and hydrology as 'the science concerned with the occurrence, distribution and circulation of water on earth'. Hydraulic studies use the principles of fluid mechanics (the basic ideas of which are derived from the principles of conservation of mass and momentum: Lane (1998)), and require knowledge of several variables which affect the transport of sediment. The water phase is generally adequately described but the sediment phase is less well

characterised given the spatial and temporal variability in particle characteristics and sediment availability. For example, transport equations for wash load are not defined as the wash load component is heavily reliant on supply (Simons & Sentürk, 1992). In addition, bed forms and channel geometry are variable (Graf, 1998) and local bank irregularities can produce energy losses and reduce the capability of the flow to transport sediment (Knighton, 1998). Therefore fluvial hydraulics is complex and simplifications are required. Consequently, results are often specific to the hydraulic conditions for which they were developed (Graf, 1998). Hydrological studies, on the other hand, investigate the nature of processes in the natural environment. These studies involve measurement of hydrological variables and aim to improve understanding of systems and to develop methods of summarising, generalising and predicting hydrological processes. Hydrological studies, like hydraulic studies, are also time- and space-specific, but interactions between variables and generalised information regarding processes may be broadly applicable to other periods and locations.

A hydrological approach is used in this study. This study aims to quantify sediment load as there are few data of upland suspended sediment fluxes. This is preferred to a hydraulic study because, as Walling & Webb (1996) stated, in most situations the sediment load of a river at a given point in space and time is several orders of magnitude less than the maximum transport capacity. In addition, Webb *et al.* (1995) postulated that the wash load cannot be readily determined from hydraulic conditions, as it is a non-capacity load. Therefore a credible simple physical law abiding transport equation cannot be determined for suspended sediment concentration.

2.4 Nature of suspended sediment

Suspended sediment is categorised as allochthonous or autochthonous. Allochthonous matter is formed outside the channel and is generally dominant. It is largely inorganic and is composed of clay minerals, mineral fragments and rock fragments (Webb & Walling, 1996). Autochthonous matter is formed within the channel and comprises micro-organisms (phytoplankton, zooplankton, bacteria) and precipitates (Webb & Walling, 1996). Suspended sediment exist as individual particles, aggregates (groups of particles formed outside of the channel) or flocs (particles which joined within the channel). The primary form of suspended sediment is flocs, a complex matrix of organic material, inorganic particles, microbial communities and pores in varying proportions (Droppo, 2001).

The nature of the suspended sediment composition and characteristics, varies with time and space. Crosby & de Boer (1995) give an example of spatial variation. Suspended sediment particles within the upper drainage basin of the Assiniboine-Whitesand River system in the prairie/parkland region of eastern Saskatchewan, Canada, primarily consisted of planktonic diatoms with a small number of flocs composed of mineral grains and diatoms bound together with clay and organic matter. In contrast, sediment in the downstream section was dominantly composed of mineral grains cemented together with clay. Temporal variation has been noted by several authors at a range of scales. Gilvear & Petts (1985) noted the heightened proportion of periphyton (i.e. algae and small crustaceans) entrained during water release from Llyn Celyn on the River Tryweryn, North Wales, and hypothesised periphyton may be an important constituent of suspended sediment in unregulated rivers during the summer and early autumn. Droppo *et al.* (2002) observed particles had lower settling velocities on the falling limb than on the rising limb and attributed this to lower densities, higher porosities and more irregular shapes of sediment on the rising limb.

Suspended sediment characteristics have been studied as an extension of sediment quantity to ascertain impacts on water quality (Neal *et al.* 1997), allow identification of sediment sources (Collins & Walling, 2002) and demonstrate enrichment and particle selectivity processes in erosion, transport and deposition (Webb *et al.*, 1995). Information regarding the characteristics of suspended sediment is more restricted than quantification of fluxes; mainly due to problems associated with obtaining sufficient suspended sediment for analysis and availability of suitable techniques. Existing research generally focuses on grain size, mineral-organic balance or geochemistry in relation to the various effects on the stream environment (e.g. Bogen, 1992) and nutrient and contamination transfer (e.g. Horowitz, 2000). Examples and outcomes of such studies are outlined in the next three sections and their impacts on suspended sediment concentrations summarised.

2.4.1 Grain size

The grain size distribution of suspended sediment varies temporally at annual and storm-event time-scales and spatially from channel cross-section to between catchment scales. Suspended sediment grain size is important for adsorption of nutrients, contaminants and radionuclides; damage to infrastructure, (e.g. hydroelectric power

stations); erosion, transport and deposition processes (Bogen, 1992); and energy expenditure and channel shape (Xu, 2002).

The grain size diameter of suspended sediment generally ranges from 1.2 μm (1.2 μm filters are commonly used to separate material in suspension from that in solution) to 0.2 mm, but it is variable, especially with regard to organic sediment given its fibrous nature (Tipping *et al.*, 1993; Wass & Leeks, 1999; Walling & Webb, 1987; University of Wales, 1977; and Fleming & Poodle, 1970). Differences in grain size are a result of different sediment source properties, preparation processes and transfer mechanisms.

When comparing grain size parameters care must be taken as two different grain size measures are used: absolute and effective. The effective grain size distribution is determined from the particle size of the *in situ* flocs or aggregates. The absolute particle size distribution is that of the individual grains; the sediment is treated to remove organics, the remaining mineral fraction dispersed and measured. Measurement procedures and potential influences on the effective particle size are given by Phillips & Walling (1995). The effective particle size is important as it influences entrainment, transport and depositional processes within channels (Droppo, 2002). The absolute particle size is used to determine information regarding the nature and origin of the sediment (Peart & Walling, 1982).

Sediment type exerts a strong control over the relationship between absolute and effective particle size distribution. The difference between the effective and absolute particle sizes can be substantial and varies from river to river. The absolute and effective grain size distributions of suspended sediment sampled from six locations were determined by Walling & Woodward (2000). At each sampling location the effective grain size distribution was substantially coarser than the absolute grain size distribution (Figure 2.2). This illustrates the importance of aggregates and flocs within British rivers and suggests that studies which examine the absolute grain size of particles under-estimate effective grain size variability. Walling & Woodward (2000) also demonstrated the variability in the relationship between the effective and absolute grain sizes during storm events.

Discharge is the dominant control over suspended sediment grain size but the response of particle size distribution and specific particle fractions to changes in discharge is not

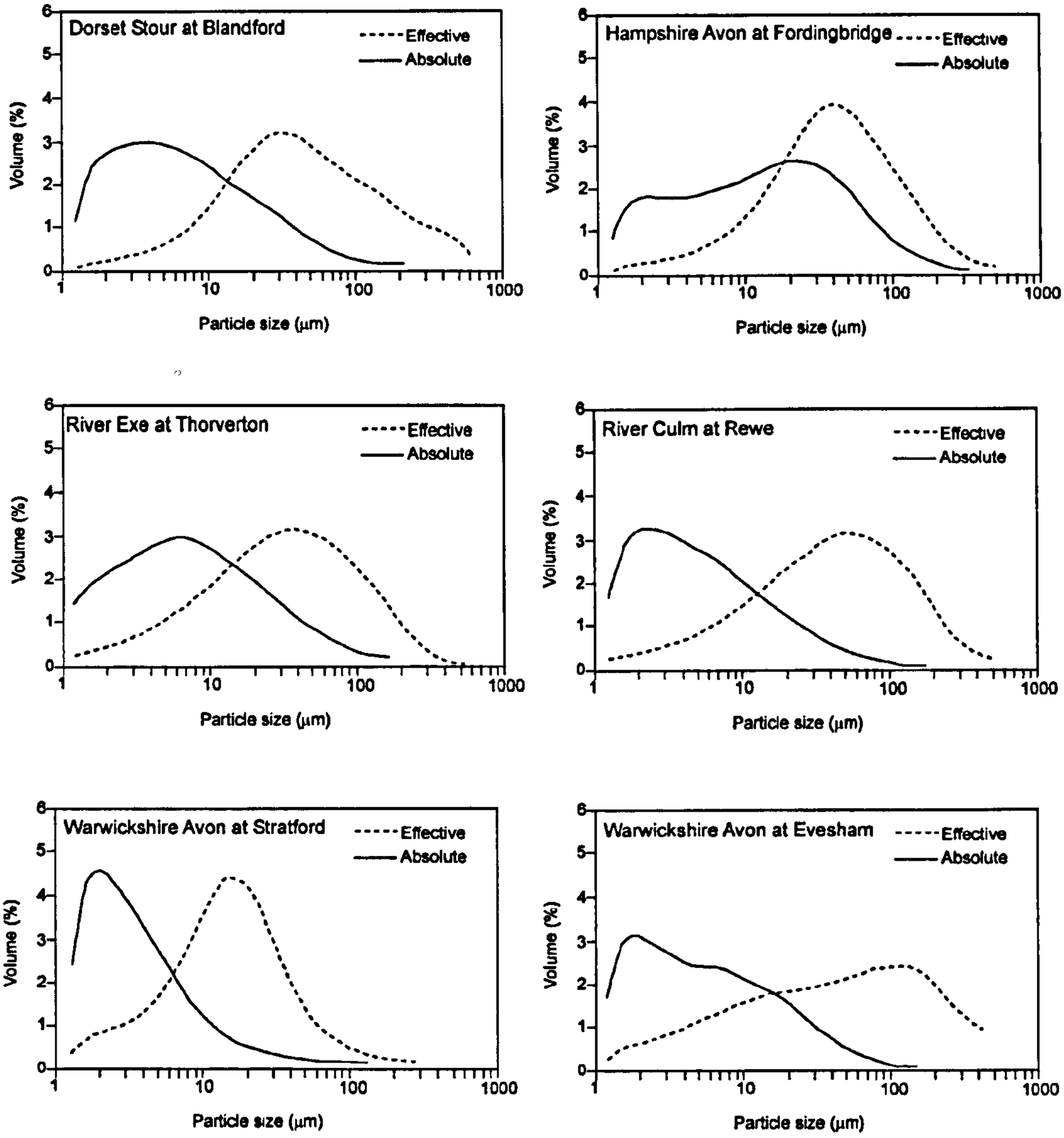

Figure 2.2. Typical effective and absolute particle size characteristics of suspended sediment samples. Source: Walling & Woodward, 2000.

consistent between or within catchments (Walling & Webb, 1987). *A priori* reasoning suggests that as discharge increases the particle size distribution will increase due to an increase in the stream power (e.g. Reid & Frostick, 1987); however, this is not always the case given the influence of sediment supply (Walling & Webb, 1987; Lenzi & Marchi, 2000; and Xu, 2002). Sediment source grain size distributions were argued to be the dominant control over the particle size distributions of suspended sediment in Norwegian rivers by Bogen (1992), although particle sizes of suspended sediment are generally finer than source samples (e.g. Stone & Walling, 1997) because of selective entrainment of smaller particles/preferential deposition of larger particles. The efficiency of transport from sediment sources to the channel also exerts an influence over the grain size distribution of suspended sediment. For example, if the transport

efficiency is lower then the proportion of fines in the suspended sediment will be higher. The transport efficiency is controlled by the amount of runoff, obstructions to flow pathways (e.g. vegetation) and the gradient of the hillslopes, coarser material is deposited on lower gradient slopes (Peart & Walling, 1982). The relative importance of transport efficiency of sediment to the channel and sediment source characteristics is likely to become less important at higher discharges (e.g. Doty & Carter, 1965).

2.4.2 Geochemistry

The geochemistry of suspended sediment is important in terms of contaminant and nutrient transfer and can also affect the physical character of the transported sediment: e.g. iron oxide promotes the formation of aggregates, and therefore coarsens the grain size distribution (Bogen, 1980). Studies which examine geochemical properties of suspended sediment rarely examine both temporal and spatial variation. However, given the proven temporal and spatial variation in suspended sediment fluxes *a priori* reasoning suggests geochemical properties will also vary with space and time.

The causes of temporal and spatial variability in geochemical properties are: different sediment sources, including the relative importance of allochthonous and autochthonous matter; interactions with water and air; and water and plant and microbial metabolism (BGS, 1992). The element mineral associations and stability of those minerals with regard to weathering can also affect sediment geochemistry (BGS, 1992). As a result of these factors, the interplay between them and the effect of grain size (e.g. Horowitz and Elrick, 1987), the temporal and spatial variation in suspended sediment geochemistry is very complex (e.g. Horowitz, 2001; Hillier, 2001 and Walling & Kane, 1982)

2.4.3 Organic-mineral balance

The organic-mineral balance of suspended sediment is important in terms of nutrient transfer, the effect on flocculation/aggregation and the transfer of organic carbon (C), as organic C comprises approximately 50% of organic matter (e.g. Naiman, 1982) and fluvial transport is the main pathway of organic C from the land to the oceans. Walling & Webb (1987) stated that suspended sediment in British rivers is typically composed of between 10% and 30% organic matter. Proportions of organic material in British rivers are highly variable and range from 1.0% to 95.2% (Table 2.1). The variations in the organic-mineral balance of suspended sediment can be partially explained by the organic-mineral balance of the sediment sources. For example, Francis & Taylor (1989)

Table 2.1. The proportion of organic matter in suspended sediment for selected British rivers.

Reference	River	Organic matter, %	
Walling & Kane (1982)	Exe, Devon		14.0
Walling & Kane (1982)	Creedy, Devon		10.0
Walling & Kane (1982)	Dart, Devon		9.0
Walling & Kane (1982)	Jackmoor Brook, Devon		9.0
Francis (1987)	Ceunant Ddu, Mid-Wales	Pre-ploughing range:	40.2-80.7
		Pre-ploughing mean:	73.4
		Post ploughing range:	69.0-95.2
		Post ploughing mean:	92.0
Francis (1987)	Nant Ysguthan, Mid-Wales	Pre-ploughing range:	41.0-74.0
		Pre-ploughing mean:	66.9
		Post ploughing range:	89.9-96.2
		Post ploughing mean:	94.0
Evans & Burt (1998)	Rough Sike, North Pennines	Storm flow:	40.0
Carling (1983)	Carl Beck and Great Eggleshope Beck, North Pennines	Range:	1.0-44.0
		Storm flow:	2.0-20.0
Hillier (2001)	River Don, Aberdeenshire	Base flow:	24
		Storm flow:	13
Robinson (1979)	Coalburn, Cumbria		50.0-75.0
Fleming (1969)	Kelvin, Scotland		15.0
	Clyde, Scotland		18.0
	White Cart, Scotland		27.0
University of Wales (1977)	Ystwyth, Mid-Wales		1.9-18.5
Wood (1977)	Rother		20.0
Collins (1973)	Sussex rivers		10.0-30.0
Finlayson (1978)	East Twin		15.0-37.0
Burt & Oldman (1986)	Peak District		30.0-40.0
Arnett (1978)	North York Moors		24.0-71.0
Arnett (1980)	North York Moors		30.0-40.0
Farr (1978)	Frome, Dorset		5.0-60.0
Labadz *et al.* (1991)	Shiny Brook, S Pennines		19.0

attributed the high proportions of organic matter in Ceunant Ddu, Mid Wales, to the dominance of peat in the catchment and the small catchment size. Variations in the organic-mineral balance can also be attributed to time of year. Walling & Webb (1987) noted a seasonal signal in the organic matter content of suspended sediment, with an increase in organic matter during the summer months given increased amounts of autochthonous matter. Discharge also affects the balance of organic and mineral sediment as the transport characteristics of mineral and organic sediment differ: organic material is buoyant (Warburton & Evans, 2001). Hillier (2001) noted a change in the relative proportions of organic and inorganic material during base flow and storm flow conditions (Table 2.1) and attributed it to dilution of the organic fraction by mineral sediment during storms and the difference in transport due to the differences in particle size and density. Wass & Leeks (1999) noted the same general relationship and identified it as non-linear; and the proportion of organic matter was much greater at lower concentrations. Carling (1983) concurred and established that the concentration of organic sediment increased as a power function with an exponent of 0.7. In contrast, Gurtz *et al.* (1980) found the proportion of organic and mineral sediment remained relatively constant and Malmquist *et al.* (1987) found a positive relationship.

Meybeck (1982) compiled information regarding the proportion of particulate organic carbon (POC) in suspended sediment of world rivers and established a general trend of decreasing POC with increasing suspended sediment concentration (SSC), and therefore increasing discharge. Walling & Webb (1987) converted the POC proportions into approximate organic matter proportions by a multiplication factor of 2.0 and placed the organic matter contents of British river suspended sediment in a global context (Figure 2.3). By global standards the suspended sediment of British rivers tends to have a higher percentage of organic matter (Figure 2.3).

2.4.4 Effects of sediment character on suspended sediment concentration

Sediment character influences the relationship between discharge and SSC and hence suspended sediment load. Assuming an abundant supply of homogeneous (equal size, density and uniform shape) sediment there would be a direct relationship between SSC and discharge (Figure 2.4A). However, if there were many smaller particles and few larger particles there might be a greater increase in SSC at lower discharges and a slower increase at higher discharges (Figure 2.4B). Conversely, if there were limited finer particles then the rate of increase in SSC at low discharges may be very slow in

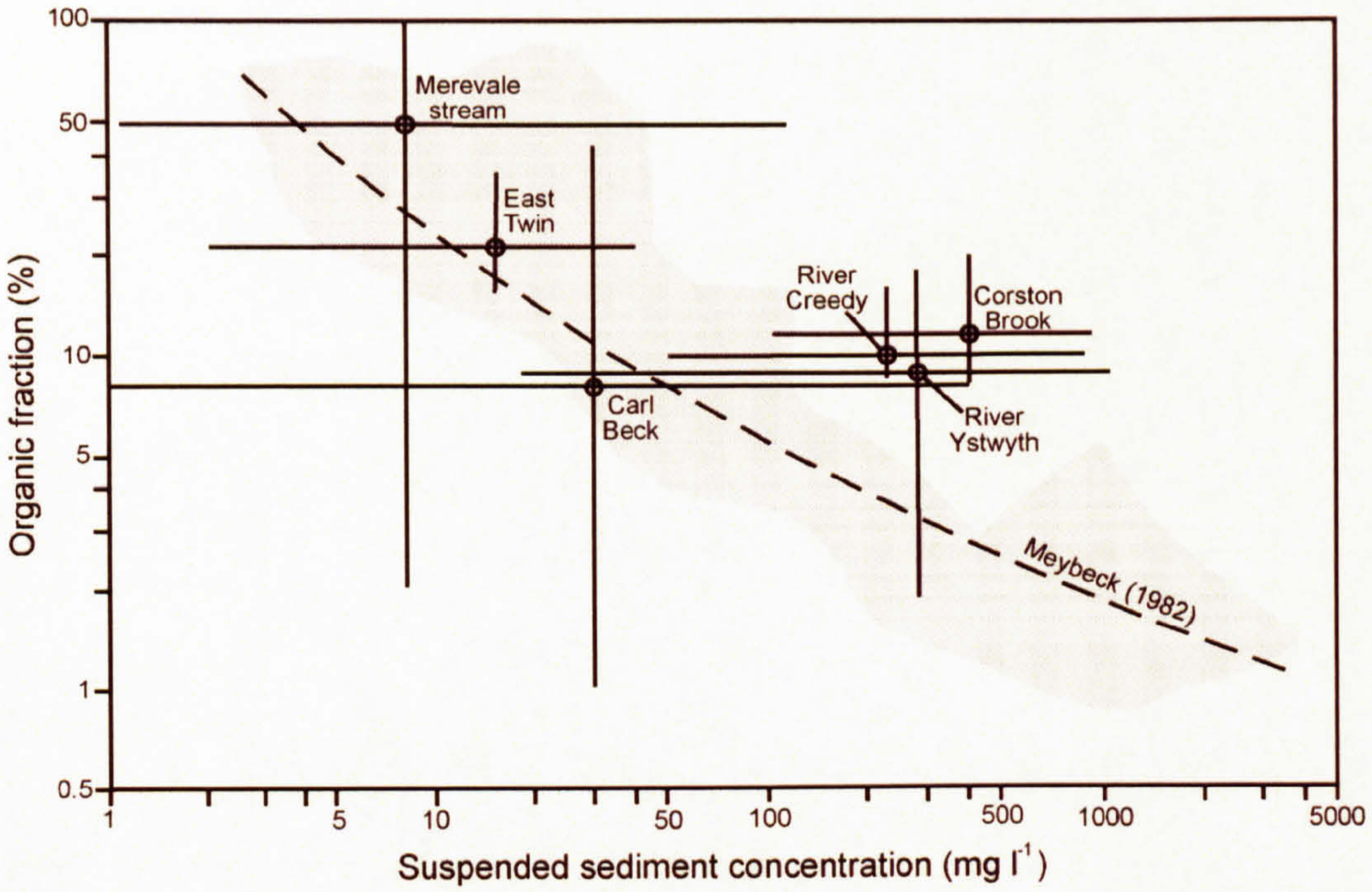

Figure 2.3. The proportion of organic matter in suspended sediment of global rivers with organic matter proportions of some British rivers superimposed (Walling & Webb, 1987).

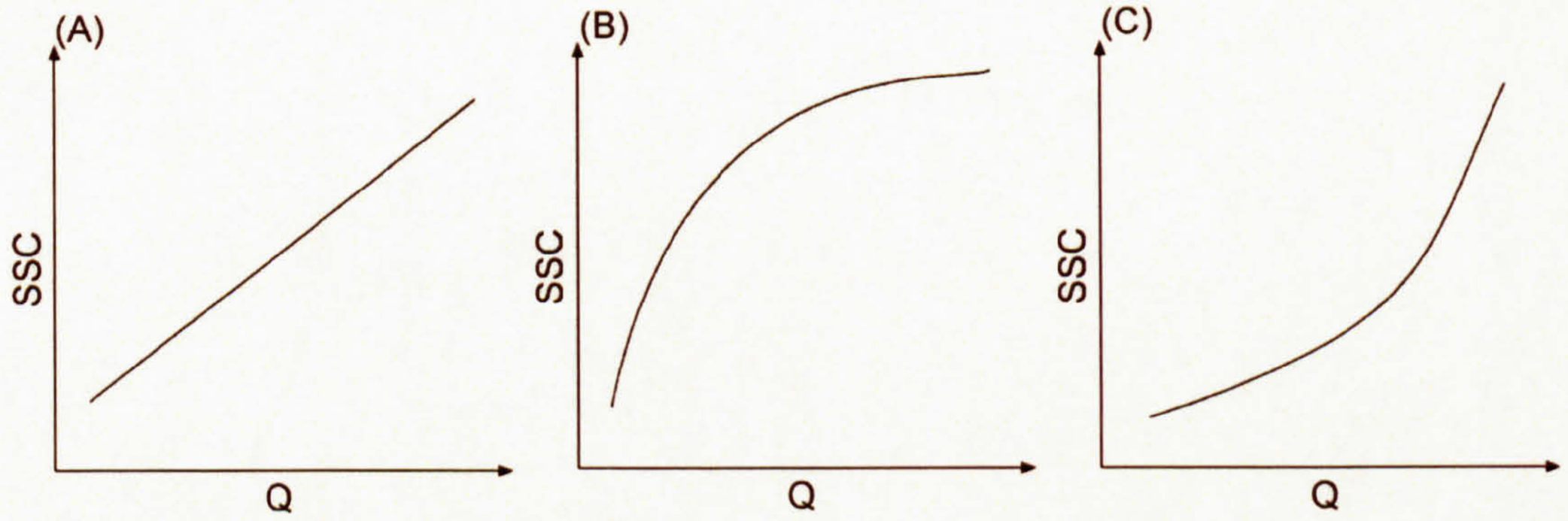

Figure 2.4. Theoretical curves demonstrating the effect of grain size distribution on the relationship between SSC and discharge. (A) assumes an abundant supply of homogenous sediment, (B) assumes more finer particles and fewer coarser particles, and (C) assumes limited finer particles and more coarser particles.

comparison with high discharges (Figure 2.4C). The actual relationship between SSC, discharge and grain size is difficult to define due to the balance between entrainment discharge and the weight of contribution of the different size fractions. This is further complicated by variation in sediment behaviour with size (Hjulström, 1935). The effect of varying particle size distributions on total SSC is demonstrated by Xu (2002) for four gauging sites on the Yellow River, China (Figure 2.5). It illustrates that the proportions of each size fraction varies with total sediment concentration, and therefore discharge. Generally, the contributions from the smaller particle size fractions increase up to total

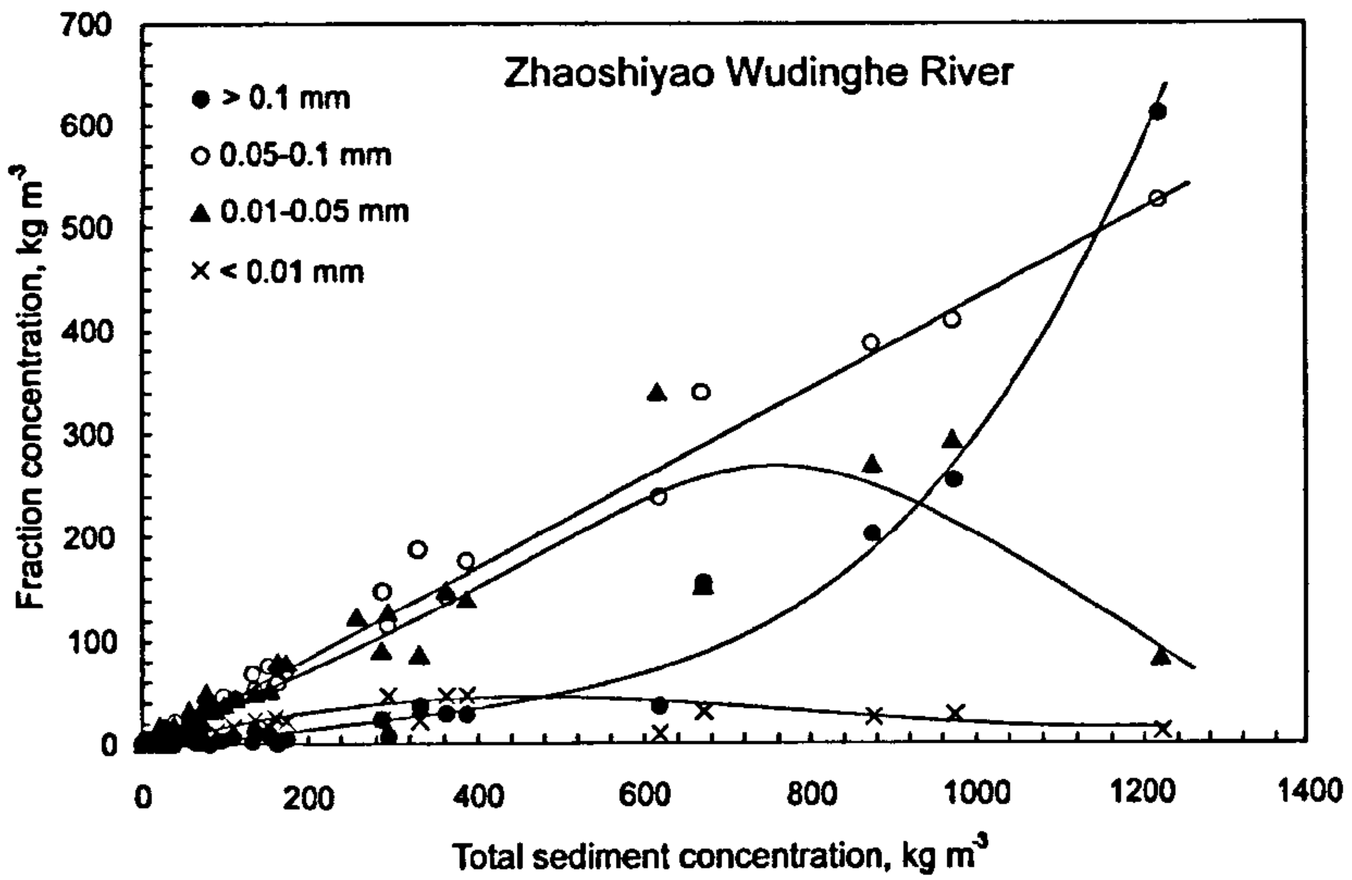

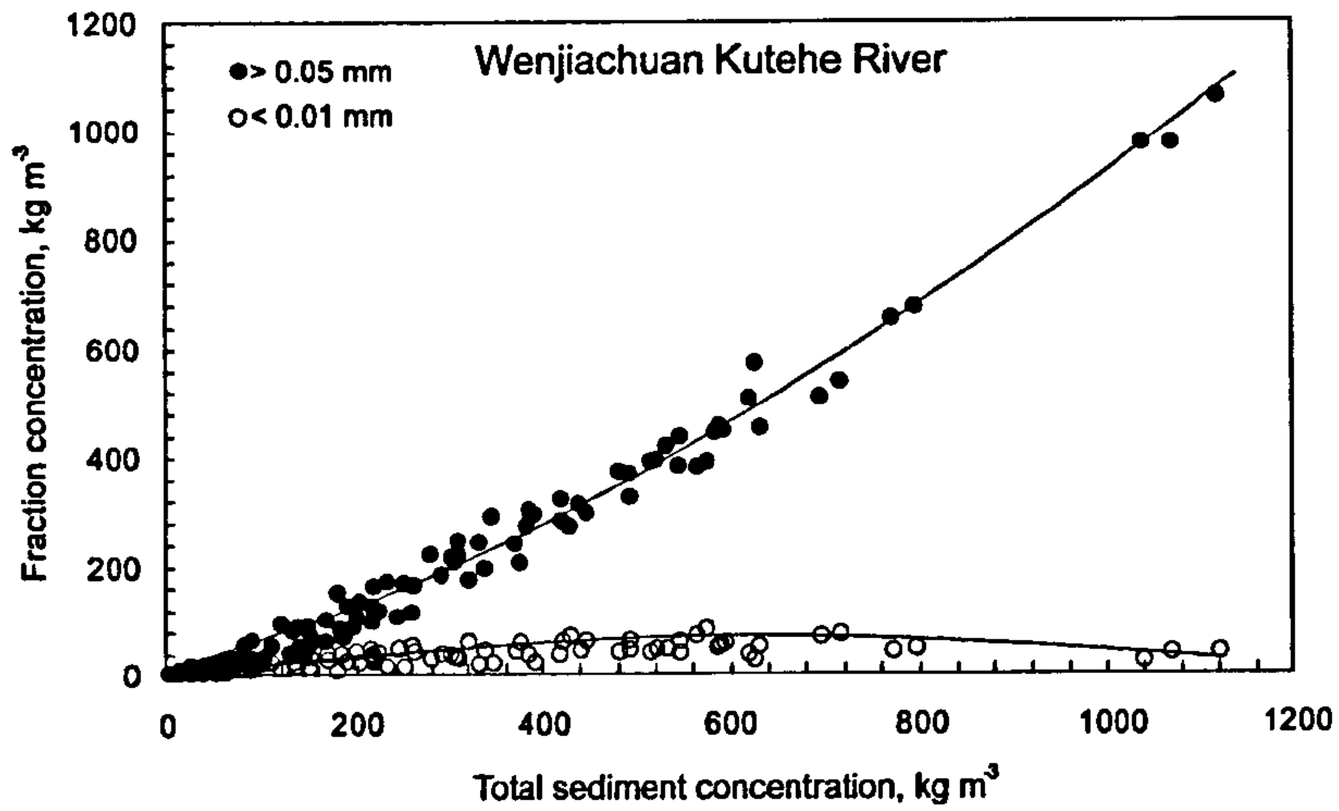

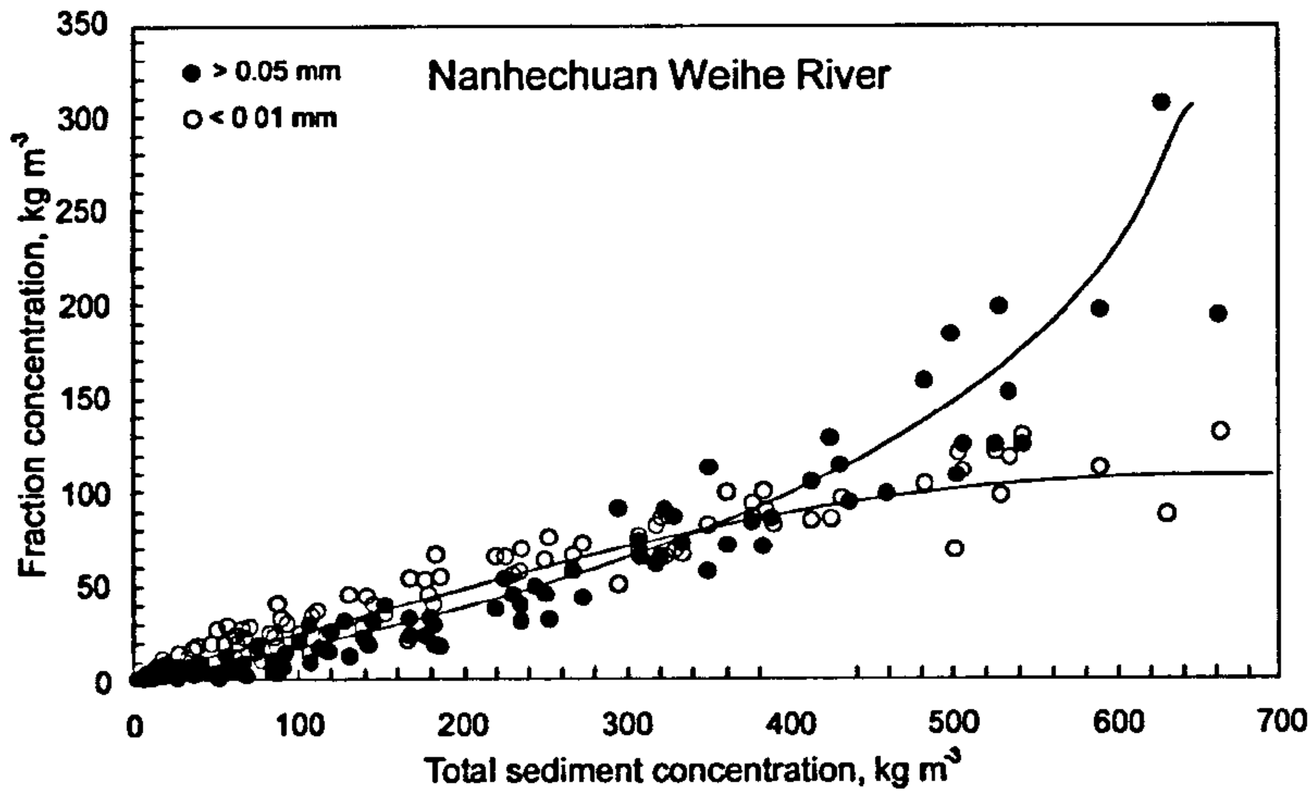

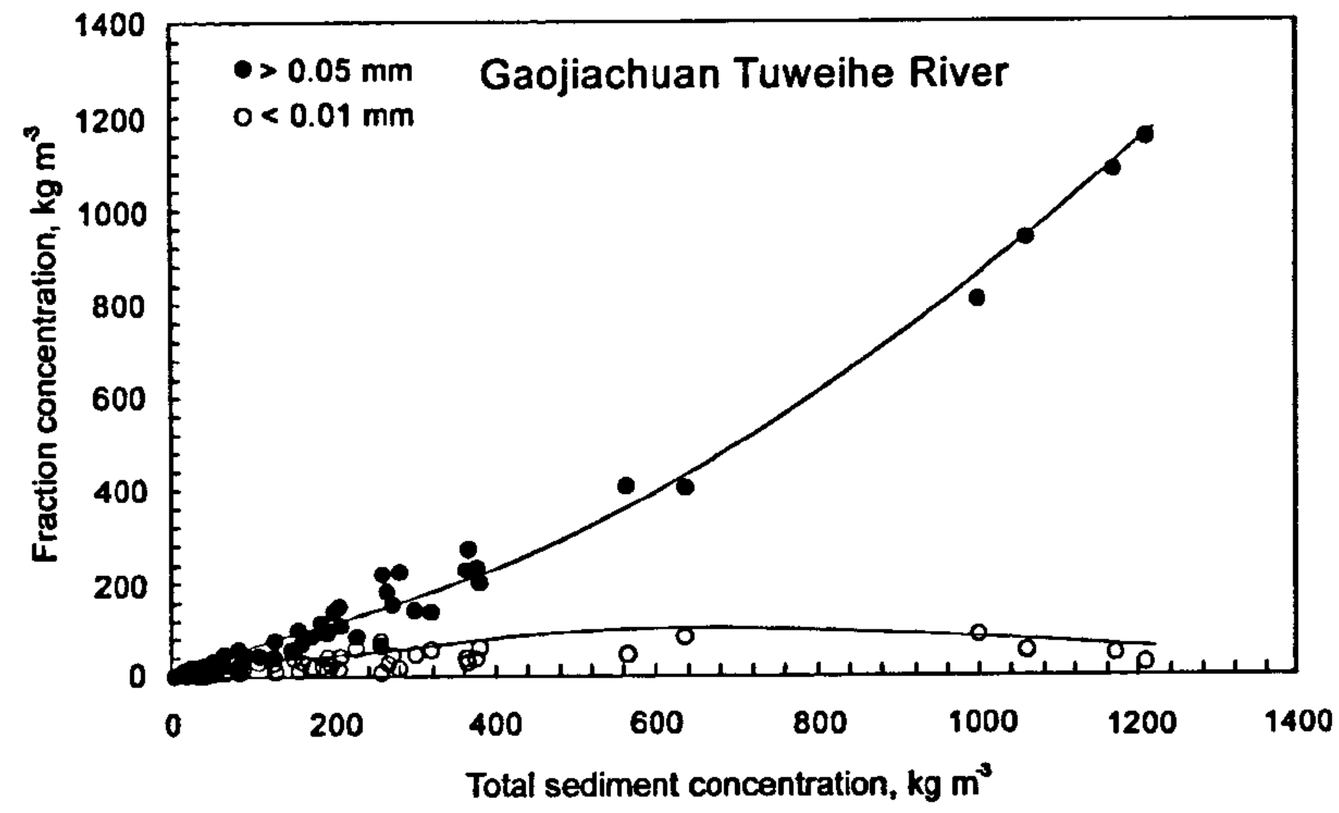

Figure 2.5. The variation in different grain-size fractions with total suspended sediment concentration for four rivers in the Yellow River catchment, China. Source: Xu, 2002.

sediment concentrations of 600 kg m^{-3} and then decrease (Figure 2.5). In contrast, the contribution from the larger grain size fractions increases with increasing discharge (Figure 2.5).

Furthermore, the organic-mineral balance is likely to have a substantial influence over this relation, especially in sites with a substantial organic component. A particular discharge will entrain larger organic particles than mineral particles given the more fibrous shape, and lower density of the organic sediment (Figure 2.6). It is assumed the relationship between grain size and discharge becomes very steep (Figure 2.6) given the buoyant nature of large peat blocks (Warburton & Evans, 2001). The dashed line on Figure 2.6 represents the maximum grain size which can be sampled by suspended sediment samplers. This illustrates that the large majority of mineral sediment is small enough to be sampled but a large proportion of organic material transported in suspension, namely the peds and peat blocks, are too large to be sampled. Mineral sediment is likely to contribute more to the total mass of suspended sediment at lower discharges (Figure 2.6) given its higher density. However, as the discharge increases large peat blocks may be entrained, therefore resulting in the dominance of organic material.

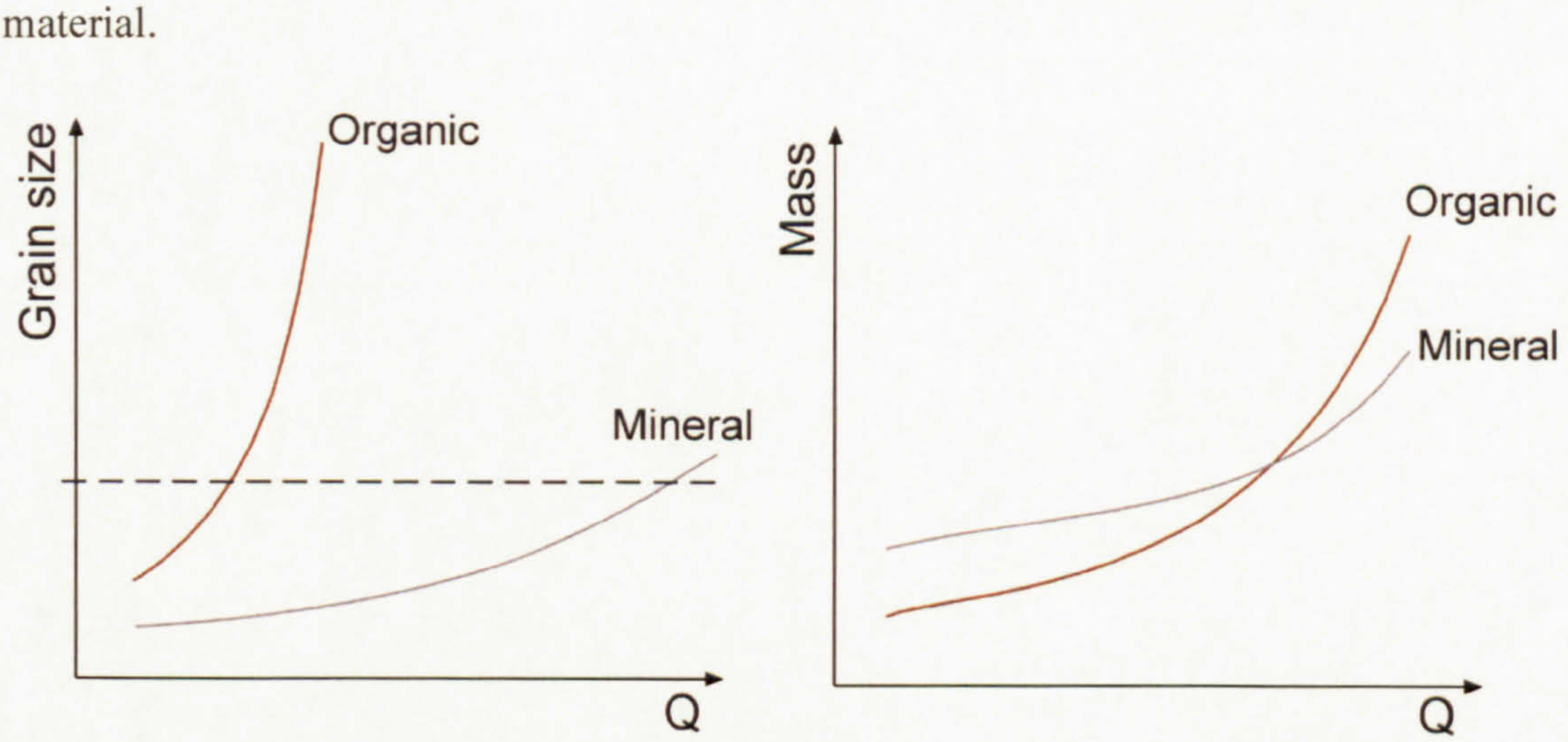

Figure 2.6. The relation between grain size, mass and discharge for organic and mineral sediment.

The organic-mineral balance is also important when considering sediment deposition. Mineral sediment of a given size will settle out at a higher velocity than equal-sized organic sediment (Figure 2.7), as a result of the difference in densities and also the difference in suspended sediment shape: mineral sediment is denser and rounder. Ferguson & Church (2004) calculate the settling velocity (w) using the submerged specific gravity (R), grain diameter (D), acceleration due to gravity (g), the kinematic

viscosity of the fluid (v, which is 1.0×10^{-6} kg m^{-1} s^{-1} for water at 20°C) and two parameters which quantify grain roundness (C_1 and C_2),

$$w = \frac{R g D^2}{C_1 v + (0.75 C_2 R g D^3)^{0.5}} . \qquad (2.1)$$

Mineral sediment was assumed to be round (C_1 = 18.0 and C_2 = 0.4) and organic sediment angular (C_1 = 24.0 and C_2 = 1.2). A submerged specific gravity of 1.7 was assumed for mineral sediment and 0.4 for organic sediment. These submerged specific gravities are representative of the study sites of this investigation (Warburton, pers. comm.). It is evident that as grain sizes increase the difference in settling velocities increases (Figure 2.7) and therefore the organic-mineral balance becomes more important. This will result in the preferential storage of mineral sediment in the fluvial system. Gravity, which promotes grain settling, is offset by upward turbulent impulses, which scale with the mean flow velocity. As a result the maximum grain size in suspension is greater in floods than in base flow and may extend to sand (which was observed on filter papers from the samples collected in this investigation). There is effectively no capacity limit on the silt and clay fractions and this washload flux is always supply-limited.

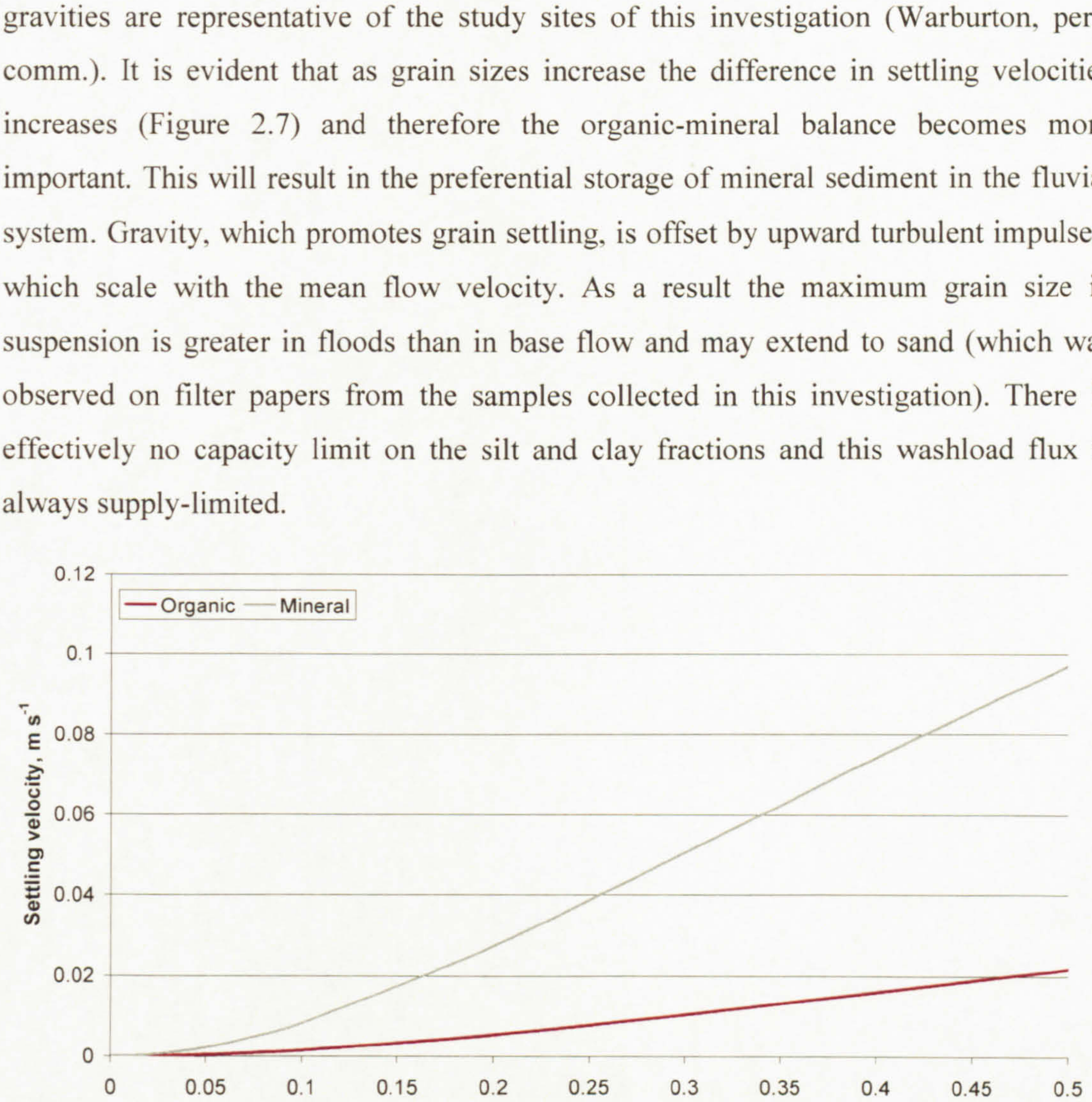

Figure 2.7. Settling velocities of organic and mineral particles calculated using the method of Ferguson & Church (2004).

These examples demonstrate the potential influence of grain size and organic-mineral balance on suspended sediment dynamics. The situation in the physical system is more

complex given the interplay between these components, affects of sediment supply and other sediment characteristics.

2.5 Suspended sediment sources

Throughout the discussion of the nature of suspended sediment the characteristics of sediment sources have been identified as a key factor. These characteristics are, in part, controlled by sediment source type. Potential suspended sediment sources types are: the channel bed, channel banks, land surface, sub-surface, tributaries, effluent discharges, and the air. In addition to these different sources, different processes can release sediment from them which can effect the sediment character (Table 2.2). For example, sediment input from the channel banks from bank collapse is likely to be coarser than sediment eroded from the banks.

Table 2.2. Potential suspended sediment sources and release processes.

Source	Process
Channel bed	Re-entrainment
	Rainfall erosion in ephemeral channels
	Erosion of channel bed forms such as bars
	Release of sub-surface material by channel bed movement
Channel banks	Bank collapse
	Erosion processes
Land surface	Overland flow (infiltration excess and saturation excess)
	Direct fall from valley sides
	Mass movements
	Gully inputs
	Disturbance, including cattle trampling, field drains etc.
Sub-surface	Throughflow
	Groundwater flow
	Soil pipes
Air	Aeolian transport
	Atmospheric deposition

The sources of suspended sediment and dominance of those sources are highly variable, through both time, from inter- to intra-catchment scales, and space, from intra- to inter-storm scales (e.g. Russell *et al.*, 2001 and Imeson *et al.*, 1984). The importance of specific sediment sources in different catchments varies (Table 2.3). It is evident that hillslope sources are generally considered important, as are channel sources (bank and bed) and tributaries (Table 2.3). However, as the data have been collected from a range of articles, each with different objectives, some sources may not have been reported. For

example, the channel bed has not been reported as a source by Labadz *et al.* (1991), but given the responsiveness of small upland catchments it is likely that sediment is stored on the channel bed and re-entrained.

Sources of sediment change with distance downstream. In the upper parts of a catchment, hillslope sources are generally more important as hillslopes tend to be steeper, drainage density higher, floodplains narrower and therefore there is stronger connectivity between the hillslopes and channel. Alternatively, downstream channel sources become more important as there is limited coupling between the hillslopes and channel given lower angle slopes, lower drainage density, wider floodplains and anthropogenic impacts.

Table 2.3. Variability in sediment sources in selected river catchments. ▒ represents a major source and ■ represents a minor source.

Reference	River	Hillslope	Bank collapse	Bank erosion	Scars	Pipes	Channel bed	Drainage	Mass movement	Tributaries	Gullies	Groundwater	Autochthonous
Asselman (1999)	River Rhine, Germany	▒			■				▒				
Burt & Gardiner (1984)	Shiny Brook, South Pennines	▒											
Francis & Taylor (1989)	Ceunant Ddu & Nant Ysguthan, Mid Wales		▒						▒				
Gilvear & Petts (1985)	River Tryweryn, North Wales		■							▒			▒
Hillier (2001)	River Don, Aberdeenshire	▒											
Hooke (2000)	Gila River, Arizona	▒		▒									
Ichim *et al.* (1984)	Rivers in Northeast Romania.												
Labadz *et al.* (1991)	Shiny Brook, South Pennines	▒											
Lewin (1974)	Maesnant, Mid Wales		▒	■									
Smith *et al.* (2003)	River Swale (Leckby Grange)		■							▒			
Walling & Webb (1987)	Devon catchments							■					
Wasson (1994)	Southern Uplands, Australia										▒		

Also, because channel gradients are steeper in the upper catchments the channels are more efficient at transporting sediment, thus there is limited in-stream storage, whereas in the lower catchment the gradient is less steep which promotes more storage within the channel (and overbank).

Suspended sediment is stored in scour holes at channel confluences, pools and riffles, topographical elements such as bars and breaks in channel slopes, slack water areas and floodplains. Sediment stored within slack water areas, the floodplain and some topographical features may be entrained from temporary storage during storm events or may be stored long-term (Schumm *et al.*, 1987).

Numerous studies have examined the contribution of channel banks to suspended sediment loads (Table 2.4). Sediment sourced from channel banks between catchments accounts for between 17% and 92% of annual suspended sediment loads (Table 2.4). Inputs of sediment from channel banks are seemingly lower in British rivers (Table 2.4). Sediment contributed by channel banks also varies spatially at an intra-catchment scale. Some authors, such as Hooke (1980) and Hasegawa (1989), found that bank erosion increased downstream, while others, such as, Lewin (1987) and Prestegaard (1988) found that bank erosion was highest in the middle reaches. Channel bank contribution has also been shown to vary temporally. For example, Lawler (1994) investigated the temporal variability of channel bank sources in response to flood events on the River Arrow, Warwickshire, using Photo-Electronic Erosion Pins (PEEP's). He concluded that bank responses were highly variable but net erosion occurred in the late winter, and summer and autumn was dominated by net deposition. Therefore it can tentatively be assumed that sediment is eroded and transported within the same event in the late winter and during the summer and autumn sediment is eroded and then deposited to await further transport.

All the factors discussed above influence the form of the storm sedigraph. The main sources are baseflow, bed surface storage, channel banks, hillslopes, gullies, and sediment released by bank collapse. The relationship between these sources is likely to be complex and variable from storm to storm, but a generalised sedigraph can be presented (Figure 2.8). Baseflow SSC is likely to be fairly constant throughout the event (Figure 2.8). Entrainment of material from the channel bed will cause a steep rise in SSC at the beginning of the storm sedigraph (Figure 2.8). Sediment derived from the

Table 2.4. The contribution of channel banks to suspended sediment loads. * denotes that channel bed scour is also included.

Reference	Location	% Sediment from channel banks
Bull (1997)	River Severn, UK	17
Ashbridge (1995)	River Culm, UK	19
Walling *et al.* (1999)	River Ouse, UK	37
Kronvang *et al.* (1997)	Denmark	92*
Rondeau *et al.* (2000)	St Lawrence River, Canada	65*
Odgaard (1987)	East Nishnabotna & Des Moines River, USA	30-40
Sekely *et al.* (2002)	Blue Earth River, USA	37
Wilkin & Hebel (1982)	Illinois, USA	50

bank (but not bank collapse) and hillslopes is likely to rise through the event as discharge increases and then tail off as discharge recedes and sediment sources are exhausted (Figure 2.8). Gully inputs and bank collapse are likely to result in steep peaks superimposed on the basic form (Figure 2.8). Bank collapse are more likely to occur on the falling limb but could occur at any time. Finally there may be other 'complex responses' caused by the effects of sediment transfer through the system, e.g. tributary inputs and hydrograph form in terms of the number of peaks and the relative importance of runoff, interflow and baseflow (Figure 2.8).

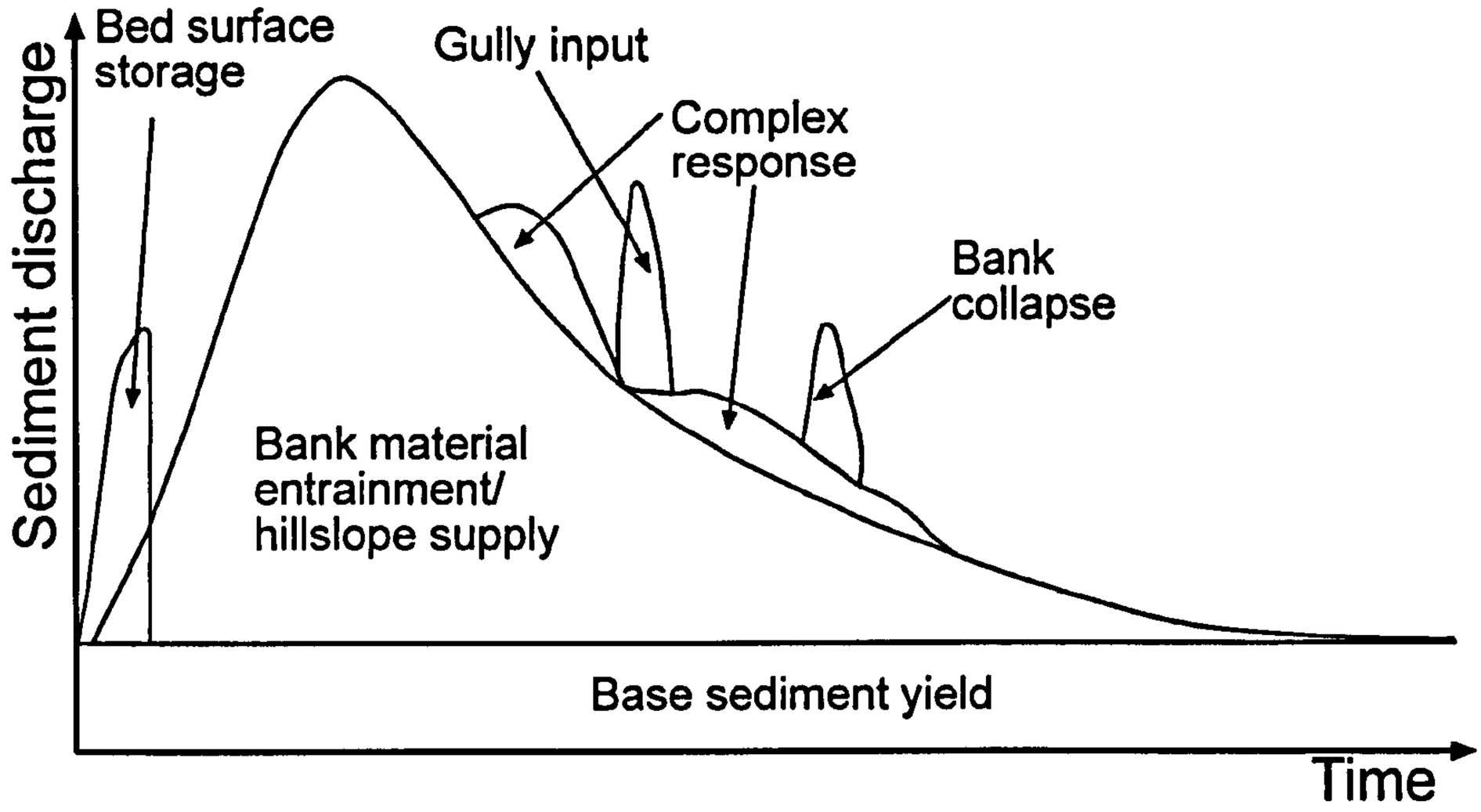

Figure 2.8. Simple schematic of the effects of different sediment sources on sedigraph form.

In summary, there are a wide range of sediment sources and different processes which release sediment from them. The range and relative contribution of sediment from the

different sediment sources vary spatially and temporally at a range of scales and affect storm sedigraph form.

2.6 Factors affecting suspended sediment dynamics

Within the literature discussion of factors affecting suspended sediment dynamics is generally polarised between large-scale studies examining the importance of factors using several catchments or small-scale studies based on one or two catchments. The large-scale studies tend to focus on large-scale characteristics, such as geology, topography and annual discharge. The catchment-specific studies generally focus on discharge as a control, with limited mention of other influences and their relative importance. Evaluating the importance of individual forcings at the catchment scale from catchment-specific studies is difficult, and arguably inappropriate given the variability in forcings between catchments. Also, within a field setting there is no reliable method of quantifying the relative importance of individual factors and the importance of interplay between them. This is further complicated by complexities superimposed by temporal variation in the various influences and catchment history.

The factors which affect suspended sediment dynamics are discussed below. They are divided into large-scale controls and small-scale controls as this is the divide evident in the literature. A comprehensive review can not be provided due to the variation in the importance of controls at different scales, both spatial and temporal. Therefore, examples are given to demonstrate the potential impact on suspended sediment dynamics and the variability in the importance of different controls. This is not an exhaustive review but intends to demonstrate the complexity of factors which affect suspended sediment dynamics.

2.6.1 Large-scale controls

Suspended sediment yields are highly variable at a global scale (Figure 2.9) as a result of heterogeneous hydrological and environmental conditions. Several studies quantitatively investigated large-scale patterns in suspended sediment and attempted to explain the similarities and contrasts by various internal and external forcings. These studies suggest that precipitation (Langbein & Schumm, 1958; Milliman & Syvitski, 1992; and Dedkov & Moszherin, 1992), discharge (Milliman & Syvitski, 1992 and Ludwig & Probst, 1996), basin area (Milliman & Syvitski, 1992), topography (Milliman & Syvitski, 1992 and Dedkov & Moszherin, 1992), geology (Milliman & Syvitski, 1992

and Dedkov & Moszherin, 1992), vegetation (Milliman & Syvitski, 1992 and Dedkov & Moszherin, 1992), and anthropogenic activity (Milliman & Syvitski, 1992 and Dedkov & Moszherin, 1992) affect suspended sediment dynamics at a large-scale. Areas with high and intense precipitation, high and irregular runoff, dissected mountain relief composed of sedimentary rocks, intense recent tectonic activity and land use change from forest to agriculture in lowland areas experienced the most intense erosion (e.g. New Zealand). Conversely areas with low erosion rates were those covered with dense forest, crystalline rock, low mountains and temperate climate (e.g. Scandinavia) (Dedkov & Moszherin, 1992).

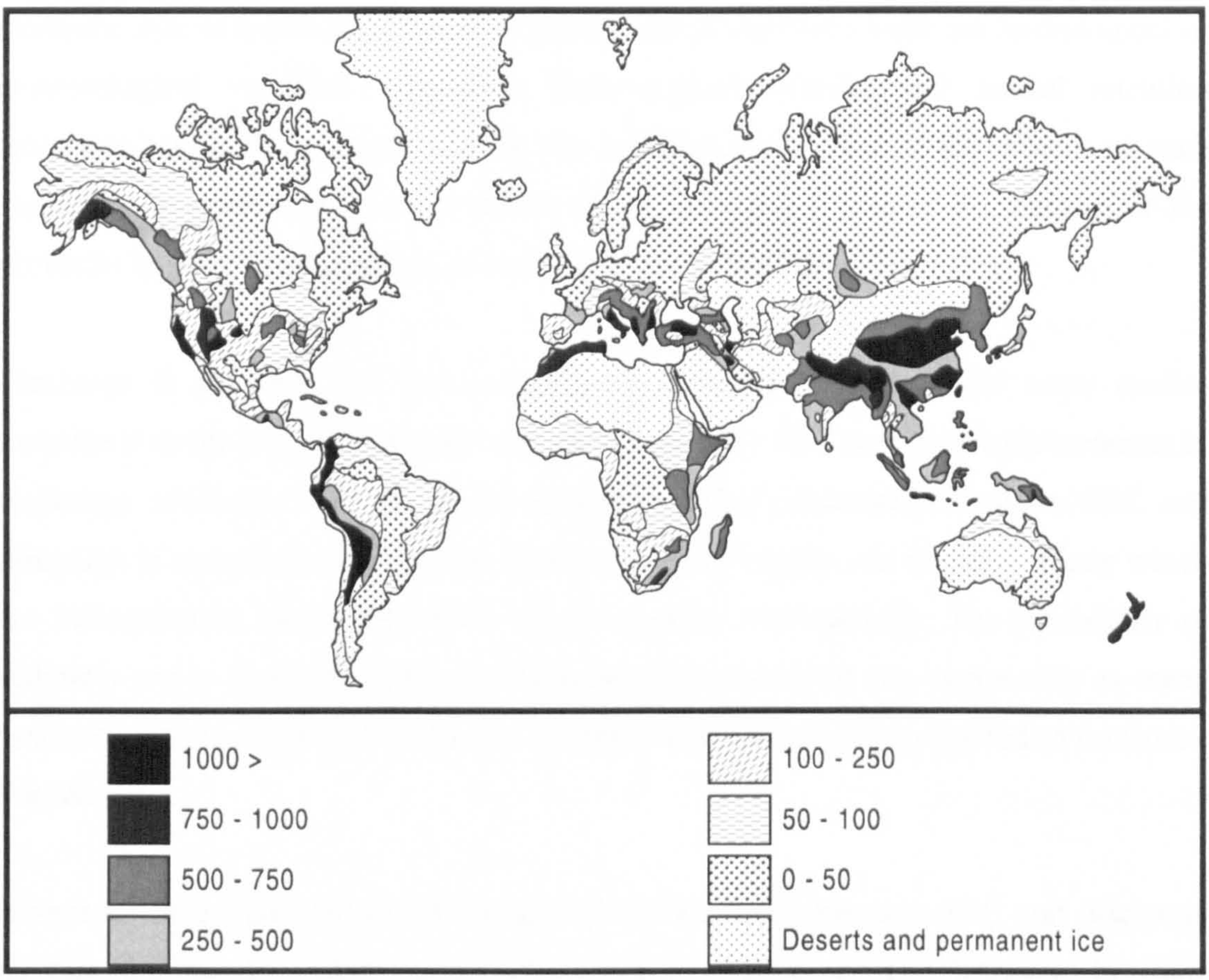

Figure 2.9. Suspended sediment yields (t km^{-2} yr^{-1}) from rivers throughout the globe. Source: Walling & Webb, 1983.

The studies by Langbein & Schumm (1958), Milliman & Syvitski (1992), Ludwig & Probst (1996), and Dedkov & Moszherin (1992) highlight the implications of spatial-scale and specific catchment characteristics which prevent the success of such large scale conjectures. High errors are likely to occur due to the interplay of many factors and individual nature of catchments. Jansson's (1988) survey of global sediment yields reinforces this. Jansson (1988) could not establish relationships between discharge,

runoff and sediment yield. The lack of relationships and trends was explained by the variation in temperature, precipitation, vegetation, seasonality (droughts and rainy season) and discharge within each climatic region.

2.6.2 Small-scale controls

This section illustrates the potential influence of controls on suspended sediment dynamics and delivery in specific catchments. It is divided into two sections: stable controls and varying controls.

2.6.2.1 Varying controls

Controls over suspended sediment dynamics which vary with time are hydrological or meteorological variables, vegetation, anthropogenic activity and natural retention structures within the channel and on the hillslope. Examples of the effects of such variables are given below. This review is not exhaustive, primarily reflective of the problems in isolating the effects of such variables in the field.

Discharge is generally the key control over suspended sediment and many studies examine it as the principal control over SSC. Generally SSC increases with increases in discharge, although there are some exceptions. The relationship between SSC and discharge is non-linear and variable due to sediment supply and dilution effects which are influenced by processes which vary temporally and spatially. The availability of sediment varies spatially within and between catchments but also temporally as many systems, and most within Britain, are sediment supply-limited as opposed to transport-limited.

Numerous investigations have illustrated the relationship between SSC and discharge through the use of rating curves (discussed in section 4.5.1). However, in some situations there is no link between discharge and SSC. For example, Stott & Grove (2001) studied the suspended sediment dynamics of Skeldal River, a proglacial river in north-east Greenland, and found that some peaks in SSC did not correlate with discharge peaks. Possible explanations were sediment input from small slides at the snout associated with melting and sediment input from unstable banks following undercutting. While this is an example within a glacial environment similar occurrences happen in rivers without a glacial influence e.g. banks have been reported to collapse on

the receding limb of floods as the support provided by the water is removed (Carling, 1983).

Stott & Grove (2001) investigated the difference between SSC and discharge relations for snowmelt and rainfall-triggered events. The relationship between SSC and discharge was highly significant for rainfall-triggered events, indicating precipitation was a strong process control. In contrast the relationship between SSC and discharge was very variable for non-rainfall triggered events, which suggests that snowmelt events provide more variable quantities of sediment to the channel, possibly from melting of snow not in contact with the hillslope, frozen ground, or a more gradual supply of runoff with a lower transport capacity.

Lenzi & Marchi (2000) investigated the effect of snow cover on sediment yields of a mountain stream in the Dolomites, Italy, and found reasonable relationships between SSC and discharge, both for events generated by floods and for events generated for snowmelt. However, there was a clear difference in the flood SSC-discharge and snowmelt SSC-discharge data clouds (Figure 2.10). The difference in data clouds was attributed to fine-grained material transported from the hillslopes during the snowmelt period and hence relatively high SSC were associated with relatively low discharges. Early snowfall and permanent snow cover throughout the winter followed by a slow and gradual melt was found to minimise suspended sediment fluxes. Conversely, a mild winter with intermittent snow cover increased suspended sediment fluxes due to the preparation of sediment for transport by freeze-thaw cycles and raindrop impact erosion. Also, rapid snowmelt floods were associated with higher suspended sediment concentrations (Lenzi & Marchi, 2000).

Some authors found the rate of change in discharge exerted a notable control over SSC (e.g. Richards, 1984). The concept was explained well by Bogen (1980) using a simple equation: higher concentrations of suspended sediment are associated with faster increases in discharge as sediment concentration at the reach output (C_o) is equal to the sediment concentration input to the reach (C_i) plus the amount of sediment entrained (ΔM), which is a result of discharge (Q), and the change in discharge (ΔQ) in a given time increment (Δt) (*n.b.* $Q + \Delta Q$ = total discharge):

$$C_o = C_i + \frac{\Delta M}{(Q + \Delta Q)\Delta t}. \qquad (2.2)$$

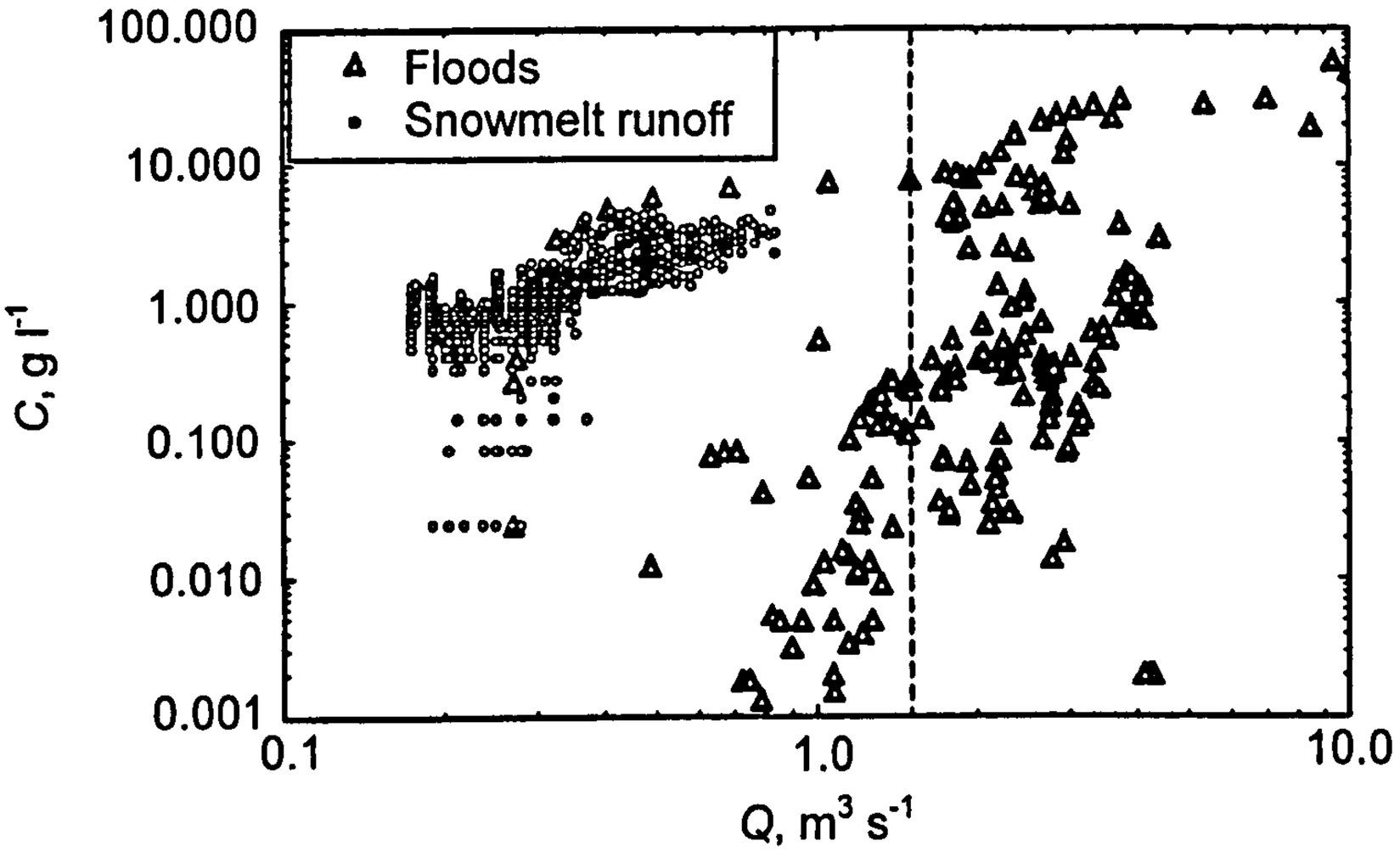

Figure 2.10. Differences in rating curve form for snow melt events and flood events. The dashed line represents a Q threshold above which bed load transport occurs. Source: Lenzi & Marchi, 2000.

Therefore if two scenarios are run with equal values for C_i, Q, ΔQ and ΔM but in scenario 1 $\Delta t = 1$ and in scenario 2 $\Delta t = 5$ then C_o will be greater for scenario 1, which experienced the quicker increase in discharge. This equation can also be used to demonstrate that if the amount of sediment eroded does not increase at a rate proportional to the increase in discharge then the sediment concentration at the output will decrease.

Other hydrological variables are rarely quantified and discussed given the problems associated with isolating their affects and the frequency with which they vary. Studies which do successfully isolate such variables tend to focus on short time-periods (e.g. storm-scale (Seeger *et al.*, 2004)). The same problems exist for meteorological variables and once again are generally examined at short-time periods.

The two principal meteorological variables which affect suspended sediment dynamics and delivery are precipitation and temperature. Temperature exerts control over suspended sediment dynamics via various processes, including: freeze-thaw, freezing of the river, snow, snowmelt and desiccation. Freeze-thaw, including the development of

needle ice, affects SSC by preparing sediment for transport and is a notable factor in many catchments (Hill, 1973; Curr, 1984; Francis, 1987; Lawler, 1986, 1987; Stott *et al.*, 1986; Wolman, 1959; Blacknell, 1981; Labadz *et al.*, 1991; and Gardiner, 1983). Desiccation was shown to be important in a peat-dominated catchment (Francis, 1990). Freezing of the channel will halt suspended sediment flux. In the British uplands complete channel freezing does not often occur, but this is important in places such as Quebec, Canada, where rivers freeze solid for approximately three months (Naiman, 1982). The intensity, as well as the amount, of precipitation is important, as intensity affects the erosive power and has subsequent affects on the discharge regime. The timing and intensity of precipitation generally varies seasonally (Figure 2.11).

The effect of meteorological conditions are interlinked with the effect of vegetation (Figure 2.11). Temperature and rainfall affect the type, extent and health of the vegetation and the type, extent and health of vegetation exert a strong control over SSC as it influences the impact of raindrop erosion, intercepts rainfall, affects the cohesiveness of the soil (binding action of roots and the provision of organic matter) and obstructs sediment transfer to the channel (Figure 2.11).

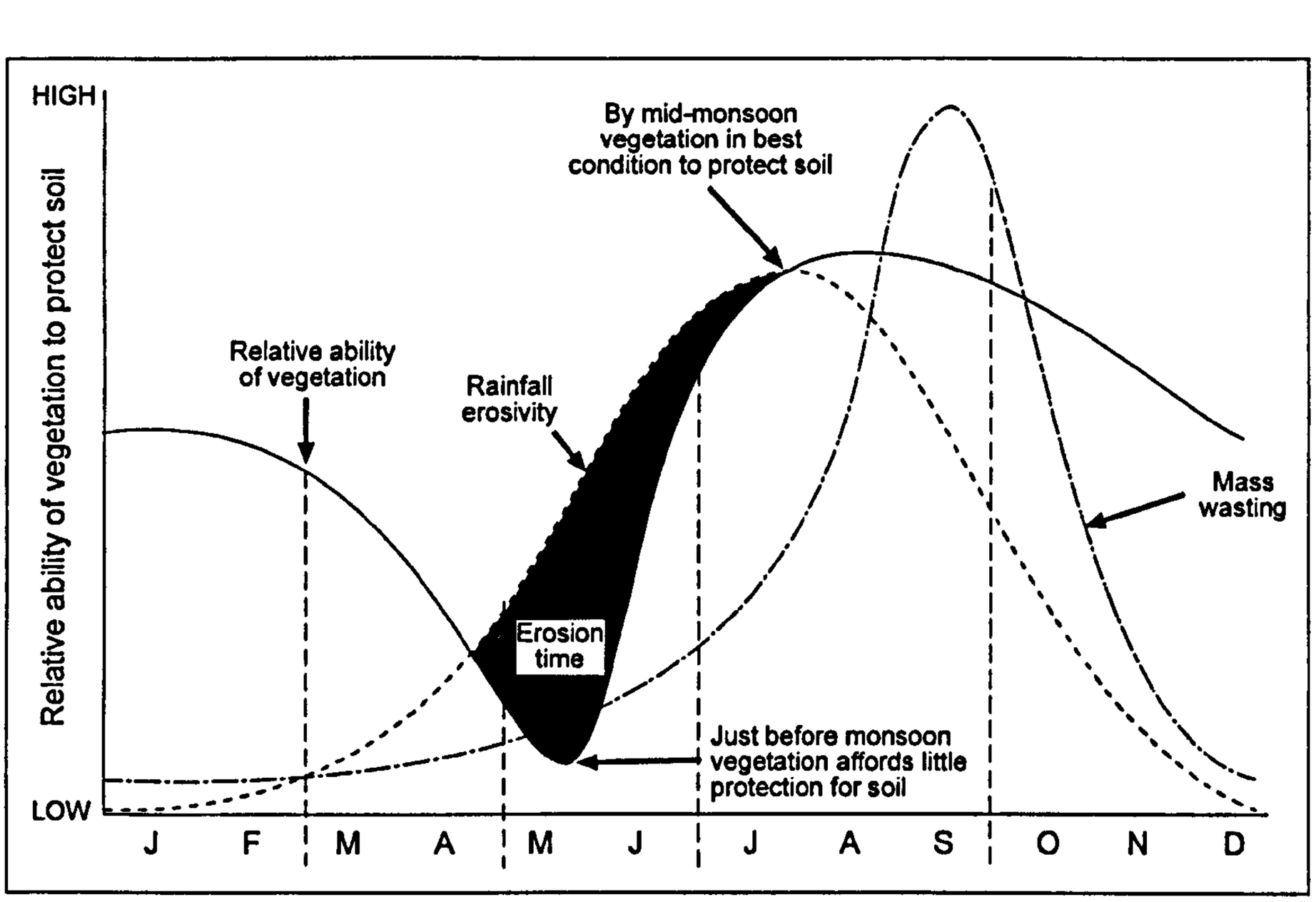

Figure 2.11. Relation between rainfall erosivity and ability of vegetation to protect soil. Based on an illustration by Galay (1987) for Nepal. Source: Morris & Fan, 1997.

Consideration of catchment vegetation in studies of suspended sediment dynamics is variable. Francis & Taylor (1989) observed that the growth of vegetation within furrows

and a vegetated buffer zone parallel to the channel reduced the potential SSC in Ceunant Ddu and Nant Ysguthan catchments, Mid-Wales. Studies which discuss the effects of vegetation are generally those which are investigating the response to land use change (e.g. Leeks & Marks, 1997 and Burt *et al.*, 1984). Within these it is difficult to isolate the effect of different vegetation types from the impact of the disturbance. For example, how much of the increase in suspended sediment flux after felling is a result of the change in vegetation cover and how much is the result of land disturbance by heavy machinery? The categorical nature of the data, the intra-annual variability of vegetation cover and the numerous ways in which it can affect suspended sediment dynamics inhibit quantified analysis of its influence.

In addition to the vegetation, meteorological and hydrological variables which control the flux of suspended sediment through sediment availability and transport capability, sediment retention mechanisms prevent and interrupt available sediment from being transported. Retention mechanisms can be natural and artificial. Vorosmarty *et al.* (1997) estimated that more than 40% of the global river discharge is intercepted by impoundments and that more than 25% of annual suspended sediment discharge to the oceans is currently trapped within reservoirs. Sediment yield at the mouth of the Mississippi River decreased by 50% between the 1950s and the 1980s due to the construction of five dams on the Missouri River, one of the Mississippi's major tributaries (Meade & Parker, 1985).

Naiman (1982) outlined the influence of various natural retention devices on suspended sediment including: physical retention devices such as debris jams, low gradient reaches, coves and eddies within meandering sections, sandbars and floodplains; and chemical process retention devices (which are more applicable to organic sediments), for example, chemical processes which promote flocculation, microbial uptake and oxidation. Gellis (1993) examined the effect of naturally generated physical retention devices (although some were of anthropogenic origin) on the suspended sediment load of Lake Loiza basin, Puerto Rico, during Hurricane Hugo. The sediment yield was lower than expected (the predicted load was 248,300 tonnes and the actual was only 99,600 tonnes) and was attributed to increased debris (uprooted vegetation, power lines, defoliated vegetation, anthropogenic structures) caused by high winds which reduced raindrop erosion and acted as dams within the channel and on the hillslopes.

Retention devices are given limited coverage in suspended sediment studies, perhaps with the exception of those examining rivers with dams. This probably reflects problems in characterising them given their generally temporary and randomly distributed nature. Also, retention devices often affect the timing of sediment delivery, not the amount of sediment delivered. Reservoirs are a common exception to this, dependent on management regime, and are fundamental for examining longer-term suspended sediment dynamics.

Anthropogenic activity also affects sediment availability and the efficiency of transport processes to and within the channel. Anthropogenic activities have been shown to have dramatic influences on sediment yield through land use change and point source inputs. Numerous authors have outlined the effects of land use change including forestry activity (e.g. Johnson, 1988), urbanisation (e.g. Walling, 1974) and ditching (e.g. Burt *et al.*, 1984). The exact effects of such activities differ between catchments (due to catchment characteristics and the nature and timing of disturbance). The responses of catchments to such disturbances are complex. For example, urbanisation may initially increase SSCs by disturbance which, in effect, prepares sediment for transport. Once disturbance ceases there may be less sediment available for transport compared with before. However, this is countered by anthropogenic inputs and higher stream powers given increased runoff as a result of the lower infiltration capacities of urban environments.

Francis & Taylor (1989) investigated the effects of ploughing on SSC in Ceunant Ddu and Nant Ysguthan, Mid Wales. Ploughing was found to cause an increase in the variability, response time and quantity of SSC; SSC was more variable and responded quicker to increases in discharge and suspended sediment load increased by 246% in Ceunant Ddu and 479% in Nant Ysguthan. Although these figures seem high, catchment area and total suspended loads of the catchments are small.

The Hades Clough catchment, southern Pennines, was ditched to improve conditions for afforestation (Burt *et al.*, 1984). The ditching had major impacts on SSCs: peak SSCs were shown to increase from pre-ditching levels by three orders of magnitude during ditching, two orders of magnitude after ditching and remained very slightly elevated six years later. Robinson (1980) devised a conceptual model of the effect of ditching on SSC (Figure 2.12). The impact of ditching differs between catchments, for example

ditches cut into well drained soils vegetated over, thus reduced sediment supply. Those cut into clay remained unvegetated and continued to provide sediment (Burt *et al.*, 1984).

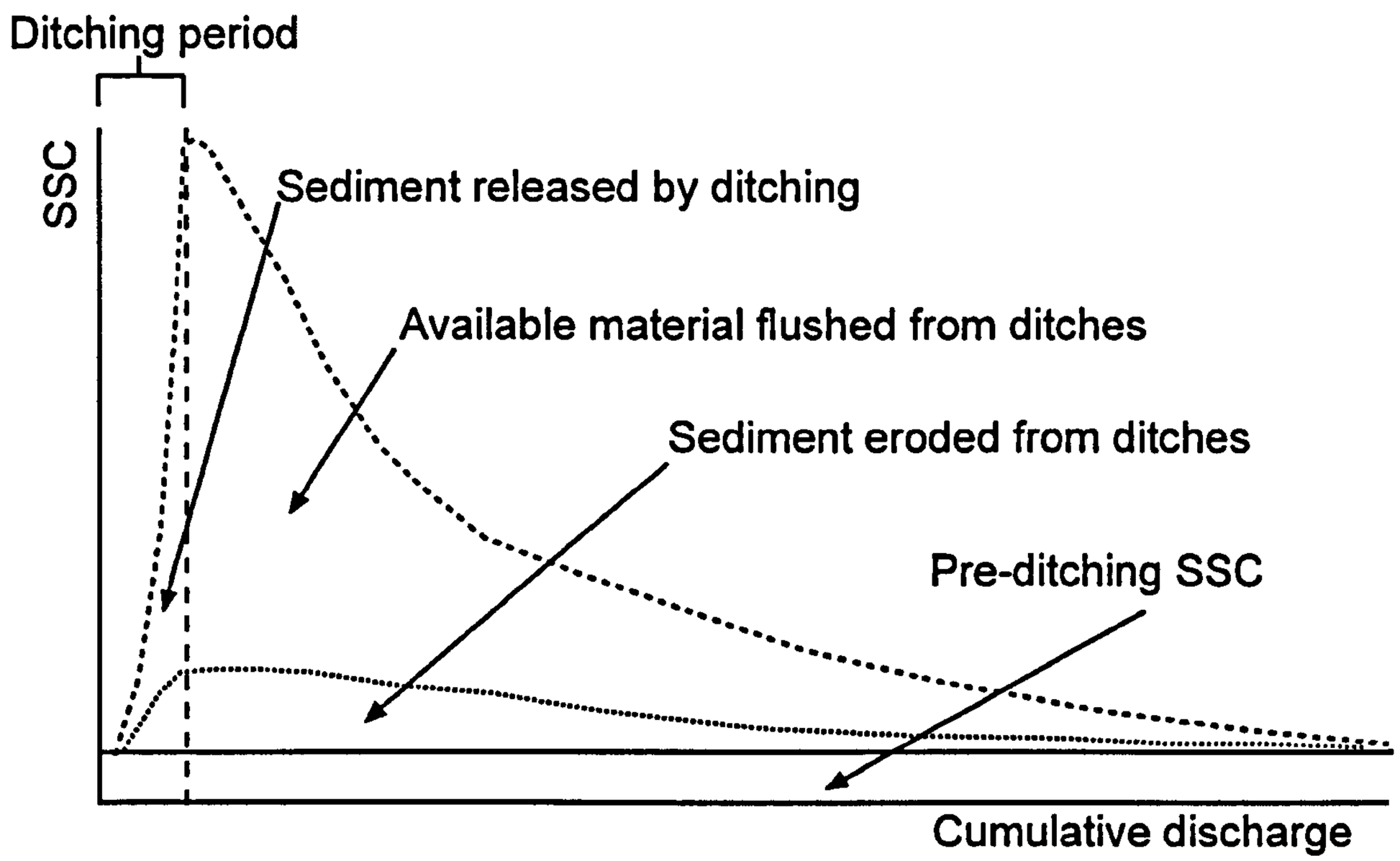

Figure 2.12. Generalised model of SSC following ditching. Source: Robinson, 1980.

In summary, discharge is commonly a very important control over suspended sediment dynamics in terms of the magnitude of discharge, the rate at which it increases and the processes responsible for its generation and these relationships vary between catchments. Temperature and precipitation are key meteorological controls over suspended sediment dynamics and delivery and interact with vegetation cover and type. However, they are rarely studied directly given the difficulties in isolating and quantifying them. Retention devices primarily affect the timing of sediment delivery. Finally, anthropogenic activity impacts suspended sediment dynamics but the extent, timing, and type of impact depends on the disturbance type and other factors.

2.6.2.2 Stable controls

Stable controls include factors such as catchment and channel morphology, topography and geology. Some examples of the effect of these factors on suspended sediment dynamics and delivery are outlined below. Given the limited number of studies which investigate more than one catchment at a small-scale there is limited information regarding the effect of some.

One of the most studied relationships within the literature is that between suspended sediment load or specific suspended sediment yield and catchment area. Generally higher sediment loads are associated with larger catchments, given the greater contributing area and higher flows. The relationship has been studied by comparing different rivers (e.g. Milliman & Syvitski, 1992) and sub-catchments of the same river system (e.g. Wass & Leeks, 1999). It is more rigorous to study the effect of scale in sub-catchments of the same river, as other characteristics, i.e. soil type and precipitation, are generally more similar. Wass & Leeks (1999) found a strong positive relationship between suspended sediment load and catchment area for the sub-catchments of the Humber system. Although this positive relationship is found for the majority of catchments some exhibit lower loads with distance downstream as a result of sediment being deposited within the system. For example, the sediment load decreased between Fassifern and Maryburn gauging sites on the Chandler River, Australia (Loughran, 1976).

Although sediment load usually increases with increased catchment area the specific sediment yield (sediment load divided by catchment area) commonly decreases. Dedkov & Moszherin (1992) suggested that this is because the systems are dominated by slope erosion. Specific sediment yield was shown to decrease with increasing catchment area in the Humber system (Wass & Leeks, 1999) and greater specific suspended sediment yields were associated with the upper reaches of Shiny Brook, South Pennines, in comparison to the lower reaches (446.6 kg km^{-2} yr^{-1} and 175.2 kg km^{-2} yr^{-1} respectively) (Labadz *et al.*, 1991). This negative relationship is commonly explained by higher rates of erosion, lower storage and/or stronger connectivity between the hillslope and channel in the upper reaches. For example, Labadz *et al.* (1991) calculated that there was a greater proportion of rainfall runoff (50%) in the upper reaches compared with the lower reaches (10%) and attributed this to steeper slopes and sparser vegetation.

However, in some catchments suspended sediment yield has been shown to have a positive relationship with catchment area. Dedkov & Moszherin (1992) suggested that systems which experience a positive relationship between catchment area and specific sediment yield are characterised by channel erosion. This was reinforced by Church & Slaymaker (1989) who found that specific suspended sediment yield decreased with increasing catchment area for undisturbed catchments in British Columbia up to 3×10^4 km^2 in area. Church & Slaymaker (1989) attributed this to the dominance of

remobilisation of Quaternary sediments over the primary denudation of the lands surface. Krishnaswamy *et al.* (2001) identified a positive relationship in the Terraba basin, Costa Rica, which was attributed to large inputs of sediment from unstable slopes near the basin mouth and agricultural activity in the downstream sections. McManus & Duck (1996) also found a positive relationship between suspended sediment yield and catchment area when examining the suspended sediment yield of 33 gauged rivers in eastern Scotland (part of the Harmonized Monitoring Program (HMP), which ran from 1975 to 1983). However, the positive relationship between specific sediment yield and catchment area was not attributed to channel erosion processes, but the large number of first order streams in the large catchments, which exposed greater lengths of channel banks and bed to erosion.

Related to the effect of catchment area is topography. Schumm *et al.* (1987) suggested sediment yield is also related to topography on the basis that sediment yield is a product of sediment released from the land by erosion processes and the quantity and conveyance of the sediment to the channel is partially controlled by the topography. It can be reasoned that certain catchment topographies promote higher suspended sediment loads. For example, catchments with steep hillslopes and limited floodplains will produce higher sediment loads than catchments with gentler hillslopes and wide floodplains if all other influences are equal.

At a smaller scale, channel form affects suspended sediment dynamics as it influences the energy available which controls the erosion, entrainment and deposition of sediment and affects the sediment source areas accessed. The effect of channel form on energy available is clearly demonstrated by the effect of 'transport' and 'deposition' reaches on SSC. Narrow, deep, fast-flowing sections with limited or no floodplain will exhibit higher SSC, if sediment is available, than wider, shallower, slower-flowing sections with broad floodplains in the same river system. Schumm (1960) observed the feedback of channel form on the balance of wash load and suspended bed load. Streams dominated by the wash load component were contained within relatively deep, narrow channels compared with those dominated by suspended bed load.

Beschta (1987) discussed the effects of catchment morphology on suspended sediment dynamics by outlining a conceptual model of erosion, entrainment, transport and deposition processes in a fluvial system. Within this model sediment mobilised in the

upper reaches is transported downstream. As distance from the headwaters increases stream gradient generally decreases promoting deposition of sediment, especially coarser grains. These zones of deposition may then activate previously stable sediment sources through processes of lateral channel migration which has consequent effects on river planform and local sediment supplies. Once transport of sediment from the headwaters decreases, the downstream channel begins to incise the recently deposited sediment, thus producing a cycle of aggradation and erosion. This active area of channel dampens the variability of suspended sediment movement in the lower reaches of the channel and as a result lower zones of rivers are less likely to experience changes in channel morphology or activation of potential sediment sources. This suggests that the monitoring location may have a substantial impact on the sediment dynamics recorded, although this may average out over time.

Bogen (1980) noted channel form influences suspended sediment yields on the grounds that the shape of the river cross-section will affect the suspended sediment sources accessed at a given discharge: there is less potential for increases in narrow, steep-sided channels than in wide, shallow channels. However, this may be partially countered by increased friction and consequently slower flows in wide, shallow channels. The effect of channel shape on SSC is demonstrated for two channel cross-sections measured in the field at Iron Crag, a small mountain torrent in the northern Lake District: the main channel which is wide and shallow and a gully which is narrow and steep-sided (Figure 2.13). As the stage increases the increases in potential sediment source area accessed varies for the different channel forms. Between L1 and L2 more channel bank is accessed in the wider, shallower, cross-section, approximately equal areas of sediment are accessed as stage rises from L2 to L3 and more sediment is accessed in the narrow, deeper, channel as stage rises from L3 to L4 (Figure 2.13). The effect of channel morphology on SSC will be very variable throughout the catchment and will also be affected by channel bank composition, i.e. if the channel banks are bedrock, the response to increases in stage will be negligible compared with those composed of soil. Also, bank failures are more likely to occur in steeper-sided channels (Figure 2.13A as opposed to Figure 2.13B).

The geology and lithology of catchments exert a strong control over SSC. Geology is important as it is a dominant control over lithology and also confines some channels. Lithology is important in terms of the ease with which sediment can be eroded (i.e.

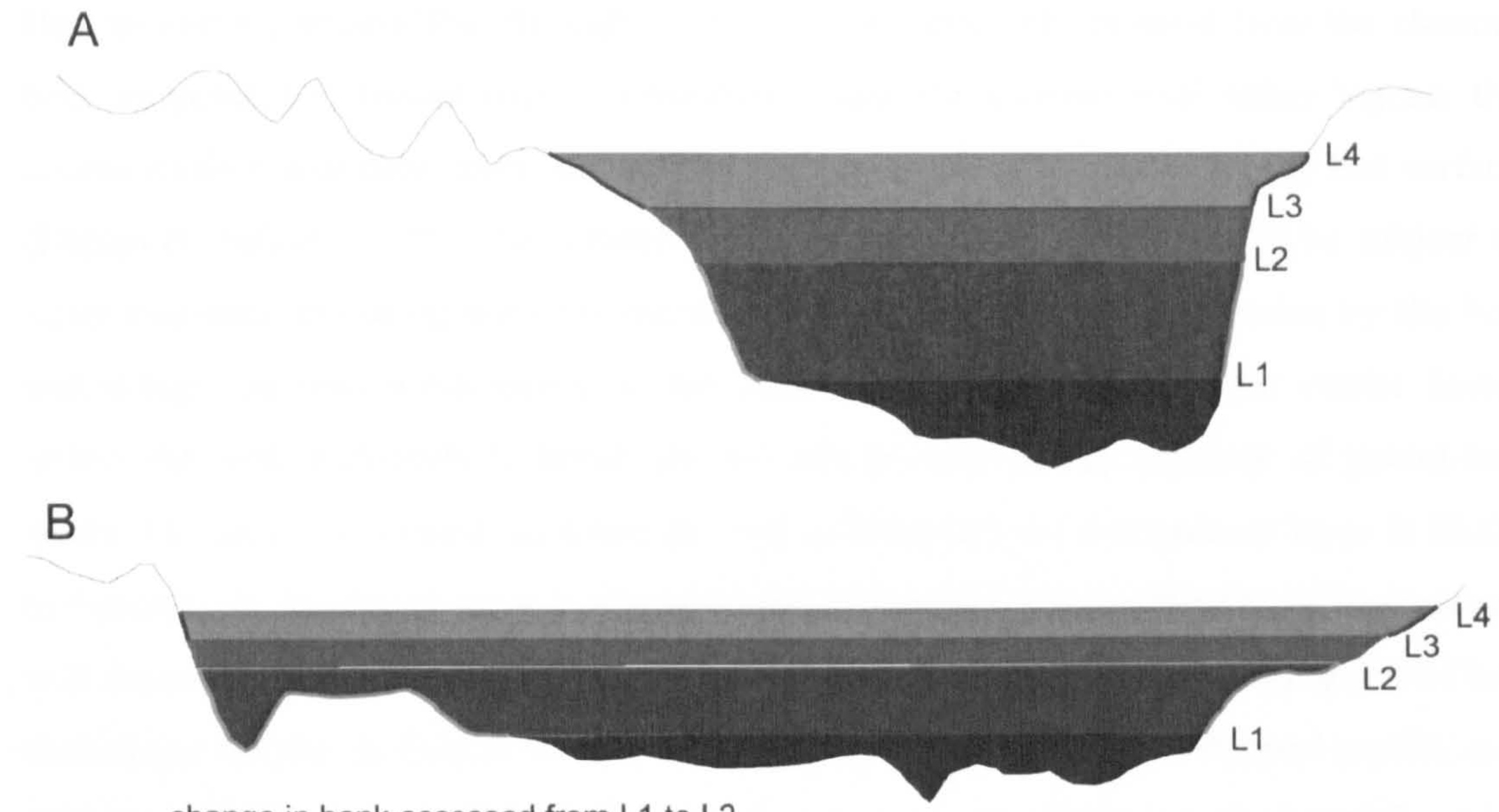

Figure 2.13. The effect of channel shape on potential access to sediment. L = water level.

degree of consolidation and cohesiveness) and the ease with which it can be transported (i.e. grain size, shape and density). Catchments with unconsolidated, less cohesive, smaller, less dense and less spherical sediment will have higher suspended sediment loads than those with consolidated, cohesive, large, dense, spherical sediment. However, there are inter-relations between these characteristics which add complications. For example, small particles are likely to be more cohesive and spherical particles are likely to be less consolidated.

The effect of bank lithology on SSC was demonstrated by Oxley (1974) by comparing two river catchments which feed Lake Ebyr, Powys. Ebyr South banks consist of unconsolidated soil with a high proportion of silt and clay, while Ebyr North banks consist of cohesive till and shale bedrock. As a result SSC were always lower in Ebyr North, even though higher discharges were often recorded than in Ebyr South. The difference in channel bed material particle size also contributed to the difference in SSC as Ebyr South had a high proportion of silt and the dominant bed grain size in Ebyr North was gravel.

The channel substrate is important: channel beds with loose, finer sediment will have higher SSCs than those with bare bedrock channel beds or those with an armour layer.

Bed armouring affects SSC through control of the supply of sediment from the channel bed. Suspended sediment that is deposited within the channel will either ingress the coarse surface sediment layer, unless this zone is saturated, or settle on the bed surface (Diplas & Parker, 1992). The sediment which settles on the surface will be subject to rapid entrainment during the next storm event, whereas protection afforded by the bed armouring prevents entrainment of the sediment which infiltrated the coarse layer, unless the bed is disturbed, which occurs infrequently in the majority of gravel-bed rivers. However, on occasions when the bed is disturbed the sub-armour layer is likely to become an important source of suspended sediment. The magnitude of importance will depend on the depth and composition of alluvium and the degree and depth of bed movement (Diplas & Parker, 1992). Bed movement may result in a stepped profile in a scatter of SSC versus discharge. Prior to bed movement supplies may start to become exhausted, then, when bed movement occurs, a supply of suspended sediment will be entrained and cause an abrupt shift in SSC-discharge relationship.

In summary, there is generally a positive relationship between suspended sediment load and catchment area and a negative relationship between specific suspended sediment yield and catchment area. These relationships can be related to catchment form and the dominant sediment sources, but exceptions do occur. Catchment form is inherently linked to suspended sediment load, although discussion of this tends to be theoretical and unquantified. Channel form affects suspended sediment dynamics by influencing the energy available and therefore erosion, entrainment, and deposition processes and by controlling the change in potential sediment source area. Catchment geology and lithology is important in terms of its erosivity, the ease with which the particles are entrained and the effectiveness of the bed armouring.

2.6.3 Interaction between controls on suspended sediment dynamics

Although the effects of catchment characteristics have been considered in turn suspended sediment dynamics within a system depend on the individual factors and the interplay between them. For example, Ternan & Murgatroyd (1984) found channel morphology, vegetation, dam and channel gradient all exerted an influence on SSC in Narrator Brook, Dartmoor. Krishnaswamy (2001) investigated sediment dynamics Terraba basin, Costa Rica – a disturbed, heterogeneous tropical basin, and attributed spatial variation to land use disturbance and rainfall erosivity, especially in relation to natural instabilities within the basin.

Limited studies attempt to assess the relative importance of different processes. Lawler (1995a) attempted to assess the changing importance of sub-aerial, entrainment and mass failure processes on channel bank sediment supply with distance downstream. He reported that: (1) Freeze-thaw decreases with altitude and hence downstream. (2) Desiccation increases with distance downstream due to decreasing precipitation and increasing temperatures and therefore evapotranspiration. (3) Entrainment peaks in the middle reaches due to increased stream power and finer particles than in the upper reaches and lower proportions of clay (therefore increasing the cohesiveness) than in the lower reaches. (4) Mass failures were predicted to increase with distance downstream as channel depth/bank size increases downstream (Leopold & Maddock, 1953). From these inferences Lawler (1995a) developed a conceptual model of downstream changes in bank erosion processes in which upstream reaches were characterised by sub-aerial processes due to low stream power and low banks, mid reaches were characterised by entrainment due to high stream power and lower reaches were dominated by mass failures as banks reach critical heights (Figure 2.14). Lawler (1995a) did not attempt to show the net effect of the processes.

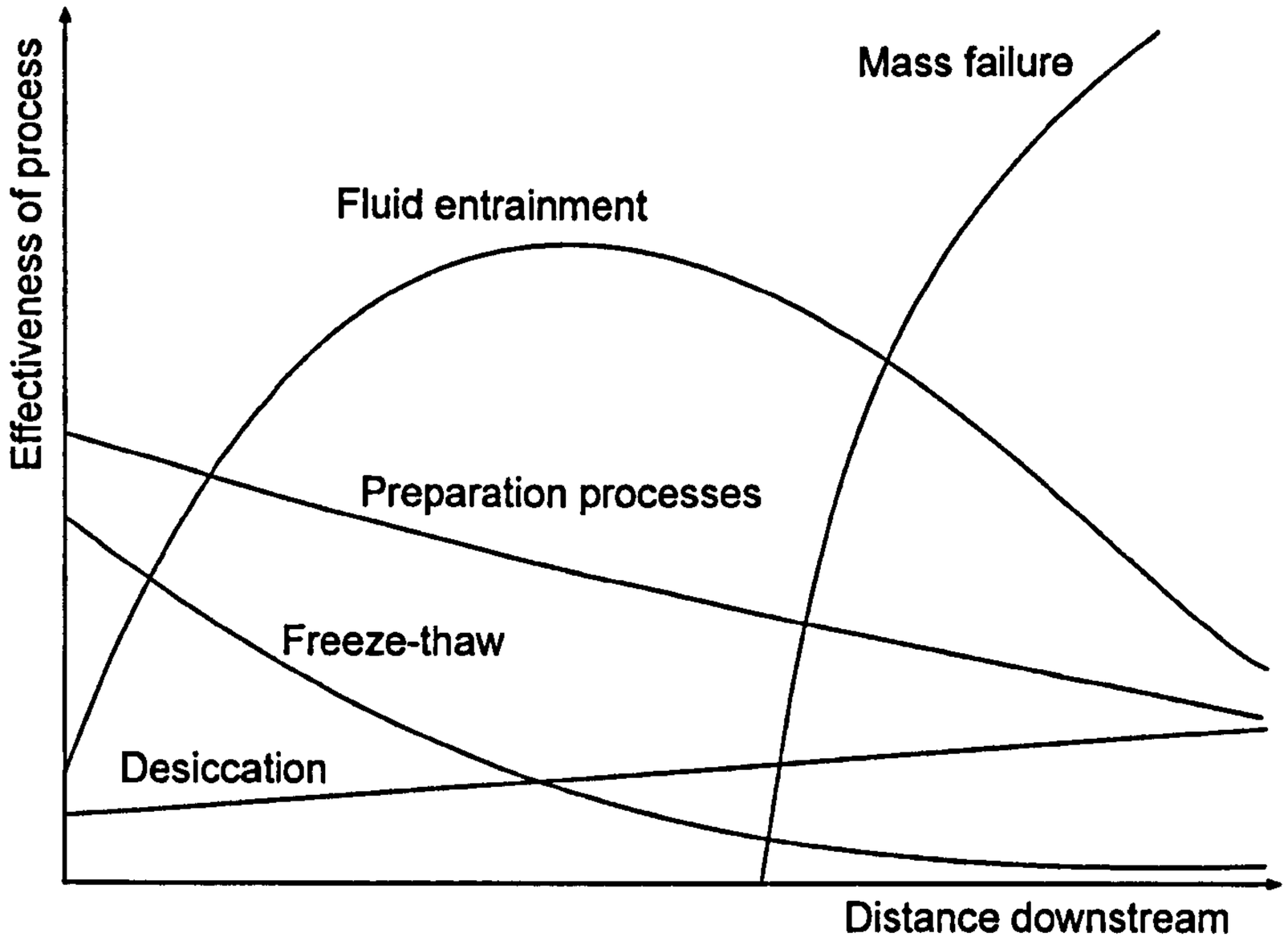

Figure 2.14. Conceptual model of bank erosion processes with distance downstream. Source: Lawler, 1995a.

2.7 Temporal variation of suspended sediment dynamics

The previous section discussed various influences on suspended sediment dynamics. Superimposed on these are temporal variations which are generally caused by sediment

supply constraints and differences in meteorological/climatic conditions. Temporal variations in suspended sediment dynamics are discussed in the following section at intra-event (hysteresis), inter-event, seasonal and inter-annual time-scales.

2.7.1 Intra-event variation in suspended sediment concentration

The relation between SSC and discharge varies between catchments, as a result of different catchment characteristics and the varying importance of different processes, and between events within the same catchment. The hysteresis between SSC and discharge has been studied by numerous authors (e.g. Bogen, 1980; Farr & Clarke, 1984; Mossa, 1989; Williams, 1989). Hysteresis is analysed by the form of SSC versus discharge plots (referred to as hysteresis loops) and is used to make inferences about the system. The form of hysteresis loops is affected by the timing and quantity of sediment and flow and the location of sediment sources in relation to the monitoring site.

Hysteresis is most commonly classified by the direction of the SSC-discharge loop: clockwise, anti/counter-clockwise and none (e.g. Asselman, 1999; Walling, 1974), although some authors define hysteresis based on the lag between SSC and discharge (e.g. Kurashige, 1994). Williams (1989) classified all the possible relationships between discharge and SSC into five categories. Class 1 hysteresis is characterised by a straight line between SSC and discharge, class 2 is a clockwise loop, class 3 is an anti-clockwise loop, class 4 is a single line with a loop, and class 5 is a figure of eight (Table 2.5). The Williams (1989) classification is the most definitive and systematic classification system available and will be used throughout this investigation. Class 6 has been added to Williams classification and is characterised by hysteresis plots with no clear form.

The type of hysteresis varies within the same catchment and the dominant type between catchments and can be used to make inferences regarding sediment supply, sources and transport mechanisms. The most common types of hysteresis reported in the literature are types 2 and 3. For example, Irvine & Drake (1987) examined hysteresis in the Ausable River, Canada: the majority of events displayed class 2 hysteresis due to the initial flushing of sediment through the system. This was also found by Bogen (1980) for the proglacial streams of Austerdalsbreen and Tunsbergdalsbreen glaciers, western Norway. Walling (1974) documented class 2 hysteresis, in a small unnamed catchment near Exeter, caused by dilution of SSC in the later stages of the flow event by increased base flow, a cause not documented by Williams (1989). Walling (1974) also

Table 2.5. Classes of SSC/Q relations as defined by Williams (1989).

Class	Relation	SSC/Q criteria	Cause
1	Single value:	$(SSC/Q)_R \approx (SSC/Q)_F$	
	A – Straight line.	The ratio of SSC/Q remains equal for all Q through the event.	Associated with a constant sediment supply throughout the event which allows SSC to increase and decrease in line with Q.
	B – Concave curve	SSC increases progressively quicker with increasing Q.	
	C – Convex curve	SSC decreases progressively quicker with increasing Q.	
2	Clockwise loop	$(SSC/Q)_R > (SSC/Q)_F$ for all values of Q	Caused by either depletion of sediment before Q has peaked due to limited supply, a prolonged flood event or the formation of a protecting armour layer prior to the peak Q.
3	Anti-clockwise loop	$(SSC/Q)_R < (SSC/Q)_F$ for all values of Q	Caused by: (1) the relative travel times of flood wave and sediment due to the difference in velocities of the flood wave and suspended sediment or by obstacles such as lakes; (2) high soil erodibility in conjunction with prolonged erosion; or (3) seasonal variability of sediment production and precipitation.
4	Single line plus loop	$(SSC/Q)_R \approx (SSC/Q)_F$ for one range of Q values $(SSC/Q)_R \neq (SSC/Q)_F$ for other range of Q values	Caused by a combination of factors outlined for class 1 and 2 or 3.
5	Figure of eight	$(SSC/Q)_R > (SSC/Q)_F$ for one range of Q values $(SSC/Q)_R < (SSC/Q)_F$ for other range of Q values	Caused by a combination of factors outlined for classes 2 and 3.
6	None	Variable, no discernible pattern	No dominant causes to produce any one relation.

$(SSC/Q)_R$ is SSC/Q on the Q rising (R) limb, for a selected Q, $(SSC/Q)_F$ is SSC/Q on the Q falling (F) limb for the same Q. Not examples of all the classes were found by Williams (1989) in the literature, namely 1C and 4. Class 6 was not defined by Williams (1989) but was added to extend the classification to cover all possible scenarios.

documented class 3 hysteresis events reflecting extended travel times of the dominant sediment source. Bank collapse during the receding limb of the hydrograph may also cause class 3 hysteresis (Carling, 1983) but depends on the form of the prior SSC-discharge relationship: if SSC peaks prior to discharge at the beginning of the event, then bank collapse on the receding limb may cause a twist in the hysteresis loop resulting in class 5 hysteresis (Ashbridge, 1995).

Asselman (1999) studied the frequency of different types of hysteresis loops for 112 storm events at a gauging station near the Rees tributary on the Rhine: 18% of events exhibited class 3 hysteresis, 23% class 6 and 59% class 2. Class 3 loops were attributed to dominant sediment inputs from upstream tributaries (Rivers Neckar and Main). The class 2 loops were attributed to sediment input from a tributary (River Mosel) nearer to the gauging station, and occurred more often in winter. Class 6 hysteresis occurred when inputs from the Neckar, Main and Mosel were approximately equal: thus when supply from the Mosel was becoming exhausted the supply from the Neckar and Main reached the gauging station, and occurred mostly in summer. Thus, hysteresis is a product of the routing and mixing of water as well as sediment supply factors.

Labadz *et al.* (1991) studied a headwater catchment in the blanket peat of the southern Pennines, Shiny Brook. The response of SSC was generally a rapid rise and rapid fall but there was some variation in the timing of the response in relation to discharge. Approximately 50% of storm events exhibited class 2 hysteresis, 30% showed class 3 hysteresis and the remainder showed class 6 hysteresis. Generally in smaller catchments class 2 hysteresis is expected as there are limited sediment sources and limited tributaries to input sediment.

Nistor & Church (in press) examined hysteresis in a gully within Russell Creek basin, Vancouver Island. Given the dominance of multi-peaked hydrograph events Nistor & Church (in press) developed a classification system, similar to that of Williams (1989), extended to include multi-peaked events. Six events were examined and four exhibited class 2 hysteresis, all of which were characterised by single- or double-peaked hydrographs, and were attributed to sediment exhaustion. The two remaining events were characterised by triple- and sextuple-peaked hydrographs and consequently the hysteresis loops showed no clear pattern. Nistor & Church (in press) found that every hydrograph peak was associated with a SSC peak but SSC peaks also occurred at other

times due to pulses of sediment unrelated to discharge. Some of these sediment pulses were related to sediment recharge during snowmelt.

Seeger *et al.* (2004) studied hysteresis in Arnás, a Mediterranean headwater catchment in the Central Spanish Pyrenees, and related the hysteresis class (classes 2, 3 and 5 were observed) to catchment conditions and runoff-generating mechanisms. Storm events were characterised by conditions prior to the event (rainfall and discharge), rainfall parameters during the event, and discharge and SSC parameters during the event. Canonical discriminant analysis was used to determine that total rainfall, antecedent rainfall 3 days before the event and soil moisture on the day of the event categorised the events into hysteresis type. Soil moisture conditions of the catchment was the dominant controlling variable as it was strongly correlated with the first discriminant function which accounted for approximately 80% of the variance of the three types of hysteresis. Class 2 hysteresis events were the most common and were characterised by a rapid increase in SSC at the beginning of the storm but overall low SSCs. Before class 2 events the catchment was relatively dry and sediment was contributed by spatially-limited, rapidly exhausted hillslope sources which were close to the channel. In comparison, class 3 events were characterised by slow rising SSC (SSC peaked after discharge). The catchment tended to be wetter, which encouraged overland flow, sediment sources were widespread, not rapidly exhausted and only connected to the channel during such high moisture conditions. Class 5 events were produced by a combination of the mechanisms outlined above for the class 2 and class 3 events: initially the catchment was very dry, so class 2 processes dominated; then high rainfall wetted up the catchment and class 3 processes dominated.

In addition to inferences regarding sediment sources and routing hysteresis, the effects of changing environmental and climatic factors on SSC and discharge can be examined. For example, Burt *et al.* (1984) used hysteresis loops to examine the effect of forest ditching on SSC. Pre-ditching hysteresis loops were predominantly class 2, which indicated sediment exhaustion, and the tightness of the loops suggested less depleted sediment stores. Hysteresis loops post-ditching were a mix of class 3 and class 2 loops and indicated a more ample supply of sediment generated by rainfall and runoff erosion (Burt *et al.*, 1984).

2.7.2 Inter-event variation in suspended sediment concentration

In sediment supply-constrained systems SSC is restricted by the sediment sources accessed during the event and exhaustion of those sources. Therefore the storm magnitude and the time elapsed since and magnitude of the last storm event are important controls on SSC, as the sediment removed by the last event will determine the amount of sediment available for transport in the next event. The effect of the last storm event on SSC has been shown to be considerable by various authors. For example, Walling & Webb (1987) reported peak SSCs of 4,000 mg l^{-1} for storm events occurring at least 30 days after the preceding storm and 400 mg l^{-1} for storm events less than 7 days since the last storm event for the River Dart, Devon. Labadz *et al.* (1991) noted hysteresis between successive storms for Shiny Brook, Southern Pennines. One event induced by 9 mm of rainfall had a peak discharge of 1.07 l s^{-1} and a peak SSC of 491.9 mg l^{-1} and an event induced by 24 mm of rainfall on the following day had a peak discharge of 2.27 l s^{-1} but a peak SSC of only 206.1 mg l^{-1}.

The effect of inter-storm hysteresis on rating curve form is clearly illustrated by Evans & Yang (in prep). A large storm in 2001 in Upper North Grain, Southern Pennines, exhausted sediment supplies and substantially altered the relationship between SSC and discharge (Figure 2.15). The rating curve was notably steeper prior to a large storm which occurred in July than after, i.e. higher SSCs were associated with given discharges prior to the storm than after the storm (Figure 2.15).

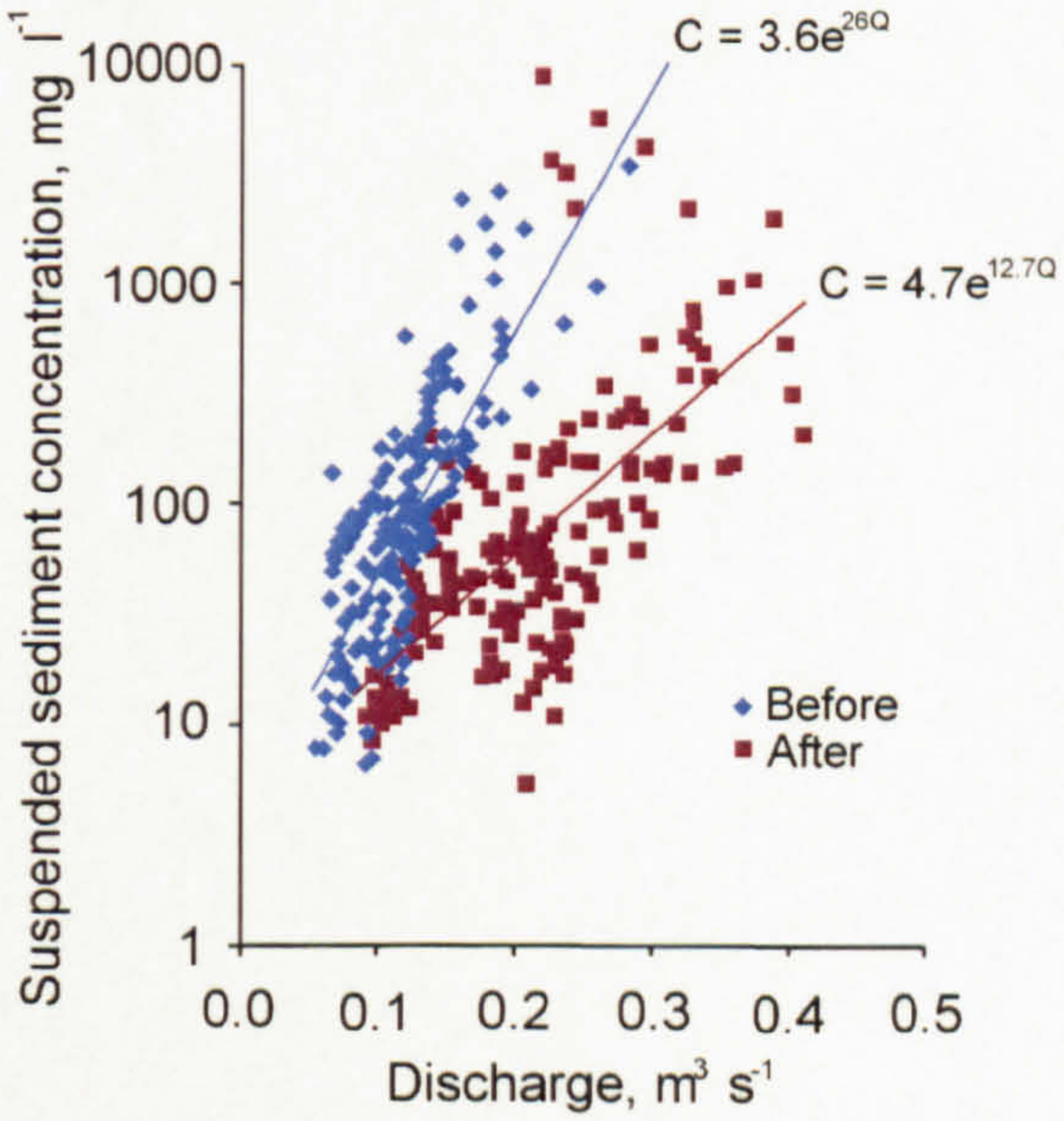

Figure 2.15. The form of the rating curve for Upper North Grain, Southern Pennines, before and after a large storm which occurred in July 2001. Source: Evans & Yang, in prep.

2.7.3 Seasonal variation in suspended sediment concentration

Seasonal variations in SSC may occur given the changes in sediment sources as a result of increased contribution from autochthonous supply during the summer months, different baseflows and different runoff-generating mechanisms. Several aspects of suspended sediment have been shown to exhibit seasonal variation, including peak flux, difference in SSC-discharge relations, variability in SSC and variation in SSC characteristics (particle size, composition etc.). Some selected examples of such variations are outlined below.

The effect of season on peak suspended sediment flux varies throughout the world given differences in the timing of seasons. For example, peak suspended sediment flux occurs in June/July in West Africa (Picouet *et al.*, 2001), the beginning of the rainfall season; in Romania suspended sediment peaks between March and May, depending on altitude (Ichim *et al.*, 1984); in Britain suspended sediment flux generally peaks somewhere between December and February, dependent on catchment characteristics and/or different meteorological conditions during the study years.

Walling & Webb (1987) divided SSC-discharge data into summer (April – September) and winter (October – March) and found a systematic difference in the winter and summer data clouds: the summer cloud plots to the left of the winter data cloud when SSC is plotted against total discharge and in the same place as the winter data cloud when SSC is plotted against stormflow discharge, although the summer data cloud is larger (Figure 2.16). Walling & Webb (1987) attributed the different data cloud locations when SSC was plotted against total discharge to the dilution of SSC by higher baseflows in the winter rather than seasonal differences in sediment supply. The larger summer data cloud, when SSC was plotted against stormflow discharge, indicates there is more variability in SSC during the summer which must be a result of more variable sediment supplies or more variability in processes which transport sediment to the channel. The usual positive trend was absent when SSC was plotted as a function of stormflow discharge (Figure 2.16). Walling & Webb (1987) suggested that this indicated a threshold SSC may be reached within storm events, thus demonstrating the limiting affect of sediment supply.

Stone & Walling (1997) observed a seasonal component in the absolute and effective particle sizes of the suspended sediment in the River Dart: October to March was

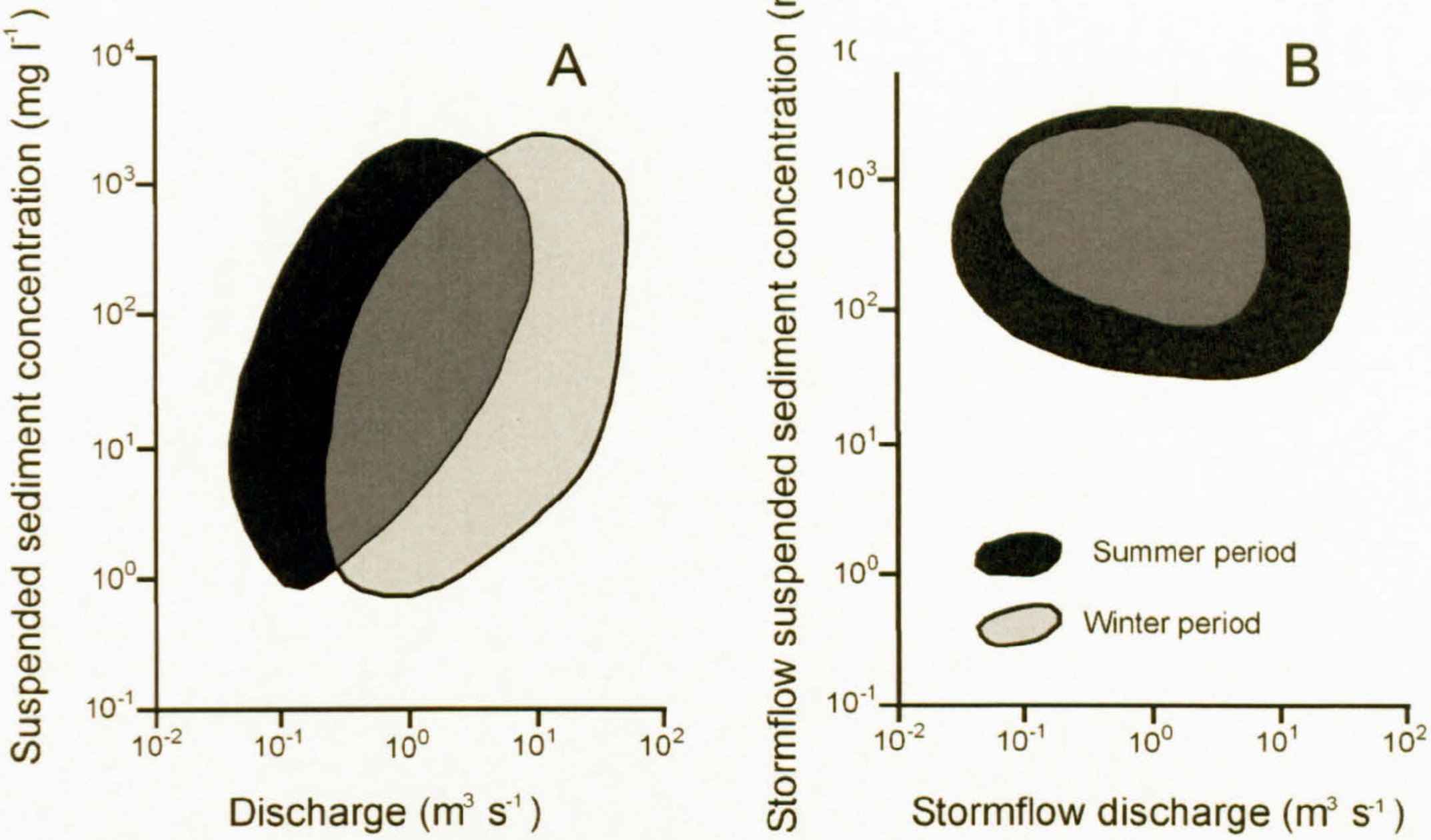

Figure 2.16. The relationship between (A) total discharge and SSC and (B) stormflow discharge and SSC. (Source: Walling & Webb, 1987).

characterised by coarser sediment compared with April to August. However, the opposite was found for sediment mobilised on the hillslopes, i.e. October to March was characterised by finer sediment compared with April to August. Therefore, hillslopes to channel transport processes were selective or the connectivity between the hillslope and the channel was weak. However, this is not representative of all catchments. For example, no clear seasonal variation existed in the absolute particle size characteristics of Jackmoor Brook, Devon, which was explained by continuity in sediment sources throughout the year (Peart & Walling, 1982).

2.7.4 Inter-annual variation in suspended sediment concentration

There is generally high inter-annual variability in suspended sediment loads as a result of different hydrological and meteorological conditions. The United States Geological Survey maintains a database containing suspended sediment loads for several years for more than 250 rivers (USGS, 2003). Two catchments, both fairly small with temperate climates, were selected from the database to indicate the variability in sediment load between years. The first catchment, Conodoguinet Creek, has an area of 2 km^2. The lowest recorded annual suspended sediment load is approximately one sixth of the highest and the coefficient of variation in suspended sediment yield is 79.2% (Figure

2.17). Stony Fork is larger with a catchment area of 19.3 km^2. The lowest annual suspended sediment load is approximately one third of the highest and the coefficient of variation is 44.6% (Figure 2.17). This pattern of higher variability in annual suspended sediment loads in small catchments was also found by Wasson (1984) for 131 Australian rivers in the southern uplands (Table 2.6). This demonstrates the responsive nature of smaller catchments and illustrates the problems with determining suspended sediment yields over short time periods, especially for smaller catchments.

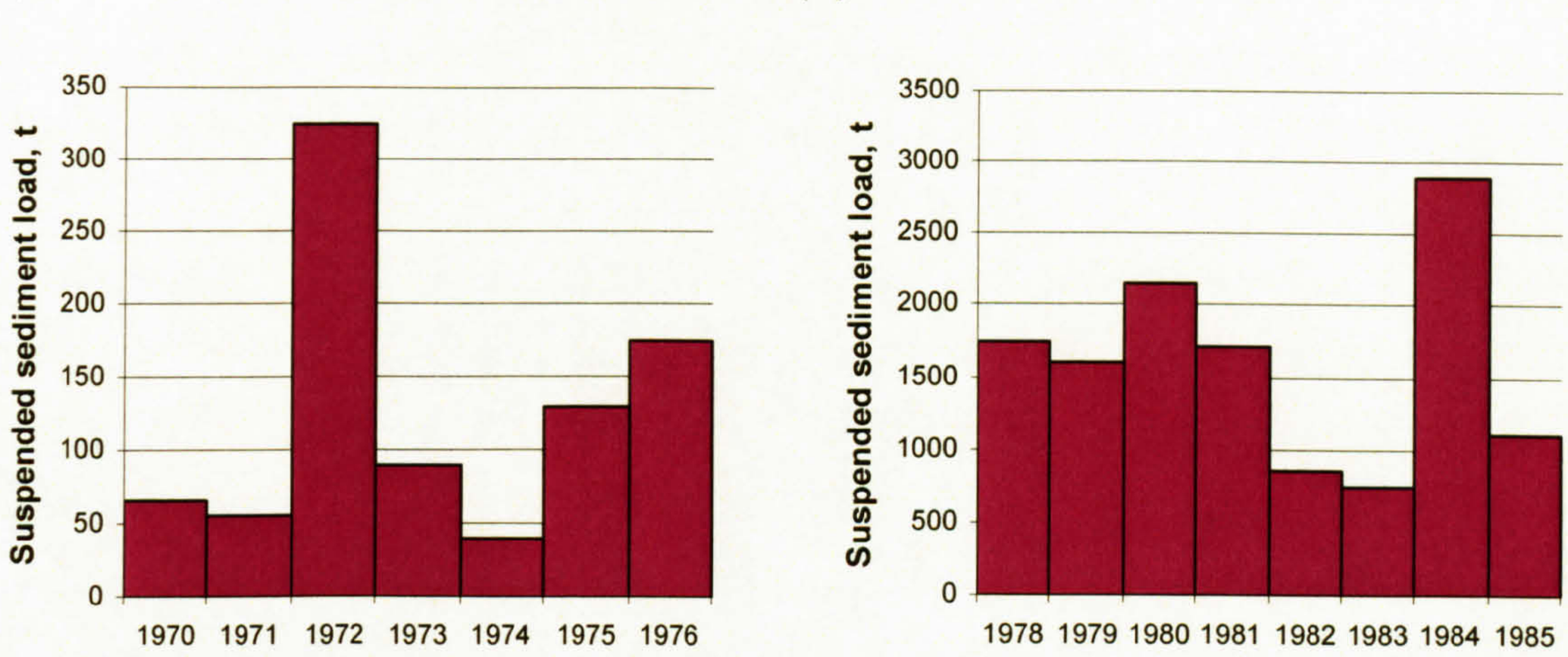

Figure 2.17. Annual loads of (A) Conodoguinet Creek, Pennsylvania (station number 01570100) and (B) Stony Fork, Pennsylvania (station number 03070455). Source: USGS, 2003.

Table 2.6. The relationship between basin area and coefficient of variation in the mean annual sediment load of 131 rivers in the southern uplands of Australia. Source: Wasson, 1984.

Basin area, km^2	**n**	**Coefficient of variation, %**
10^5-10^4	2	32
10^4-10^3	21	187
10^3-10^2	21	133
10^2-10^1	7	162
10^1-10^0	10	211
10^0-10^{-1}	41	208
10^{-1}-0	23	478

Inter-annual variability has been quantified for British rivers, and a selection of these is outlined below. Walling (1977b) calculated suspended sediment loads for the River Creedy, Devon, for two consecutive years based on turbidity records and rating curves. The suspended sediment load was almost three times as high in the second year of measurement. Wass & Leeks (1999) illustrated the annual and inter-annual variability of suspended sediment loads of two British rivers: the Humber and Swale. The sediment

yield from the Humber from October 1994 to November 1997 was 699,861 t. Out of the 699,861 t 53% was transported from October 1994 to November 1995, 14% from October 1995 to November 1996 and 33% from October 1996 to November 1997. The suspended sediment yield of the River Swale (Catterick Bridge) varied from 92.1 to 17.8 t km^{-2} yr^{-1} in consecutive years. Al-Ansari & McManus (1979) calculated the annual specific suspended sediment loads for the River Earn, Central Scotland, at Forteviot and Kinkell. The loads were approximately double in 1974 compare with 1973 for both catchments: the loads were 78,000 t in 1973 and 151,000 t in 1974 in Forteviot, and 44,000 t and 108,000 t in Kinkel. Labadz *et al.* (1991) estimated sediment load of Shiny Brook to be 199 kg in 1984/5 and 240 kg in 1985/6.

Annual suspended sediment loads were established for Kirkton and Monachlye, West Scotland, from 1983 to 1987 (Johnson, 1988). The loads were very variable with a maximum and minimum of 1956 t and 292 t in Kirkton, and 1027 t and 228 t in Monachyle (Figure 2.18). However, this is not all natural variability as both catchments underwent land use change, in Kirkton the roads were upgraded and forest felled and Monachlye was ploughed, at the end of 1985.

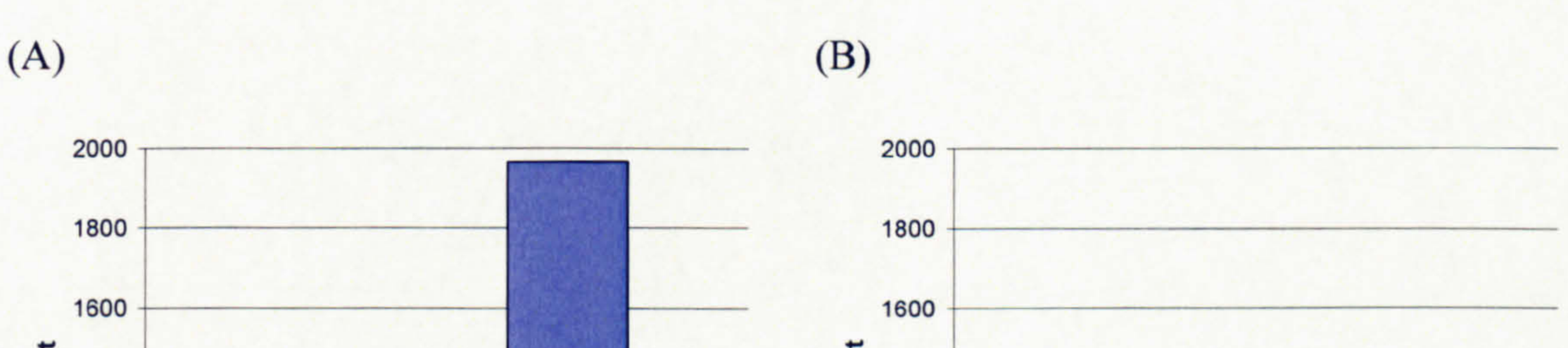

Figure 2.18. Variability in annual suspended sediment loads at (A) Kirkton, and (B) Monachlye, West Scotland. Data sourced from: Johnson, 1988.

Given that there is commonly a substantial variation in suspended sediment loads between years it is not possible to monitor a catchment for one year, calculate the load and declare that load as representative of the catchment. Given the complexity of the various controls on suspended sediment dynamics it is not possible to correct annual loads to provide an 'average' annual yield. Therefore, loads should be declared as specific for that year, or long-term monitoring should be undertaken and the average taken, assuming no environmental change occurs.

2.7.5 Summary

Temporal variation occurs in the amount, source and character of suspended sediment which depends on catchment characteristics and meteorological conditions. Temporal variation is examined at a range of scales, from intra-event to inter-annual. Generally, the temporal variation is lower, the longer the time period studied as averaging occurs, (with the exception of case studies revealing a marked adjustment to the system, for example land use change). Temporal variation prevents general statements being made regarding a catchment, unless the catchment has been monitored for a sufficient time period.

In summary, suspended sediment dynamics at an event time-scale are commonly examined using hysteresis loops. The different loop forms can be attributed to antecedent catchment conditions and sediment sources. Consequently, catchments are characterised by different dominant loop forms and likely sediment sources can be derived. In addition, in very general terms, hysteresis loops can be used to infer the effect of changing environmental conditions.

Time since and magnitude of the last storm have substantial impacts on the relationship between SSC and discharge and are responsible for some of the variability in SSC-discharge relations in the same catchment. The importance will vary with catchment characteristics and hydrological conditions, i.e. the speed and effectiveness at which the sediment preparation processes operate, and will also vary temporally within the same catchment.

There is seasonal variation in suspended sediment dynamics. However, the arbitrary nature, i.e. summer is from April to September regardless of weather conditions, may obscure some patterns. Also, the effect of particularly large storms may dampen or

obscure the seasonal signal. For example, the large storm in July in Upper North Grain, Southern Pennines (Figure 2.15). Given this seasonal variation it is important to consider the effect of season when investigating the character and dynamics of suspended sediment.

2.8 Importance of the magnitude and frequency of events

Magnitude-frequency analysis of flood events is common place, but in contrast sediment yields from individual storms and the associated magnitude and frequencies are seldom quantified. Knowledge of the magnitude and frequency of events (e.g. do high magnitude low frequency or low magnitude high frequency events dominate sediment transport?) could improve estimated yields and aid the development of sediment control management (Hicks, 1994).

Finlayson & McMahon (1988) examined the relative importance of high frequency, low magnitude and low frequency, high magnitude discharge events in world streams and found that low frequency, high magnitude events were more important. Based on this Olive & Rieger (1992) postulated that low frequency, high magnitude events are more important in terms of suspended sediment transport. However, it is possible that sediment exhaustion may result in lower magnitude, higher frequency events being more important in some rivers.

Magnitude-frequency analysis of sediment transport in British rivers has concentrated on the percentage of sediment transported in a percentage of time (Table 2.7). The majority of sediment is transported in a short time period, so that high magnitude, low frequency events are more important in terms of sediment transfer in British rivers. This reinforces the view of Olive & Rieger (1992) and suggests that while British rivers may experience sediment exhaustion there is enough time between events for sediment stores to replenish. Webb & Walling (1984) suggested that variations in magnitude-frequency relations are influenced by catchment scale and sediment availability. For example, different proportions of time to transport 50% of the load of the Barle, Dart and Creedy can be related to constraints on sediment sources; sediment sources of the River Barle are only accessed during extreme events, whereas sources are gradually accessed in the River Dart and Creedy catchments.

Table 2.7. The percentage of time taken to transport a given percentage of suspended sediment. All results are based on annual studies except those by Walling & Webb (1987) which was based on suspended sediment loads from 1976-1981.

Reference	River	% of sediment	% of time
Webb & Walling (1984)	Creedy	90	7
Webb & Walling (1984)	Creedy	1.3	20
Wass & Leeks (1999)	Swale	90	11
Wass & Leeks (1999)	Trent	90	25
Walling & Webb (1987)	Barle	50	0.2
Walling & Webb (1987)	Dart	50	0.35
Walling & Webb (1987)	Creedy	50	0.75
CEH (2004)	Plynlimon catchments	80	5
Wilkinson (1971)	Gullet Sike	22	0.0003
	Winter	50	0.14
	Summer	50	1.10
	Winter	90	0.60
	Summer	90	1.30
	West Grain	17	0.0003
	Winter	50	0.14
	Summer	50	0.12
	Winter	90	1.00
	Summer	90	1.20
	Langden Brook	18	0.0003
	Winter	50	0.12
	Summer	50	0.10
	Winter	90	0.75
	Summer	90	1.00
Smith *et al.* (2003)	Swale (Catterick to Leckby Grange)	66	<5

The contribution of major storms to annual suspended sediment loads is variable between years and is likely to be a noteworthy control over the inter-annual differences in suspended sediment loads. For example, between 7.0% and 22.8% of the total annual yield of the River Creedy, Devon, was transported on the day of maximum daily yield over a nine year period (Webb & Walling, 1998). Hicks (1994) used magnitude frequency relationship analysis to qualitatively assess the potential transferability of sediment yield calculated from one year to other years by examining the relationship between storm sediment yield and storm return period. This provides a useful indication of the possible errors and potentially allows more accurate load estimates, especially estimates of long-term loads. However, the effects of changing sediment availability due to natural (e.g. base level) and anthropogenic (e.g. urbanisation) factors remain unknown.

2.9 Suspended sediments within Britain

Suspended sediment concentrations in British rivers are low in a global context (Figure 2.9). Concentrations seldom exceed 5000 mg l^{-1} and generally remain below 500 mg l^{-1}. Coupled with low discharges this leads to low annual suspended sediment loads. Annual specific suspended sediment yields of British catchments range from less than 1 t km^{-2} yr^{-1} to nearly 500 t km^{-2} yr^{-1} with an average of 50 t km^{-2} yr^{-1} (Walling & Webb, 1987). Within the Britain there is limited information regarding patterns in suspended sediment yield at a national scale. Walling & Webb (1987) compiled a map of suspended sediment yields within the Britain from various sources (Figure 2.19), although several studies have been undertaken since. Despite the spatial coverage being poor Walling & Webb (1987) generalised: (1) loads greater than 100 t km^{-2} yr^{-1} are primarily associated with upland areas which experience more than 1000 mm yr^{-1} precipitation and high sediment delivery ratios due to small-medium catchment size. (2) Lowland areas have lower sediment yields, less than 25 t km^{-2} yr^{-1}, which reflects low precipitation, low sediment delivery ratios, low relief and larger catchments. (3) A group of catchments in Mid Wales and Mendip Hills have very low sediment yields (<5 t km^{-2} yr^{-1}), reflective of resistant bedrock and limited anthropogenic activity. However, the compiled studies were undertaken in different years and therefore the difference in specific suspended sediment yield will be influenced by temporal variability. Also, different monitoring and modelling techniques were used and this can lead to substantially different load estimates.

Time-scales of suspended sediment studies within the Britain are generally short as a result of restricted research frameworks. The main exception to this is research by Walling and associates of the River Exe catchment and sub-catchments, Devon, some of which have been monitored since 1980.

2.9.1 British uplands

There are few direct estimates of British upland suspended sediment loads (Table 2.8 & 2.9). Existing estimates of suspended sediment yields from upland catchments are based on SSC sampling (Table 2.8) or analysis of reservoir cores (Table 2.9). Reservoir studies allow the determination of longer-term suspended sediment fluxes but do not offer the high resolution information that monitoring-based studies provide. Very few monitoring studies within upland Britain have established long-term suspended sediment records. The two notable exceptions to this are Plynlimon, Mid-Wales (Kirby

Table 2.8. Monitoring studies of British upland suspended sediment loads. Fuller outline if studies in Appendix A, Table A.1.

Reference	River	Region	Area, km^2	Annual load, t	Specific sediment yield, t km^{-2} yr^{-1}
Crisp (1966)	Rough Sike	North Pennines	0.83	93	112.0
Wilkinson (1971)	West Grain	North Pennines	1.51	77.4	51.1
	Langden Brook	Central Pennines	15.34	843	55.0
Oxley (1974)	Ebyr North	Montgomeryshire	0.07	0.779	11.1
	Ebyr South		0.09	1.125	12.5
Carling (1983)	Carl Beck	North Pennines	2.18	54	24.8
	Great Eggleshope Beck	North Pennines	11.68	141	12.1
Burt *et al.* (1984)	Hades Clough	West Yorkshire	0.22	No loads. Pre-ditching SSC 200 mg l^{-1}, post ditching frequently >1000 mg l^{-1}	
Duck (1985)	Ogle Burn	Central Scotland	13.0	83	6.4
Johnson (1995)	Kirkton	West Scotland	6.85	Pre-felling 1983: 321	46.9
				Pre-felling 1984: 275	40.1
				Pre-felling 1985: 526	76.8
				Post-felling 1986: 4353	635.5
				Post-felling 1987: 599	87.4
				Post-felling 1988: 4044	590.4
				Post-felling 1989: 3610	527.0
	Monachyle	West Scotland	7.70	Pre-ploughing 1983: 293	42.8
				Pre-ploughing 1984: 280	40.9
				Pre-ploughing 1985: 326	47.6
				Post-ploughing 1986: 934	136.4
				Post-ploughing 1987: 909	132.7
				Post-ploughing 1988: 493	72.0
				Post-ploughing 1989: 1419	207.2
Francis (1987)	Ceunant Ddu	Mid-Wales	0.342	Pre-ploughing: 1.257	3.7
				Post-ploughing: 3.048	8.9
	Nant Ysguthon	Mid-Wales	0.135	Pre-ploughing: 0.088	0.7
				Post-ploughing: 0.443	3.3
	River Severn	Mid-Wales	0.94	62.3 (32.4 organic)	66.3
Labadz *et al.* (1991)	Shiny Brook	West Yorkshire	0.004	1984/5: 0.198	49.6
				1985/6: 0.240	60.0
Kirby *et al.* (1991)	Severn	Mid-Wales	8.70	-	-
	Tanllwyth	Mid-Wales	0.89	10.7	12.1
	Hore	Mid-Wales	3.08	Pre-felling: 75.2	24.4
				Felling year: 175.9	57.1
	Hafren	Mid-Wales	3.67	130.0	35.3
-	Cyff	Mid-Wales	3.13	19.1	6.1
	Iago	Mid-Wales	1.02	-	-
	Gwy	Mid-Wales	3.98	-	-
Leeks & Marks (1997)	Tanllwyth	Mid-Wales	0.89	Pre-felling 1995: 21.6	24.3
				Post felling 1996: 39.0	43.8
	Hafren	Mid-Wales	3.67	1995: 59.1	16.1
				1996: 84.7	23.1
	Severn	Mid-Wales	8.70	1995: 138.4	15.9
				1996: 127.0	14.6
	Cyff	Mid-Wales	3.13	1996: 16.7	5.3
Evans & Warburton (in press)	Rough Sike	North Pennines	0.83	1998: 35.9	43.3
				*1999: 39.3	47.3
				*2000: 36.8	44.3
				*2001: 36.2	43.6

Studies which use the same data sets as Johnson (1995) and Kirby *et al.* (1991) are not included. For example, Stott *et al.* (1986), Stott (1987b), Johnson (1988a, 1988b, 1994), Good (1986), Moore & Newson (1986), Francis & Taylor (1987) and Francis (1990). * Evans & Warburton (in press) annual suspended sediment loads for 1999-2001 were derived from the 1997/1998 suspended sediment rating curve.

Table 2.9. Sediment yields of British upland catchments determined from reservoir sedimentation studies.

Reference	Site	Region	Vegetation	Area, km^2	Altitude, m	Method	Sediment yield, $t\ km^{-2}\ yr^{-1}$
Winter (1950)*	Grassholme	North Pennines	Moorland	78.7	275-670	Empirical	173.1-236.1
	Blackton	North Pennines	Moorland	34.1	282-472	Empirical	130.3-175.6
Young (1958)	Loxley	Yorkshire	Moorland & forest	11.1	274-489	Survey	9688.3 $m^3\ km^2\ yr^{-1}$
Labadz *et al.* (1991)							(recalculated) 113.4
McManus & Duck (1985)							(recalculated) 52.5
Walling & Webb (1981)							(recalculated) 49.7
Hall (1967)	Catcleugh	Northumberland	Moorland	40.0	250-550	Survey	114.0
Walling & Webb (1981)							(recalculated) 43.1
Ledger *et al.* (1974)	North Esk	East Scotland	Moorland	7.0	350-600	Survey	26.0
	Hopes	East Scotland	Moorland	5.0	300-550	Survey	25.0
Stott (1985, 1987b)	Trentabank	South Pennines	Moorland	2.2	258-475	Survey	34.5-49.3
Burt (unpub) in Soutar (1989)	Holmestyes	South Pennines	Moorland				Pre-ploughing: 3.2
							Post ploughing: 51.3
Duck & McManus (1990)	Harperleas	Central Scotland	Moorland & forest	3.4	259-522	Survey	13.8
	Glenquey		Moorland	5.6	287-643	Survey	15.1
	Holl		Moorland & forest	4.0	204-440	Survey	72.3
	Carron Valley		Moorland & forest	38.7	225-570	Survey	141.9
	Earlsburn		Moorland	2.9	367-460	Survey	68.2
	North Third		Moorland	9.3	171-441	Survey	205.4
Labadz *et al.* (1991)	Wessenden (4 reservoirs)	South Pennines	Moorland	15.1	-	Survey	Mean, total: 203.7
							Mean, organics: 38.8
White *et al.* (1996)	77 rivers	South Pennines	Moorland, pasture & forest	1.2-114.9	-	Coring	Mean, total: 124.5
							Mean, organics: 20.5
Hutchinson (1995)	Howden	Peak District	Moorland	32.0	236-628	Coring	127.7
Foster & Lees (1999)	Barnes	SE Scotland	Moorland	1.78	250-400	Coring	23.5
	Fontburn		Coniferous forest	27.7	190-440	Coring	9.4
Halcrow (2001)	Upland, some sediment control (21 rivers)	Britain	Moorland	-	-	-	Mean: 92.7
	Upland, no sediment control (36 rivers)	Britain	Moorland	-	-	-	Mean: 132.9
Holliday (2003)	Burnhope	North Pennines	Moorland	17.8	400-478	Coring	33.3

*Winter (1950) used two methods, one based on published river silt contents and the second from silt records from the channels (but insufficient data). Volumes given by Winter (1950) were converted to weights using a specific gravity of 2, as established by Winter (1950).

et al., 1991) and Balquhidder, Scotland (Johnson, 1994) which were established in 1979 and 1981 respectively.

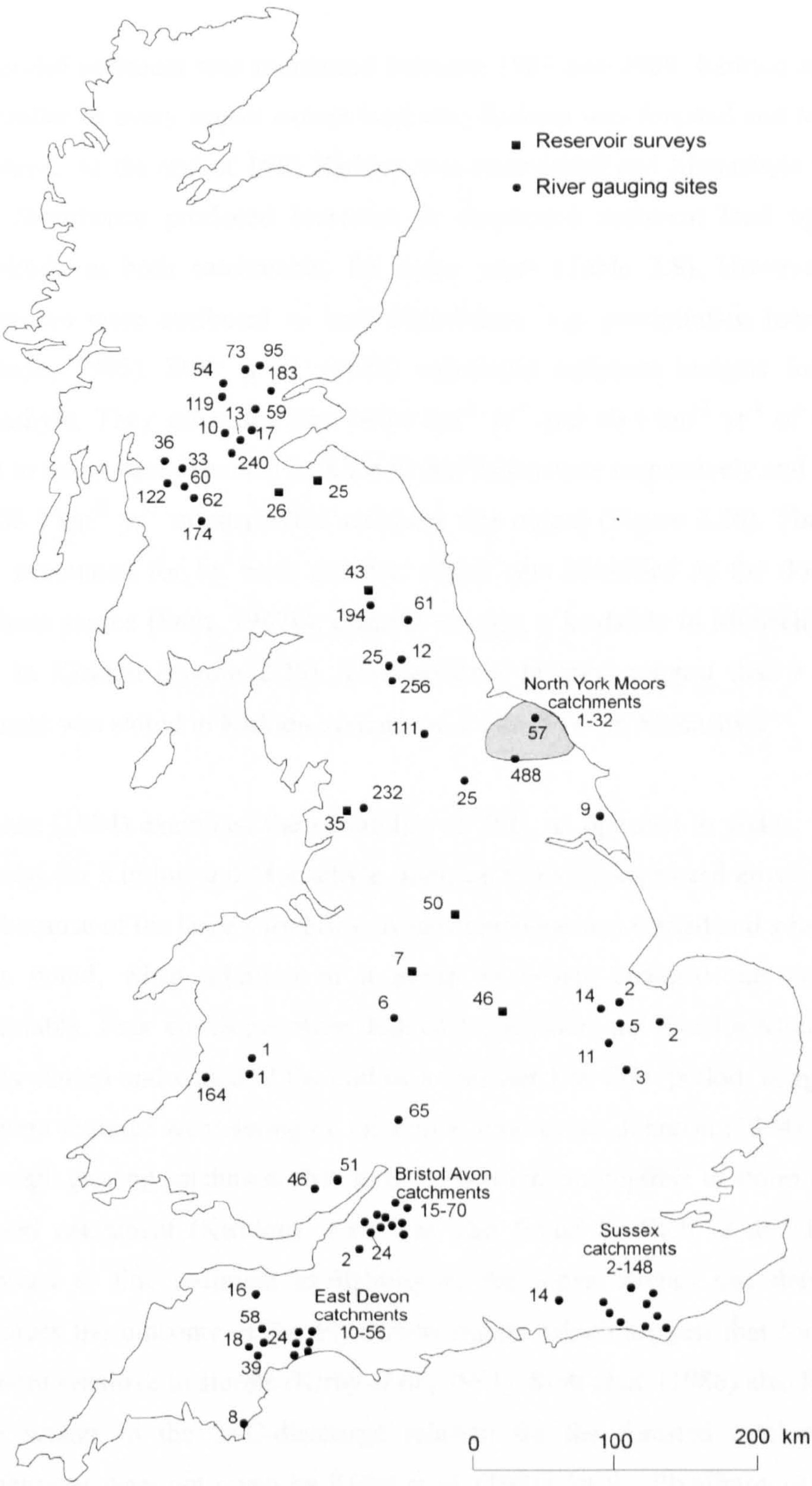

Figure 2.19. National variation of suspended sediment yields in t km^{-2} yr^{-1} for mainland Britain. Source: Walling & Webb, 1987.

Various aspects of suspended sediment dynamics and delivery have been investigated in Kirkton and Monachyle (the paired catchments at Balquhidder). An overview of the research undertaken at Balquhidder between 1981 and 1991 is given by Johnson (1995).

Suspended sediment was monitored between 1983 and 1989. Kirkton and Monachyle are similar in every aspect except land use: Kirkton was forested and Monachyle was moorland. At the end of 1985 Kirkton was clear-felled and Monachyle was ploughed. This disturbance produced increases in suspended sediment load by an order of magnitude in both catchments, for some years (Table 2.8). However, not all the differences were attributed to land disturbance, e.g. precipitation increased in 1986 (Johnson, 1995). Stott *et al.* (1986) calculated sediment budgets for Kirkton and Monachyle. They estimated that 140 t km^{-2} yr^{-1} and 40 t km^{-2} yr^{-1} of sediment were input to the stream networks in Kirkton and Monachyle respectively and 131 t km^{-2} yr^{-1} and 38 t km^{-2} yr^{-1} of suspended sediment was output (Figure 2.20). These differences were accounted for by bank erosion, which was identified as the dominant natural sediment source (Stott, 1987b); channel storage; a landslide in Monachyle; and debris jams in Kirkton (Figure 2.20). The sediment budgets suggest that 9 t km^{-2} yr^{-1} of sediment was stored in Kirkton system and 2 t km^{-2} yr^{-1} in Monachyle.

Johnson (1994) examined the variability of SSC, as opposed to yields, in the ten year data sets for Kirkton and Monachyle. Johnson (1994) constructed envelopes around the data because of the large variability. A new envelope was started and a break in the time series noted, when addition of a group of points changed the existing envelop appreciably. Four envelopes were defined for Kirkton and five for Monachyle and the breaks started and ended at the end of a summer low flow period, suggesting that the sediment regimes were acting on an annual time cycle. Johnson (1994) also noted that the rough grazing catchment (Monachyle) was less susceptible to storm events than the forested catchment (Kirkton). This was also found by Stott *et al.* (1986) and was attributed to fine sediment availability in the forest ditches and debris jams. This reinforces the outcome of the Plynlimon studies which suggest that forest catchments are more sensitive to storms (Kirby *et al.*, 1991). Stott *et al.* (1986) also found there was more scatter in the SSC-discharge relation for the forested catchment. The data distributions were not given by Kirby *et al.* (1991) for the Plynlimon catchments so no direct comparisons can be made.

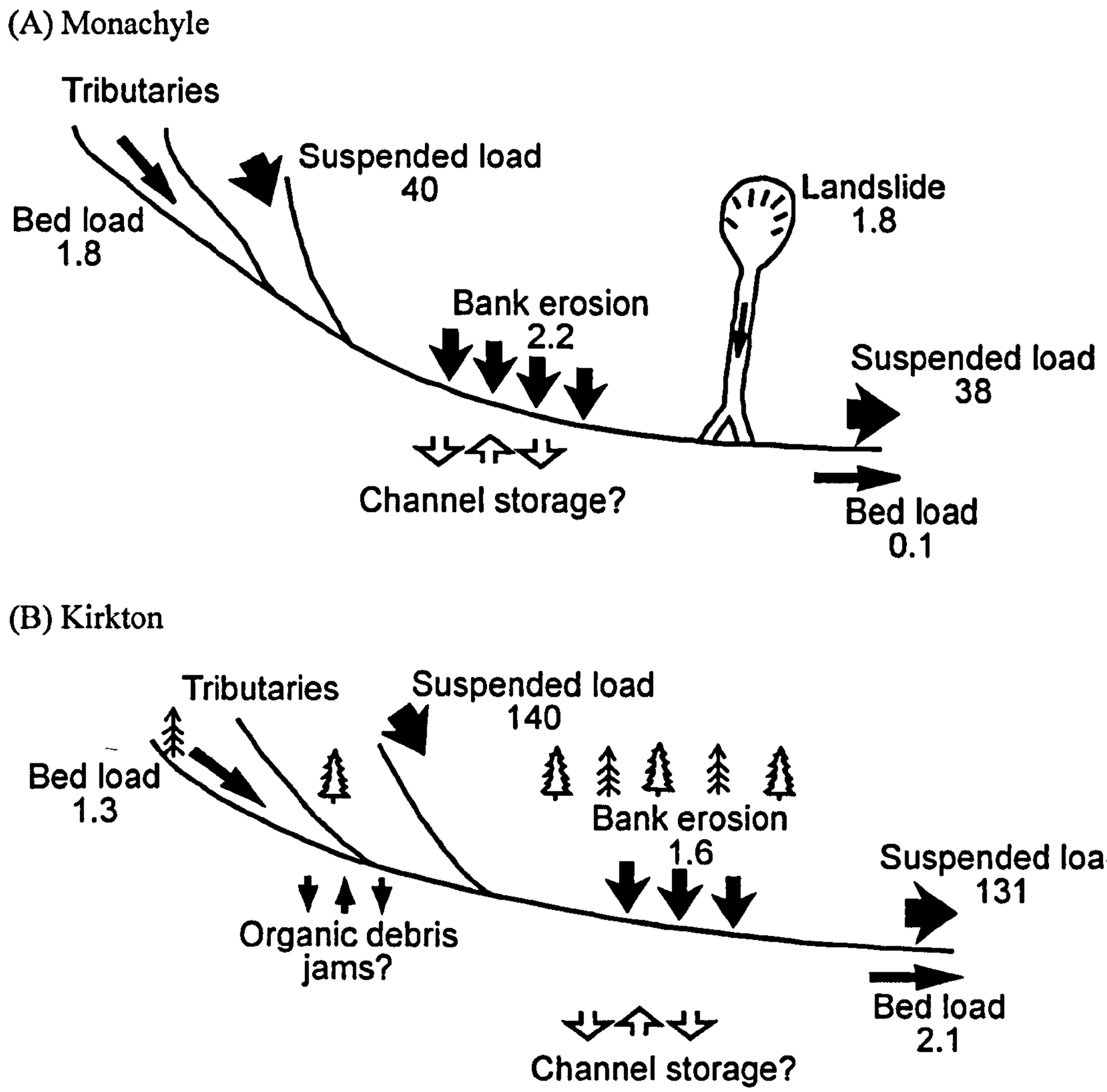

Figure 2.20. Sediment budget for (A) Monachyle, and (B) Kirkton, Scotland, based on 1985 sources and 1982-1985 outputs. All figures in t km^{-2} yr^{-1}. Source: Stott *et al.*, 1986.

Johnson (1994) established that a year after ditching occurred in Monachyle no change in sediment variability was evident. However, sediment yield post-ditching remained higher and more variable than before, even two years later. A delay in sediment response has not been noted in similar studies, e.g. Robinson & Blyth (1982), but is indicative of meteorological conditions not catchment response, e.g. limited storm events in Monachlye. This illustrates the interplay between controlling factors. Clear felling in Kirkton produced an increase in sediment variability. There was a subsequent increase in sediment variability from 1990-1992 which was not related to clear-felling activity. This second increase was attributed to increased mean daily rainfall and was not mirrored in Monachyle, probably because Monachyle has more natural protection. Johnson (1994) commented on the difficulty associated with isolating the effects of land use, climate and hydrological change on sediment fluxes.

Efforts in establishing suspended sediment loads for Kirkton and Monachlye also demonstrates some important methodological considerations. Stott *et al.* (1986) examined the use of seasonal categorisation of data to improve suspended sediment load estimates for Kirkton and Monachlye. They concluded it was important to collect data from all seasons to capture the potential temporal variation in the SSC-discharge relationship. The relationship between SSC and discharge was poor for the winter as a result of the effect of snow (Stott *et al.*, 1986). The harsh and unusual climates of the catchments precluded the use of standard seasons; instead Stott *et al.* (1986) suggested seasons should be defined by meteorological conditions. This is a sensible approach given the arbitrary nature of season classifications, even for catchments with less extreme climates. However, the criteria for defining the seasons will remain, to some degree, arbitrary and this will vary inter-annually. These studies also demonstrate the importance of model development on suspended sediment load estimates. Johnson (1988 & 1995) calculated different suspended sediment loads for 1983 to 1987, some of which were markedly different (Table 2.10), e.g. 1986 Kirkton load was double (cf. Johnson (1995) compared with Johnson (1988), Table 2.10). This appears to be related to methodology because Johnson (1988) calculated separate rating curves for each year and used linear regression back-transformed using the log-normal correction factor. Johnson (1995) also used a rating curve approach but grouped the data into discharge classes and used the mean SSC and discharge values of each class to derive the rating curve.

Table 2.10. Load estimates (t) for Kirkton and Monachyle as determined by Johnson (1988) and Johnson (1995).

Study period	Johnson (1988)	Johnson (1995)	Difference, %
Kirkton:			
1983	483	321	50.0
1984	292	275	6.2
1985	386	526	–26.6
1986	1965	4353	–54.9
1987	986	599	64.6
Monachlye:			
1983	337	293	15.0
1984	296	280	5.7
1985	228	326	–30.1
1986	1027	934	10.0
1987	860	909	–5.4

The Plynlimon suspended sediment studies are summarised in Kirby *et al.* (1991) with other research undertaken at Plynlimon. Given the summary nature of the report the suspended sediment studies are not outlined in detail and suspended sediment yields were only calculated for some of the sub-catchments (Table 2.8). However, rating curves of all catchments were given (Figure 2.21). The difference in suspended sediment yields (Table 2.8) and rating curve form (Figure 2.21) illustrates the variability in suspended sediment dynamics across the 19.25 km^2 study area. Examination of the specific suspended sediment yields, altitude and catchment area shows no clear patterns (Table 2.8). However, there are similarities in the form of the regression lines in accordance with the vegetation type. The Severn and Hafren are characterised by forest and moorland and the gradients are very similar (Figure 2.21). The two steepest regressions are associated with forested catchments (Figure 2.21) and the regressions for Cyff and Iago, which are characterised by moorland and pasture, plot in the same region of the graph (Figure 2.21). As the gradient of regression lines represents the increase/decrease in SSC for a given increase/decrease in discharge this suggests that there is some continuity between sediment controlling factors between catchments with the same vegetation cover. From this it can be stated that the forest catchments are most sensitive to change in discharge, the catchments containing both moorland and pasture are the second most sensitive and the catchments containing a combination of forest and moorland are the least sensitive.

The main land use types of the British upland catchments included in suspended sediment studies are moorland, grassland, or forest; and some were ditched or ploughed (Table 2.8). There is no simple correlation between land use and specific suspended sediment yield (Figure 2.22). The lack of correlation may be explained by: the distribution of land cover in the catchment; the influence of factors, such as lithology and land use change, over suspended sediment delivery and dynamics may subsume the effect of land cover; the different study years (1966 to 1998), over which short-term climatic change has been noted (Longfield & Macklin, 1999); and/or different monitoring equipment, sampling regimes and modelling methods (Table 2.8).

Differences in monitoring and modelling methods and the effect of inter-annual variability in meteorological conditions question the validity of any generalisations obtained from the comparison of different studies undertaken at different times using different methods. For example, Crisp (1966) and Evans & Warburton (in press) both established suspended sediment loads for Rough Sike, Northern Pennines. Crisp's

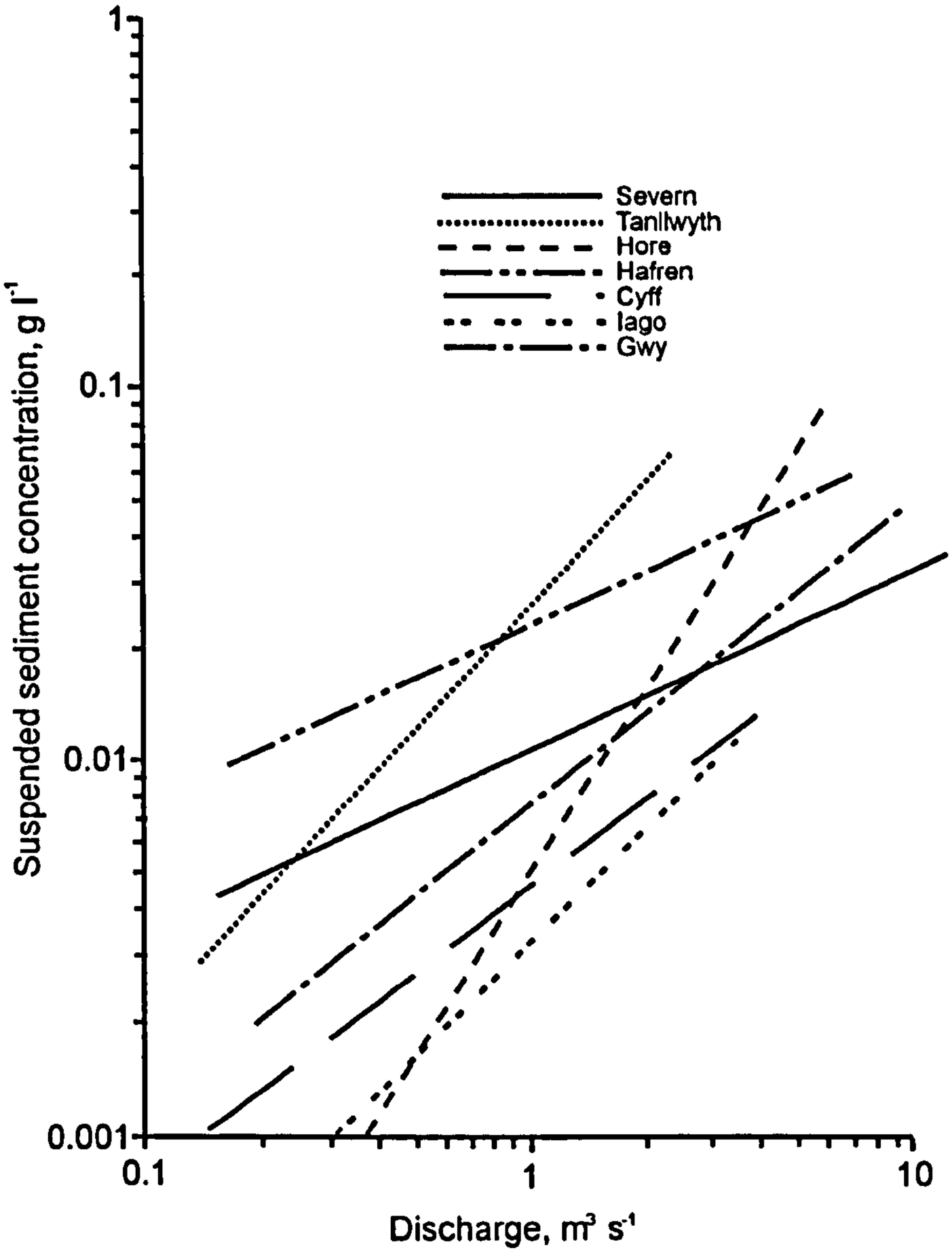

Figure 2.21. Suspended sediment rating curves for the Plynlimon catchments. (Adapted from: Kirby *et al.*, 1991)

(1966) estimate was approximately three times that of Evans and Warburton's (in press) and while the majority of the differences may be attributed to decreased erosion in the catchment, the influence of the different monitoring and modelling methods (Table 2.8) cannot be fully tested.

Annual suspended sediment loads in British upland catchments vary from 0.09 t in Nant Ysguthon, mid Wales (Francis & Taylor, 1989) to 1965 t in Kirkton, West Scotland (Johnson, 1988) (Table 2.8). The specific suspended sediment yields vary from 0.7 t km^{-2} yr^{-1} to 2869 t km^{-2} yr^{-1} for these same catchments (Table 2.8), with an average of 80.4 t km^{-2} yr^{-1} for all the catchments. This is higher than the average specific suspended sediment yield suggested for British catchments by Walling & Webb (1987). Upland catchments tend to be small, often have a peatland component and are generally characterised by flashy discharge regimes as the high drainage densities and low

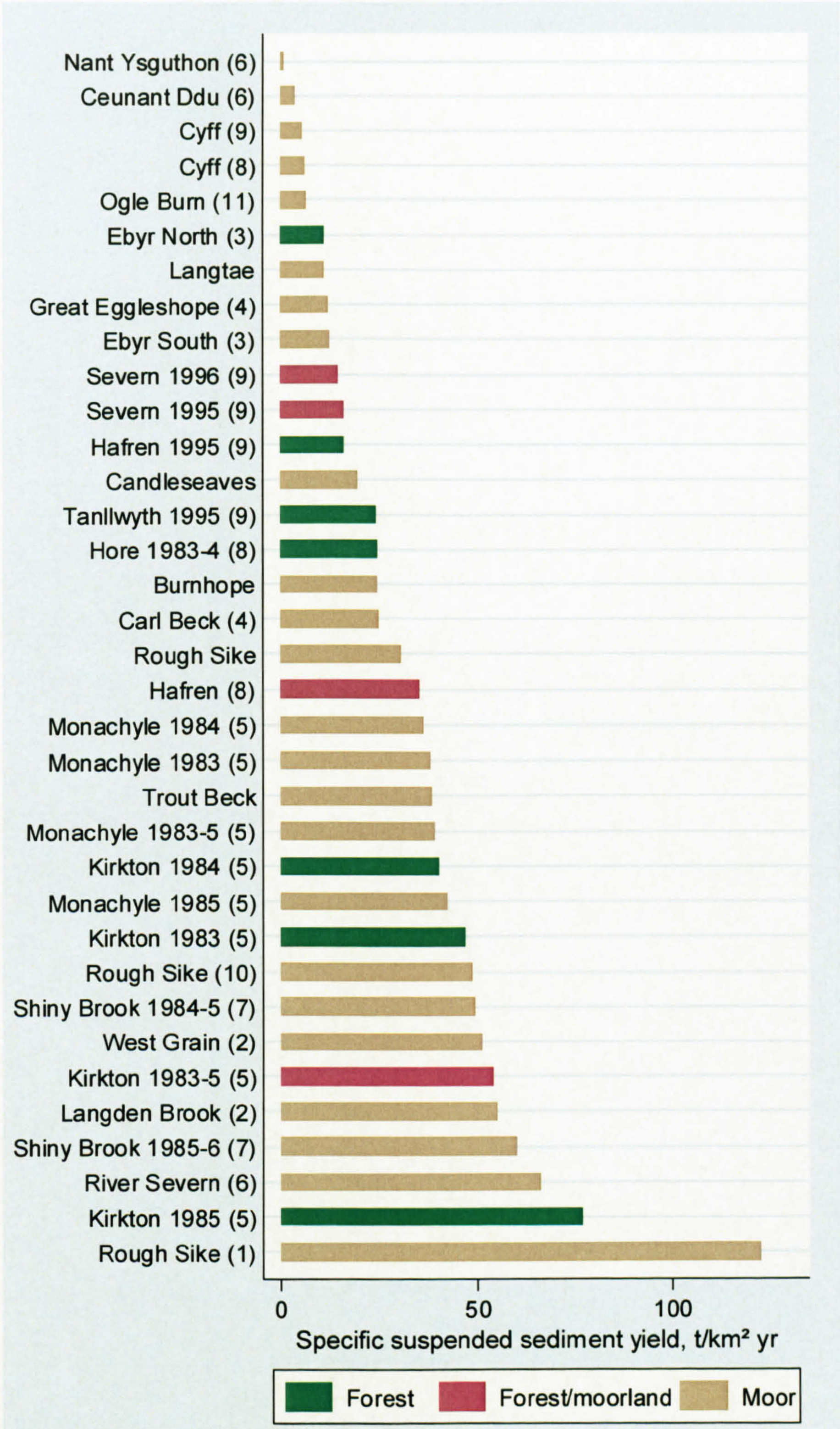

Figure 2.22. Specific suspended sediment loads of undisturbed British upland catchments colour-coded by catchment land use type. (1) Crisp, 1966; (2) Wilkinson, 1971; (3) Oxley, 1974; (4) Carling, 1983; (5) Johnson, 1995; (6) Francis, 1987; (7) Labadz *et al.*, 1991; (8) Kirby *et al.*, 1991(9) Leeks & Marks, 1997; (10) Evans & Warburton (in press); and (11) Duck, 1985. See Table A.1 for more information.

infiltration rates of peat promotes surface runoff, producing large and rapid storm discharges (Burt & Gardiner, 1984 and Burt *et al.*, 1984). For example, Labadz *et al.* (1991) noted that there was little evidence of any delayed flow in Shiny Brook, i.e. stream stormflow was mostly derived from overland flow with a small contribution from through flow. High suspended sediment yields in upland catchments are a result of overland flow, which transports sediment to the channel; large area of banks exposed to flow, as a result of the high drainage densities; and high stream powers given the quick delivery of water to the channel. In addition, hillslope to channel connectivity is generally higher than in lowland catchments given the typically higher gradient slopes and drainage densities.

Some upland suspended sediment loads and yields are anomalously low (Table 2.8). This is often the result of limited mineral sources in the catchment and the low density of peat. The low density of peat is influential as the dry weight of suspended sediment is used to calculate sediment loads and yields. For example, the specific sediment yields of Nant Ysguthon and Ceunant Ddu are very low, even after land disturbance (Table 2.8). Organic material composed between 60% and 94% of the suspended sediment. In addition, to its low density, peat banks are relatively resistant to erosion given its fibrous nature (Evans & Burt, 1998), although freeze-thaw and desiccation are effective at preparing peat for transport (Francis, 1987).

Suspended sediment loads and yields are generally expressed in mass. However, given the differences in dry densities, the impact on the landscape varies depending on the mineral-organic balance of the sediment system. Warburton (pers comm.) suggests that densities of 0.15 and 1.2 t m^{-3} are representative of organic and mineral sediment, respectively, in northern England catchments. Therefore, the volumetric impact of erosion on the landscape is substantially less if the suspended sediment is predominantly mineral than if it is predominantly organic.

Suspended sediment dynamics are controlled by sediment supply and transport processes. While studies of upland suspended sediment dynamics have illustrated discharge is generally the dominant control over SSC, it is not the only control. Carling (1983) established that the transport of suspended sediment was always less than the transport capacity of the flow, as determined by hydraulic equations, which indicates the supply-limited nature of the catchment. Furthermore, clockwise hysteresis within storm

events was evident, and the loops became more open as sediment sources became progressively more exhausted throughout the season (Carling, 1983). In Rough Sike, peak SSC typically preceded peak discharge by one hour due to sediment exhaustion as sediment available for transport was flushed from the system (Evans & Burt, 1998). Sediment exhaustion is noted as a controlling factor in most upland catchments. Carling (1983) divided total flow into stormflow and baseflow to assess if dilution by base flow was occurring and being mistaken for sediment exhaustion as postulated by Walling & Webb (1982). Walling & Webb (1982) surmised that the effect of dilution in flashy streams, such as those studied by Carling (1983), would be insignificant, and Carling's (1983) results agreed with this. Furthermore, the sedigraphs of several storms were very spiky on the falling limb and were not related to changes in flow. Evans & Burt (1998) attributed this phenomenon to irregular inputs of sediment due to bank collapse.

Both Crisp (1966) and Evans & Burt (1998) investigated the suspended sediment dynamics of Rough Sike, Northern Pennines. Crisp (1966) noted that the bulk of sediment was transported during individual events. Evans & Burt (1998) supported this and noted that the relationship between SSC and discharge was much stronger for the rising limb than the falling limb. Wilkinson (1971) also documents the importance of high magnitude, low frequency events in the transport of suspended sediment for West Grain and Langden Brook, Pennines.

Few studies have examined total sediment load but those that have indicate that suspended load is the dominant component. Wilkinson (1971) found that the majority of sediment was transported in suspension in two upland catchments in the North of England (Table 2.11). Johnson (1995) also found that suspended sediment was responsible for the majority of sediment transport, although the dissolved load was not quantified (Table 2.11).

Table 2.11. Percentage of sediment transported in each phase. Dissolved load was not quantified for Monachyle and Kirkton. Source: Wilkinson (1971) and Johnson (1995).

Site	Suspended	Dissolved	Bed
West Grain	65	26	9
Langden Brook	60	24	15
Monachlye	99.3-99.9	-	0.1-0.7
Kirkton	94.0-99.7	-	0.3-6.0

Weathering processes are important in preparing the sediment for transport. Freeze-thaw and desiccation were noted to be important in peatland catchments in in Mid-Wales (Francis, 1987). Needle ice, which is related to freeze-thaw cycles, and peat fans at the end of gully networks were identified as controls in Rough Sike, North Pennines, by Evans & Burt (1998), although their contribution to suspended sediment was variable. Periods of drought are also known to be of importance, as suggested by Francis (1987) for peatland catchments, and Oxley (1974) who observed that SSCs were noticeably higher following a drought period. The effect of season on the relationship between SSC and discharge has been noted by several authors (e.g. Wilkinson, 1971 and Stott *et al.*, 1986). In contrast, there was no clear division between rating curves for different seasons for Carl Beck and Great Eggleshope Beck (Carling, 1983).

In summary, few studies of suspended sediment have been undertaken in the British uplands. This is despite the dominance of the suspended transport phase; the impact of land disturbance associated with forestry, agriculture and moorland gripping; and the potential improved scientific understanding gained from studying catchments with fewer influences. Existing studies have shown that land disturbance, vegetation cover, lithology, organic-mineral balance, meteorological conditions and catchment size are important influences over suspended sediment dynamics. Sediment exhaustion was an important influence in all of the studies.

This review of suspended sediment in the British uplands has led to the identification of several knowledge gaps:

(1) Few studies have investigated the difference in suspended sediment dynamics in more than one catchment (e.g. Oxley, 1974; Stott *et al.*, 1986; Johnson, 1988, 1994; and Francis & Taylor, 1989), but the focus of these tends to be on the implications of land use change. Given the different methodologies employed by different authors and the different time periods of study no firm generalisations, regarding upland suspended sediment dynamics, can be made.

(2) The aim of most investigations appears to be to establish suspended sediment loads. Within-storm variation in the SSC-discharge relationship or the spatial variability in suspended sediment are not greatly studied. There is limited information regarding variation in the nature of suspended sediment properties.

(3) No single study has directly examined more than two catchments in different regions of British uplands. Therefore, it is difficult to make generalisations

regarding the relative influence of catchment characteristics and meteorological conditions over suspended sediment dynamics.

(4) A large variety of monitoring and modelling methods are used and limited attention is given to the effects of the various methods on load estimations.

2.10 Chapter summary

There are various sources of suspended sediment and different processes release sediment from each. The dominance of the different sources and releasing processes varies spatially and temporally and partially controls the character of the sediment. The factors affecting the dynamics of suspended sediment are complex and include internal and external influences. The literature is generally polarised: it examines either large-scale or small-scale controls; coupled with interactions between different influences and spatial and temporal variations operating at a range of scales. This inhibits any generalisations of the dominant controls over suspended sediment dynamics to be made.

Suspended sediment dynamics vary temporally from the intra-event to inter-annual scales. Hysteresis is used to analyse within-storm SSC-discharge relations which allows inferences on the nature of the sediment delivery system and likely sediment sources to be made. Some authors also discuss inter-event hysteresis and seasonal variation. Inter-annual variability in suspended sediment yield is high, especially for smaller catchments. This results from changing meteorological conditions and land use. Low frequency, high magnitude events were found to contribute a higher percentage of the annual load in British rivers.

Suspended sediment fluxes in the Britain are low in a global context but within a British context fluxes are generally higher in upland areas. Relatively few studies have been undertaken in the British uplands despite the high fluxes and the potential insight into sediment systems provided by small catchments. Variations in suspended sediment loads and yields cannot be attributed to catchment characteristics with confidence given the different monitoring and modelling methods and time periods of study. Some studies investigated more than one catchment but none compared more than one catchment in different regions over the same time period. Therefore only limited generalisations can be made on the basis of existing studies.

This review highlights two main gaps in the literature with regard to suspended sediment studies which this thesis will address. (1) There is limited knowledge of the relative importance of local and regional controls. (2) There are relatively few studies in British upland catchments, especially using the same monitoring and modelling techniques to allow direct comparisons of loads, yields, hysteresis, spatial variation, and the importance of magnitude and frequency between catchments.

Chapter Three: SUSPENDED SEDIMENT MONITORING

3.1 Overview

This section introduces the different approaches used to determine catchment suspended sediment loads and outlines the systematic monitoring programmes which have been undertaken in Britain. Sampling regimes are described, both statistical and non-statistical, and sampling techniques are explained, including their suitability for different sampling regimes. Examples of the effects of sampling regime on suspended sediment yield estimates are given to demonstrate the importance of developing an appropriate sampling regime. Finally, some problems and considerations of suspended sediment sampling are highlighted. While this is primarily a review of suspended sediment monitoring methods, it helps define suitable methods for monitoring suspended sediment flux in the British uplands (objective 1).

3.2 Introduction

The suspended sediment yield from a drainage basin is generally estimated by measuring suspended sediment and discharge at the catchment outlet (e.g. Smith *et al.*, 2003), by monitoring erosion within the catchment (e.g. Hadley & Shown in Walling, 1994), or by studying lake or reservoir cores (e.g. Foster & Lees, 1999). Lake or reservoir cores are useful for studying long-term sediment dynamics but do not allow spatial or short term variability (i.e. inter and intra storm) to be examined. Soil erosion monitoring techniques are preferential if the aim of the study is to quantify land denudation but are problematic if the aim is to quantify sediment flux out of a catchment because of the effect of storage within the catchment (especially within catchments with weak connectivity between the channel and hillslopes) and obtaining data representative of the catchment as a whole can be difficult, even in small

catchments. Therefore, monitoring suspended sediment concentrations and discharge is the preferred method for this investigation, as it allows examination of spatial and short-term variability and does not suffer the problems of storage associated with soil erosion monitoring.

Recently in Britain there have been two large-scale programmes which involved systematic monitoring of suspended sediment: the Land-Ocean Interaction Study (LOIS) and the Harmonised Monitoring Programme (HMP). The HMP began in 1975 and aimed to investigate river water quality of all gauged rivers in Great Britain (McManus & Duck, 1996). However, a monthly, or less frequent, sampling regime was employed (McManus & Duck, 1996) which has been shown to be inaccurate by various authors (e.g. Walling *et al.*, 1992) as high flow events, which transport the majority of suspended sediment, are often under-sampled.

LOIS aimed to quantify the fluxes and transformation of sediment, nutrients and contaminants from headwaters to the coastal shelf. The project ran from 1992 to 1998 and the study area comprised the river catchments, estuaries and coastal zones between Great Yarmouth and Berwick-upon-Tweed. The rivers sub-study involved 42,000 km^2 of land and established and maintained monitoring of discharge, sediment, nutrients, metals and organic micro-contaminants of the Humber River system, and to a lesser extent the Rivers Tweed and Tyne (Barrett, 2002).

Apart from these programmes there is no adequate, standard and long-term national suspended sediment sampling programme within Britain. As a result data are limited and coverage varies spatially and temporally. Also, because monitoring is undertaken by different investigators protocols and regimes differ. Therefore, when comparing studies it is not apparent if differences or similarities reflect processes and characteristics of the river systems or the monitoring methods. It would thus be ideal to establish a national sampling regime and protocols. There is a suspended sediment database, collected using uniform methods, in the USA which is operated by the United States Geological Society (USGS). The database consists of two sets of records: (1) daily samples from rivers throughout the USA, and (2) periodic samples.

In summary, contemporary monitoring is the most appropriate way of obtaining sediment load estimates and examining spatial and short-term temporal variation in

sediment delivery. However, there are no current national monitoring schemes and no standard protocol for monitoring suspended sediment in British rivers.

3.3 Field sampling equipment and regimes

Measurement of suspended sediment concentration (SSC) is problematic because of temporal and spatial variability (especially given the potential cross-sectional variability in SSC within the channel cross-section); and the stochastic response of SSC to controlling factors. There are different suspended sediment sampling methods. The selected method depends on equipment and time available, the sampling regime required, and the purpose of study. No single ideal method exists to measure SSC continuously. There are several possible combinations of sampling methods and regimes (Table 3.1). These are fully explained in the following sections.

3.3.1 Sampling methods

The main methods of sample collection are discussed below in order of sophistication and the possible sampling regimes noted for each. The samplers differ in their expense, sample volume, frequency at which samples are taken and flexibility in terms of the different sampling regimes they can achieve (Table 3.1).

3.3.1.1 Grab samplers

Grab samples are taken (by hand) using pre-rinsed wide necked bottles. Grab samples are advantageous as they can be taken as and when required and no expensive equipment is needed. Grab samples are commonly taken while standing on the river bank which may result in over-estimation in suspended sediment concentration because of their proximity to sediment sources (e.g. the bank) or an under-estimation as the sample is taken closer to the surface (Carling, 1984) or because the flow is slower, reflecting increased friction by the channel edges. Also, the samples are not guaranteed to be from a fixed location, both laterally and horizontally. Gulp samples are often used in studies which use fixed-interval sampling regimes, i.e. one sample every two weeks (e.g. Hope *et al.*, 1997a), and they are especially useful in studies examining the spatial variability in suspended sediment as otherwise several costly auto-samplers would be required. Gulp samples are also used to take samples of 'interesting' conditions and storm samples if fieldworkers are on site at the time to augment automated sample collection.

Table 3.1. Possible combinations of the main sampling method and sampling regimes and the key characteristics of the sampling methods.

Sampling method	Sampling regime							Sampling method characteristics			
	Flow proportional	Continuous	Quasi-continuous	Fixed-interval	Storm	Spatial	Arbitrary	Statistical	Expense	Volume, l	Frequency of samples	Flexibility
Grab				■	■	■			Low	Various	Variable	Intermediate
Rising stage					■				Low	< 5	On rising limb	Low
Depth-integrated				■	■	■			Intermediate	< 1	Variable	Intermediate
Time-integrated mass		■			■				Low	N/A	Continuous	Low
Siphon and filter		■			■				Intermediate	N/A	Continuous	Low
Auto-samplers	■		■	■	■		■		High	0.5 – 10	Fixed interval or variable	High
Turbidity			■	■	■		■		High	N/A	Regular	High

3.3.1.2 Rising stage samplers

Rising stage samplers are bottle samplers attached to a structure at a fixed height above the water surface. The samplers are filled when the river stage rises; therefore samples are only taken on the rising limb of flow events. Although relatively inexpensive, rising stage samplers are not as widespread as other sampling techniques, mainly because the falling limb cannot be sampled and therefore reliable suspended sediment load estimates cannot be made. In addition multi-peaked hydrographs cast doubt on the legitimacy of the samples, i.e. when was it taken and if the rising stage sampler was collected on the first rising limb did the second rising limb contaminate it? Loughran (1976) used rising stage samplers to ascertain suspended sediment concentration on the rising limb of flow events in the Chandler River, Australia.

3.3.1.3 Depth-integrated samplers

Depth-integrated samplers are devices which collect water throughout the depth of the water column. This is considered superior to fixed-point sampling methods (i.e. auto-samplers, grab samplers, rising stage samplers, siphons, turbidity and time-integrated samplers) as any differences in suspended sediment throughout the water column are captured and an 'average' obtained. However, depth-integrated samplers require an operator and therefore the number of samples and timing of sampling are restricted. Also, applications of depth-integrated sampling are limited as either an operator has to wade into the river or cable systems have to be used. There are different depth-integrated samplers available and the principal differences are in weight, dimensions and water sampler container size: some available samplers and examples of the sampling technique are given by Walling (1994, Table 3.3 & 3.4). Depth-integrated samplers can be used within fixed-interval, arbitrary, spatial and storm (if operators are on site at the time) sampling regimes.

3.3.1.4 Time-integrated mass samplers

A time-integrated mass sampler (TIMS) was developed by Phillips *et al.* (2000) (Figure 3.1) to obtain bulk samples of fine suspended sediment. TIMS are orientated in line with the flow, water flows in through the restricted inlet pipe, enters the larger chamber, velocity decreases, sediment settles out and water flows out of the outlet.

Phillips *et al.* (2000) rigorously tested the performance of the TIMS, including the effect of frictional resistance of the inlet tube, the flow structure within the main body, and the

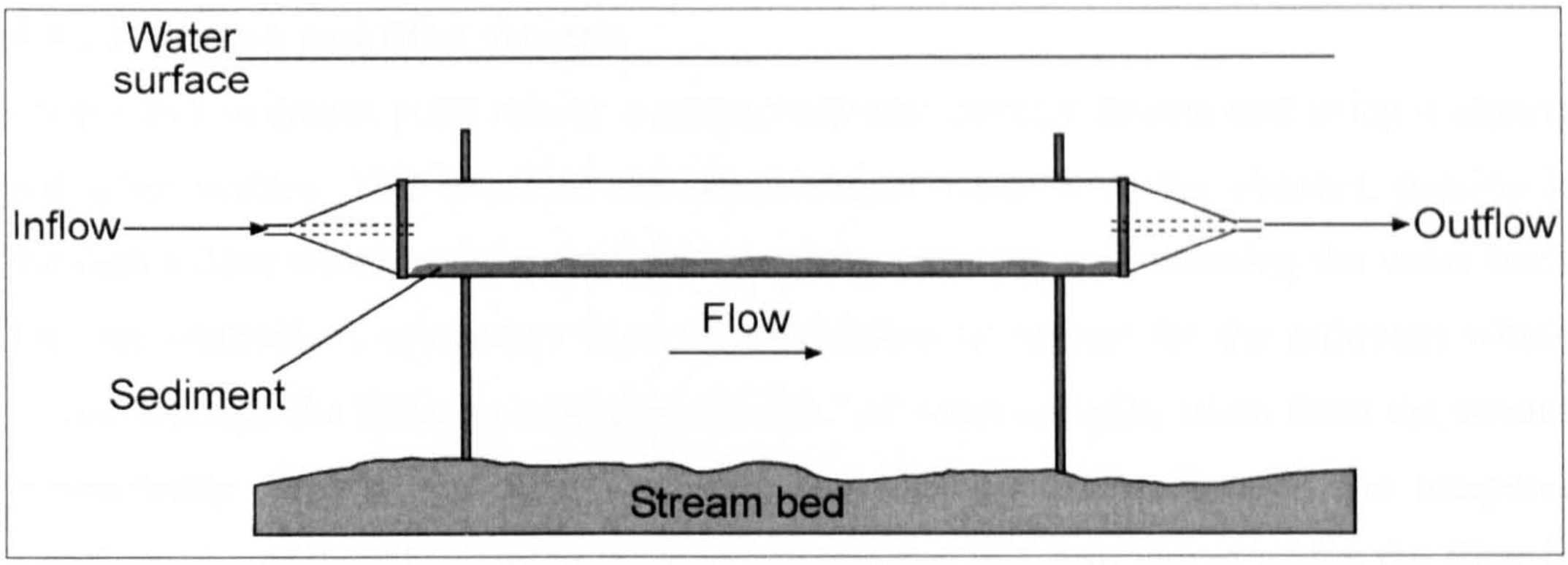

Figure 3.1. A time-integrated mass sampler.

efficiency. Efficiency was measured in flume experiments by two methods: the total mass and the grain size distribution retained in the sampler compared with that of the stream water. The flume experiments showed between 31% and 71% of sediment was retained within the sampler, with higher sediment retention associated with higher velocities (Phillips *et al.*, 2000). Sediment from all particle size fractions was retained but higher proportions of the coarser fractions; this bias increased with velocity. The difference between the particle size distribution of inflowing water and that of the sediment retained in the TIMS was found to be statistically significantly different except when flow velocities were low and suspended sediment relatively coarse (Phillips *et al.*, 2000). However, Phillips *et al.* (2000) report that improved results could be expected in field conditions as dispersed mineral sediment was used in the flume experiments, whereas in the field aggregates will be derived from sediment sources and flocs may form (Droppo, 2000), thus coarsening sediment sizes and therefore increasing the chance of retention in the TIMS. TIMS have advantages over other techniques as bulk sediment samples can be accumulated without taking large volumes of water, and the samplers are relatively economical, easy to construct and can be deployed in most channels. The disadvantages of TIMS are that the samples are taken at a fixed depth, which may be problematic in shallow streams: to sample continuously the TIMS have to be located close to the bed and therefore when stage rises some coarser load may be sampled. Also, the sampler does not sample a strictly representative sample size or grain size distribution, the channel velocity and inlet velocity may differ, and the efficiency is difficult to establish in field settings. Within limits of the errors, TIMS can be used to sample suspended sediment continuously, to estimate storm yields and can be distributed throughout catchments to capture spatial variability. Phillips *et al.* (2000), Russell *et al.* (2000) and Ankers (2003) report field applications of TIMS.

3.3.1.5 Siphon and filter systems

Suspended sediment yield can be continuously and directly determined using a siphon and filter system. This involves siphoning stream water from the channel, passing it through a filter which retains a proportion of the sediment, and releasing the water back into the channel. A correction factor is established to correct for the sediment which passes through the filter by analysing the SSC of water samples taken from the stream concurrently. Siphon and filter sampling provides no information on the temporal variation of suspended sediment yield at a resolution less than that at which the filter is changed. There is a trade-off between retaining as much sediment as possible, and therefore achieving a more accurate measure of sediment yield, and the frequency which the filter has to be emptied to prevent blocking when selecting the filter membrane size. Crisp and Robson (1979) used a siphon and filter set up to monitor sediment flux in Rough Sike. A high proportion of suspended material passed through the filter mesh (filter mesh was 0.33 mm by 0.26 mm). Crisp & Robson (1979) established a correction factor of 1.8 (i.e. only 56% was retained by the filter). Crisp & Robson (1979) generally emptied the filter daily but during storm events as often as every half hour. Siphon and filter systems can be used to monitor suspended sediment continuously, assess storm yields and spatial variation if several systems are available.

3.3.1.6 Automated samplers

Automated samplers, or auto-samplers, are devices which can be programmed to perform predefined sampling regimes; therefore no operator is required at the time of sampling. The most basic auto-sampler will take samples at set intervals, allow the sampling program to be delayed until a defined time, or triggered by a rise in stage using a float switch. The more complex auto-samplers can operate with several bottle configurations (in terms of volume and number) and can be triggered by various conditions (e.g. change in turbidity: Lewis & Eads, 2001), precipitation, or after a given a volume of flow (American Sigma, 1998). The interval between samples can be varied within one programme (this allows more samples to be taken at the beginning of the storm), and more than one bottle per sample may be used or more than one sample placed in each bottle (for example, if an 'average' was required for a day). In addition, several auto-samplers can be deployed in a cascade. Auto-samplers are preferred because of their versatility, limited operator assistance, accuracy of timing and static sampling location. Auto-samplers are perhaps the most common method of water sample collection in suspended sediment studies (e.g. Evans & Burt, 1998 and Fenn,

1989) and they allow fixed-interval, storm, arbitrary (if the particular sampler can be set to take a sample when a defined threshold is reached) and spatial (if more than one auto-sampler is available) sampling. However, the samplers are costly and have to be located in a secure position in terms of proximity to the channel and potential interference from people and animals.

3.3.1.7 Turbidity meters

Turbidity is a measure of the optical property of a substance (in this context stream water) which causes light to be scattered and absorbed. There are two types of turbidity measurement: turbidimetry and nephelometry. Turbidimetry is the measurement of the attenuation of a beam of light of a known intensity, whereas nephelometry is the measurement of the degree of scattering of a beam of light of a known intensity (e.g. Lawler, 1995b). Both techniques are based on the principle that light is scattered and absorbed by particles in its path. Turbidity measurements have to be calibrated against water samples collected and analysed for SSC as the concentration, size distribution, shape, orientation, surface conditions, refractive index of particles, refractive index of suspension medium and the wavelength of light used all affect the turbidity readings. The difference in these factors leads to variation in the form and strength of the relationship between SSC and turbidity. Bubbles, water colour, variable particle size and variable particle density are the most influential factors which affect the SSC-discharge relationship. Johnson (1992) noted the inappropriateness of using turbidity to determine SSC in headwater catchments. Density is likely to be of special importance in study sites with mineral and organic sediment components because a large but less dense organic particle will scatter/absorb more light than a small but dense mineral particle. Foster *et al.* (1992) noted the impact of particle size on turbidity measurements and found that substantial proportions of organic material complicate the relationship between turbidity and SSC. The relationship is also complicated by spatially and temporally varying particle size distributions (Peart & Walling, 1982). The strength of the relationship between SSC and turbidity is potentially a major source of error in suspended sediment load estimates. However, Olive & Rieger (1988) suggest that the increased accuracy introduced by the quasi-continuous nature of turbidity recordings outweighs the inaccuracies introduced by the SSC-turbidity relationship. Turbidity measurement is either a continuous or a quasi-continuous method of suspended sediment monitoring, but unlike siphon systems and time-integrated mass samplers it allows fixed-interval, storm and arbitrary regimes to be sub-sampled from the record.

Turbidity is advantageous given the low level of operator input but algal growth over the light source and/or sensors can be problematic, although many sensors are now self-cleaning.

3.3.1.8 Other

The above methods are not the only ways in which suspended sediment is monitored but those which are most common. Other methods, some of which are fairly experimental, include: acoustic, nuclear, vibrating tube, differential pressure, impact, video microscopy and other optical techniques similar to turbidity (Wren *et al.*, 2000) (Table 3.2).

Table 3.2. Principles of other types of suspended sediment measurement.

Method	Operating principles	Example reference
Acoustic	Bursts of sound are emitted and SSC derived from the proportion back-scattered.	Thorne *et al.* (1991)
Nuclear	Measurement of either the back-scatter or the transmission of gamma/X-rays.	Welch & Allen (1973)
Vibrating tube	River water routed through a continuously vibrating tube which is electronically monitored.	Skinner (1989)
Differential pressure	Uses pressure transducers to determine the specific weight of sediment/water mixes.	Lewis & Rasmussen (1996)
Impact	Based on the principle of momentum transfer: the impact rate of sediment particles hitting a sensor is measured and related to mass, velocity and impact angle.	Van Rijn & Schaafsma (1986)
Video microscopy	Sediment/water mix is filmed *in situ* and then examined by image analysis software.	Baier & Bechteler (1996)

3.3.2 Sampling regimes

There are several sampling regimes which can be adopted in studies of suspended sediment. These depend on the objectives of the study. The sampling regimes can be categorised as statistical or non-statistical (Figure 3.2). Non-statistical sampling is more common than statistical sampling, and less specialist equipment is required to facilitate it.

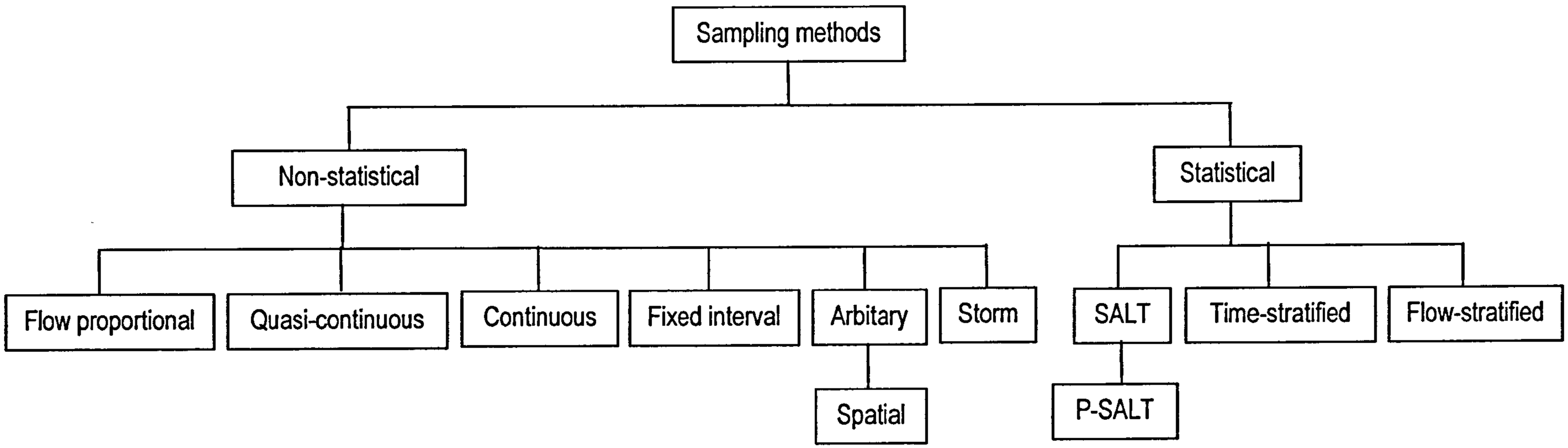

Figure 3.2. The different types of statistical and non-statistical sampling regimes. SALT = selection at list time, P-SALT = piecewise selection at list time.

3.3.2.1 Non-statistical sampling

Non-statistical sampling regimes consist of flow-proportional, continuous, quasi-continuous, fixed-interval, storm, spatial and arbitrary (Figure 3.2). Flow-proportional sampling involves a sample being taken after a fixed volume of flow. Olive & Rieger (1988) doubt the applicability of flow-proportional sampling as it assumes that SSC changes in proportion to discharge, which is not necessarily the case, especially in sediment-supply limited systems. Continuous sampling is the uninterrupted sampling of suspended sediment and quasi-continuous sampling is continual but interrupted, e.g. every 15 minutes. Fixed-interval is sampling at equal set intervals, the precise equality of sampling intervals being dependent on the technique used. Storm sampling is the purposeful sampling of flow events, commonly triggered by a float switch which detects a rise in stage. Spatial sampling involves sampling at various locations concurrently, although in practice this may not be concurrent dependent on equipment and the number of fieldworkers. Finally, arbitrary sampling is simply sampling at arbitrary times, often at interesting instances.

3.3.2.2 Statistical sampling

Statistical or probability sampling methods (Figure 3.2) provide unbiased estimates and allow variance (a measure of efficiency) to be calculated. Probability sampling also rationalises the number of samples taken, thus reduces costs and makes more effective use of the data (Thomas and Lewis, 1995). In contrast, estimates based on non-statistical samples have indeterminable bias and lack valid variance estimators. However, there are two substantial drawbacks with probability sampling. First, it requires previous knowledge of the relationship between the variables under examination. Therefore studies which aim to establish the relationship between SSC and Q would have to establish the relationship using non-statistical sampling and then apply probability sampling to provide unbiased estimates and calculate the variance. Second, there is not a mechanism to take into account the variability in the SSC-discharge relations (hysteresis) and this variability undermines some of the basic principles on which the probability sampling techniques are based.

The validity and use of probability sampling can be explained by an analogy: if there was a database of 10,000 river catchments detailing catchment area and total channel length within each catchment, then the total channel length of all catchments could be determined by sampling a few catchments and multiplying up the results. If non-

statistical sampling, in this example simple random sampling (SRS), was used *n* catchments would be randomly selected, the total channel length for each catchment summed, divided by *n* and multiplied by 10,000 (the total number of river catchments). However, if there were 9,000 small catchments, 900 medium catchments and 100 large catchments this could lead to a biased result. Alternatively, if statistical sampling, in this example probability proportional to size (PPS), was used each catchment would be given a probability of being selected in accordance to its area (the 'auxiliary variable'), with larger catchments having a higher chance of being selected (i.e. large catchments: 9 in 10, medium catchments: 9 in 100 and small catchments: 1 in 100). Then *n* catchments would be selected, the total channel length in each catchment assessed, a per catchment mean calculated and multiplied by 10,000. If the total channel length in the 10,000 catchments is replaced with storm suspended sediment yield, the total channel length in each catchment with a suspended sediment sample and the area of each catchment with discharge (the auxiliary variable), then this concept can be directly related to suspended sediment sampling. Therefore, there is more chance that suspended sediment samples will be taken at higher discharges on the basis that periods of higher discharge contribute more suspended sediment to the total yield (based on an example in Thomas, 1985).

Applying statistical sampling to suspended sediment is a substantial undertaking as it requires prior knowledge of the variables under study and their relationship, and development of an algorithm to control sampling. However, it transfers much of the work from the data analysis stage to the planning stage. Four probabilistic sampling methods have been applied to suspended sediment studies: selection at list time (Thomas, 1985), piecewise selection at list time (Thomas, 1988a, 1989), time-stratified (Thomas & Lewis, 1993) and flow-stratified (Thomas & Lewis, 1995). All four methods require an automated sampler, stage/discharge gauge and a programmable data logger.

Norick (1969) developed selection at list time (SALT) sampling (a refinement of PPS sampling), to sample timber volume and was first used to estimate suspended sediment yields by Thomas (1985). Essentially the probability of taking a sample is proportional to the sample's contribution to the total suspended sediment yield. In comparison to SALT, P-SALT increases the sampling rate at low flows and decreases it at high flows and therefore produces better data for small storms and periods interrupted by station

visits (necessary for bottle changing etc.). However, P-SALT can lead to increased variance in comparison with SALT because the optimal number of samples may not be taken for a given stage. Time-stratified sampling divides the hydrograph into time periods of different lengths based on current stage and change in stage. Time periods are shorter for high stages and rapidly changing stages and longer for lower, more stable stages. Time-stratified results in more even temporal distribution of samples than SALT, and it ensures adequate sample sizes and hence good precision for both small storms as well as large storms (Thomas and Lewis, 1993). However, time-stratified does not work well if a long recession limb is overlapped by the rising limb of the next storm and it is sensitive to reduction in the number of samples, especially for complex hydrographs. Flow-stratified is similar to time-stratified but divides the hydrographs by discharge/stage as opposed to time: each of the flow classes is randomly sampled during the time it is occupied. Unlike time-stratified, flow-stratified time period sizes are not known until the end of the monitoring period and non-contiguous samples from the same flow class are placed in the same group, based upon whether they are rising or falling and magnitude (e.g. high rising, mid rising, low rising, high falling, mid falling and low falling). Flow-stratified works well for total load over long periods with many peaks.

SALT was tested on data collected from Casper Creek, California (Thomas, 1985). The rating curve was developed from 541 rating pairs collected in 1978-1980 and was then used to calculate SSC for each 30 minute period during 1980. The suspended sediment yield was calculated using a combination of both SALT and SRS. The SRS procedure was used to select samples during base flow periods and SALT during storm flow periods. Six samples from the SRS and 39 from the SALT categories were sampled (only six were sampled from the SRS as their flows and sediment concentrations were very low), and the load estimate calculated. This was repeated 50 times to produce a distribution of yields from which the mean yield and variance could be calculated. The mean total suspended sediment yield was calculated to be 204.7 tons which was a 0.6% underestimate of the true yield (sum of the 30 minute intervals yields) with a standard deviation of 11.0 tons.

TS was tested on data from five storms on Mad River, California. Water discharge and turbidity were recorded continuously and pumped samples taken to establish the relationship between turbidity and SSC. Suspended sediment and discharge were then

established at 10 min intervals. Although this data set does not represent actual loads, they were taken to be 'true' for the purpose of the investigation. The results were good; for example, the suspended sediment load for one storm was only 6.8% less than the 'true' load (Thomas and Lewis, 1993).

3.3.2.3 The effect of sampling regime on sediment load determinations

This section illustrates the influence sampling strategy can have on suspended sediment load calculations, the variability which can exist in the yield estimates using the same sampling technique but different data, and the variability in storm estimates depending on storm magnitude.

The effect of sampling strategy on suspended sediment load estimations has been investigated by several authors. This is commonly accomplished by obtaining a high resolution data set (synthetic or empirical) and sub-sampling it to simulate various sampling regimes. For example, Olive & Rieger (1988) generated three synthetic ten hour storm event series of discharge and SSC with an interval of one minute. The three events were: (1) a single peaked hydrograph SSC peaking prior to discharge, (2) a double peaked hydrograph with SSC peaking prior to discharge and depleting, and (3) a multi-peaked hydrograph with a SSC series with no discernible pattern. Two aspects of the sampling regime were investigated: different sampling intervals (5, 10, 15, …., 120 minutes) and the timing of the commencement of sampling (i.e. will the SSC peak be sampled?). Relatively small errors were associated with sampling intervals of less than 30 minutes and the starting point was critical, especially for intervals of greater than one hour (Figure 3.3).

Yaksich & Verhoff (1983) investigated the effect of sampling strategy on suspended sediment load estimations of the Maumee River, Ohio. Daily data (determination method not stipulated) were used and the sediment load calculations from the full data set were used as the standard to assess the effectiveness of storm sampling and lower resolution fixed-interval sampling. Storm sampling resulted in more accurate load estimates than reduced fixed-interval sampling (Table 3.3). The storm sampling may have produced more accurate load estimations than the standard load calculated from the daily data, as it is likely that high flow events were under-sampled. Yaksich & Verhoff (1983) recommended that five to ten samples should be taken during base flow conditions and 15-20 samples from the largest two or three flow events. However, while

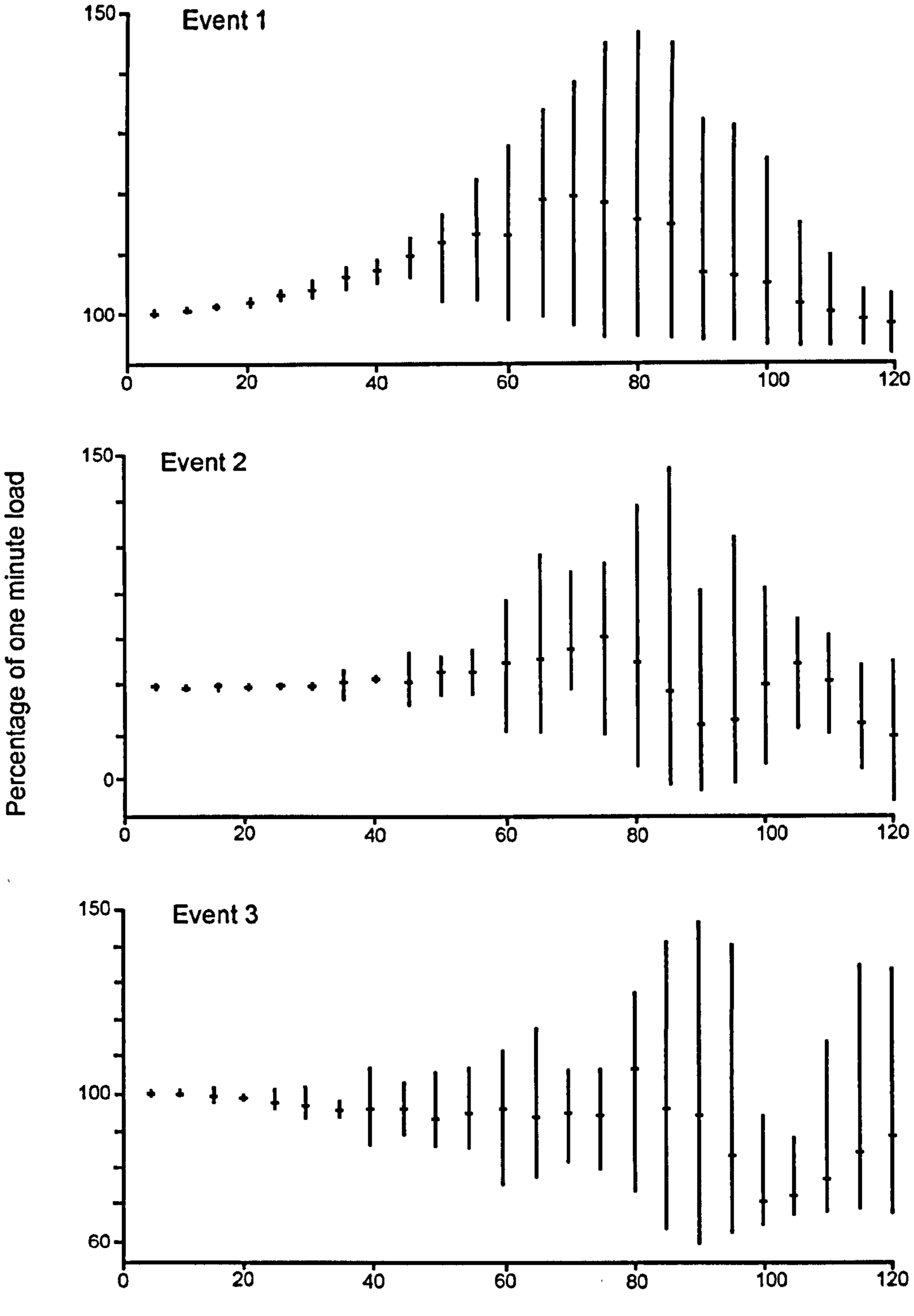

Figure 3.3. Variations in suspended sediment loads caused by varying sampling interval and sampling start point for three simulated storm events. Source: Olive & Rieger (1988).

sampling the two largest storms produced reasonable results for the Maumee River it is not a recommended approach, especially in systems which are sediment supply-limited, as the full range of relationships between SSC and discharge may not be captured.

Table 3.3. The variability in load estimates for the Maumee River, Ohio, dependent on sampling strategy used. Load was estimated using flow integral method. Load was estimated using the flow integral method. Source: Yaksich & Verhoff, 1983.

Sampling strategy	Number of samples	Load, tonnes per day	Error, %
Daily (actual load)	365	3,000	-
Four times per month	48	2,073	± 40
Four flow events	48	3,133	± 13
Three flow events, without largest	36	1,939	± 19
Three flow events, with largest	36	3,074	± 13
Two flow events, with largest	24	3,440	± 13
High flow event	17	2,709	± 25

Fenn (1989) developed rating curves based on fixed interval sampling for six ablation seasons in the Glacier de Tsidjiore Nouve basin. The sampling interval was four hours for two of the seasons and one hour for the other four seasons. Rating curves developed from the four hour interval samples had noticeably lower R^2 values (Table 3.4). This may be an indicator of an inferior sampling strategy, perhaps caused by sampling at the same times each day and therefore sampling the same point in the daily cycle.

Table 3.4. Linear regression parameters for ln Q and ln SSC for the Glacier de Tsidjiore Nouve basin. n = number of observations, a = intercept, b = gradient. No value of a is given for 1985 as there is an error in the source Source: Fenn, 1989.

Season	Interval, hr	n	a	B	R^2
1977	4	557	0.97 ± 0.82	0.92 ± 0.13	0.25
1978	1	1440	-1.81 ± 0.18	1.29 ± 0.03	0.82
1981	1	2287	-1.16 ± 0.30	1.22 ± 0.05	0.54
1982	4	565	4.58 ± 0.52	0.32 ± 0.08	0.10
1984	1	332	-5.73 ± 0.92	1.85 ± 0.67	0.69
1985	1	519	-	0.92 ± 0.10	0.38
All	-	5700	-0.85 ± 0.15	1.15 ± 0.02	0.60

Thomas (1988) sub-sampled a data set of 4450 ten minute interval SSC (derived from turbidity) and Q pairs using four different sampling methods in order to establish the role of sampling technique in suspended sediment yield bias. The four methods were: random sampling – data points were sampled at random from the sample population; systematic sampling – samples were chosen at a fixed interval; flow-proportional – a sample after a fixed proportion of the water yield for the sample period had passed; and selection at list time (SALT) sampling (section 3.3.2.2). Each of the sampling methods was repeated 25 times and approximately 50 data points were sampled each time. The replicates were conducted to indicate the potential variability in yield estimates resulting from the samples selected. The random and stratified sampling methods are time-

proportional techniques and the associated rating curves exhibited lower gradient and intercepts than the discharge-proportional methods (flow proportional and SALT). The rating curves produced by each of the four methods for each sample set of data were used to calculate sediment yields for the data period, uncorrected and corrected (using the log-normal correction factor) (section 4.5.1.1) for back-transformation bias. The mean sediment yield calculated from the twenty-five SALT rating curves was the most accurate, but the flow-proportional method exhibited less variance. Variance of the estimates increased for all sampling methods when the log-normal correction factor was applied. The time-proportional methods under-predicted suspended sediment yield. A rating curve developed using all the data had a slope and intercept similar to those of the time-proportional methods, thus indicating that more data do not necessarily produce better estimates. Thomas (1988) also calculated three storm yields using the systematic and flow-proportional rating curves. The results were consistent with the yields calculated for the whole time period: the flow-proportional rating curves out-performed the systematic rating curves, and both produced better estimates for smaller storm events.

Walling *et al.* (1992) used a two year turbidity data set to assess the impact of sampling strategies on suspended sediment load estimates of the River Exe at Thorverton, Devon. Fifty simulated data sets were established (using different start dates and times) for weekly, fortnightly and four weekly intervals. The precision of the resultant load estimates were low: weekly sampling produced sediment load estimates (interpolation procedure) for the two year period from 20 to 130 × 10^3 t; fortnightly from 5 to 150 × 10^3 t; and four weekly from just above 0 to 155 × 10^3 t. Suspended load was increasingly under-estimated as sampling interval increased.

Al-Ansari *et al.* (1988) also investigated the effect of sampling strategy on load estimates but on the Euphrates, which is more transport- than sediment supply-limited and has a regulated flow regime. Daily data were sub-sampled to investigate the practicality of reducing the sampling interval to two, three or four samples per month. The results showed that four samples a month was preferable, but all the results were within 20% of the actual loads.

The superiority of storm sampling over fixed-interval sampling, especially in smaller catchments with flashier regimes, is clearly illustrated by a study of the River Creedy,

Devon (Walling, 1977a). Turbidity and discharge were monitored continuously, and subsequently a one hour sampling interval was identified to be adequate to define the two records. From this hourly record, weekly samples were extracted and a rating curve developed, but the resultant rating curve was found to be inadequate due to under-sampling of high flow events (Walling, 1977a).

Walling & Webb (1988) investigated the effect of using just regular weekly samples and a combination of regular weekly samples and storm samples on the suspended sediment loads of the Rivers Dart, Creedy and Exe, Devon. The data series were between two and ten years in length (Table 3.5) and consisted of hourly SSC and discharge values. The storm samples were divided into two groups defined by discharge and samples were taken randomly for each group, the numbers dependent upon the relative frequency of flows within each class. The regular sampling grossly under-estimated the total suspended sediment load: the estimated suspended load of the River Dart was only 5% of the actual load. The River Exe showed an improvement in accuracy and precision with the addition of the storm samples; the Dart and Creedy showed limited improvement. Walling & Webb (1988) also examined the difference in load estimates determined from the hourly data compared with the load estimated from a rating curve developed using all the data. The rating curve, even when bias-corrected, greatly under-estimated the load as determined from the hourly data (Table 3.5). Walling & Webb (1988) attributed the large difference between the actual loads and the estimated loads (Table 3.5) to under-sampling of storm events, scatter in the SSC-discharge relationship, seasonal patterns, difference between SSC and discharge response to storm events and sediment exhaustion.

Table 3.5. The actual load, load as determined form regular weekly samples, regular samples and storm samples, a rating curve and a rating curve corrected for bias for the Rivers Dart, Creedy and Exe. Source: Walling & Webb, 1988.

River	Area, km^2	Record length	Actual load, t	Regular, t	Regular & storm, t	Rating, t	Bias-corrected rating, t
Dart	46	1975-1985	24,499	897	1,570	862	2,145
Creedy	262	1972-1980	82,863	16,125	23,936	15,443	39,579
Exe	601	1978-1980	41,402	3,010	7,886	2,754	9,212

Sampling strategies recommended by authors are not always transferable between catchments (Johnson, 1992). The effect of sampling interval on sedigraphs varies between storms and catchments. Sample SSC and discharges series from two storms monitored at Trout Beck and one storm from Burnhope were selected. The sampling

interval for all three storms was 15 minutes. Sampling intervals of 30, 45 and 60 minutes were simulated and storm sedigraphs drawn (Figure 3.4) and storm yields errors calculated (the load calculated from the 15 minute interval series was taken as the actual load) (Table 3.6). The example SSC series from Trout Beck show that altering the sampling interval has a larger impact on peaked sedigraphs (Figure 3.4). This is because there is more chance of not sampling the peak SSCs and the sedigraph becomes much more subdued. Irregular sedigraphs, such as that for Burnhope (Figure 3.4), are smoothed by reducing the sampling interval (Figure 3.4). Therefore sampling at greater intervals obscures the pulsed nature of sediment flux. The storm loads errors were all less than 6.5% and were all under-estimates with the exception of the 45 minute interval data for the 1st April Trout Beck storm (Table 3.6). This suggests that increasing the sampling interval will have a limited effect on the annual suspended sediment load, especially as most sediment is transported during storms. However, the representativeness of the three selected storms is unknown.

Table 3.6. Actual loads for each storm, t, calculated from the 15 minute data and the percentage errors resulting from increasing the sampling interval for two storm events in Trout Beck and one in Burnhope.

Interval, minutes	Trout Beck 7th November	Trout Beck 1st April	Burnhope 25th October
15	**548.0**	**1719.7**	**2831.2**
30	-6.1	-1.4	-0.9
45	-2.9	0.7	-1.7
60	-5.2	-5.8	-2.1

3.3.2.4 Sampling issues and considerations

Foster *et al.* (1992) reported inadequate sampling is the most important source of errors in load estimations. The location of the sample station is of utmost importance in suspended sediment monitoring at the cross-section and river reach scale. The distribution of suspended sediment throughout the water column, both vertically and horizontally, can affect estimated suspended sediment loads. Therefore, it is imperative that the sampling location within the channel cross-section is representative (either it represents the average SSC in the cross-section or there is no variability throughout the cross-section), if accurate flux estimates are required. However, there is not always a systematic variation in the distribution of SSC at different discharges within a channel cross-section (Johnson, 1992). Sampling location should be within the middle of the channel to minimise bias introduced by the effect of friction with the bank on water flow and the proximity to a potential sediment source. The vertical position of the

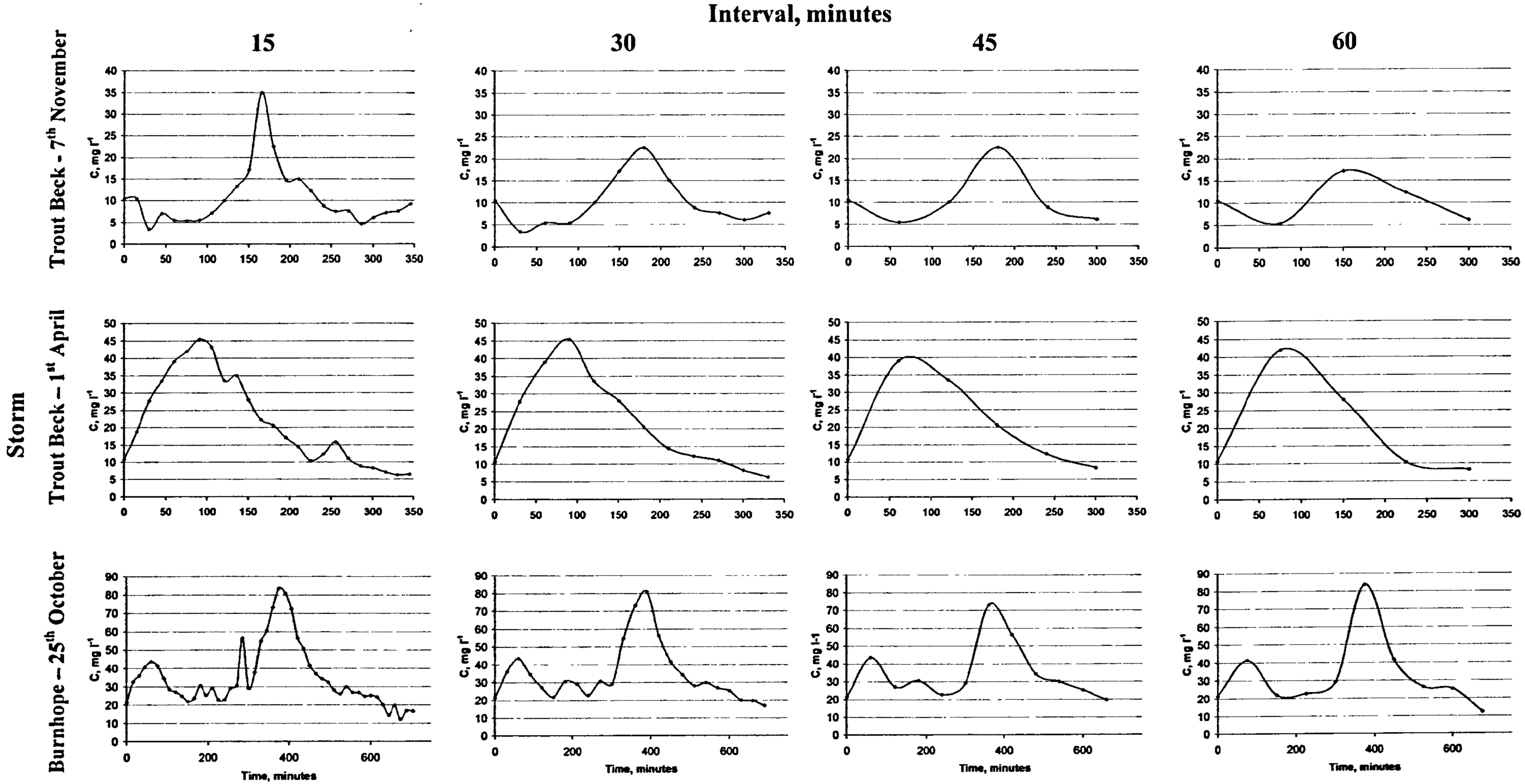

Figure 3.4. The effect of sampling interval on the sedigraph form of three storms.

sampling would ideally be 0.6 of the depth, from the channel bed (Phillips *et al.*, 2000) as it is the level of average velocity. However, if a permanent *in situ* sampler is being used (i.e. auto-sampler), then the intake should be set at a level low enough to sample the low flows. The easiest way to ensure a representative sample is taken is to chose a sampling site after a section of turbulent water, e.g. after a weir, as turbulence promotes mixing. However if a turbidity meter is being used turbulent water should be avoided as it can distort the relationship between turbidity and SSC. If there is doubt regarding the degree of mixing and representation of a sampling location, then a calibration study can be undertaken. This involves taking samples throughout the cross-section of the channel at a range of discharges and examining SSC for variation. If there is large variation, then a cross-sectional variation co-efficient can be derived by weighting the actual sample location SSC accordingly. The potential magnitude of error caused by cross-sectional variability is demonstrated by Horowitz *et al.* (1989), who found that SSC (determined by point samples) varies by up to 250% in the Arkansas River, Colorado. Carling (1984) illustrated that the distribution of suspended sediment is approximately equal throughout shallow rough bedded streams. However, narrow deep streams were shown to transport more suspended sediment closer to the bed with increasing discharge, as the efficiency of sediment transfer to the surface by turbulence is reduced.

The sampling location at the reach scale is also important. Within some rivers there may be stretches where overbank flow occurs more often. The reduction of flow velocities on the floodplain will cause sediment to fall out of suspension when the river overtops the bank. Therefore, the SSC may be significantly greater upstream of a reach where overbank flow often occurs than downstream of that section. Leeks (pers comm) observed this at two nested gauging sites with no tributary inputs between in Plynlimon, Mid-Wales.

Time is an important consideration within suspended sediment studies, in terms of not only the temporal variation in suspended sediment dynamics but also sampling considerations. First, it is key that SSC data are matched up correctly with discharge data. Olive & Rieger (1988) noted a 12% change in load when the SSC series was offset by ten minutes. Second, intervals between samples, especially storm samples, should be set to maximise the storm coverage at as high a resolution as possible. Third, the time period over which the suspended sediment samples are taken should be long enough to allow the full range of SSC-discharge relations to be captured.

3.4 Chapter summary

On the basis of this review auto-samplers, grab samplers and time-integrated samplers were chosen to sample suspended sediment within this study (Figure 3.5). Auto-samplers were chosen because of the logistics of being on site, especially given the upland nature of the study areas, to take samples and their programmability, i.e. they can be used to take fixed-interval samples and be triggered by storm events. Gulp samplers were selected to take spatial sample sets, as insufficient auto-samplers were available, and to augment samples obtained by the auto-sampler. Time-integrated samplers were deployed to obtain bulk samples of sediment for analysis. Turbidity was not selected given the variable particle sizes and densities of mineral and organic sediment and the dark water colour which is characteristic of peatland catchments.

The sampling regimes chosen were: storm, fixed-interval, spatial, continuous and arbitrary (Figure 3.5). Storm sampling was the primary sampling regime associated with the auto-sampler, although some fixed-interval samples were also taken at some sites. The gulp samplers were operated under arbitrary and spatial sampling regimes. The arbitrary samples were taken if the river was in flood and the auto-sampler was not activated to augment the auto-sampler record and the spatial samples to investigate the spatial variation in SSC within the channel network. The time-integrated mass samplers, by their nature, were operated under a continuous regime and were spatially distributed throughout the channel network. The aim of the above explained sampling approach was to characterise suspended sediment through time and space within the catchments and to allow properties other than quantity, to be examined.

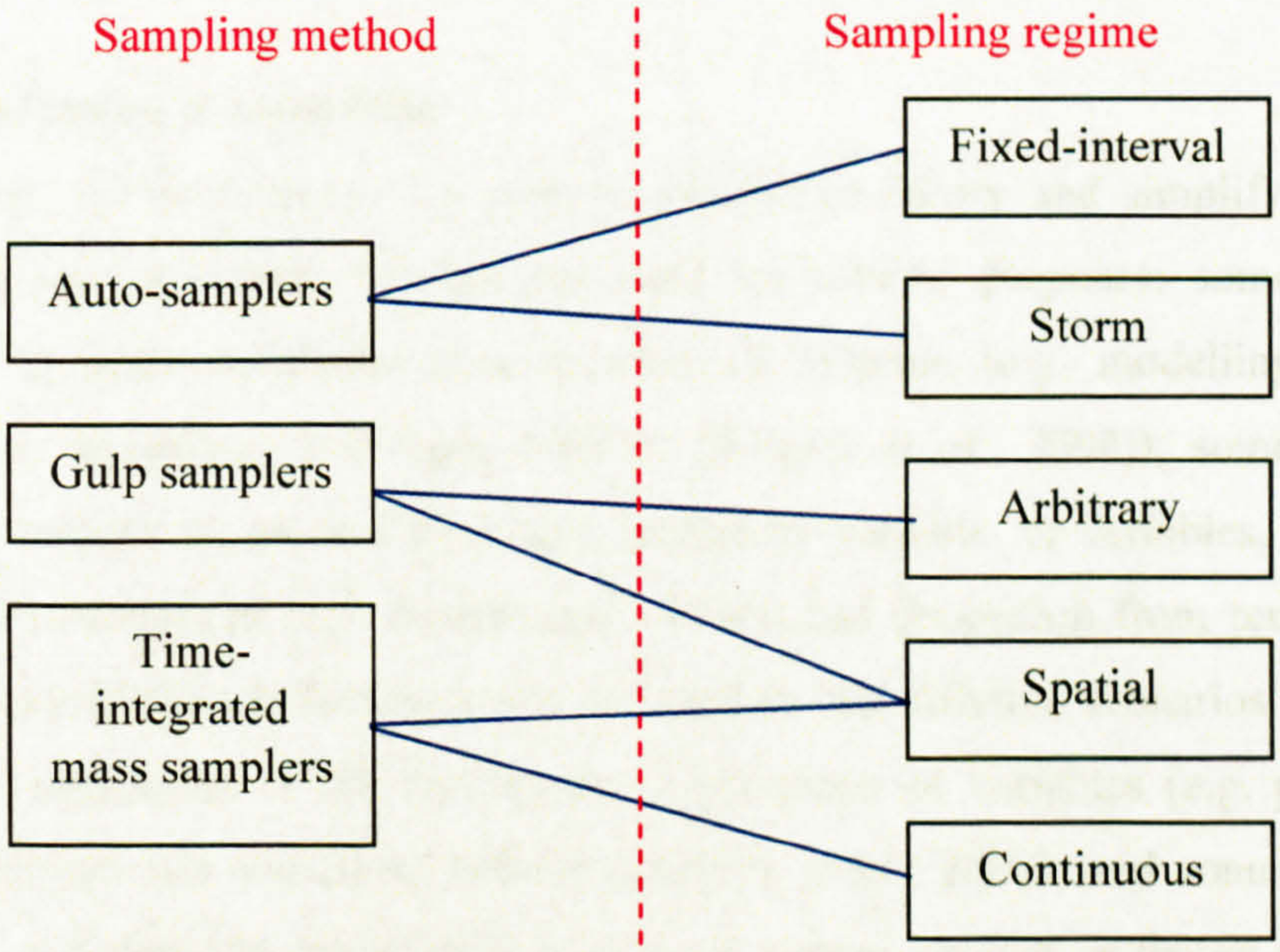

Figure 3.5. Sampling methods and associated sampling regimes selected for this study.

Chapter Four: SUSPENDED SEDIMENT MODELLING

4.1 Overview

This chapter outlines methods of modelling suspended sediment concentration from discharge. It begins with a general introduction to modelling (excluding hardware models) including its role, advantages and limitations. The types of model applicable to suspended sediment studies are then outlined. Then specific model types (rating curves, generalised linear models, time series analysis, artificial neural networks and a hydrograph partitioning method) are described, including application procedures, advantages, disadvantages and examples from the literature. Load estimation techniques, which are applied to suspended sediment data series, are then reviewed and assessed. While this is primarily a review of suspended sediment modelling methods, it helps define suitable methods for modelling suspended sediment flux in the British uplands (objective 2).

4.2 Introduction to modelling

Models are representations of a system, process or theory and simplify the physical structures and processes. Models are used for several purposes: some models are designed to replicate phenomena in physical systems (e.g. modelling pore water pressure to determine river bank stability (Rinaldi *et al.*, 2004)); some are used to predict a variable or process from an explanatory variable, or variables, to reduce the need for measurement (e.g. determining erosion and deposition from remotely sensed data (Pickup & Marks, 2000)); some are used to run different scenarios dependent on the initial conditions or the importance of processes or variables (e.g. predictions of climate change and associated effects (Doherty *et al.*, 2000); and some illustrate the processes and variables involved in a physical system, process or theory (e.g. sediment

budgets (Holliday, 2003)). The complexity of models is diverse: some are as basic as a flow chart, outlining the main components of a system, e.g. the fate of sediment once it has entered a channel (Figure 4.1), while others are extremely complex and require powerful computers, e.g. climate prediction models.

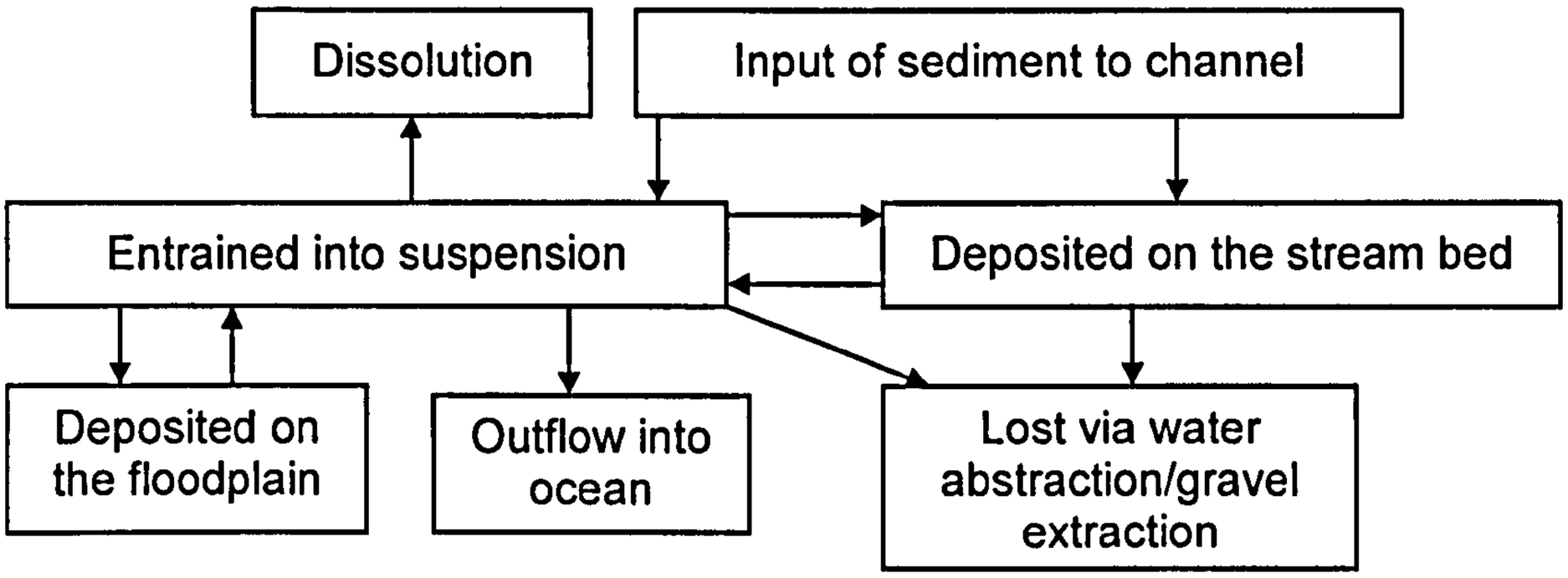

Figure 4.1. Flow chart model of the fate of sediment once it has entered the channel.

The main disadvantage, but also an advantage, of models is that it is not possible to completely capture systems or processes within the physical environment, i.e. models are always simplifications of the real world. For example, many suspended sediment models (such as rating curves and time series models) attempt to relate discharge to SSC with no reference to the mechanical processes involved in transporting sediment (e.g. Asselman, 2000; Gurnell & Fenn, 1984). Also, models are only as good as the data and assumptions used to construct them. For example, most models will only produce results of value at the same or lower resolution as the input data; if inaccurate data are input into a model inaccurate results will be output; and if the form of the model is not optimal, for example, attempting to predict suspended sediment concentration stage as opposed to discharge, then the model outcomes will be poor. The main advantage of models over laboratory and field investigations is that individual variables and processes can be isolated and varied, and once set up models are economical in terms of time and cost.

Models rarely give 'the answer' and therefore it is beneficial to view models as instruments designed to assess and evaluate the relative importance of different processes and variables and to enable 'what if' scenarios to be run. Climate prediction models are a good example: starting conditions and variables can be changed to evaluate what may happen and which variables and processes are most influential (e.g. Anon, 2004). Models which produce incorrect results are often just as useful, as they

may uncover an unexpected or unrealised process or variable, provoke deeper thought or cause the case study to be viewed from a different perspective.

Model verification is an important component of model building, as it allows some qualification and/or quantification of the model performance. Verification procedures are specific to the type of model. In the simplest form verification may involve examining a flow chart (e.g. Figure 4.1) and checking no components are missing while others require numerical or graphical verification. Numerical verification commonly involves the calculation of a figure of merit which supposedly encapsulates the discrepancy between the model output and the observed data, such figures as the determination coefficient (R^2) or root mean square error (RMSE). Graphical verification involves visually checking the model outputs with observed data and/or examining diagnostic plots to identify any anomalous data which may be affecting the model.

4.3 Types of model

There are various types of model and various ways in which models are classified. Models are either deterministic, stochastic, or contain elements of both. Deterministic models are those which give the same output every time, given a set of inputs and conditions. Alternatively, stochastic models contain a stochastic or random component and therefore if the model were run several times with a given set of inputs, the outputs would be different. The following section introduces black box, process, mass balance, and conceptual models relevant to suspended sediment studies. Black box and mass balance models are deterministic, although may include a stochastic component. Process-based models may be deterministic, stochastic, or contain both deterministic and stochastic components.

Black box models involve the input of data and conversion to output data by some mechanism, often by a data transformation or fitting technique e.g. regression. Therefore, no knowledge regarding the physical processes within the system is gained or assumed. However, in some scenarios, it is possible to gain some understanding by examining the effect of changing one variable while holding other variables constant. Process models are those which include representations of the processes within a system. Mass balance models are often process-based, but are differentiated from process models as the various components (inputs, outputs, flows and storage) of the model balance. Finally, conceptual models are those which do not involve any

quantification but illustrate the linkages between different components within a system and the various pathways, lack process detail and are often theoretical. Conceptual models often precede the development of the other types of model.

With reference to SSC-discharge rating relations, black box modelling is the most common, specifically rating curves: discharge is the input (Q), SSC is the output and within the black box power function relates Q to SSC (Figure 4.2).

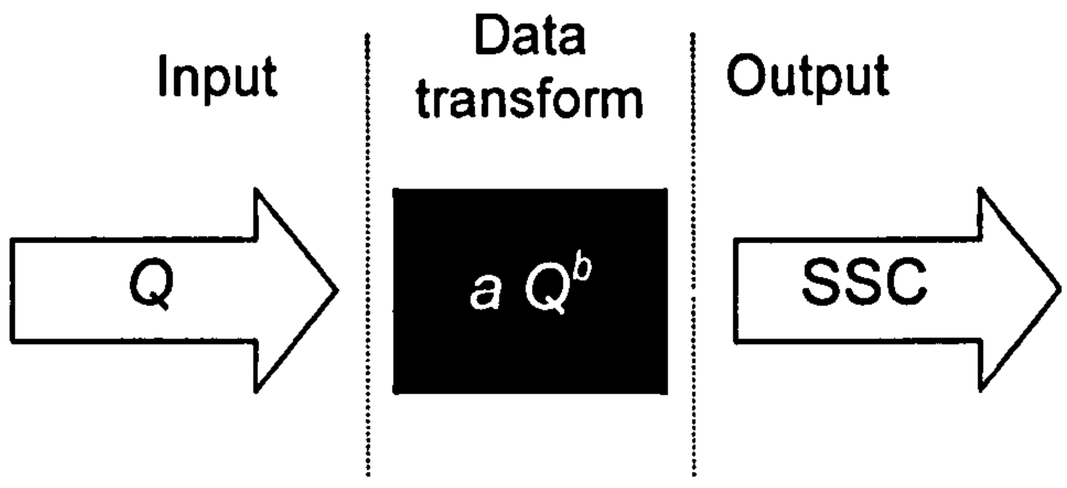

Figure 4.2. Schematic of a black box model for SSC and Q.

Although rating curves are a black box approach, some incorporate process knowledge. For example Van Sickle & Beschta (1983) incorporated a sediment supply function and many authors divide data into rising limb and falling limb (e.g. Ferguson, 1986) or seasons (e.g. Walling, 1977a) and produce a regression equation for each. Such adaptations to the basic black box rating curve approach could be described as 'process-orientated', but are not conventional process models.

It would be extremely complex to produce a process model of SSC, given the numerous variables which influence SSC and the complex interactions between them. An example related to SSC of a process model is one which models the suspension of particles from a river bed developed by Kurashige (1996). Within the model Kurashige (1996) used the diameter of the 65th percentile of the bed sediment distribution (D_{65}), density of the grains (ρ), density of the river water (σ), acceleration due to gravity (g), tractive force on the river bed (τ), and equivalent roughness height of the bed (k_s) to calculate the maximum grain size lifted from the bed:

$$d_{\max} = 0.834 \frac{\tau}{(\sigma - \rho)\, g} \left\{ \ln\left(\frac{10.4\, D_{65}}{k_s} + 1 \right) \right\}^2 . \qquad (4.1)$$

It was the knowledge of the processes involved in lifting a particle into suspension and the associated physical laws that enabled a process model to be constructed. The outcome of this grain lifting model was then used to estimate SSCs of Hiyamizusawa Brook, Japan (a small, sand bedded, headwater catchment).

An example of a mass balance model relating to suspended sediment is a catchment sediment budget. Sediment budgets allow insight into the components within a system and can be useful management tools. Holliday (2003) developed a sediment budget for Burnhope reservoir, Northern Pennines (Figure 4.3). The inputs of sediment are shoreline erosion and tributaries, the stores are shoreline storage and the reservoir, and the output of sediment in the reservoir outflow. The dominant sources of sediment influx are the tributaries (548 t) and the major store of sediment is the reservoir (592 t).

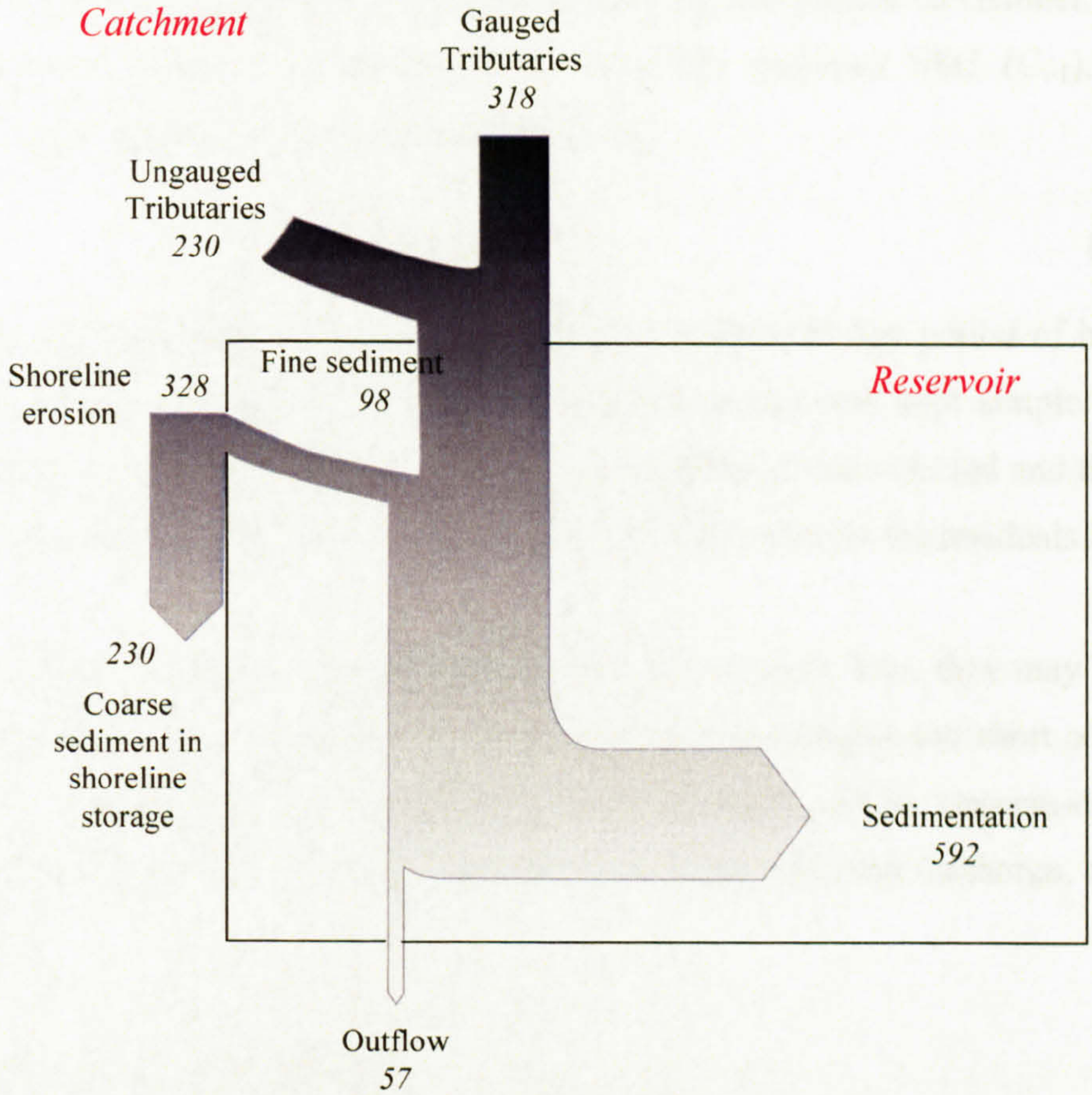

Figure 4.3. A mass balance model in the form of a sediment budget for Burnhope reservoir. Source: Holliday, 2003.

A conceptual model for SSC within a river would outline the various sources and sinks of suspended sediment (Figure 1.1). This can be useful as it outlines the possible influences on suspended sediment concentration, including those which are difficult to

quantify (e.g. quantity of sediment derived from precipitation within the channel). For example, the dominant sources of sediment in an urbanised area may be anthropogenic inputs, entrainment from the bed and sediment input from upstream and the dominant sinks of sediment are likely to be deposition on the channel bed and output to the downstream channel. In contrast the dominant sediment sources in upland channels are likely to be hillslope supply, tributaries, gully inputs and entrainment from banks, the bed and floodplain and the dominant sinks of sediment are likely to be deposition on the bed and floodplains and sediment output to the downstream reach.

An example of a suspended sediment model with a stochastic component is a transfer function (a form of time series analysis). Transfer functions contain an underlying deterministic trend and a stochastic or random component. Such models have been used by Gurnell & Fenn (1984) and Lemke (1991) among others. Fenn (1989) developed a transfer function model for the Tsidjiore Nouve Glacier proglacial channel, Switzerland. Instantaneous SSC was estimated (C_i) from the previous SSC (C_{i-1}), the current discharges (Q_i) and the future discharge (Q_{i+1}):

$$C_i = 1.03\, C_{i-1}\, (Q_{i+1} / Q_i)^{1.9027}. \qquad (4.2)$$

The model was developed from an arbitrarily selected 25 day period of hourly spaced SSC and discharge series. The transfer function model was kept simple: the constant was fixed at zero, an equation with only one coefficient was selected and the noise term was dropped when predicting values as the expected value of the residuals is zero.

This section has given examples of different model types, how they may be applied to studies of suspended sediment dynamics and their advantages and short comings. From this it is evident that black box models, some of which may be 'process-orientated' are most suitable for establishing a relationship between SSC and discharge, as required in this study.

4.4 Model selection criteria

When selecting a model a key factor is the purpose of the investigation, in terms of scale (both temporal and spatial) and what is being investigated (load or dynamics). For example a suspended sediment model may be required to examine and understand sediment dynamics, or to give an accurate load estimate for a specified period, or produce a more transferable load estimate model (in terms of time and possibly space).

In order to select the most appropriate model it is common to develop more than one model and make a judgement on which is the 'best' model. To give guidance selection criteria are often established. For example, Cox *et al.* (in review) outlined seven criteria for choosing a model:

(1) **Summary**: Should capture the main features/behaviour in the system which is relevant to the concerns of the investigation. In statistical terms a model should provide some measure of average components and a measure of variability.

(2) **Physical basis:** Should ideally be based on physical principles.

(3) **Physical plausibility:** If it is not possible to have a physically based model then it should at least be physically plausible.

(4) **Goodness of fit:** The model should predict close to observations, but this can be problematic. For example a closer fit may be achieved by increasing model complexity but this may not increase scientific insight. Also an improved fit may cause over-fitting, i.e. the relationship becomes too specific to the data it was derived from. Assessing goodness of fit is generally done by examining single numbers, such as R^2, but residual plots should also be examined.

(5) **Simplicity:** Should be simple enough to understand but complex enough to gain insight into the system characteristics.

(6) **Computability:** Facilities to develop the model in the restricted time framework are required.

(7) **Comparability:** The potential to compare the outcomes of models with other examples in the literature.

Many studies rely on a measure of fit to indicate the 'best' model (Table 4.1). The most common measure is R^2. However, it is bad practice to rely on one numerical indicator to evaluate model fit as it may obscure problems with the model fit or assess the model in a way which is not reflective of what the model is being developed for.

4.5 Models applicable to suspended sediment dynamics

Suspended sediment studies generally require a model as the majority of monitoring techniques are discontinuous and continuous methods are problematic in some catchments. Rating curves and time series analysis are the predominant methods of suspended sediment modelling within the literature. There is some limited material on the application of generalised linear models (GLM) to derive rating curves, artificial neural networks and hydrograph partitioning techniques. The type and level of

Table 4.1. Examples of measures of model fit used in suspended sediment studies.

Measure	Equation	Notes	Example reference
R^2	$R^2 = \left[\frac{\sum (Q-\overline{Q})(C-\overline{C})}{\sqrt{\left[\sum (Q-\overline{Q})^2 \sum (C-\overline{C})^2\right]}}\right]^2$	Square of the correlation between two variables: indicates the variability in C which is 'explained' by Q.	Evans & Burt (1998)
Root mean square error (RMSE)	$\left[\frac{1}{n}\sum_{i=1}^{n}\left(\hat{C}-C\right)^2\right]^{0.5}$	Positive square root of the mean square error which is the average of the squared residuals. Assumes that larger prediction errors are of more importance than smaller errors.	Dolan *et al.* (1981)
Akaike's Information Criterion (AIC)	$\mathrm{AIC} = (n \ln [2\pi / n] + n + 2) + n \ln R + 2m$	Penalises for increased numbers of parameters. If too many observations the residual sum of squares predominates over the number of model parameters.	Asselman (2000)
Mean absolute percentage error (MAPE)	$\frac{1}{n}\sum_{i=1}^{n}\left(\frac{\lvert C-\hat{C}\rvert}{C}\right)100$	Gives the mean error in absolute terms so that under- and over-predictions do not cancel each other out.	Fenn (1989)
Sample-error sum of squares	$SS_E = \sum_{i=1}^{n}\left(C-\hat{C}\right)^2$	Measures fit summing the squared differences between observed and fitted concentrations.	Crawford (1991)
Prediction sum of squares		Involves the deletion of each observation in turn, a rating developed each time, the concentration predicted and the differences between each observation and predicted value squared and summed.	Crawford (1991)

Number of observations (n), the number of model parameters (m) and the residual sum of squares (R), discharge (Q), mean discharge ($\overline{Q}$), mean SSC ($\overline{C}$), predicted SSC ($\hat{C}$), actual SSC (C).

complexity of the models used indicate the nature of the problem under examination. Some studies simply aim to construct a relationship between discharge and SSC (e.g. Asselman, 2000), whereas others attempt to explain the variability in the discharge-SSC relationship by examining other variables such as temperature and rainfall (e.g. Hodson & Ferguson, 1999). To some degree this depends on whether the aim is to quantify the stream suspended sediment load or to make inferences regarding the nature of sediment dynamics within the system. The main types of suspended sediment models are discussed below, with various adaptations, considerations and reference to specific examples. All the approaches are inter-linked as all develop SSC from discharge. However, they are discussed in discrete sections defined by the methodologies: rating curves, rating curves derived by GLMs, time series analysis, artificial neural networks and hydrograph partitioning.

4.5.1 Rating curves

The concept behind rating curves is to establish a relationship between SSC and discharge at a given location. This relationship is used to examine dynamics (e.g. Asselman, 2000), establish loads by combining it with a quasi-continuous discharge record (e.g. Evans & Warburton, in press) or to indicate change in the environment over time (e.g. Marron, 1989) or space (e.g. Loughran, 1976).

The development of a rating curve begins with a plot of SSC against Q. Assuming there is a monotonic relationship (i.e. there is no turning point within the data trend), a smooth curve is fitted to remove any idiosyncrasies in the data and to simplify the relationship. There are various means of fitting the curve. Most rating curves have a power function form (e.g. Walling, 1977a & Asselman, 2000) with concentration (C) being related to discharge (Q) by two empirically derived parameters (a and b):

$$C = a\,Q^{b}. \tag{4.3}$$

Power functions are a good choice for suspended sediment rating curves as the limiting form is correct: it passes though the origin which makes physical sense (i.e. if $Q = 0$ then SSC = 0). In comparison, if a linear function was fitted the intercept would most likely be positive or negative which is physically unlikely.

The two general approaches used in the rating curve literature for the derivation of a and b are: a non-linear least squares method (e.g. Crawford, 1991) or through imposing

linearity between SSC and Q by transformation and performing ordinary least squares (OLS) regression (e.g. Jansson, 1985). The predominant reasons for transforming the variables are to make the scatter of data points more linear and more homoscedastic, as these are important assumptions of linear regression. Thus equation 4.3 can be transformed to:

$$\ln C = \ln a + b \,.\, \ln \mathrm{Q}. \qquad (4.4)$$

Some studies use the $\log_{10}$ transformation while others use the natural logarithm, which is denoted as ln or $\log_e$. The choice does not affect the outcome of the model. The natural logarithm has been chosen in this study on the basis that routines in the statistical package used are based on ln and equations based on the inverse of natural logarithms (exponential) are 'cleaner' than those based on the inverse of $\log_{10}$.

There are several assumptions of linear regression which should be satisfied to ensure a 'good' model. These include: serially uncorrelated randomly distributed residuals with a zero mean, constant variance (homoscedasticity) and normal distribution and a linear relationship between the variables (most important) (Poole and O'Farrell, 1971). However, linear regression is fairly robust and therefore if the assumptions are not quite met (i.e. the error distribution is not quite normal) the effect is often negligible.

Deriving a and b iteratively for a non-linear relationship, as compared with OLS after linearity has been forced by transformation, is beneficial as bias correction is not necessary (as the errors are additive, not multiplicative). However, there are several problems with deriving a and b iteratively (Crawford, 1991). First, solutions for a and b do not always converge. Second, errors are assumed to be independent, but often are not. Third, errors are assumed to be identically and normally distributed but are often highly skewed and not identically distributed: e.g. Jansson (1985) noted that variance of residuals generally increases with increasing discharge.

Crawford (1991) compared four models: log-transformed OLS regression corrected for bias by smearing (SM), log-transformed OLS regression corrected for bias by the Bradu-Mundlak estimator (BME), non-linear least squares by deriving a and b iteratively and weighted non-linear least squares by deriving a and b iteratively, using the inverse of the variance of individual observations as weights. (Table 4.2). Crawford (1991) concluded that the estimates of a and b were more precise when determined by

bias-corrected log-transformed OLS regression and the accuracies of the bias-corrected log-transformed OLS regression and weighted non-linear least squares methods were higher than the accuracy of the non-linear least squares method. With respect to sediment loads the bias-corrected log-transformed OLS regression models gave the most accurate and precise estimates and the accuracy of the weighted non-linear least squares method was comparable but less precise. The assessment criteria used were the sample-error sum of squares and prediction error sum of squares.

Table 4.2. The rating equations for the Big Blue River and Wabash River derived by different methods. Source: Crawford, 1991.

Model	Big Blue River	Wabash River
OLS with SM correction	$C = 0.974\,Q^{1.715}$	$C = 0.405\,Q^{1.583}$
OLS with BME correction	$C = 1.014\,Q^{1.715}$	$C = 0.410\,Q^{1.583}$
Non-linear least squares	$C = 23.341\,Q^{1.122}$	$C = 10.219\,Q^{1.110}$
Weighted non-linear least squares	$C = 1.056\,Q^{1.684}$	$C = 0.327\,Q^{1.628}$

Other means of curve fitting are moving average, locally-weighted scatter plot smooth (LOWESS) (e.g. Krishnaswamy *et al.*, 2001) and local polynomial. These methods allow different relationships between SSC and discharge to be established throughout the data set. These methods are advantageous as the form of the data is followed more closely; however, the curve cannot be extrapolated or easily compared with other studies as they are not summarised by a few parameters. Krishnaswamy *et al.* (2001) found that a LOWESS model gave consistently lower sediment yields that those based on the standard rating curve model, attributed to discharge values in the record which exceeded those in the model (when this occurred the concentrations were assumed to be the highest recorded concentration). However, the LOWESS model predicted more accurately within the sampled range of the data range.

4.5.1.1 Back-transformation bias

A fundamental problem with rating curves for which the variables are logarithmically transformed is back-transformation bias. This bias arises because of the difference between log space and original data space: log space is multiplicative and the original data space is additive. This can be demonstrated by a simple example (Table 4.3). The mean of the set of observations is 4.0 and ln 4.0 is 1.4, the mean of ln X is 1.3 and the back-transform is 3.7: this is 0.3 lower than the mean of the original data (Table 4.3), i.e. the mean of X does not equal the exponential of the mean of ln X.

Table 4.3. A simple illustration of the back-transformation problem.

Observation	X	ln X
1	2.0	0.7
2	3.0	1.1
3	4.0	1.4
4	5.0	1.6
5	6.0	1.8
Mean	4.0	1.3
Log transform/back-transform	1.4	3.7

The mean of any set of observations will always be equal or greater than the back-transform of the mean of the log transformations for the same set of observations. Therefore, when applied to rating curves fitted by OLS regression the means of ln C are always under-estimates of the log transformed mean of C at any given value of Q. This is because, by definition, the sum of the residuals is equal to zero. However, when the data are back-transformed the sum of the back-transformed residuals is always positive, as demonstrated above, (unless the regression line is a perfect fit) given the multiplicative nature of log transformed data (Singh & Durgunglu, 1989). The effect back-transformation bias has on rating curves can be substantial. For example, suppose for a given Q the linear regression trend line bisected the difference between two ln C points of 1.6 and 3.9 (corresponding to 5 and 50 mg/l respectively). The mean and point of optimal dissection is 27.5 mg l^{-1}. But if the data is log transformed then the mean is 15.8 mg l^{-1}, a substantial 11.7 mg l^{-1} or 43% under-estimation. Back-transformation bias is mostly a problem for a and b as the effect of multiplicative bias is physically justifiable for the error term as C generally exhibits more variation at higher values of Q.

Three main correction factors have been developed to correct back-transformation bias: the log-normal correction factor (LNCF), smearing (SM) and the Bradu-Mundlak estimator (BME). The LNCF is a parametric technique and therefore the errors are assumed to be normally distributed. It multiplies all the predicted values by a measure of the average expected under-estimation of the predictive values due to the difference in raw data and logarithmically transformed data space. The LNCF can overcompensate for bias if sample size is large (i.e. greater than 30) or if the standard deviation is small (i.e. less than 0.5) (Helsel & Hirsch, 1992). LNCF is based on the standard error of the estimate of C (s),

$$\text{LNCF} = \exp(s^2/2). \tag{4.5}$$

SM is a non-parametric technique; i.e. it can be applied regardless of the distribution of the errors although the errors should be independent. SM aims to estimate the expected response on the non-transformed scale after fitting a linear regression on a transformed scale by distributing (or smearing) excess in one observations residual to other observations (Duan, 1983). SM is based on the difference between ln C and estimated ln C,

$$\mathrm{SM} = \frac{1}{n}\sum_{i=1}^{n} \exp^{\ln C_i - \ln \hat{C}_i} \tag{4.6}$$

SM avoids the overcompensation of LNCF and has been implemented in geographical literature (e.g. Horowitz, 2000) but to a lesser extent than the LNCF. Essentially both SM and the LNCF increase the intercept but do not change the gradient of the trend line. The BME is a minimum variance unbiased estimator (Cohn *et al.*, 1989 & 1992) and is a parametric technique. A unique correction is generated for each value of the explanatory variable based on the magnitude of potential under-estimation of each prediction given the difference in raw data space and logarithmically transformed data space. BME is based on the degrees of freedom in the regression equation (m), an estimate of variability (V) and the standard error (s),

$$\mathrm{BME} = \left(\frac{m+1}{2\,m}\right)\left(\left[1-V\right]s^2\right), \tag{4.7}$$

$$V = \frac{1}{N} + \left[\frac{\left(\ln Q - \ln \overline{Q}\right)^2}{\sum_{i=1}^{N}\left(\ln Q - \ln \overline{Q}\right)^2}\right]. \tag{4.7a}$$

The BME is least common in the literature. It BME performs marginally better than SM if the residuals are log-normally distributed (Helsel & Hirsch, 1992). Although Cohn *et al.* (1989) demonstrated that the BME was superior to both uncorrected data and LNCF corrected data it is rarely used. This is due to the more complex procedure compared with both SM and the LNCF and its lack of usage and thus lack of comparative studies in the literature.

Several studies have applied the various bias correction techniques with variable success. Ferguson (1986) used hourly turbidity data from Foster *et al.* (1985) to

illustrate the value of the LNCF. The data used were at hourly intervals for a 52 week period and the true load was 9.85 tonnes. The uncorrected load estimation from the rating curve was much lower than the actual load and the LNCF corrected estimation was a slight under-estimation (Table 4.4). Jansson (1985) also found the LNCF resulted in under-estimates. Ferguson (1986) applied the LNCF to seven field data sets and nine computer-simulated data sets. The LNCF gave results within 3% of the true load for the nine simulated data sets and between 91% and 104% for the field studies. Singh & Durgunoglu (1989) compared three estimates of suspended sediment load: uncorrected log-transformed linear regression, LNCF corrected log-transformed linear regression and non-linear regression (Table 4.4). Singh & Durgunoglu (1989) regard the non-linear regression estimates as the best estimation method based on lower sum of squares of untransformed residuals: however, no comparison with actual load was made. Koch & Smillie (1986) compared uncorrected, LNCF corrected and SM corrected load estimates of the Yampa River and Little Snake River, north west Colorado. No actual load estimates were available for comparison but both corrected values were in excess of the uncorrected loads, especially the SM correction. The SM corrected load was considered the most sound as the residuals were not normally distributed so the LNCF was deemed unsuitable.

Table 4.4. Examples of annual suspended sediment loads, t yr^{-1}, as estimated by actual data, non-linear regression and linear regression uncorrected for bias and corrected by LNCF and SM.

Reference	River	Actual	Non-linear	Correction factor		
				None	LNCF	SM
Ferguson (1986)		9.85		5.62	8.97	
Koch & Smillie (1986)	Yampa			4.14×10^5	5.76×10^5	7.32×10^5
	Little Snake			1.37×10^6	1.90×10^6	3.42×10^6
Singh & Durgunoglu (1989)	Salamonie		8.09×10^2	4.25×10^2	6.22×10^2	
	Elkhorn Creek		6.08×10^2	3.45×10^2	4.68×10^2	

There has been some resistance to the application of the LNCF. Miller (1988) accepted that it was justified when calculating suspended sediment yield. But when estimating SSC for a given discharge Miller (1988) argued the uncorrected value of SSC was more representative. This was based on reasoning that the uncorrected back-transformation of SSC at a given discharge represents the median SSC whereas the bias-corrected SSC gives the mean and the median is generally taken as the more representative indicator of

skewed data. Ferguson (1988) agreed that the median SSC would be a more 'typical' SSC but determinations of SSC are likely to be in order to check that a threshold value is not being exceeded and therefore the mean should be used.

Walling & Webb (1988) also questioned the application of the LNCF when estimating annual load of the River Creedy using a suite of rating curves developed from log C and log Q for two consecutive years. Prior to the application of the LNCF only one out of the eight load estimates was an under-estimate and therefore the LNCF resulted in a larger over-estimation. Walling (1977a) attributed the over-estimation to positive hysteresis which characterised individual storm events. As the rising limb of an event is of much shorter duration but generally has a much higher SSC than the falling limb, the regression line will be higher than representative of the system, thus building in a 'correction' for back-transformation bias. However, most studies develop separate regressions for the rising and falling limbs if there is a noteworthy difference in the form of the relationship.

4.5.1.2 Inter-annual differences in model form

Suspended sediment loads are often calculated for just one year. This could produce misleading load estimates as suspended sediment load can be highly variable between years (section 2.7.4). Also, calculating suspended sediment load from a rating curve developed with data from a different time period can produce highly inaccurate yield estimates. For example, Fenn *et al.* (1985) applied sediment rating curves to hourly SSC samples from a proglacial stream: Tsidjiore Nouve, Switzerland. The principal aim of the investigation was to evaluate the applicability of rating curves to proglacial streams. The main outcomes were that rating curves can not be applied to time periods with different conditions but 'global rating curves' calibrated from a time period during which a range of basic SSC-discharge relationships occurred can produce 'acceptable' suspended sediment load predictions. Fenn (1989) built on this by developing seven rating curves, six from individual years and one using the data from all years. Fenn (1989) clearly illustrates the annual differences between rating curve form (Table 4.5) and consequently confirms that a rating curve from one year should not be applied to another year, given the different hydrological and meteorological conditions and geomorphological response. Fenn (1989) calculated the sediment load for the six ablation seasons from each of the rating curves. The calculated suspended sediment loads ranged from 34% to 239% of the actual loads. The rating curve developed from

the data from all years performed better overall than any of the year-specific rating curves and ranged from 64% to 200% of actual loads. This is because the longer sampling period incorporates the majority of SSC-discharge relationship forms. Fenn (1989) quantified the rating curves' performance by calculating the mean absolute percentage error (MAPE, see Table 4.1). The rating curve model with the lowest MAPE was developed from the 1982 data (Table 4.5). However, the MAPE's of the other models based on data from one season indicate that a rating curve based on one season should not be applied to other seasons (Table 4.5).

Table 4.5. The MAPE of each annual rating curve for Tsidjiore Nouve when applied to all years of data. Source: Fenn, 1989.

Year	Model	MAPE
1977	$\ln C = 0.9731 + 0.9220 \ln Q$	81.2
1978	$\ln C = -1.8143 + 1.2851 \ln Q$	39.4
1981	$\ln C = -1.6150 + 1.2223 \ln Q$	60.6
1982	$\ln C = 4.5833 + 0.3184 \ln Q$	35.4
1984	$\ln C = -5.7349 + 1.8506 \ln Q$	46.2
1985	$\ln C = -0.6801 + 0.9232 \ln Q$	49.2
All	$\ln C = -0.8490 + 1.1470 \ln Q$	38.0

4.5.1.3 Multiple rating curves

The scatter about sediment rating curves is generally attributed to changes in sediment supply, which in turn, is a result of variable hydrological, meteorological and geomorphological conditions. For example, SSC at a given discharge on the rising limb of a flood event is commonly higher than SSC at the same discharge on the falling limb due to sediment depletion. The same principle occurs on a seasonal time scale: floods which occur early in the hydrological year generally have higher SSCs than floods of the same magnitude that occur later in the hydrological year (Beschta, 1978 and Asselman, 1999). Several authors have attempted to reduce the scatter by sub-dividing the data according to hydrological and/or meteorological conditions. The most common data divisions are by limb (e.g. Evans & Burt, 1998) and season (e.g. Holliday, 2003). Furthermore, some authors divided the data by discharge-generating conditions e.g. storm flow and diurnal flow (e.g. Richards, 1984).

Numerous studies have examined season as an influence on SSC. For example, research by Walling (1974) on a small catchment near Exeter showed the benefit of dividing the data into summer and winter. The scatter plot of SSC as a function of Q illustrated that season had a strong influence and the summer rating curve plotted above the winter

rating curve. Walling (1974) attributed the heightened summer rating curve to more available sediment during the summer due to dry and dusty surface conditions, coupled with the high erosive powers of intense convectional rainfall and higher baseflows and sediment exhaustion effects during the winter.

Walling (1977a) examined the effect developing separate rating curves from data sub-sets as defined by limb and season on load estimates for the River Creedy, Devon (Table 4.6). Five estimates of load were made for two years: the continuous record (actual load), a single rating curve, seasonal rating curves, rising/falling rating curves and rising/falling seasonal rating curves (Table 4.6). Splitting the data into rising limb and falling limb produced the most accurate estimates which is contrary to the findings of Walling (1974). This apparent contradiction could be the result of different catchment characteristics or more 'standard' summer and winter weather in the study year of Walling (1974).

Table 4.6. Load estimations for the River Creedy, Devon. Source: Walling, 1977a.

Method	Suspended sediment load, tonnes		Error, %	
	1972-1973	1973-1974	1972-1973	1973-1974
Continuous	7,412.7	20,577.4	-	-
Single	9,429.7	33,648.2	+27.2	+63.5
Summer/winter	8,533.9	33,138.5	+15.1	+61.0
Rising/falling	7,708.6	26,898.6	+4.0	+30.7
Summer/winter & rising/falling	7,100.7	26,895.4	-4.2	+30.7

Holliday (2003) examined the effect of season on suspended sediment in Burnhope Burn, Northern Pennines, by sub-dividing the data into spring, summer, autumn and winter and by using Fourier analysis. The load derived from the seasonal rating curves was lower than the load estimate derived from the rating curve based on all data. Unfortunately no judgement can be made as to which is better as there was no estimate of actual load. Examination of the seasonal rating curves showed that the autumn and spring models were a better fit, as indicated by R^2, than the model developed from all the data (Table 4.7). However, the relation between SSC and Q in the winter was weak and in the summer was very weak (Table 4.7).

It is not surprising that there is not a consistent seasonal relationship between studies as seasons are arbitrary classifications. For example, summer might be generalised to consist of convective rainfall events (therefore high intensity), higher proportions of

Table 4.7. Regression models for Burnhope Burn, Northern Pennines, in 2000/2001. Source: Holliday, 2003.

Data	*n*	Model form	R^2
All	1203	log C = 1.1569 log Q + 1.8258	0.71
Spring	73	log C = 1.0812 log Q + 2.3380	0.76
Summer	194	log C = 0.5702 log Q + 0.7341	0.06
Autumn	560	log C = 1.0163 log Q + 1.4982	0.73
Winter	372	log C = 1.3757 log Q + 1.9093	0.59

autochthonous matter, generally low discharges and consequently more bed sediment storage. Also, longer periods between high flow events allowing more time for sediment preparation. Alternatively, winter might be generalised with stratiform rainfall, more allochthonous material, generally higher discharges, less bed sediment storage, freeze-thaw cycles producing sediment for transport, snow cover and frozen ground stabilising sediment, shorter time periods between high flow events and therefore less time for sediment preparation. However, in the uplands there may be freeze-thaw cycles in a summer month and convective rainfall also occurs in winter. As a result, seasonal rating curves are not always successful, except in environments where there are distinct differences between seasons.

Data are often divided by limb and separate rating curves developed for each (e.g. Farr & Clarke, 1984). This is based on the reasoning that if sediment exhaustion occurs then SSC is likely to be higher on the rising limb than on the falling limb for a given Q. However, there may not be a clear distinction between rising and falling limb rating curves given variability in available sediment between storms.

Crisp & Robson (1979) used a siphon and filter technique to quantify peat discharge from Rough Sike, Upper Teesdale (a study site of this investigation). Crisp & Robson (1979) developed a suite of rating curves from the siphon data for Rough Sike: all data points, rising limb, peak, falling limb and base flow (Table 4.8). The R^2 values for all these regressions were above 85% except for base flow. On the basis of the results of the study Crisp & Robson (1979) made several conclusions. First, base flow discharges should be treated separately from the other flow states when establishing the relationship between suspended sediment transport and discharge. Second, SSC is higher during the rising limb than the falling limb at equal discharges. Third, sediment concentration (C in mg l^{-1}) is related to discharge (Q in m^3 s^{-1}) by

$$C = 900\ Q^{2.1444}. \qquad (4.8)$$

Table 4.8. Linear regression parameters for $\log_{10} Q$ and $\log_{10} C$ for Rough Sike. n = number of observations, a = intercept, b = gradient. Source: Crisp & Robson, 1979.

Flow state	n	a	b	R^2
Rising limb	47	5.7±0.3	2.5±0.3	0.87
Peak	28	5.5±0.3	2.5±0.3	0.89
Falling limb	113	5.3±0.2	2.3±0.2	0.89
Base flow	24	2.6±0.4	0.8±0.5	0.30
All	212	5.3±0.2	2.1±0.1	0.87

Evans & Burt (1998) also developed a rating curve for Rough Sike. The methodology involved a rating curve of SSC (established from water samples from an automated sampler triggered by stage) as a function of discharge. The regression parameters and R^2 values as established by Evans & Burt (1999) and Crisp & Robson (1979) are considerably different (Tables 4.8 & 4.9). Evans & Burt (1998) attribute the higher R^2 values to the difference in SSC determination methods: Crisp & Robson (1979) averaged SSC over a longer time period (minimum 30 minutes), in comparison with spot samples as used by Evans & Burt (1998), and studied coarser grain size fractions. The difference in parameter values could also be due to different hydrological, geomorphological and meteorological conditions producing different suspended sediment dynamics. This is reinforced by the vastly different yields: Crisp & Robson (1979) estimated than annual load as 93 t and in comparison Evans & Warburton (in press) (using the same data as Evans & Burt (1998)) estimated the yield as 37.1 t.

Table 4.9. Linear regression parameters for $\log Q$ and $\log C$ for Rough Sike. n = number of observations, a = intercept, b = gradient. Source: Evans & Burt, 1998.

Flow state	n	a	b	R^2
All	252	1.2	0.35	0.21
Rising limb	47	1.7	0.68	0.48
Falling limb	205	1.0	0.20	0.10

However, while the majority of studies conclude that rating curves are problematic due to scatter and attempt to reduce the scatter by subdividing the data, the basic rating curve is still the most accurate technique to estimate loads for some catchments. For example, Al-Ansari *et al.* (1988) concluded a basic rating curve was a satisfactory technique for suspended sediment load determination of the Euphrates at Haditha, Iraq. Twelve estimates of sediment load were made from nine years of logarithmically transformed daily data. Ten of the estimates were based on linear regression. One was

developed from all the data and the remaining nine from the data sub-divided into: individual years; months; high and low water seasons; spring, summer, autumn and winter; rising and falling limb; and discharge classes of 100, 200 and 300 $m^3 s^{-1}$ (to eliminate the influence of more data at lower discharges: e.g. Jansson, 1985). However, the simple linear regression based on all the data proved to produce the most accurate estimate of annual sediment load. Al-Ansari *et al.* (1988) postulated that this was due to the large catchment (the Euphrates which drains 444,000 km^2), a relatively low specific suspended sediment yield (1.4×10^7 t yr^{-1}), trapping of substantial amounts of sediment in reservoirs and a regulated flow regime.

4.5.1.4 Adaptations to rating curve model form

Several models have been developed from the standard rating curve technique in an attempt to improve the accuracy and comparability. The developments include variations on the basic form of the suspended sediment rating curve model in an attempt to improve model fit and the incorporation of explanatory variables other than discharge in an attempt to integrate better measures of sediment transfer processes.

Several authors have added additional variables with the aim of explaining more variability in the SSC-discharge relationship and identifying important controls. For example, Holliday (2003) investigated the affect of season using Fourier analysis based on sine and cosine variables: sin [2 π FOY] and cos [2 π FOY] where FOY is fraction of year. Multiple regression of log C as a function of log Q, sine variable and cosine variable indicated that log Q was the most influential variable but the sine and cosine variables were statistically significant. Unfortunately there was not a full year data set to test this but the data that was available showed a peak during early winter and a trough during summer (Holliday, 2003).

Richards (1984) applied sediment rating curves to the proglacial stream; Storbreen in Norway. The data set used was small (16 days with a sample taken every two hours); however, it gave some valuable insights into suspended sediment dynamics. Initially a simple log-log linear regression rating curve was developed but the results were inaccurate: the load was under-estimated by 22% and only 21% of the variability in SSC was explained by Q. Change in Q, calculated by subtracting the preceding Q from the present Q and dividing it by two, was added to the regression as a second explanatory variable. Change in Q also indicates whether Q was rising or falling

(positive during rising and negative during falling). Adding change in Q resulted in an increase of 29% of the variability in SSC explained and an improved load estimate (over-estimation by 10%). Richards (1984) noted that different processes were controlling suspended sediment concentration during different conditions, i.e. during storm flow and diurnal (melt) flow. Therefore the data were divided into storm flow and diurnal flow and a multivariate (Q and change in Q) rating curve produced for each. The diurnal flow regression indicated that change in Q was the controlling variable (Q coefficient was not significantly different from 0) but only explained 10% of the variance in SSC. However, 46% of the variation in SSC was explained by Q and change in Q during periods of storm flow. The loads estimated by the storm flow and diurnal flow regressions result in an over-estimation of total load for the 16 day period of just under 10%: the most accurate estimation. Richards (1984) notes that such a division in data may not be possible or practical, except for short time periods, and therefore suggests a multiple regression with Q, change in Q, temperature and precipitation (at appropriate lags) may be optimal for proglacial streams.

Walling (1974) applied stepwise multiple regression using stormflow Q at the time of sampling, the relation of the sample to hydrograph peak, the flow level preceding the hydrograph and the index of flood intensity (calculated by hydrograph peak-flow level preceding hydrograph/time of rise (Bobrovitskaya, 1967)) as explanatory variables. These extra explanatory variables explained 70% of the variance in SSC, compared with 33% by Q alone. Several authors have also adopted a multivariate approach (e.g. Hodson & Ferguson, 1999).

Walling (1974) also used multiple regression to study the impact of hydrological and meteorological factors on maximum storm period SSC, total storm sediment load, and discharge-weighted mean SSC. Total storm rainfall, maximum storm intensity, storm duration, kinetic energy of the storm (as by Wischmeier & Smith, 1958), peak Q, peak quickflow Q, intensity of rise, total quickflow runoff, flow level preceding hydrograph rise, antecedent precipitation index, soil temperature at 1 cm depth, and a measure of season (cosine of $2\ \pi\ D\ /\ 365$, sine of $2\ \pi\ D\ /\ 365$, D = Julian day) were used as explanatory variables. These explanatory variables explained 80% of the variation in peak and mean storm SSCs and 96% of the variation in storm load. In all three regressions rainfall, streamflow, antecedent conditions and seasonal variables were most important. However, due to interdependence between them it is not possible to ascertain

the relative importance of each. Orthogonalised regression, a technique based on principal components analysis, was applied to identify the relative importance of each variable. This indicated the most important variables for maximum and mean storm SSC were total rainfall, maximum rainfall intensity, total kinetic energy and the sine season variable. In contrast the controlling factors over storm yields were peak quickflow Q, peak Q, rainfall amount, rainfall energy and sine season.

Several authors have investigated the effect of different forms of the basic rating curve. Jansson (1985) tested the impact of model form on suspended sediment load estimates for the River Ljusnan, Sweden. The methods were: a regression equation developed iteratively by the least squares technique on the power function model; log-transformed linear regression; log-transformed linear regression with the data divided into two discharge groups; and log-transformed linear regression of the mean SSC of twenty defined discharge classes (Table 4.10). The power function and discharge class models produced the most accurate sediment loads, corresponded to graphs with higher gradients and lower intercepts, and modelled the higher SSC values more accurately. In comparison the log-transformed linear regression model under-predicted SSC at high values of discharge and therefore resulted in a gross under-estimation of load (Table 4.10). The mean SSC model produces good results because the grouping reduced the number of data points at low discharge values and limited scatter. However, on further examination it was evident that this method over-predicted SSC at low discharge and under-predicted SSC at high discharge. The power function also under-estimated SSC at lower discharge (Jansson, 1985). This pattern of the best models under-predicting at lower discharges indicates the minor role lower discharges play in suspended sediment transportation (Crisp & Robson, 1979).

Table 4.10. Suspended sediment loads of the River Ljusnan, Sweden, (dates not given) calculated by various methods. Source: Jansson, 1985.

Model	Load, t	R^2
True load	52,855	-
$C = a\,Q^b$	50,441	0.69
$\log C = \log a + b \log Q$	17,228	0.49
$\log C = \log a + b \log Q$ (for $Q>10 m^3 s^{-1}$ and $Q<=10 m^3 s^{-1}$)	33,137	($Q>10 m^3 s^{-1}$) 0.53 ($Q<10 m^3 s^{-1}$) 0.03
$\log L = \log a + b \log Q$	17,228	0.81
$\log C_{mean} = \log a + b \log Q_{class}$	50,850	0.86

Jansson (1996) also studied the Reventazón river, Costa Rica, and established the most appropriate rating curve. The first model was log-log linear regression and was corrected for bias as graphical evidence indicated the trend line lay too low. There was a clear break-point in the data at 185 $m^3 s^{-1}$ and due to this a single rating curve under-estimated load. This was resolved by producing two regression curves: one for discharge less than 185 $m^3 s^{-1}$ and one for discharge greater than 185 $m^3 s^{-1}$. However, the number of data points at low discharges levered the <185 $m^3 s^{-1}$ regression line to a position which was too low and hence load was still under-estimated. Therefore Jansson (1996) divided the data into twenty discharge classes, calculated the mean SSC for each and applied a log-transformed linear regression model. By using the mean SSC of discharge classes the disproportionate number of data points at low discharge values did not lever the regression line. This approach has also been used by US Army Corps of Engineers (1975), Verhoff *et al.* (1980) and Walling & Webb (1981) among others. A break-point in the data was still evident so two regression lines were developed as before (Figure 4.4).

Jansson (1996) also attempted to find the 'effective discharge interval' i.e. the discharge range in which the majority of sediment is transported. This was achieved by comparing the sediment load for each discharge class and the frequency of occurrence of the discharge class. The effective discharge interval for the Reventazón River was 40-210 $m^3 s^{-1}$ and therefore the rating curve should be as close as possible a fit during this discharge range. This is a useful and beneficial gauge of the accuracy of a rating curve, placing importance in the fit where it is most crucial, rather than its overall fit evaluated in a statistical sense.

Asselman (2000) developed four types of rating curves using four different data sub-sets for the River Rhine, Germany (Table 4.11). The suspended sediment load estimates were generally good (less than 20% error) when calculated for a four year period (1979-1983) (Table 4.11). However, annual load estimates suffered from higher errors, i.e. ~60% (Asselman, 2000). The log-transformed rating curves generally gave low estimates, especially at high Q (Table 4.11). Under-estimations were less for the bias corrected log-transformed rating curves (Table 4.11). The least squares non-linear and least squares non-linear with additive constant (p) gave the best estimates (Table 4.11). The analysis of residuals for all four models indicate that none is a statistically a good fit and hence Asselman (2000) choose the model (least squares non-linear with additive

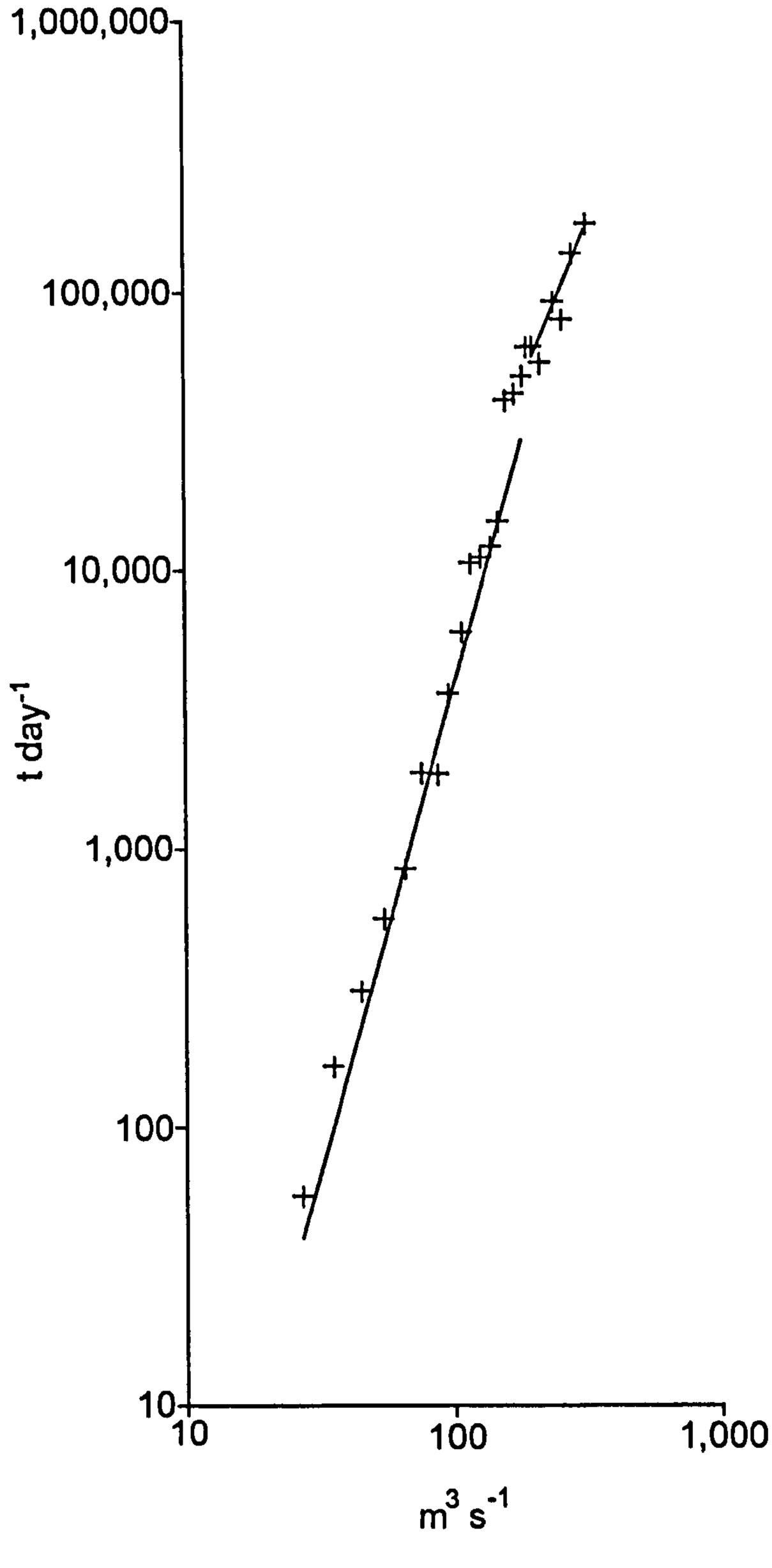

Figure 4.4. Rating curve with turning point. Each cross represents the mean SSC in each Q class. Source: Jansson, 1996.

constant rating divided by stage and season) with the highest efficiency (R^2). However, an increase in R^2 is expected when additional variables (season and stage) are entered into the model. Asselman (2000) still concluded that the least squares non-linear with additive constant model divided by stage and season is the optimum model, when taking all sites and measures of model fit into consideration.

Table 4.11. Types of regression model used by Asselman (2000) and the percentage difference between actual loads and estimated load for the Rhine at Andernach. Rating curves developed from 1979-1983 data series.

Data categorisation	Least squares non-linear ($C = a\,Q^b$)	Log-transformed linear ($C = \log a + b \log Q$)	Bias corrected log-transformed ($C = \exp(2.651\,S^2)$)	Least squares non-linear with additive constant term ($C = a\,Q^b + p$)
Season	0.0	-18.3	-9.7	2.6
Limb	1.4	-14.3	-5.0	1.2
Season & limb	-2.0	-14.1	-5.2	0.7
All	-0.1	-18.5	-11.4	0.2

Another less conventional rating curve technique was used by Walling (1977a). He developed a suite of rating curves from logarithmically transformed data but also fitted a linear trend line by eye on the grounds that this allows more weight to be given to the high discharge portion of the plot, i.e. the portion of the plot which has more effect on sediment loads (Figure 4.5). While this seems reasonable, load calculation based on this technique showed large over-estimations (134% and 280% for 1972-1973 and 1973-1974 respectively). This suggests that least squares linear regression introduces a bias towards under-estimation when the fact that most sediment is transported at high discharges is taken into consideration (Walling, 1977a). However, loads calculated by the eye-fitted method were gross over-estimates, inconsistent when applied by different people, and hence not recommended for load calculation.

The above adaptations of model form are fairly basic and do not require much, if any, extra information. In contrast, Van Sickle & Beschta (1983) developed a 'grey box' modelling technique, i.e. the main processes and feedbacks of the sediment delivery system were incorporated, but the numbers of variables, equations and parameters were minimised. Initially Van Sickle & Beschta (1983) incorporated a simple sediment supply variable: the total amount of sediment available upstream of the sampling location was assumed to be one store and was gradually depleted. To achieve this an extra term was added to the sediment rating curve formula in which $C(t)$ is SSC at time t, $Q(t)$ is discharge at time t, $S(t)$ is sediment stored at time t, S_o is maximum sediment stored at beginning of the rainy season and a, b, p and r are empirically defined parameters,

$$C(t) = a\,Q(t)^b \cdot p \cdot \exp\left[r\,\frac{S(t)}{S_o}\right]. \qquad (4.9)$$

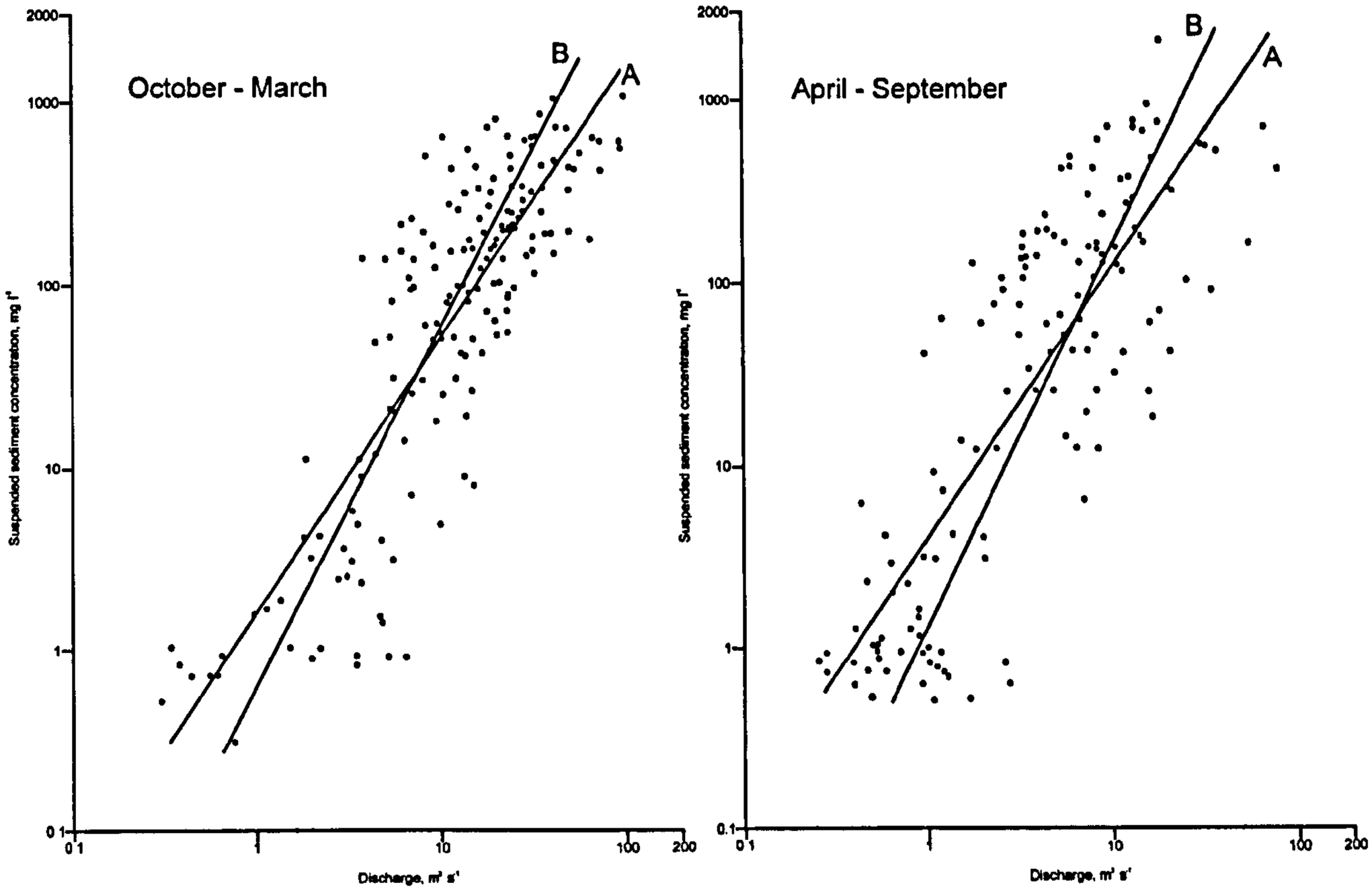

Figure 4.5. Comparison of OLS regression (A), and eye-fitted (B) rating curves. Source: Walling, 1977a.

Essentially the extra part of the equation expresses the relative change in SSC due to changes in available sediment. The exponential function was chosen to control the decrease in sediment supply as sediment concentration, at an event or seasonal time scale has been shown to be exponential as opposed to linear in form (Van Sickle & Beschta, 1983). The change in sediment supply was based on the sediment discharge past the sampling point. Consequently, the standard rating curve equation is multiplied by a factor which decreases as time progresses, thus reducing the estimate of SSC. To model the effect of diffuse sediment sources sediment inputs were introduced between storm events. The model developed by Van Sickle & Beschta (1983) yielded better results than the standard rating curve when applied to four storm events: ratios of the model error to conventional rating curve model error were 0.46, 0.95, 0.52 and 0.78.

Van Sickle & Beschta (1983) developed a second model which involved a distributed sediment supply component and hence was more realistic than the first lumped model. The distributed model worked on the principle that as Q increases the number of sediment storage compartments accessed increases and each compartment is depleted in accordance with sediment supply and Q. The compartments are defined as horizontal sections across the bank profile (Figure 4.6).

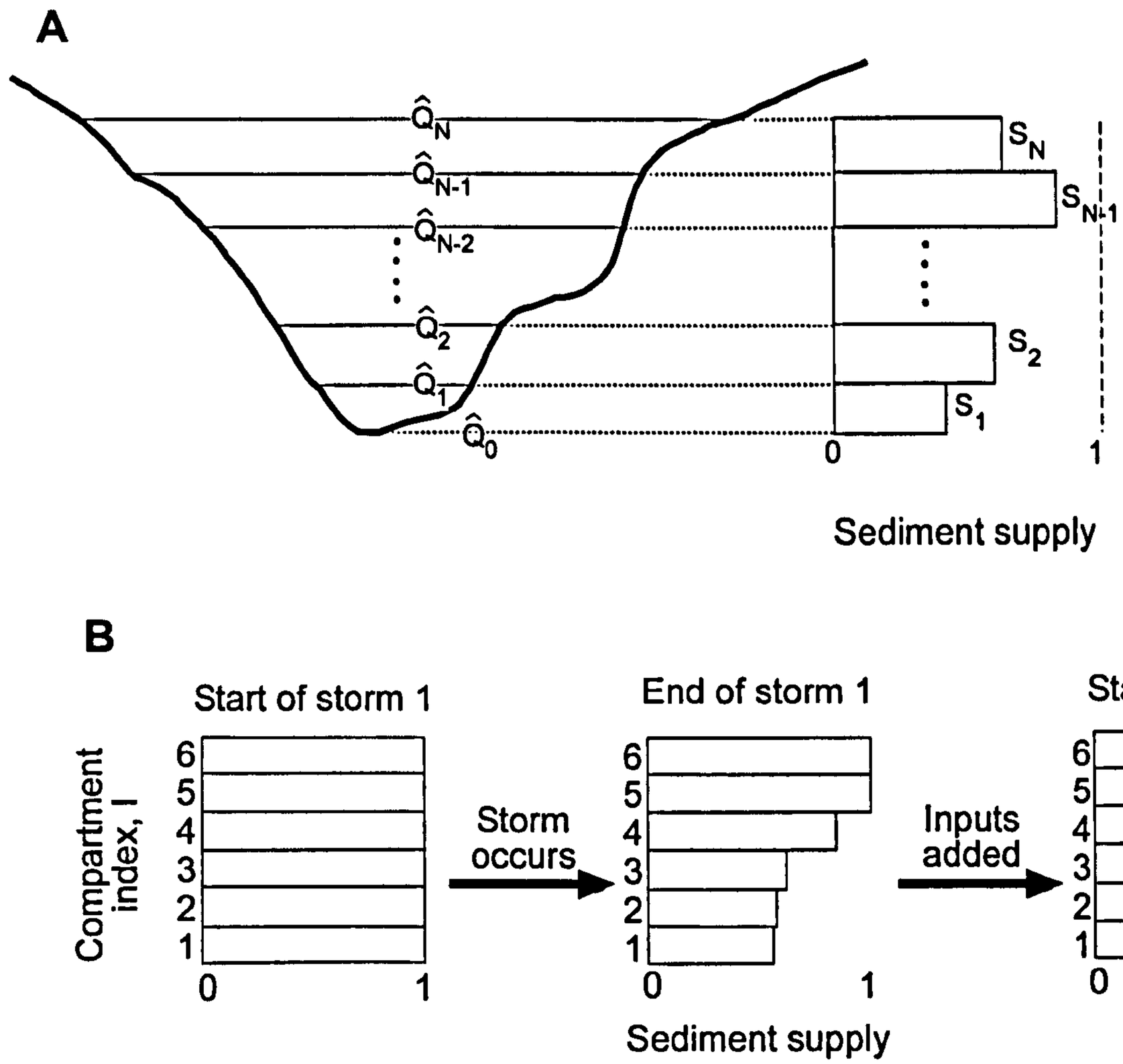

Figure 4.6. Van Sickle & Beschta's (1983) distributed model. A – Changes in sediment supply at different stages. B – Depletion and re-charging of the sediment supply compartments in accordance with storm events.

This does not imply that only sediment from the banks is included; it also allows for material re-suspended from the bed due to increased turbulence, sediment released from obstructions (e.g. a branch) at the onset of defined discharges and additional sources of sediment due to the headward expansion of the channel. The rate of sediment depletion in each compartment is based on the following equation:

$$\frac{d\,S_i(t)}{dt} = -a \cdot Q(t)^b \cdot p \cdot \exp\left[r\,\frac{S_i(t)}{S_i(t_0)} \right] \qquad Q(t) \geq Q_{i-1}$$

$$= 0 \qquad\qquad Q(t) < Q_{i-1} \qquad (4.10)$$

In order to calculate total sediment storage (S_T) at time t, the storage in each compartment is summed:

$$S_T(t) = \sum_{i=1}^{N} S_i(t)\,, \qquad (4.11)$$

Total sediment transport (T) at time t is the loss from each compartment summed:

$$T(t) = -\sum_{i=1}^{N} \frac{d\, S_i(t)}{dt}, \tag{4.12}$$

and C is then calculated by:

$$C(t) = \frac{T(t)}{Q(t)}. \tag{4.13}$$

The distributed model was more successful when applied to the same four flood events in comparison with the lumped model, as it was more responsive to changes in streamflow and sediment supply, had smaller concentration errors and allowed for distributed inputs. The distributed model had the major advantage of allowing direct storage estimates for several sites accessed at different discharges to be entered. Van Sickle & Beschta (1983) argued that of the two models the lumped model had the greater predictive potential, but was not shown statistically superior to the standard rating curve. The distributed model was deemed more useful as a predictive tool and could use hydraulic geometry relations (e.g. Yang *et al.*, 1981) to test assumptions about the relative availability at different flow regimes. However, both models require a quantitative knowledge of sediment supply. While this is an attractive method no other applications of Van Sickle & Beschta's (1983) model are known, most likely reflecting data demands.

4.5.1.5 Model parameter interpretation

Although the parameters of the rating curve model have no physical meaning they have been found to correlate with catchment characteristics. For example, Bogardi (1961) established a good relationship between b and the average width of the catchment, mean discharge, ratio of highest to lowest discharge and the mean discharge per unit catchment area for twelve Hungarian rivers. Furthermore, Walling (1974) attributed the magnitude of b to the nature and grain size of the suspended sediment load. Larger values of b were associated with rivers with a considerable quantity of sand-sized suspended sediment which required transported higher velocities to transport it. Therefore, the gradient of the rating curve increased as the discharge and consequently, sediment availability, increased. Smaller values of b were associated with rivers whose load was almost entirely clay and silt-sized. As a result, the increased transport competence of the stream at higher discharges was of little importance. Sarma (1986), also discusses the magnitude of b in terms of suspended sediment grain sizes.

On the basis of such studies attempts have been made to predict the parameters for ungauged basins based on catchment characteristics. For example Rannie (1977) developed an equation which predicted the rating curve form of unmonitored catchments. The study was based on fifty US river catchments with no lake or reservoirs and a catchment area of less than 300 square miles. Rannie (1977) found the parameters were related in the following relationship

$$b = 1.581 - 0.155 \log a, \qquad (4.14)$$

and the rating curve of an unmonitored catchment was predicted by using the mean annual runoff, $ft^3\ s^{-1}\ mile^{-2}$; maximum relief, feet; and basin area, square miles, or mean relief, feet. However, large percentage errors (143% to 285%) in the sediment load estimation were associated with the application of this technique.

As mentioned above, model parameters have been interpreted with regard to the physical characteristics and processes of the fluvial systems. However, care must be taken when relating the *a* and *b* parameters as steep gradients (high *b* values) are more likely to have high (positive or negative) intercepts (*a*) than less steep gradients. Asselman (2000) undertook an in-depth examination of rating curve forms from gauging sites within the River Rhine catchment (Figure 4.7). The steepness of the rating curves for gauging sites on the Rhine and its tributaries decreased downstream (Figure 4.7A). Based on this observation Asselman (2000) used scatter plots of *b* versus *a* to infer the nature of the sediment transport regime (Figure 4.7B). However, the tendency for high values of *b* to promote high values of *a* must be taken into consideration. The points produced three lines (Figure 4.7B) and points on the same line were assumed to have a similar sediment transport regime. The highest line (i.e. those which have a larger *b* value for a given values of *a*) (Figure 4.7B) was attributed to sediment transport regimes where a large proportion of the annual sediment was transported during high discharges. Conversely, the lowest line (i.e. those which have a lower value of *b* for a given value of *a*) (Figure 4.7B) were populated by data points from streams characterised by more sediment transport at relatively low discharges.

Asselman (2000) also investigated the steepness of the SSC-discharge ratings. She reasoned that steep rating curves (those with high b values) should be characteristic of river sections with low sediment transport at low discharge values and large increases in sediment transport with a given increase in discharge, thus indicating that the power of

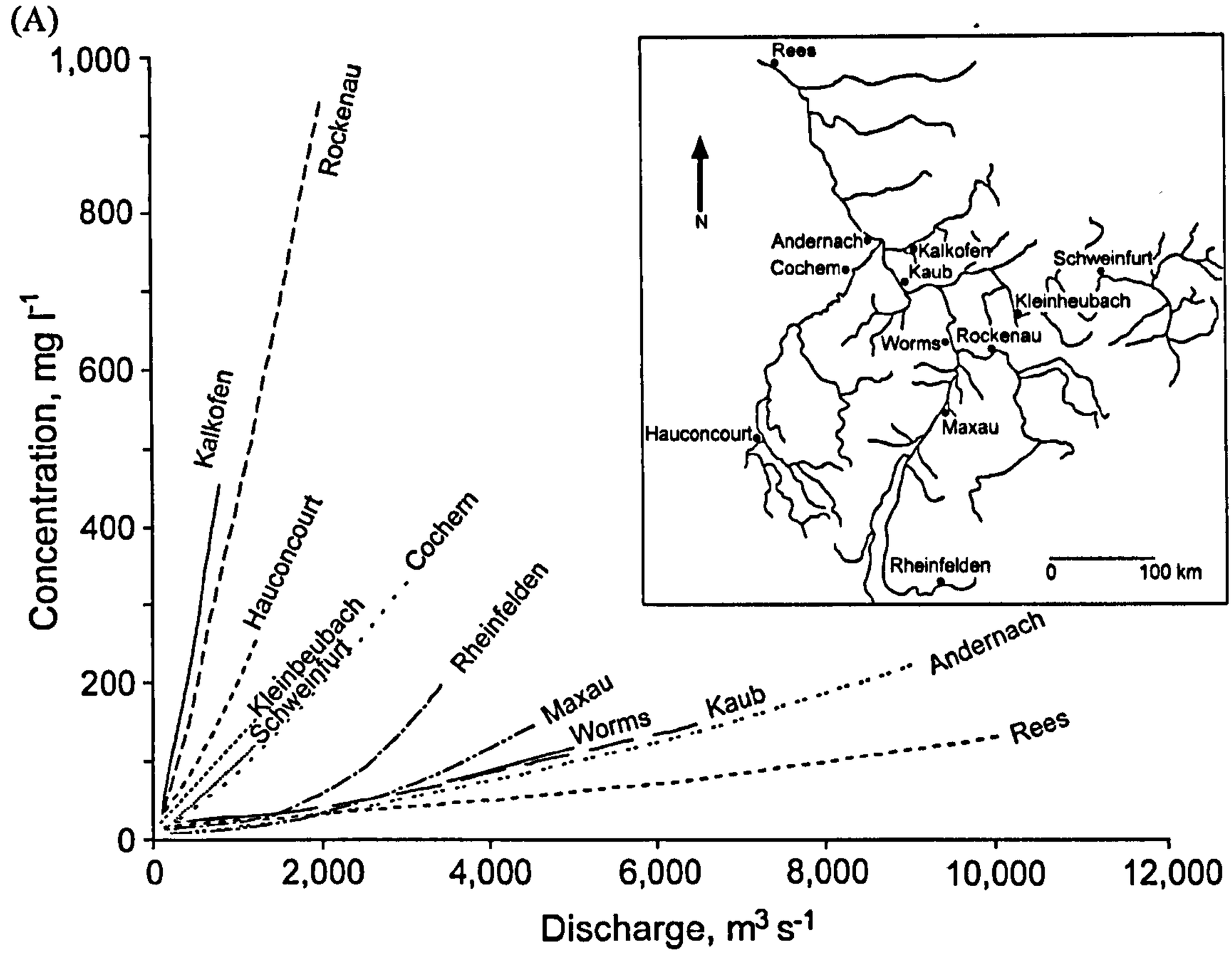

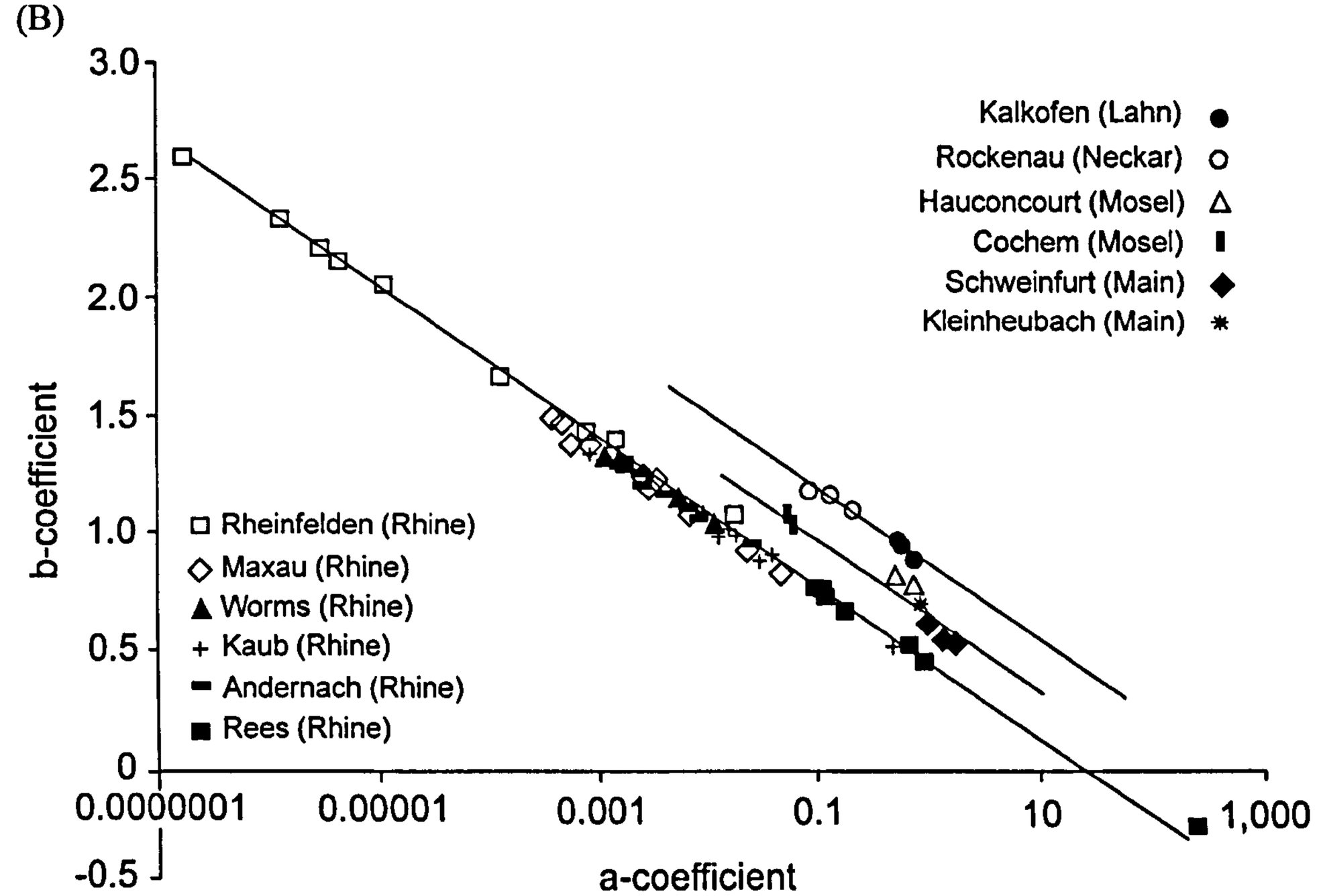

Figure 4.7. (A) Variation in rating curve form on the River Rhine and its tributaries with distance downstream and (B) correlation between the *a* and *b* coefficients with an inset of the gauging site locations. Source: Asselman (2000).

the river to erode material during higher discharges is high or that important sediment sources are accessed at higher discharges. Conversely, less steep rating curves should be characteristic of rivers with sufficient sediment ready for transport at the majority of discharges. This can be partially attributed to a grain size control. Peters-Kümmerly (1973) attributed the value of *b* solely to the erosive power of the river, which is in partial agreement with Asselman (2000), and Rannie (1977) ascribed high b values to sensitive systems and low b values to less sensitive systems. While this is not explicitly what Asseleman (2000) proposed, it is what she inferred: high b values indicate rivers with a large variability in SSC for a given discharge range, and low b values indicate rivers with less variability in SSC for a given discharge range due to plentiful sediment supply. To test the hypothesis Asselman (2000) calculated the amount of sediment transported during discharges equal to or less than the average discharge and during the 10% of the time at the highest discharges for study sites on the Rhine and its tributaries. This analysis showed sites on the main channel transported 25-35% of sediment at discharges equal to or less than the average discharge and approximately 35% during the very high discharges which occur for 10% of the time. These percentages remained constant with distance downstream the Rhine. In contrast the tributaries transported between 10% and 20% of sediment at discharges equal to or less than average discharge and between 60% and 80% during the higher discharges. Asselman (2000) accounted for these differences in sediment transport regimes by the influence of scale: given the lower discharges in tributaries a given increase in discharge will have more affect, in terms of sediment sources accessed and erosive power, in a tributary than in the main channel.

More authors interpret the meaning of *b* than the meaning of *a* given the potential influence of *b* on the value of *a* (high gradients are more likely to be associated with high intercepts). However Rannie (1977) suggested *a* indicates the level of process in absolute terms and therefore reflects catchment characteristics and Peters-Kümmerly (1973) suggest *a* represents an index of erosion severity with high values indicating intensively weathered material which are easily transported.

Asselman (2000) also conducted an interesting analysis on the relationship between the *a* and *b* parameters. Several rating curves were developed for each study site from different periods of the data by non-linear least squares. The parameters were then plotted with *b* as a function of *a*. All the points from all the study sites on the Rhine

exhibited a strong negative relationship. The same relationship was identified by Thomas (1985). This suggests that there is a common point at which all the rating intersect. The common point does not vary with time (as the relationship between *a* and *b* was based on rating curves produced for each study site with different sections of the same data series) it is postulated to be a result of catchment characteristics which do not vary with time, e.g. relief, area, drainage density. However, Asselman (2000) could not attribute this to a single catchment characteristic.

4.5.2 Rating curves derived by generalised linear models

In research where a simple model linking response and explanatory variable(s) is required, such as between SSC and discharge, linear regression is frequently applied. However, as outlined previously the assumptions of linear regression necessitate data transformation prior to model formulation. The transformation of data adds an extra step into the analysis and results in back-transformation bias which necessitates yet another step or bias in the results. Generalised linear models (GLMs) are a family of alternative linear models which can be used to relate response and explanatory variables and do not require data transformation or bias corrections.

GLMs were introduced by Nelder and Wedderburn (1972) and since then have been incorporated in many statistical computer packages. Nelder and Wedderburn (1972) did not develop the whole suite of GLMs as many forms already existed under other guises (linear regression, ANOVA, inverse linear regression, logistic regression, log-linear regression, dilution assay, survival analysis and probit analysis), but grouped them as a suite of models with the same aim and using similar techniques (Lane, 2002).

There are two principal differences between GLMs and traditional linear regression. First, the response variable can be in the form of any of a wide range of distributions (Table 4.12). Hence no transformations are necessary, as the distribution is specified in the model. The gamma distribution is especially useful as it allows a skewed distribution which is advantageous as both SSC and Q are bounded by zero and hence susceptible to asymmetry. Second, a link function is specified which relates the mean of the response to a scale on which the effects in the model combine additively. Therefore, instead of the mean of the transformed response variable it is the transformed mean of the response variable (the difference between these are shown in Table 4.3, section 4.5.1.1). The link function can take any of a number of forms (Table 4.13). GLMs are

advantageous if the errors are non-normally distributed, the variance is not constant and the effects of the explanatory variable(s) combine multiplicatively, as opposed to additively, on the response variable (Lane, 2002): all of which can be true for SSC-discharge relations.

Table 4.12. Possible distributional forms of the response variable of GLMs. Source: StataCorp., 2003a.

Distribution	Definition
Normal/Gaussian Inverse normal	Variance is independent of the mean
Binomial/Bernoulli Negative binomial	Variance is equal to $Np(1\text{-}p)$ where the mean is Np where N = the number of trials and p = the probability of the trial being a success.
Poisson	Variance is equal to the mean
Gamma	Variance is proportional to the square of the mean, i.e. the coeeficient of variation is constant.

The number of distributional forms, link functions and valid combinations vary between software packages. The most common distributional forms, link functions and valid combinations are given in Table 4.13.

Table 4.13. Definitions of GLM link functions and possible distribution and link function combinations. Φ^{-1} = the inverse Gaussian cumulative, n = number, μ = mean of response variable, k = 1 if negative binomial is the selected distribution and $\#_k$ if the negative binomial $\#_k$ is selected. Source: StataCorp., 2003a.

Link function	Definition	Normal	Inverse normal	Binomial	Negative binomial	Poisson	Gamma
Identity	$= \mu$	X	X	X	X	X	X
Log	$= \ln(\mu)$	X	X	X	X	X	X
Logit	$= \ln(\mu / (1 - \mu))$			X			
Probit	$= \Phi^{-1}(\mu)$			X			
Complementary log-log	$= \ln(-\ln(1 - \mu))$			X			
Odds power	$= ((\mu / (1 - \mu))^n - 1) / n$			X			
Power	$= \mu^n$	X	X	X	X	X	X
Negative binomial	$= \ln(\mu / (\mu + k))$				X		
Log-log	$= -\ln(-\ln(\mu))$			X			
Log-complement	$= \ln(1 - \mu)$			X			

GLMs have several advantages over the traditional linear regression methods. First, it is preferable to adjust the form of the model than to adjust the data as adjusting the data

abstracts from the physical system and necessitates some form of back-transformation. Second, GLMs allow for a greater range of distributional forms and thus allow for different relationships between the mean and the variance. Third, there are no back-transformation problems as with linear regression. Fourth, there is no difficulty with zero counts. These cause problems when transformed with linear regression as it is not possible to log zero. Fifth, controlling the link function and the distributional form independently allows the scale at which the effects are examined and the variance behaviour of the response to be separated (Lane, 2002).

GLMs are less accessible than linear regression due to unfamiliarity, especially with the distributional forms and the computation procedures. This is perhaps the reason why GLMs are not more widely used. There are several disadvantages of GLMs (Lane, 2002) but only one has an impact on this investigation: the effects of the explanatory variable(s) are not linear and hence it is not possible to state that a unit change in the explanatory variable results in a change of a fixed magnitude in the response variable, unless an identity link is used. However, this is also the case with linear regression developed from transformed data.

Cox *et al.* (submitted) developed five rating curves for Trout Beck (a study site of this investigation). Three were based on the linear regression of ln C on ln Q, one was simply back-transformed into data space, one was back-transformed and bias corrected by smearing (SM), and one was back-transformed and bias corrected by the lognormal correction factor (LNCF). The other two rating curves were GLMs: one with a log link and a gamma error family and one with a log link and a Gaussian error family. The rating curves were all broadly similar in form (Figure 4.8) and the root mean square error (RMSE) and correlations coefficients were essentially the same. Cox *et al.* (in review) concluded that GLMs are a valuable and flexible alternative to the more traditional linear regression techniques which avoid the problem of back-transformation.

4.5.3 Time series analysis

Time series analyses (TSA), specifically transfer functions, are also used to quantify suspended sediment (e.g. Lemke, 1991). However, transfer functions are less commonly used given their complex nature and heavy data demands for model development and calibration. Transfer functions have been more often applied in glacio-fluvial studies or when quasi-continuous turbidity data are available (e.g. Gurnell, 1984).

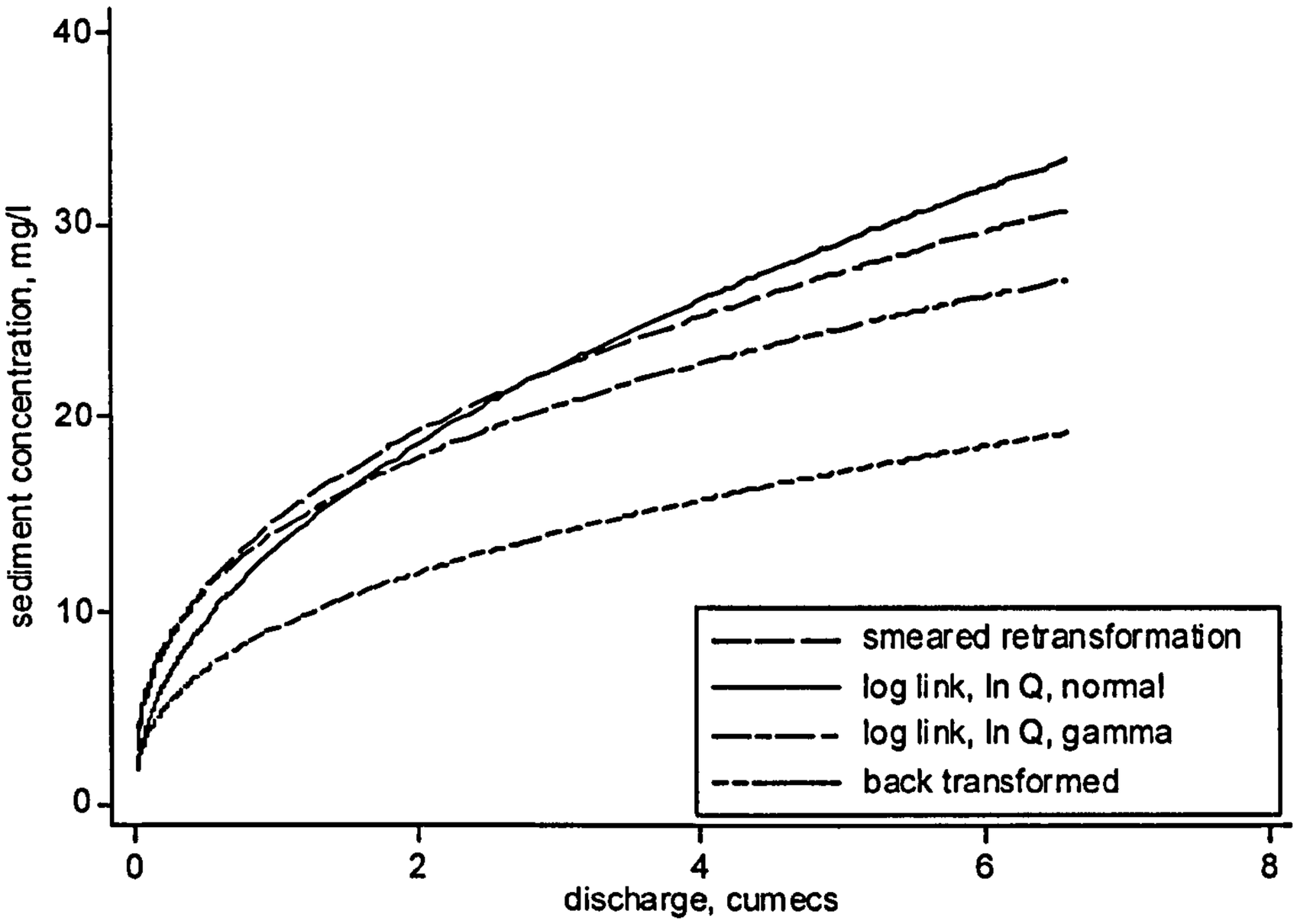

Figure 4.8. The five rating curves developed for Trout Beck. Source: Cox *et al.*, in review.

TSA is the investigation of a sequence of observations occurring in time or space. They have been used in a range of fields including economics, marketing, process control and the physical sciences. In essence TSA is the development of a statistical model which is representative of a statistical process that generated an observed time series. The objectives of TSA are to describe, explain, postdict, predict and control.

There are two main sub-divisions of TSA: the time domain and the frequency domain, and numerous variants within them (Figure 4.9). The time domain approach establishes the relationship between time series in accordance with time and characterises the data in the same form as the data were observed. Alternatively the frequency domain investigates the time series by the pattern of sine and cosine waves of different scales necessary to reproduce it, i.e. spectral analysis. The time domain variants of TSA are commonly used in suspended sediment studies, although some glacio-fluvial studies use the frequency domain.

Within time domain TSA there are models which require stationary or non-stationary time series (Figure 4.9); the majority of applications are based on stationary time series. Stationarity is the concept that the time series is similar in terms of the processes

responsible for the outcome and therefore the mean and variance is approximately constant throughout the series. This is often defined by statistical measures, e.g. different segments of the time series have approximately equal mean and/or variance. Also, the correlation which exists between variables should be a function of the time interval between observations and not controlled by absolute position within the time series. Suspended sediment time series may be stationary or non-stationary, dependent on the time-scale of analysis and if there has been a change in the processes controlling SSC, i.e. at an annual time-scale the series may be considered non-stationary if the production of autochthonous matter is substantial during the summer months, or land use change may produce non-stationarity (e.g. Johnson, 1994). If the time series under investigation are non-stationary then the data can be transformed, stratified or a non-stationary time series model used.

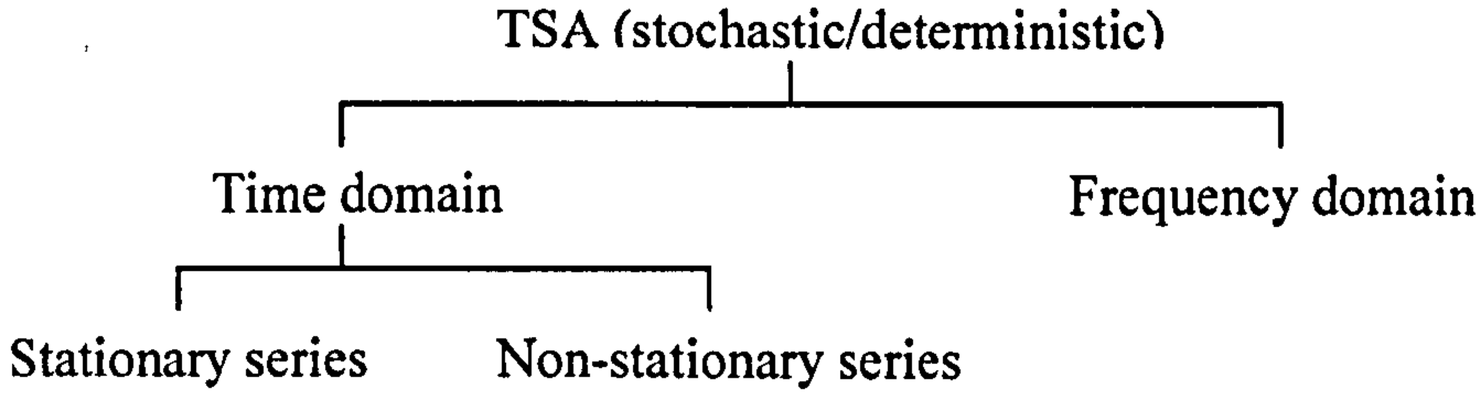

Figure 4.9. Some of the variants of TSA.

Time series are either deterministic (observations can be predicted exactly by previous values) or stochastic (observations are only partly predictable from previous variables: there is a deterministic component of cycles, trends or seasonality superimposed with a stochastic variation). If the relationship is stochastic then the observed time series is one of several possible time series produced by the underlying stochastic process. Hence the time series model can be viewed as specifying the form of the underlying process. For example, if the relationship between discharge and SSC were purely deterministic, for any given discharge time series the same SSC time series would result. However, stochasticity means that a given discharge time series could result in several different SSC time series.

There are four types of stochastic processes particularly relevant to suspended sediment studies: random, moving average (MA), auto-regressive (AR) and mixed MA and AR (ARMA). Random processes consist of independent values with no memory of previous values. MA processes are those in which the current observation depends on

the current random error plus the random error of one or more previous observations and therefore retains memory. AR processes are those in which the current observation depends on one or more previous observations plus a random error (a similar concept to regression except that the values are regressed on previous values in the same series) and hence generally retains longer-term memory than MA. ARMA is a combination of both AR and MA processes.

The majority of TSA SSC studies translate the input series (discharge) into the output series (SSC) by fitting a transfer function and noise model to the time series. The transfer function and noise component are calculated together so that any pattern in the noise can be differentiated from the transfer function, therefore preventing bias of the transfer function by the noise component (Gurnell & Fenn, 1984).

The principal difference between TSA and other statistical techniques used to study suspended sediment concentration is that autocorrelation is assumed to exist between successive observations (e.g. hysteresis). In other forms of statistical analysis independence between successive values is an assumption of the model and if violated can introduce error. Also, TSA commonly requires a time series of equally spaced data and therefore data requirements are more rigid than those demanded by other statistical methods. This is a substantial disadvantage of TSA with respect to modelling suspended sediment. There are some examples of TSA performed with sparse or irregularly spaced data (e.g. Bierkens *et al.*, 1999 and Parzen, 1984), but these are not generally suitable for suspended sediment studies as they risk abstracting beyond the limits of the data.

Lemke (1991) developed transfer functions for two catchments: Crow Creek and Nodaway River, Iowa. Discharge-SSC transfer function models were developed for both catchments and a multiple input (discharge, precipitation and air temperature) model was developed for Crow Creek. The discharge, SSC, precipitation and air temperature data were at daily intervals. Lemke (1991) recommended use of transfer functions as the developed models fitted the data well and were generally good representations of the system given allowance for delays and systems inputs and responses.

After finding sediment rating curves inappropriate because of serial autocorrelation Gurnell & Fenn (1984) investigated the use of TSA, specifically transfer function

models. Gurnell & Fenn (1984) developed transfer functions and rating curves for the proglacial stream of the Glacier de Tsidjiore Nouve, Switzerland, from hourly samples of discharge and SSC from two ablation seasons: 1st June to 30th July 1978 and 29th June to 23rd July 1981. In comparison with the rating curves the transfer functions gave better predictions of suspended sediment load. However, during one time period the transfer function prediction was only 56% of the actual suspended sediment load. This was explained by a major outburst of water from the glacier leading to water flowing on a different route across an old moraine, but the estimate was still superior to those from rating curves. This illustrates the need to sample the full range of SSC-discharge relations to achieve accurate predictions. Fenn (1989) compared load estimates derived from transfer functions and rating curves for Tsidjiore Nouve for several ablation seasons. The transfer function out-performed the various rating curve models: the average difference between the transfer function model load and actual load (as derived directly from the SSC-discharge records) was 5 % in comparison with the 35.4 – 81% associated with the rating curves. The transfer function was more temporally robust than the rating curves. Rating curves developed from one ablation season gave very inaccurate results when applied to other ablation seasons, whereas the transfer function gave reasonable estimates.

Irvine & Drake (1987) also found a transfer function model to be superior to a rating curve model. Irvine & Drake (1987) applied regression and transfer function ARMA models to daily discharge and SSC data from April to September for 1970, 1974, 1977 and 1980 from the Ausable River, southern Ontario. They reported problems of transfer function parameter instability: parameter estimates changed substantially from one year to the next. However an 'average' model using all data provided satisfactory results and predictive errors were less than those associated with the rating curve models. Data demands were reported as problematic for transfer function model development.

Caroni *et al.* (1984) also described similar model parameter instabilities as noted by Irvine & Drake (1987), but examined the change on an event, as opposed to seasonal, time-scale using half-hourly interval rainfall, discharge and SSC measurements from Pigeon Roost Creek, Mississippi. The differences in model parameters for the transfer function models developed for distinct storms were explained by the complex interactions within the fluvial system which caused individual responses to individual events. However, if an annual suspended sediment yield estimate were required, Caroni

et al. (1984) postulated that the average model (developed from all data) may perform acceptably, a common conclusion to most studies of this kind.

Transfer functions are most suited to fixed-interval and continuous SSC records and therefore are most commonly applied to pro-glacial streams (e.g. Fenn, 1989) or less responsive rivers for which daily sampling is adequate (e.g. Lemke, 1991). They are not suitable for responsive, remote rivers for which turbidity is a poor proxy for SSC, i.e. British upland rivers.

4.5.4 Artificial neural networks

Artificial neural networks (ANN) are also known as neurocomputing, neural networks, connectionism and parallel distributed computing and are a form of artificial intelligence. ANNs is a verified and fairly mature technique which extends computing potential from simple arithmetic and data retrieval to more complex information processing procedures. There are several different types of ANN and they are categorised as either supervised, used to map one or more inputs to one or more outputs, or unsupervised, concerned with categorising data (Openshaw and Openshaw, 1997). The most widely researched and used (resulting in the best performance when applied to input-output function approximation) are multi-layer forward-feed networks (Rumelhart *et al.*, 1986). Other types include Hopfield maps (Hopfield, 1982), self-organising feature maps (Kohonen, 1982) and counter-propagation networks (Hecht-Nielsen, 1988).

The concept of ANNs was first introduced by McCulloch and Pitts (1943) but the technique was not widely popular until the 1980s. Applications range from speech recognition, image analysis and robotics. Within physical geography ANNs have been employed to forecast river flow (Abrahart and See, 2000), forecast floods (Campolo *et al.*, 1999 and Cameron *et al.*, 2002), synthesise reservoir inflow series (Raman and Sunilkumar, 1995), generate rainfall data (French *et al.*, 1992), predict water quality parameters (Maier and Dandy, 1996) or snow water equivalent from multi-channel brightness temperatures (Chang & Tsang, 1992), model rainfall-runoff relationships (Hsu *et al.*, 1995), study groundwater reclamation problems (Ranjithan *et al.*, 1993), predict air temperature (Cook & Wolfe, 1991) and study suspended sediment (Yitian & Gu, 2003; Cigizoglu, 2004).

The rationale behind the development of ANNs was to imitate the ability of the human brain to learn by example. However, it is important to remember that ANN merely derives ideas and inspirations from biology and the study of brains: the link between them is very tenuous. The process by which ANNs learn is described by Mogili & Sunol (1993) as a process in which a computer program improves its performance, gains knowledge and solves new problems, in a given domain. Mogili & Sunol (1993) also commented that ANNs are not appropriate for knowledge acquisition, as they do not allow knowledge extraction in the form of rules. This is because ANNs are a data-based modelling approach, not theory-based, and as such are a 'black box' pattern-recognition approach. ANNs have no algorithms (arithmetical/computational procedures), which are core in most computer models; instead ANNs 'learn' and then generalise from the specific to the abstract. In summary "ANNs have the ability to learn the underlying relationships between inputs and outputs (as opposed to the exact relationship), they are well suited to modelling natural systems, where complex relationships exist between the inputs and outputs, and data are often incomplete and noisy" (Maier and Dandy, 1996, p1014).

An ANN is composed of several computational elements, called nodes or neurons (represented by the circles in Figure 4.10). The basic ANN form or 'architecture' consists of an input layer, hidden layer(s) and an output layer (Figure 4.10). Each node in the output layer represents an output variable (i.e. the variable(s) being modelled) and each input node represents an input variable from which the output variable is derived. The number of nodes in the hidden layer and the number of hidden layers are variable. Additional hidden layers are reported to be necessary for more complex relationships but care must be taken as excess hidden layers can lead to a model which is too specific (i.e. it cannot generalised) (Openshaw and Openshaw, 1997). Moreover, the more hidden layers, the more weights and hence the slower the training process (Shamseldin, 1997). Each node is connected to each node in the next layer and there are no connections between nodes in the same layer. Parameters are associated with each of these connections and are known as weights. The weights are summed by the nodes and the result transformed by a transfer function (the most commonly used transfer function is the sigmoidal function). Therefore the output of each node is a smooth nonlinear transformation of the inputs. The number of nodes in the hidden layers is crucial as it controls the sensitivity of the ANN. Too few will result in poor modelling; too many will induce over-fitting of the data, i.e. data noise will be modelled (Masters, 1993). The

number of nodes is commonly determined by trial and error. Inputs from one layer move forward to the next in parallel hence the name parallel, distributed modelling. Model training (also know as learning and analogous to statistical model calibration) entails comparing the output values generated by the ANN with the actual values and changing the weights to minimise error. The most common method is the back propagation algorithm.

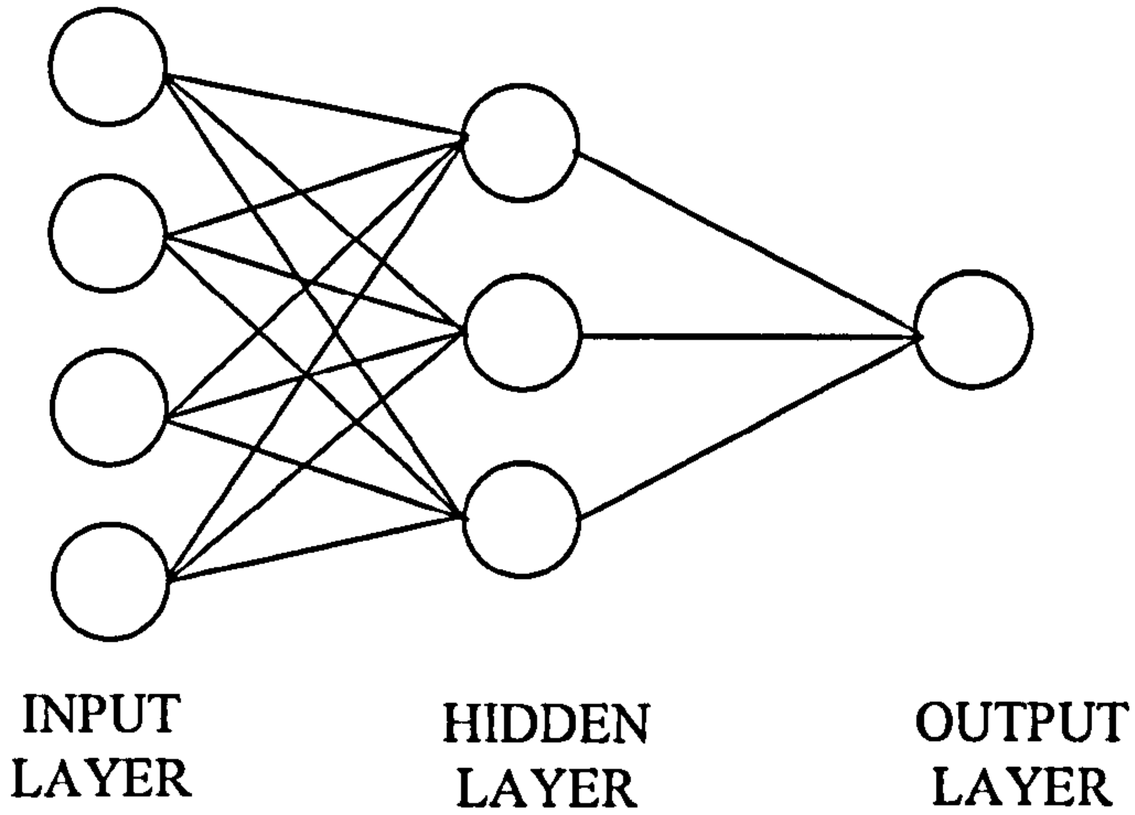

Figure 4.10. An example of an ANN structure.

Openshaw and Openshaw (1997) describe ANNs as a "brittle" technology which produce either extremely good results or extremely poor results in comparison with conventional methods which generally produce mediocre results. The ability of ANNs to model non-linearity, tolerate noisy data, process different data types (e.g. categorical and continuous) and model more than one output with virtually no knowledge of the processes and patterns being model and without making any assumptions about the nature of the data makes ANNs a very adaptable technique. However, ANNs are generally black box and data-driven and problems arise if there is a major change in the system being studied and cannot be extrapolated from.

Maier and Dandy (1996) presented ANNs as a viable technique for the forecasting of water quality parameters using salinity in the Murray River, Australia, as a case study. The aim was to predict salinity at Murray Bridge 14 days in advance to avoid saline water being pumped to Adelaide. Daily salinity levels were available for Murray Bridge and four sites upstream, flow records for two sites upstream of Murray Bridge and stage data for Murray Bridge and six sites upstream. This array of data was input to an ANN and promising results obtained: the average absolute percentage error of the 14 day

salinity prediction was 6.5% when obtained as part of a real time forecasting simulation for 1991. Therefore Maier & Dandy (1996) proposed that ANNs are a viable method for forecasting water quality parameters. However, no comparison was made with a more conventional model.

There have been some applications of ANNs to sediment dynamics. Abrahart & White (2000) compared soil loss estimates from different types of land use/management from four limited data sets (n = 22, 56, 32, & 7 but the data were combined) as obtained by multiple linear regression and a feed-forward ANN. The data were from agricultural land in Malawi and the different land use/managements were: (1) complete physical conservation works and formal land use plan, (2) intensive uncontrolled arable farming, (3) complete physical conservation works but no formal land use plan, and (3) eucalyptus plantation. Four explanatory variables were used for both the regression and ANN: rainfall, peak rainfall intensity, runoff, runoff coefficient and also four fuzzy set membership variables which were based on land use and management for each catchment. The ANN had one hidden layer with eight nodes and one output node (no justification of architecture was given) and used the back-propagation algorithm. While the ANN approach produced similar predicted soil loss to those obtained by regression the solution was a tighter fit to the data (Figure 4.11) and was more flexible in response to changing circumstances, i.e. land use. The ANN approach also included 'jittering' of the data which allowed the level of generalisation of model fitting to be increased. While this example is not specific to suspended sediment dynamics some of the process controls may be the same, and it illustrates the worth of ANN in modelling limited data sets.

Cigizoglu (2004) applied a feed-forward ANN to 29 years of daily mean flow and suspended sediment load data from two locations on the Schuylhill River, Philadelphia. Cigizoglu (2004) developed several ANN models, all of which out-performed other methods of sediment load assessment (Table 4.14). The applicability of ANNs to hysteresis studies was also investigated. The ANN managed to provide a hysteresis loop from data spanning over 150 days, whereas the sediment rating curve, by its nature, did not reproduce hysteresis. Cigizoglu (2004) noted the superiority of ANNs over the conventional methods of prediction due to the non-linear dynamics, generalisation of the whole data set, and lack of constraints or assumptions.

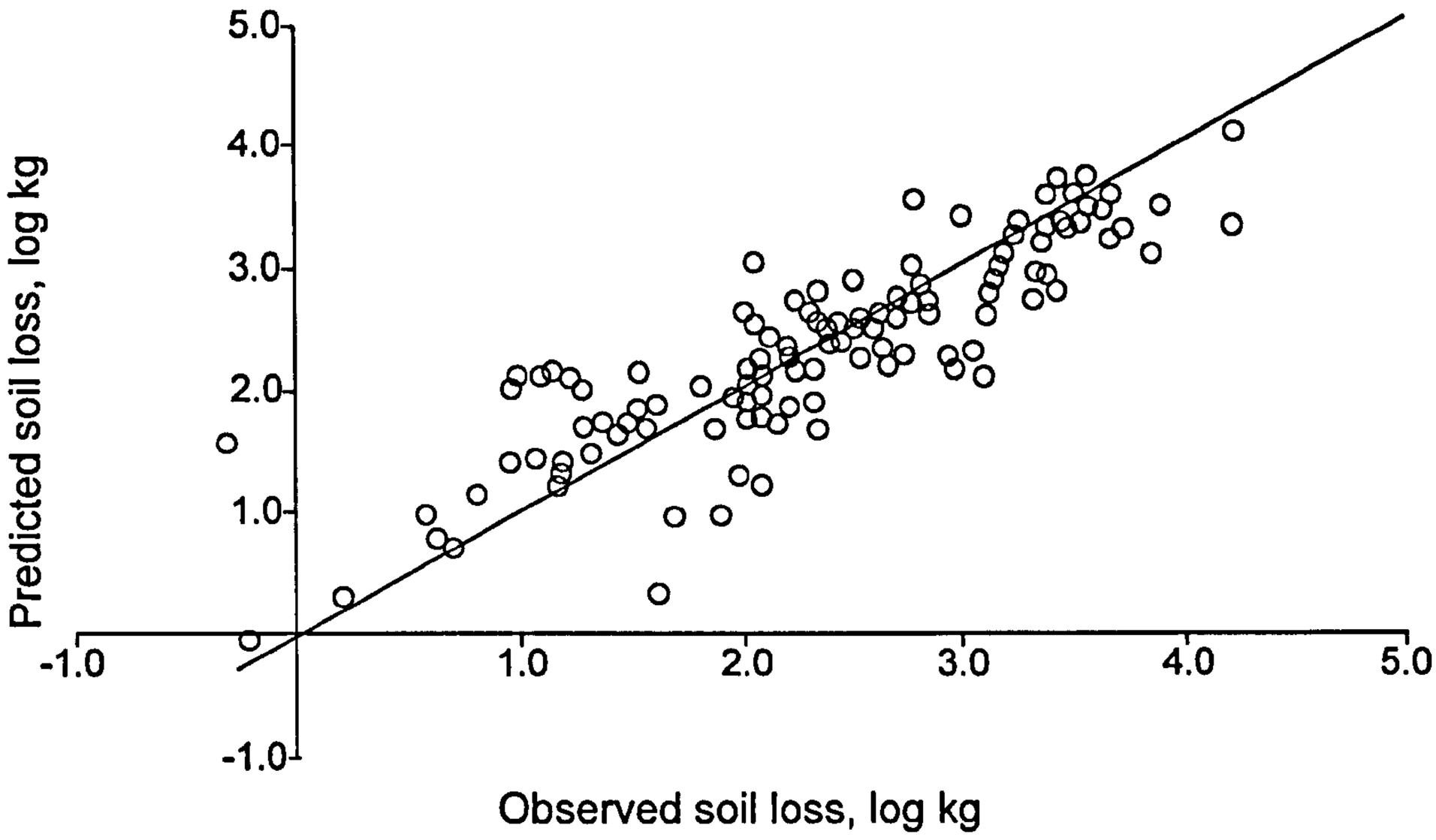

Figure 4.11. Predicted soil loss as a function of observed soil loss for predictions derived by (A) multiple linear regression and (B) ANN. Source: Abrahart & White, 2000.

Table 4.14. The inputs and outputs of the various models for the Schuylhill river, Philadelphia, developed by Cigizoglu (2004). The optimum ANN architecture (performance was assessed by R^2 and RMSE) and compared to TSA and regression models.

ANN Architecture	Inputs & outputs	R^2	RMSE	Comparison with other models
4:5:1	Four previous suspended sediment loads from the downstream station used to predict the current day suspended sediment load at the same station.	0.24	35×10^6 t day^{-1}	Performed better than an autoregressive model with the same inputs.
10:6:1	Ten previous flows from the downstream station used to predict the current day flow at the same station.	0.51	5886 m^3 s^{-1}	Performed better than the above suspended sediment ANN, due to the higher autocorrelation between flows in comparison with sediment loads.
10:6:1	Nine upstream sediment loads (including current day) and a periodicity component used to predict current day sediment load at the downstream station.	0.50	2.2×10^7 t day^{-1}	Performed better than linear multiple regression with the same inputs.
6:4:1	Five flow values (including the current day) and a periodicity component from the downstream station used to predict the downstream sediment load.	0.91	3.9×10^6 t day^{-1}	Performed better than a standard rating curve, which significantly underestimated observed sediment load.

More complex ANNs examining suspended sediment have been developed. Yitian & Gu (2003) developed an ANN which modelled flow and sediment transport in the river system around Dongting Lake, China. The ANN architecture was based on the river network form. Mass conservation was used as the transfer function and was satisfied at each node by a water (w) continuity equation (4.15) and a sediment (s) continuity equation (4.16) using the layer position in the neural network (k); index for the nodes in the previous (i) and current (j) layers; the water/sediment storage/deposition (V); the water/sediment discharge (Q); the weights (ω); the number of nodes in the previous layer (N_k); the sediment transport rate (Q_s) which is equal to the product of discharge (Q) and sediment concentration (C); and time (T).

$$\frac{\partial V_{w,j}^{k+1}}{\partial T} = \sum_{i=1}^{N_k} \omega_{i,j}^{w,k+1} \, Q_{w,i}^{k} \, Q_{w,j}^{k+1}, \tag{4.15}$$

$$\frac{\partial V_{s,j}^{k+1}}{\partial T} = \sum_{i=1}^{N_k} \omega_{i,j}^{s,k+1} \, Q_{s,i}^{k} \, Q_{s,j}^{k+1}. \tag{4.16}$$

Separate simulations were run for sediment transport and water flow due to data availability. Daily discharge and non-point source surface runoff data from 1981-1983 were used to calibrate the ANN for water flow and the 1984 data were used to verify it. The R^2 for the calibration and verification periods were 0.995 and 0.985 respectively and the average error (difference between observed and predicted divided by observed) was 3% and the maximum 6%. Annual sediment discharges at Dongting Lake and various tributaries for 1956-1979 were used to calibrate the sediment ANN and data for 1980-1988 were used to validate it. The R^2 values were 0.997 for the calibration period and 0.986 for the validation period. This study clearly demonstrates that ANNs are capable of modelling flow and sediment transport and, especially with regards to sediment transport, the model is robust enough to be transferred between years. Basing the ANN structure on the river network and the incorporation of the mass conservation functions adds some process knowledge to the model.

4.5.5 Hydrograph partitioning models

Hydrograph partitioning models, sometimes known as cascade tank models, are used in hydrological investigations (e.g. Sugawara, 1961) to analyse the different runoff components of a river but have rarely been applied to suspended sediment studies. Cascade tank models consist of a series, generally three, 'tanks' arranged in a cascade

which represent different layers in the soil profile and separate quickflow, interflow and baseflow components. Applications to suspended sediment studies involve the separation of hydrographs into quickflow, interflow and baseflow components using the cascade tank and the relationships between the SSC series and the different discharge component series are analysed.

The elementary cascade tank model introduced by Sugawara (1961) was used by Okunishi *et al.* (1990) to separate the different components of hydrographs in order to model suspended sediment. Okunishi *et al.* (1990) used hourly time series of rainfall, discharge and suspended sediment from the River Dart to develop the cascade tank model. Hydrographs with a range of peak discharges, preferably multi-peaked hydrographs, were used to adjust the cascade tank parameters. Walling & Kane (1982) and Peart and Walling (1986) established that most suspended sediment transported by the River Dart originated from slopes and so the quickflow component was of most importance in terms of the origin of SSC within the stream. Therefore Okunishi *et al.* (1990) calculated the sediment concentration of quick flow by subtracting the baseflow sediment load from the total sediment load. The calculated quickflow SSC fitted the observed data well except there was a marked difference on the rising limb. Analysis also showed that if quickflow discharge was constant then SSC declined and was attributed to sediment exhaustion effects. Okunishi *et al.* (1990) ignored the interflow component of the storm hydrograph.

Okunishi *et al.* (2000) applied an adapted cascade tank model (Fukushima, 1988) to Yendacott catchment, Devon: a small lowland catchment with subdued relief and predominantly agricultural land. The modified cascade tank was calibrated using multi-peaked long-duration hydrographs. It was suggested that interflow contributed to suspended sediment concentration in the Yendacott catchment and therefore multiple regression was used to calculate the SSC of the quickflow and interflow components; for reasons unexplained by the author saturation overland flow was ignored in the analysis. The SSC of baseflow was ignored, as there were some inaccurate SSC measurements during low flow periods reflecting errors concerning the turbidity meter and the limited contribution of baseflow to total sediment load. The analysis showed that the variation in the SSC of Hortonian overland flow was more variable and an order of magnitude higher than for interflow, except during one high flow event. This exception was explained by a small amount of overland flow and an over-estimation of

peak discharge by the tank model. In general, this approach modelled SSC well but there was a systematic trend for the calculated SSC to peak lower and earlier than the observed values and; the calculated SSC to be over-estimated on the falling limb. This indicates that the varying balance between Hortonian overland flow SSC and interflow SSC during flow events. The variability in overland flow was explained by the variation in the source area of Hortonian overland flow as opposed to sediment exhaustion. The variation in interflow could not be explained (Okunishi *et al.*, 2000).

4.6 Load estimation techniques

It is evident from the literature that there are numerous ways suspended sediment discharge can be calculated once SSC and Q series have been established. Phillips *et al.* (1999) assessed the accuracy and precision of 22 load estimation techniques (Figure 4.12) at different sampling frequencies (weekly, fortnightly and monthly) and catchment scales. This was an important investigation as it established the most accurate and precise method to quantify suspended sediment loads from different catchments sampled at different frequencies: high resolution (15 minute interval) data was available for six sites and was sub-sampled at a variety of frequencies; and infrequent (weekly to monthly) samples were available for a further 23 sites. However, no one load estimation technique was consistently more accurate and precise. Sampling interval was noted to have a variable influence on accuracy but precision clearly decreased as sampling interval increased. Both accuracy and precision were affected by basin scale; both measures decreased as basin size decreased (Phillips *et al.*, 1999).

Dolan *et al.* (1981) also compared various load estimation techniques in an attempt to establish the most accurate and precise method. While most of the methods involved were simple averaging techniques with the data divided into daily, monthly, quarterly, six month or annual time scales or, regressions with the data subdivided into flow stratifications, quarterly, six month or annual time-scales. Beale's ratio estimator stratified by flow was also used (Figure 4.12). The Beale's ratio estimator is a form of statistical estimation in which the annual flow is divided into Q intervals, the average C calculated for each interval, the probability of each Q interval assessed and then multiplied by C and Q for that interval to give total load for that interval. The total loads for each interval are then summed to give total annual load. The root mean square error indicated that Beale's ratio estimator was the best technique, especially when sampling was biased towards high and low flows.

Logarithmically transformed linear regression
$\ln C = \ln a + b \ln Q$

- Data stratified into June-Nov and Dec-May
- Data stratified into March-May, June-Aug, Sept-Nov and Dec-Feb
- Data stratified into rising and falling limb
  - Data stratified into rising and falling limb and March-May, June-Aug, Sept-Nov and Dec-Feb
- Corrected by lognormal correction factor
- Corrected by smearing
- Corrected by $C_n = \frac{C_{S_2}}{C_2} CM1_i$ (Phillips *et al.*, 1999)
- Corrected by $C_n = \left(\frac{C_1}{aQ_1^b} + \frac{t}{T}\left(\frac{C_2}{aQ_2^b} - \frac{C_1}{aQ_1^b}\right)\right) aQ^b$ (Walling, 1984)

Interpolation methods

- Method 1: $L = K\left(\sum_{i=1}^{n} \frac{C_i}{n}\right)\left(\sum_{i}^{n} \frac{Q_i}{n}\right)$
- Method 2: $L = K\sum_{i=1}^{n}\left(\frac{C_i Q_i}{n}\right)$
- Method 3: $L = K\frac{\sum_{i=1}^{n} C_i Q_i}{\sum_{i}^{n} Q_i}\overline{Q_r}$
- Method 4: $L = K\left(\sum_{i=1}^{n} \frac{C_i}{n}\right)\overline{Q_r}$
- Method 5: $L = K\sum_{i=1}^{n}\left(C_i \overline{Q}_p\right)$

Beale's ratio

$$BRE = \left(\frac{1 + \frac{1}{n}\frac{S_{lq}}{\overline{lq}}}{1 + \frac{1}{n}\frac{S_q^2}{\overline{q}^2}}\right) \qquad S_{lq} = \left(\frac{1}{n-1}\right)\left[\sum_{i=1}^{n}(Q_i^2 C_i) - n \times \bar{q} \times \bar{l}\right] \qquad S_q^2 = \left(\frac{1}{n-1}\right)\left[\sum_{i=1}^{n}(Q_i^2) - n \times \bar{q}^2\right]$$

- Data stratified according to whether Q is above or below the mean
- Data stratified according to whether Q is above or below the median

Flow duration rating
$L = \sum_{i}^{ns}(Q_{m_i} \times C_{m_i} \times P_{c_i})$ (Walling, 1984)

- Corrected by lognormal correction factor
- Corrected by smearing

Flow interval
Q divided into equal intervals, mean Q and C calculated for each class and multiplied to give mean load. Total load is calculated by summing the product of each occurring Q and the associated load for the respective Q class. (Verhoff *et al.*, 1980 &Walling, 1984)

Quickflow/baseflow
$L = K(\overline{C_q Q_q}) + K(\overline{C_d Q_d})$ (Phillips *et al.*, 1999)

Figure 4.12. Load estimation techniques as compiled by Phillips *et al.* (1999).

C_i = instantaneous C, C_{ri} = instantaneous corrected C, C_1 = measured C for the previous sample, C_2 = measured C for the next sample, C_{S2} = estimated concentration at time of next sample, Q_i = instantaneous Q, $Q_1 = Q$ at time of collection of C_1, $Q_2 = Q$ at time of collection of C_2, T = time interval between the collection of C_1 and C_2, t = time interval between the collection of C_1 and C_{ri}, n =number of samples, Q_{mi} = median value of Q for the Q interval, $C_{mi} = C$ associated with Q_{mi} (estimated using method 1), P_{ci} = % of Q record associated with Q class, $\overline{C_q}$ = mean quickflow C, $\overline{C_d}$ = mean delayed flow C, CM_i = instantaneous C as estimated by method 1, $\overline{Q_r}$ = mean Q for period between samples, $\overline{Q_q}$ = mean quickflow Q, $\overline{Q_d}$ = mean delayed flow Q, $\overline{Q_p}$ = mean Q for the period of record, $\bar{q}$ = mean flow associated with the sample concentration, $\bar{l}$ = mean load for the occasions on which sample concentrations were obtained, L = total load.

4.7 Chapter summary

This section outlined rating curves, time series analysis, artificial neural networks and hydrograph partitioning models deemed to be appropriate for modelling suspended sediment. No one modelling approach can be declared superior, as their success will depend on what is being modelled, the data available and the trade-off between model complexity and required accuracy and precision. However, if a non-standard rating curves (e.g. those developed using GLMs), artificial neural network or a hydrograph partitioning model is developed then, given their limited application, a basic rating curve model or transfer function should be developed alongside for comparative purposes.

The modelling techniques selected on the basis of this review for this study are rating curves. The methods chosen for rating curve development are OLS regression of naturally log-transformed SSC and discharge and GLMs with a gamma or Gaussian distribution and an identity or log link.

OLS regression was chosen on the basis that it is suitable for the data collected; is the prevalent method in the literature which allows direct comparisons to be made; there are several adaptations that can be developed to allow some degree of process to be incorporated into the model; and the model parameters can be interpreted with reference to the physical system. GLMs were selected as some aspects of these are statistically superior to regression, i.e. back-transformation bias is not an issue; they have a simple one-step procedure; allow different distributions and relationships between the explanatory and response variables, i.e. the model is adjusted to fit the data rather than the data transformed to fit the model; and to the author's knowledge the effect of using a GLM as opposed to an OLS regression model on load estimates has not been investigated previously. GLMs could also be adapted in the same manner as the linear regression models to allow inclusion of some process knowledge. However, this will not be undertaken as identifying patterns is more complex due to the non-linear form of the output and the number of models considered in this study has to be rationalised, given the number of sites.

TSA was not selected given the data demands: collecting a continuous data set at intervals small enough to capture the flashy response of upland streams is problematic. Hydrograph partitioning and ANN methods are more experimental and were not chosen

given the limited nature of the available data sets and the need for rigorous model development given their limited application in determining the relationships between SSC and discharge in the literature.

Chapter Five: STUDY AREAS

5.1 Overview

This chapter provides background on the six study sites of this investigation: Trout Beck, Rough Sike (tributary of Trout Beck), Swinhope Burn, Burnhope Burn, Langtae Burn and Candleseaves. The location, catchment characteristics (geology, soil type, vegetation cover, meteorology and catchment statistics) and rationale for study site selection are given for each. More detailed information is given for Trout Beck and Rough Sike because more background information is available as they are within the Environmental Change Network (ECN) Moor House and Upper Teesdale National Nature Reservoir (NNR) site, where many scientific studies have been undertaken over the last fifty years. This is appropriate because it is in these catchments, where detailed information is available, more in-depth investigations were undertaken, e.g. spatial sampling of suspended sediment.

5.2 Location

This investigation examines suspended sediment delivery and dynamics in upland catchments. There is no statutory definition of upland (or lowland) Britain (Anon, 2003), which is perhaps due to the indistinct nature of the upland/lowland boundary; although arable cultivation can produce a falsely sharp boundary (Atherden, 1992). The definition of the upland-lowland divide can depend on the discipline in which it is being studied. For example, a geomorphologist may loosely define upland and lowland areas by periglacial features, whereas a botanist may define the boundary by plant species. Other measures of the boundary are (1) the absence or scarcity of anthropogenic influence, such as infrastructure, buildings, boundaries and cultivation (Fielding & Haworth, 1999); (2) the cause of the morphology of the landscape: glacial erosion and mass movement generally dominate in upland areas whereas glacial deposition, fluvial

signatures and anthropogenic influence are broadly dominant in lowland areas; (3) a threshold altitude, e.g. 300 m (Atherden, 1992) or 400 m (Ballantyne & Harris, 1994); (4) all land north of a transect connecting the mouths of the Tees and Exe estuaries (Atherden, 1992); and (5) physical characteristics: climate, soil fertility, topography, vegetation type etc. Some classifications are based on a combination of these characteristics. For example, upland was defined as an area with steep slopes, a maximum elevation above 400 m and a thin/discontinuous drift cover by Ballantyne & Harris (1994) and by a combination of several characteristics which gives the area a certain "upland feel" by Atherden (1992). Naturally, many of the upland defining factors are linked to altitude; climate, soil fertility, vegetation type and the abundance or scarcity of anthropogenic activity are all partially influenced by altitude. In this study all land above 400 m is used to define upland.

All the study sites are in northern England (Figure 5.1), five in the north Pennines and one in the northern Lake District. Rough Sike is a tributary of Trout Beck and both are contained within Moor House and Upper Teesdale NNR, northern Pennines. Langtae Burn, Burnhope Burn and Swinhope Burn are in Upper Weardale, the valley to the east of Teesdale. Candleseaves is in the northern Lake District. The grid references of the principal monitoring stations in each catchment are given in Table 5.1.

5.3 Catchment characteristics

The solid and drift geology, soil types, vegetation cover, meteorology and various catchment statistics are outlined below for each study catchment. Catchment photographs are given on Figure 5.2 and catchment maps on Figure 5.3.

5.3.1 Geologies and soil type

The geology and soil cover types of the study sites are broadly similar with the exception of the geology of Candleseaves (Table 5.2). The Pennine catchments are underlain by sedimentary rocks and Candleseaves is underlain by igneous and metamorphic rocks (Table 5.2). Also, all of the catchments except Candleseaves have a surficial geology of glacial drift (Table 5.2), which buffers the influence of the underlying bedrock. Raw oligo-fibrous peat soils dominate each catchment and there is varying proportions of Cambic stagnohumic gleys and Cambic stagnogleys (Table 5.2). The characteristics of the soil types and associated geology are given in Table 5.3. Given the ECN status of the Trout Beck and Rough Sike catchments more detailed

Table 5.1. Catchment grid references, study periods, meteorological characteristics and statistics.

Characteristic	Trout Beck	Rough Sike	Swinhope	Langtae	Burnhope	Candlesaves
Grid reference	NY761337	NY756356	NY897347	NY832384	NY831387	NY279301
Study period	1st October 2001 – 30th September 2002	1st June 1997 – 31st August 1998	18th April 2002 – 17th April 2003	12th July 2000 – 20th March 2001	16th May 2000 – 20th March 2001	1st May 2003 – 30th April 2004
Precipitation, mm yr^{-1}	2052	2184* (1638)	1964	1800* (1475)	1962* (1736)	1887
Average temperature, °C	6.6	8.3	7.4	7.2†	7.2†	7.7
Maximum temperature, °C	21.9	23.9	26.8	19.7†	19.7†	27.0
Minimum temperature, °C	-8.7	-8.7	-9.7	–0.6†	–0.6†	-1.0
Area, km^2	11.83	0.76	3.70	3.00	11.80	0.003
Length, km	7.5	3.0	5.5	9.9	17.5	0.1
Shape**	Rounded	Elongated	Rounded	Elongated	Rounded	Elongated
Stream pattern**	Dendritic	Dendritic	Dendritic	Dendritic	Dendritic	Single thread
General aspect	West	West	West	West	West	East
Average channel slope, m km^{-2}	0.03	0.06	0.07	0.08	0.05	0.08
Relief range, m	525-848	570-746	405-608	400-705	400-746	475-640
Stream order	4	2	3	2	3	1
Drainage density, km km^{-2}	3.15	3.50	2.07	2.30	2.16	210.0
Mean flow, m^3 s^{-1}	1.35	0.06	-	0.22	0.51	0.23*
Peak flow, m^3 s^{-1}	44.68	1.87	-	0.90	2.86	10.45*
Total channel length, km	37.3	2.66	7.7	6.9	25.5	0.63
Land use	Grazing, recreation	Grazing, recreation	Grazing, recreation	Grazing, recreation	Grazing, recreation	Grazing, recreation

*Estimated annual rainfall records as incomplete records due to foot and mouth (Langtae and Burnhope) or equipment malfunction (Rough Sike). Only 0.65 and 0.85 of the year were monitored for Langtae and Burnhope respectively. ** See Figure 4.3 for catchment maps. †Temperature was not recorded at Burnhope and Langtae but mean monthly minimum and maximum values averaged from 1992-1999 were available (Holliday, 2003).

Burnhope: gauging site

Burnhope: catchment view

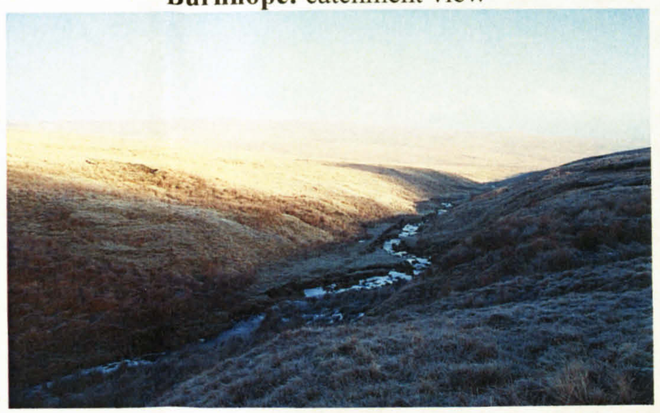

Langtae & Burnhope: catchment view

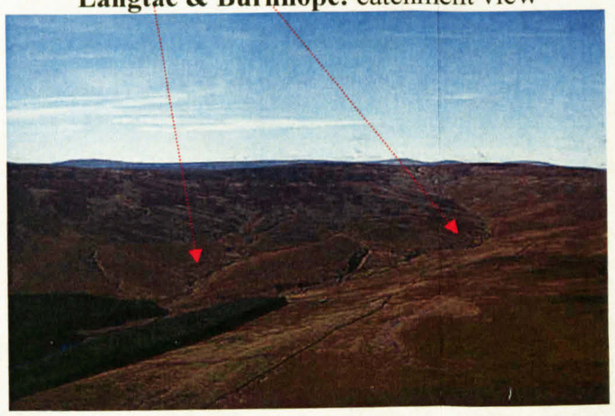

Candleseaves: gauging site

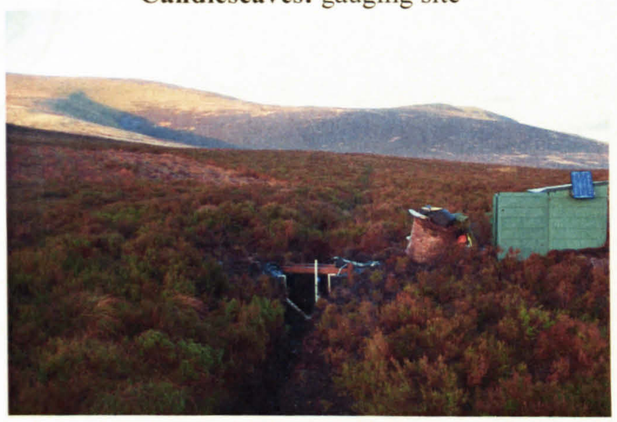

Candleseaves: catchment view

Rough Sike: gauging site

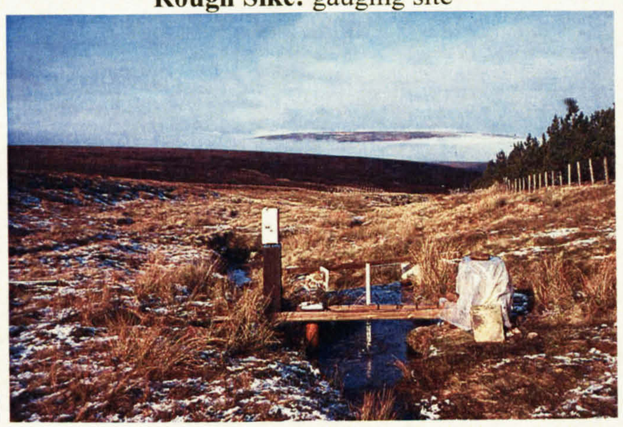

Rough Sike: catchment view

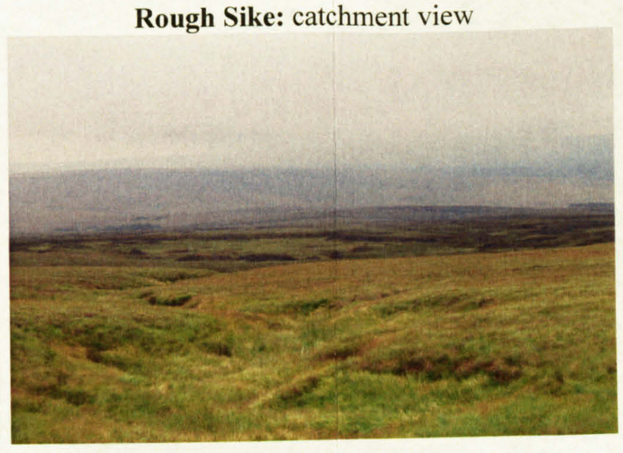

Swinhope: gauging site

Swinhope: catchment view

Trout Beck: gauging site

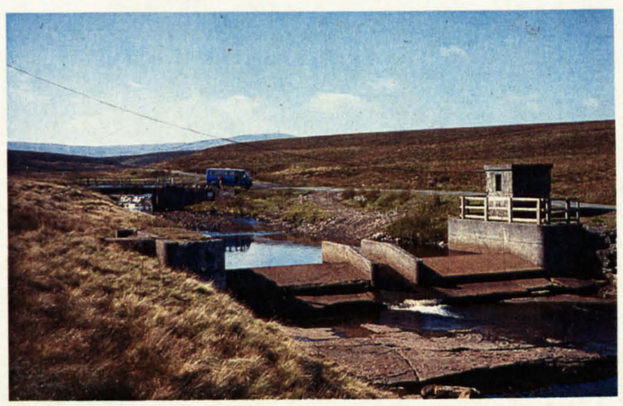

Trout Beck: catchment view

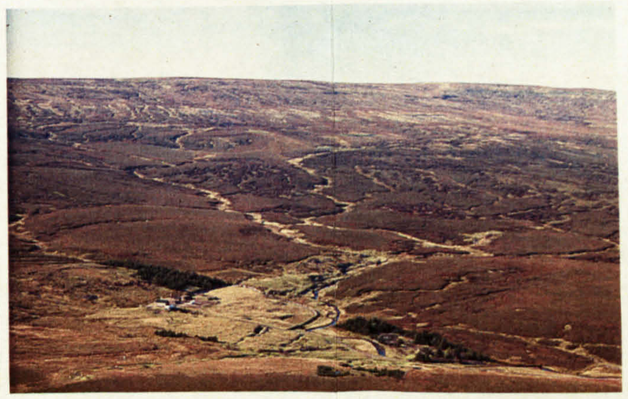

Figure 5.2. Photographs of gauging site and general catchment views for each of the study sites. Red circles indicate the gauging sites on the catchment views, where appropriate.

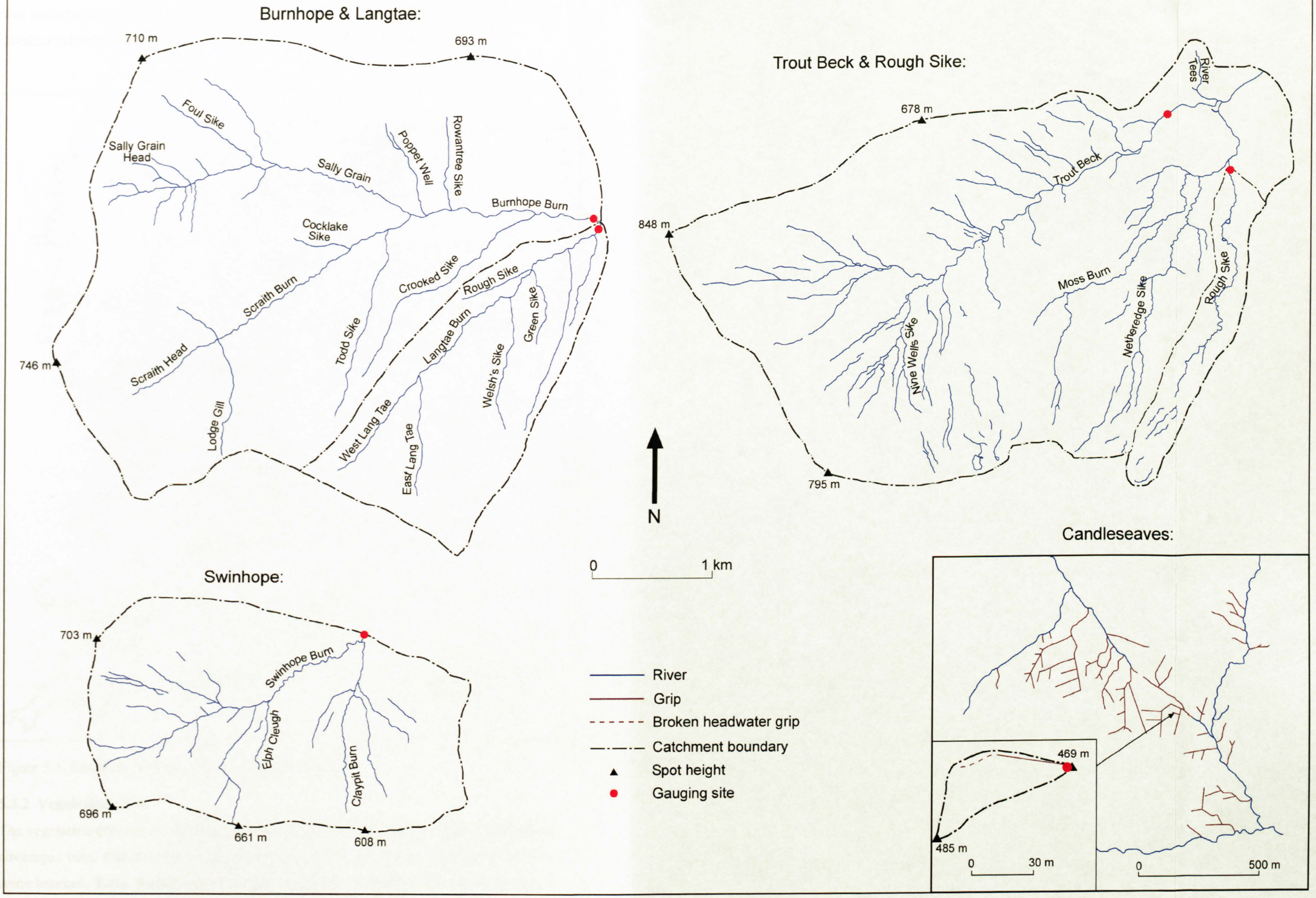

Figure 5.3. Catchment maps for each of the study sites. All catchments drawn to the same scale except Candleseaves.

background information is available. Detailed soil, vegetation and geology mapping was undertaken and GIS coverages developed (ECN, 2004) (Figure 7.3, 7.4 & 7.5). This detailed information is not available for the other study catchments.

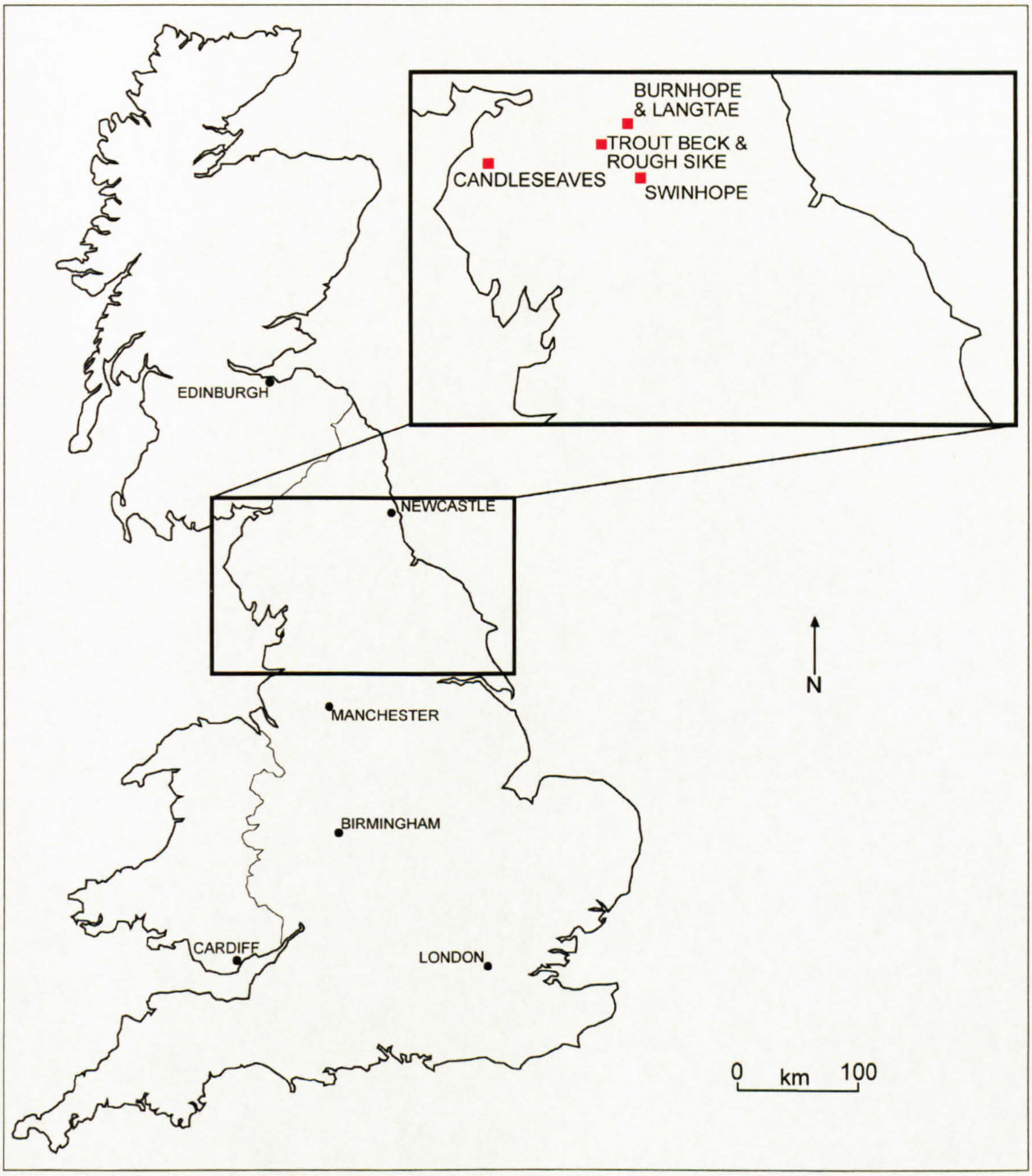

Figure 5.1. Location of study sites in northern England.

5.3.2 Vegetation cover

The vegetation types in all six study catchments are broadly similar (Figure 5.2) but the coverages vary. Candleseaves is dominated by heath with patches of rough grass and some bracken. Trout Beck/Rough Sike are dominated by heath on the flatter areas and rough grasses in the steeper sections and along the channels. There are also patches of

Table 5.2. Catchment geologies and soil type. The geologies of Trout Beck, Rough Sike, Langtae, Burnhope and Swinhope were sourced from the British Geological Survey (1993a). The hard rock geology of Candleseaves was sourced from the British Geological Survey (1993b) and the surficial geology from the Geological Survey of Great Britain, 1973). The soil types of all study sites were sourced from the Soil Survey of England and Wales (1983).

Geology and soil types \ Study site	Burnhope	Candleseaves	Langtae	Rough Sike	Swinhope	Trout Beck
Hard rock geology:						
Carboniferous limestone						
Carboniferous coal sills						
Carboniferous grit sills						
Carboniferous sandstones						
Ordovician mudstones						
Ordovician silty mudstones						
Ordovician siltstones						
Ordovician sandstone						
Surficial geology:						
Alluvium						
Glacial drift						
Hill peat						
Soil type:						
Cambic stagnohumic gley						
Cambic stagnogley						
Raw oligo-fibrous peat						

Table 5.3. Soil types, associated geology and soil and site characteristics of the study sites. Source: Soil Survey of England and Wales, 1983.

Soil type	Geology	Soil & site characteristics
Cambic stagnogley soils	Drift from Palaeozoic sandstone and shale.	Slowly permeable seasonally waterlogged fine loamy, fine loamy over clayey and clayey soils.
Cambic stagnohumic gley soils	Drift from Palaeozoic sandstone, mudstone and shale.	Slowly permeable seasonally waterlogged fine loamy, fine loamy over clayey upland soils with a peaty surface horizon. Coarse loamy soil affected by groundwater in places. Very acid where not limed.
Raw oligo-fibrous peat soils	Blanket peat	Thick very acid raw peat soils. Perennially wet. Hagged and eroded in places.

rushes, bracken and isolated coniferous tree plantations. Bracken, heath and rough grasses dominate at Burnhope and Langtae. Finally, Swinhope is dominated by rough grasses, especially in the lower section of the catchment. There are areas of heath in the upper catchment and patches of bracken and isolated deciduous and coniferous trees throughout. Although there are isolated patches of trees in some catchments none can be described as forested (forest cover is estimated to be less than 1% of the total catchment area).

In addition to variations in the relative coverage of vegetation types there is variation in proportion of unvegetated ground in each catchment. Candleseaves is completely covered by vegetation, as is the vast majority of Swinhope, Burnhope and Langtae (there are some bare patches adjacent to mining areas and river channels). Trout Beck and Rough Sike have noteworthy patches of unvegetated ground and bare peat haggs, 18.5% and 22.5% respectively (ECN, 2004).

5.3.3 Meteorological characteristics

The meteorological characteristics of the study catchments for the year for which suspended sediment loads were calculated are given in Table 5.1. Annual precipitation records were not available for Rough Sike, Langtae or Burnhope due to foot and mouth and equipment failure. Estimates were derived by calculating the average proportion of rainfall that occurred within the missing dates over a 10 year time period from the ECN Moor House record (ECN, 2004) and multiplying the existing records by this[1].

The meteorological characteristics of the study year are given for each catchment as are more relevant to this study than long-term averages. Variation in these characteristics may be partially reflective of inter-annual variability as opposed to between site variability. The annual precipitation ranges from 1800 mm to 2350 mm (Table 5.1). The average temperatures of the study sites are fairly similar: 6.6 – 8.3°C (Table 5.1). The minimum and maximum temperatures differ (Table 5.1) but this may be a result of different locations, shielded/unshielded and sampling strategies rather than a reflection of true differences in catchment conditions.

1

Site	Missing period	Correction factor	Standard error, %
Rough Sike	1st December 1997 – 4th March 1998	1.33	7
Langtae	21st March 2001 – 11th July 2001	1.22	5
Burnhope	21st March 2001 – 15th May 2001	1.13	4

5.3.4 Catchment statistics

The form of study sites includes rounded and elongated catchments with dendritic and single thread channel patterns and a range of stream orders (Table 5.1 and Figure 5.3). The study catchments have a range of catchment areas, 0.003 to 11.83 km^2, and therefore allow the effects of scale to be examined; although some are of similar size to allow the role of other catchment characteristics to be investigated (Table 5.1). The catchments also have a range of average channel slopes, drainage densities and flows (Table 5.1). The land use of all the catchments is the same (grazing and recreation) but this is representative of British upland land use. The relief of the catchments is variable and ranges from a minimum of 400 m a.s.l. to a maximum of 848 m a.s.l (Table 5.1).

5.4 Rationale for site selection

The main criteria for site selection were: the desire to monitor sites representative of the British uplands, use of established monitoring infrastructure, accessibility, logistics of undertaking a water monitoring program in a remote location and possible links to existing and past research (Table 5.4). Candleseaves was specifically chosen to investigate the effects of moorland gripping, a widespread practice in the British uplands which is now beginning to be reversed. Rough Sike and Trout Beck were both monitored to investigate the effects of scale in the same catchment while other characteristics are uniform and also because of the wealth of existing data given the ECN status of the site. Burnhope and Langtae, although not nested, allow comparison of very similar catchments in most aspects except scale. Swinhope and Langtae offer the chance to compare catchments of the same scale as do Trout Beck and Burnhope. The study sites are all within northern England which, although it does not give good spatial coverage of Britain, was necessary for logistical reasons.

Table 5.4. Existing infrastructure and existing data at the study sites.

Existing infrastructure and data \ Study site	Burnhope	Candleseaves	Langtae	Rough Sike	Swinhope	Trout Beck
Existing Q recording infrastructure	■	■	■	■	■	■
Existing precipitation recording infrastructure	■	■	■	■	■	■
Existing temperature recording infrastructure		■		■		■
Existing SSC records	■	■	■			
Existing automatic weather station				■		■
Historic suspended sediment load study				■		

5.5 Chapter summary

In summary the study sites have broadly similar soil types and vegetation covers but they fall into two groups in terms of the geology: Candleseaves is underlain by igneous and metamorphic rocks whereas the remaining catchments, which are all in the Pennines, are underlain by sedimentary rocks. In terms of catchment statistics the study catchments primarily differ in terms of scale, gradient, stream order, drainage density and flow. The annual precipitation of the study catchments ranges from 1800 mm yr^{-1} at Langtae to 2184 mm yr^{-1} at Rough Sike. This is likely to be more a reflection of inter-annual variability as opposed to a genuine climatological difference. The study sites are representative of upland catchments within Britain, and while not spatially distributed throughout Britain, will allow valuable insights into suspended sediment dynamics and fluxes in upland catchments.

Chapter Six: FIELD AND LABORATORY METHODS

6.1 Overview

This chapter outlines the field monitoring techniques and frameworks for each site. The laboratory methods are described and linked to the field sampling regime.

6.2 Field monitoring

Field data collection involved methods used to record discharge; precipitation; surface moisture; surface wetness; and sampling of suspended sediment (auto-samples, gulp samples and time-integrated mass samples) and source sediment (surface and channel bed). There is a need for collection of these basic data as limited records exist for small upland catchments. The suspended sediment sampling methods used were selected after careful consideration of the methods outlined in Chapter 3 and their applicability to the upland environments of the study sites. Additional field monitoring was undertaken in Moor House and Upper Teesdale NNR, which incorporates Rough Sike and Trout Beck, to examine the spatial controls over suspended sediment delivery. The justification for this was the wealth of background information available given its ECN status and because of the nested nature of Rough Sike and Trout Beck catchments, which allows the effect of scale to be examined with relatively similar catchment characteristics.

6.2.1 Discharge

Different methods were used to monitor discharge at the study sites, given the presence of existing infrastructure (Table 6.1). At all sites the discharge measurement interval was 15 minutes. Discharge measurements were provided by the Environment Agency

Table 6.1. Summary of the field data collection undertaken at each site.

Field data type	Burnhope	Candleseaves	Langtae	Swinhope	Rough Sike	Trout Beck
Discharge:						
Interval, minutes	15	15	15	15	15	15
Method	Velocity-area	V-notch weir	Velocity-area	Velocity-area	Rectangular weir	Crump weir
Annual record period	16/05/00 – 20/03/01	01/05/03 – 30/04/04	12/07/00 – 20/03/01	18/04/02 – 17/04/02	01/08/97 – 31/07/98	01/10/01-30/09/02
Notes	Incomplete annual record due to foot and mouth		Incomplete annual record due to foot and mouth	Higher stages not correlated with Q		Gaps in record filled in by correlation with Upper Tees gauging site
Precipitation:						
Interval, minutes	15	15	15	15	60	60
Method	Tipping bucket	Tipping bucket	Tipping bucket	Tipping bucket	Automatic weather station	Automatic weather station
Notes					Gap from 01/12/97 – 04/03/98	
Surface moisture:	None	None	None	None	Hourly	None
Surface wetness:	None	None	None	None	Hourly	Hourly
Suspended sediment:						
Auto-sampler:						
Fixed-interval	701 at 6 and 12 hr intervals	0	458 at 6 and 12 hr intervals	0	0	129 at 8 hr intervals
Storm	503 at 5 and 15 minute intervals	206 at 5 minutes intervals for the first 13 samples and 10 for the last 11.	0	572 at 10 minute intervals	522 at 5, 15, 30 and 40 minute intervals	224 at 15 minute intervals
TIMS:						
Number	0	0	0	3	21, some subsequently removed by high flows	
Time period				26/02/03 – 23/04/04	10/07/02 – 16/10/03	
Gulp samples:	0	0	0	2 sets of 3 from 1 event	9 sets of 9 from 4 events	
Sediment sources	None	None	None	None	Range of samples from potential sources: peat banks, soil, floodplain sediment, till.	
Bed sediment storage	None	None	None	None	8	

(EA) for Trout Beck: stage was measured by a pressure transducer at a crump weir and transformed into discharge using an established stage-discharge relationship. There is a short gap in the record due to data loss during foot and mouth (01/10/01 to 11/11/01). However, the River Tees is monitored in close proximity to the EA gauging station on Trout Beck (Figure 6.1) and a regression relationship relating the two sites allowed the missing discharge measurements for Trout Beck to be calculated.

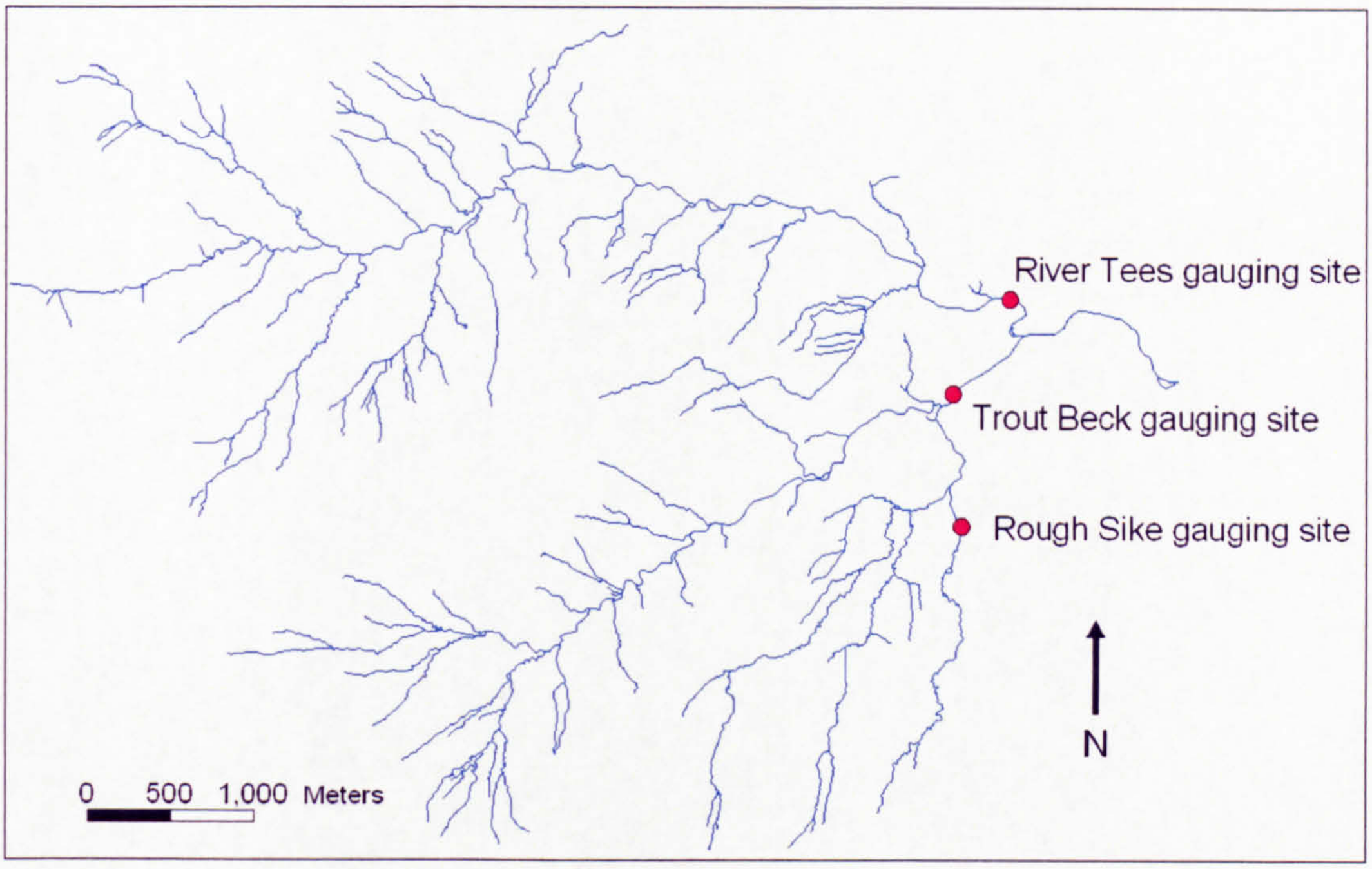

Figure 6.1. Location of Trout Beck, Rough Sike and River Tees gauging sites.

Local stage was recorded every 15 minutes at Rough Sike, Candleseaves, Burnhope, Langtae and Swinhope using pressure transducers and Campbell CR10X, CR10 and CR500 data loggers. The pressure transducers were housed in stilling wells to damp the effect of water surface disturbance (Figure 6.2). A rating between stage and discharge was established and the stage record converted to discharge.

At Swinhope discharge was established by the velocity-area method. Velocity was measured using a Valeport electromagnetic velocity meter at 0.6 of water depth (Riggs, 1985) in 10 cm wide cells across the channel (this ensured at least ten readings were taken). The same method was used for Burnhope and Langtae (Holliday, 2003). Due to the travel distance to Swinhope and the flashy nature of the system the highest discharges in the study period were not measured and it was not possible to reliably extrapolate the stage-discharge curve to the maximum stage using the methods suggested by Herschy (1995). However, it was possible to reliably extrapolate the stage-

Figure 6.2. Example of typical sampling equipment at Swinhope. Rain gauge is approximately 5 m to the right.

Figure 6.3. Weir at Candleseaves

discharge curve to the bankfull discharge, as determined by Warburton (pers. comm.), as there are no abrupt changes in the channel form.

Stage was recorded at Rough Sike at a sharp-edged rectangular weir. The stage record was converted into discharge using an empirical relation for sharp-edged rectangular weirs and this was calibrated in the field. Stage was recorded at Candleseaves at a V-notch weir (Figure 6.3) and an empirical relation for 90° V-notch weir was used to derive discharge and was calibrated in the field.

Bed movement (erosion or deposition), ice, aquatic growth and human induced change potentially introduce error into stage-discharge relationships (Herschy, 1998). Human disturbance is of limited concern at the study sites due to their remote locations and there is limited aquatic growth given the climate. Ice may have occasionally influenced the relationship (ice on the water surface would cause an over-estimation in discharge) but not as significantly as in rivers which experience long-term and thick ice cover. Bed movement is the most likely cause of error in the stage-discharge relationship at the study sites of this investigation. To gauge if there was substantial bed movement at Swinhope, Burnhope and Langtae during the study period measurements of the bed level from a datum were taken periodically. The bed at all three sites was stable during the monitoring period.

Other potential sources of error in discharge measurements arise from instrumental bias and operator error. Herschy (1998) stated attainable uncertainties (95% level) of 5-10% for electromagnetic discharge measurement such as those at Swinhope, Burnhope and Langtae; 5% for crump weirs as at Trout Beck; 2% for thin plate V notch as at Candleseaves; and 5% for rectangular weirs as at Rough Sike. Attempts were made to minimise errors by taking repeat measurements and no substantial errors were detected.

6.2.2 Precipitation

Rainfall was recorded at all seven study sites. The rainfall data for Trout Beck and Rough Sike was provided by ECN (2004), measured hourly by an automatic weather station (Table 6.1). Rainfall at Candleseaves, Burnhope, Langtae and Swinhope was measured using tipping bucket rain gauges (Figure 6.4) in conjunction with Campbell data loggers (Table 6.1). The loggers recorded the number of tips in every 15 min interval which were converted into millimetres.

Figure 6.4. Tipping bucket rain gauge at Swinhope.

Snowfall was not measured directly at any of the study sites. This is unfortunate due to the proven difference of suspended sediment response to rainfall and snowmelt-induced runoff (Lenzi & Marchi, 2000). However, snowmelt was monitored indirectly by the rainfall gauges as snow which landed in the rain gauge top melted and this was recorded. Furthermore, there was no substantial snowfall in the study periods.

6.2.3 Surface conditions

Soil moisture was measured using a gypsum block 20 cm under the grass and this data was only available for Rough Sike. Surface wetness is defined as the number of minutes the ground surface was wet for per hour and were only available for Trout Beck and Rough Sike. Surface wetness and soil moisture were measured hourly (Table 6.1) by the automatic weather station maintained by ECN (ECN, 2004) at Moor House and Upper Teesdale NNR.

6.2.4 Suspended sediment

Suspended sediment was measured using three different sampling techniques: auto-samplers, time-integrated mass samplers (TIMS) and gulp samplers.

6.2.4.1 Automated samplers

Two types of auto-sampler were used (Rock and Taylor and American Sigma 900/900MAX) but the main difference relevant to this study is that the Rock and Taylor samplers have a 48 bottle capacity and the Sigma samplers a 24 bottle capacity. The

bottle volumes for both samplers was 500 ml. The intake nozzles were located to minimise sample contamination by bed and bank material but low enough in the channel to ensure low flows were sampled. The auto-samplers were run on one of two sampling regimes: fixed-interval or storm-triggered. Fixed-interval sampling was undertaken at Trout Beck, Langtae and Burnhope and the intervals were either 6, 8 or 12 hours (Table 6.1). Storm sampling, using a level switch, was undertaken at all sites except Langtae. The intervals between the samples in the storm-triggered sampling were 10 minutes at Swinhope; 15 minutes at Trout Beck; 5, 15, 30 and 40 minutes at Rough Sike; 5 and 15 minutes at Burnhope; and 5 minutes for the first 13 samples and 10 minutes for the remaining 11 at Candleseaves (Table 6.1). The different sampling intervals were chosen to ensure complete storm events were sampled at the highest possible resolution and reflect the responsiveness of the system. Logistics (e.g. access to the sites), disturbance by livestock, technical problems, and prolonged spells of low stage prevented regular sampling throughout the entire study period.

6.2.4.2 Time-integrated mass samplers

Time-integrated mass samplers (TIMS) (Figure 3.1), as designed by Phillips *et al.* (2000), were used to collect time-integrated bulk sediment samples. The TIMS were constructed of 95 cm lengths of 9 cm diameter polyvinylchloride pipe sealed with plastic caps threaded with 8 mm internal diameter hosepipe inlet/outlet tubing. Funnels were placed over the end caps, with the inlet/outlet tubing threaded through, to reduce hydrodynamic disturbance. The TIMS were fixed approximately 8 cm above the channel bed using metal stakes and cable ties. The internal diameter of the TIMS constructed for this study was reduced from 98 mm, as designed by Phillips *et al.* (2000), to 90 mm due to the logistics of collecting several throughout the stream network.

Twenty-one TIMS were originally deployed throughout the stream network at Moor House (Figure 6.5) and were emptied and reset approximately every month (Figure 6.6). However, access problems and high river stage caused variable deployment times and some TIMS were lost during high flow events (Figure 6.6). Three TIMS were deployed at Swinhope and were emptied and reset approximately every month, access and river stage allowing. One TIMS was deployed at Candleseaves approximately 5 m upstream from the gauging site and was emptied once per month. The TIMS were emptied into 5 l water containers in the field to allow continuous monitoring of suspended sediment.

No TIMS were deployed in Burnhope or Langtae (Table 6.1).

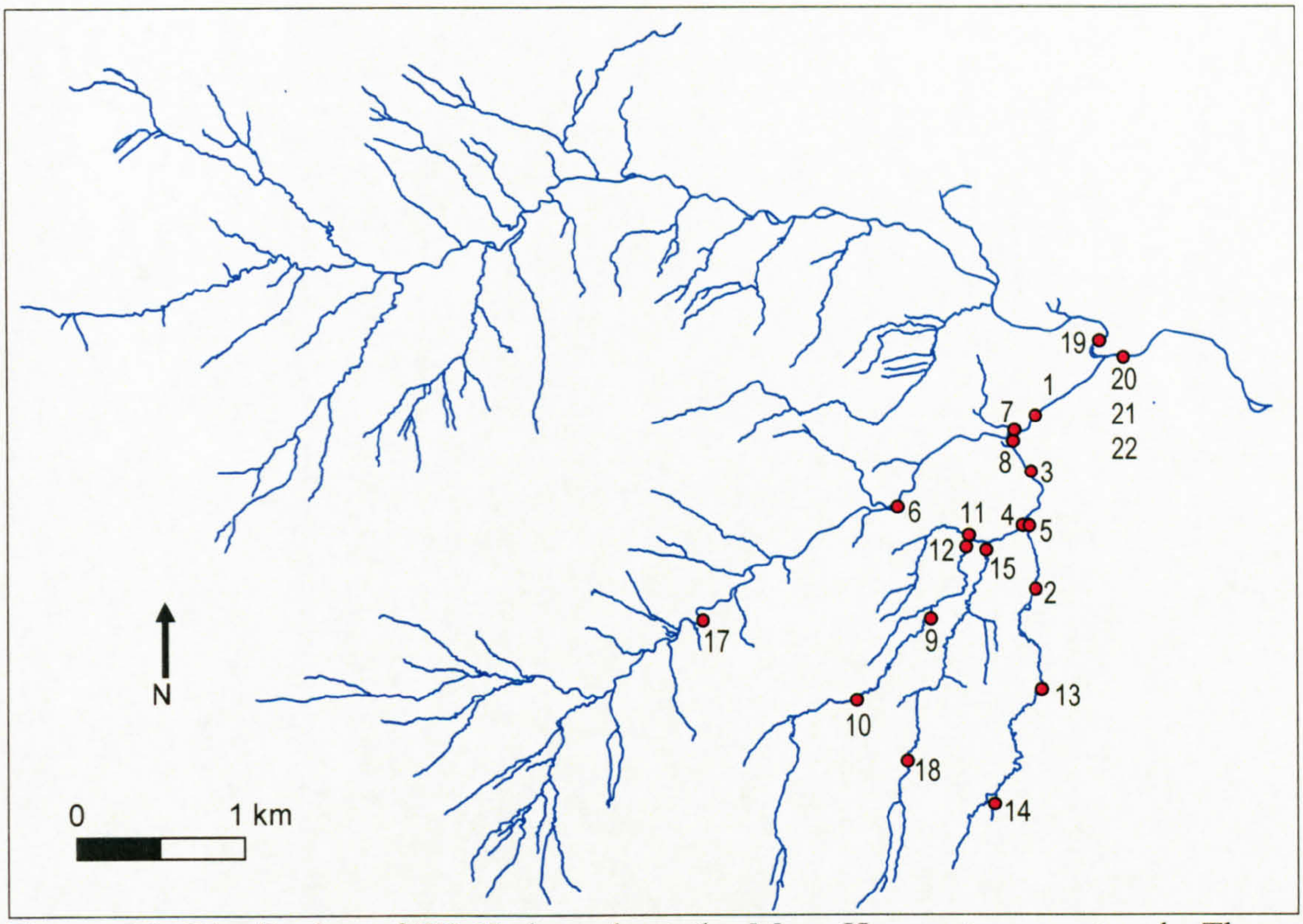

Figure 6.5. Distribution of TIMS throughout the Moor House stream network. The entire stream network is displayed in order to show the contributing catchments to each TIMS.

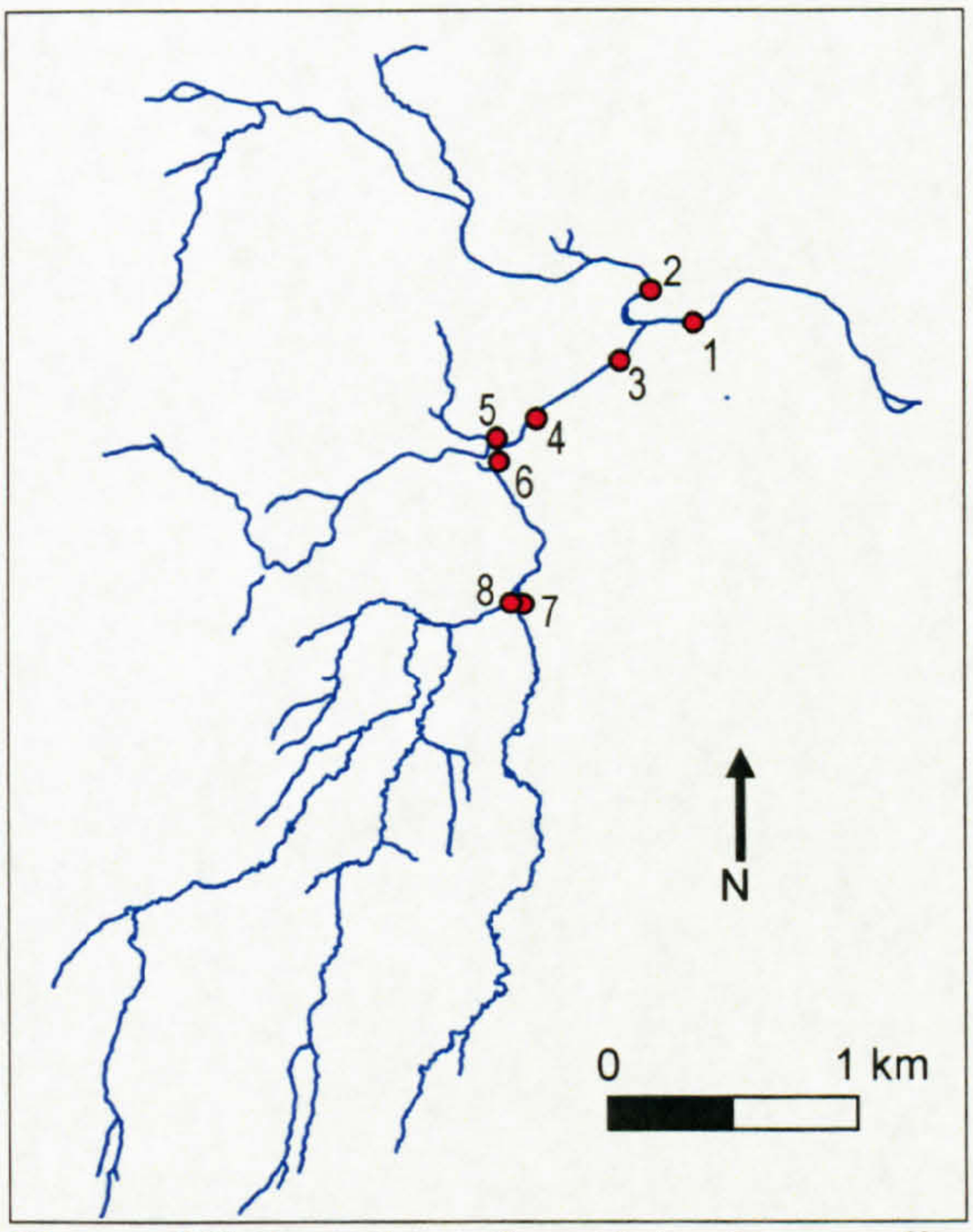

Figure 6.7. Location of spatial gulp sampling points in the Moor House stream network.

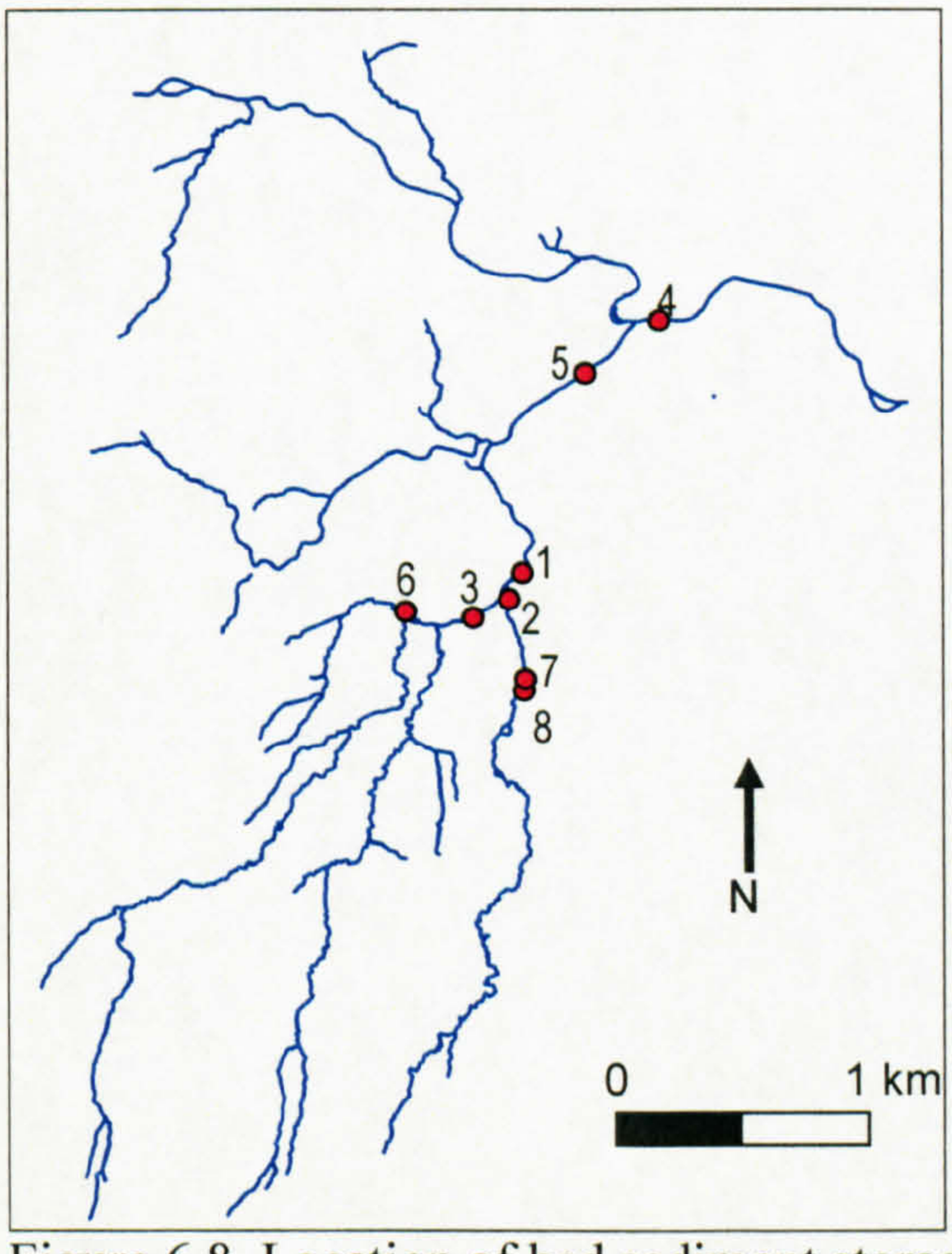

Figure 6.8. Location of bed sediment storage experiments in the Moor House stream network.

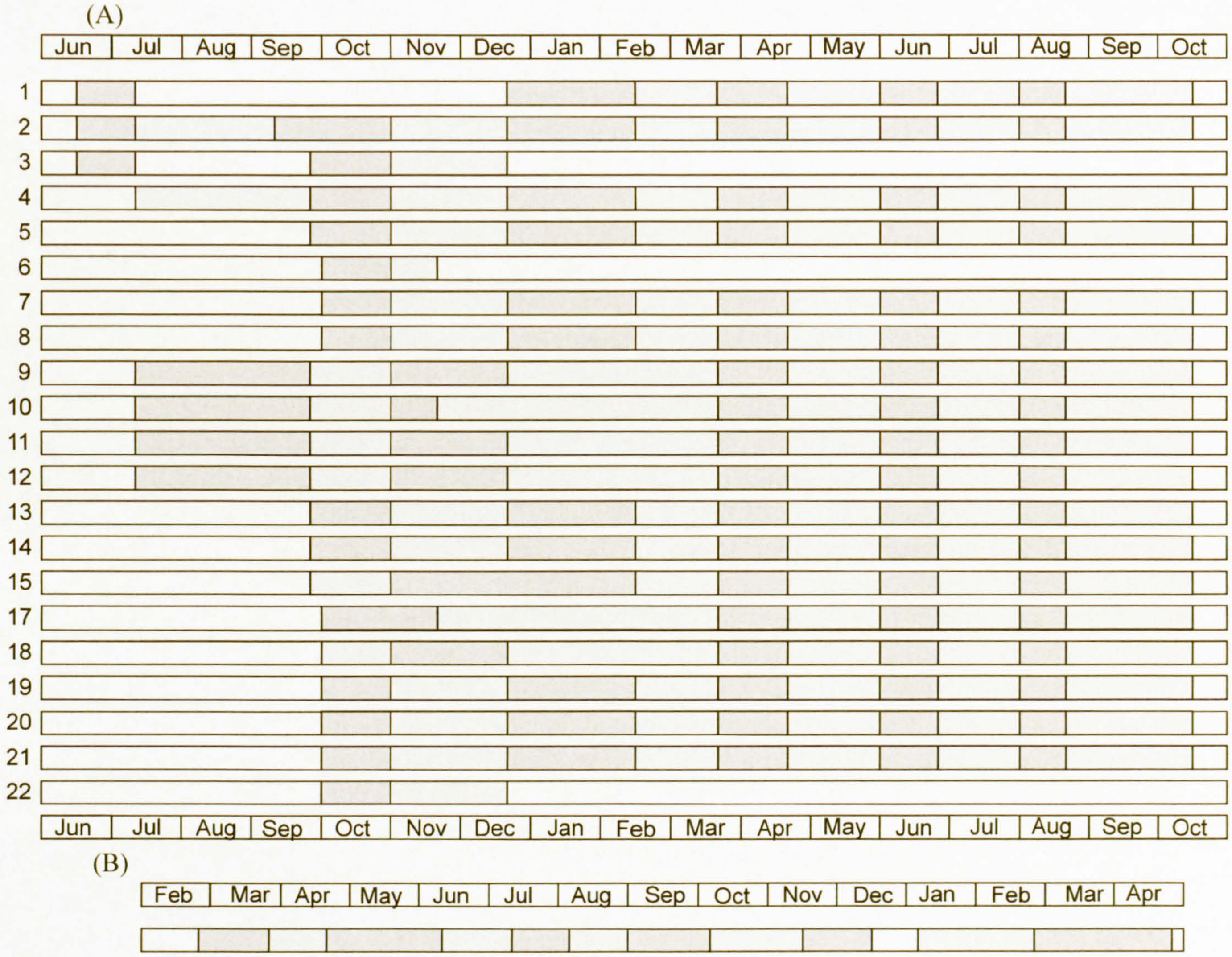

Figure 6.6. Calendar of TIMS deployment times at (A) Moor House and (B) Swinhope. All three TIMS at Swinhope were reset at the same time. Shaded boxes (light and dark) represent deployment periods, white boxes represent gaps in the record (due to the TIMS being washed away).

6.2.4.3 Gulp samplers

Gulp samples were taken using 500 ml wide-necked sample bottles which were pre-rinsed at the sampling location. The samples were taken as far from the stream bank as possible to avoid any local bank erosion and low velocity effects. Nine sets of gulp samples (during five high flow events) were taken at eight locations in Moor House and Upper Teesdale NNR (Figure 6.7) to allow the spatial variability of SSC to be assessed (Table 6.1). Spatial samples were also taken at Swinhope but only two sets were taken during one storm event (the samples were taken by hand and therefore were reliant on the discharge conditions during site visits) (Table 6.1).

6.2.5 Sediment source samples

Sediment source samples were collected from the Rough Sike and Trout Beck catchments using a stainless steel trowel and sealed in a plastic bag. The trowel was cleaned between each sample. Sediment source samples were only collected from the Trout Beck and Rough Sike catchments as these catchments are the focus of the examination of the spatial controls on suspended sediment delivery. The samples were colleted in order to compare them with the suspended sediment sampled retained by the TIMS.

6.2.6 Bed sediment storage

Bed sediment storage experiments were undertaken in the channel network at Moor House (Figure 6.8). The specific locations were chosen to ensure a range of flow velocities, bed surface sediment distributions and coverages of periphyton were sampled. The experiments were undertaken on the 9th and 10th of July 2002 and the flow conditions remained stable over these two days. These experiments were only undertaken within the Moor House channel network as it was the focus of the examination of the spatial controls over suspended sediment delivery. The method outlined by Lambert and Walling (1988) was used to assess bed sediment storage. The procedure was as follows:

(1) A steel ring was inserted into the channel bed ensuring there was no through-flow of water.

(2) The water level in the ring was noted by taking three depth measurements. These were combined with the ring area to calculate the volume of water isolated in the ring.

(3) The location in the stream network, within the local channel area and flow conditions were noted.

(4) The water in the ring was agitated for one minute and three 500 ml samples were taken. This simulates a flood event with no bed movement.

(5) The bed surface was gently agitated for one minute and three 500 ml samples were taken. This simulates a flood event with limited bed movement.

(6) The bed surface was vigorously agitated for one minute and three 500 ml samples were taken. This simulates a flood event with severe bed movement.

(7) Sediment samples were collected from the surface and sub-surface (the boundary defined by the depth of the largest clast on the surface) of the channel next to the water's edge. These samples were not taken where the bed sediment storage experiment was conducted as the fine fraction would be under-sampled.

6.3 Laboratory analysis

This section outlines the laboratory methods used to determine the suspended sediment concentration (SSC) of the auto-sampler, spatial and bed sediment storage water samples; the grain size of the bed sediment storage samples; the dry sediment weight of TIMS samples; the geochemistry of the TIMS and sediment sources samples; and the organic matter content of the TIMS sediment samples.

6.3.1 Determination of suspended sediment concentration

The SSC of the auto-sampler, gulp samples, and bed sediment storage samples were determined using a vacuum filtration method:

(1) Whatman GF/C 47mm glass microfibre filter papers (retain particles >1.2 μm) were placed in numbered tin dishes and weighed to an accuracy of 0.0001 g (m_1).

(2) The volume (in ml) of the sample was measured using a measuring cylinder (v).

(3) The associated filter paper was placed on a filter holder under vacuum.

(4) The sample was poured into the filter holder.

(5) The measuring cylinder and sample bottle were rinsed with distilled water to remove any remaining sediment.

(6) When no water remained in the vacuum pump the sides were rinsed with distilled water to ensure all sediment was on the filter paper.

(7) The filter paper was removed and placed back in the tin dish.

(8) Steps 2 to 7 were repeated with the remaining samples.

(9) The tin dishes containing the filter papers were placed in an oven at 105°C for 24 hours.

(10) The tin dishes were places in a desiccator to cool.

(11) The filter papers and tin dishes were reweighed (m_2).

The volume and mass data were then entered into a spreadsheet and SSC, in mg l^{-1}, calculated by:

$$SSC = (m_2 - m_1)/v. \quad (6.1)$$

This is the standard method and filter paper size used in the literature and therefore allows direct comparison of the results. Some samples contained too much sediment to be efficiently measured by vacuum filtration and the following procedure was followed:

(1) The water levels were marked on the sample bottles.

(2) Glass beakers were numbered and weighed to 0.0001 g (m_1).

(3) The sample bottles were shaken, the contents poured into the beakers and any remaining sediment flushed out with distilled water.

(4) The sample bottles were filled up to the mark with tap water, emptied into a measuring cylinder and the volume recorded (v).

(5) The beakers were placed in an oven at 105°C until all the water evaporated and the sediment dried.

(6) The beakers, with dried sediment, were reweighed (m_2).

The SSC was calculated using the same formula as (6.1).

If there was a delay between collection and processing the water samples were stored in a fridge at 3°C to prevent algal growth given the bias that this would introduce. During summer months samples were inspected on return to the laboratory and if algal growth had occurred while in the field, samples affected in this manner were discarded.

6.3.2 Time-integrated mass sampler processing

The TIMS samples in the five litre water containers were stored in a fridge at 3°C until processed. The dry weights of the sediment were determined by the following method:

(1) Large glass tanks were labelled and rinsed with distilled water.

(2) The TIMS samples were emptied into the tanks and any remaining sediment was flushed out with distilled water.

(3) The tanks were covered and left until the sediment settled out (up to one week).

(4) Excess water was siphoned off.

(5) Sediment was left to air dry in the tanks.

(6) Sample bags were labelled, placed on the balance and the balance zeroed.

(7) The sediment was brushed out the tanks into the sample bag which was then reweighed to 0.0001 g.

Once bagged the samples were stored in a fridge ready for future analysis.

6.3.3 Geochemical analysis

Some of the TIMS and sediment source samples were analysed for 44 elements (Table 6.2). All except Al, Ca, Mg, Na and Si were determined using a Perkin Elmer ELAN 6100 DRC PLUS inductively-coupled mass spectrometer (ICP-MS) using Primar-MS calibration standard solution. Al, Ca, Mg, Na and Si were determined used a VARIAN 220-FS atomic absorption spectrometer (AAS) using AA standard solution. An ICP-MS was used to allow rapid analysis of a wide range of elements at low concentrations. Al, Ca, Mg, Na and Si were analysed separately using AAS as the concentrations were very high. Prior to analysis the samples were disaggregated and oven dried at 105°C for 24 hours. A representative 0.5 g sub-sample was taken and digested using a total digest method (9 ml of concentrated nitric acid and 3 ml of hydrofluoric acid for 15 minutes using a microwave system) (US EPA Method 3052).

Table 6.2. Analysed elements sorted by element group.

Element group	Element
Alkali metal	lithium (Li), sodium (Na), potassium (K).
Alkali earth metal	magnesium (Mg), calcium (Ca), strontium (Sr), beryllium (Be).
Semi-metal	silicon (Si), antimony (Sb), arsenic (As), boron (B).
Basic metal	aluminium (Al), thallium (Tl), lead (Pb), bismuth (Bi).
Transition metal	yttrium (Y), scandium (Sc), molybdenum (Mo), silver (Ag), cadmium (Cd), titanium (Ti), vanadium (V), chromium (Cr), manganese (Mn), iron (Fe), nickel (Ni), cobalt (Co), copper (Cu), zinc (Zn).
Non-metal	selenium (Se).
Rare earth	samarium (Sm), ytterbium (Yb), neodymium (Nd), dysprosium (Dy), lanthanum (La), erbium (Er), lutetium (Lu), terbium (Tb), europium (Eu), thulium (Tm), gadolinium (Gd), praseodymium (Pr), cerium (Ce), holmium (Ho).

6.3.4 Particle size analysis – coarse fraction

The particle size distributions of the bed sediment storage samples were determined by the standard method:

(1) The sediment was air dried.

(2) Clasts larger than 32 mm were removed.

(3) The sediment finer than 32 mm was placed into a sieve stack ranging from 32 mm to < 63 μm and shook on a sieve shaker for ten minutes.

(4) The contents of each sieve were weighed.

(5) The percentage of sediment in each grain size class was calculated.

The finer than 63 μm fraction was not analysed given the problems measuring organic sediment with available equipment (laser granulometer).

6.3.5 Organic matter analysis

The organic matter content of sediment is determined by dissolving or destroying the organic matter. Dissolving the organic matter is problematic as no solvent has been found which induces all the organic matter into solution. Destruction of the organic matter is also difficult as the inorganic fraction has a tendency to be affected. Organic matter is destroyed by either oxidation or burning. Incomplete oxidation tends to give variable results and therefore loss-on-ignition (LOI) (burning) is most widely used and was used in this study. However, LOI is also an imperfect measure of the organic content as some weight loss may be due to the dehydroxylation (loss of structural water) and decomposition of inorganics, especially in clay-enriched soils with low organic content (e.g. Howard and Howard, 1990). Several studies have been undertaken to evaluate the optimal temperature and heating time (e.g. Storer, 1984). The findings from these studies indicate that a temperature of 400 to 450°C for 8-16 hours removes all of the organic and minimises the decomposition of the inorganic fraction and dehydroxylation (Nelson and Sommers, 1996). Based on this the procedure followed for LOI was:

(1) Representative 2.0 – 5.0 g sub-samples of sediment were disaggregated.

(2) The sub-samples were oven dried at 105°C for 24 hours.

(3) Empty crucibles were weighed to 0.0001 g (m_c).

(4) The sediment sub-samples were placed into the crucibles and the mass recorded to 1/1000th g (m_o).

(5) The crucibles were placed in a muffle furnace at 400°C for 16 hours.

(6) The crucibles were removed and placed on a wire rack to cool for 15 minutes.

(7) The crucibles were placed in a desiccator and left to cool completely.

(8) The crucibles were reweighed to 0.0001 g (m_i).

The percentage organic matter was then calculated by:

$$100\ [(m_o - m_i) / (m_o - m_c)]. \qquad (6.2)$$

6.4 Chapter summary

This chapter outlines the field and laboratory methods used to obtain the data for subsequent analysis. The methods selected are the standard methods within the literature deemed most suitable to upland environments. This allows direct comparison with existing studies.

A summary of the field data collection methods and associated information is given in Table 6.1. The field data collection strategy is motivated by two facets of investigation:

(1) Establishing relationships between SSC and discharge for each of the study sites, including examination of the variations in the SSC-discharge relationship between storm events. The variation in the SSC-discharge relationship is examined with reference to antecedent catchment conditions and storm characteristics. This requires discharge, precipitation, surface moisture, surface wetness and auto-sampler SSC data (Figure 6.9).

(2) Examining the spatial controls on suspended sediment delivery. This focuses on Moor House and Upper Teesdale NNR given the wealth of information already available as a result of its ECN status. The discharge, TIMS sediment, gulp sample SSC, sediment source and bed sediment storage field data collection are required for this (Figure 6.9). The links between the samples collected and the various laboratory analyses are also summarised in Figure 6.9.

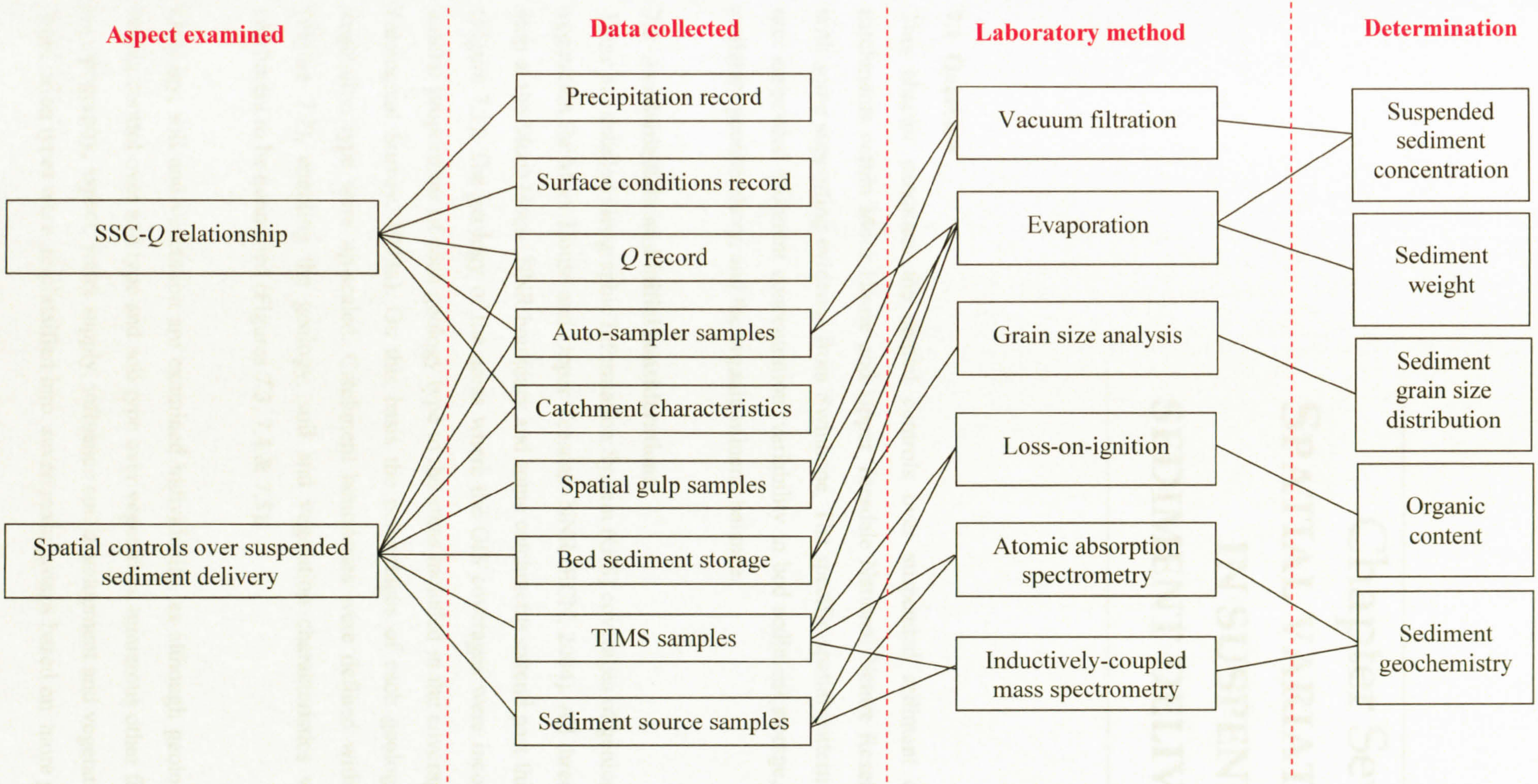

Figure 6.9. The relations between the aspects of suspended sediment dynamics and delivery examined in this study, data collected and the laboratory analysis. Catchment characteristics refers to catchment area, geology, soil type and vegetation cover obtained from maps and GIS coverages sourced from ECN (2004). TIMS: time-integrated mass sampler.

Chapter Seven: SPATIAL VARIATION IN SUSPENDED SEDIMENT DELIVERY

7.1 Overview

This chapter examines the spatial controls over suspended sediment delivery in catchments within Moor House and Upper Teesdale National Nature Reserve (NNR), with some supporting evidence from Swinhope. The specific spatial patterns examined are: suspended sediment concentration, variability in bed sediment storage, suspended sediment geochemistry, and the organic-mineral balance.

7.2 Available data and initial considerations

There are detailed Geographic Information System (GIS) coverages of geology, soil and vegetation for Moor House and Upper Teesdale NNR (ECN, 2004). All three coverages stop at the Moor House NNR boundary and some catchments extend past this boundary (Figure 7.1). The geology of the areas where the GIS coverages were incomplete had similar proportions of each geology type to the areas included in the coverages (British Geological Survey, 1993a). On this basis the percentages of each geology, soil and vegetation type were up-scaled. Catchment boundaries were defined within the GIS (Figure 7.2), enabling the geology, soil and vegetation characteristics within each catchment to be quantified (Figures 7.3, 7.4 & 7.5).

Geology, soil and vegetation are examined individually, as although geology exerts a strong control over soil type and soil type over vegetation, numerous other factors, such as topography, aspect, water supply, influence soil development and vegetation growth. Vegetation types were re-classified into seven main groups based on more generalised

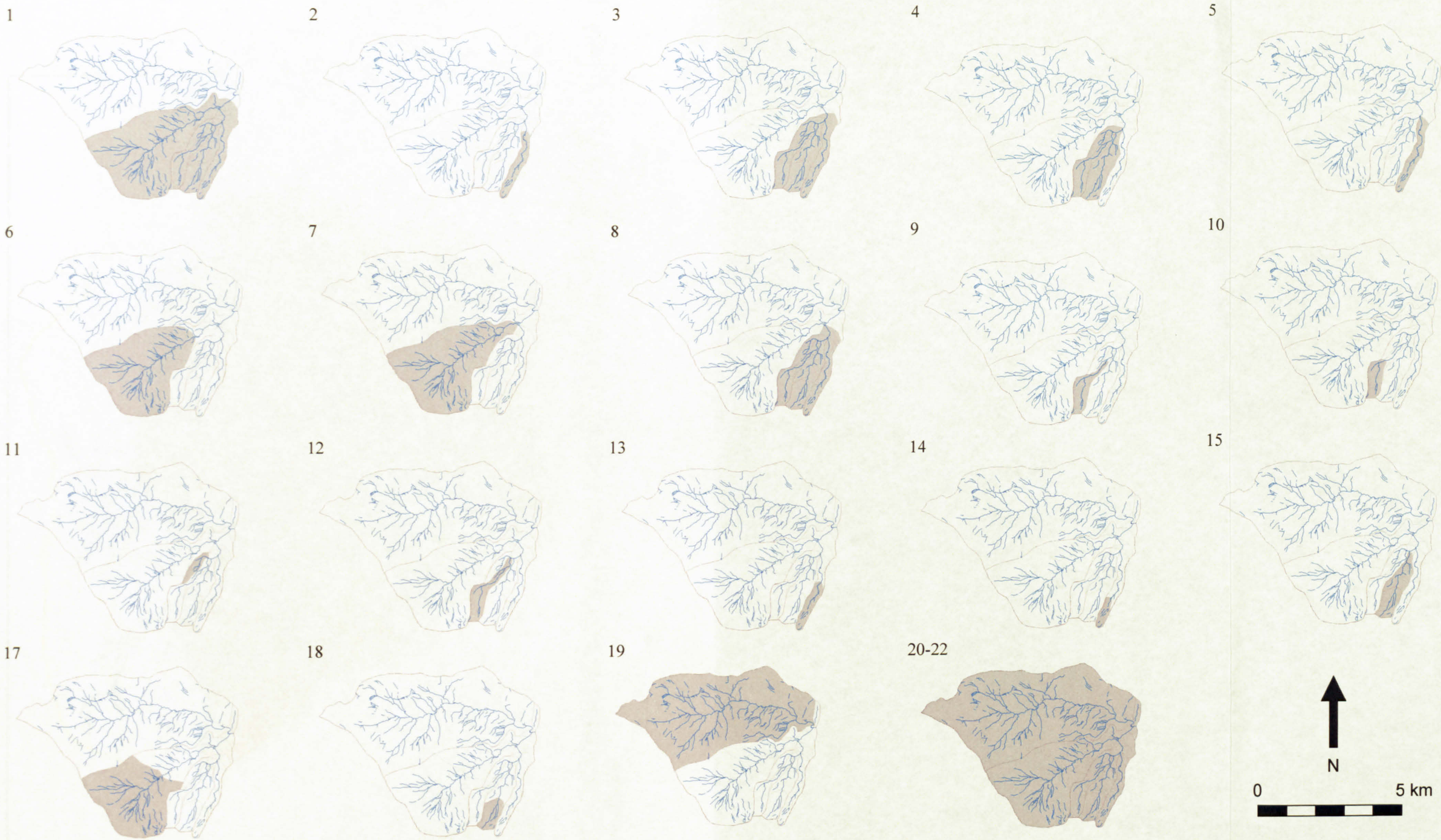

Figure 7.2. Key to the TIMS catchments to assist in identification of the catchments on the geology, soil and vegetation maps (Figures 7.3, 7.4 & 7.5).

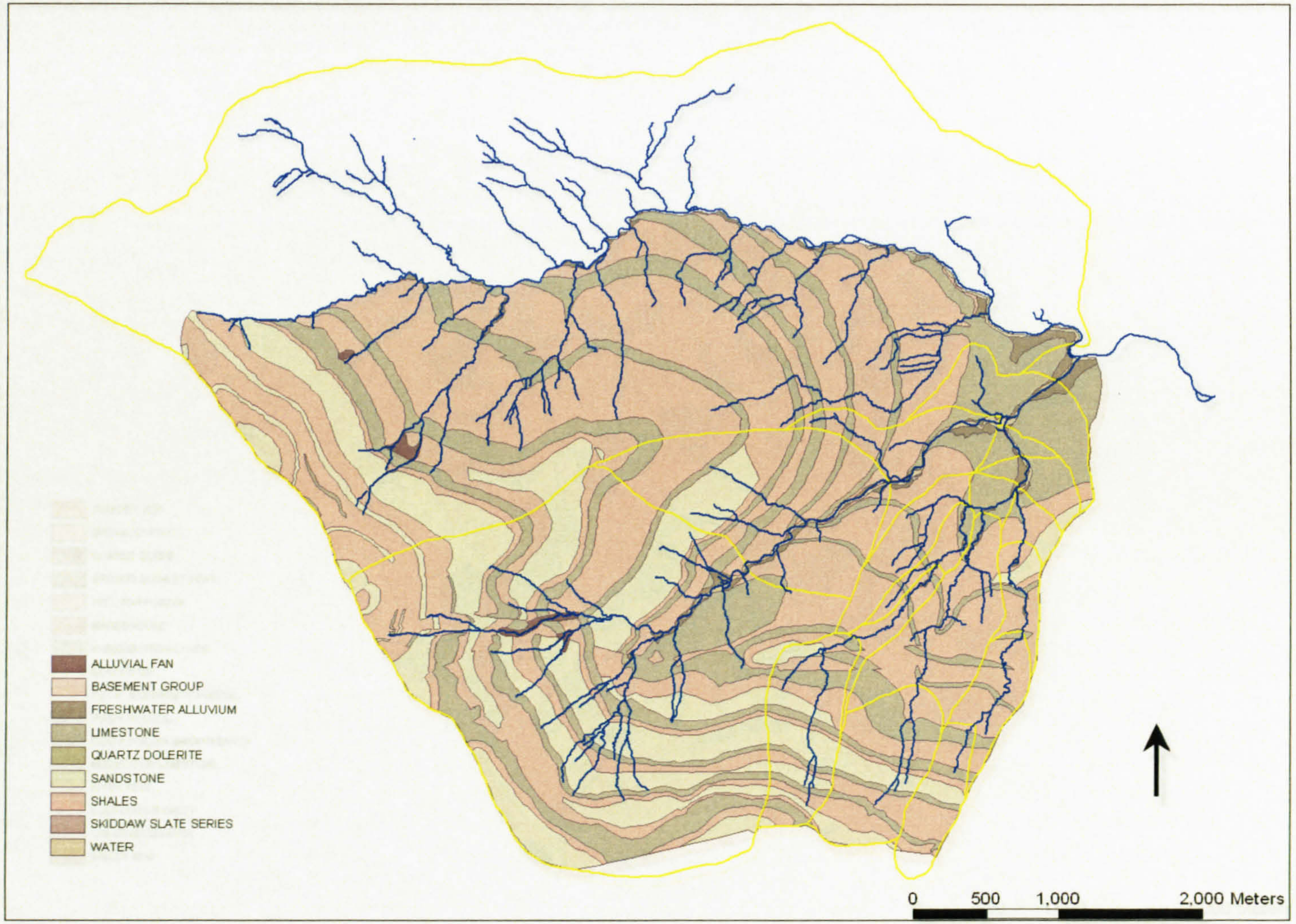

Figure 7.3. The geology types of the TIMS catchments in Moor House and Upper Teesdale NNR. The yellow lines are the catchment boundaries. Refer to Figure 7.2 for key to catchments.

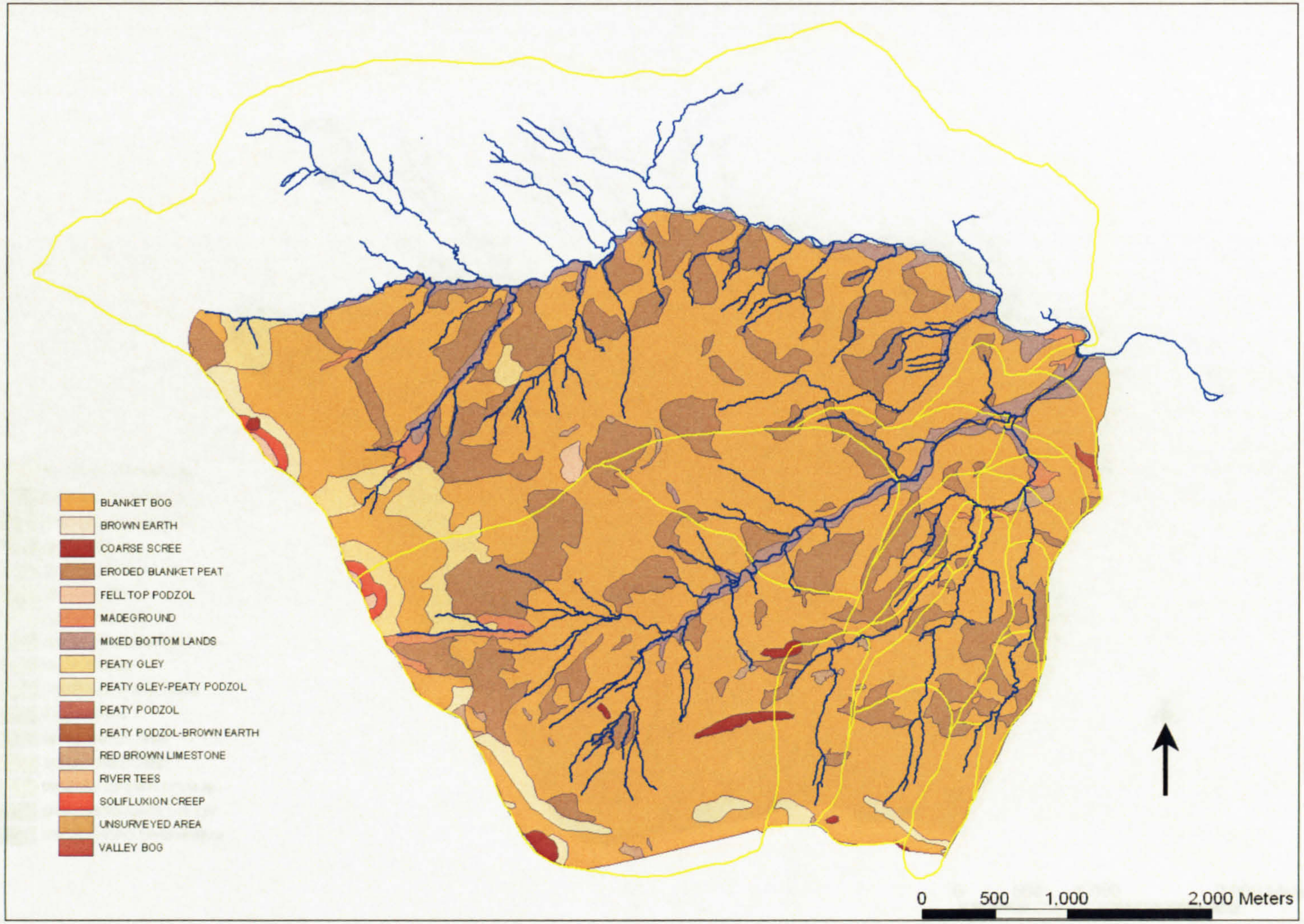

Figure 7.4. The soil types of the TIMS catchments in Moor House and Upper Teesdale NNR. The yellow lines are the catchment boundaries. Refer to Figure 7.2 for key to catchments.

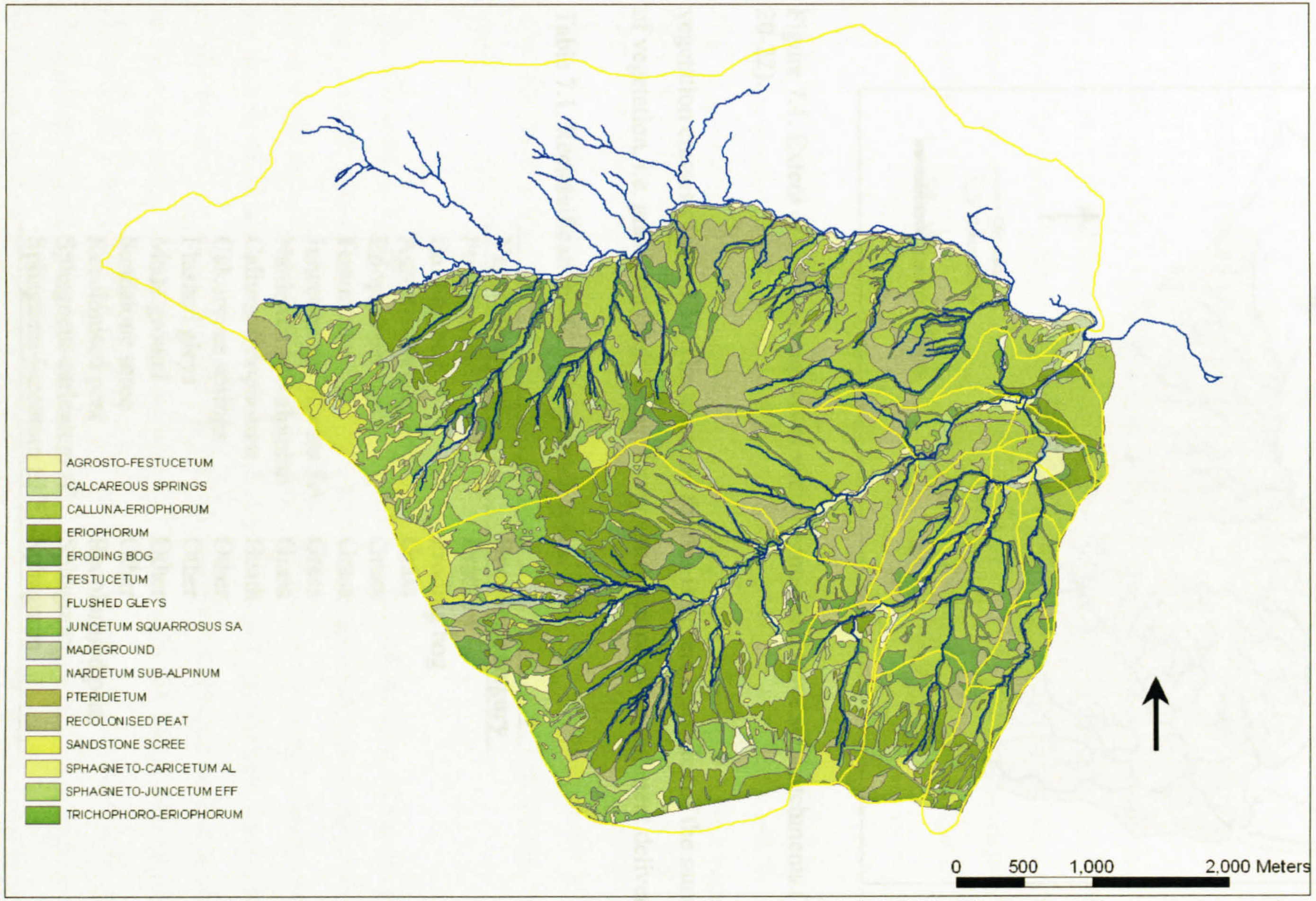

Figure 7.5. The vegetation types of the TIMS catchments in Moor House and Upper Teesdale NNR. The yellow lines are the catchment boundaries. Refer to Figure 7.2 for key to catchments.

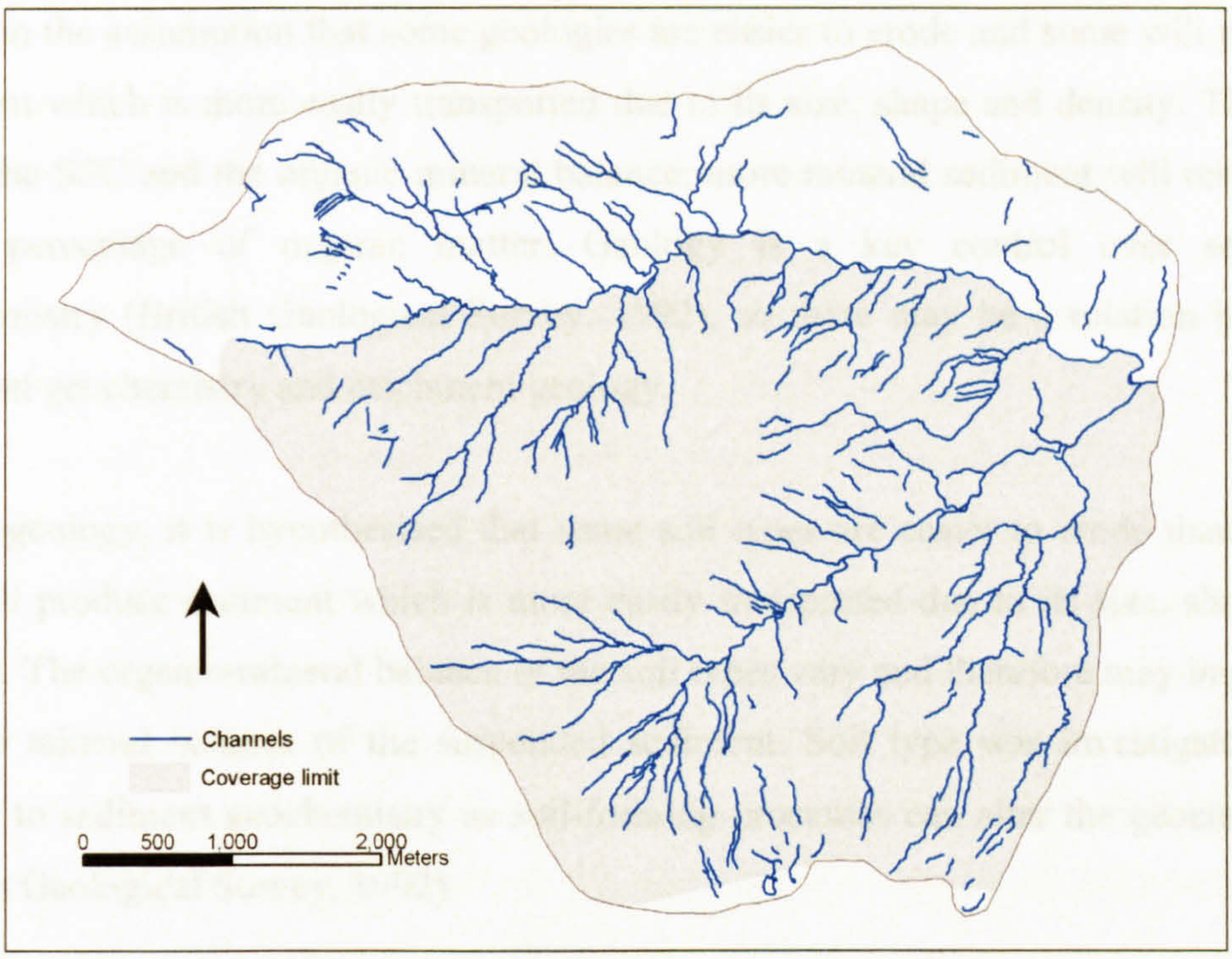

Figure 7.1. Extent of GIS in comparison with the most extensive sub-catchments (TIMS 20-22).

vegetation classes (Table 7.1). The rationale for this is different species of the same type of vegetation, i.e. grass, are likely to have very similar impacts on sediment delivery.

Table 7.1. Reclassification of GIS vegetation types.

Vegetation type	Broader category
Pteridietum	Bracken
Eroding bog	Eroding bog
Agrosto-festucetum	Grass
Eriophorum	Grass
Festucetum	Grass
Juncetum squarrosus SA	Grass
Nardetum sub-alpinum	Grass
Calluna-Eriophorum	Heath
Calcareous springs	Other
Flushed gleys	Other
Made ground	Other
Sandstone scree	Other
Recolonised peat	Recolonised peat
Sphagneto-caricetum AL	Sphagnum
Sphagneto-juncetum EFF	Sphagnum

Geology, soil type and vegetation cover were examined to assess if the dominance of a particular type was associated with higher SSCs, a particular sediment geochemistry signature and the organic-mineral balance of the sediment. Investigation of geology is

based on the assumption that some geologies are easier to erode and some will produce sediment which is more easily transported due to its size, shape and density. This will affect the SSC and the organic-mineral balance; more mineral sediment will result in a lower percentage of organic matter. Geology is a key control over sediment geochemistry (British Geological Survey, 1992), so there may be a relation between sediment geochemistry and catchment geology.

As for geology, it is hypothesised that some soil types are easier to erode than others and will produce sediment which is more easily transported due to its size, shape and density. The organic-mineral balance of the soil types vary and therefore may impact on organic mineral balance of the suspended sediment. Soil type was investigated with respect to sediment geochemistry as soil-forming processes can alter the geochemistry (British Geological Survey, 1992)

Vegetation was related to SSC and the organic-mineral balance to determine if lower SSCs are associated with particular vegetation types which protect the soil from rain drop erosion; binds the soil with roots and organic matter; and obstructs flow paths, and therefore sediment delivery, to the channel. Also, one cover type is eroding bog (i.e. no vegetation cover), which allows the impact of bare soil/peat on SSC to be investigated. Vegetation cover was considered with respect to sediment geochemistry as plant microbial metabolisms can alter sediment geochemistry (British Geological Survey, 1992).

The SSC and bed sediment storage results are discussed in light of the individual catchment characteristics. The TIMS catchments were grouped, using cluster analysis, given the number. Cluster analysis is a means of determining natural groupings. There are numerous variations of cluster analysis, each with several possible variations, and no one method is accepted as being universally better than any of the others. Most types of cluster analysis are based on a measure of dissimilarity, of which there are several (StataCorp., 2003b). Everitt *et al.* (2001) and Kaufman & Rousseeuw (1990) provide comprehensive introductions to cluster analysis. The average linkage method with the Euclidean distance as the measure of dissimilarity was used in this investigation as Kaufman & Rousseeuw (1990) suggest that it is reasonably robust and works well for many applications. Following the cluster analysis, dendrograms, which are tree structures indicating catchment groups, were drawn. The dendrograms allow groups at

different levels of dissimilarity to be defined. A threshold of the dissimilarity distance of 5 was selected to define the geology, soil and vegetation catchment groups. The mean percentage of each geology, soil and vegetation type was calculated for each group.

Catchment size was also determined for each of the SSC, bed sediment storage and TIMS catchments to allow the effect of scale to be investigated. The position in the channel network is also discussed. Scale and position in the channel network are worthy of consideration given factors such as hillslope connectivity and the ratio of submerged bank area to volume of water. Scale is examined on the basis that smaller catchments are likely to have higher SSC and higher organic matter contents given the likely stronger hillslope connectivity, and higher ratio of submerged bank area to volume of water, and lower proportion of mineral sediment sources. Position in the channel network is examined as catchment area is not always representative of the strength of hillslope connectivity and ratio of submerged bank area to volume of water. For example, in some cases a first order catchment may be larger than a second order catchment.

7.3 Suspended sediment concentration

This section examines the relationship between catchment scale, stream order and SSC. Variation in (1) fixed-interval SSC samples taken simultaneously on Trout Beck and Rough Sike and (2) spatially distributed storm samples taken in the Moor House channel network are described and related to catchment characteristics.

7.3.1 Rough Sike & Trout Beck fixed-interval suspended sediment concentrations

SSC samples were taken simultaneously at two locations within Moor House NNR: Trout Beck and Rough Sike (Figure 6.1). Synchronised automated samplers were programmed to take one sample every eight hours from 27th March 2002 to 11th July 2002; however, for logistical reasons small gaps exist in the data set. These data allow the influence of spatial scale to be examined without any interference from temporal variability as the auto-samplers took samples at exactly the same time.

7.3.1.1 Catchment characteristics

The area of Rough Sike is approximately 15 times smaller than Trout Beck (Table 7.2). The soil types are fairly similar for both catchments but the geologies and vegetation covers differ (Table 7.2). In terms of vegetation, Trout Beck has a higher percentage of

grass and a lower percentage of heath and eroding blanket bog. In terms of geology, Trout Beck has a much lower percentage of shale and a higher percentage of limestone and sandstone (Table 7.2).

Table 7.2. Catchment area and percentage cover of different vegetation, soil and geology types of the Rough Sike and Trout Beck gauging site catchments. The values of eroding bog and eroded blanket peat derived from the vegetation and soil classifications are very different and are a result of the classification systems used by ECN (2004).

	Trout Beck	**Rough Sike**
Area, km^2	11.83	0.76
Vegetation:		
Grass	41.2	21.7
Heath	33.4	46.4
Recolonised peat	11.6	11.3
Eroding bog*	9.9	20.2
Sphagnum	1.4	0
Other	2.2	0.3
Bracken	0.2	0
Soil:		
Mixed bottom lands	2.8	0
Made ground	1.1	0
Solifluxion	0.3	0
Valley bog	0.1	0
Coarse scree	0.9	0.1
Fell top podzol	0.1	0
Eroded blanket peat*	18.5	22.5
Blanket bog	71.1	75.8
Peaty-gley peaty-podzol	2.2	1.6
Peaty-gley	1.8	0
Red brown limestone	1.0	0
Geology:		
Shale	48.7	71.2
Limestone	27.4	16.1
Sandstone	23.9	12.6

7.3.1.2 Comparison of Trout Beck & Rough Sike suspended sediment concentrations

Comparison of the instantaneous SSC measurements shows that, on average, the SSC of Trout Beck is lower than Rough Sike (Figure 7.6), and a paired t-test indicated that the difference is statistically significant at 9% probability. The mean of the instantaneous SSC of Trout Beck is lower than that of Rough Sike: 1.9 mg l^{-1} and 2.4 mg l^{-1} respectively. The variability, as indicated by coefficient of variation, in SSC is greater

for Trout Beck (200%) than for Rough Sike (95%) (standard deviation is 3.8 mg l^{-1} for Trout Beck and 2.3 mg l^{-1} for Rough Sike).

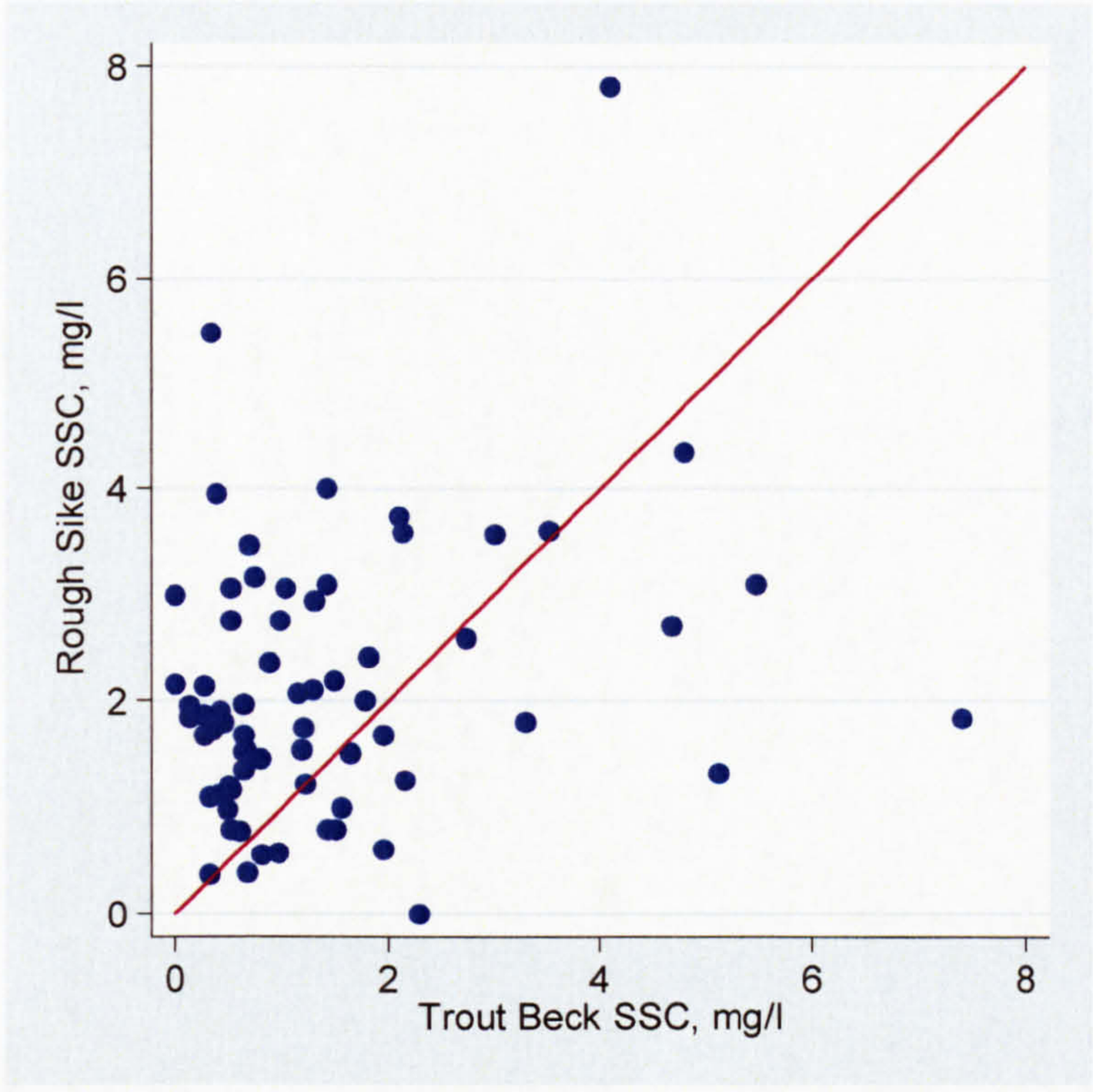

Figure 7.6. The relationship between SSC at Trout Beck and Rough Sike. Red line = 1:1.

The lower SSC in Trout Beck in comparison with Rough Sike can be explained by dilution of the SSC, deposition of sediment between the gauging sites and/or sediment supply. It is hypothesised that sediment is more readily available in the Rough Sike catchment due to several factors:

(1) Rough Sike has a higher proportion of organic sediment, which can be transported at lower velocities than denser mineral fractions. This is supported by the soil covers of the two catchments. Rough Sike is characterised by 22.5% eroding blanket peat and 75.8% blanket bog in comparison with 18.5% and 71.1% respectively in Trout Beck (Table 7.2).

(2) Rough Sike has a larger proportion of channel banks susceptible to erosion.

(3) Rough Sike is steeper, 0.06 in comparison with 0.03 for Trout Beck, and therefore has a higher unit stream power.

(4) Rough Sike has a higher drainage density, 3.50 km km^{-2} in comparison with 3.15 km km^{-2}.

Alternatively, the decrease in SSC between Rough Sike and Trout Beck could be caused by dilution by clear-water runoff with a lower SSC from the channels which join the channel between the Rough Sike and Trout Beck gauging stations (Figure 6.1). The channel most likely to have a lower SSC is Trout Beck, given its higher order, larger catchment area, gentler hillslopes and therefore weaker connectivity between hillslopes and the channel.

The greater variability in the SSC of samples taken at Trout Beck suggests more complex sediment delivery mechanisms are operating in the larger catchment. This complexity is explained by an increased range of sediment sources and longer travel distances, both of which result in sediment being delivered to the gauging site at different times. The greater variability in soil types in Trout Beck in comparison with Rough Sike (Table 7.2) may also promote higher variability in SSC in terms of greater variability in the particle characteristics (size, shape and density), which influence the processes of erosion, entrainment and deposition.

Some inferences regarding the effect of geology, soil and vegetation type on SSC can be made. No conclusive statements can be made as only two catchments are examined and the effect of scale can not be isolated. Rough Sike has a higher percentage of shale than Trout Beck and less limestone and sandstone (Table 7.2). Shale, limestone and sandstone are all sedimentary rocks but all weather differently. Limestone is primarily weathered by dissolution (Sparks, 1986) and therefore produces limited particles for transport. Sandstone breaks down into quartz particles which are generally quite coarse and resistant to further weathering (Sparks, 1986). As a result the particle sizes are often too coarse to travel in suspension. Shales are composed of clay-sized material (Sparks, 1986), are easily weathered from banks and the stream bed and produce material suitable for suspension. Therefore, higher percentages of shale may promote higher SSCs.

The vegetation types also differ between the two catchments: Rough Sike has a higher proportion of eroding bog and heath and a lower percentage of grass in comparison with Trout Beck (Table 7.2). The higher percentage of eroding bog may promote the higher SSC associated with Rough Sike; however, the connectivity between the eroding bog area and channel will control the impact. Lower SSCs are associated with runoff from grass-covered areas in comparison with heath-covered areas at Moor House (Clement,

in prep) due to greater disruption to flow pathways and sediment retention. Therefore the higher SSCs sampled from the Rough Sike catchment may also be attributable to the lower percentage grass cover and the higher proportion of heath.

7.3.2 Comparison of spatial storm sample suspended sediment concentrations

At Moor House spatially distributed water samples were collected during storm events to allow insight into variability in SSC within the channel network over a range of discharges. Results are presented on three sets of eight samples, which were taken during one event, and supplemented by two sets of eight spatial samples collected from a further three events.

7.3.2.1 Catchment characteristics

The distribution of spatial SSC sampling points enables the effect of catchment area on sediment delivery to be investigated (Figure 7.7).

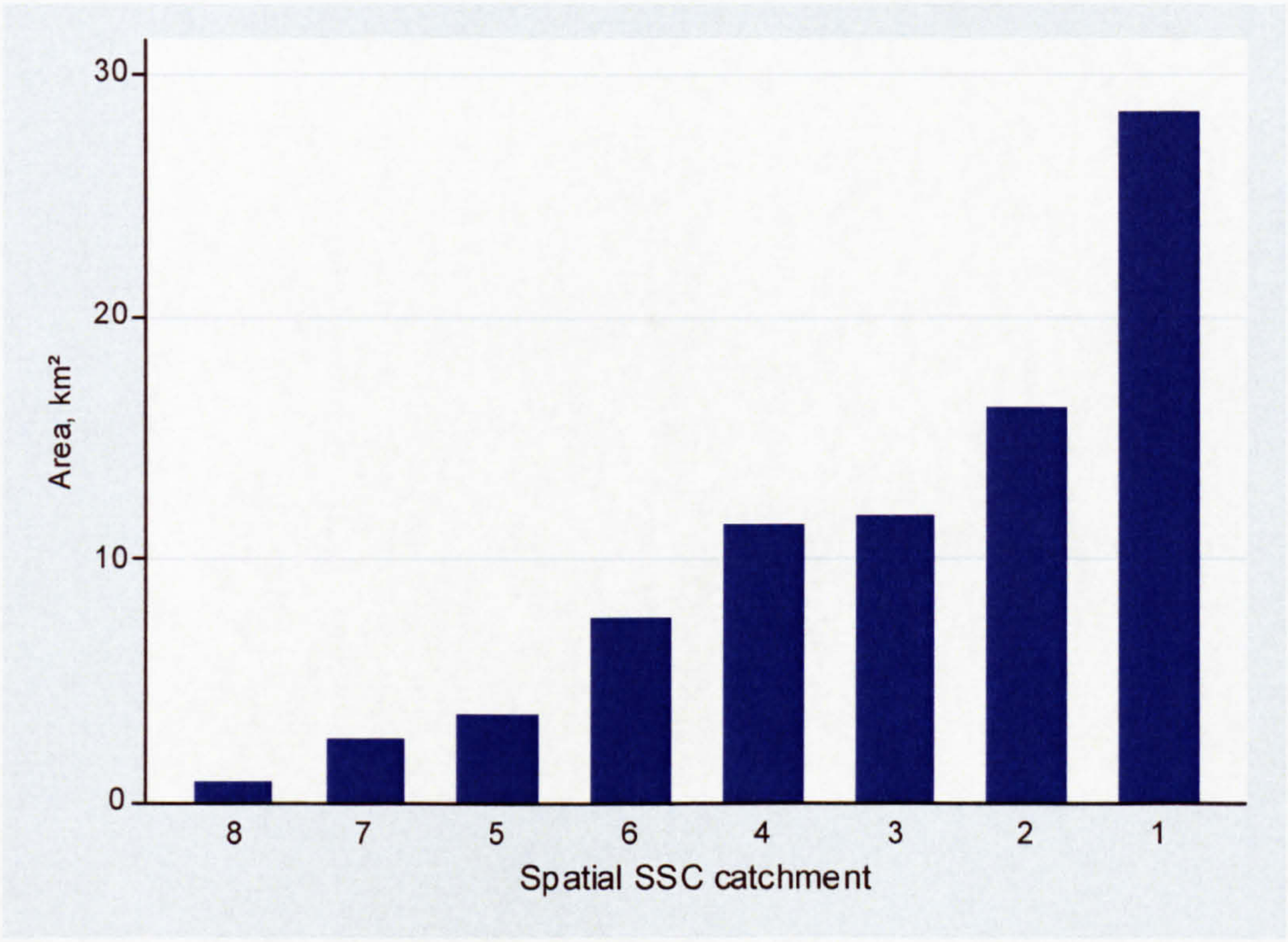

Figure 7.7. Catchment area of the spatial SSC catchments.

The geology of the spatial sampling catchments are similar in as much as they all contain shale, limestone and sandstone (Figure 7.8). The percentage of limestone in each catchment is fairly constant at around 20%, whereas the percentage of shale varies from 45% to 70% and the percentage of sandstone from 12% to 30% (Figure 7.8).

(A)

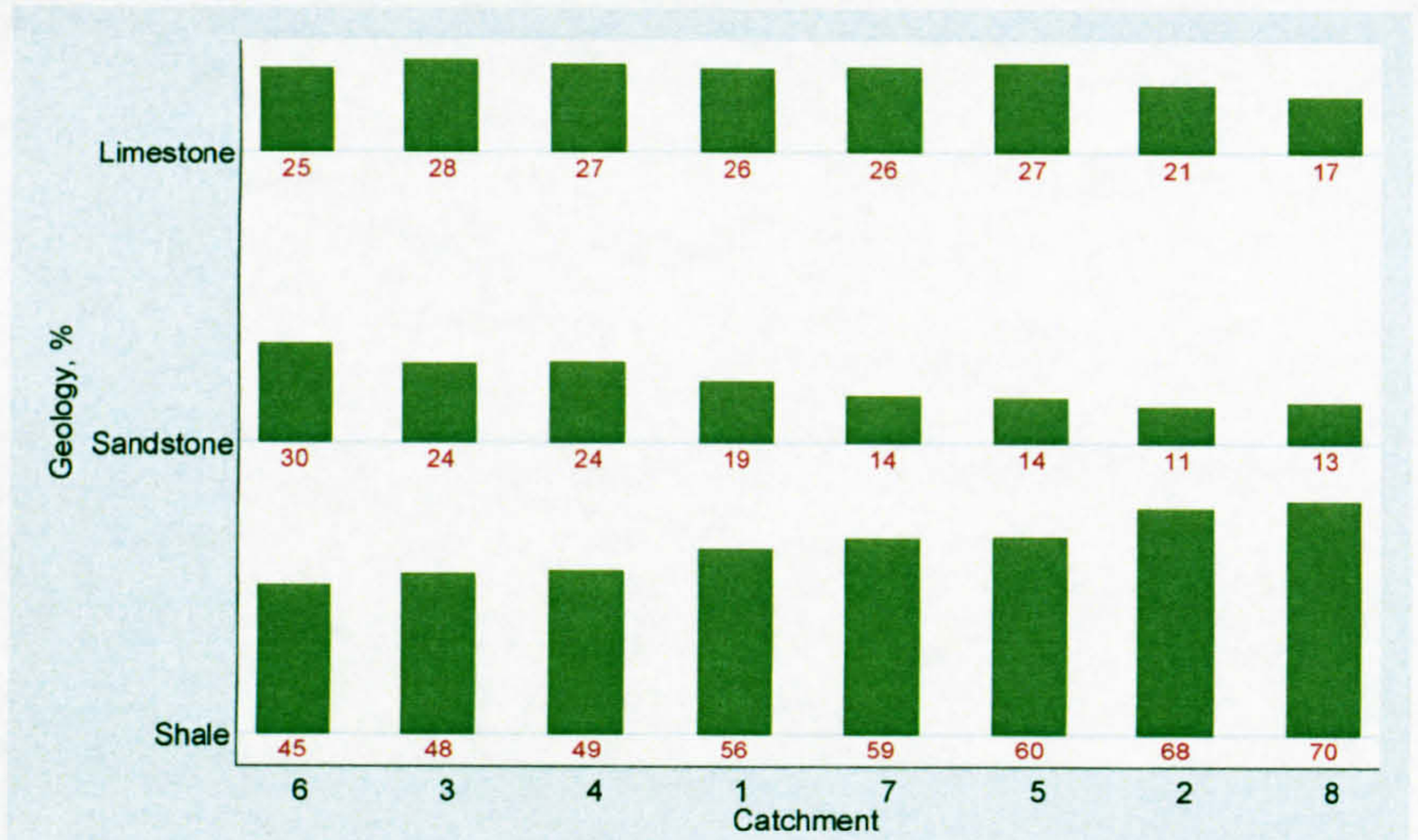

(B)

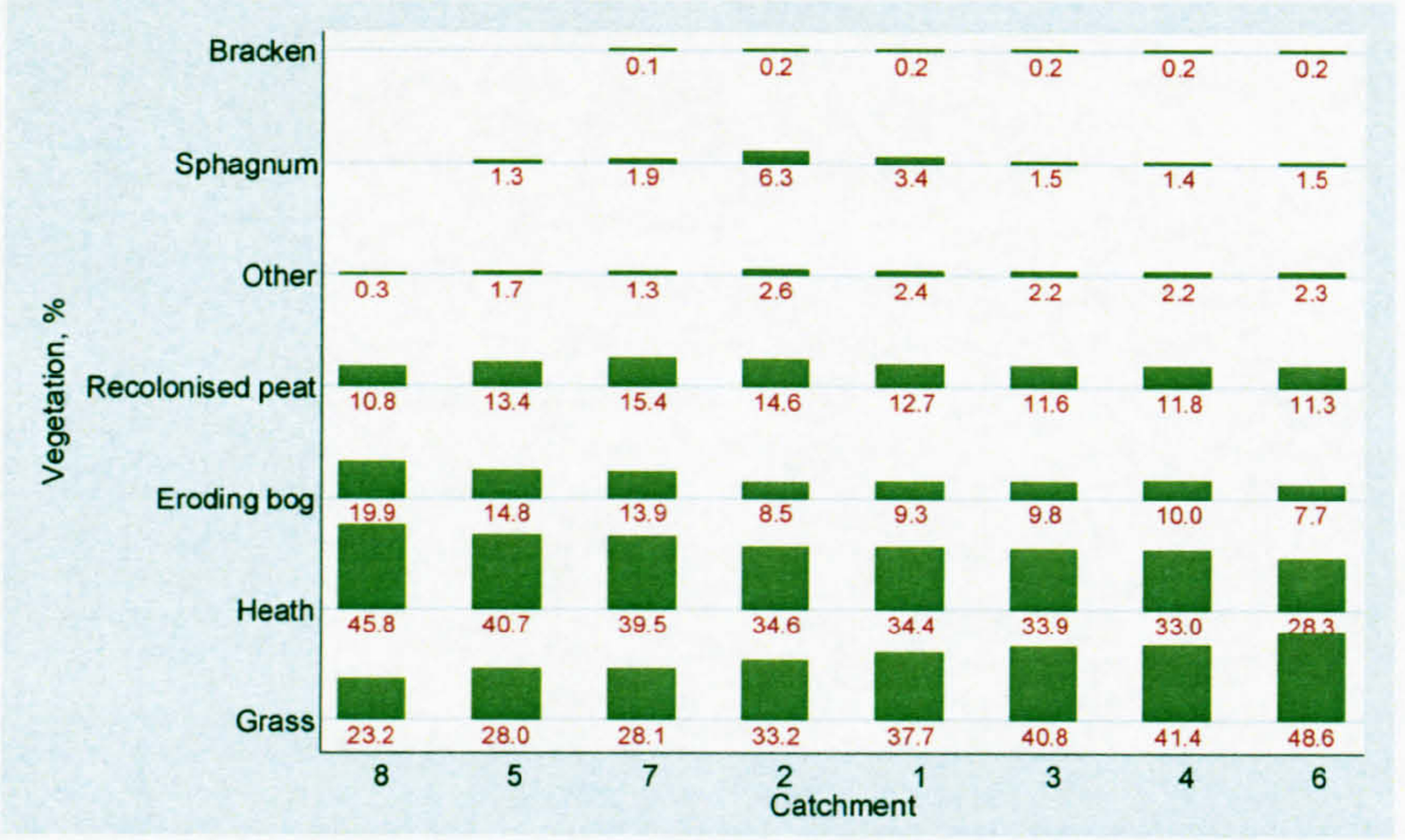

(C)

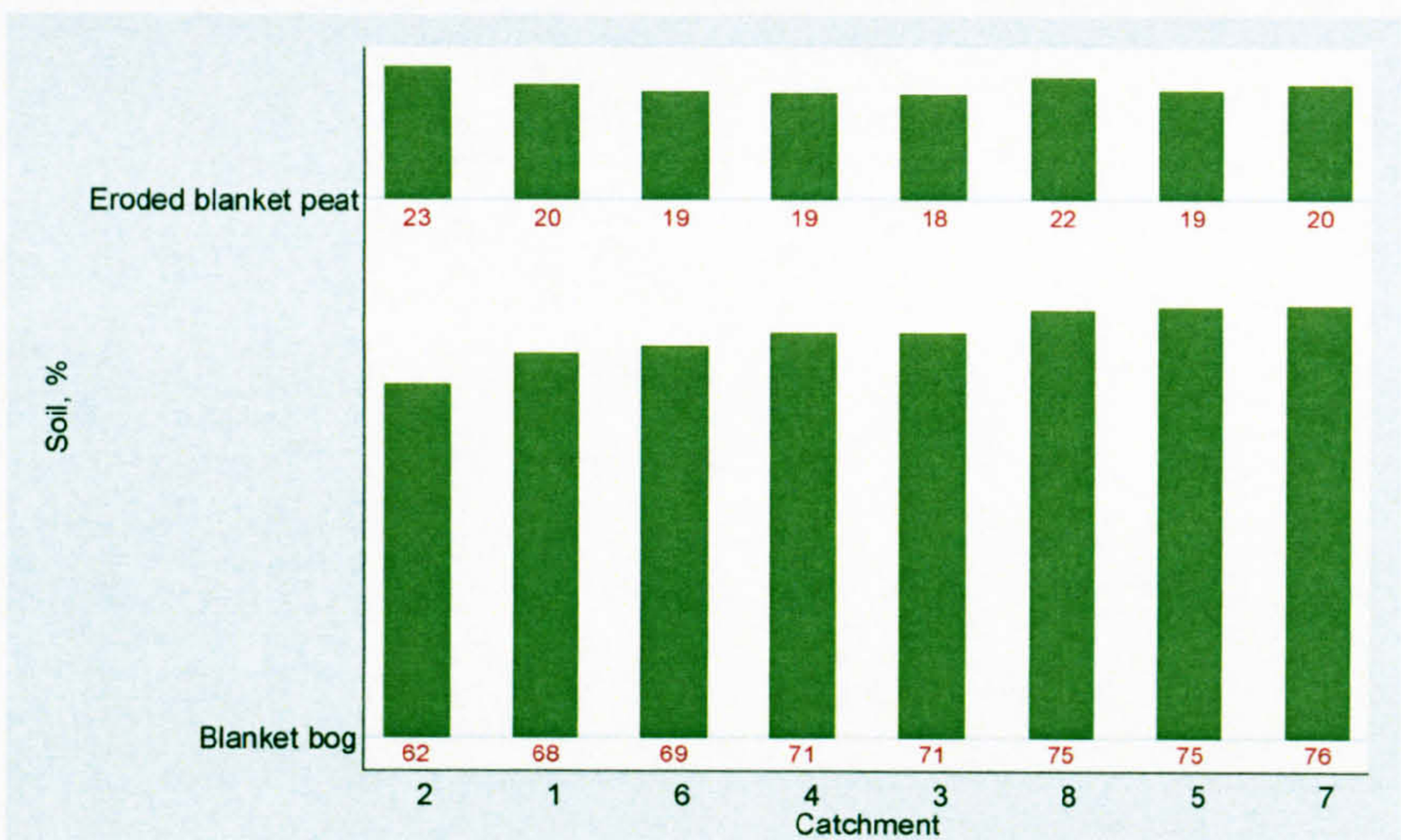

(C cont.)

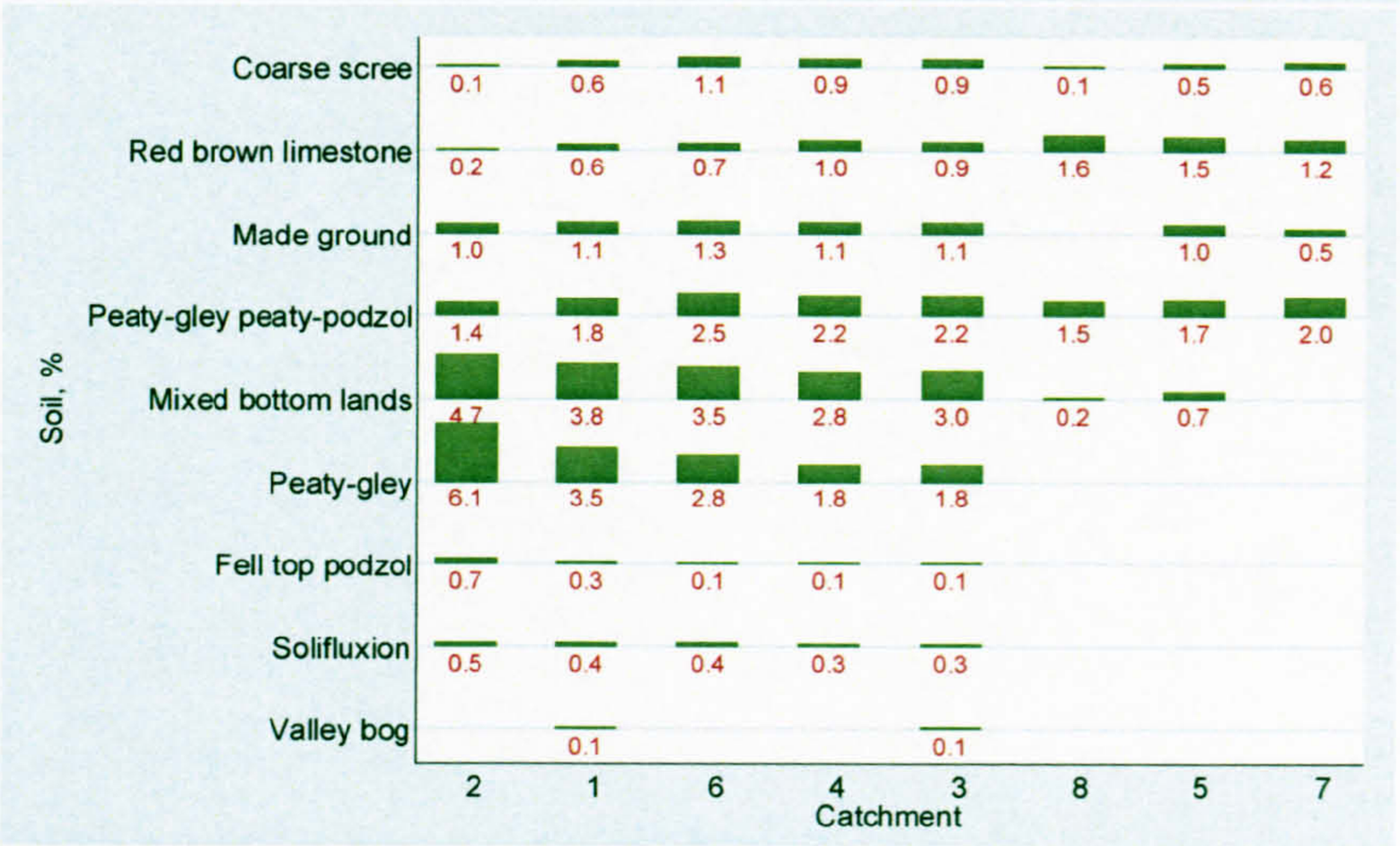

Figure 7.8. Percentage of each (A) geology, (B) soil, and (C) vegetation type in the spatial SSC sampling catchments. Two graphs are given for soil to allow the proportions of the less dominant types to be examined. The catchments are ordered by the proportion of the dominant type.

The dominant vegetation cover in all catchments is grass and heath, which together account for approximately 70% of the vegetation cover (Figure 7.8). The most variable aspect of the vegetation cover in the relative proportion of grass (22%-52%) and heath (30%-45%) (Figure 7.8). Each catchment also contains between 10% and 15% of recolonised peat and between 5% and 20% eroding bog (i.e. unvegetated). Bracken, sphagnum and other (Table 7.1) are limited and variable between the catchments (Figure 7.8).

All the catchments contain between 60% and 75% blanket bog and the percentage of eroding blanket peat is approximately 20% for each (Figure 7.8). The other soil types comprise no more than 15% of each catchment. The largest variation in soil cover is the percentage cover of blanket bog and the percentage cover of mixed bottom lands and peaty-gleys (Figure 7.8).

On the basis of these classifications there are no particularly distinctive sub-catchments: there is a continuum in the coverages as opposed to distinct groups. This is expected as the catchments are nested (Figure 7.2).

7.3.2.2 Comparison of spatial storm sample suspended sediment concentrations

Three sets of eight spatial samples were taken within the channel network (Figure 6.7) at Moor House during a storm event on 17th January 2002. The storm lasted approximately 12 hours and had a distinct symmetrical single peak (Figure 7.9). The first set was taken on the rising limb (08:50 to 09:11, $Q = 5.21$ m^3 s^{-1}), the second set at the peak (10:53 to 11:19, $Q = 6.10$ m^3 s^{-1}), and the final set on the falling limb (12:47 to 13:09, $Q = 4.72$ m^3 s^{-1}) (Figure 7.9). The timings of the rising limb, falling limb and peak are obtained from the Trout Beck gauging site (Figure 6.1 or adjacent to sample point 4 on Figure 6.7).

On the rising limb the highest SSCs occurred in the lower order streams (Figure 7.9). At the peak discharge the SSCs decreased at all but three sampling locations, which were all in the higher order channels (Figure 7.9). On the falling limb SSC decreased throughout the system and were greater in the lower order channels (Figure 7.9). This suggests that SSCs are generally higher in the lower order channels. These data give several insights into the suspended sediment dynamics within the system.

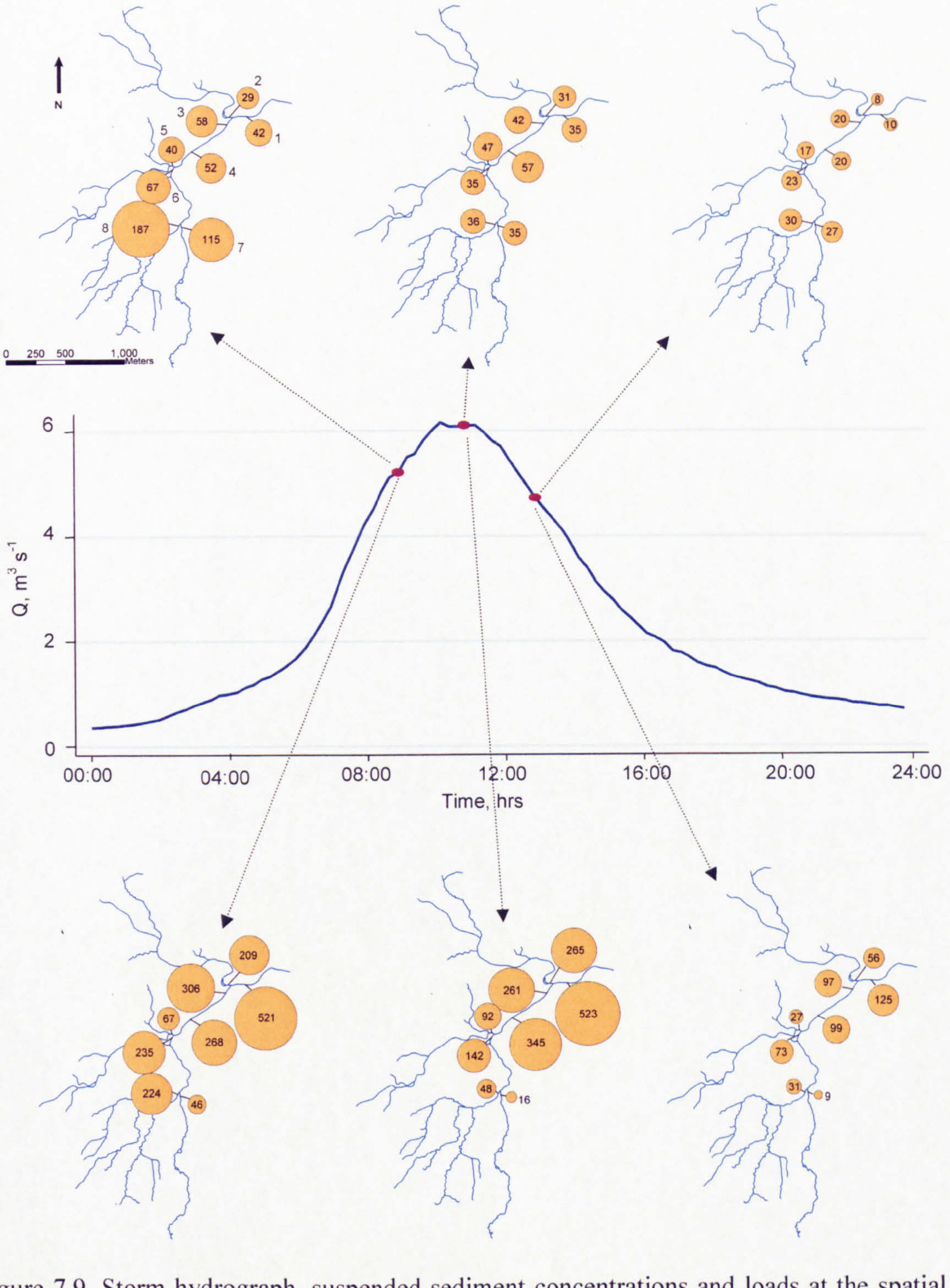

Figure 7.9. Storm hydrograph, suspended sediment concentrations and loads at the spatial sampling locations for the event on the 17th January 2002. Figures in the proportional circles are the SSC in mg l^{-1} (upper diagrams) and suspended sediment load in kg s^{-1} (lower diagrams).

The decreases in SSCs between the rising limb and peak, and the rising limb and falling limb, occur given the hysteresis between SSC and discharge (section 2.7.1). There was a rise in SSC at sampling locations two, four and five between the rising limb and peak sample sets (Figure 7.9) which may be due to an episodic sediment input (e.g. bank collapse) or the progression of a sediment wave through the system. It could also be due to the arrival of a secondary flood peak, but there is no evidence of this on the storm hydrograph (Figure 7.9).

The higher SSC in the lower order channels on the rising limb (Figure 7.9) can be explained by:

(1) Stronger coupling between the hillslope and channel in the lower order channels.
(2) Banks supplying more sediment because there is more channel bank per volume of water in the lower order streams; or the composition of the channel banks is more prone to erosion in the lower order channels.
(3) The lower order channels are steeper and therefore, more erosive.
(4) The SSC in the higher order channels were diluted by higher flows of water poorer in sediment.
(5) Deposition occurred in the higher order channels as a result of change in channel morphology: typically narrow and deep in the lower order channels and broad and shallow in the higher order channels, although the peat fraction is unlikely to be deposited. There is some evidence of sediment deposition in the field in slack water areas, for example, at the channel margins just upstream from the Trout Beck gauging site.

The most likely explanations are stronger coupling and more sediment supply by stream banks. On the falling limb, more bank sediment supply, deposition and dilution may explain why SSCs were greater in the lower order channels, in comparison with the higher order channels (Figure 7.9).

Sediment load was calculated to give insight into the contribution of the sub-catchments to the total downstream load. Discharge recordings were only available for Trout Beck gauging site (Figure 6.1) so the approximate discharges of the sampling locations were calculated using the catchment area weighted method. The SSC were then multiplied by discharge to give instantaneous sediment load in kg s^{-1}.

The suspended sediment loads increased downstream with the exception of sample points three and four at the peak and on the falling limb (Figure 7.9). There are four possible explanations for this: (1) measurement error; (2) deposition occurred between the sampling points; or (3) an episodic input of sediment. Field observations suggest limited sediment deposition occurs between sample points three and four; the channel is broad, shallow and moderately fast-flowing. Therefore, it is most likely that measurement error or an episodic input of sediment accounts for the difference. The 84 kg decrease appears too high to be attributable to measurement error and so is attributed to an episodic input from a source local to point four or perhaps the movement of a sediment wave through the system. It is difficult to reach a firm conclusion given the assumptions of the method. Also, a sediment peak could travel down the reach in a shorter time than the time interval between samples three and four.

Comparison of the diagrams illustrating SSC with those illustrating load conveys the importance of discharge in sediment loads. The importance is evident in comparison of sampling points with the highest loads and those with the highest SSCs: generally the sampling points with low SSCs but high discharges (e.g. sample point one) have higher loads than those with high SSCs but low discharges (e.g. sample point eight) (Figure 7.9).

Patterns of highest, lowest and intermediate loads are broadly similar between the sample sets: sampling location 1 always has the highest load, sampling location 7 the lowest load, sampling location 4 the second or third highest (Figure 7.9). A scatter plot matrix of the relative load of each sub-catchment, calculated by summing the loads of all the catchments and then calculating the percentage each catchment represents, at the different stages of the storm event illustrates this trend clearly (Figure 7.10). This suggests that throughout the event there was continuity between the sampling locations in terms of the relative sediment loads. This could be due to constant relative sediment supply given similar connectivity, potential sources and the longevity of the sources between catchments. However, the most probable explanation of the seeming continuity in loads is the dominance of discharge, i.e. the relative discharge of each sampling location sub-catchment is constant because of the calculation method and therefore any variable by which the discharges are multiplied by will be imprinted with this pattern. There is most scatter on the graph of peak as a function of rising limb (Figure 7.10). It

was expected that there would be more scatter between the relative loads of the rising and falling limbs due to the contrast in available sediment.

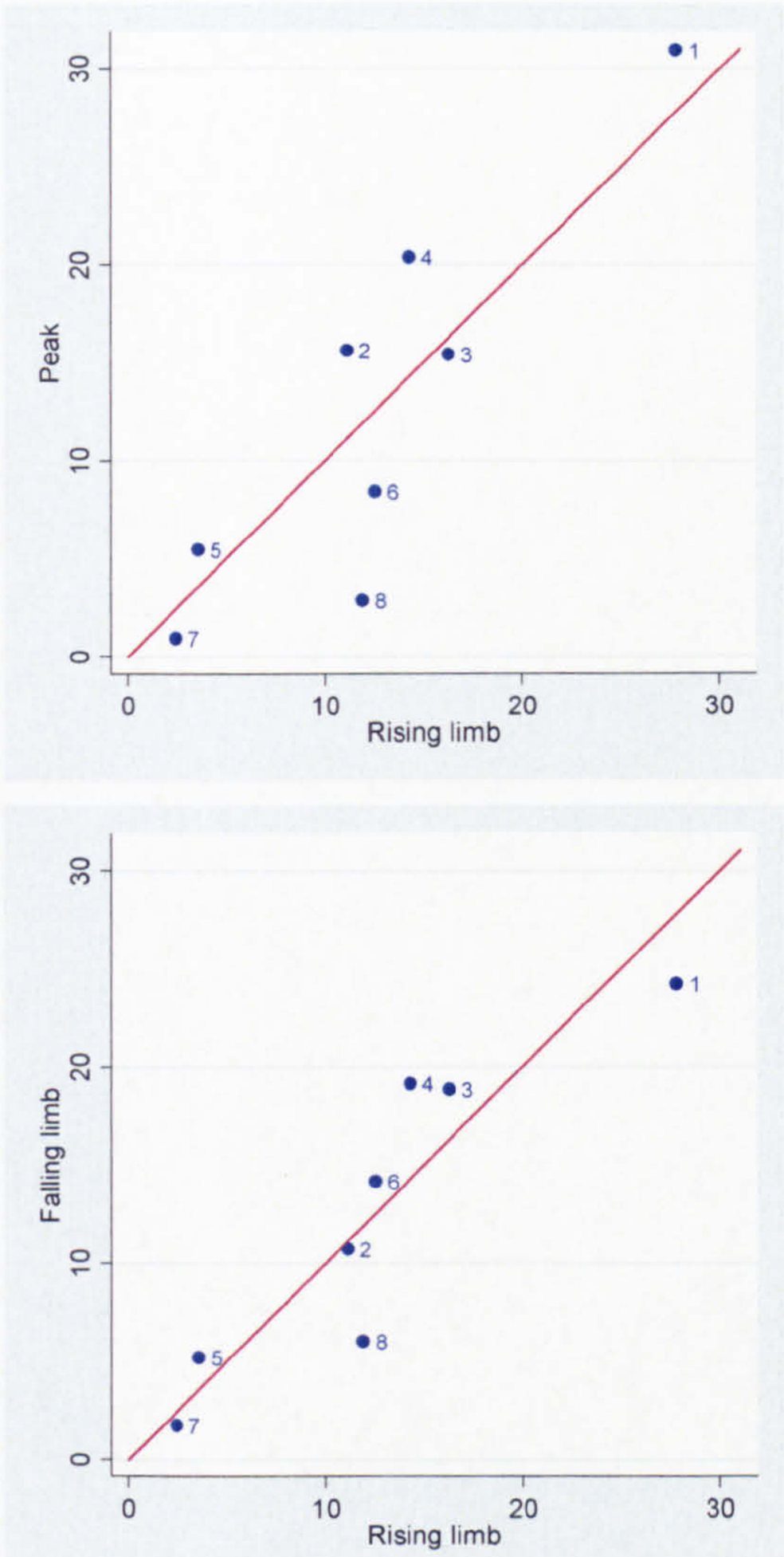

Figure 7.10. Graph matrix of the percentage of total suspended sediment load at each SSC spatial sampling point on the rising limb, falling limb and peak. $y = x$ is uperimposed for reference.

Other spatial samples were taken during three events using the same sampling points as those used on 17th January 2002. It was not possible to obtain another set of spatial samples which captured the rising limb, peak and falling limb but the three other sets show the variation between the rising limb and peak (6th February 2002), primary and secondary falling limb (21st – 22nd November 2002) and two points on the falling limb (6th November 2002). This gave insight into the between-storm variability in SSC in the channel network.

The 6th February event shows a similar pattern as the 17th January event in terms of higher SSC on the rising limb than at the peak (Figure 7.11). The differences in the values are less despite being taken at broadly similar discharges (Figures 7.9 & 7.11). This can be explained by the pattern of discharge prior to sampling: the 17th January event was a single peaked event which began from base flow, whereas the 6th February event was part of a multi-peaked hydrograph and therefore sediment supplies will already have been depleted.

The event on the 21st – 22nd October was multi-peaked and both sets of spatial samples were taken on a falling limb (Figure 7.12). The SSCs between the sampling sites, although higher on the first falling limb, remain fairly constant with relation to each other: the three highest SSC were obtained at sites 3, 4 and 5, the lowest at site 8. This suggests that through different stages of the storm events the relation between SSC at the different locations may stay fairly constant. This probably indicates that the system is transport-limited, but it has already been shown by the events on 17th January and 6th February that it is more likely to be supply-limited. Therefore, there may be some form of uniformity in the rate of sediment exhaustion sources in the sub-catchments. This could be caused by similar sediment source types and sizes in each sub-catchment.

The spatial sample sets taken during the 6th November event were both sampled on the same falling limb (Figure 7.13). These samples show SSCs declined at all the sampling locations except one (samples site 6) (Figure 7.13). The SSCs may have been declining because the flood wave moved out of the system, dilution by storm flow or because sediment was falling out of suspension given the lower velocities. The increase in SSC at the sampling point 6 could be attributed to a local source, such as a bank collapse.

The spatial variation in SSC during storm events so far has focussed on location in the channel network. Location in the channel network and catchment area are closely related: lower order catchments are smaller. In terms of the geology, soil type and vegetation cover no conclusive patterns can be identified. This is attributed to the broadly similar nature of the catchments (Figures 7.8) and suggest that at the storm scale processes associated with the storm (discharge generating processes and activation of sediment sources) are more dominant controls over SSC than the catchment characteristics.

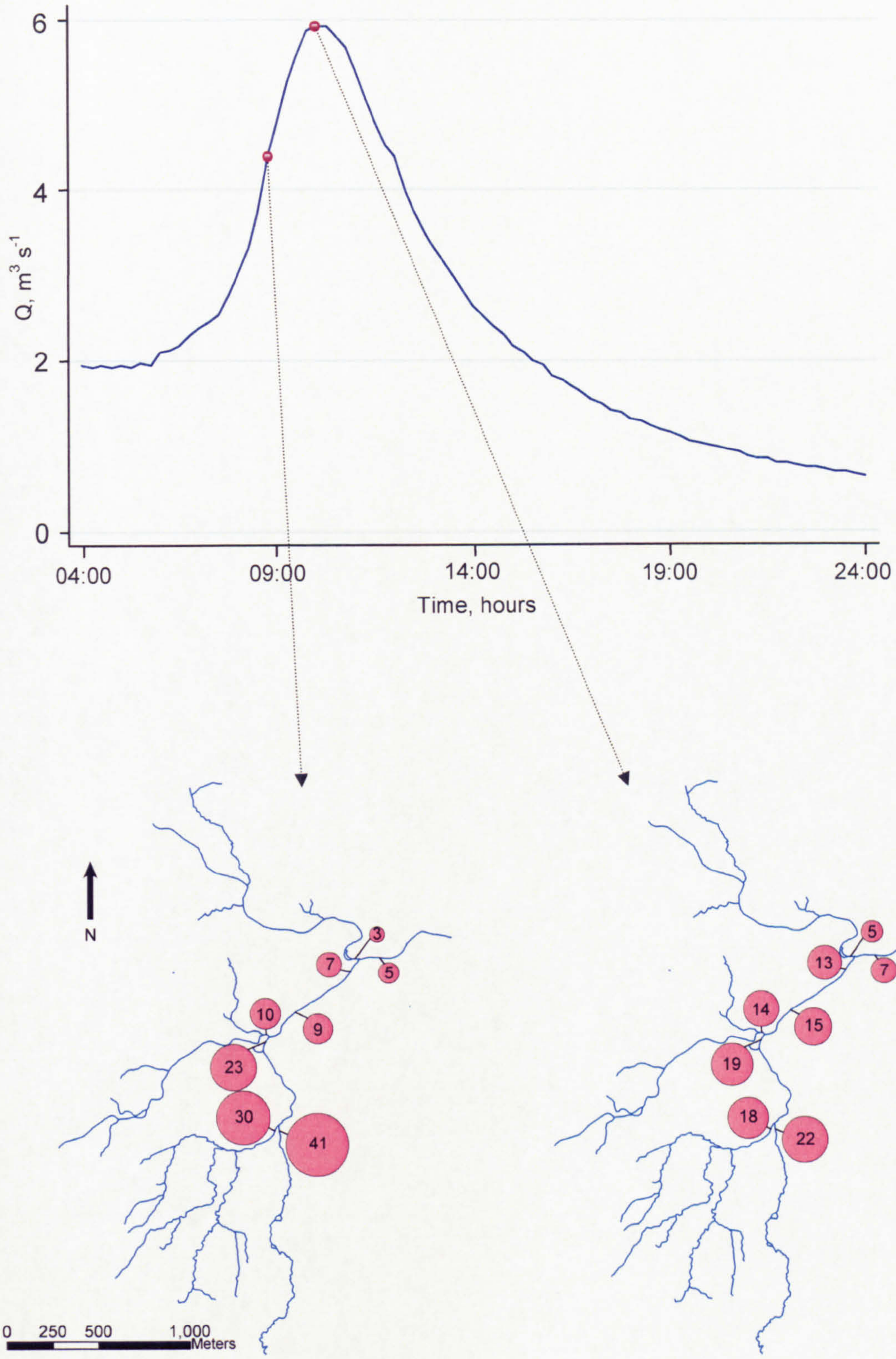

Figure 7.11. Storm hydrograph and spatial suspended sediment concentrations at the spatial sampling locations for the event on the 6th February 2002. Figures in the proportional circles are the SSC in mg l^{-1}.

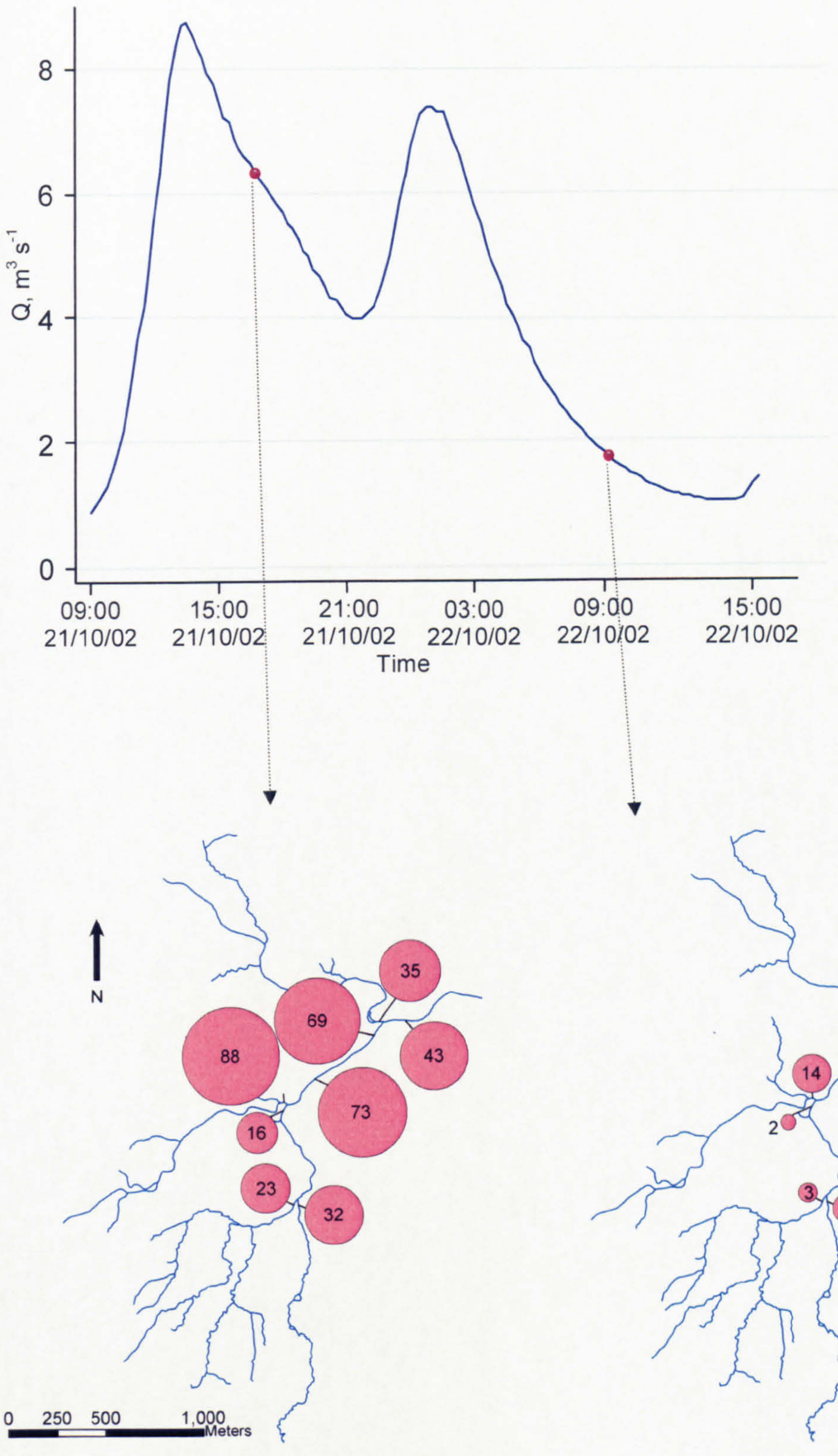

Figure 7.12. Storm hydrograph and spatial suspended sediment concentrations at the spatial sampling locations for the event on the 21st – 22nd October 2002. Figures in the proportional circles are the SSC in mg l^{-1}.

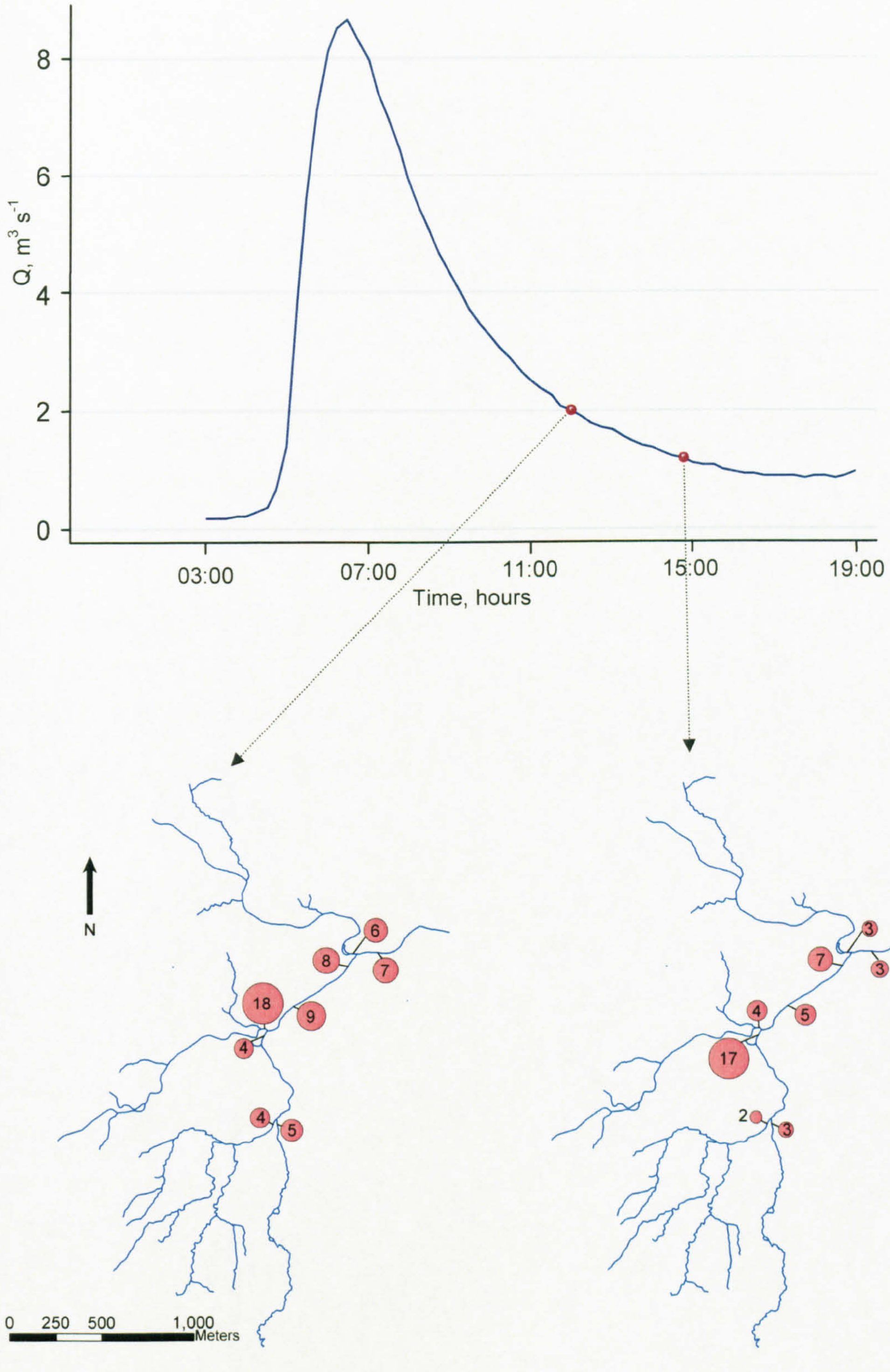

Figure 7.13. Storm hydrograph and spatial suspended sediment concentrations at the spatial sampling locations for the event on the 6th November 2002. Figures in the proportional circles are the SSC in mg l^{-1}.

7.3.5 Summary

Analyses of the Trout Beck and Rough Sike auto-sampler and spatial storm SSC data sets have shown:

(1) More sediment is supplied by the smaller, lower order catchments, although the variability in SSC is higher in the higher order catchments, given more complex patterns of sediment supply and delivery.

(2) Catchment geology and vegetation cover may exert some control over the auto-sampler data, but no firm conclusions can be made as they can not be isolated from the effect of catchment scale. No patterns between geology, soil type, vegetation cover and spatial storm SSC could be identified given the lack of variation between catchments, or their limited influence in comparison with the effect of storm-scale processes on sediment delivery.

(3) The system is supply-limited.

(4) Discharge is the dominant control over suspended sediment load.

7.4 Bed suspended sediment storage

The section examines the variability in river bed suspended sediment storage. The section begins with a description of the experiment, outlines the hypothesis and then discusses the outcomes. The catchment characteristics are not quantified given the point nature of these experiments.

7.4.1 Description of experiment

The storage of sediment on and within the bed in the Moor House channel network was investigated. The aim of this experiment was to examine the potential variability in suspended sediment supplied by the bed. Eight sites were chosen based on the flow regime and nature of the bed sediment (Figure 6.8 & Table 7.3). This approach, as opposed to a random sample site selection method, was chosen to ensure that the magnitude of the potential differences in SSC as a result of entrainment from sediment stored on and within the bed was captured. Sites were selected on the apparent velocity, the apparent size distribution of bed surface sediment and the existence of periphyton, as they influence sediment stored on the bed surface and the protection afforded by bed armouring. All the experiments were undertaken within a two day period, during which the discharge remained stable. The experiment involved isolating a section of channel bed and agitating the water only, to simulate no bed movement; the bed surface, to

simulate slight bed movement; and the deeper bed, to simulate severe bed movement (section 6.2.6 for outline of procedure).

Table 7.3. Flow conditions and channel bed characteristics of the bed sediment storage experiment locations.

Location	Flow	Channel bed
1	Intermediate flow, flat	Predominantly finer sediment and periphyton. No large clasts.
2	Fairly slow flow	Down stream from a bedrock section. Range of particle sizes. Periphyton.
3	Fairly flat, slow flow.	Bedrock with loose clasts and finer sediment on top.
4	Fairly fast flowing, riffle	Mostly pebbles – boulders with limited finer particles.
5	Fast flowing	Pebbles – boulders with some overlain finer sediment
6	Fairly fast flow	Predominantly pebbles – boulders. Some periphyton.
7	Flat and slow flowing	Fine sediment. No periphyton.
8	Flat, intermediate flow	Predominantly pebbles with some cobbles. finer particles and periphyton

7.4.2 Hypotheses

The hypotheses for this analysis are: (1) slower-flowing sections have higher SSCs and faster-flowing sections have lower SSCs; (2) the more extreme the bed disturbance the greater amounts of suspended sediment supplied; (3) locations with coarser particle size distributions have lower SSCs and locations with finer particle size distributions have higher SSCs; and (4) locations with periphyton will potentially have higher SSCs during the water only agitation, dependent on the amount of mineral sediment stored on the bed surface.

7.4.3 Findings

As expected the SSCs were consistently lower when only the water was agitated and higher when the deep bed was agitated: the SSCs during water agitation ranged from 50 to 1,573 mg l^{-1}, the SSCs of bed surface agitation ranged from 429 to 7,622 mg l^{-1} and finally the SSCs of bed agitation ranged from 2,306 to 19,854 mg l^{-1} (Figure 7.14). The difference in the SSCs in each stage of agitation varied substantially between sampling locations (Figure 7.14). The highest concentrations during water agitation were associated with the sampling locations with a higher portion of finer sediment on the

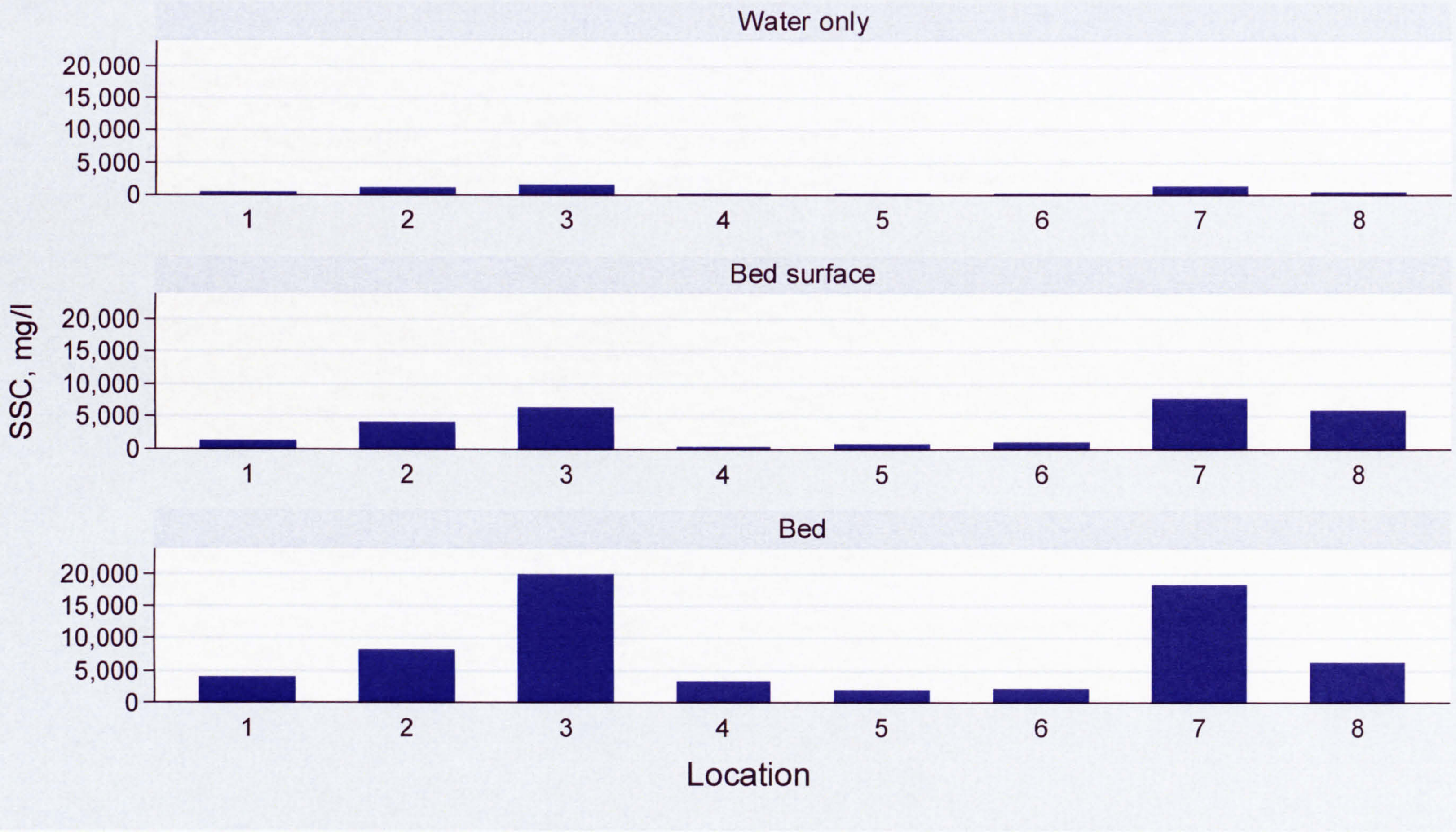

Figure 7.14. SSC of bed sediment storage samples when the water only, bed surface and deeper bed were agitated.

bed surface with the exception of location 2 (Figure 7.14 & 7.15): there is a higher proportion of the finer particle sizes in the surface sediment of locations 1, 3, and 7 (Figure 7.15). Periphyton may have caused the high SSC at location 2 (Table 7.3). There is also a correlation between the flow regime and SSCs of water only agitation: low SSCs were associated with the faster-flowing sections and high SSCs were associated with the slower-flowing sections (Table 7.3 & Figure 7.14).

The patterns in the bed surface agitation results are similar to the water only agitation results; however, there are some differences. The highest SSC was obtained at location 7 as opposed to location 3 (Figure 7.14). This can be explained by periphyton present at location 3 but not at location 7. The periphyton will have been disturbed during water only agitation and increased the SSC at location 3. However, when the bed surface was disturbed more mineral particles will have been suspended at location 7 due to the finer particle size distribution (Figure 7.15). Mineral particles are denser than periphyton and therefore would have resulted in a higher SSC. There are other such inconsistencies which can not be explained by the existence or lack of periphyton. The SSC at location 2 is higher than that of location 8 when only the water was agitated but when the bed surface was agitated the SSC of location 8 was higher than that of location 2. Also, location 6 had the lowest SSC, location 5 the second lowest and location 4 the third lowest when only the water was agitated but when the bed surface was agitated location 4 had the lowest SSC, location 5 the second lowest and location 6 the third lowest (Figure 7.14). Although every attempt was made to agitate each location with equal vigour unequal agitation could be the cause of this pattern.

The results of the deep bed agitation experiment yields almost identical results, in terms of locations which gave the highest SSC, as water only agitation (Figure 7.14) and therefore can be attributed to flow conditions and particle size distribution; the particle size distribution of the sub-surface is very similar to the surface (Figures 7.14 & 7.15).

Examination of the differences in particle size distribution of the surface and sub-surface layers at each location shows that the sub-surface layer typically has a finer particle size distribution than the surface layer, with the exception of location 7 (Figure 7.16). This is expected and is indicative of a surface armour layer. Field observations (Table 7.3) showed that location 7 was dominated by fine sediment, which looked like a

recent deposit, which explains the very similar surface and sub-surface grain size distributions (Figure 7.16) and lack of armour layer.

(A)

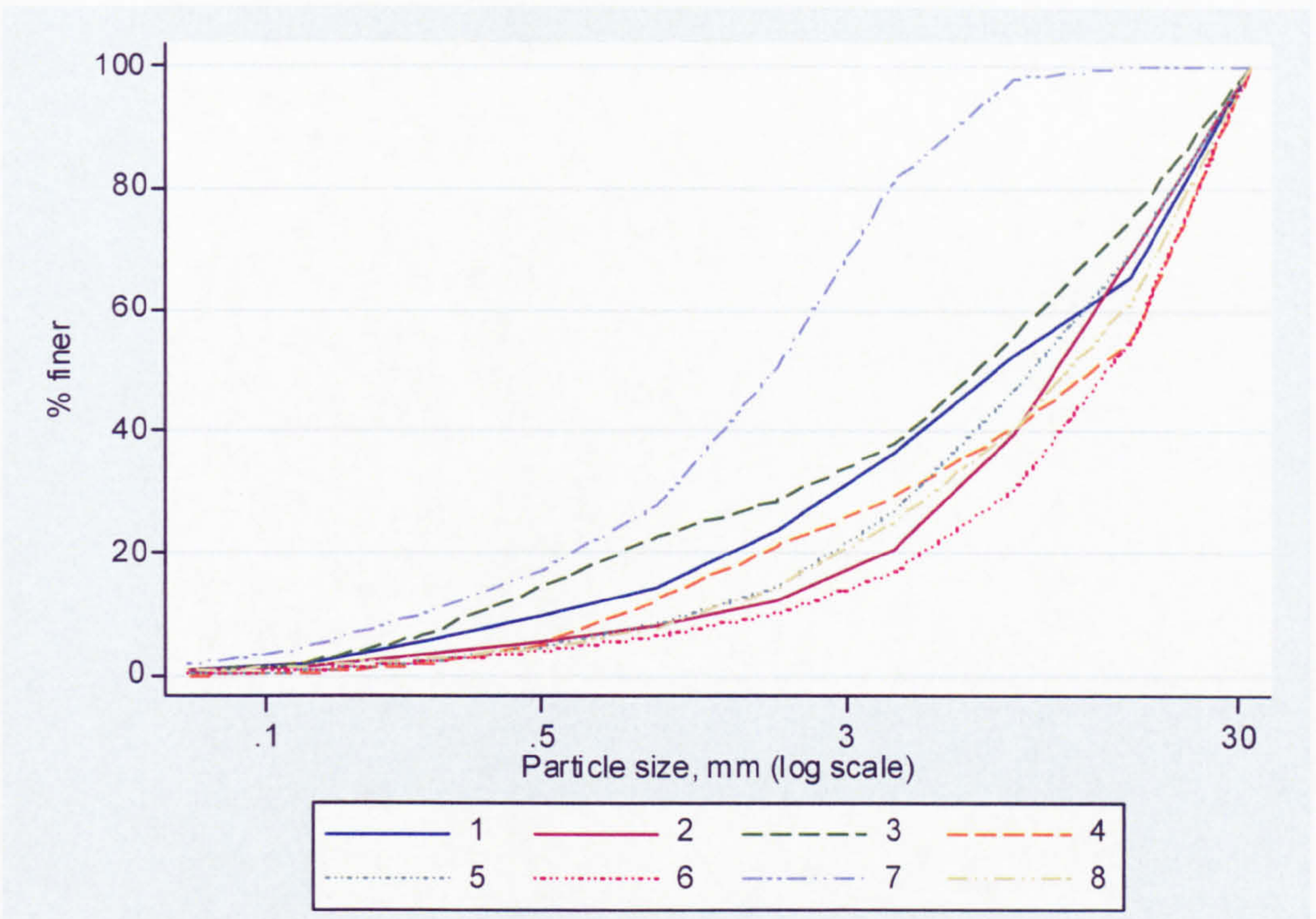

(B)

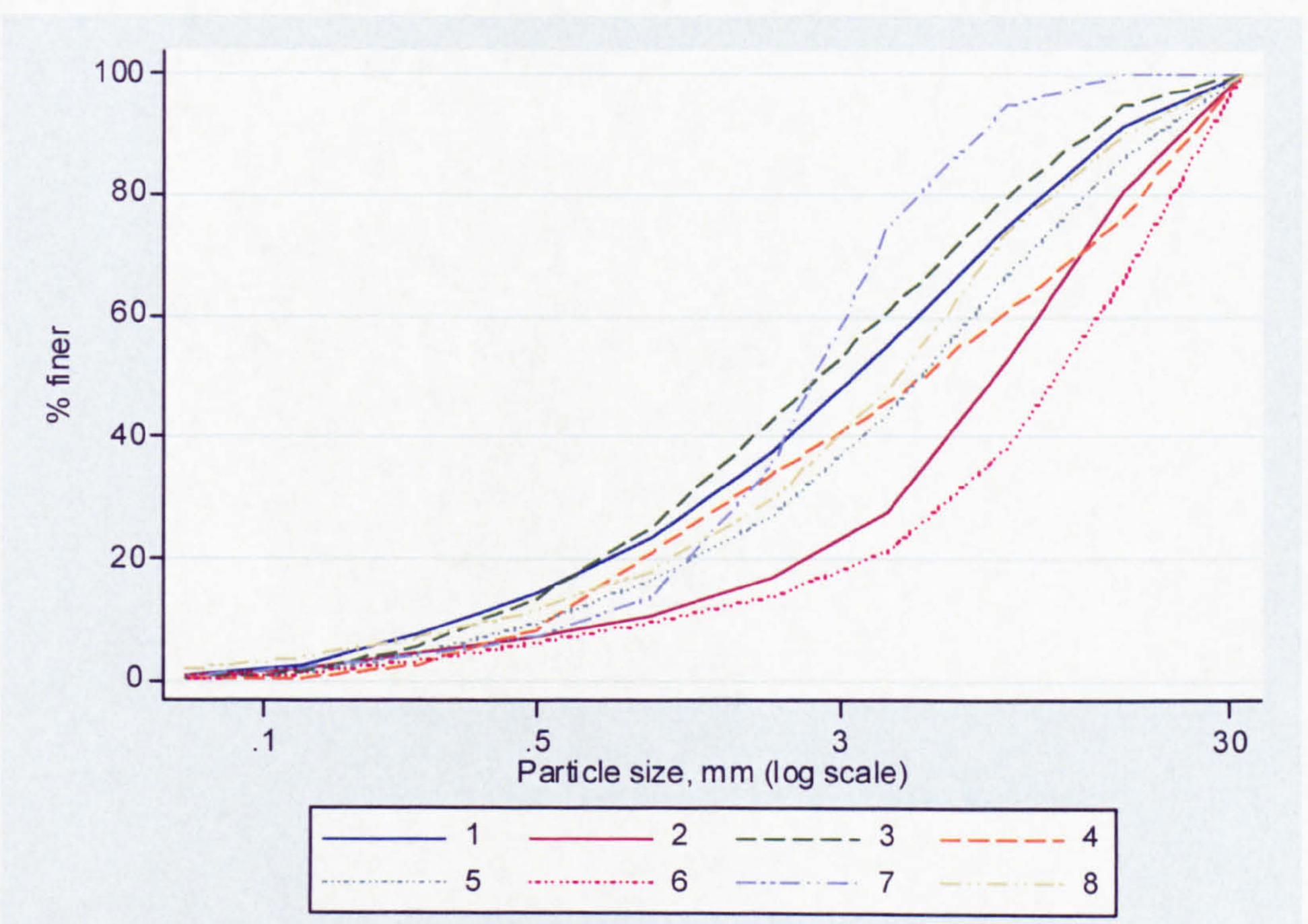

Figure 7.15. Particle size distribution (up to 32 mm) of the (A) bed surface and (B) bed sub-surface. Larger particles were not included as they were measured, as opposed to weighed, in the field. Note logarithmic x-axis scale.

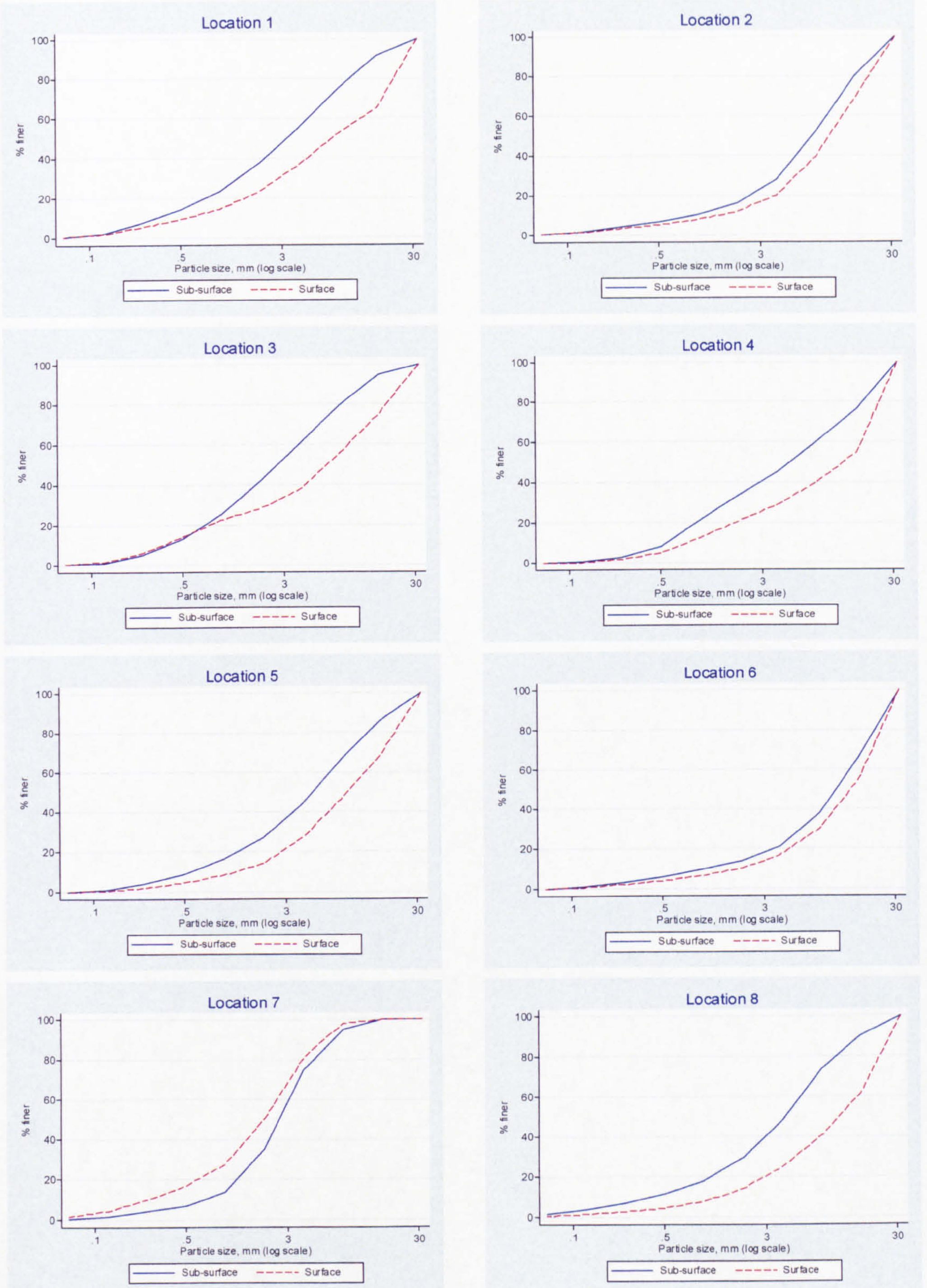

Figure 7.16. Bed surface and sub-surface grain size distributions for each bed sediment storage location. Larger particles were not included as they were measured, as opposed to weighed, in the field. Not the logarithmic x-axis.

7.4.4 Summary

The bed sediment storage experiments show the potential spatial variability of SSC during bed disturbance events of different magnitudes. The variability is primarily linked to the flow regime, existence of periphyton and the particle size distribution of the bed sediment. These factors are reliant on local channel form, i.e. broad channel cross-sections promote slow flow, which promotes deposition on the bed and consequently bed sediment storage is relatively high. These experiments could aid the explanation of spatial variability in SSC which is not explained by catchment characteristics. The results also demonstrate, especially sample locations 7 and 8, the extent and small spatial scale at which bed sediment storage, and therefore SSC, varies. During most floods either the bed is not disturbed at all or there is some limited, patchy bed surface disturbance. Therefore the results of the surface water agitation are most relevant when considering the spatial variability in SSC caused by bed surface storage for the majority of events, but not large events.

7.5 Organic-mineral balance

The spatial and temporal variation of organic matter content of sediment retained in the time-integrated mass samplers (TIMS) is examined in the following section. The analysis focuses on Moor House but is supplemented by results from Swinhope. The organic matter content is related to: position in the channel network; catchment size; and catchment geology, soil and vegetation.

7.5.1 Catchment characteristics

The distribution of catchment sizes within the study area is uneven. Most are fairly small (Figure 7.17), but this is typical of upland peatland catchments. The catchment areas vary from 0.31 to 28.46 km^2 (Figure 7.17).

The TIMS catchments were grouped by the relative proportions of geology, soil and vegetation type using cluster analysis (section 7.2). The groups are a useful tool to enable patterns to be identified and generalisations made. The cluster analysis was done separately for geology, soil and vegetation so it was possible to ascertain the importance of each and as there are limited correlations between the geology, soil and vegetation types (Figures 7.3, 7.4 & 7.5), given the influence of other factors such as aspect and slope. The most important control over suspended sediment dynamics is likely to be soil type as this is more sensitive to erosion and transfer to the channel than the underlying

geology. The presence/absence of vegetation is likely to be of higher importance than the particular type of vegetation.

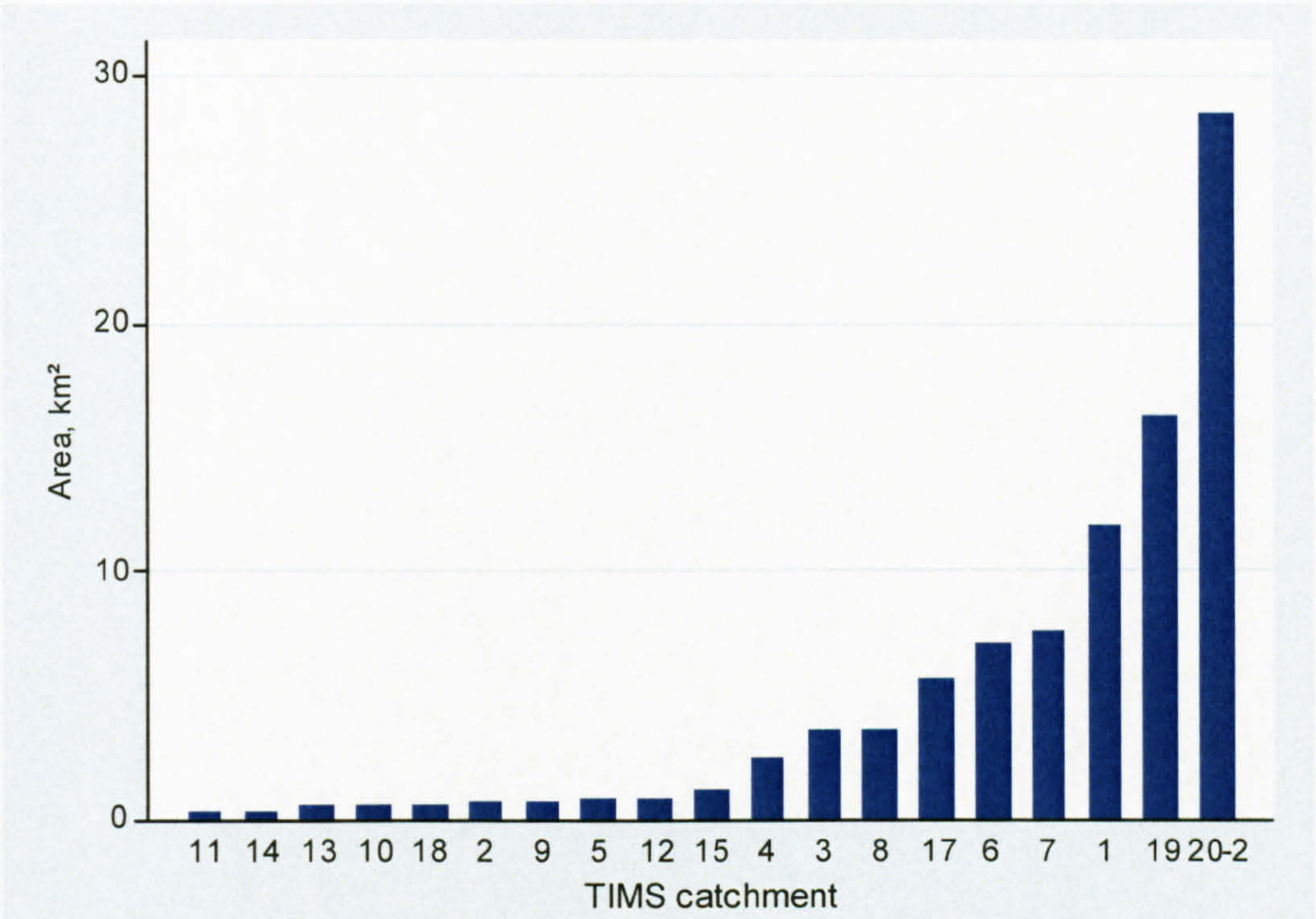

Figure 7.17. TIMS catchment areas.

7.5.1.1 Geology

The dendrogram generated by cluster analysis of geology suggests that the catchments can be divided into seven groups (Figure 7.18). All the TIMS geology catchment groups contain shale, sandstone and limestone (Figure 7.18). Catchment 11 stands out from the other catchments as it is the only catchment without any sandstone (Figure 7.18). The remaining catchment groups all contain approximately the same percentage of limestone (30%) but differ in the percentage cover of shale, which ranges from 15% to 35% and sandstone which ranges from 35% to 65% (Figure 7.18)

7.5.1.2 Soil

The dendrogram generated by cluster analysis of soil types suggests the catchments should be divided into six groups (Figure 7.18). The TIMS catchment groups as defined by soil are broadly similar: dominated by blanket bog with a notable proportion of eroding blanket peat and varying amounts of mixed bottom lands, peat-gley peaty-podzols, peaty-gleys, made ground, red brown limestone, coarse scree, solifluxion,

valley bog and fell top podzols (Figure 7.18). Catchment 11, again, is distinct and is characterised by 50% eroding blanket peat and 50% blanket bog (Figure 7.18). Three of the remaining catchment groups (19; 1, 6, 7, 17 & 20-22; and 2, 3, 4, 5, 8, 13 & 15) have similar percentages of eroding blanket peat, but differ in the percentage cover of blanket bog and other soil types (Figure 7.18). The remaining catchment groups (9, 10, 12 & 18 and 14) have a lower percentage cover of eroding blanket peat, a higher percentage of blanket bog and about 5% peaty-gley peaty-podzol (Figure 7.18).

7.5.1.3 Vegetation

The dendrogram generated by the cluster analysis of vegetation covers suggests the catchments should be divided into eight groups (Figure 7.18). In terms of vegetation cover catchment 11 is distinctive with 50% heath, 40% recolonised peat and 10% eroding bog (Figure 7.18). The proportion of eroding bog, i.e. bare ground, is of key importance. The remaining catchment groups are broadly similar in as much as they all contain grass, heath, recolonised peat, eroding bog and no more than 10% of sphagnum, bracken and other combined (Figure 7.18). It is the percentages of grass and heath which appear to define the catchment groups, although the eroding bog contents of TIMS 2 & 5 catchment group and TIMS 3, 4, 8, 13 & 15 are higher than for the other groups (Figure 7.18).

7.5.2 Spatial variation

Logistical constraints meant that it was not always possible to reset all the TIMS on the same day and some of the samplers were removed by high flows. To ensure only spatial variation in the organic matter content of TIMS sediment was investigated, not duration of deployment, only the results from eighteen TIMS (1, 2, 4, 5, 7, 8, 9, 10, 11, 12, 13, 14, 15, 17, 18, 19, 20 and 21) over six deployment periods (18/03/03 – 16/10/03) were examined. The organic-mineral balance from three TIMS deployed at Swinhope from 26/02/03 to 23/04/04 supplement the results from Moor House.

7.5.2.1 Moor House

The most obvious feature of the data from Moor House is that TIMS 11 generally has the highest organic matter content (Figure 7.19): the mean organic matter content of TIMS 11 over the six deployment periods is almost 20% more than the next highest mean organic matter content (Table 7.4). TIMS 14 consistently has one of the lowest

Geology:

Soil:

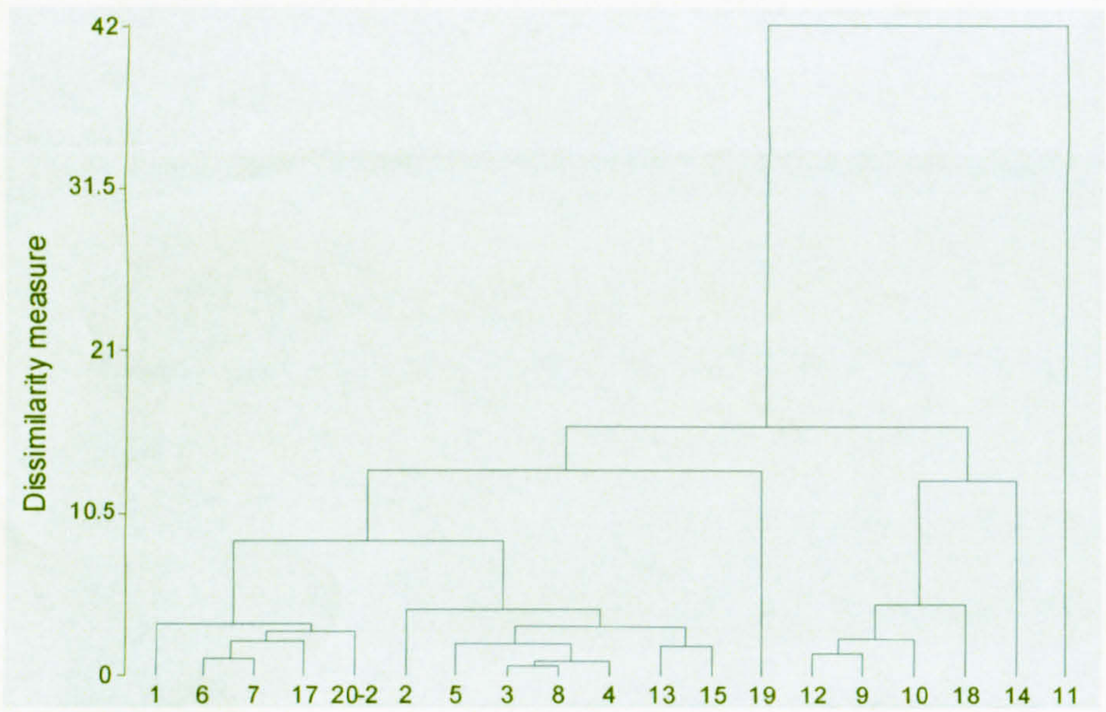

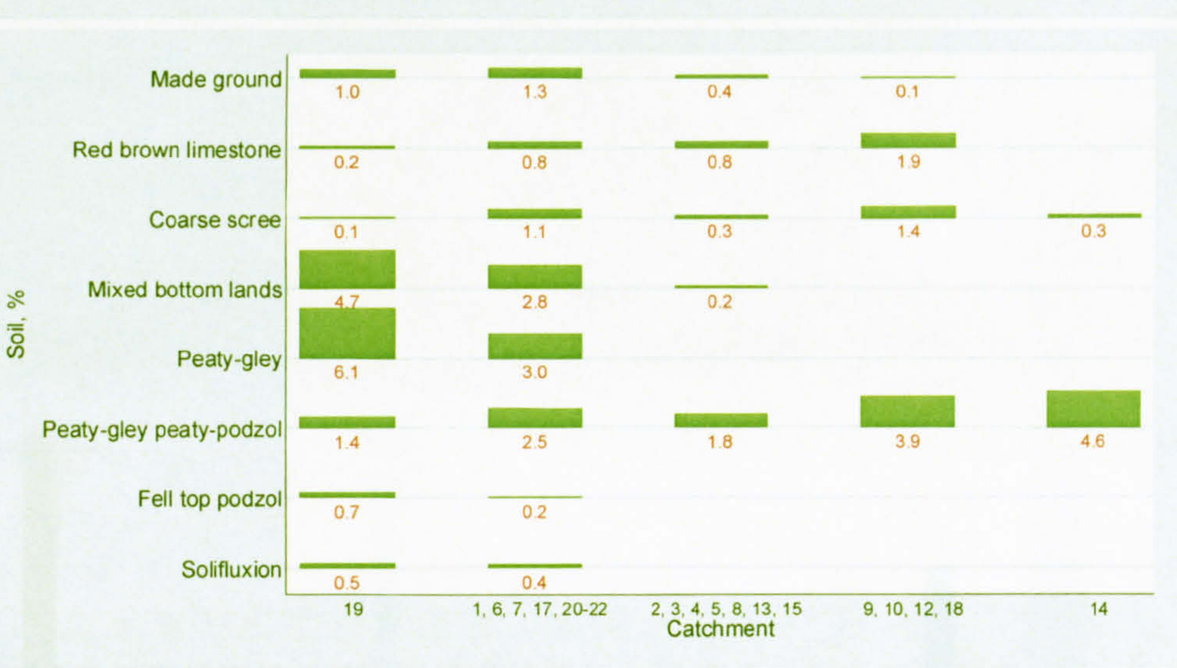

Vegetation:

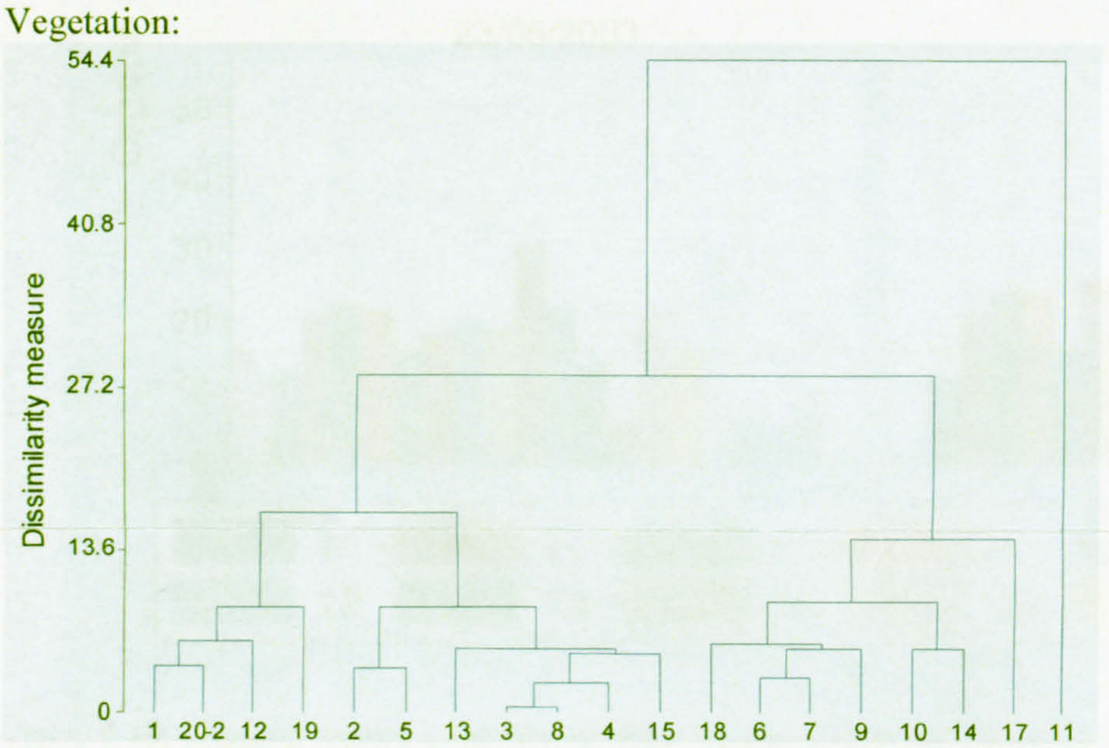

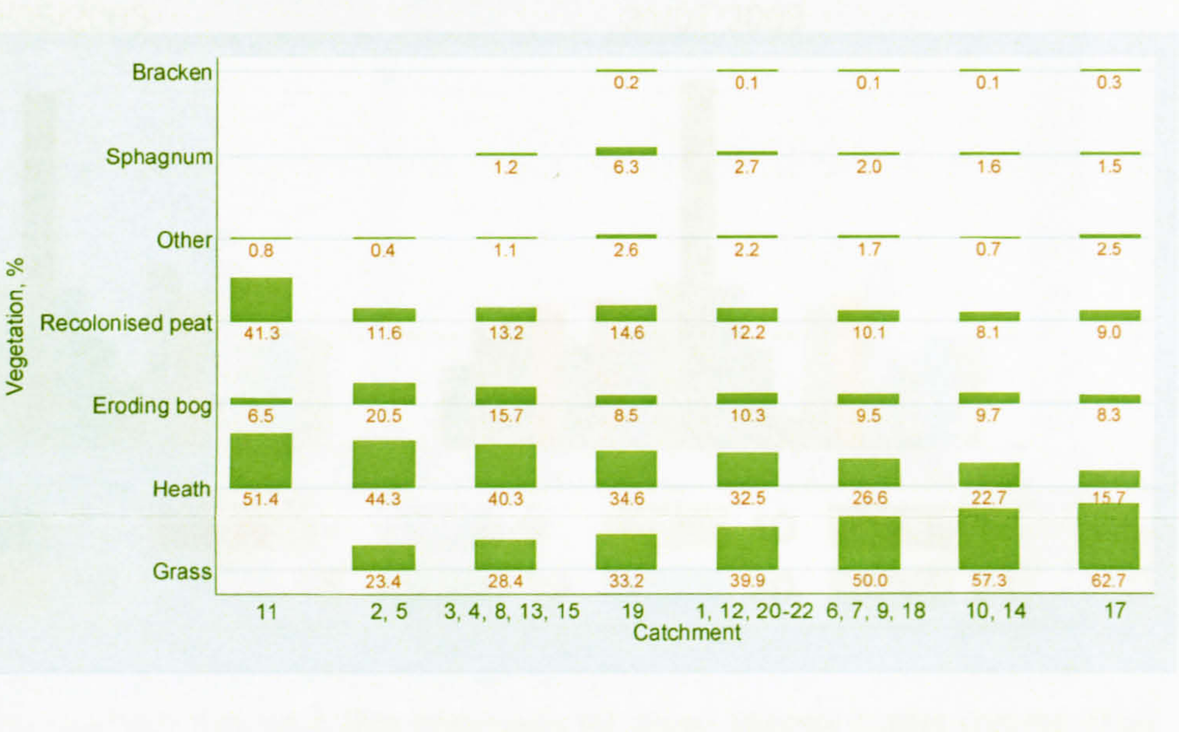

Figure 7.18. TIMS catchment cluster analysis dendrograms for geology, soil and vegetation and the mean percentages of each geology, soil and vegetation type in the catchment groups as defined by cluster analysis. Two graphs of mean percentages of soil type are given to allow examination of the less dominant soil types.

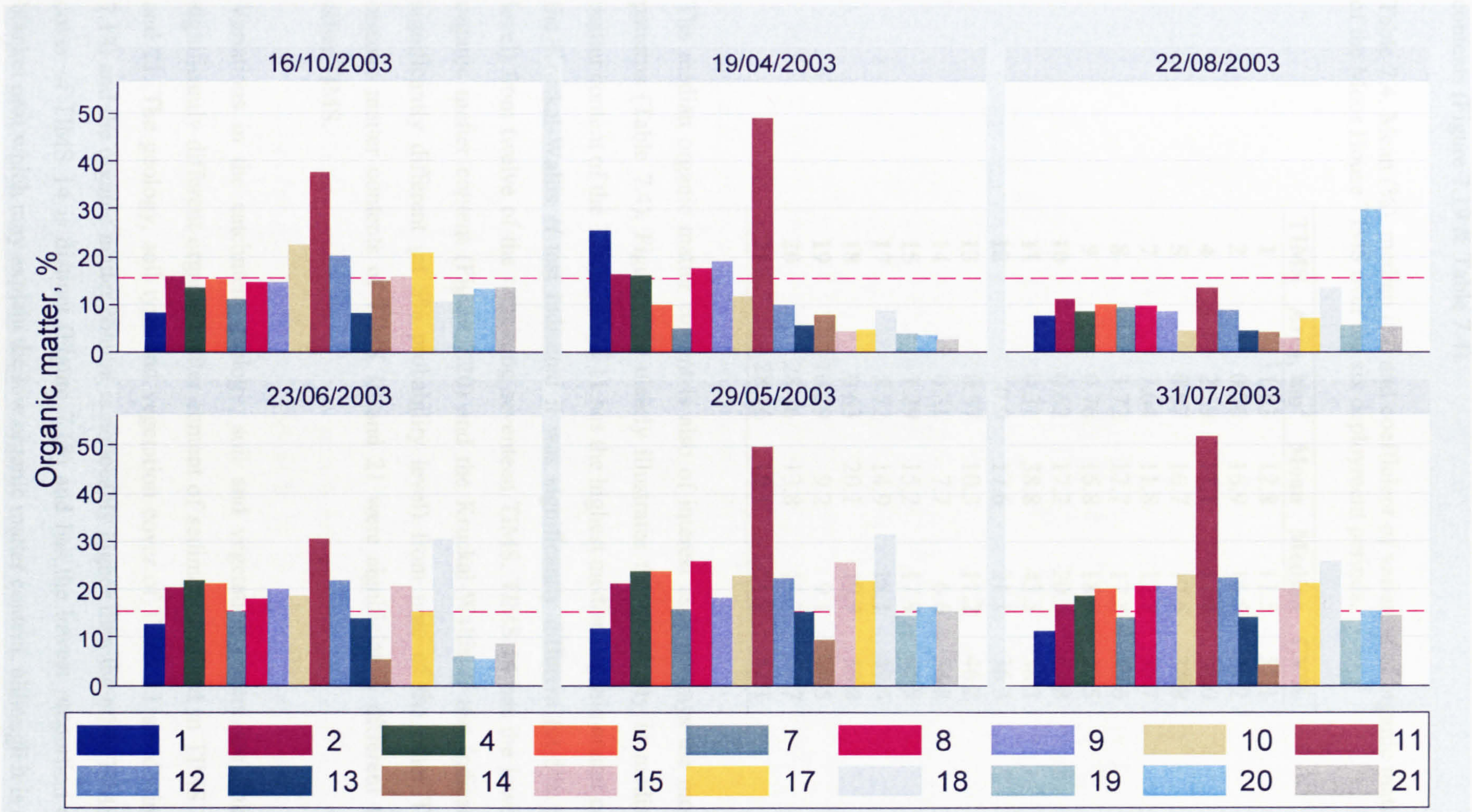

Figure 7.19. Organic matter contents of Moor House TIMS for six deployment periods. The dash line represents the mean organic matter content of all TIMS throughout the monitoring period. Note the different y-axis scales.

organic matter contents and TIMS 13, 19, 20 and 21 also have low organic matter contents (Figure 7.19 & Table 7.4).

Table 7.4. Mean (%), median (%) and coefficient of variation of organic matter content of the Moor House TIMS over the six deployment periods.

TIMS	Area, km^2	Mean	Median	CV%
1	11.83	12.8	11.5	51.1
2	0.76	16.9	16.5	21.2
4	2.59	17.1	17.4	33.0
5	0.87	16.7	17.6	34.8
7	7.64	11.8	12.7	35.7
8	3.72	17.7	17.8	30.6
9	0.76	16.8	18.6	27.5
10	0.62	17.2	20.5	43.8
11	0.31	38.8	43.5	38.3
12	0.9	17.6	21.1	36.3
13	0.57	10.3	11.2	46.2
14	0.31	7.7	6.6	54.8
15	1.29	15.2	17.9	61.8
17	5.72	14.9	18.1	49.6
18	0.63	20.1	19.7	50.8
19	16.29	9.2	9.1	49.5
20	28.46	13.8	14.2	67.7
21	28.46	10.1	11.2	52.1

The median organic matter content is also of interest as it portrays the more general patterns (Table 7.4). Figure 7.20 clearly illustrates the variability in median organic matter content of the TIMS. TIMS 11 has the highest median organic matter content and the Kruskal-Wallis *H* test indicated it was significantly different (at 5% probability level) from twelve of the remaining seventeen TIMS. TIMS 14 has the lowest median organic matter content (Figure 7.20) and the Kruskal-Wallis *H* test indicated it was significantly different (at 5% probability level) from nine of the other TIMS. The organic matter contents of TIMS 19 and 21 were significiantly different from eight other TIMS.

Variations in the catchment geology, soil and vegetation covers are linked to the significantly different organic matter content of sediment retained in TIMS 11, 14, 19 and 21. The geology, soil type and vegetation cover of TIMS 11 are distinct (Figure 7.18) and the organic matter content is noticeably higher than the other TIMS. The soil cover of TIMS 14 is distinct (Figure 7.18) and has the lowest proportion of eroding blanket peat which may explain the low organic matter content, although it is dominated

by blanket bog (Figure 7.18) and has limited mineral stores. The soil cover of TIMS 19 and the geology of TIMS 21 are distinct (Figure 7.18).

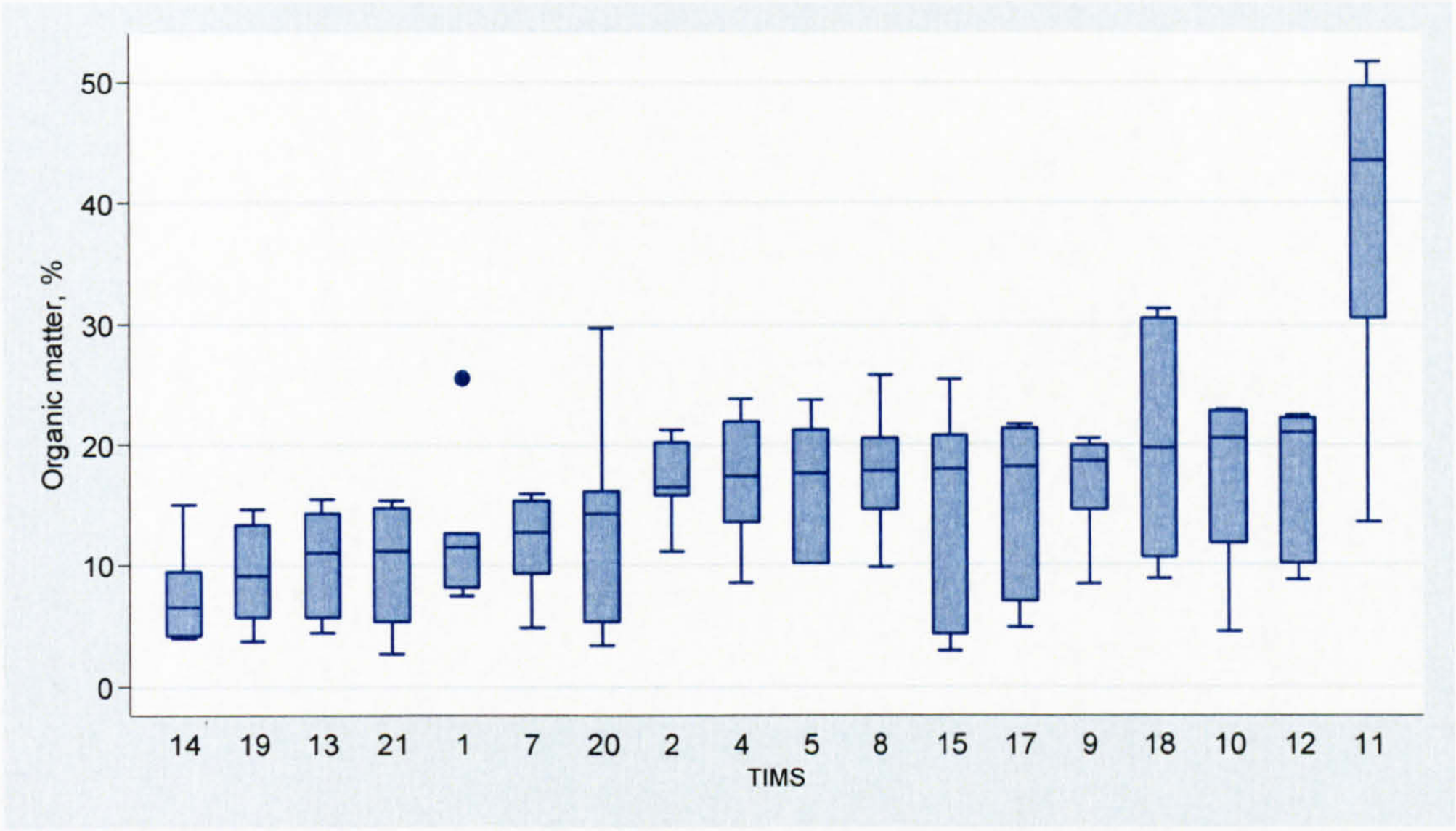

Figure 7.20. Box plots of the organic matter content, ordered by the median organic matter content, of TIMS sediment from the Moor House channel network.

The variability in the organic matter content of the TIMS sediment is of interest as it indicates variability in sediment sources over time. The greatest variability, as indicated by the interquartile range (>30%), occurs in catchments 11, 15, 17 and 18 (Figure 7.20). The higher variability of organic matter content of these TIMS can not be related to soil type, vegetation cover or geology as they are all in different catchment groups as defined by soil, vegetation and geology (Figure 7.18). There is no trend with catchment scale (Figure 7.17) but there is a weak trend with position in the channel network: catchments 11, 15, 17 and 18 are all located in upper catchments (Figure 6.5). However, some TIMS located in the upper catchments, for example TIMS 14, exhibit very low variability (Figure 7.20). The lack of pattern between catchment characteristics and position in the channel network and variability in the organic matter content suggests that connectivity between the sources and channel and the rate at which sediment sources are exhausted are controlling factors. Source connectivity and exhaustion are difficult to measure at a catchment-scale at a high enough temporal resolution to capture the variability. This indicates the mis-match between scales at which influential factors are measured and the scales at which processes operate.

There is no clear pattern in the mean organic matter content with position in the stream network (Figure 7.21). There is possibly a weak trend, with the exception of upper Rough Sike (TIMS 13 and 14), TIMS 8, TIMS 12 and TIMS 21, for the organic matter content to decrease with position in the channel network (Figure 7.21). The higher percentage of organic matter at TIMS 8 can be explained by the input from TIMS 11 (Figure 7.21). This overall pattern could be attributed to a smaller proportion of organic sediment supply in the higher order catchments, in comparison with the lower order catchments, as a result of the more extensive mineral-dominated floodplains and lower connectivity between hillslope and channel. Larger peat peds and blocks may be transported in the lower order catchments, but were not sampled as the TIMS inlet is too small. Such blocks and peds will abrade into smaller particles as they are transported. This may explain the lack of clear pattern between organic matter content and position in the stream network.

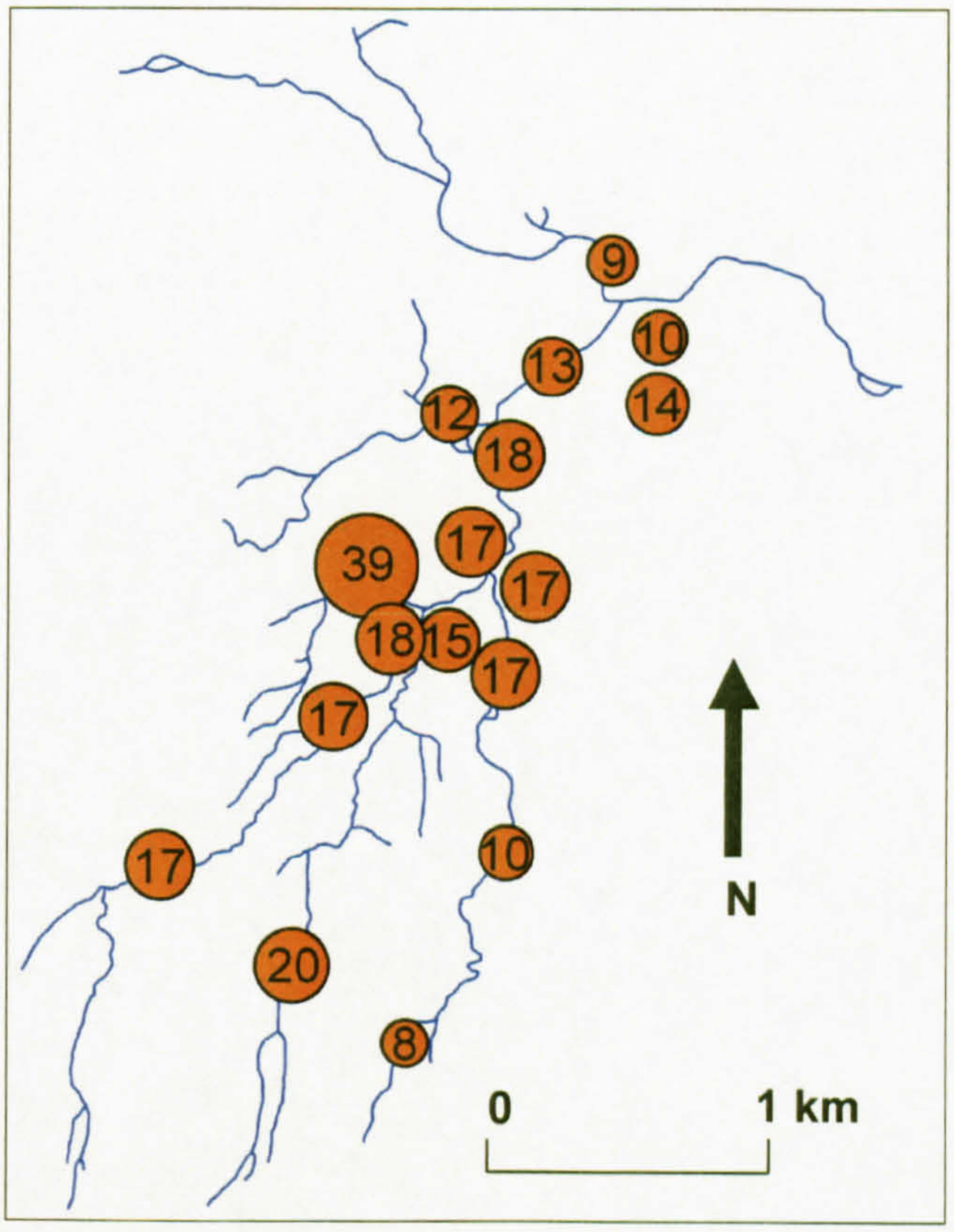

Figure 7.21. Organic matter content (%) of TIMS throughout the Moor House network.

Examination of organic matter content of TIMS sediment and the catchment groupings as determined by geology and vegetation cover indicates that there is no relation between geology or vegetation and organic matter content, except that the geology and vegetation cover of TIMS 11 catchment is distinct from all other catchments. However,

there is a relation between soil type and the organic matter content for the catchments with the higher (above 15%) organic matter contents (2, 4, 5, 8, 9, 10, 11, 12, 15 and 18) (Table 7.4):

(1) TIMS 11 has the highest organic matter content and also has distinct soil coverage: 50% blanket bog and 50% eroding blanket peat (Figures 7.18 & 7.19).

(2) Catchments 9, 10, 12 and 18 compose a soil group with 81.4% blanket bog, 11.4% eroding blanket peat, 3.9% peaty-gley peaty-podzol, 1.9% red brown limestone, 1.4% coarse scree and 0.1% made ground (Figure 7.18).

(3) Catchments 2, 4, 5, 8, 15 compose a soil group with 76.0% blanket bog, 20.5% eroding blanket peat, 1.8% peaty-gley peaty-podzol, 0.8% red brown limestone, 0.4% made ground, 0.3% coarse scree and 0.2% mixed bottom lands (Figure 7.18). Catchment 3 and 13 are also in the same group but TIMS 3 was removed by high flows during the time period examined and TIMS 13 had an organic matter content of 10.3% (Figure 7.19).

These catchment groups have the highest proportions of organic soil (blanket bog and eroding blanket peat), with the exception of catchment 14 (Figure 7.18). This suggests that the high proportions of organic matter may be due to limited supply of soil containing mineral sediment.

Examination of the effect of catchment area on organic matter content indicates the mean organic matter content decreases with increasing catchment area up to 20 km^2 and then stablises (Figure 7.22). As suspended sediment in the smaller catchments has a higher organic matter content and the organic fraction of suspended sediment is less likely to be deposited, given its buoyant nature, the lower organic matter content of TIMS sediment from the larger catchments is likely to be caused by dilution with mineral sediment. This could be explained by changes in the dominant source types: more organic-dominated sources (peat bank and hillslope sediment) in the smaller catchments, more mineral-dominated (floodplain sources) in the larger catchments. This makes physical sense, especially with regard to floodplain (mineral-dominated) sources, which occur more frequently and are more extensive in the lower catchments.

7.5.2.2 Swinhope

Spatial variation in organic matter content was also investigated using three TIMS at Swinhope. TIMS B and C were in tributaries approximately three metres upstream from their confluence and TIMS A was approximately ten metres downstream from the

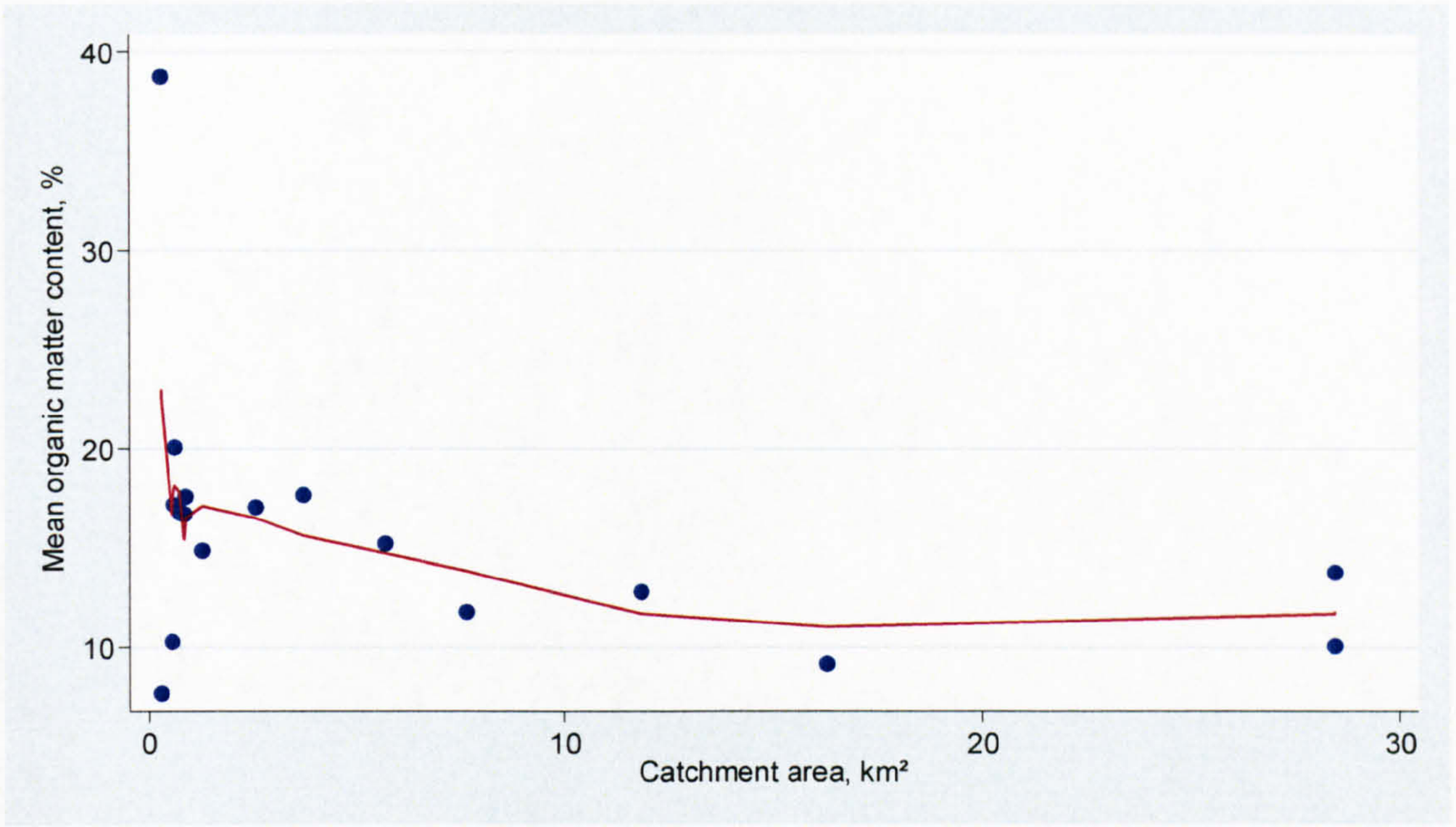

Figure 7.22. Mean organic matter content as a function of catchment area for Moor House TIMS. A LOWESS smooth has been superimposed to illustrate the generall trend.

confluence. TIMS B commonly has the highest organic matter content (Figure 7.23) and has the highest mean organic matter content out of the three TIMS: 17.8% in comparison with 14.2% for TIMS A and 15.0 for TIMS C. However, the Kruskal – Wallis *H* test concluded that there was no significant difference (at 5% probability level) between the organic matter contents of the three TIMS.

Catchment B has the lowest percentage of raw oligo-fibrous peat soils and therefore it is unexpected that the sediment has the highest organic matter content. As for Moor House, this indicates the difference between the importance of sediment source characteristics and overall catchment characteristics: it does not matter which soil types exist or dominate within the catchment if they are not connected to the channel network.

The coefficients of variation of TIMS A, B and C are 35.6%, 28.8% and 41.2% respectively. This indicates that there is least variability in the organic matter content of the sediment transported in the TIMS B catchment and the most variability in the TIMS C catchment (Figure 7.23). This suggests that there is more variability in the sediment source types in catchment C. For example, there may be some organic-dominated sources which are only accessed during high flow events.

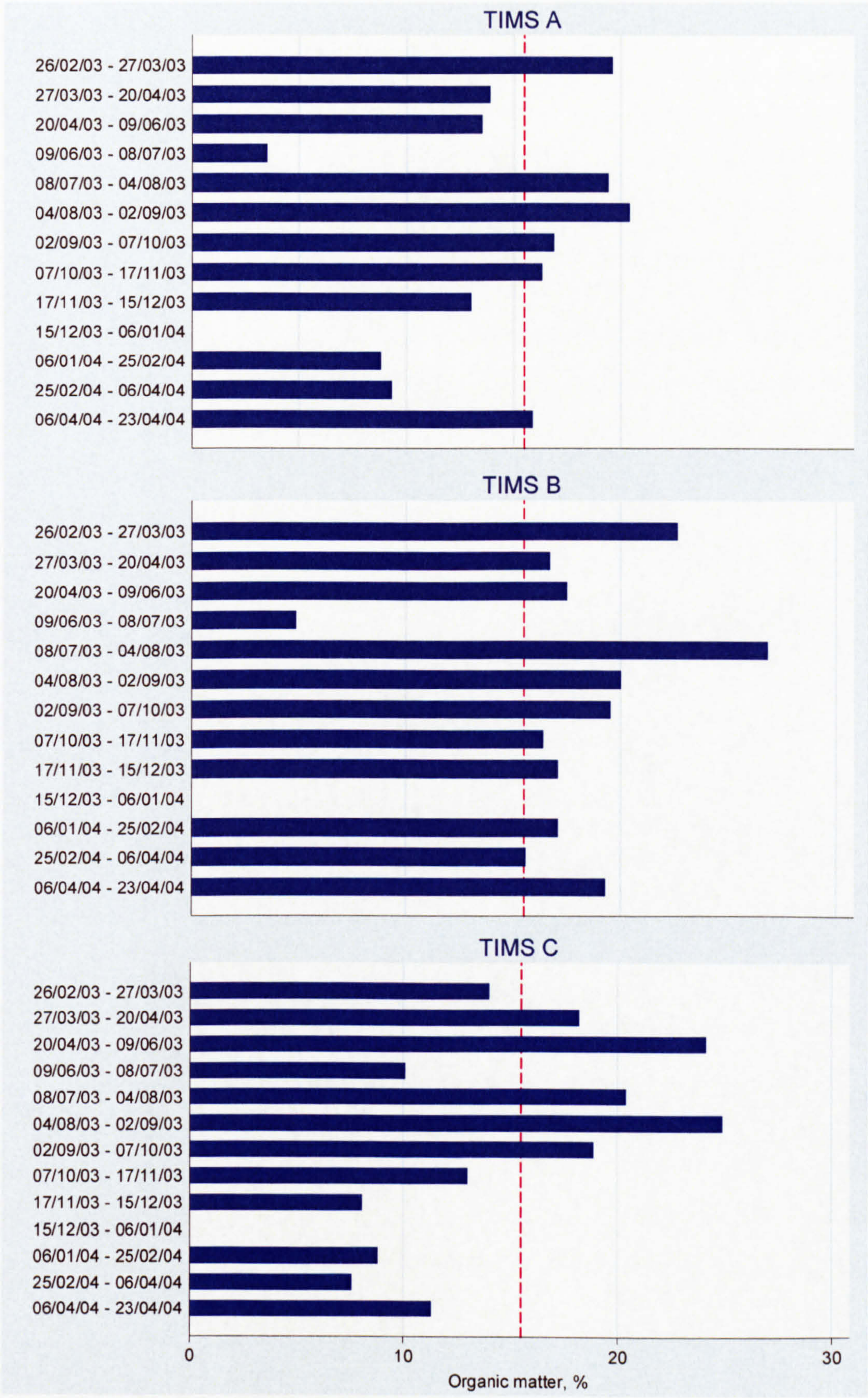

Figure 7.23. Organic matter content of the three TIMS at Swinhope. The dashed line represents the mean organic matter content of all samples at all locations. The samplers were not deployed between 15/12/03 and 06/01/04 due to technical difficulties.

There is a relationship between location in the channel network and organic matter content: the lower order catchments (B & C) have higher organic matter contents. This follows that the smaller catchments have higher organic matter contents. This could be related to the dominance of hillslope sources in the upper catchments, as discussed previously. However, given the close proximity of the three TIMS sampling locations it is unlikely. A possible explanation is that sediment falls out of suspension where catchments B and C combine, as there is a pool and slow-flowing section. However, this would promote the deposition of mineral sediment and therefore enrich the organic matter content of TIMS A. TIMS B and C are located in shallower channel sections than TIMS A, are therefore fixed closer to the bed and as a result are more likely to over-sample mineral bed sediment than TIMS A. Another possible explanation is that the higher discharges after the confluence entrain a higher proprtion of mineral sediment, thus decreasing the percentage of organic matter retained in TIMS A. Other possible explanations for this pattern are sampling and analysis error, especially given the differences were found to be statistically insignificant. Higher discharges after the confluence, sampling and analysis errors are the most likely causes, although proximity to the bed may also exert an influence.

7.5.3 Temporal variation in organic matter content

The following section outlines the monthly variation in the organic matter content of suspended sediment collected in the TIMS at Moor House and Swinhope over a period of approximately a year. The TIMS were deployed from 10/07/02 to 16/10/03 at Moor House and 26/02/03 to 06/04/04 at Swinhope and were reset approximately once a month.

The organic matter content of suspended sediment is governed by: (1) the production of organic matter within the stream environment, (2) the supply of allochthonous organic matter and (3) transport processes. Previous research (e.g. Walling & Webb, 1987) suggests the organic matter content of sediment peaks during summer months, due to the influence of autochthonous sediment sources and the higher proportions of organic matter transported during low flows given the lower density of organic sediment (e.g. Hillier, 2001). Organic matter commonly consists of 50% organic carbon (Ball, 1964).

Ankers (2003), who deployed 60 TIMS in various catchments in Devon, found that organic carbon peaked in summer and early autumn and attributed this to increased

primary productivity given the higher temperatures and the change in balance of sediment sources. Organic carbon is observed to decrease during storm events (e.g. Carling, 1983 and Hillier, 2001) and therefore is lower during the winter when there are more storms.

7.5.3.1 Moor House

The organic matter content of the Moor House TIMS sediment varies from 2% to 52%. Temporal patterns in the variation of organic matter content of TIMS in the Moor House channel network are evident; however, there is not a clear seasonal signal (Figure 7.24). The organic matter content of most TIMS is lowest in April, and again in late June and September (Figure 7.24). Peaks are observed in most TIMS in March, late May and August (Figure 7.24). Throughout the winter months (October to March) the organic matter content remained fairly constant (Figure 7.24). Troughs in the summer months, when organic matter content is hypothesised to be high, could be explained by large storm events which contribute high percentages of mineral sediment. Given the generally low flows during the summer one large event would have more effect than during the winter. There is substantial variability in the magnitude of the peaks and troughs of organic matter contents between the TIMS catchments (Figure 7.24). Ankers (2003) also found this for the range of TIMS catchments in Devon.

Figure 7.24. illustrates the general temporal patterns in organic matter content of TIMS but obscures any patterns that may be evident in individual TIMS records. Figure 7.25 shows the temporal variation in organic matter contents of individual TIMS, sorted by the median organic matter content. While there is seasonal variation no consistent seasonal trend is apparent (Figure 7.25). No relation could be found between catchment size, geology, soil type, vegetation cover or position in the channel network and the type or severity of the temporal variation.

Given the coarse resolution and the influence of production of autochthonous matter, the supply of allochthonous matter, and transport processes, especially the negative relationship between organic matter and discharge, it is not surprising that the seasonal variation in organic matter content is highly variable. If the organic matter content had been monitored continuously/quasi-continuously and moving averages taken more of a trend may have been apparent.

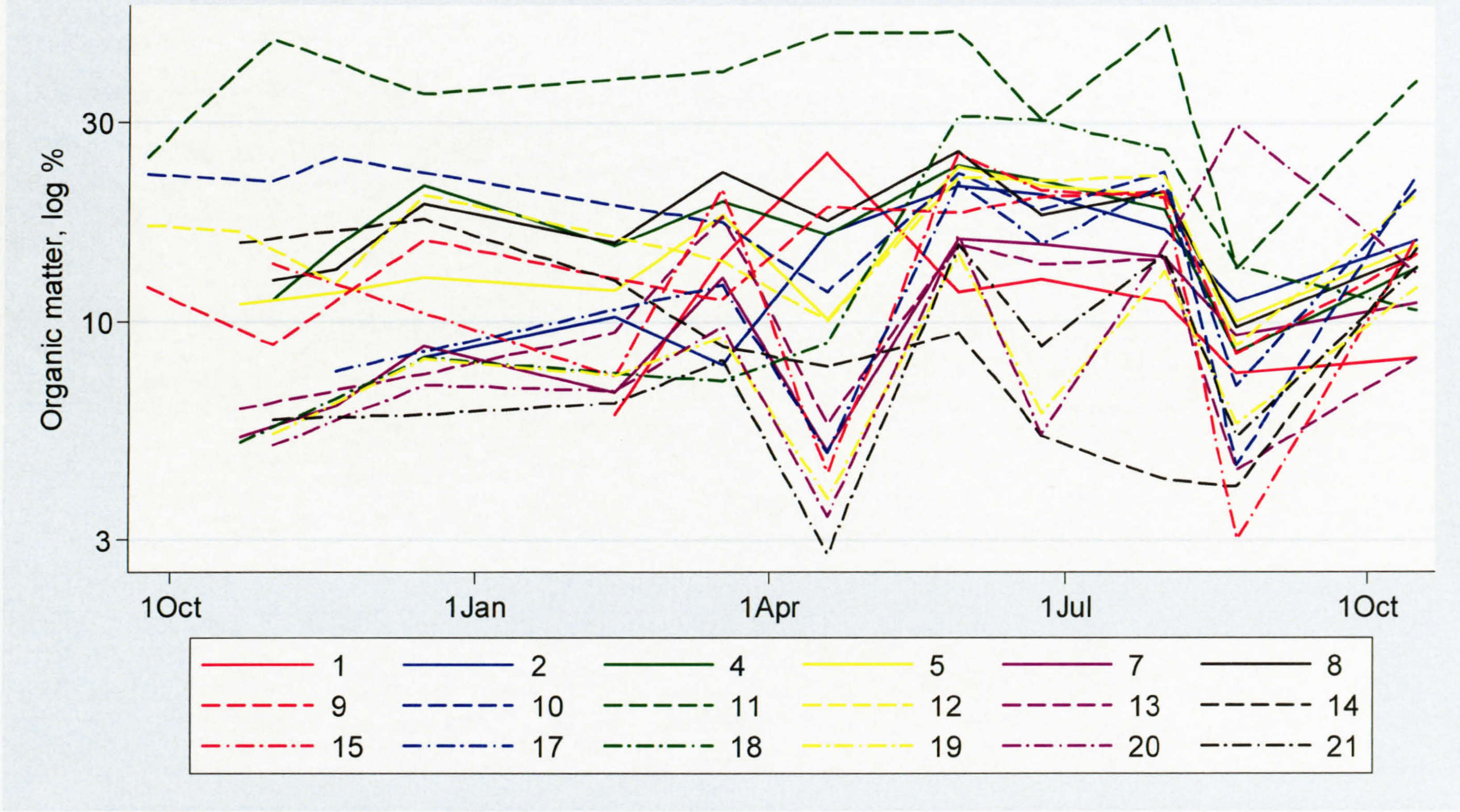

Figure 7.24. Temporal trends in organic matter content of TIMS sediment in the Moor House channel network. Each line represents a TIMS. Note the logarithmic scale on the y-axis.

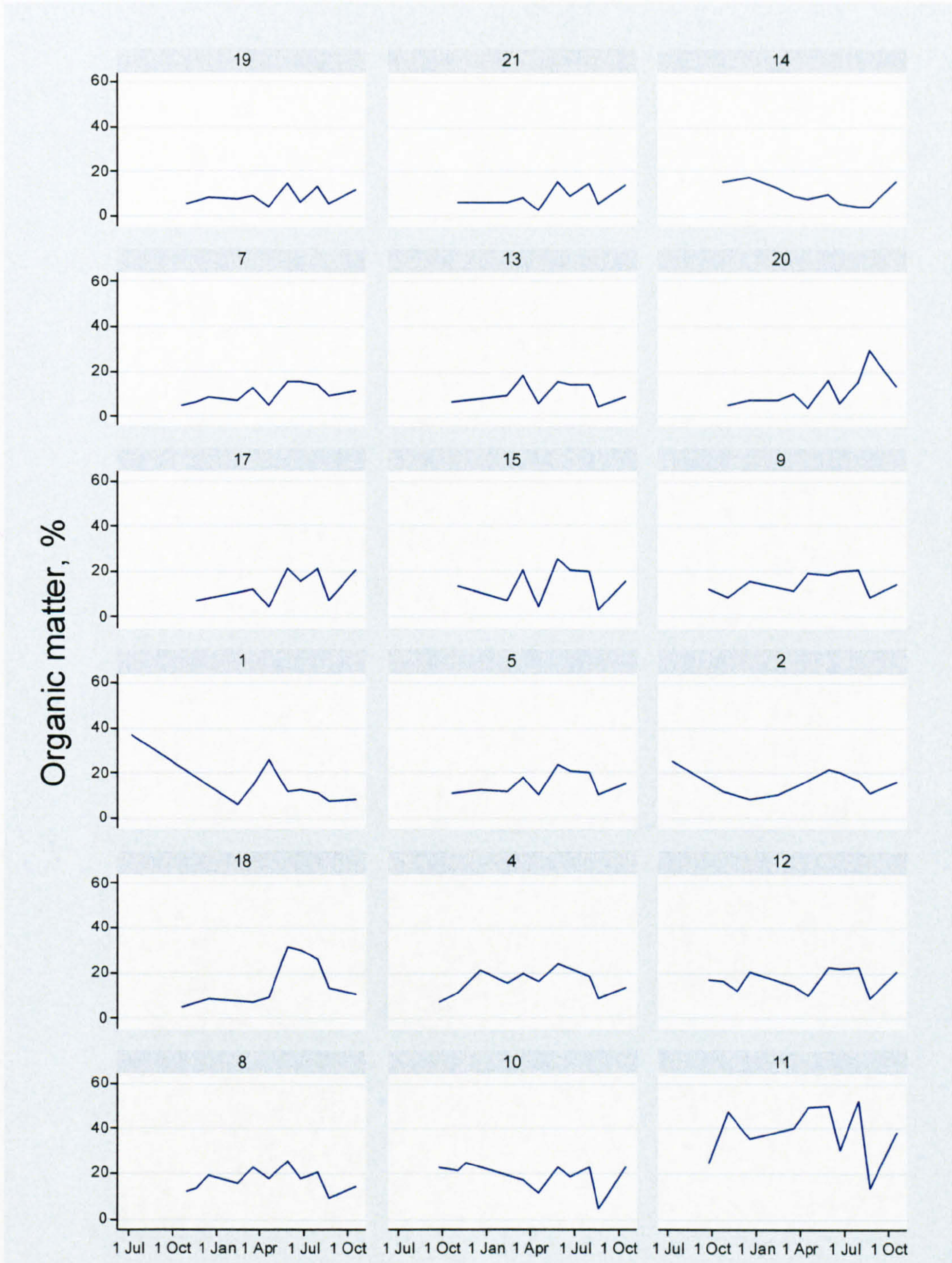

Figure 7.25. Temporal trends in the organic matter content of each of the TIMS in the Moor House channel network. TIMS are ordered according to the median organic matter content.

During field collection of the TIMS at Moor House some of the inlets were found to be temporarily blocked by stream debris (vegetation, peat blocks and clasts in some of the more active reaches). These blockages during deployment may also have interfered with the seasonal signal at Moor House.

7.5.3.2 Swinhope

The organic matter content of TIMS sediment was also investigated at Swinhope and varied from 3% to 27%. With the exception of the July TIMS samples the seasonal signal is much more evident (Figure 7.26). This is apparent in the organic matter contents of each TIMS and very apparent in the mean content of all three TIMS: organic matter content peaks from June to September at ~22% and troughs from February to April at ~12% (Figure 7.26). The seasonal pattern indicates that there is variability in the sediment sources throughout the year. The increase in the organic content of the sediment during the summer months can be attributed to increased productivity, in particular within the channel. In addition to changes in sediment sources, sediment transport processes may affect the relative proportions of organic and mineral sediment. During the winter months discharges are generally higher and therefore transport capacities are greater. Given that mineral particles generally require more energy to be transported as they are denser than organic particles, it follows that there will be a higher proportion of mineral sediment transport during the winter compared with the summer.

The low organic matter content of the TIMS sediment in July could be explained by a large storm event. One large event is evident in the stage record and is of comparable magnitude with the largest storm events in June and August (Figure 7.27). However, the discharge does rise very steeply (Figure 7.27). The rainfall record indicates that the third most intense rainfall occurred within the July TIMS deployment period (Figure 7.28), which may have released sediment from mineral sources and transported it to the channel, thus causing the uncharacteristically low organic matter content.

7.5.4 Summary

There are four key findings from the analysis of the organic matter content of TIMS sediment from the Moor House and Swinhope channel networks:

(1) There are statistically significant differences in the spatial variation in organic matter content within the Moor House channel network, which can be related to variability in soil cover in the catchments. There are some links between geology and vegetation and variations in organic matter content. In contrast, the spatial variation in the organic matter content of sediment at Swinhope was insignificant. This may reflect the closer proximity of the TIMS at Swinhope as opposed to true differences between the systems.

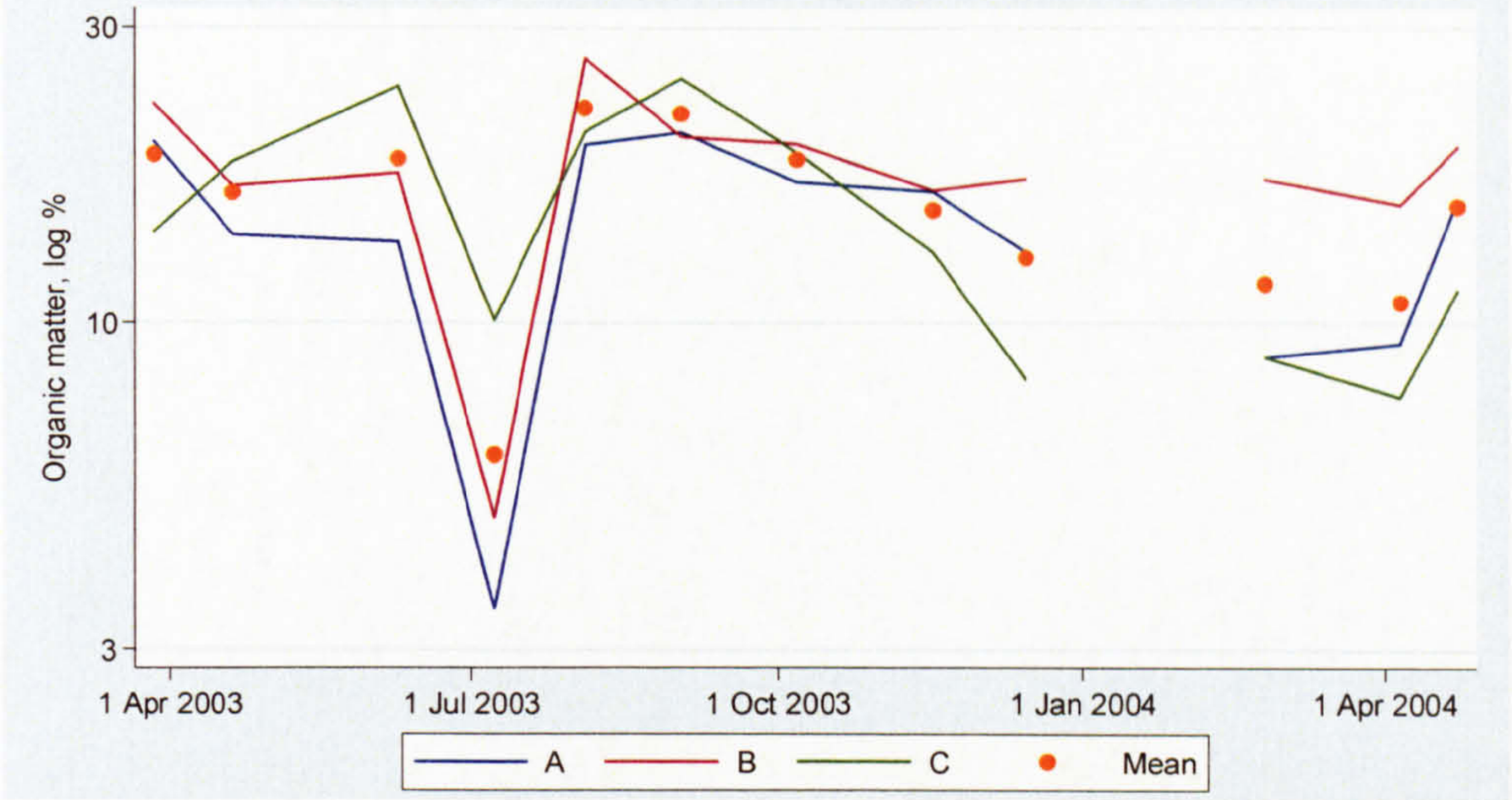

Figure 7.26. Organic matter content of TIMS sediment from the Swinhope channel network. Each line represents a TIMS. The TIMS were not deployed between 15/12/03 and 06/01/04 due to field difficulties. Note the logarithmic scale on the y-axis.

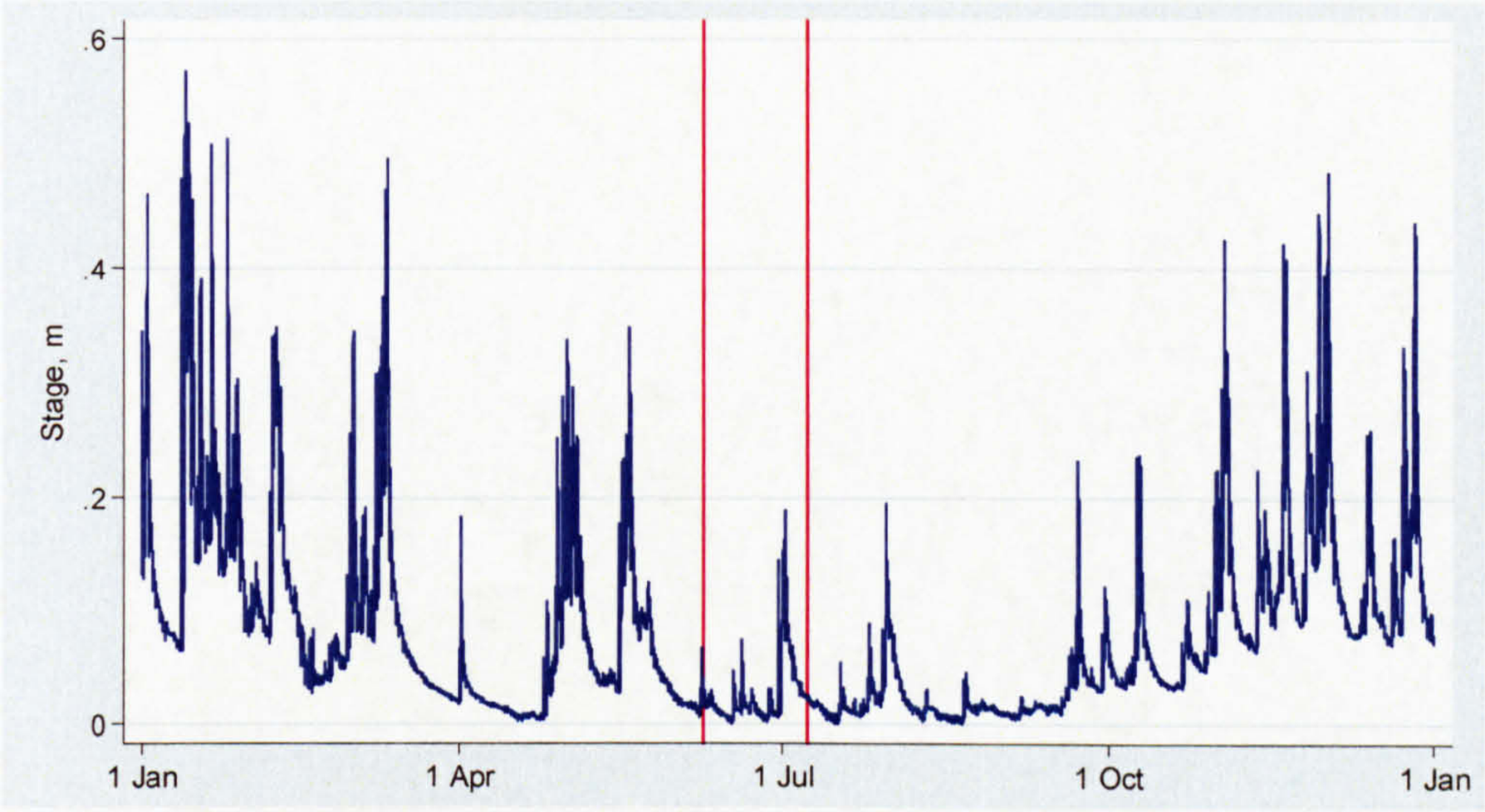

Figure 7.27. Stage record for Swinhope. The red lines indicate the period for which the TIMS had an uncharacteristically low organic matter content.

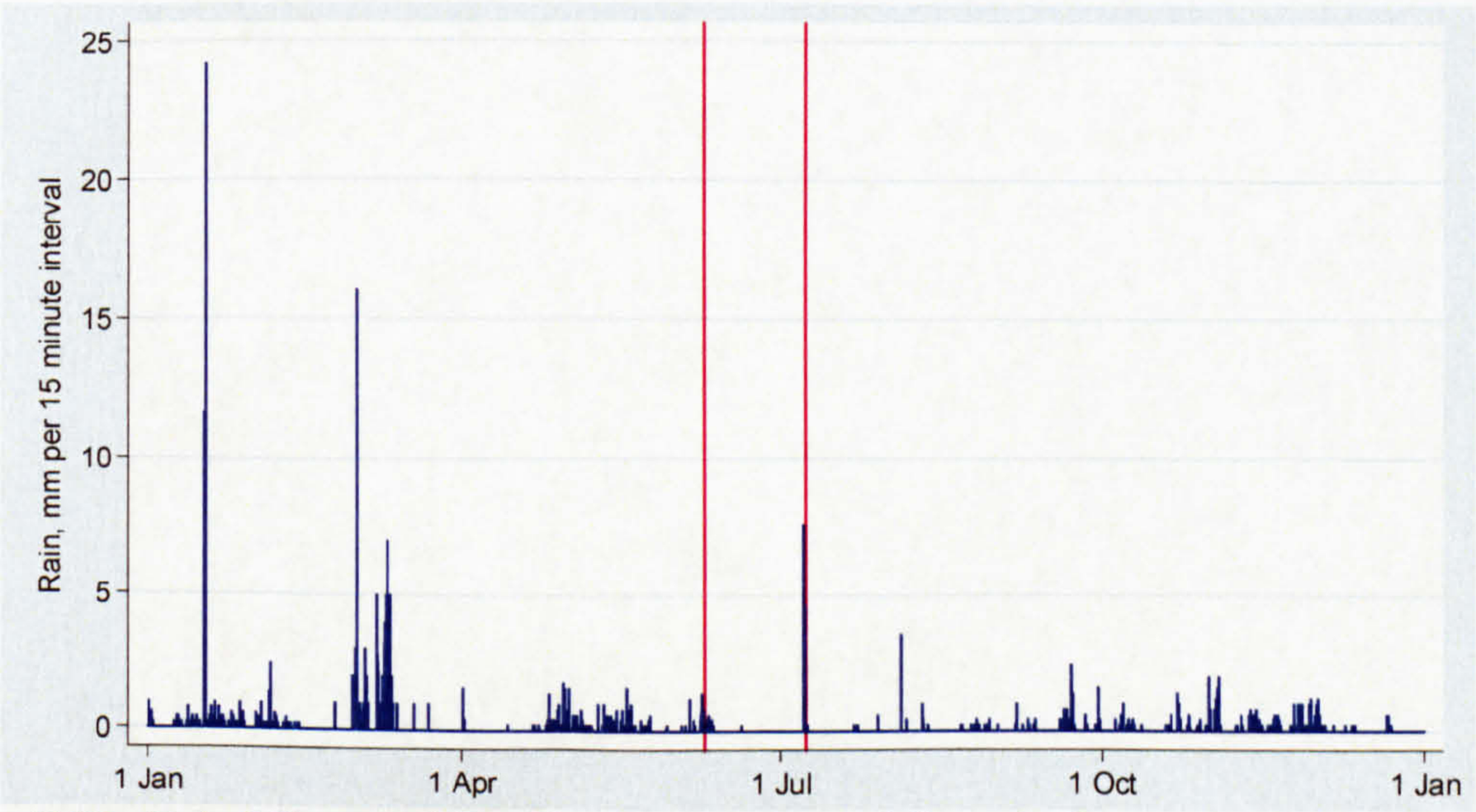

Figure 7.28. Rainfall record for Sinwhope. The red lines indicate the period for which the TIMS had an uncharacteristically low organic matter content.

(2) Organic matter content decreases with catchment area and distance downstream. Multiple organic sediment sources throughout the catchments and mineral sediment supplied by channel banks, floodplains and bars, which are not classified on the soil map, may obscure this pattern.

(3) Decreases in organic matter content are likely to be a result of increased contributions of mineral sediment sources as organic material is unlikely to be deposited given its low density.

(4) It was expected that approximately the same temporal patterns in organic matter would be evident at Moor House and Swinhope, given their broad similarity and close proximity. There was a pattern in the organic matter content of TIMS sediment deployed at Moor House, but no seasonal trend. In contrast, there was a clear seasonal signal at Swinhope. The lack of clear seasonal signal at Moor House may be explained by the dominance of peat at Moor House, in comparison with Swinhope: the majority of the hillslopes at Moor House are covered with peat and many of the channel banks are composed of peat and peat deposits are less extensive at Swinhope, are located in the upper catchment, and a lower proportion of the channels have peat banks. Therefore, the seasonal signal at Moor House could be attributed to substantial transfer of mineral sediment during the summer months during storms damping the autochthonous organic signal and/or interference of the signal by the greater number of allochthonous organic sources throughout the catchment. At Swinhope the input of autochthonous organic sediment during the summer and the effect of the seasonal flow regime may be more influential on the relative percentages of organic and mineral transfer.

7.6 Principal component analysis of sediment geochemistry

The following section examines the spatial variation in suspended sediment geochemistry using principal component analysis (PCA). PCA is introduced, the analysis procedure and framework for interpretation outlined, the results presented and the findings summarised. The results are examined in light of the catchment characteristics as outlined in section 7.5.1. This facet of the investigation is more exploratory in nature than the previous sections and offers insights into linkages between the suspended sediment and geochemical systems. The hypothesis being tested is to examine trends between the geochemical properties of sediment captured in the time-integrated mass samplers (TIMS) from Moor House in relation to catchment

characteristics, the geochemical composition of sediment sources and the possible effect of in-stream processing.

PCA is a multivariate exploratory data analysis technique used to get a sense for data sets which may not have explanatory and response variables. It is used to seek identification and understanding of any structure in the data and to suggest hypotheses of relationships between variables (Chatfield & Collins, 1980). Principal components (PC) are derived from the covariances or correlations between variables: correlations are preferred if the variables are assumed to be of equal importance, but are on different measurement scales. The PCs are linear combinations of the original variables, and capture the majority of the variation in the original data, but are completely uncorrelated with each other. Eigenvalues and eigenvectors are calculated from the correlation or covariance matrix. The eigenvalues are the variances of the PCs. The eigenvectors are the coefficients which relate the PC to each original variable. The PCs are calculated by summing the product of the standardised value of each original variable and the associated eigenvector element. If all the variables are positively correlated, then the first PC, a weighted average of the variables, can often be regarded as a measure of size. However, if there are some negative correlations then interpretation of PCs is more difficult and is done by examining the eigenvectors, selecting variables which are dominating each individual PC and trying to make some link between them.

There are three main uses of PCA. First, to identify new, hopefully meaningful, variables (Chatfield & Collins, 1980). An example of this is research into the factors which govern stream water quality. For example, Haag & Westrich (2002) sampled ten water quality properties (chlorophyll-a, biochemical oxygen demand in five days, electrical conductivity, pH, water temperature, ammonium nitrogen, nitrite nitrogen, nitrate nitrogen, phosphate and dissolved oxygen) and discharge every two weeks over five years at six locations along the River Neckar, Germany. PCA was performed and four PCs were retained which captured 72% of the variance in the original data. Haag & Westrich (2002) examined the dominant controls over each PC (i.e. the variables with the highest eigenvector coefficients), applied knowledge of controls and influences on water quality and consequently were able to associate biological processes with PC1, discharge with PC2, seasonal influences with PC3 and wastewater influences with PC4. The second main use is to decrease dimensionality to aid future analysis, for example identification of groups and clusters and production of suitable variables for statistical

techniques (e.g. multiple regression) for which mutually independent variables are desired and to eliminate singularity problems if the number of observations is less than the number of variables (Chatfield & Collins, 1980). Worrall *et al.* (2003a) applied PCA to a two year weekly sampling set of pH, conductivity, alkalinity, Na, K, Ca, Mg, Fe, total N, SO_4, Cl and colour measurements of precipitation, soil water and stream water samples from Moor House NNR (a study site of this investigation). The aim of the study was to identify controls over runoff composition. Five PCs were retained which explained 90% of the variance in the original data. In contrast to Haag & Westrich (2002) the bulk of the PCA interpretation in Worrall *et al.*'s (2003a) study was graphical and no interpretations of the PCs were made. Aided by other data analysis techniques PCA led to conclusions regarding controls of runoff flow pathways and hydrochemistry. The third use is to eliminate variables which contribute little or no extra information (Chatfield & Collins, 1980) and thus rationalise data collection requirements.

7.6.1 Analysis

The sediment was analysed for 44 elements including a selection of the most common rare earth elements and a suite of the most common metals (Table 7.5). Specific elements were not selected as this data analysis was exploratory and the purpose was to identify trends and patterns, not to quantify concentrations of specific elements.

Table 7.5. Analysed elements sorted by element group.

Element group	Element
Alkali metal	lithium (Li), sodium (Na), potassium (K).
Alkali earth metal	magnesium (Mg), calcium (Ca), strontium (Sr), beryllium (Be).
Semi-metal	silicon (Si), antimony (Sb), arsenic (As), boron (B).
Basic metal	aluminium (Al), thallium (Tl), lead (Pb), bismuth (Bi).
Transition metal	yttrium (Y), scandium (Sc), molybdenum (Mo), silver (Ag), cadmium (Cd), titanium (Ti), vanadium (V), chromium (Cr), manganese (Mn), iron (Fe), nickel (Ni), cobalt (Co), copper (Cu), zinc (Zn).
Non-metal	selenium (Se).
Rare earth	samarium (Sm), ytterbium (Yb), neodymium (Nd), dysprosium (Dy), lanthanum (La), erbium (Er), lutetium (Lu), terbium (Tb), europium (Eu), thulium (Tm), gadolinium (Gd), praseodymium (Pr), cerium (Ce), holmium (Ho).

A pilot study of the geochemical variability within the TIMS samples was undertaken. Three data sets were generated: (1) raw, (2) ranked, and (3) logarithmically transformed. The data were ranked to increase the robustness of the analysis and enable investigation of the relative difference in elemental concentrations between the sampling sites. The data were logarithmically transformed to reduce skew. This pilot study indicated the geochemical data should be used in its raw form, as ranking the data abstracted the analysis too far from the actual data and comparison of the principal components derived from the raw and logarithmically transformed data resulted in the same overall patterns.

Before PCA the quality of the analytical determinations was checked to prevent inaccurate determinations from influencing the results. Determinations with high standard errors may result in the PCA modelling the errors as opposed to the patterns in the data. The data were also checked for cross-correlations between elements: elements with high cross-correlations were removed to clarify the structure. Se was discounted due to the high (200%) standard errors in the analytical determinations. A correlation matrix between elements was calculated and variable pairs with a correlation coefficient greater than 0.90 identified (Table 7.6). From these pairs Dy, Ho, Ce, K, Na and Bi were retained as every other element shows correlations above 0.90 with one or more of these elements. This combination of elements was chosen as it represents the least number of elements required. A graph matrix of the elemental data was also drawn to check for any abnormalities in the data but none were evident. Elements which did not notably influence the outcomes of the PCA were eliminated as it is preferable to have fewer variables than observations.

After the elements eliminated by cross-correlations and poor analytical determinations were removed 27 elements remained: Li, Be, B, K, V, Mn, Fe, Co, Cu, Zn, Sr, Cd, Sb, Ba, Tl, Pb, Bi, Ce, Ho, Sc, Dy, Eu, Na, Mg, Ca, Al and Si. These 27 elements were analysed by PCA using the correlations between the elements, not the covariances, to prevent elements with higher average values from exerting more influence than those with lower values. Four separate PCA were undertaken: (1) on all 27 elements for TIMS samples only; (2) on elements which correlated with the PCs of (1) at greater than 0.75 (as indicated by the correlation coefficient); (3) on all 27 elements for TIMS and source sediments; and (4) on elements which correlate with PC of (3) at greater than 0.75 (as indicated by the correlation coefficient) for TIMS and source sediment samples. The

Table 7.6. Element pairs with > 0.90 correlation coefficient.

Element 1	Element 2	Correlation coefficient	Element 1	Element 2	Correlation Coefficient
K	Ti	0.944	Dy	Yb	0.944
K	Cr	0.941	La	Pr	0.981
Ti	Cr	0.986	La	Y	0.976
As	Bi	0.915	La	Nd	0.930
Mo	Bi	0.901	Er	Lu	0.923
Ag	Na	0.923	Er	Tm	0.933
Ce	La	0.918	Er	Yb	0.980
Ce	Tb	0.920	Lu	Tm	0.992
Ce	Gd	0.960	Lu	Yb	0.936
Ce	Pr	0.973	Tb	Tm	0.913
Ce	Y	0.965	Tb	Gd	0.987
Ce	Sm	0.954	Tb	Sm	0.989
Ce	Nd	0.995	Tb	Nd	0.921
Ho	Er	0.953	Tm	Yb	0.931
Ho	Lu	0.943	Gd	Sm	0.999
Ho	Tb	0.978	Gd	Nd	0.959
Ho	Tm	0.966	Pr	Y	0.997
Ho	Gd	0.948	Pr	Nd	0.982
Ho	Sm	0.953	Y	Nd	0.976
Ho	Yb	0.908	Sm	Nd	0.952
Dy	Er	0.972			

PCA was repeated with a reduced number of elements to ensure the number of variables (elements) was less than the number of observations (samples). The results of the PCA undertaken with all 27 elements were not investigated in detail, but the PC plots were checked to ensure the same patterns were evident on the PC plots obtained from the reduced number of elements PCA.

7.6.2 Framework for interpretation of the PC plots

The geochemical signature of stream sediment is derived directly from the parent material but may be chemically modified by reactions with the air, water and plant and microbial metabolisms (British Geological Survey, 1992). The element mineral association and the stability of those minerals will also affect the stream sediment geochemistry (British Geological Survey, 1992). The distribution of selected elements in stream sediment throughout the Lake District and surrounding area was surveyed by the British Geological Survey (1992). Samples were primarily from first and second order streams at a density of one sample per 1.6 km^2: thirteen were taken in the Trout Beck system. Due to the strong control of parent material, examination of the spatial variation in suspended sediment geochemistry is more successful in heterogeneous catchments and most applications of PCA are centred on distinguishing observations into groups based on characteristics that *a priori* reasoning suggests. While the

characteristics of each of the TIMS catchments are not distinct, the variable proportions of geology, soil and vegetation types should promote different sediment characteristics.

The chosen PCs were graphed against each other and structures identified. Each element was correlated with each PC to determine their importance. Several relationships and patterns were evident on the PC plots. The relationships and patterns in the higher order PC plots are the most important as the higher the order of the PC the more of the variability it explains, i.e. PC1 explains 58% and PC2 explains 17% (Figure 7.30). These patterns will be examined in order to:

(1) Assess the impact of the slightly different catchment characteristics in terms of geology, soil type and vegetation cover. For example some elements are low in limestone compared with mudstones and sandstones (e.g. V (British Geological Survey, 1992)) so therefore TIMS samples in catchments with higher proportions of limestone may plot in a different region on the PC graphs.

(2) Compare sediment source and suspended sediment geochemistry. This will potentially allow the dominant sediment sources to be ascertained if each type of source samples (peat, soil, floodplain and glacial till) proves to have consistent geochemical signatures.

(3) Establish if the geochemistry of a TIMS after a confluence reflects the geochemistry of the TIMS on each branch of the channel network before the confluence. This will allow inferences to be made regarding the degree of mixing between the confluence and TIMS and the dominance of each tributary in terms of sediment load and stream velocity.

(4) Establish if the geochemistry of successive TIMS in the channel network is related. In principle samples from successive TIMS should have similar geochemistry as the catchments are nested. However, in-stream processing and the influence of local sources may result in different geochemical signatures.

(5) Investigate if the sediment geochemistry of TIMS in the same river cross-section are similar. If the sediment is well-mixed across the river section the geochemical signatures should be similar. Inadequate mixing and the influence of local bank sources may result in different signatures.

(6) Investigate if TIMS in the same point in the channel network (e.g. all first order streams) have similar geochemistry on the basis that sediment source

will be broadly similar. For example, a higher proportion of sediment delivered by runoff is expected in the upper catchments than in the lower catchments.

The TIMS sample set used was collected on 18/12/02 and samples from TIMS 1, 6, 10, 15 and 17 were missing. However, the samples available allow examination position in stream network, upstream changes and point in channel cross-section to be examined (Figure 7.29).

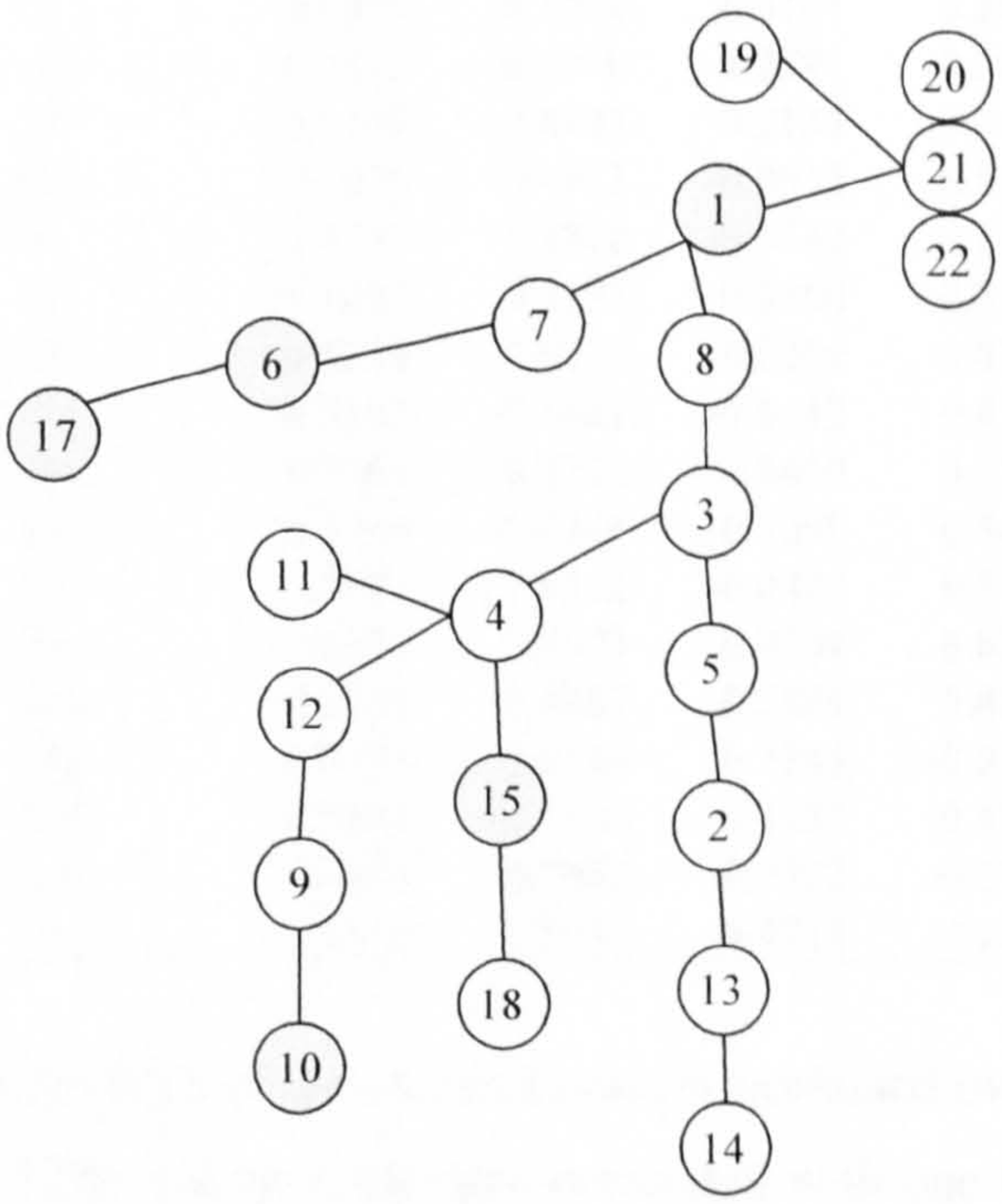

Figure 7.29. Schematic of TIMS location in the network (see Figure 6.5 for location on a catchment map). Shaded TIMS were missing as they were removed by high flows or insufficient time in the field.

7.6.3 PCA of TIMS sediment only

Each element was correlated against each PC to identify which elements contributed most to each PC (0.75 was taken as a threshold): Be, B, V, Cu, Sr, Bi, Ce and Ho contributed most to PC1; Sb and Al contributed most to PC2; and Zn was the only element which had a high correlation with PC3 (Table 7.7). All the other elements were discarded and PCA was repeated with the above eleven elements. This was done to ensure the number of observations was more than the number of variables.

Table 7.7. Correlations between each element and PC1-PC4 calculated from 27 elements. Figures in bold are those above the chosen 0.75 threshold.

	PC1	PC2	PC3	PC4
Li	0.6912	0.4880	-0.0811	-0.2921
Be	**0.8279**	0.3277	-0.1924	0.3345
B	**0.8583**	0.0289	-0.4288	0.2009
K	0.6716	0.4753	-0.5415	0.0332
V	**0.9681**	-0.0658	-0.0597	0.1471
Mn	0.4155	0.1608	0.6135	0.2017
Fe	0.4052	0.7216	0.3605	0.0844
Co	0.5589	0.7050	0.1789	-0.2456
Cu	**0.8268**	0.1458	-0.0352	-0.1207
Zn	0.3935	0.1468	**0.7649**	0.1471
Sr	**0.8395**	-0.1914	-0.0101	0.2843
Cd	-0.1142	0.4770	-0.2791	0.3824
Sb	-0.1160	**0.8441**	-0.2138	-0.3563
Ba	0.2070	0.4953	-0.0615	0.6724
Tl	0.5399	0.2820	-0.5842	0.1530
Pb	0.1483	0.1273	0.8360	0.3311
Bi	**0.8519**	-0.0677	0.2501	-0.0730
Ce	**-0.9103**	-0.1623	-0.0142	0.0161
Ho	**-0.9163**	0.2327	0.0400	0.1567
Sc	0.3269	-0.6269	-0.3099	0.5408
Dy	-0.7293	0.6362	-0.0427	0.1458
Eu	-0.6321	0.3673	0.0504	0.6384
Na	-0.2563	0.4067	0.2809	0.4158
Mg	-0.7278	0.6136	0.2243	-0.0386
Ca	0.5836	0.1103	0.4457	-0.4787
Al	0.0383	**0.7885**	-0.0822	-0.2709
Si	-0.5910	0.5081	-0.4718	-0.1075

The first four PC of the PCA of the eleven elements explained over 90% of the variation in the data (Figure 7.30) and each variable correlated with one PC at over 0.75 (Table 7.8). This information partially explains why some of the elements contribute to the PCs and also the likelihood of in-stream processing. A graph matrix of the PCs was drawn (Figure 7.31) and compared with the graph matrix of the PCs derived from the 27 elements (Figure 7.32) and the same patterns were evident. Therefore it can be concluded that Be, B, V, Cu, Sr, Bi, Ce, Ho, Sb, Al and Zn summarise the patterns of elemental abundance in the TIMS. Clustering on the PC plots is not as tight as on some published examples (e.g. Worrall *et al.*, 2003a) but this is perhaps expected due to the homogeneous nature of the catchments i.e. while the proportions of geology, soil and vegetation types vary they all contain the same types.

Several patterns and relationships are evident on the PC plots and can be discussed in light of the interpretation framework outlined above. The most obvious feature is that TIMS 11 is an outlier in all plots, except PC4 as a function of PC3 (Figure 7.31). There

Table 7.8. The distribution of elements (BGS, 1992) and correlations between each element and PC1-PC4 calculated from: 11 elements for TIMS sediment only, and eight elements for source and TIMS sediment. Figures in bold are those above the chosen 0.75 threshold. * Source: BGS, 1992.

Element	TIMS sediment only				TIMS and source sediment				Distribution*
	PC1	PC2	PC3	PC4	PC1	PC2	PC3	PC4	
Li					**0.8944**	-0.3419	0.1183	0.1718	High levels over Pennine block.
Be	**0.8677**	0.2681	-0.1315	0.1047	**0.9495**	0.0593	-0.0156	-0.1981	High levels throughout Teesdale. Possible link with mineralization.
B	**0.8901**	0.0746	-0.3349	0.2372					Patchy distribution over Carboniferous rock. High in upper Teesdale.
V	**0.9770**	-0.0434	-0.0715	-0.0277					Complex and patchy over the Pennines. Lower concentrations associated with limestone and higher concentrations with sandstones and mudstones.
Fe					0.6791	0.6538	-0.1381	-0.256	Higher levels association with mudstones and shale. Possible association with mine contamination.
Co					**0.9279**	0.0864	0.2553	-0.1264	Mostly low over Carboniferous rocks. Complex patterns over Pennine block. Possible secondary enrichment.
Cu	**0.8423**	0.1723	0.1605	0.2628	**0.9073**	-0.2032	-0.1618	0.1887	Low over limestone. High where there is mineralization and mining activity.
Sr	**0.8854**	-0.2926	-0.0184	0.1184					High over the Pennine block. Associated with limestone.
Bi	**0.8321**	-0.0778	0.3511	-0.0548					Low but high anomalies over Pennine block. Associated with mineralization and Zn and Cu.
Ce	**-0.8747**	-0.2389	0.1085	0.3709	0.1879	**0.8843**	-0.3681	0.1947	No information.
Ho	**-0.8941**	0.1048	0.1735	0.1697					No information.
Sb	-0.1380	**0.8668**	0.2024	0.3765					Generally low except in areas of mineralization. Coincides with Zn.
Al	-0.0222	**0.9195**	-0.0021	-0.3578					No information.
Zn	0.4030	-0.1320	**0.8660**	-0.0879					Distribution influenced by mining and mineralization. Variable away from mineralization.
Mg					0.0297	**0.8702**	0.4493	0.1784	Very low over Carboniferous rocks.

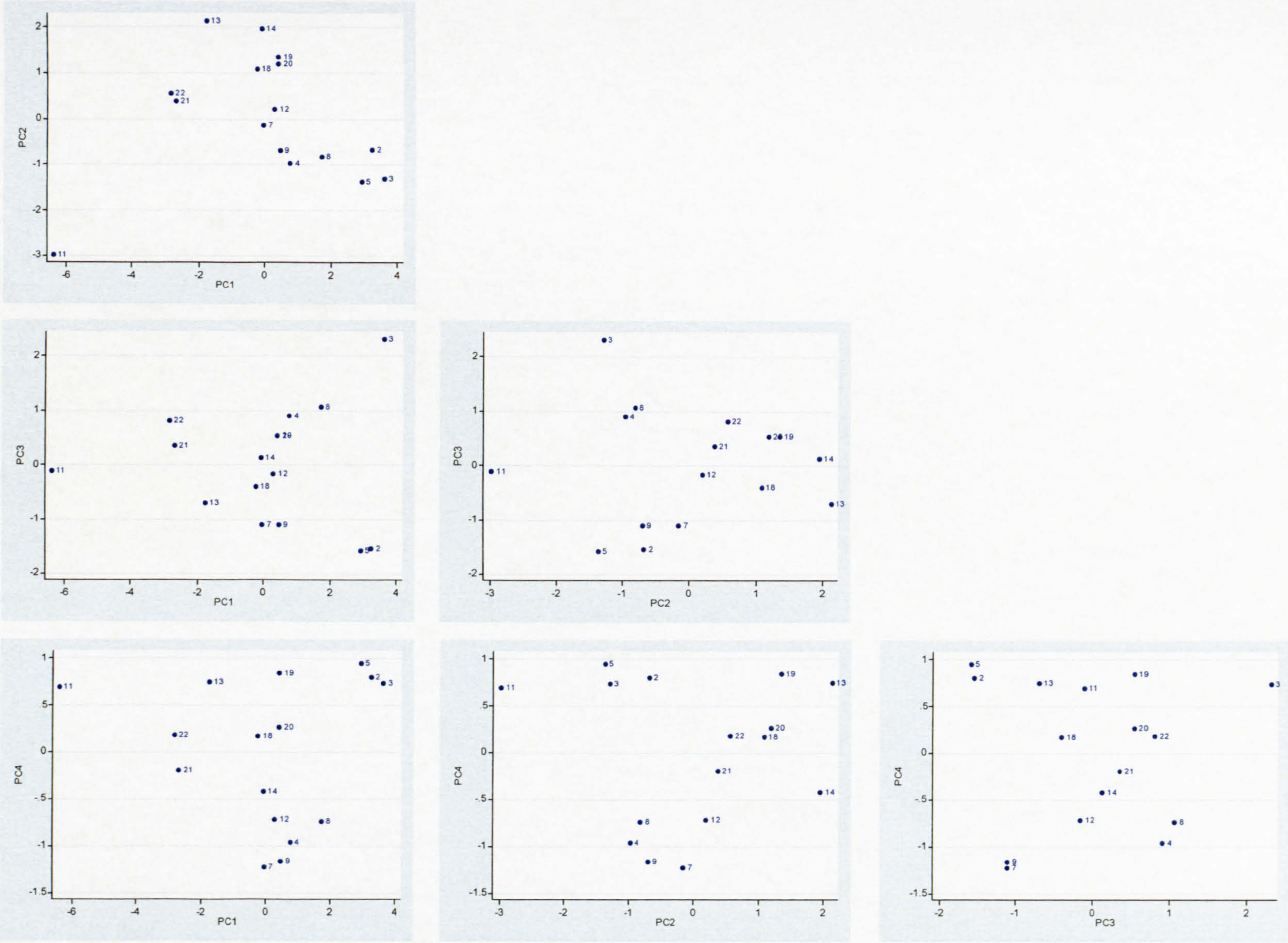

Figure 7.31. PC plots for the TIMS samples only based on 11 elements.

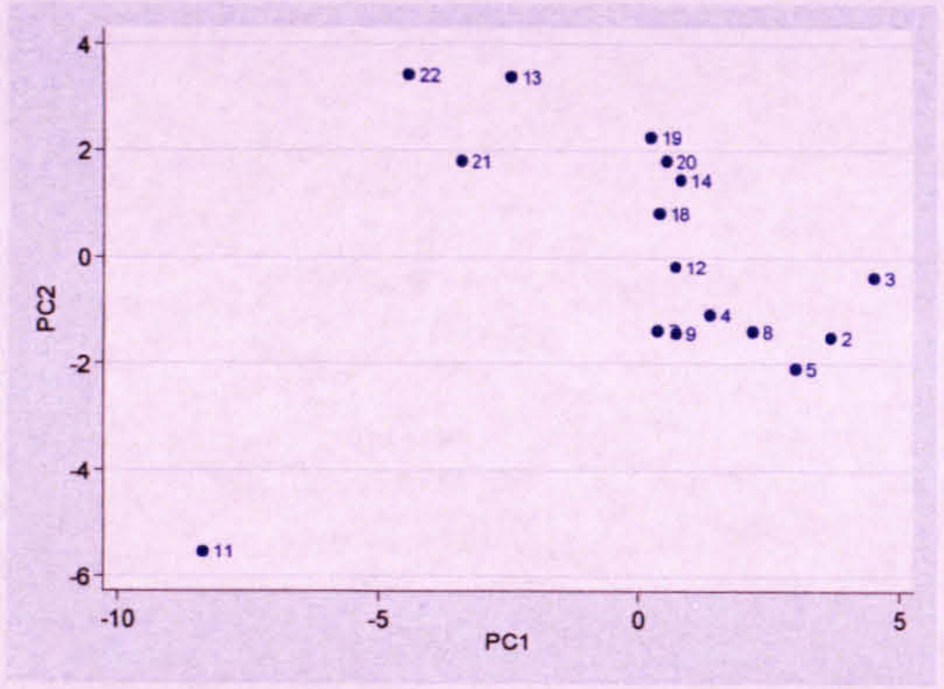

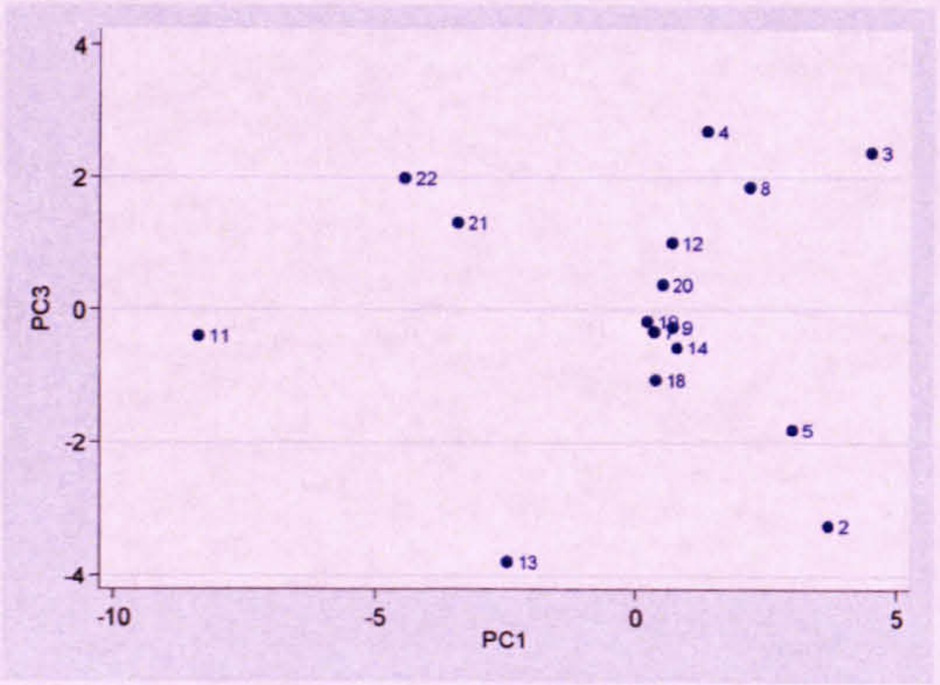

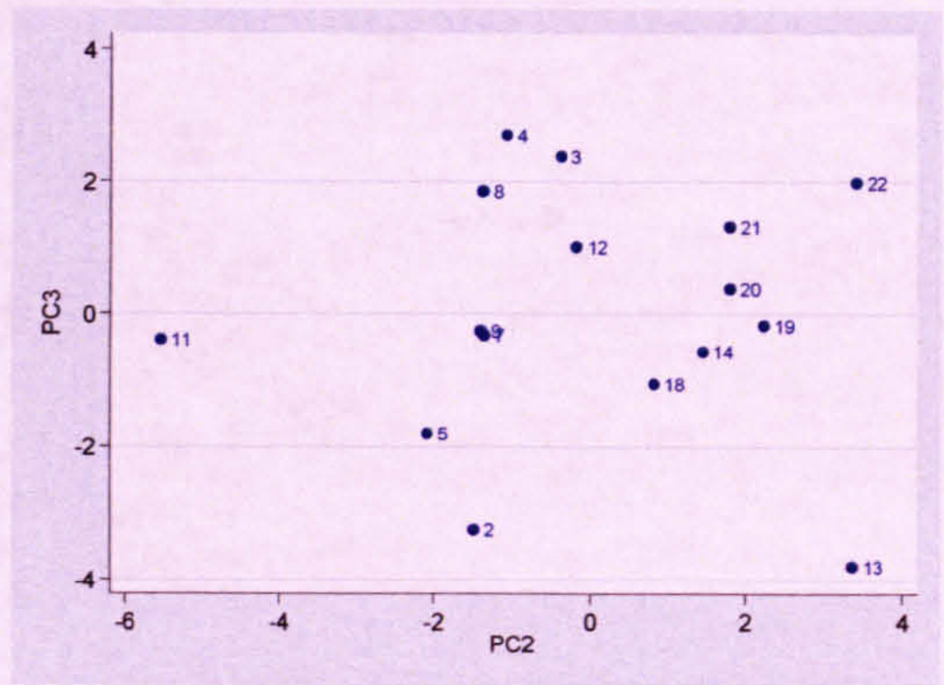

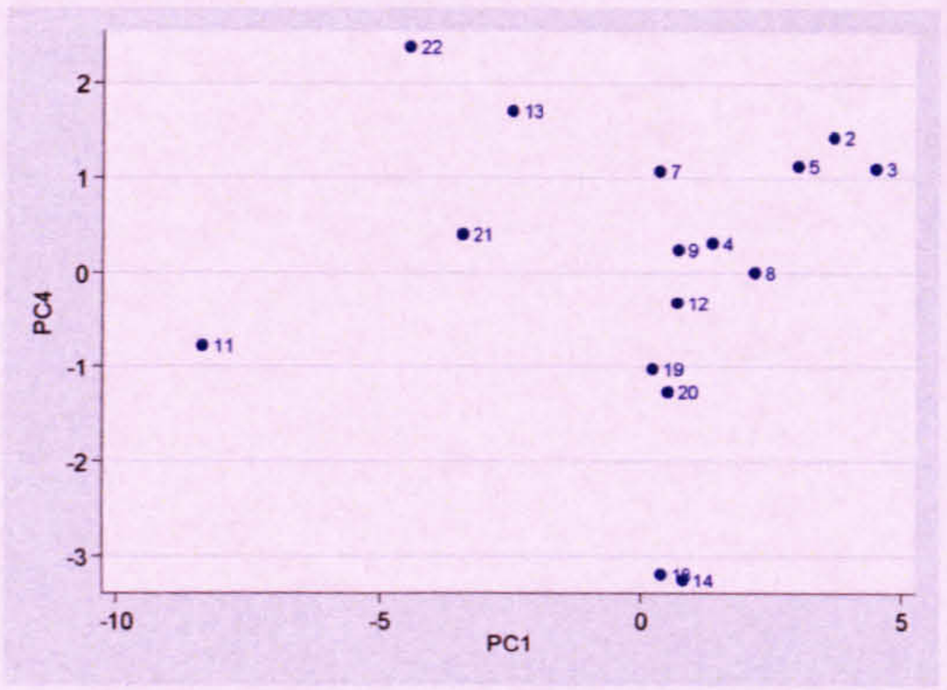

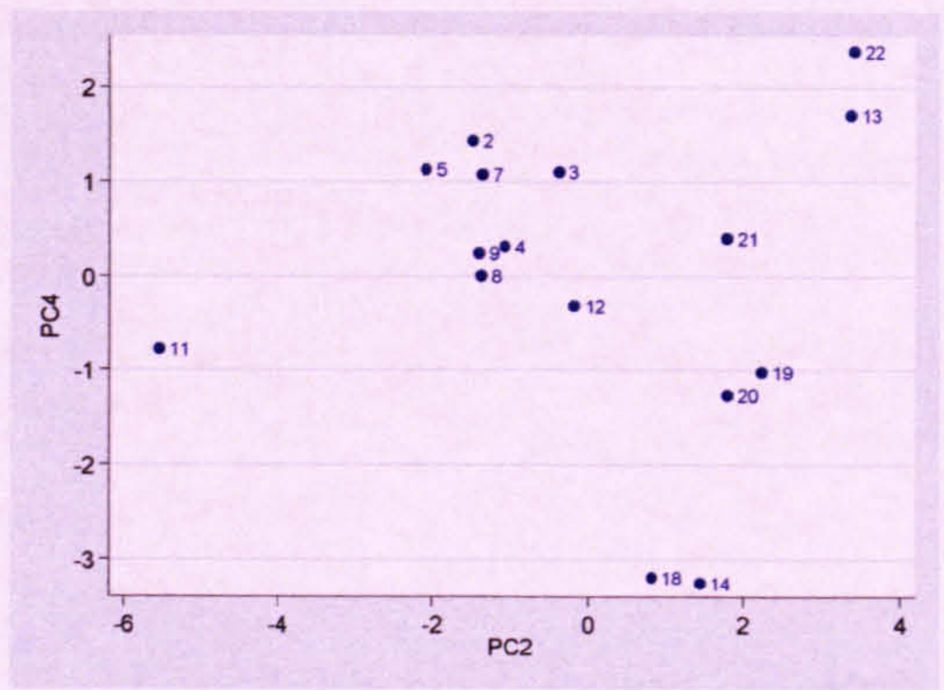

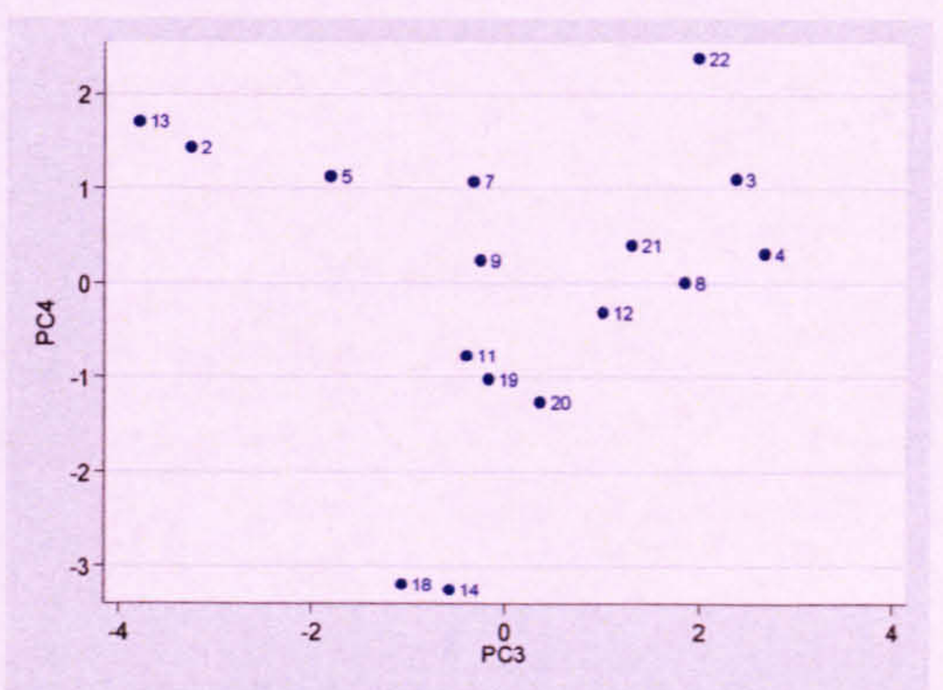

Figure 7.32. PC plots for the TIMS samples only based on 27 elements.

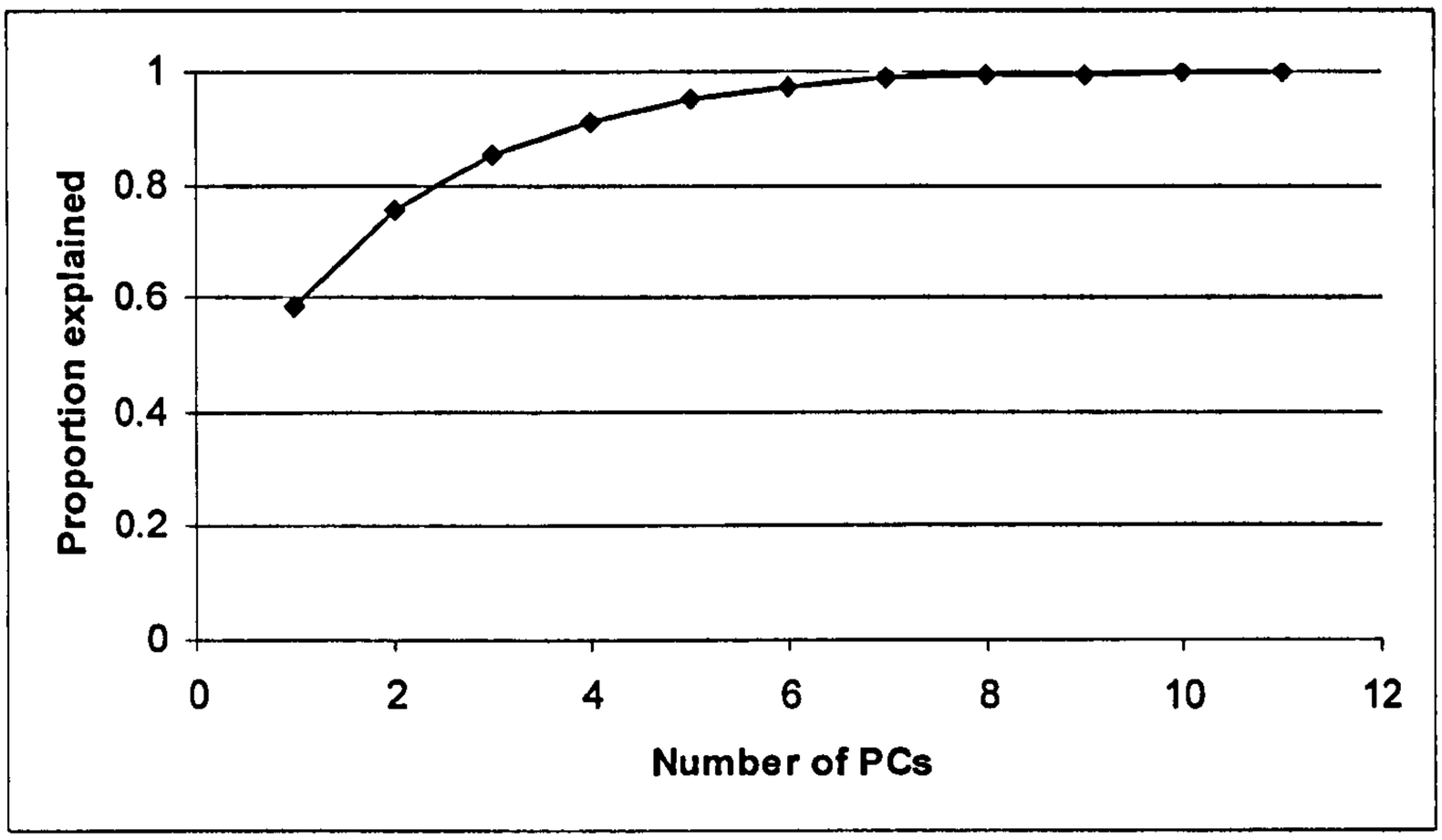

Figure 7.30. The cumulative proportion explained with increasing number of PCs calculated from 11 elements.

could be doubt regarding the validity of this data point: however, the TIMS 11 catchment is also unique in terms of its geology, soil type and vegetation cover (Figures 7.18). The catchment of TIMS 11 is the only one with discernibly different geology/soil type/vegetation cover and therefore no more inferences can be made regarding the effect of geology, soil type and vegetation cover.

The locations of TIMS 19-22 allow inferences to be made regarding the geochemistry of sediment at different locations in the same channel cross-section and sediment dynamics at tributaries. TIMS 21 and 22 are always in close proximity, especially in the plot of PC1 versus PC2 (Figure 7.31). This is expected as TIMS 22 is on the right bank side and TIMS 21 in the centre of the same channel cross-section. However, TIMS 20 is on the left bank side of the same cross-section but is not grouped with TIMS 21 and 22 (Figure 7.31). TIMS 20 is very close to TIMS 19, especially in the plots of PC1, PC2 and PC3. Due to the location of TIMS 19-22 (Figure 7.29) these two features could be explained by insufficient mixing, due to velocity differences, of water and sediment from Trout Beck and the River Tees by the time it reaches the TIMS 20-22 sampling cross-section. No more inferences can be made regarding sediment mixing within a channel cross-section, as TIMS 20-22 were the only TIMS to be deployed in the same cross-section.

There is clustering, to various degrees, of TIMS 2, 3, 5 and 8 on the PC plots (Figure 7.31). These are downstream of each other in the channel network (Figure 7.29) and are

the only successive TIMS which cluster, with the exception of TIMS 19 and 20. TIMS 2 and 5 are often closer, which is expected as there are no tributary inputs between them and are nested and therefore have similar soil type, vegetation cover, and to a lesser degree, geology (Figure 7.18). TIMS 4 and 8 are adjacent in most of the PC plots which is perhaps expected as TIMS 4 is upstream from TIMS 8 (Figure 7.29). However, TIMS 3 is located between TIMS 4 and 8 in the channel network but, while it is in the vicinity in the PC3 versus PC1 and PC3 versus PC2 plots, is not clustered with them (Figure 7.29 & 7.31). This could be explained either by insufficient mixing of water and sediment from Rough Sike and Netheredge before the TIMS 3 location or by a strong local influence on the sediment supplied to TIMS 3. A local sediment supply is perhaps the most likely cause as the right-hand bank is actively eroding upstream from TIMS 3, but the clustering of TIMS 3 with TIMS 2 and 5 (upstream catchments (Figure 7.31) suggests that insufficient mixing may be the cause.

TIMS 7 and 9 are consistently adjacent on all of the PC plots but there is no obvious explanation: they are not adjacent in the channel network and have different catchment geologies, soil types and vegetation covers (Figure 7.18). There appears to be no pattern between the PC of TIMS in the same location in the channel network (e.g. first order channel).

Much of the interpretations above are based on the evident clustering of TIMS on the PC plots and can be attributed to catchment characteristics and/or the physical setting within the channel network. However, it is important to note that, based on the reasoning above, some clusters are missing. For example, while the relation of sediment from before and after a confluence is evident in the case of TIMS 19 and 20 there is no relation between TIMS 11, 12, 15 and 4 or TIMS 4, 5 and 3. This could be due to the dominance of local sediment sources, blocking of the TIMS inlet, height of the inlet from the bed, input from tributaries or in-stream processing. The British Geological Survey (1992) reported that Be, B, Zn, Sr weather slowly, Sr is easily weathered and immobile fractions, V is generally immobile, Cu weathers rapidly under acid conditions and has an affinity for organic matter and Bi weathers easily (Table 7.8). No information was given for Ce, Ho or Al (Table 7.8). Cu and Bi both strongly correlate with PC1, so in-stream processing between TIMS may hide some relations, although there are at least five immobile/slowly weathering elements in the PC (Table 7.8).

7.6.4 PCA of source and TIMS samples

PCA was applied to the TIMS dataset discussed above and sixteen sediment source samples: four soil, four peat, four floodplain and four till. These were not included in the original analysis as the source samples are a different type of sample. This analysis does not examine the relations between the TIMS, as this was done in the previous section, but the relations between source samples and TIMS samples in an attempt to infer sediment provenance.

The same elements as before were discarded on the basis of quality of analytical determination and correlations between elements. PCA of the remaining 27 elements was undertaken and the correlation between the elements and each PC were calculated (Table 7.9). Only eight elements correlated with a PC at 0.75 or above: Li, Be, K, Fe, Co, Cu with PC1 and CE and Mg with PC2 (Table 7.9). All other elements were discarded and PCA was repeated with the eight remaining elements.

The eight remaining elements explained 95% of the variance in the geochemical data between the TIMS sampling locations (Figure 7.33) and the same broad patterns exist on PC plots derived from the 27 elements (Figure 7.34) as from the 8 elements (Figure 7.35). All eight elements are correlated with a PC at greater than 0.75 except Fe (Table 7.8).

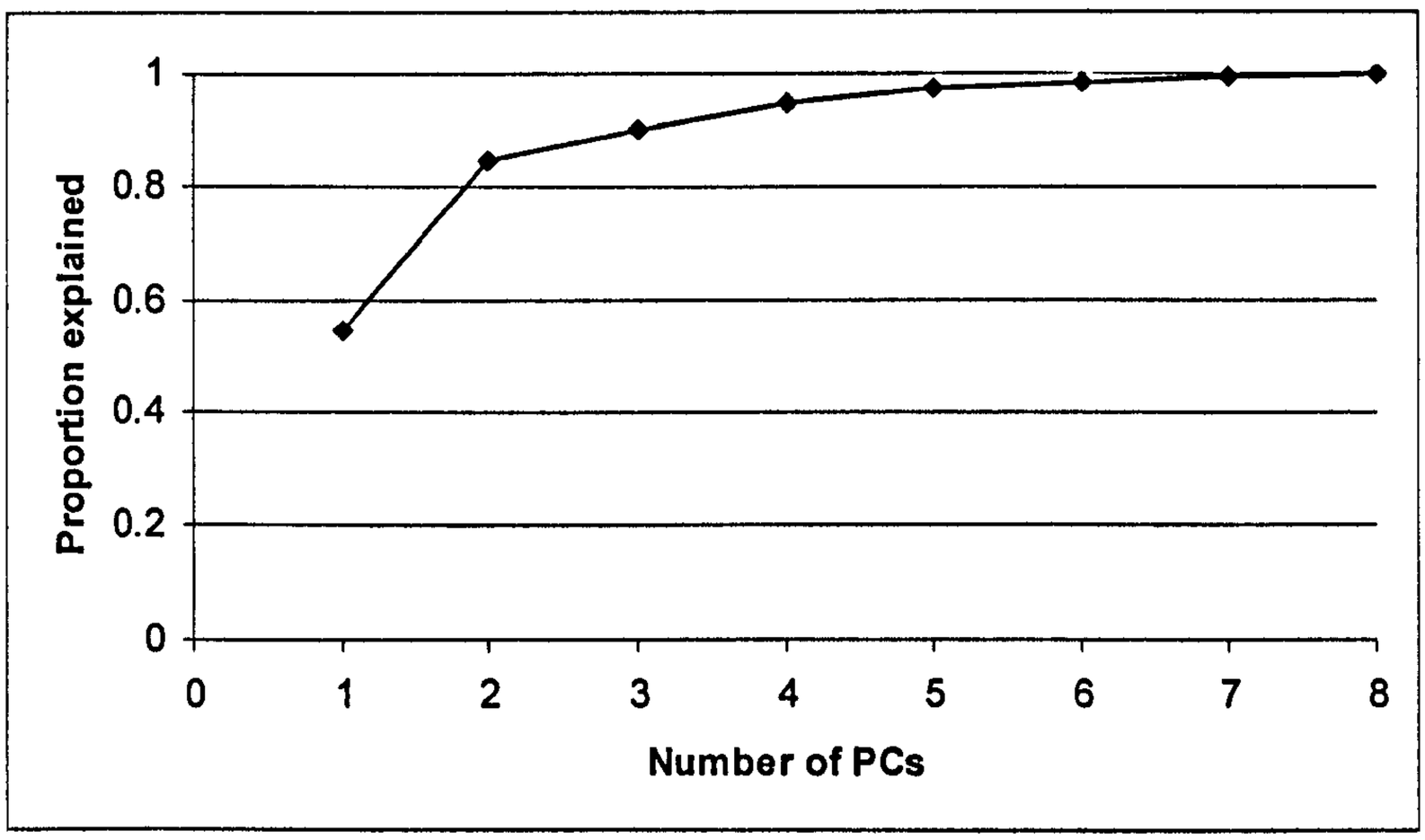

Figure 7.33. The cumulative proportion explained with increasing number of PCs calculated from 8 elements.

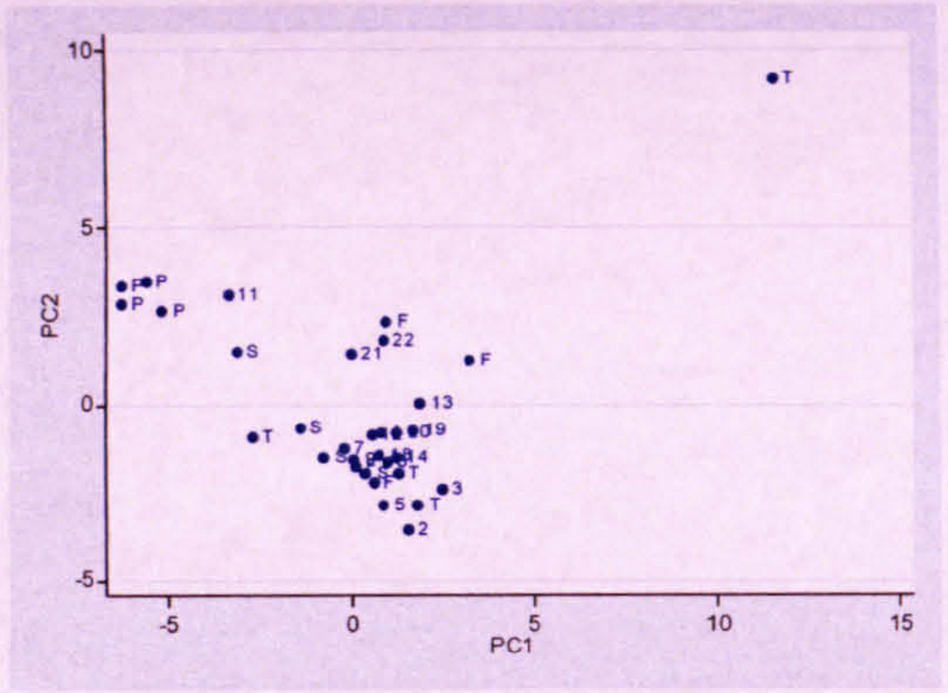

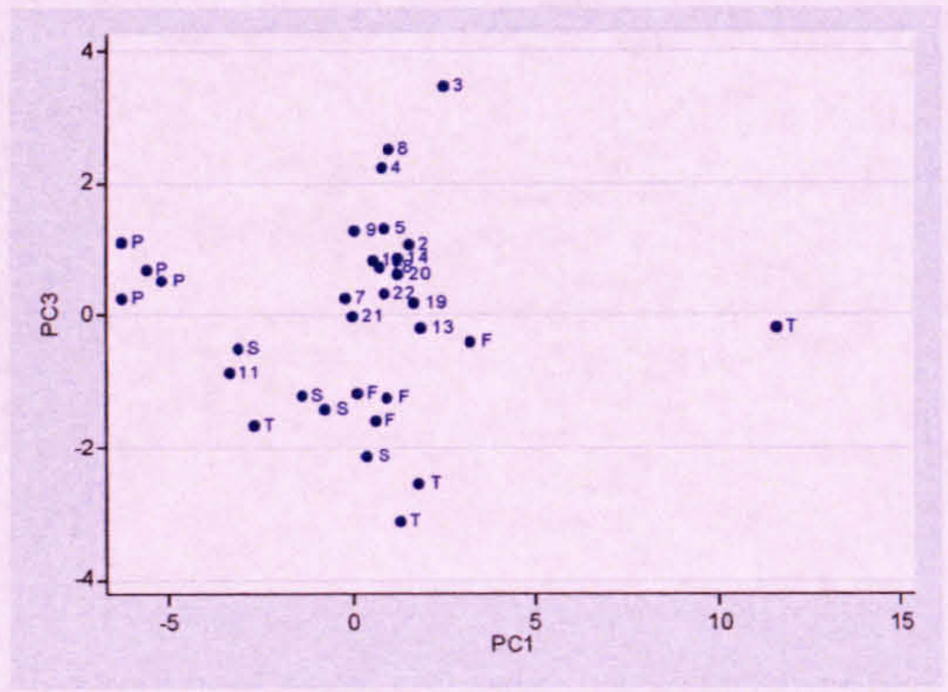

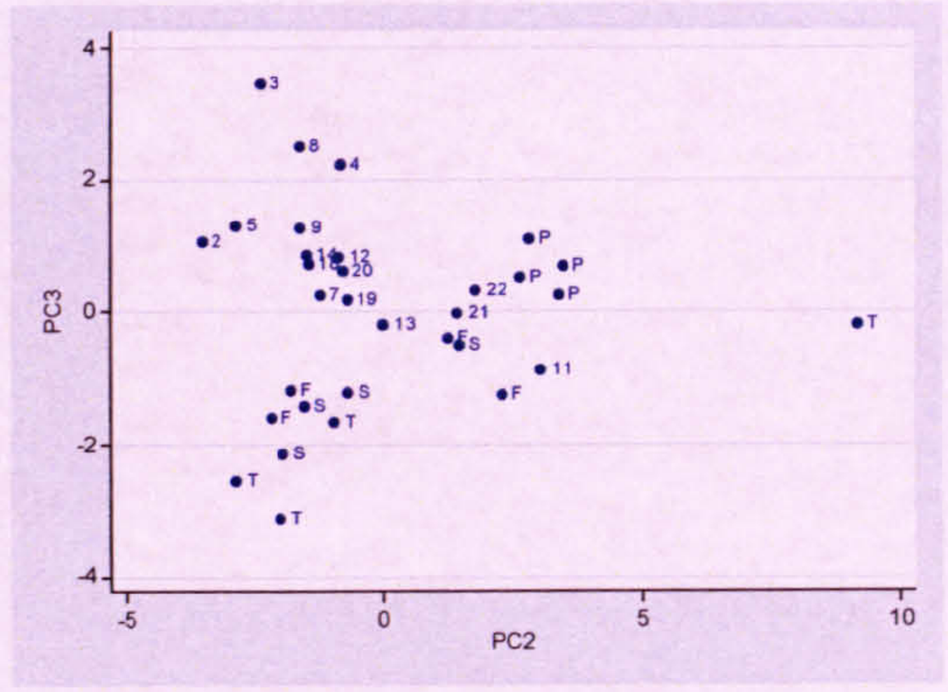

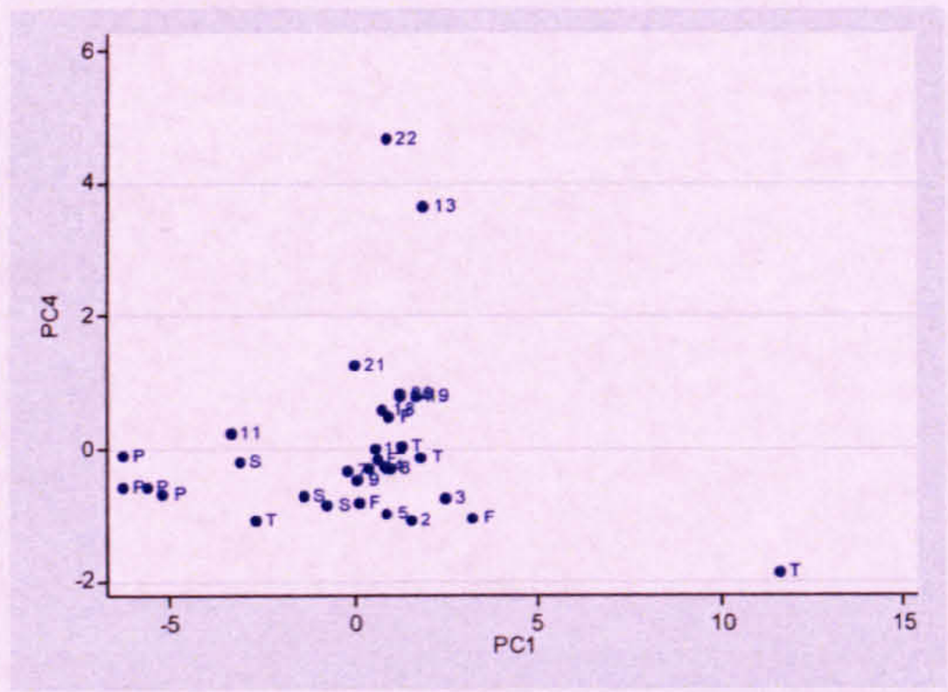

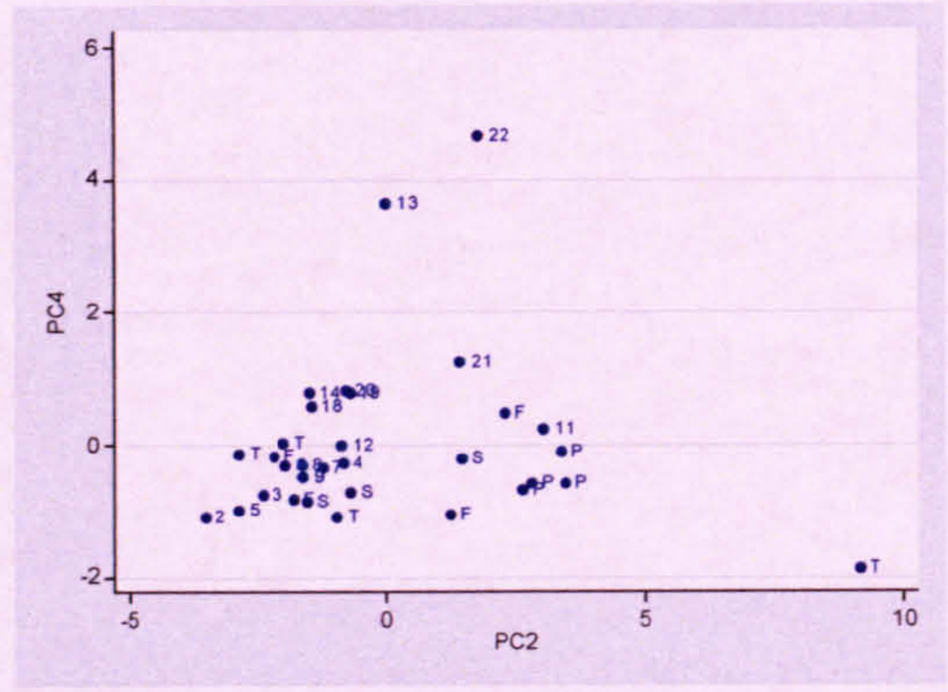

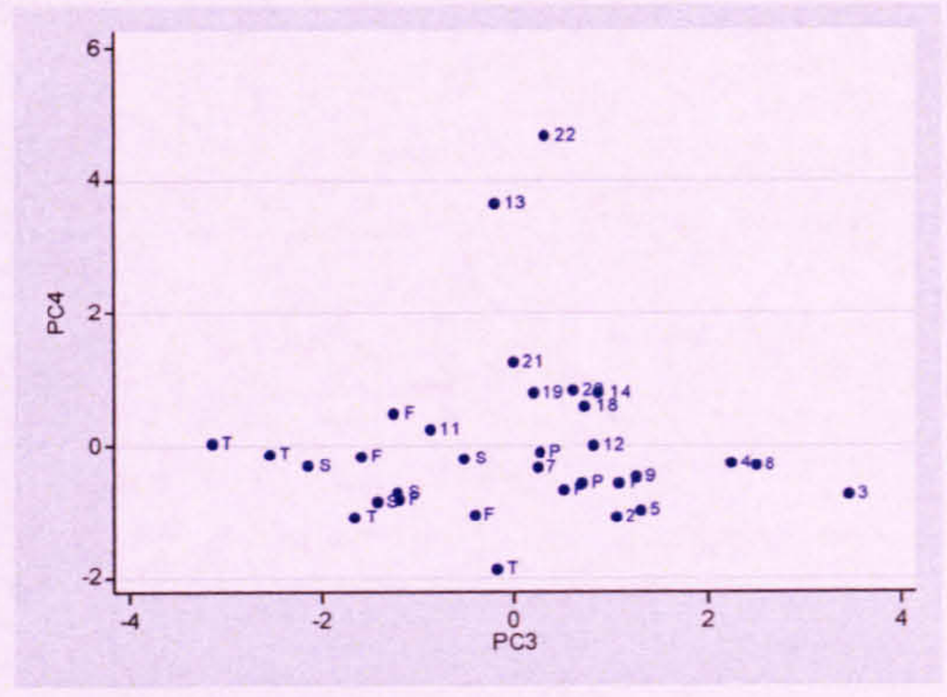

Figure 7.34. PC plots for the TIMS and sediment source samples based on 27 elements.

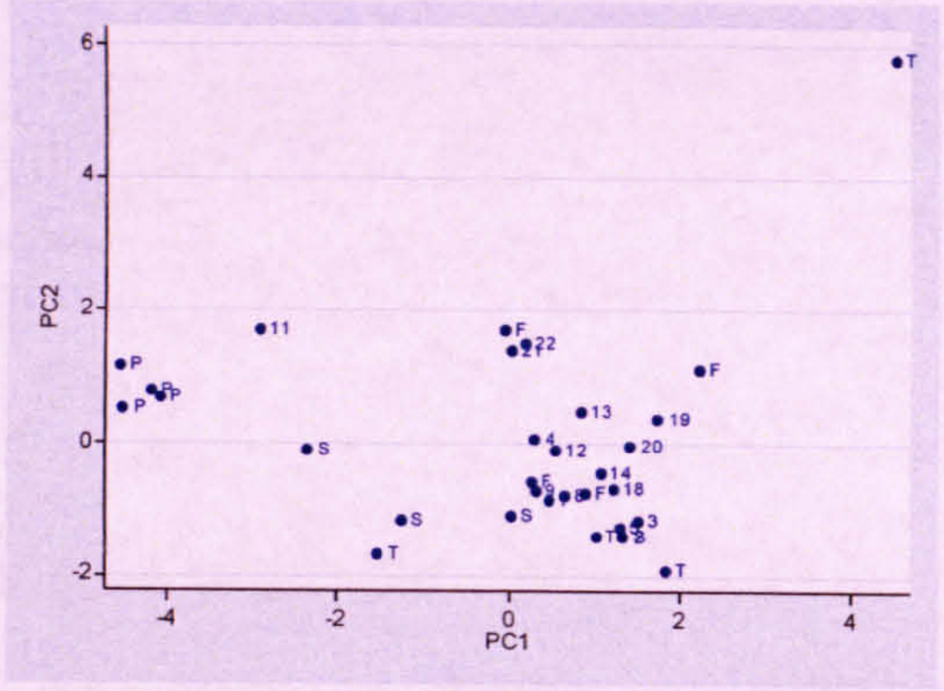

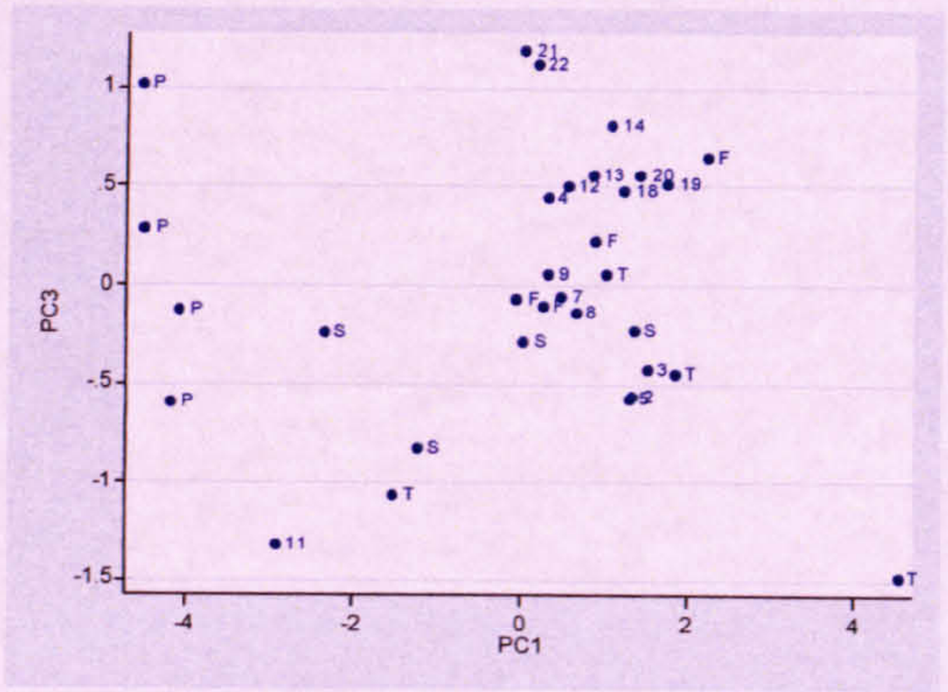

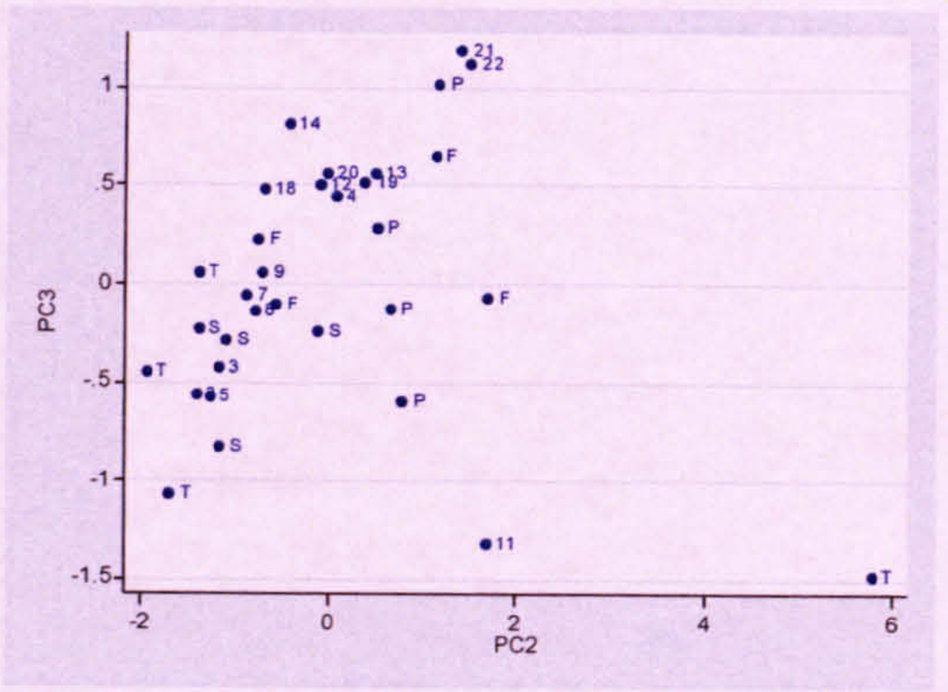

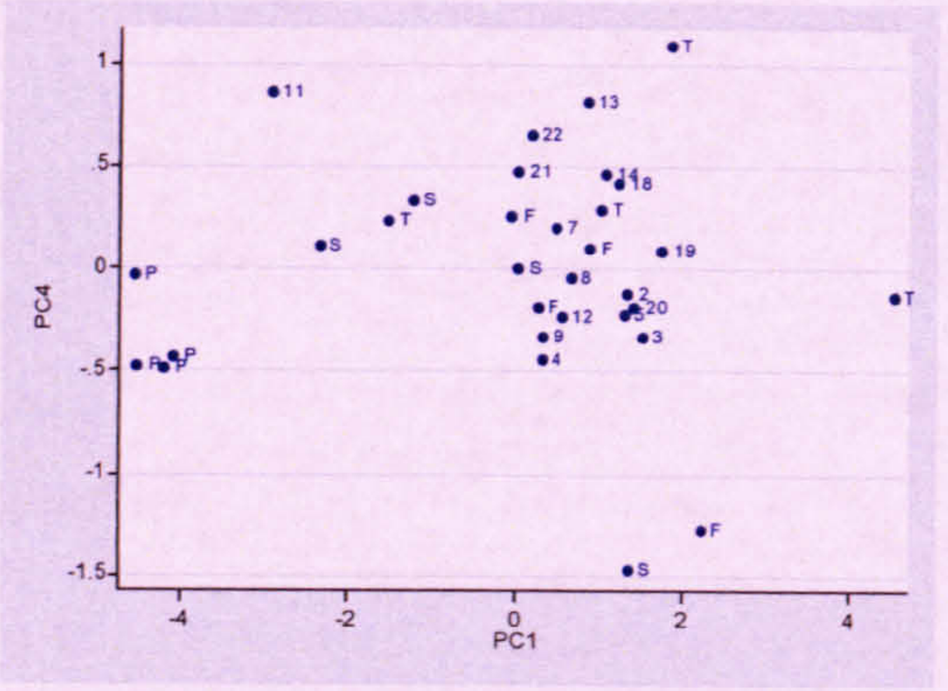

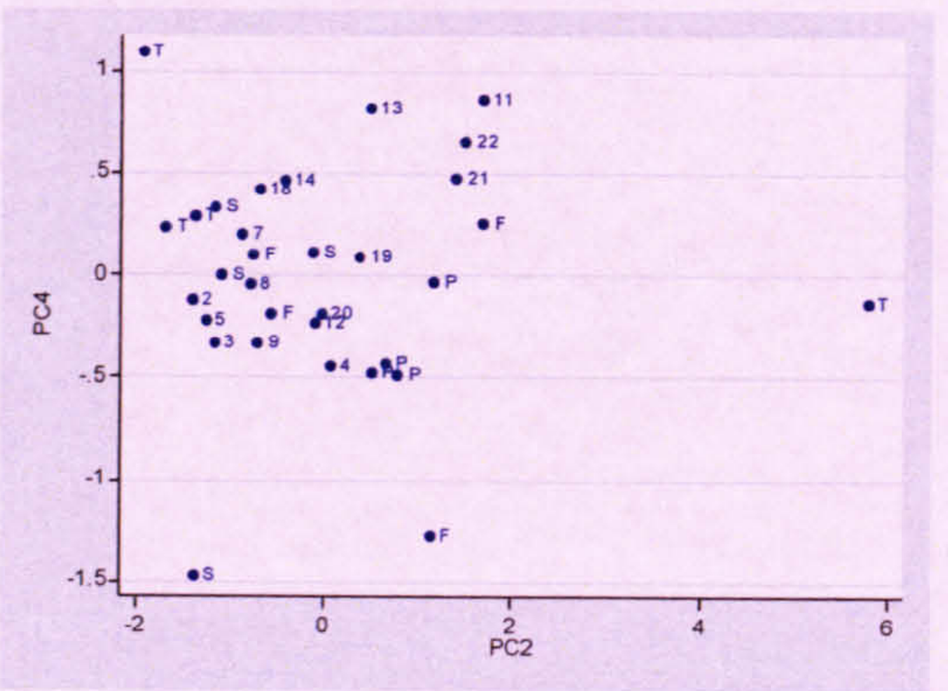

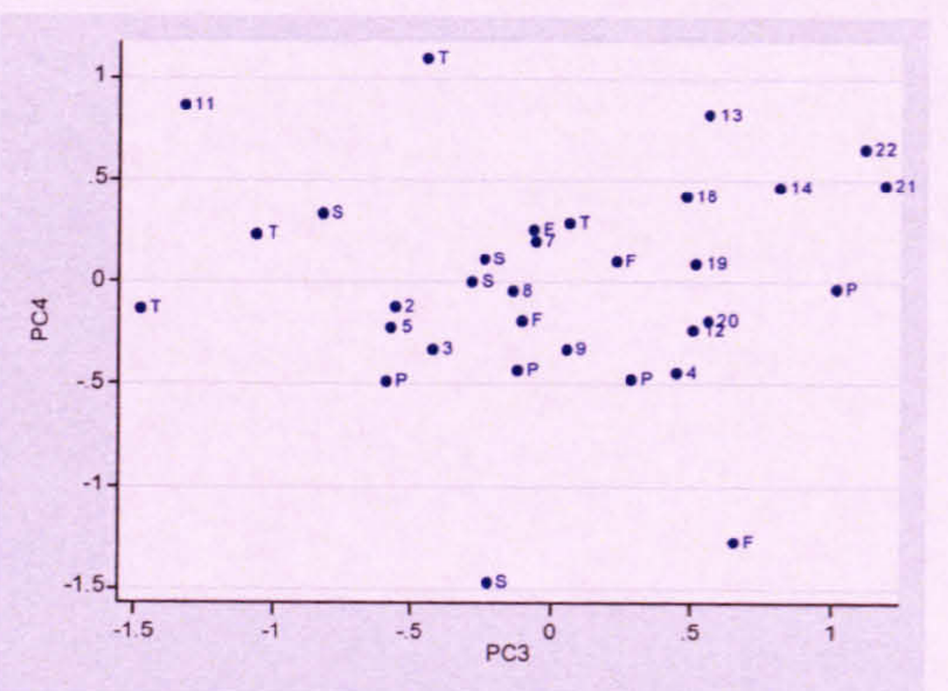

Figure 7.35. PC plots for the TIMS and sediment source samples based on 8 elements.

The sediment source samples are not in discrete clusters with the exception of peat (Figure 7.35). This is most likely attributable to localised differences, i.e. geology, soil type, vegetation cover and mining activity. As peat is derived from vegetation remains, the geochemistry is likely to be relatively similar compared with the geochemistry of different rock types and soil types. The spread of each source sample type can be used to infer the possible dominant sediment source types for each TIMS catchment.

Table 7.9. Correlations between each element and PC1-PC4 calculated using 27 elements. Figures in bold are those above the chosen 0.75 threshold.

Element	PC1	PC2	PC3	PC4
Li	**0.7531**	-0.5735	-0.1060	0.1281
Be	**0.9205**	-0.2161	0.1861	0.0443
B	0.6615	-0.6702	0.0858	-0.0390
K	**0.7704**	-0.5319	-0.2591	0.0027
V	0.7120	-0.5966	-0.1145	-0.2324
Mn	0.7063	0.5313	0.1650	-0.2128
Fe	**0.8314**	0.4556	0.1110	-0.1312
Co	**0.8687**	-0.1933	0.0188	0.1075
Cu	**0.8346**	-0.4044	-0.0420	-0.0198
Zn	0.7466	0.2617	0.4386	0.0095
Sr	0.4901	-0.6011	0.5016	0.0097
Cd	0.3108	0.0814	0.0813	0.5594
Sb	0.5679	0.3317	-0.4417	-0.0009
Ba	0.6861	0.6552	0.0724	-0.2265
Tl	0.5143	-0.4531	0.0268	0.0388
Pb	0.6834	0.6578	0.0898	-0.2463
Bi	0.6944	-0.2670	0.3804	-0.1259
Ce	0.4398	**0.8145**	-0.0767	-0.0272
Ho	0.5012	0.7185	0.0070	0.2945
Sc	0.7248	-0.1166	-0.4815	-0.2793
Dy	0.5398	0.7649	-0.1101	0.1978
Eu	0.6616	0.6757	0.0488	-0.2197
Na	0.1573	-0.0203	-0.0536	0.6602
Mg	0.1965	**0.7519**	-0.0246	0.5018
Ca	0.2754	-0.3252	0.6715	0.2558
Al	0.6623	-0.3896	-0.4055	0.2101
Si	0.6765	-0.3333	-0.4297	0.1977

TIMS 11 is consistently in close proximity to the peat source samples, although it is also close to soil and till data points (Figure 7.35). This suggests that peat sources are more dominant than for any other TIMS but the sediment also contains soil and glacial till sediment. This is reinforced by the dominance of peat in the catchment characteristics compared with the other TIMS catchments (Figure 7.18). TIMS 2, 3 and 5, which are in succession in the channel network (Figure 7.29), are plotted in close proximity on the PC plots and are encircled by soils and till source sample points (Figure 7.35) suggesting that soil and till source dominate. TIMS 7, 8 and 9 are in close proximity on the PC plots and are encircled by floodplain, soil and till sample points (Figure 7.35) suggesting that floodplain, soil and till sources are dominant. The final

group of TIMS on the PC plots consists of TIMS 4, 12, 13, 14, 18, 19, 20, 21 and 22 and are encircled by floodplain source samples on the PC2 as a function of PC1 plot and by peat and floodplain sources on the PC3 as a function of PC2 and PC3 as a function of PC1 plots (Figure 7.35) suggesting that peat and floodplain sources dominate. Field observations confirm these suggestions in so far as the source types suggested exist in the catchments. However, generally each sediment source type is present in each catchment and the generalisations are not always consistent with expectations. For example, the PCA suggests that sediment in TIMS 20-22 primarily originates from peat and floodplain sources. However, TIMS 20-22 are located in a shallow broad channel section with a broad floodplain with limited exposed peat surfaces (Figure 7.36). The peat may have been transported from upstream but the PCA did not suggest that peat was a dominant sediment source in the TIMS 7 and 8 samples, and these are the upstream TIMS. Therefore the dominant sediment sources as suggested by PCA should be taken tentatively.

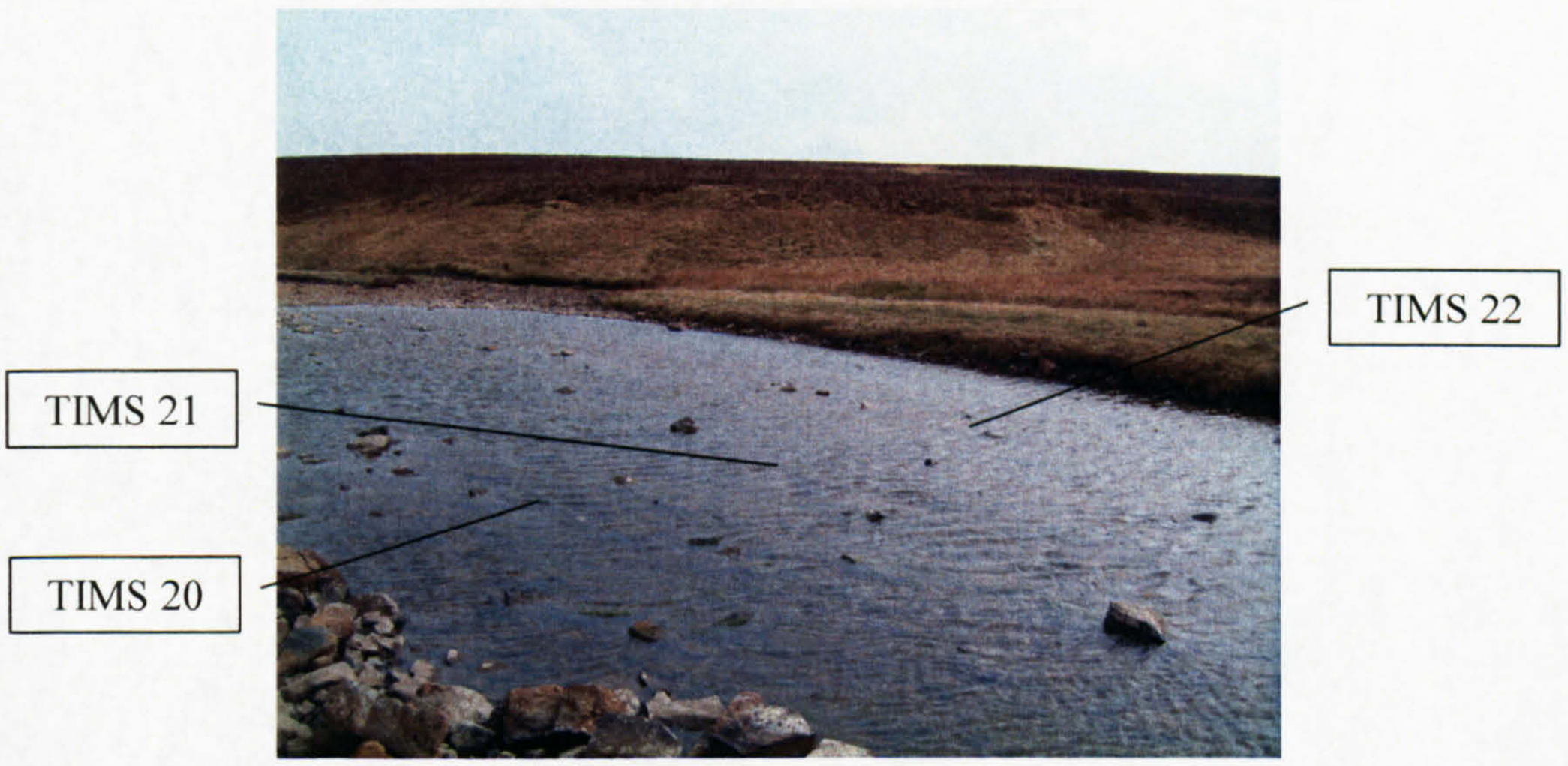

Figure 7.36. Physical setting of TIMS 20-22.

7.6.5 Summary

PCA has proven to give some interesting insights into sediment behaviour and character within the Moor House channel network. It has shown the influence of catchment geology/soil/vegetation, the similarities and differences in sediment geochemistry in successive TIMS samples and before and after confluences and differences in sediment geochemistry across a channel cross-section. The PCA also showed that there is no relation between position in the stream network (e.g. first order streams) and sediment geochemistry, not all successive TIMS have similar sediment geochemistry and the

inputs of sediment from tributaries are not uniform at every confluence. It has also shown that there are some geochemical relations between TIMS sediment for which a physical reason could not be found. The effect of in-stream processing on the PCA is expected to be limited as Cu and Bi are the only elements which are easily weathered.

The PCA of the TIMS and sediment source samples show, with the exception of peat, the diverse geochemistry of sediment source samples of the same type. Likely dominant sediment sources for each TIMS could be suggested but were not definite. The loose clustering on the 'TIMS-only' PCA plots and the variability in the geochemistry of the same source type sediments indicates a continuum in the geochemical character as opposed to distinct groups.

7.7 Chapter summary

This chapter demonstrates spatial variability in the quantity and characteristics of suspended sediment at Moor House and Swinhope. The following conclusions can be drawn:

(1) SSC are higher in the lower order channels, most likely due to the better hillslope-channel connectivity, more bank per unit area of flow, higher stream powers given higher gradient and fewer locations for sediment deposition.
(2) The systems appear to be supply-limited.
(3) Soil type exerts site specific control over sediment quantity and character but no general relationships could be found.
(4) Location in the channel network, and by association, catchment size, is related to the organic-mineral balance of suspended sediment at Moor House. Decrease in organic matter content result due to dilution with mineral sediment and distance downstream.
(5) There is evidence of a seasonal trend in the organic matter contents of sediment at Swinhope. Storm events obscure any seasonal signal in the organic matter content of sediment at Moor House.
(6) Sediment sources of the same type have diverse geochemistry (with the exception of peat sources); there is a continuum in suspended sediment geochemistry as opposed to distinct groupings.
(7) Local channel form, which controls the flow regime, bed particle size distribution and existence of periphyton, affects the amount of bed sediment

storage, which explains some of the spatial variation in suspended sediment delivery.

(8) Distinct variations were not really expected given the close proximity/nested nature and similar characteristics of the study catchments. Also, the different spatial scales at which catchment characteristics can be assessed, field monitoring can be undertaken, and at which processes operate, complicate the identification of spatial controls.

Chapter Eight:
SUSPENDED SEDIMENT RATING CURVE DEVELOPMENT

8.1 Overview

As previously outlined (Chapter 4), several techniques can be used to predict the relationship between suspended sediment concentration and discharge. This chapter focuses on rating curves, the different models that can be used to construct them and the different variables and data-subsets used. It begins by outlining an analysis framework, including model choice, data selection and indicators of model fit. For each catchment data characteristics are presented, models developed and load estimates derived. The discussion of these results is the focus of chapter nine.

8.2 Rating curve analysis framework

Rating curve model types can be broadly divided into linear regression, generalised linear models and smoothing approaches (such as LOWESS and local polynomial). Smoothing approaches, while advantageous as they allow the form of the data to be followed more closely, will not be applied as they cannot be extrapolated or easily compared between catchments (due to the number of site-specific model parameters). Of the possible linear regression approaches, ordinary least squares regression was selected due to its prevalence in the literature, suitability to the study data sets and ease of application (section 4.5.1). Data transformation of SSC and Q was undertaken prior to linear regression given the ideal of normally distributed residuals with equal variance and a linear relationship between SSC and Q. Results were either uncorrected for back-transformation bias, or corrected by the log-normal correction (LNCF) factor, smearing (SM) or the Bradu-Mundlak estimator (BME) (Figure 8.1).

Six generalised linear models (GLM) were also developed: gamma-identity with Q as the explanatory variable, gamma-identity with ln Q as the explanatory variable, gamma-log with Q as the explanatory variable, gamma-log with ln Q as the explanatory variable, Gaussian-log with Q as the explanatory variable and Gaussian-log with ln Q as the explanatory variable (Figure 8.1). The Gaussian distribution is more appropriate when there is equal variance in SSC over the range of Q, while the gamma distribution is more appropriate when the variability in SSC increases over the range of Q. The identity link is appropriate when there is a linear relation between SSC and Q, the log link is appropriate when there is a power or exponential relation between SSC and Q.

There are a large number of combinations possible in terms of the model input variables. These include: all data; data categorised by hydrograph limb, season (4), split-year (April-September and October-March), limb and split-year; lagged SSC/Q series, additional explanatory variables including change in Q and time of year (incorporated by sine and cosine functions); and the Q class method. The reasoning behind including such variables is to capture some of the processes responsible for the variability in the SSC-Q relationship. If all these models were developed here it would lead to more than 20 models (dependent on how many lags and derivatives of the Q class method were developed) per model type. If developed for all model types. If applied to all six study site data sets (uncorrected, LNCF, SM and BME corrected linear regression and three GLM models each with Q and ln Q as the explanatory variable) this would result in at least 200 models. If this framework was applied to all six study sites then 1200 models would be developed. As a result a clear framework for model development is needed so that the number of models does not become unworkable. Establishing a strict model development framework is also essential to ensure similar models are developed for each site to allow inter-catchment comparisons.

8.2.1 A strategy for model selection

One of the objectives of this study is to assess the worth of GLMs in the development of rating curves, and consequently load estimates, and compare them with rating curves derived by linear regression. Therefore, rating curves were developed for each of the study sites using linear regression and each of the GLMs and annual load estimates were calculated from each. The linear regression estimates were back-transformed using each of the correction factors (LNCF, SM and BME). As all model types can be independently justified this resulted in a basic matrix of ten load estimates for each

study site (Figure 8.1) and allow the variability in load estimates resulting from the different basic model forms to be investigated.

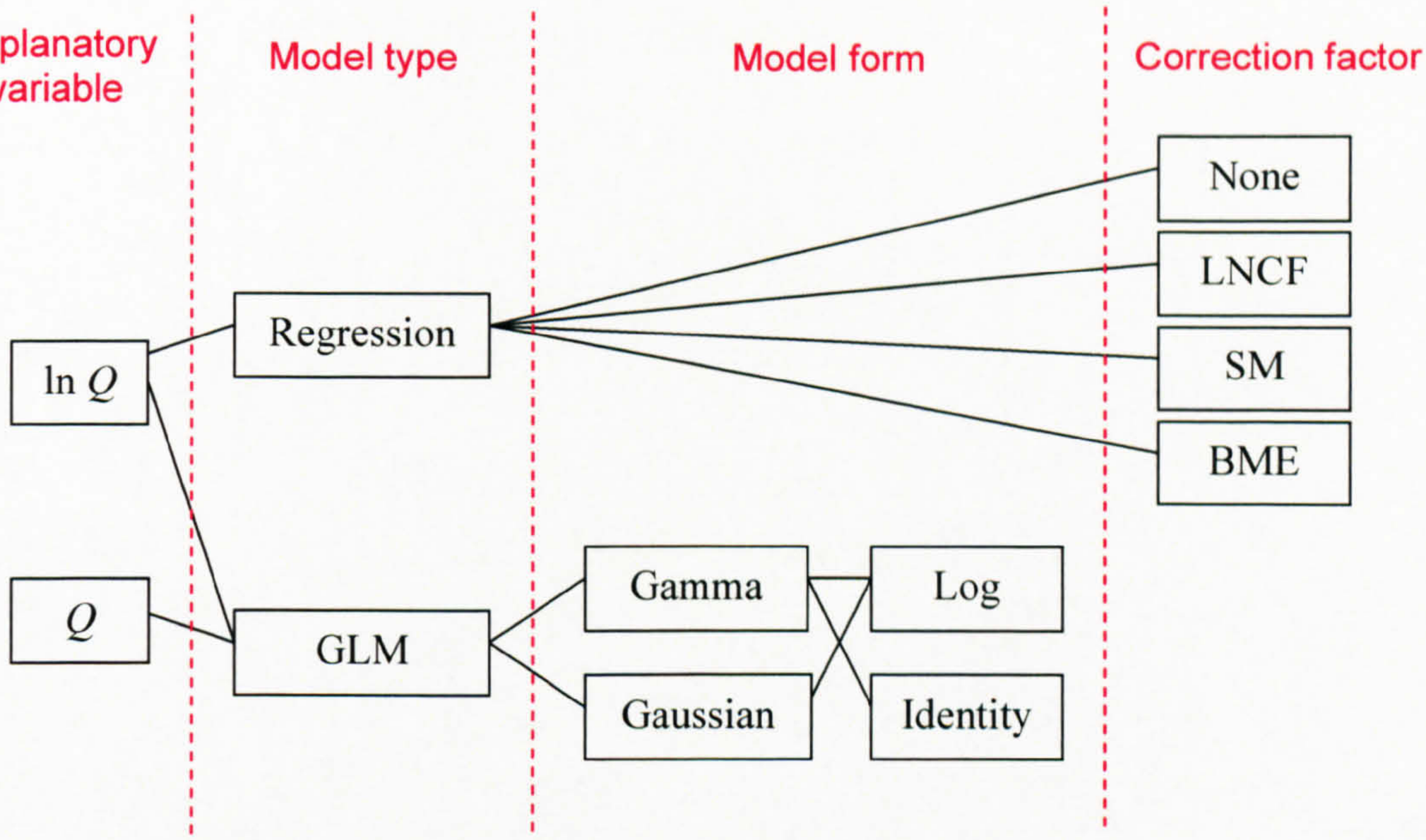

Figure 8.1. Model framework for the suite of basic rating curves.

The effect of dividing the data sets into various sub-sets (Table 8.1), was investigated using the linear regression approach. The standard linear regression rating curve was also adapted by adding change in Q as an additional explanatory variable (Table 8.1). Change in Q also incorporates whether it is the rising or falling limb: positive values are rising, negative values are falling limb (section 4.5.1.4). A Q class method rating curve was also produced (a standard format of all data and 20 Q classes were selected and linear regression developed using the untransformed mean SSC and Q for each class) (section 4.5.1.4). These choices lead to the development of 15 models, some of which combined to produce seven load estimates. For each application the annual load over the period of SSC monitoring load was calculated and compared with the annual load derived from the basic linear regression model developed from all data. No back-transformation correction factors were applied as the suitability of the correction factor has to be assessed on a case-by-case basis and if difference correction factors were applied to different data sub-sets direct comparisons could not be made. Also, the relative differences in load estimates would remain the same. These models, based on the same basic linear regression model form, allow the variability in load estimates produced by the variation of input parameters to be determined.

Table 8.1. Definition of the Q data sets from which the various rating curves were developed.

Variable	Definition
Limb	If $Q_i > Q_{i-1}$, limb = rising If $Q_i \leq Q_{i-1}$, limb = falling
Split-year	Summer = April to September Winter = October to March
Season (4)	Spring = March to May Summer = June to August Autumn = September to November Winter = December to February
Limb & split-year	Summer-rising = April to September & $Q_i > Q_{i-1}$ Summer-falling = April to September & $Q_i \leq Q_{i-1}$ Winter-rising = October to March & $Q_i > Q_{i-1}$ Winter-falling = October to March & $Q_i \leq Q_{i-1}$
Time of year	Sine = sin (2 π FOY) Cosine = cos (2 π FOY) where FOY = day of year / 365
Lag	$Q_L = Q_{t-1}$
Change in Q	$\Delta Q = Q_i - Q_{i-1}$
Q class	Intervals vary for each catchment

While basing the adaptations on linear regression may appear counter to the objective of assessing the value of GLMs in rating curve development, using the GLM approach would multiply the number of models by a factor of six and the effect of categorising the data is more apparent on linear regression plots due to the spread of the data, making it easier to identify trends and infer the physical processes responsible. This is clearly evident from Figure 8.2 which shows the spring, summer, autumn and winter rating curves for Rough Sike derived using linear regression (Figure 8.2A) and a Gaussian-log GLM with Q as the explanatory variable (Figure 8.2B). In addition, using linear regression allows direct comparison with existing studies, none of which used GLM.

8.2.2 Load estimation

There are various methods by which loads can be estimated from simultaneous recordings of SSC and Q (section 4.6, Figure 4.12). Within this study the loads are calculated from the estimated instantaneous SSC from the various models ($\hat{C}_i$), instantaneous discharge (Q_i) and time between samples (t)

$$\hat{L} = \sum_{i=1}^{n} \hat{C}_i \, Q_i \, t \; . \qquad (8.1)$$

(A)

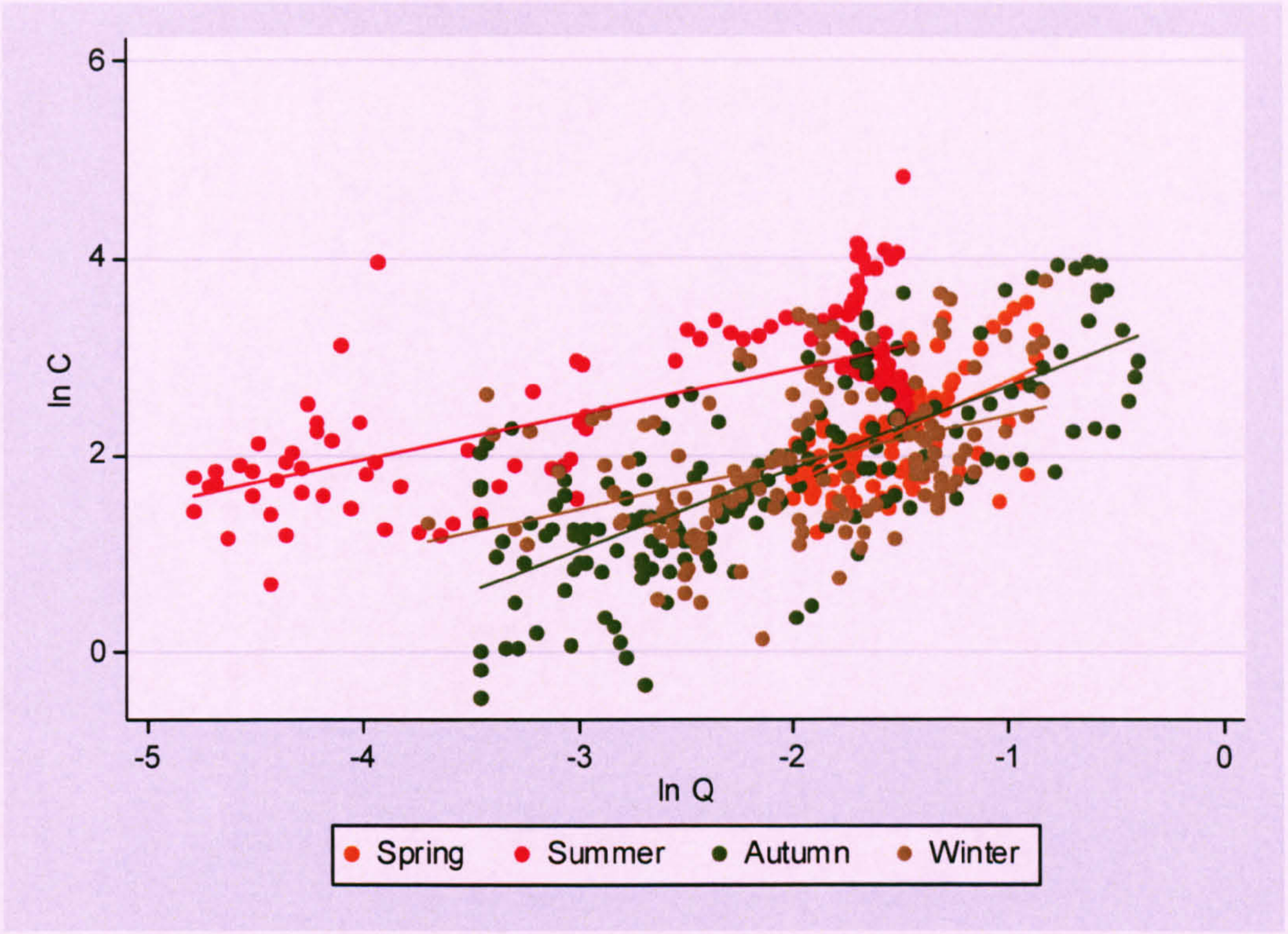

(B)

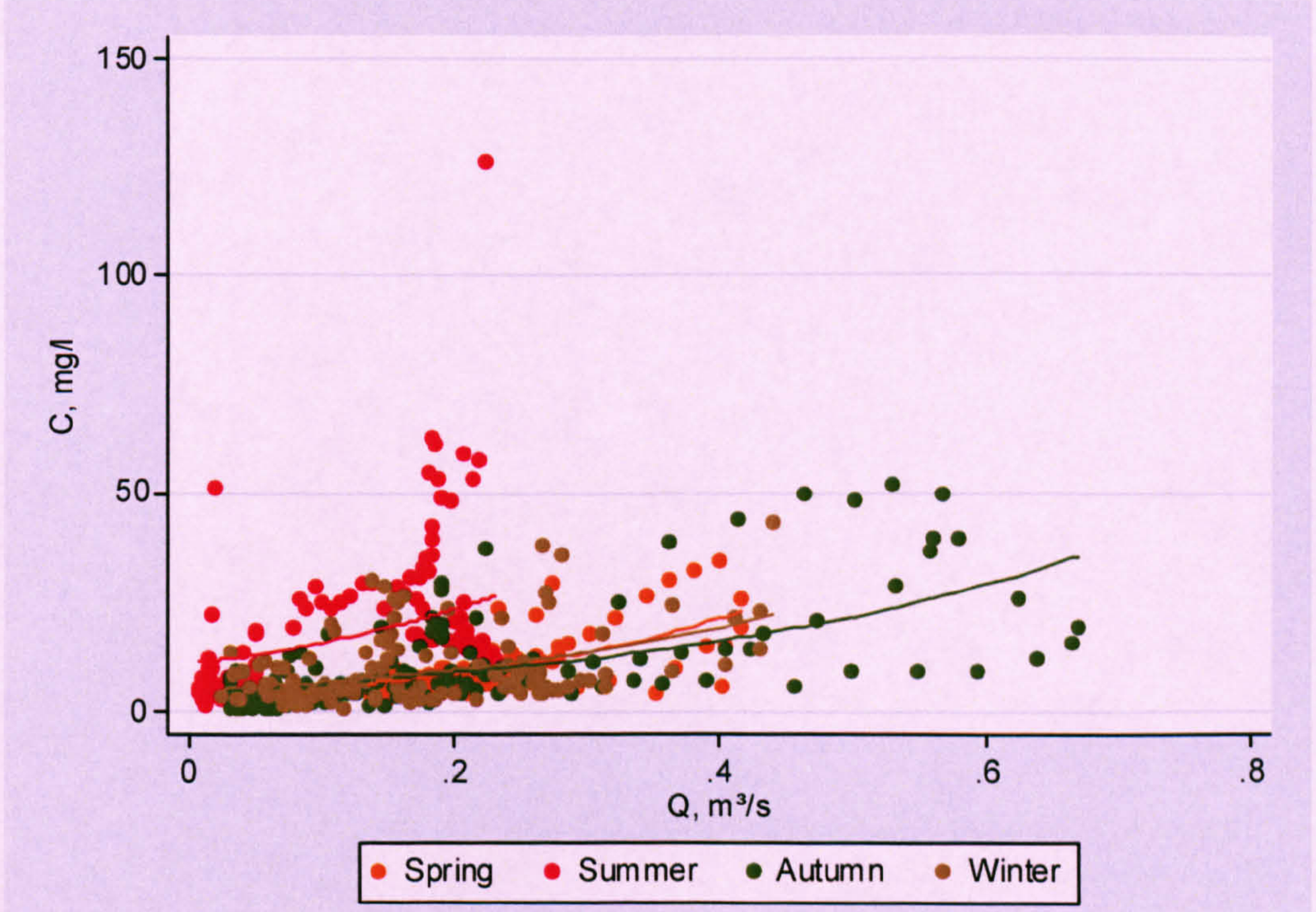

Figure 8.2. Comparison of sediment rating curves for Rough Sike derived for spring, summer, autumn and winter using (A) linear regression and (B) Gaussian-log GLM with Q as the explanatory variable.

This method was chosen as it is the standard way in which to integrate frequent SSC and Q series. No other load estimation techniques are employed as Phillips *et al.* (1999) gives a comprehensive overview of the various methods and the limited nature of the data sets used in this investigation would prevent such rigorous examination as that undertaken by Phillips *et al.* (1999).

8.2.3 Model validation procedure

A model validation procedure has been developed (Figure 8.3). It involves calculating the coefficient of determination (R^2) and root mean square error (RMSE) as measures of fit; examining diagnostic plots to assess if the model assumptions are met and to highlight any oddities in the data; examining the rating curves with reference to the data points; and comparing the actual and predicted storm period load estimates (Figure 8.3).

R^2 is a measure of correlation between two variables (in this case actual and predicted SSC) and is expressed as a value between zero and one (Table 4.1). The higher the value of R^2, the better the model fit. The R^2 value is different if calculated from the raw and transformed data. Care must be taken when applying R^2 to ensure it gives a true indication of model fit. For example, if there is a cloud of data points and then one point at a distance, a misleadingly high R^2 value will be given (Figure 8.4). R^2 also returns a low value if there is noteworthy scatter around the regression line, a characteristic of suspended sediment rating curves, even though the model is a good generalisation of the underlying form of the relationship.

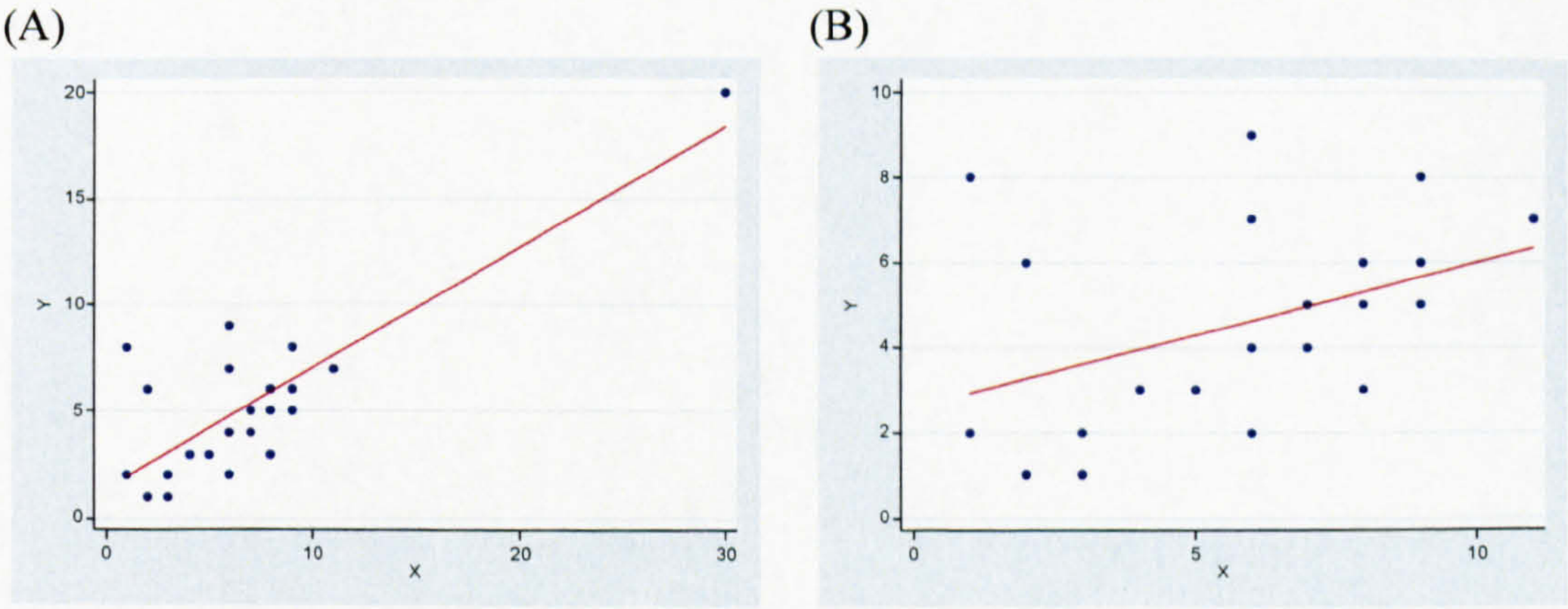

Figure 8.4. The effect of outliers on R^2. (A) R^2 of 0.68 due to influence of outlier and (B) R^2 of 0.17 as outlier removed.

The RMSE is the positive square root of the average of the squared residuals. The use of RMSE implies that errors at larger values of the explanatory variables are more

Prior to model development **Post model development** **Model selection**

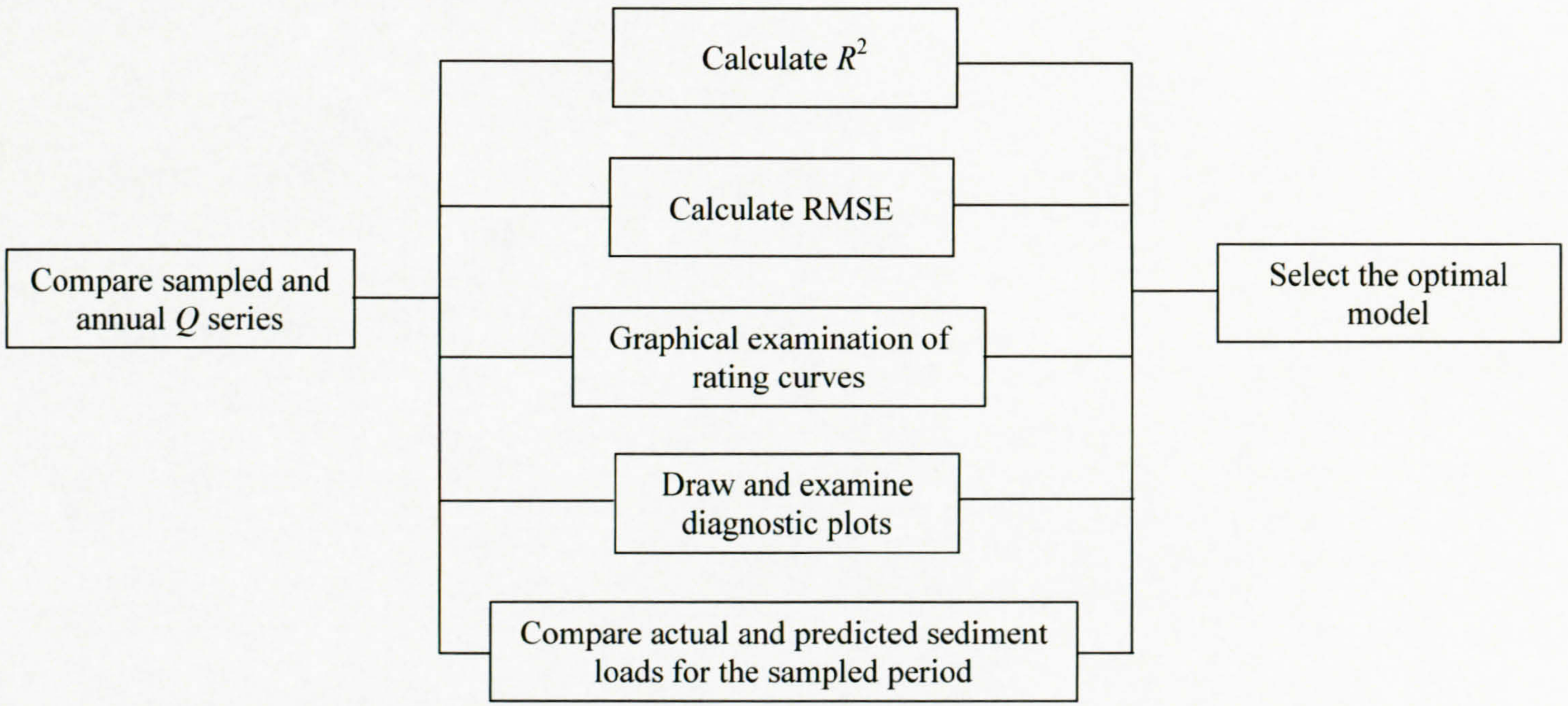

Figure 8.3. Model validation procedure.

important than errors at smaller values of the explanatory variables. RMSE is calculated from the predicted and actual SSC for all observations (Table 4.1) and a smaller RMSE indicates a better model fit. RMSE is expressed in the same units as the response variable and therefore differs if calculated from the raw or transformed data. For the 10 basic models the RMSE was calculated from SSC and Q, not ln C and ln Q. The RMSE is less affected by outliers than R^2: for example the RMSE are 2.23 and 2.15 for Figure 8.4 A & B respectively.

Several model diagnostic plots were generated for each model: residual distribution, observed versus predicted, quantiles of fitted minus mean and quantiles of the residuals and residuals versus fitted values. Where possible deviations from the 'ideal' diagnostic plot were explained with reference to the physical geo-system. The diagnostic plots reflect the relationship between SSC and discharge and the suitability of the model choice.

If the model is a good fit the residuals distribution plots should show a normal distribution with equal variance throughout the range of the explanatory variable unless a gamma distribution is chosen. Figure 8.5A is an example of a good residual plot as the residuals are approximately normally distributed and the variance is approximately equal over the range of ln Q. In contrast, Figure 8.5B shows non-normally distributed residuals and unequal variance.

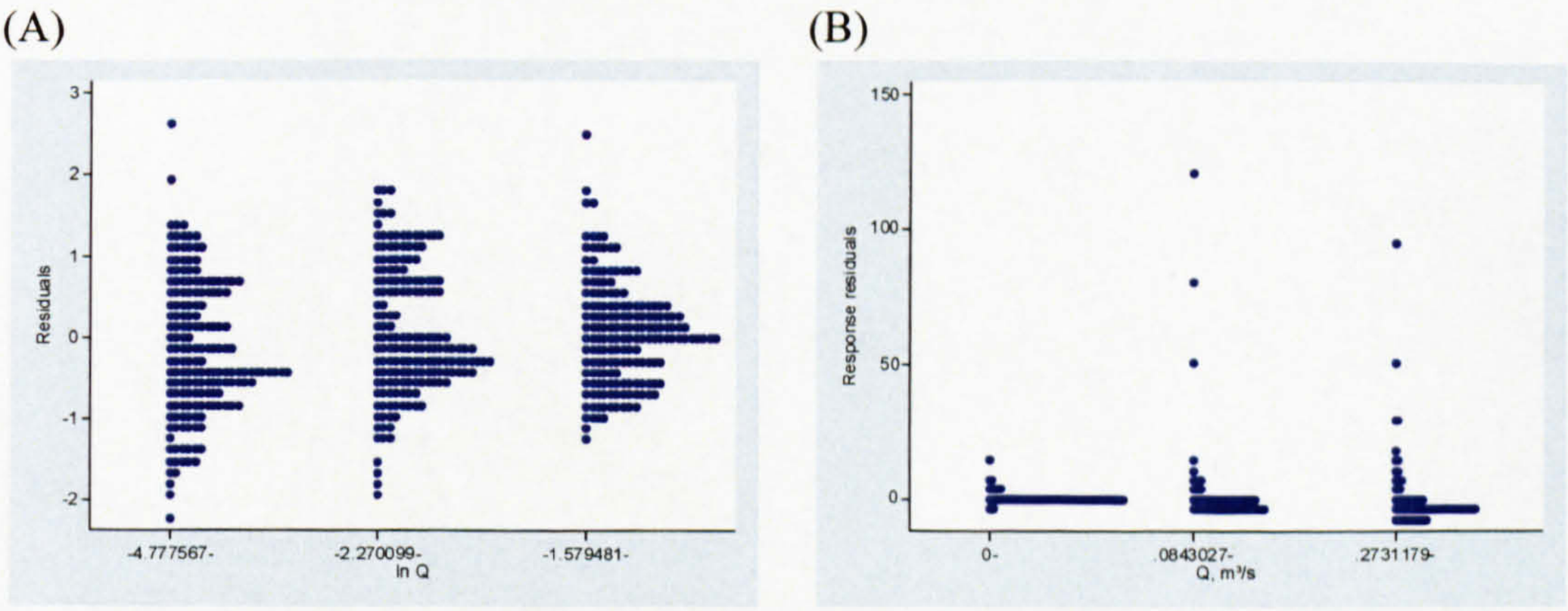

Figure 8.5. Residual distribution plots: (A) Approximately normally distributed residuals with equal variance (linear regression of ln C on ln Q using all data from Rough Sike) and (B) non-normally distributed residuals with unequal variance (Gaussian-identity GLM using all data with Q as the explanatory variable for Langtae).

The data cloud should be narrow and of even width around the observed equals predicted line on the observed versus predicted plot. Figure 8.6A is an illustration of a

good observed versus predicted as the band is of even width. The band is quite broad but this is indicative of the variability in SSC. In contrast Figure 8.6B is an example of a observed versus fitted plot indicating poor model fit: the band is of very variable width.

(A)

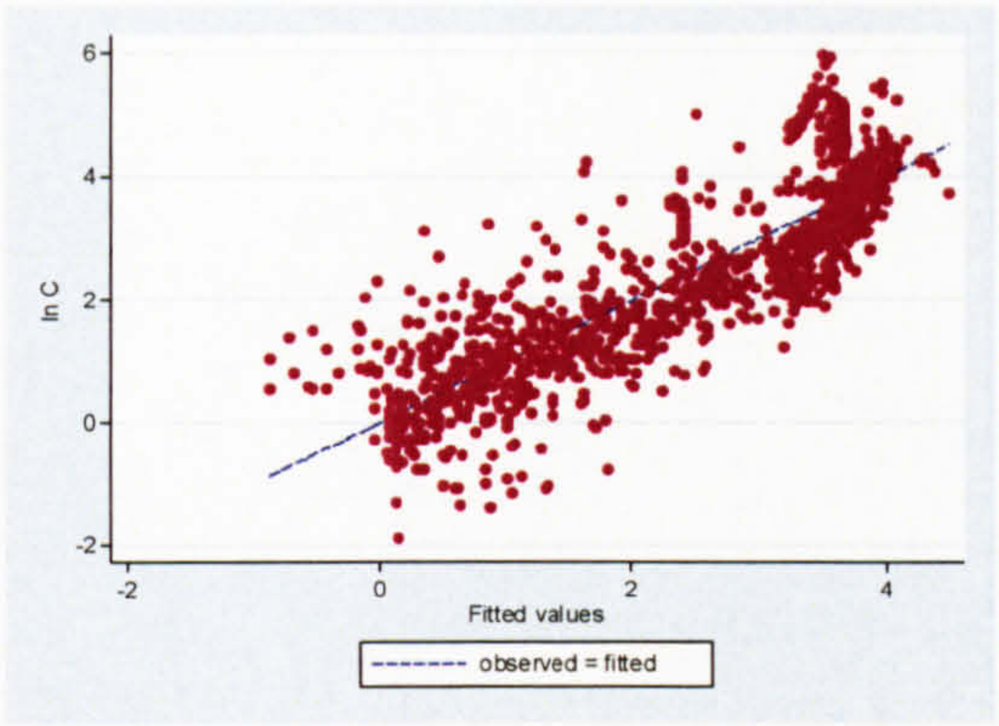

(B)

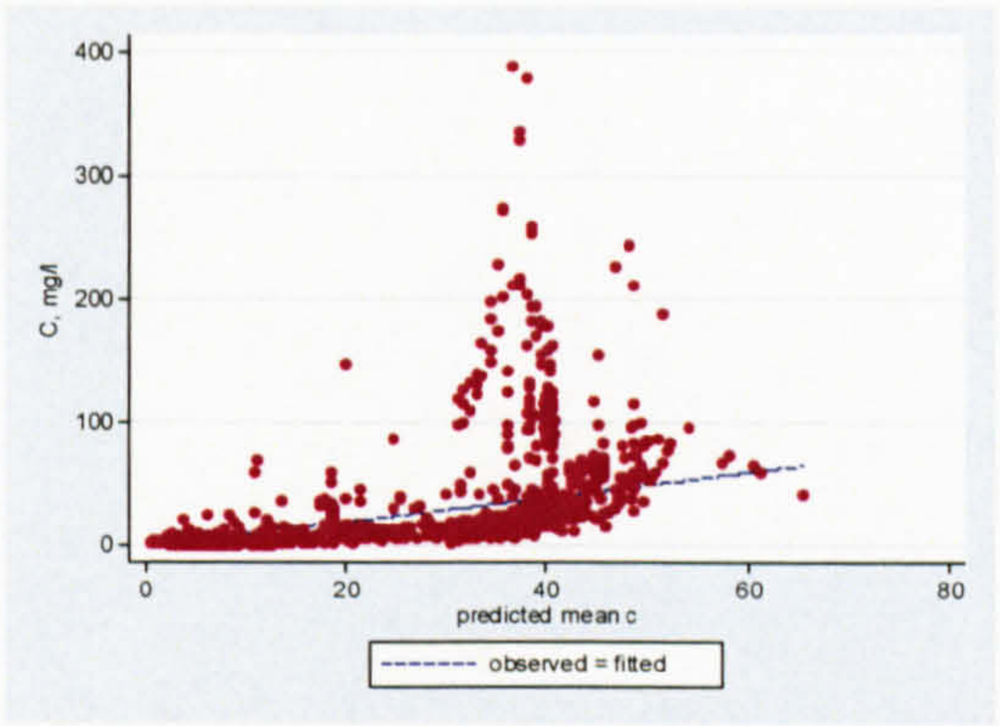

Figure 8.6. Observed as a function of predicted plots. (A) Approximately normally distributed data cloud (linear regression of ln C on ln Q using all data from Burnhope) and (B) unequal data cloud (gamma-identity GLM using all data with Q as the explanatory variable for Burnhope).

There should be no structure (i.e. clusters and trends) in the residual versus predicted values plot (Figure 8.7) as structure indicates that the model is not a good generalisation of the data. However, if a gamma distribution is selected the magnitude of residuals may increase at higher predicted values. Figure 8.7A is therefore an example of a residual versus predicted plot from a well fitting model. In contrast, Figure 8.7B is derived from a very poorly fitting model as there are clusters in the data and a general trend for residuals to decrease with increases in predicted values.

(A)

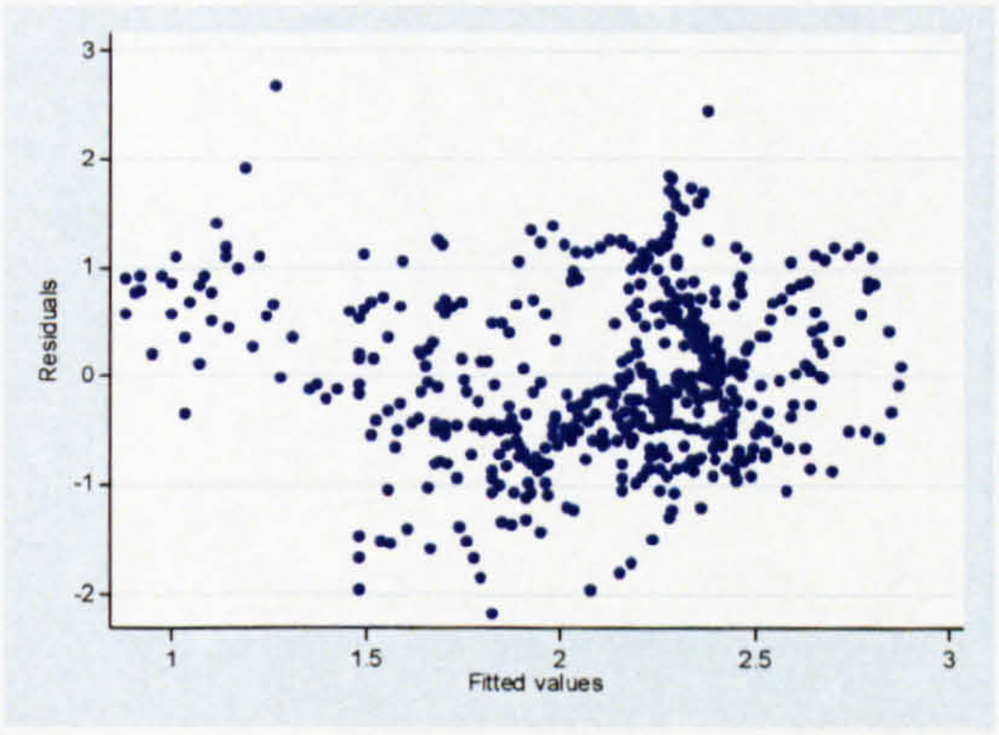

(B)

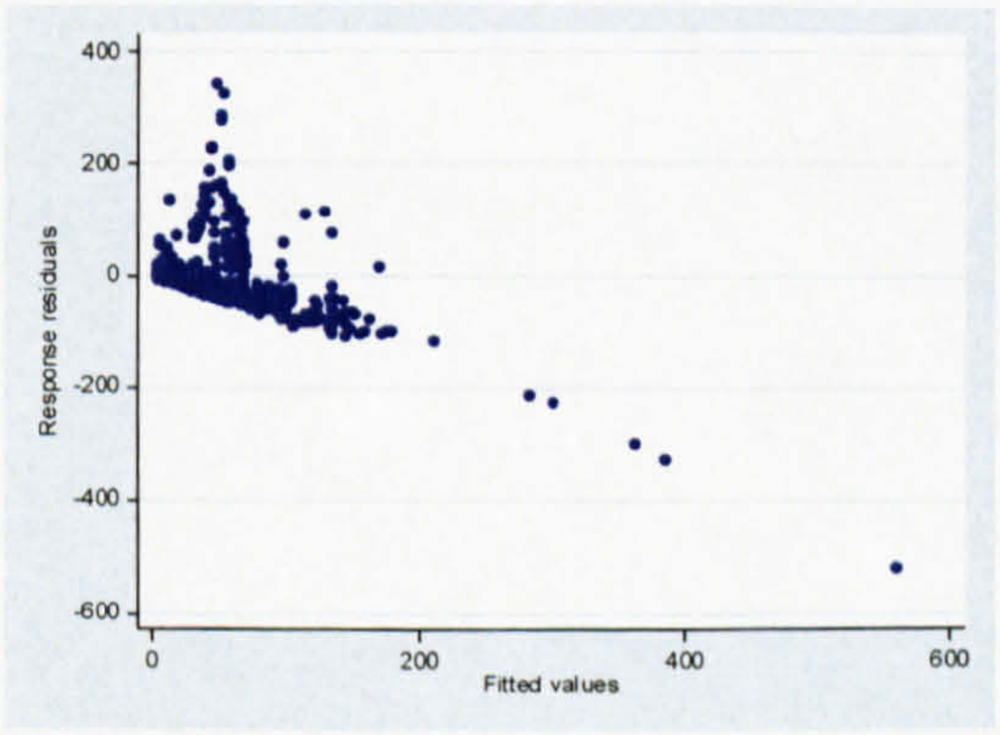

Figure 8.7. Residuals as a function of predicted plots. (A) Data cloud with no structure (linear regression of ln C on ln Q using all data from Rough Sike) and (B) structured data cloud (Gaussian-log GLM using all data with Q as the explanatory variable for Burnhope).

Quantile plots give an indication of the variability in the data and allow idenitification of finer structure. Two quantile plots are given side-by-side: fitted minus mean versus fraction of the data and residuals versus fraction of the data. Both curves should exhibit a rotated s-shape (as on a cumulative frequency graph of a Gaussian distribution). The shape of the fitted minus mean plot indicates the general form of the relationship and the residual plot gives an insight into the distribution of the residuals. In terms of assessing model fit it is the residual plot which is of more importance. Ideally, the curve will approximately symmetrical (i.e. an equal number and size of positive and negative residuals) unless a gamma distribution is assumed, have a low angle and very limited spread (Figure 8.8A). In contrast Figure 8.8B shows a residual plot which is asymmetric, with higher errors at higher discharge values, and has a steep gradient.

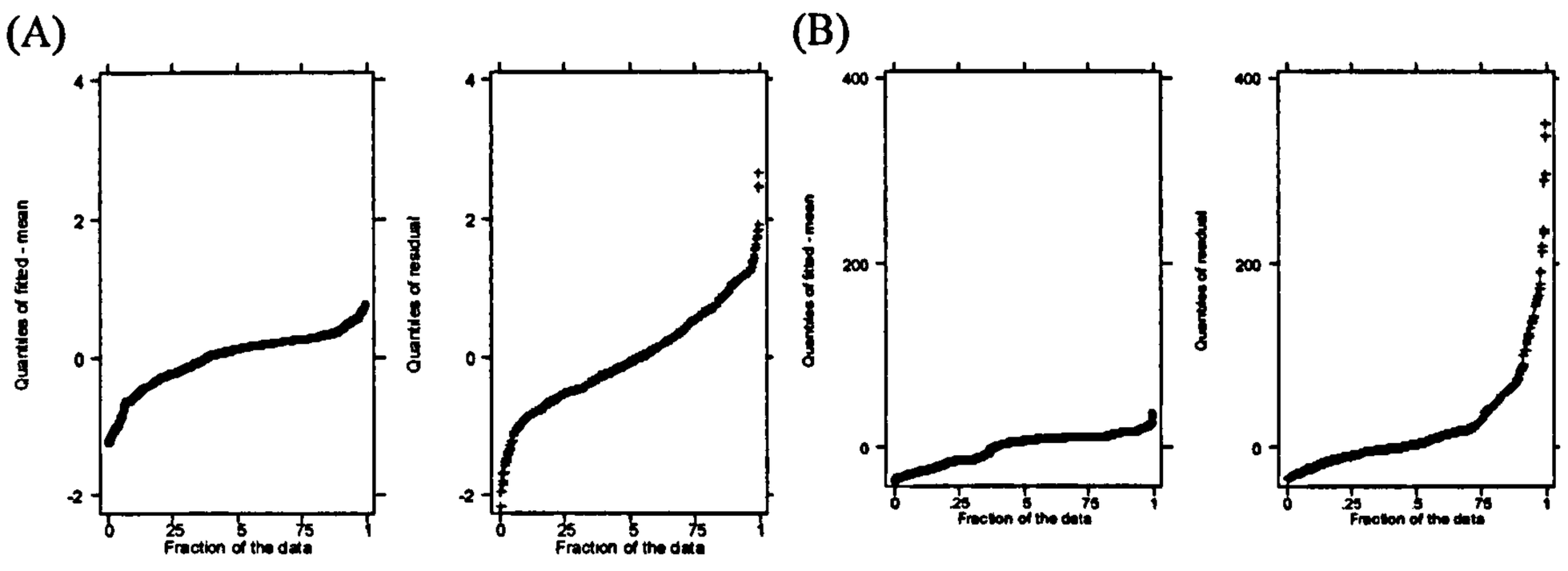

Figure 8.8. Quantile plots – note y-axis scales. (A) Fairly straight lines (linear regression of ln C on ln Q using all data from Rough Sike) and (B) bumpy lines with a high gradient (Gaussian-identity GLM using rising limb data with Q as the explanatory variable for Burnhope).

The actual loads for the storms for which SSC was measured were calculated using equation 8.1 and compared to the predictions produced by each of the models. This suggests which of the models is the most accurate; although it must be remembered the period for which SSC was monitored only represents a small proportion of the annual record and is biased towards storm events.

These measures of model fit are considered in light of the similarity or contrast in the distributions of the sampled and annual Q series given the potential effect of the distribution, especially with regard to the storm period estimate, and graphical examination of the fit of the rating curve to the data and the optimal model selected. There is no hierarchy as to which is the best indicator of model fit as they assess

different aspects of model fit and often it is the relative difference between them which is important. For example, if R^2 was selected as the superior measure but only differed by 0.01 between models but the sampled period load estimates varied from 5% to 70% more weight should possibly be given to the sampled period load estimates.

8.3 Rating curve development

In the following section each study site is examined in turn. The SSC, sampled Q and annual Q series characteristics and distributions are described. The ten basic rating curve models are developed, annual load estimates calculated, their fit assessed and the optimal model selected. The adapted models are then developed for each site, annual load estimates made and the relative value of each adaptation discussed.

8.3.1 Burnhope

8.3.1.1 Data characteristics and distributions

The Burnhope data set is the largest and consists of a combination of fixed-interval and storm sampling (Table 8.2). The storm sampling consisted of ten storms of mainly 48 samples in each (Table 8.2).

Table 8.2. Type, number and dates of samples taken in the Burnhope catchment.

Sample type	Number	Details
Fixed-interval	701	16th May 2000 – 7th March 2001
Storm		
Total:	503	
Per storm:	48	25th Oct 2000
	48	2nd Nov 2000
	48	7th Nov 2000
	48	12th Nov 2000
	48	28th Nov 2000
	48	8th Dec 2000
	48	22nd Jan 2001
	48	23rd Jan 2001
	71	10th Feb 2001
	48	7th Mar 2001

Approximately a third of the sampled SSC were taken on the rising limb and two thirds on the falling limb (Table 8.3). In comparison only 15% of values in the 10 month Q record (truncated due to foot and mouth) were categorised as rising limb (Table 8.3). A wide range of SSC values were sampled and almost the complete range of discharges was included in the sampled period (Table 8.3 & Figure 8.9). However, the mean Q of the sampled Q series is double that of the 10 month record as a result of the storm

Burnhope:

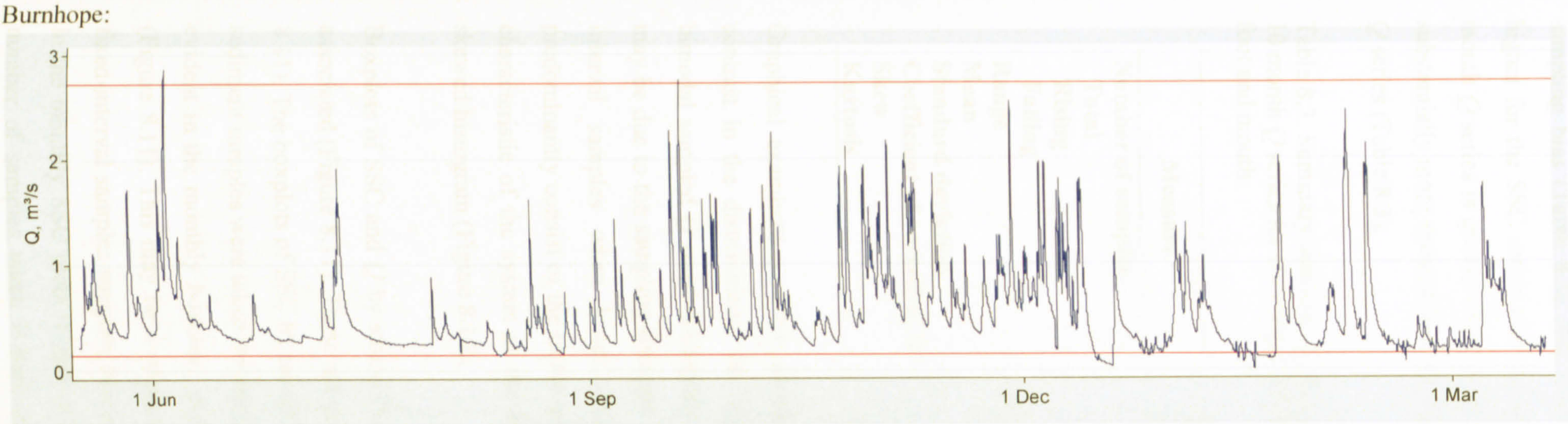

Candleseaves:

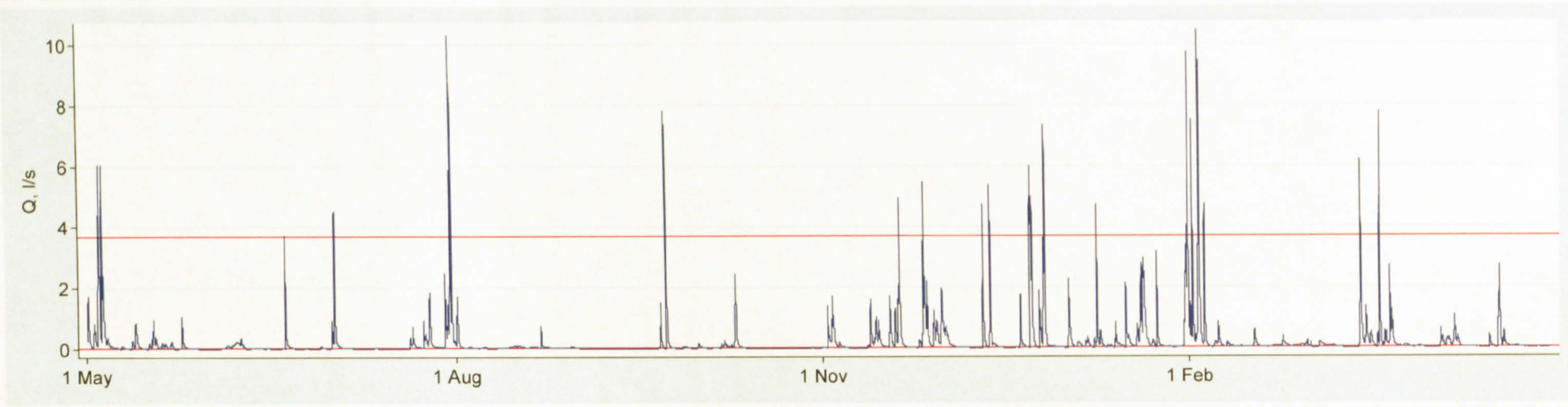

Langtae:

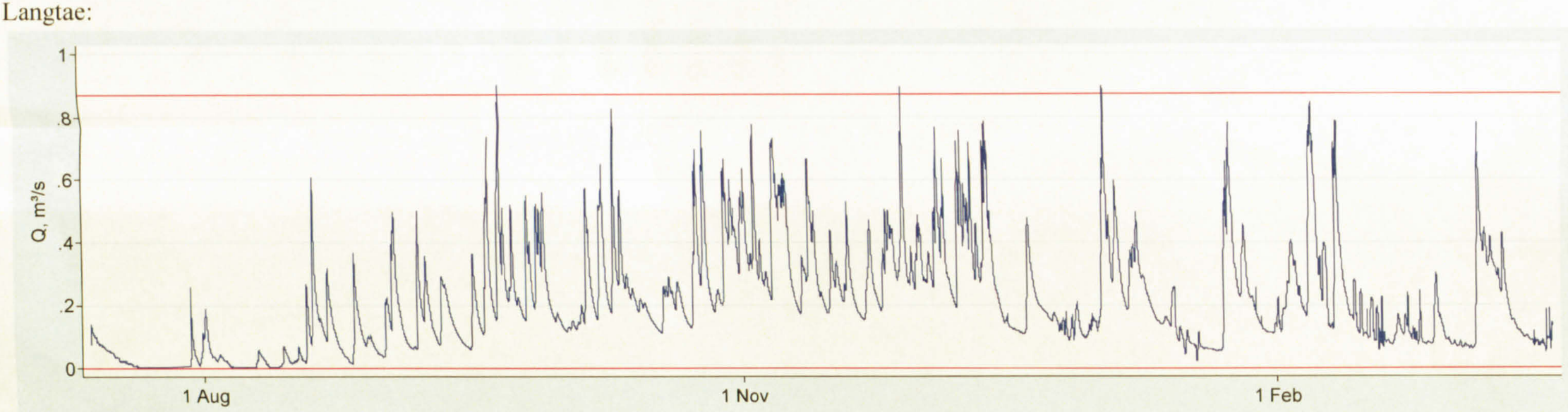

Rough Sike:

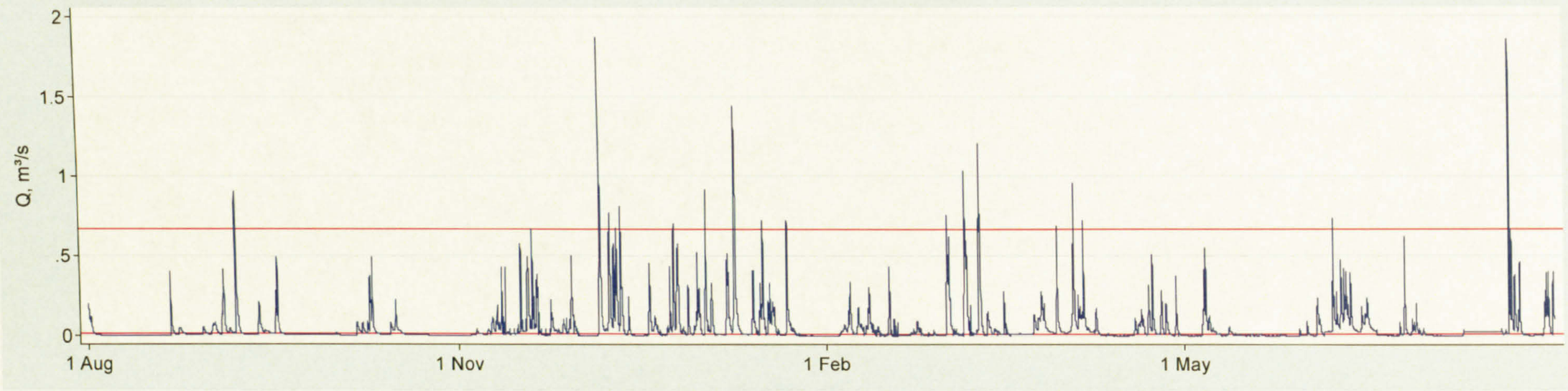

Trout Beck:

Figure 8.9. Annual discharge hydrographs for each catchment except Swinhope (due to calibration problems). Note: only 10 month record for Burnhope and 8 month record for Langtae. The red lines denote the highest and lowest discharges at which SSC was sampled.

sampling bias (Table 8.3). The coefficient of variation is approximately three times higher for the SSC series than for the sampled Q series and the variability in the 10 month Q series is greater than for the sampled Q series (Table 8.3). The SSC series is substantially more skewed and tail weighted, as indicated by kurtosis, than the sampled Q series (Table 8.3).

Table 8.3. Summary statistics of the sampled SSC (mg l^{-1}) and Q (m^3 s^{-1}) series and the 10 month Q series for Burnhope. Unfortunately the annual Q series was truncated due to foot and mouth.

Measure	SSC sampled period		10 month record
	SSC	Q	Q
Number of samples:			
Total	1204		29552
Rising	391		5069
Falling	812		24483
Range	0.2 - 389.1	0.15 - 2.72	0.00 - 2.86
Mean	29.0	1.04	0.51
Standard deviation	45.8	0.61	0.37
Coefficient of variation, %	157.9	58.3	72.2
Skew	3.16	0.20	1.96
Kurtosis	16.52	1.61	7.57

Graphical examination of the distribution of sampled SSC and Q series show the contrast in the distributions: the high peak and skew of SSC in comparison with bimodal sampled Q series histogram (Figure 8.10). The bimodal distribution of the Q may be due to the sampling strategy: the first peak is primarily composed of the fixed-interval samples when lower discharges were sampled and the second peak predominantly consist of the storm samples biased towards higher discharges. It is not a characteristic of the system as the 10 month Q series produces a smooth, positively skewed histogram (Figure 8.10).

Boxplots of SSC and Q by storm illustrate the variability in SSC and Q is not closely associated (Figure 8.11). There are generally more outliers on the SSC boxplots (Figure 8.11). The boxplots of SSC by month show that, with the exception of April, suspended sediment samples were taken throughout the year (Figure 8.11). A seasonal trend in Q is evident in the monthly boxplots, peaking in the winter and troughing in the summer (Figure 8.11). This may be a result of the sampling strategy, but the high number of fixed-interval samples suggests this is a real seasonal signal. This trend is not reflected in the monthly SSC plots (Figure 8.11). However, this may be a consequence of the number of samples taken in each month, as more samples were taken in the winter

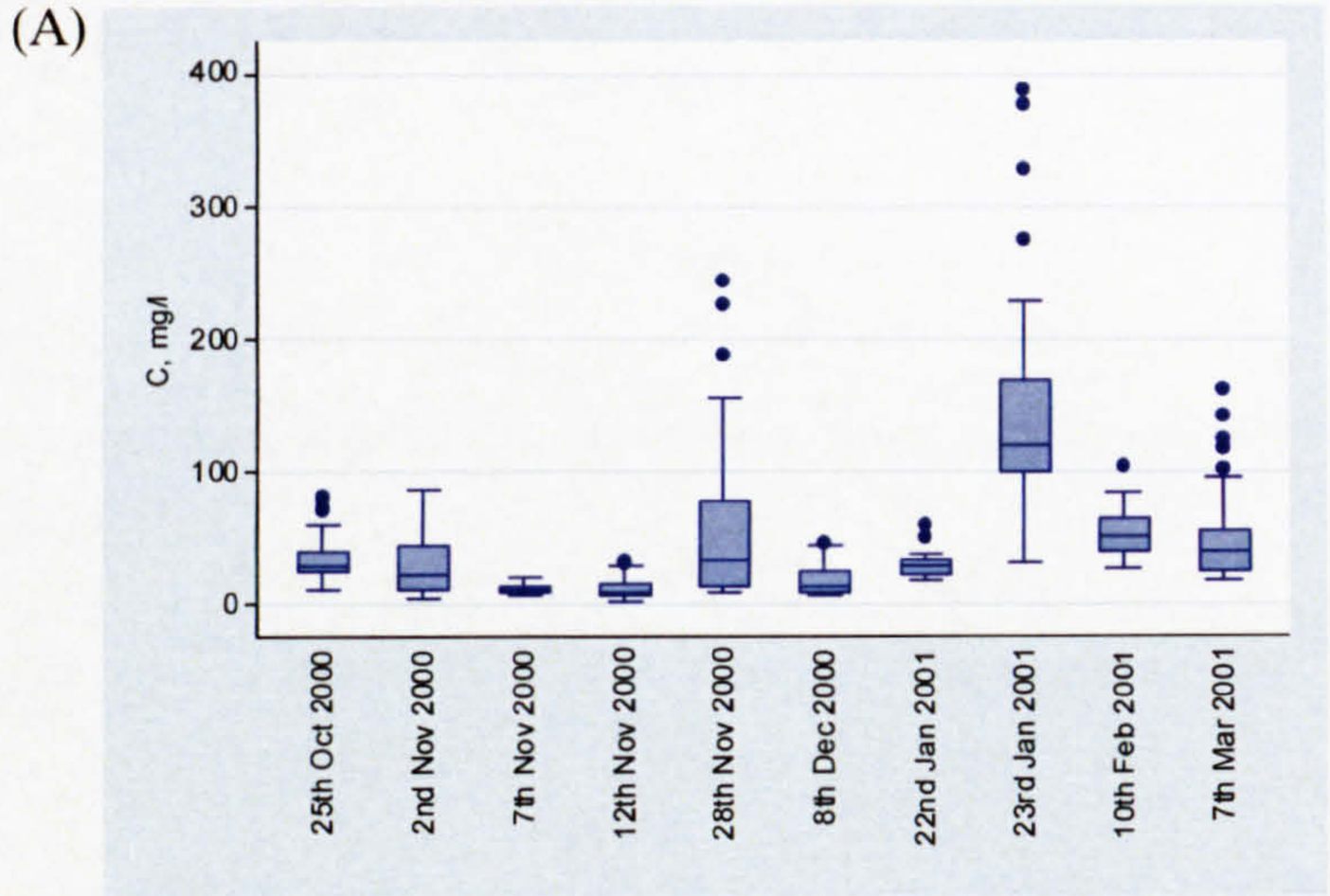

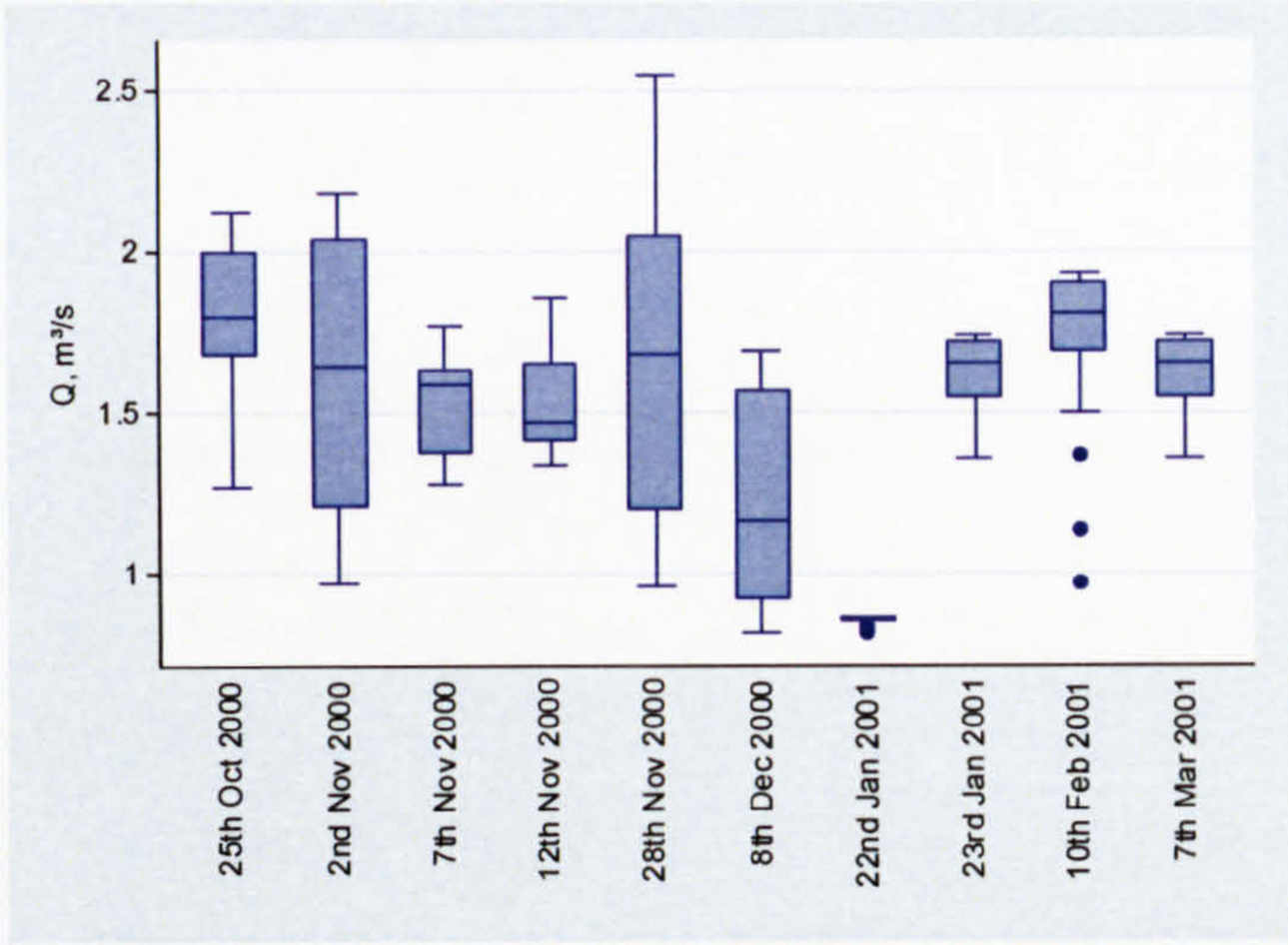

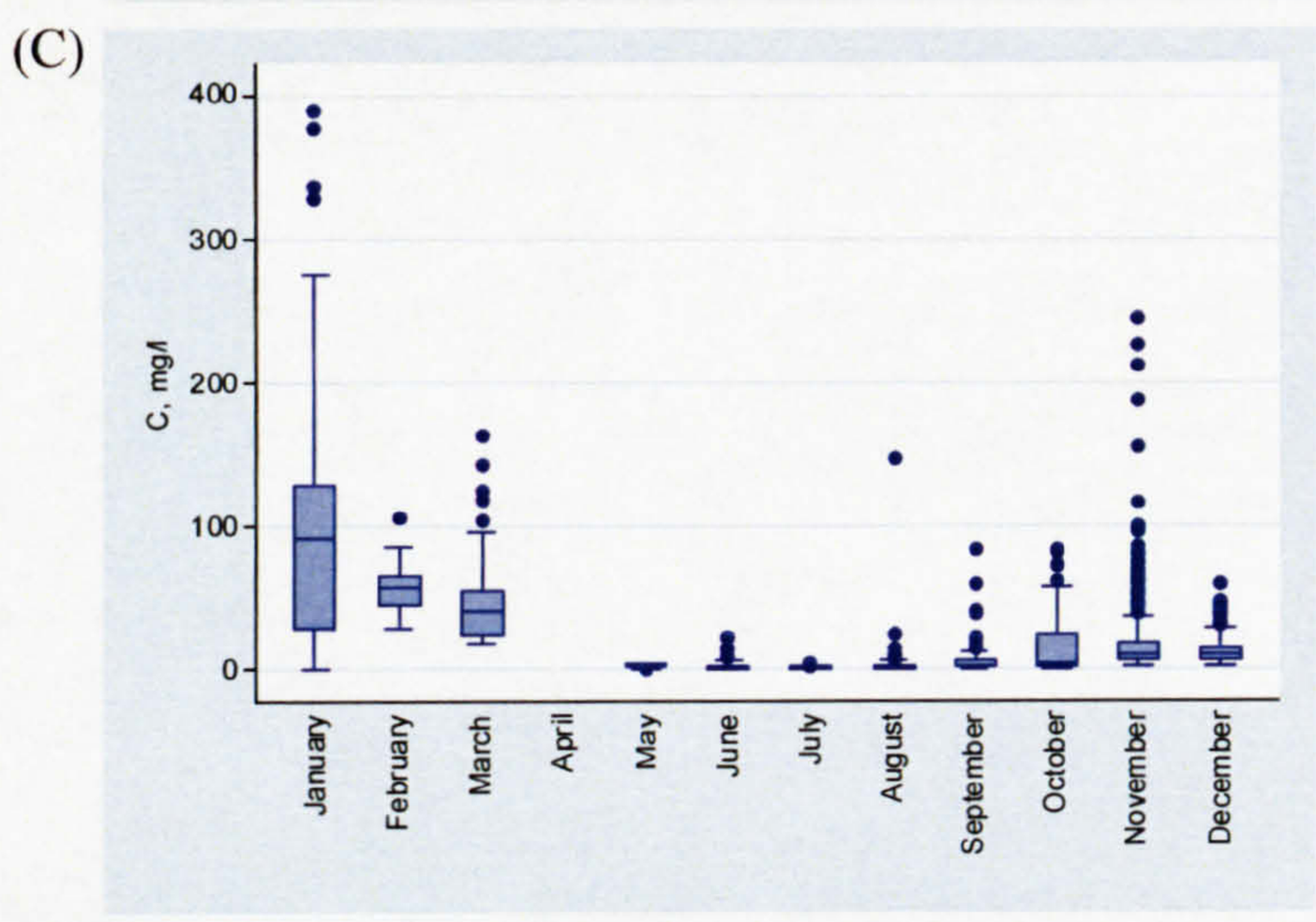

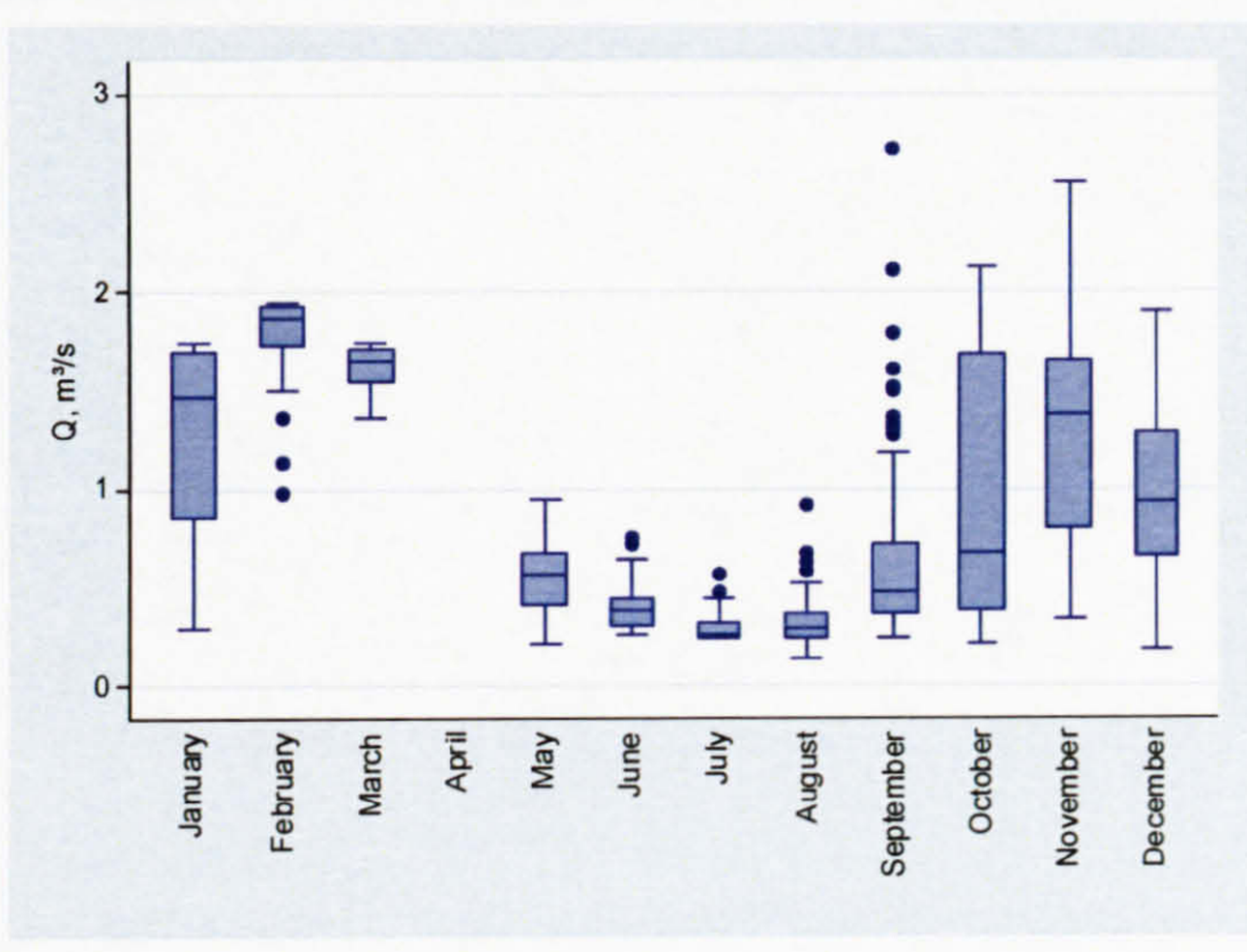

Figure 8.11. Boxplots illustrating the distribution of (A) SSC by storm, (B) Q by storm, (C) SSC by month, and (D) Q by month for Burnhope.

months (Table 8.4), and the higher the number of samples the greater the variability is likely to be.

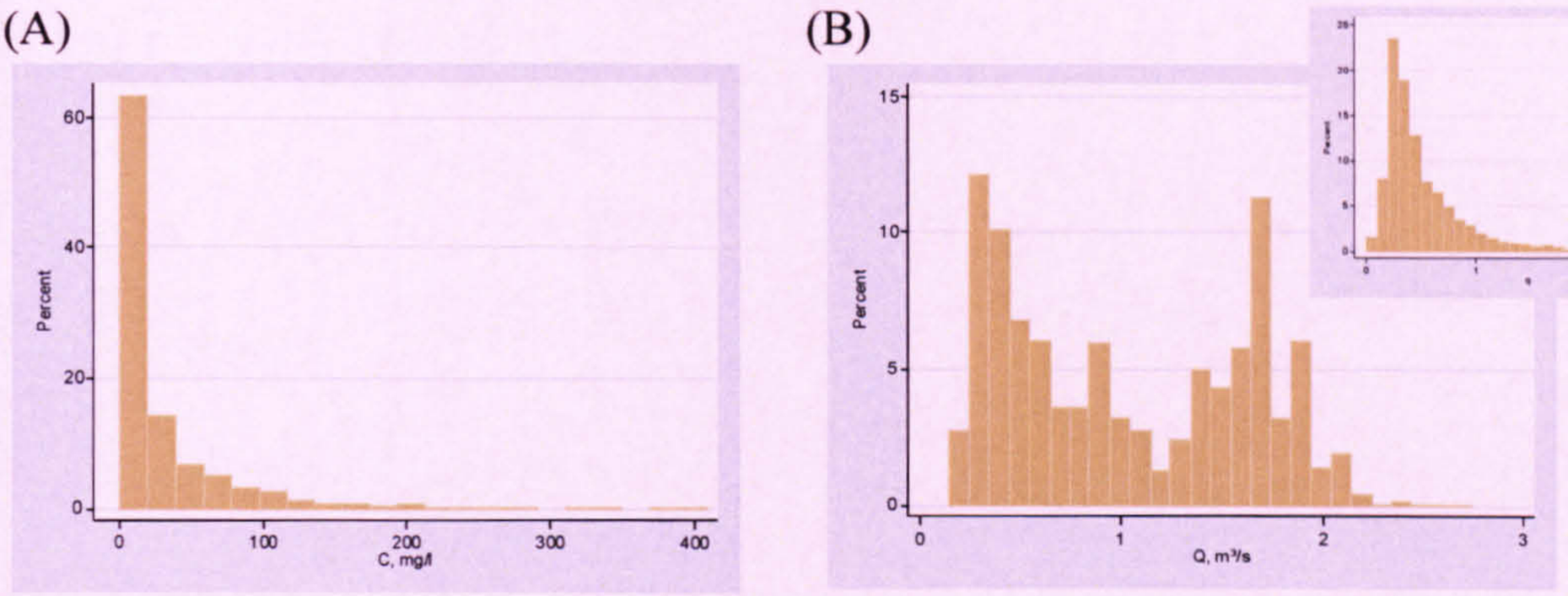

Figure 8.10. Distributions of sampled (A) SSC and (B) Q series with an inset of the distribution of the 10 month Q record for Burnhope.

Table 8.4. Number of SSC samples taken in each month for Burnhope.

Month	Number of samples
January	164
February	95
March	48
April	1
May	26
June	65
July	47
August	83
September	108
October	148
November	305
December	114

In summary the sampled series is biased towards the rising limb which may lead to over-predictions in suspended sediment load if sediment exhaustion is an influence in the catchment. The sampled Q series covers almost the full range of Q in the 10 month series so errors will not be introduced by extrapolation of the curve. Although the distributions of the sampled and 10 month series are very different the accuracy of the sampled period load estimate should be a reasonable measure of model fit. Samples were taken throughout the year, which suggests that the full range of SSC-Q relations will have been sampled. However, storm sampling was only undertaken during the winter.

8.3.1.2 Basic rating curves

Out of the basic rating curve models, the R^2 values indicate that the linear regression model is the worst fit and the gamma-identity with Q as the explanatory variable and the gamma-log and Gaussian-log models with ln Q as the explanatory variable are the best fit (Table 8.5). The RMSE also suggests that the gamma-log and Gaussian-log models with ln Q as the explanatory variables are superior (Table 8.5). In contrast, the diagnostic plots suggest the linear regression model is more appropriate because the linear regression model residuals are approximately normally distributed with equal variance, no structure is evident in the residuals plots and the quantile plots are fairly smooth and symmetrical. In contrast the GLM diagnostic plots show non-normally distributed residuals, structure in the residual plots and a long tail in the residual quantile plots at the higher quantiles, although this is acceptable if a gamma distribution is assumed.

Graphical examination of the basic model rating curves shows that, with the exception of the corrected linear regression models, the rating curves are quite different (Figure 8.12). The congruence of the LNCF, SM and BME corrected regression models (Figure 8.12) is testament to the approximately normal distribution of the residuals. The gamma-log model with Q as the explanatory variable is very different from the other rating curves, its gradient increases sharply at high values of Q (Figure 8.12); depending on the distribution of Q, this may result in very large load estimates. The gamma-identity model with ln Q as the explanatory variable is a physically implausible model as it predicts negative SSC values for low values of Q (Figure 8.12).

Despite being physically implausible, the most accurate sampled period load estimate was produced by the gamma-identity curve with Q as the explanatory variable: the model under-predicted the sampled period load by just 7% (Table 8.5). This reflects the importance of high discharges in sediment transfer. The second most accurate model is linear regression uncorrected for bias (Table 8.5). The bias towards sampling SSC on the rising limb (Table 8.5), assuming the system is sediment-limited, may have compensated for the back-transformation bias. With the exception of the gamma-identity curve with Q as the explanatory variable all the GLMs provide less accurate estimations of load than the linear regression models, with or without back-transformation bias correction (Table 8.5).

Table 8.5. Basic Burnhope rating curve equations, associated R^2 and RMSE values, predicted 10 month loads, monitored period predicted loads and percentage difference between actual and predicted load for the monitored period. 10 month loads were calculated from 16th May 2000 to 20th March 2001. The R^2 and RMSE values for linear regression relate to C not ln C. UC = uncorrected, LNCF = corrected by the log-normal correction factor (1.41), SM = corrected by smearing (1.46), and BME = corrected by the Bradu-Mundlak estimator.

Model	Equation	R^2	RMSE	n	10 month load, t	Monitored period Load, t	Monitored period % difference
Linear regression	$\ln C = 1.83 \ln Q + 2.66$	0.32	39.95	1203			
UC:					171.3	18.7	–11.2
LNCF:					241.2	26.3	25.1
SM:					249.9	27.2	29.6
BME:					229.0	26.3	25.0
Gamma–identity, Q	$C = 25.26 Q - 3.21$	0.57	39.72	1203	287.7	19.6	–6.8
Gamma–log, Q	$C = \exp(2.14 Q + 0.50)$	0.46	46.08	1203	255.8	35.7	69.9
Gaussian–log, Q	$C = \exp(1.18 Q + 1.96)$	0.55	38.57	1203	437.7	26.9	28.2
Gamma–identity, ln Q	$C = 13.12 \ln Q + 15.79$	0.53	44.53	1203	125.9	11.3	–46.3
Gamma–log, ln Q	$C = \exp(1.80 \ln Q + 3.04)$	0.57	37.81	1203	251.5	26.8	27.4
Gaussian–log, ln Q	$C = \exp(1.68 \ln Q + 3.15)$	0.57	37.75	1203	285.8	28.0	33.4
					Actual:	**21.0**	

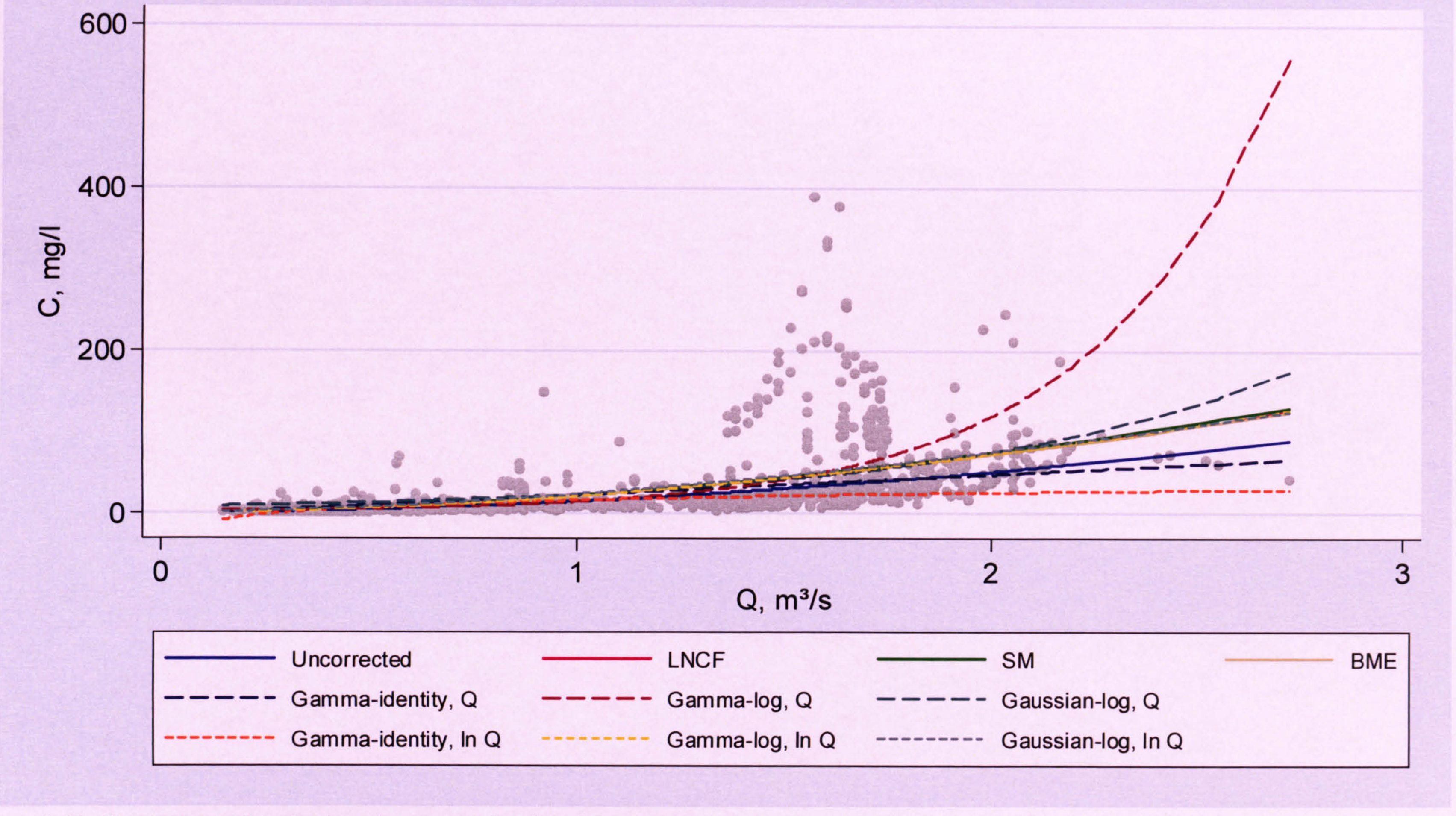

Figure 8.12. Comparison of the basic rating curves developed for Burnhope.

R^2, RMSE, residual plots, graphical examination of the rating curves and the accuracy of the sampled period load estimate each suggest that different models are superior. However, the gamma-identity model with Q as the explanatory variable is selected as the best model on the basis that R^2 is the highest, RMSE is only 2 mg l^{-1} more than the lowest RMSE, the unequal variance in the residuals is more acceptable as a gamma distribution is assumed and the sampled period load estimate is the most accurate. Although the sampled and 10 month Q distributions are different the full range of Q was sampled and therefore the load estimation should be a fairly good indicator of model fit.

8.3.1.3 Adapted rating curves

Fifteen adaptations of the basic linear regression rating curve were developed which resulted in seven load estimates (Table 8.6). A lagged model was not developed, as the monitored period load estimate indicates that a zero lag was the most appropriate.

Developing separate rating curves for the rising and falling limb data did not result in notably better models in terms of R^2 and RMSE (Table 8.6). However, the sampling period load estimate derived from the two models was more accurate, although only by 3% (Table 8.6). The gradient of the rising limb models was greater than that of the falling limb model, indicating there was a greater increase in ln C for a given increase in ln Q (Figure 8.13 & Table 8.6). The rising limb and falling limb data clouds are indistinct (Figure 8.13).

The regression models derived from the split-year data sub-sets are a poorer fit in terms of R^2 and comparable in terms of RMSE than the model derived from all data (Table 8.6). There is a substantial difference in the gradient of the summer and winter models. The summer curve has a lower gradient suggesting that for a given increase in ln Q, ln C increases by a smaller amount in summer compared with winter (Figure 8.13 & Table 8.6). SSC is only predicted to be higher in summer than in winter at very low discharges (Figure 8.13). There is no clear separation in the data clouds, except that data points at lower values of ln Q are dominated by summer samples, and conversely data points at higher values of ln Q are dominated by winter samples (Figure 8.13). Developing split-year models increases the accuracy of the sampled period suspended sediment load by 4% (Table 8.6).

Table 8.6. Adapted linear regression rating curve equations for Burnhope, associated R^2 and RMSE values, predicted 10 month loads, monitored period predicted loads and percentage difference between actual and predicted load for the monitored period. 10 month loads were calculated from 16th May 2000 to 20th March 2001. The R^2 and RMSE values for linear regression relate to ln C not C. None of the load estimates are corrected for back-transformation bias.

Model	Equation	R^2	RMSE	n	10 month load, t	Monitored period Load, t	Monitored period % difference
All data	$\ln C = 1.83 \ln Q + 2.66$	0.71	0.83	1203	171.3	18.7	–11.2
Limb:							
Rising	$\ln C = 1.88 \ln Q + 3.02$	0.61	0.85	391	170.9	19.3	–8.0
Falling	$\ln C = 1.63 \ln Q + 2.42$	0.71	0.74	812			
Season (4):							
Spring	$\ln C = 2.34 \ln Q + 2.49$	0.76	0.75	74	162.5	16.2	–22.9
Summer	$\ln C = 0.73 \ln Q + 1.31$	0.06	0.91	195			
Autumn	$\ln C = 1.50 \ln Q + 2.34$	0.73	0.59	561			
Winter	$\ln C = 1.91 \ln Q + 3.17$	0.59	0.77	373			
Split–year:							
Summer	$\ln C = 1.18 \ln Q + 1.90$	0.31	0.82	329	156.0	19.5	–7.0
Winter	$\ln C = 1.79 \ln Q + 2.73$	0.61	0.80	874			
Limb & split–year:							
Summer – rising	$\ln C = 1.50 \ln Q + 2.37$	0.43	1.03	43	157.9	19.8	–5.7
Summer – falling	$\ln C = 1.05 \ln Q + 1.75$	0.26	0.78	286			
Winter – rising	$\ln C = 1.73 \ln Q + 3.11$	0.49	0.81	348			
Winter – falling	$\ln C = 1.62 \ln Q + 2.49$	0.66	0.69	526			
Lag	Lag did not improve load estimate						
ΔQ	$\ln C = 1.82 \ln Q + 4.09 \Delta Q + 2.66$	0.72	0.82	1203	174.6	18.9	–10.0
Time of year	$\ln C = 1.36 \ln Q + 0.53 \sin [2 \pi \text{FOY}] + 0.55 \cos [2 \pi \text{FOY}] + 2.56$	0.77	0.73	1203	151.9	16.2	–23.0
***Q* class**	$\ln C = 1.37 \ln Q + 2.61$	0.87	0.51	21	171.3	18.7	–11.2
					Actual:	**21.0**	

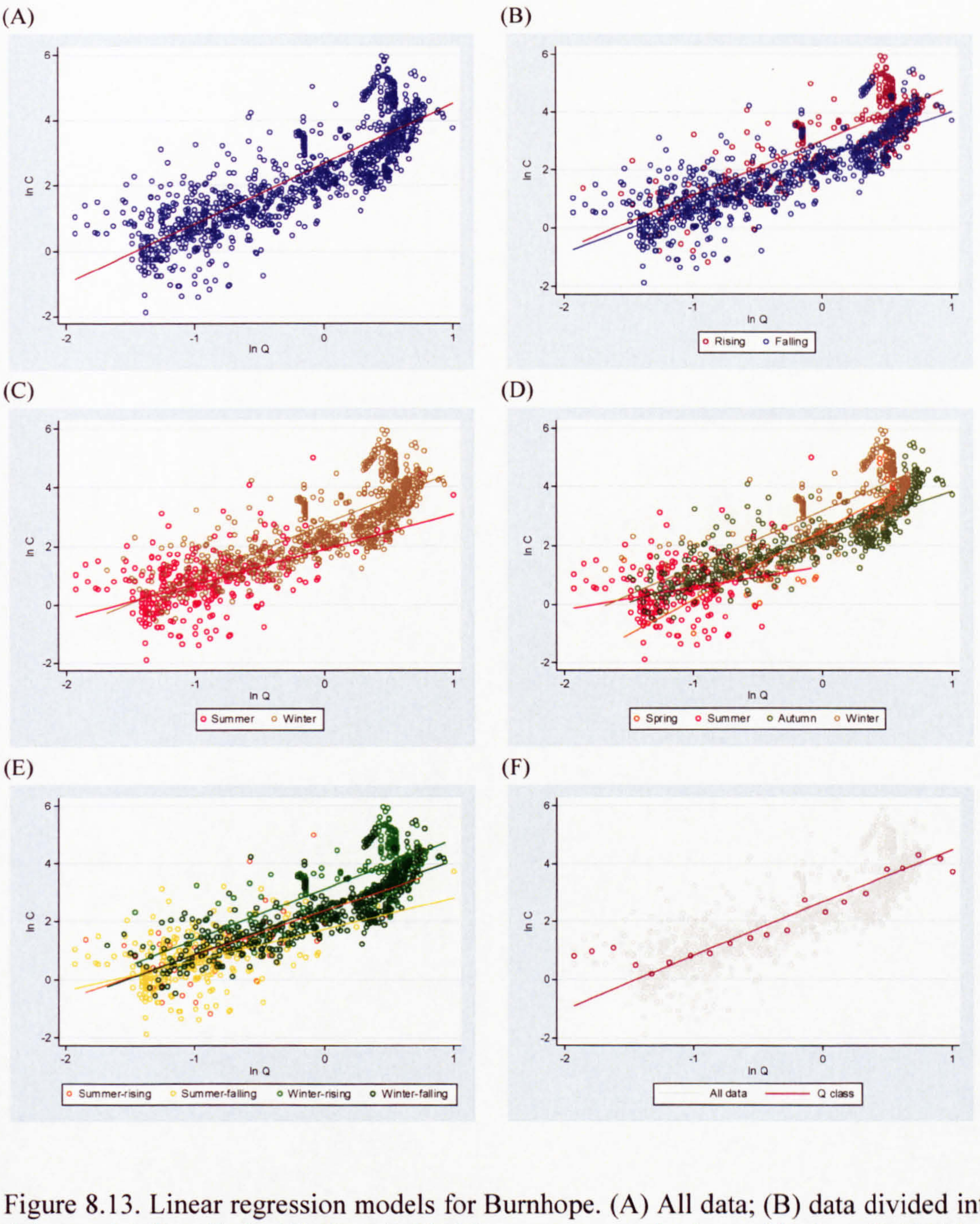

Figure 8.13. Linear regression models for Burnhope. (A) All data; (B) data divided into rising and falling limb; (C) data divided into summer and winter; (D) data divided into spring, summer, autumn and winter; (E) data divided into summer-rising, summer-falling, winter-rising, winter-falling; and (F) *Q* class method.

The gradients of the seasonal regression models are all quite different: the gradient is highest for spring, then winter, then autumn and lowest for summer (Table 8.6 & Figure 8.13). The R^2 and RMSE values indicate the summer model is a poor fit (Table 8.6). These four separate models result in a less accurate load estimate than if just one regression model was developed from all the data and the R^2 and RMSE are variable in comparison with the all data model (Table 8.6).

Categorising the data by split-year and limb results in the most accurate load estimation, which is perhaps not surprising given that rising and falling and split-year models both increased the accuracy (Table 8.6). However, in comparison with the regression model based on all data the R^2 and RMSE values indicate poor model fits (Table 8.6). The gradient of the regression lines are broadly similar for all models except the summer-falling model but the intercepts differ (Table 8.6 & Figure 8.13).

The model fit, in terms of R^2, RMSE and sampled period load estimate, is very similar if change in Q is added as an extra explanatory variable (Table 8.6). R^2 and RMSE values indicated a superior model fit if sine and cosine variables were added as additional explanatory variables, but the resultant sample period load estimate was over 10% less accurate than the basic linear regression model (Table 8.6). The Q class method decreased the accuracy of the sampled period load estimate by over 20% even though the R^2 and RMSE errors suggest a notably better model fit (Table 8.6). The principal difference between the Q class and basic linear regression model is the Q class regression gradient is 0.5 lower (Table 8.6 & Figure 8.13). Therefore under-predictions, mostly at higher ln Q, must have caused the decrease in model accuracy.

In summary, the largest improvement in sampling period load estimate was achieved by categorising the data by split-year and limb. However, the improvement was only 5.5% (Table 8.6). R^2 indicated that out of the fifteen models only four were a better fit than the all data model. In contrast, RMSE indicated that all but three of the models were an improved fit (Table 8.6).

8.3.2 Candleseaves

8.3.2.1 Data characteristics and distributions

Thirteen storms were sampled at Candleseaves and no fixed-interval samples were

taken (Table 8.7). Storms were not sampled throughout the year: no storms were sampled in late summer/early autumn or late winter/early spring (Table 8.7).

Table 8.7. Type, number and dates of samples taken in the Candleseaves catchment.

Sample type	Number	Details
Fixed-interval	0	
Storm		
Total:	306	
Per storm:	24	1st May 2003
	24	17th May 2003
	23	19th June 2003
	19	30th June 2003
	24	21st July 2003
	24	28th July 2003
	24	2nd November 2003
	24	17th November 2003
	24	28th November 2003
	24	12th December 2003
	24	7th January 2004
	24	23rd January 2004
	24	7th February 2004

Approximately two thirds of the samples were taken on the rising limb (Table 8.8). In comparison approximately two thirds of the Q measurements were taken on the falling limb during the annual monitoring period. Sampled SSC ranged from approximately 0 to over 100 mg l^{-1} (Table 8.8). Only approximately one third of the range of the annual Q record was sampled (Table 8.8 & Figure 8.9) and the mean and standard deviation of the annual Q series are lower than the sampled Q series (Table 8.8). The coefficient of variation indicates that both sampled data series are highly variable, with SSC more so than Q (Table 8.8). The annual Q record is much more variable than both the sampled series (Table 8.8) and from this it can be postulated that the population SSC is likely to be even more variable. SSC and Q are both positively skewed, with SSC more so than sampled Q (Table 8.8). The kurtosis of the SSC series is also higher than the kurtosis of the sampled Q series: the SSC distribution has more tail weight (Table 8.8 & Figure 8.14). The skew and kurtosis of the annual Q are notably higher than the sampled series Q and SSC series (Table 8.8), and therefore the annual SSC series is potentially more skewed and tail weighted.

Table 8.8. Summary statistics of the sampled SSC (mg l^{-1}) and Q (m^3 s^{-1}) series and the annual Q series for Candleseaves.

Measure	SSC sampled period		Annual record
	SSC	*Q*	*Q*
Number of samples:			
Total	306		35136
Rising	215		12330
Falling	91		19809
Range	0.2 - 113.6	0.02 - 3.69	0.00 - 10.45
Mean	6.7	0.72	0.23
Standard deviation	12.75	0.89	0.71
Coefficient of variation, %	190.7	123.6	310.50
Skew	5.09	1.85	6.74
Kurtosis	32.24	5.83	61.65

Graphical examination of the sampled SSC and Q series illustrates the more peaked and skewed nature of the SSC series (Figure 8.14). The bias of sampling higher flows is evident from comparison of the annual and sampled Q series distributions (Figure 8.14).

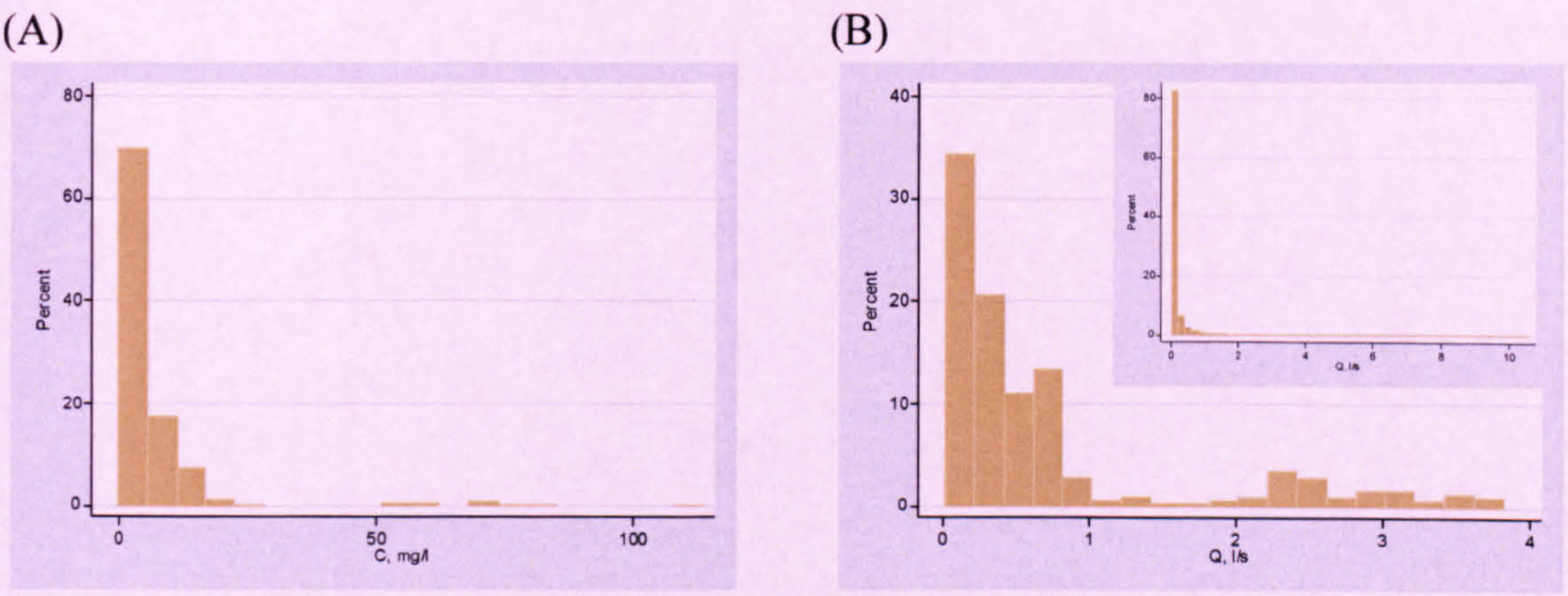

Figure 8.14. The distribution of (A) sampled SSC and (B) sampled Q with an inset of the distribution of the annual Q record for Candleseaves.

Box plots of the SSC and Q for each storm show that there are more outliers in the SSC series (Figure 8.15). The Q value distributions vary more between storms than the SSC distributions (Figure 8.15). The 19th June event has a much larger range of SSC (Figure 8.15) and will cause scatter in the rating curve models developed and decrease the model fit.

The monthly box plots of the SSC and Q series clearly illustrate periods in the year when no samples were collected (Figure 8.15). The gap from August to October can be attributed to low flows and therefore there was very little sediment transfer during that period. The variation in SSC was greatest in June and this was not a consequence of the

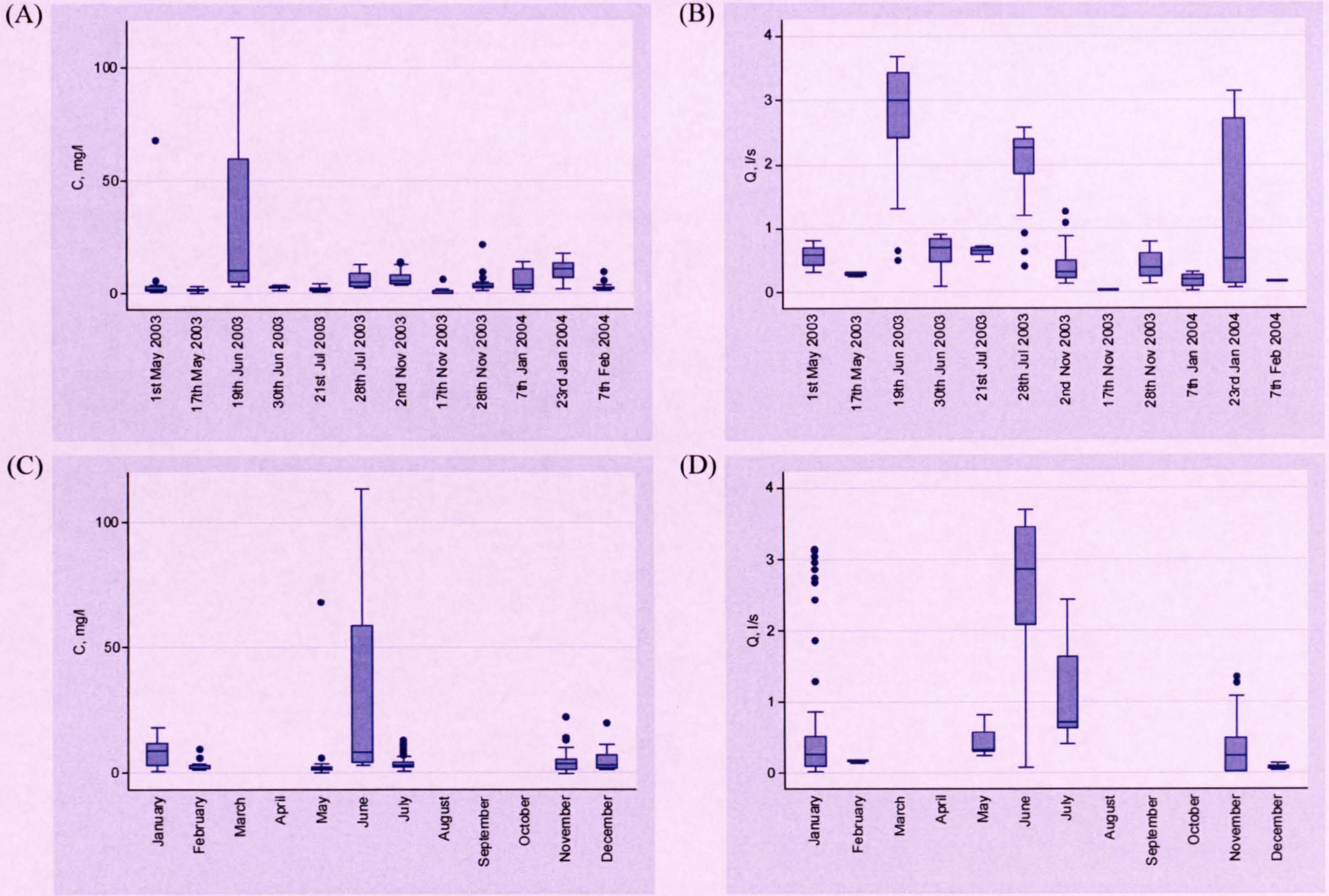

Figure 8.15. Boxplots illustrating the distribution of (A) SSC by storm, (B) Q by storm, (C) SSC by month, and (D) Q by month for Candleseaves.

number of samples collected, as only six fewer samples were collected in June than in any other month except February and December (Table 8.7). The variation in SSC is low in November, especially taking into consideration that at least 24 more samples were taken than for any other month (Figure 8.15 & Table 8.7). The distribution of SSC in June is reflected in the distribution of Q (Figure 8.15). Generally there appears to be more variation in the distribution of the Q series and there are a notable number of outliers in January, which is not reflected in the distribution of SSC (Figure 8.15).

In summary, due to more samples being taken on the rising limb in the sampled series in comparison with the annual record an over-prediction of sediment load may occur if sediment exhaustion is an important factor in the catchment. Only the lower third of the annual Q range was sampled and therefore errors may result due to extrapolation of the rating curve. Combined with the difference in distributions between the sampled and annual Q series, this casts doubt on the worth of the sampled period load estimate as an indicator of model fit. Lastly, the distribution of the samples throughout the year is poor, which suggests that all SSC-Q relations may not have been captured.

8.3.2.2 Basic rating curves

R^2 suggests the Gaussian-log and gamma-log models with Q as the explanatory variable are the best models and that linear regression is one of the poorest (Table 8.9). The RMSE suggests that the Gaussian-log model with Q as the explanatory variable is marginally superior (Table 8.9). The diagnostic plots indicate that the linear regression model is a fairly good fit: residuals are approximately normally distributed with a constant variance, the residuals are randomly distributed when plotted as a function of the predicted values and approximately the same number of data points are under- and over- predicted to approximately the same magnitude with the exception of a cluster of data points with very low ln C values. The diagnostic plots for the GLM models suggest that all the models are a fairly poor fit. The residuals are non-normally distributed and have unequal variance throughout the range of Q/ln Q, although this is acceptable for the gamma models. The observed as a function of predicted plot shows that most values of C are over-predicted with a few values grossly under-predicted. The residual versus fitted plots have structure in the scatter and a few very large residuals when Q was the explanatory variable. However the scatter is fairly even, except at high values of ln Q, when ln Q was used as the explanatory variable and this is acceptable if a gamma distribution is assumed. The quantile plots show the data is very highly positively

Table 8.9. Basic Candleseaves rating curve equations, associated R^2 and RMSE values, predicted annual loads, monitored period predicted loads and percentage difference between actual and predicted load for the monitored period. Annual loads were calculated from 1st May 2003 to 30th April 2004. The R^2 and RMSE values for linear regression relate to C not ln C. UC = uncorrected, LNCF = corrected by the log-normal correction factor (1.59), SM = corrected by smearing (1.74), and BME = corrected by the Bradu-Mundlak estimator.

Model	Equation	R^2	RMSE	n	Annual load, kg	Monitored period Load, kg	Monitored period % difference
Linear regression	$\ln C = 0.25 \ln Q + 1.54$	0.27	12.95	300			
UN:					33.6	0.40	–53.6
LNCF:					53.4	0.64	–26.2
SM:					58.4	0.70	–19.4
BME:					51.5	0.65	–25.1
Gamma–identity, Q	$C = 3.80 Q + 3.83$	0.32	12.11	306	85.3	0.85	–1.9
Gamma–log, Q	$C = \exp(0.47 Q + 1.44)$	0.34	12.01	306	225.8	0.91	5.4
Gaussian–log, Q	$C = \exp(0.51 Q + 1.36)$	0.34	12.00	306	275.6	0.94	8.6
Gamma–identity, ln Q	$C = 1.76 \ln Q + 8.51$	0.24	12.41	300	57.0	0.70	–18.9
Gamma–log, ln Q	$C = \exp(0.31 \ln Q + 2.13)$	0.28	12.30	300	62.9	0.75	–13.8
Gaussian–log, ln Q	$C = \exp(0.53 \ln Q + 2.19)$	0.30	12.20	300	80.5	0.90	3.9
					Actual:	**0.87**	

skewed. The ill-fitting nature of these models is largely attributable to some very large residuals at high values of Q/ln Q.

Graphical comparison of the different models shows four groups of models: (1) uncorrected linear regression; (2) the corrected linear regression models and gamma-identity based on ln Q; (3) Gaussian-log model based on ln Q and gamma-identity based on Q; and (4) Gaussian-log and gamma-log both with Q as the explanatory variable (Figure 8.16). All the models are broadly comparable, with notable differences occurring only at high discharges, as some are more influenced by the high SSC outliers (Figure 8.16).

Comparison of the percentage difference between modelled and observed loads indicates that the GLMs give consistently better predictions that the linear regression models (Table 8.9). The most accurate prediction was given by the gamma-identity model with Q as the explanatory variable: suspended sediment load was under-predicted by just 1.9% (Table 8.9). The best linear regression estimate was that corrected by smearing and was a 19.4% under-prediction (Table 8.9).

In terms of R^2 and RMSE the models are very similar: R^2 varies from 0.24 to 0.34 and RMSE from 12.00 to 12.95 mg l^{-1}. Only a small proportion of the annual Q range was sampled and therefore the validity of the sampled period load estimate is uncertain. Therefore, the most appropriate model should be selected on the basis of the diagnostic plots and graphical examination of the rating curves. On this basis linear regression corrected for bias by SM was chosen. SM was chosen as opposed to LNCF, despite the approximately normal distribution of residuals with equal variance, as there was a 0.15 difference between the SM correction and the LNCF.

8.3.2.3 Adapted rating curves

Examination of scatter plots of ln C and ln Q data show serial autocorrelation in the data (Figure 8.17). Clusters of samples from bottle sets from the auto-sampler are clearly evident and ideally more samples would be taken to avoid one bottle set biasing the results. However, no more bottle sets could be taken as the grip was blocked, which would have caused a change in the sediment dynamics.

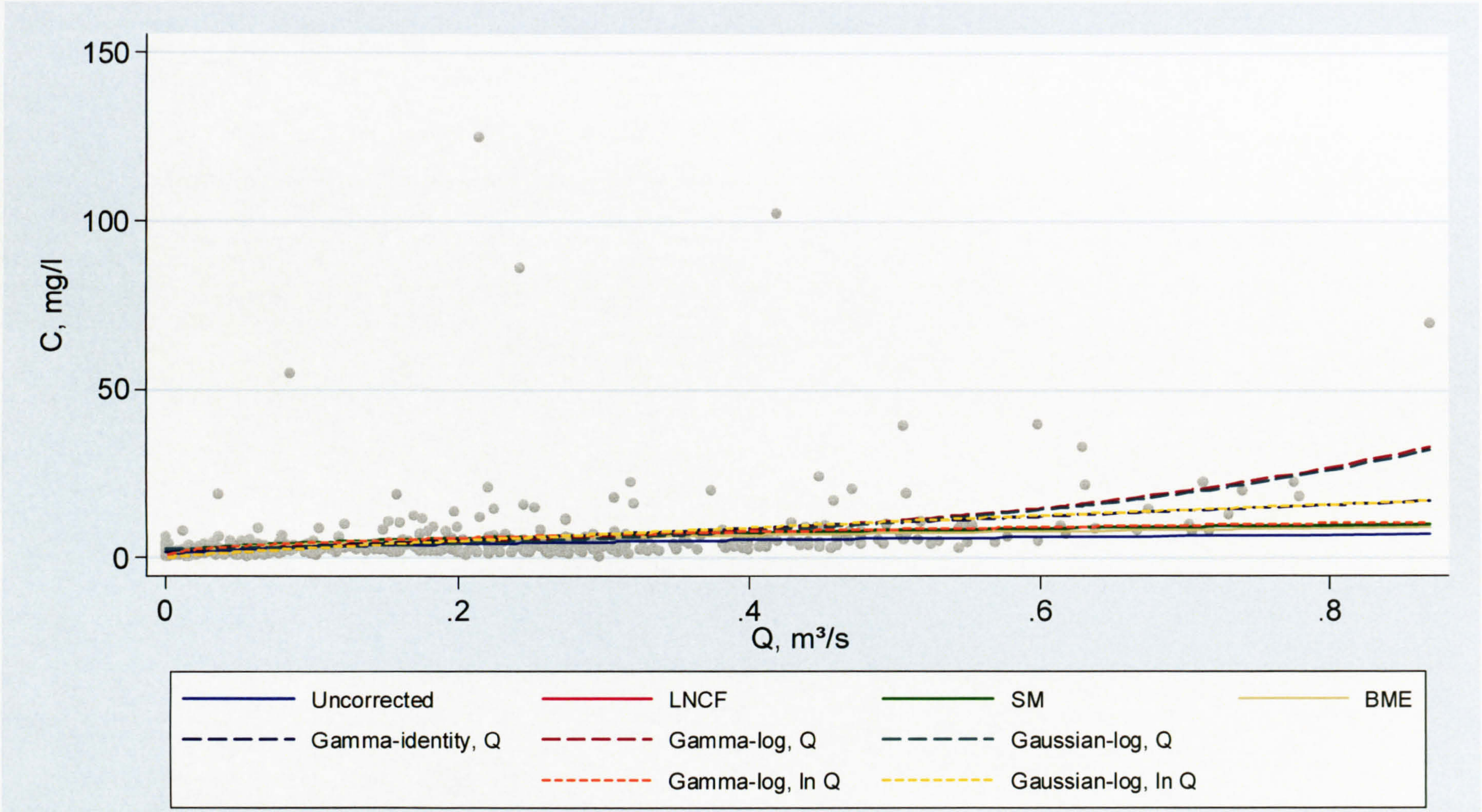

Figure 8.20. Comparison of the basic rating curves developed for Langtae.

(A)

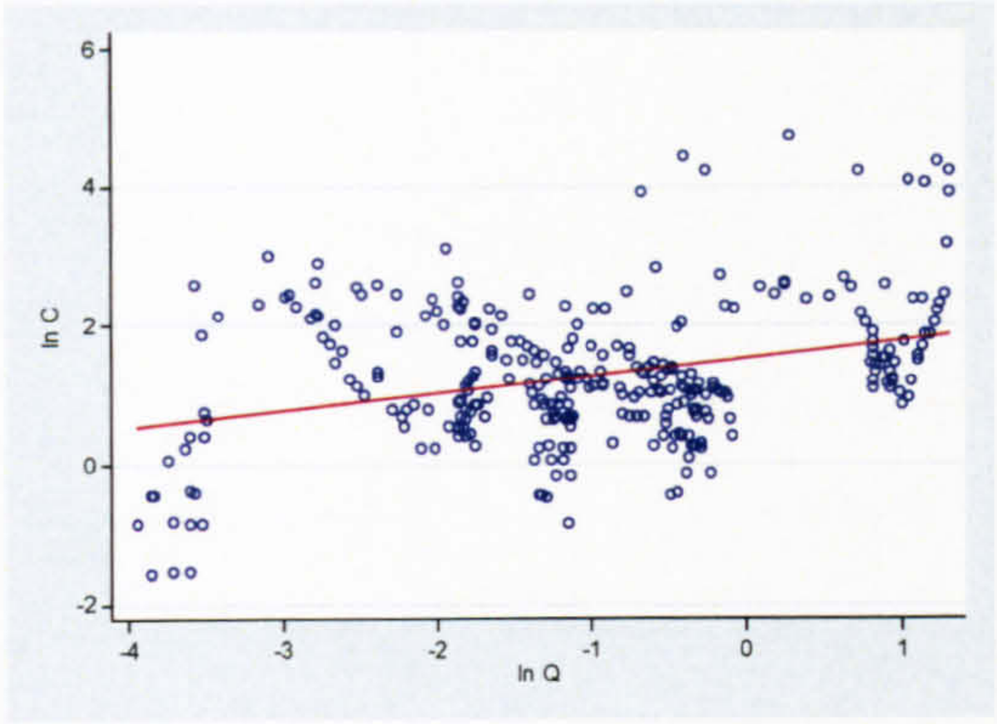

(B)

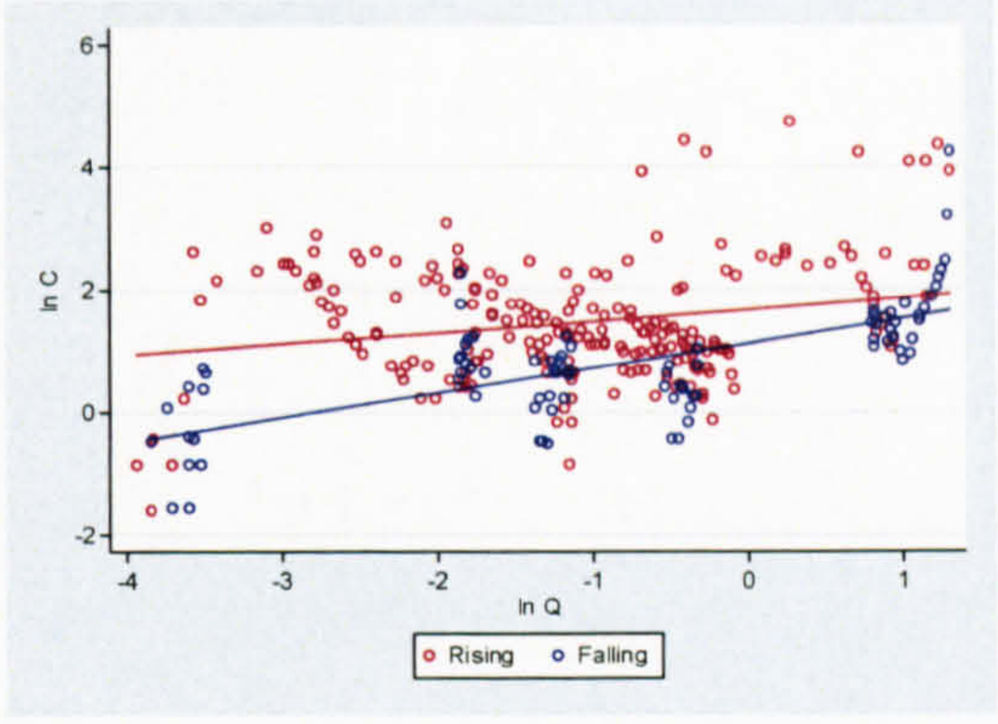

(C)

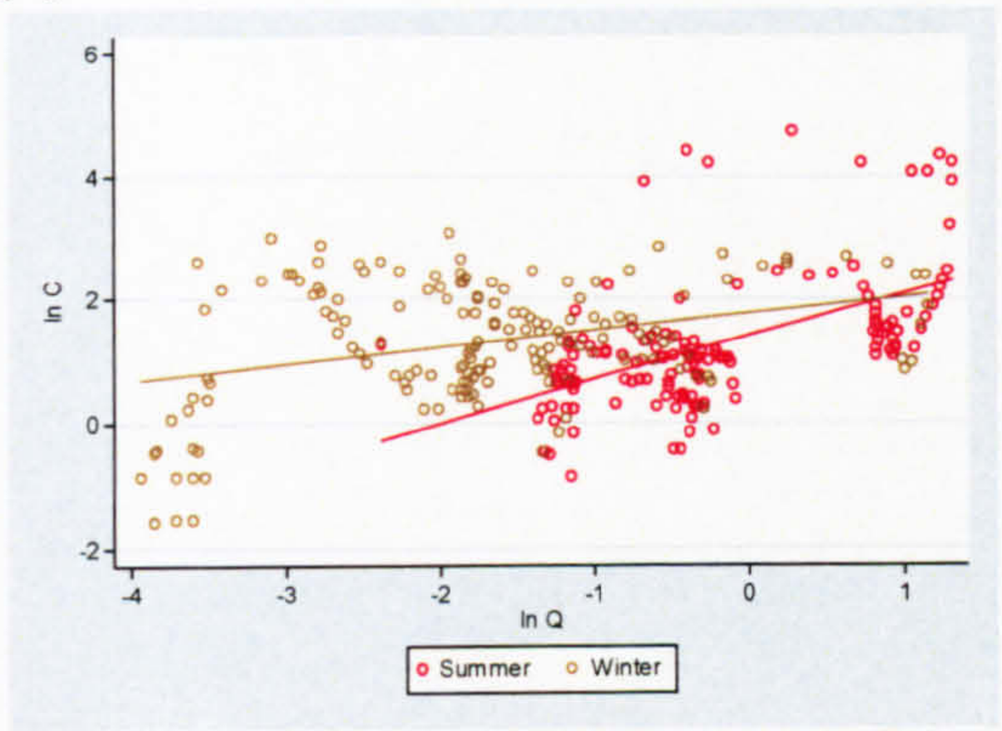

(D)

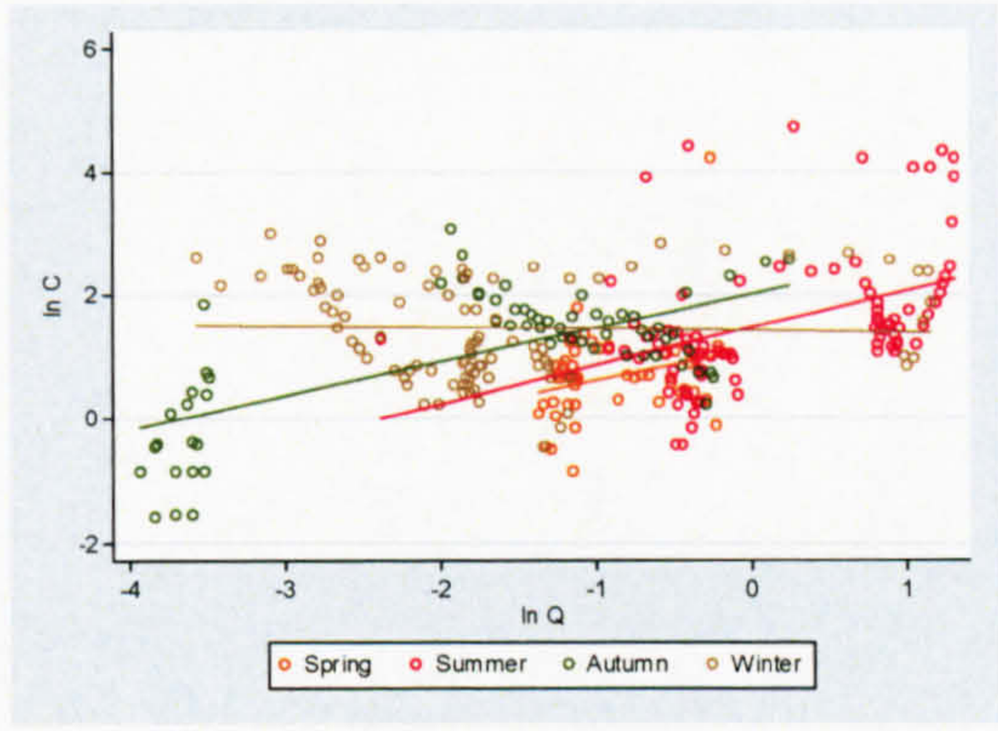

(E)

(F)

(G)

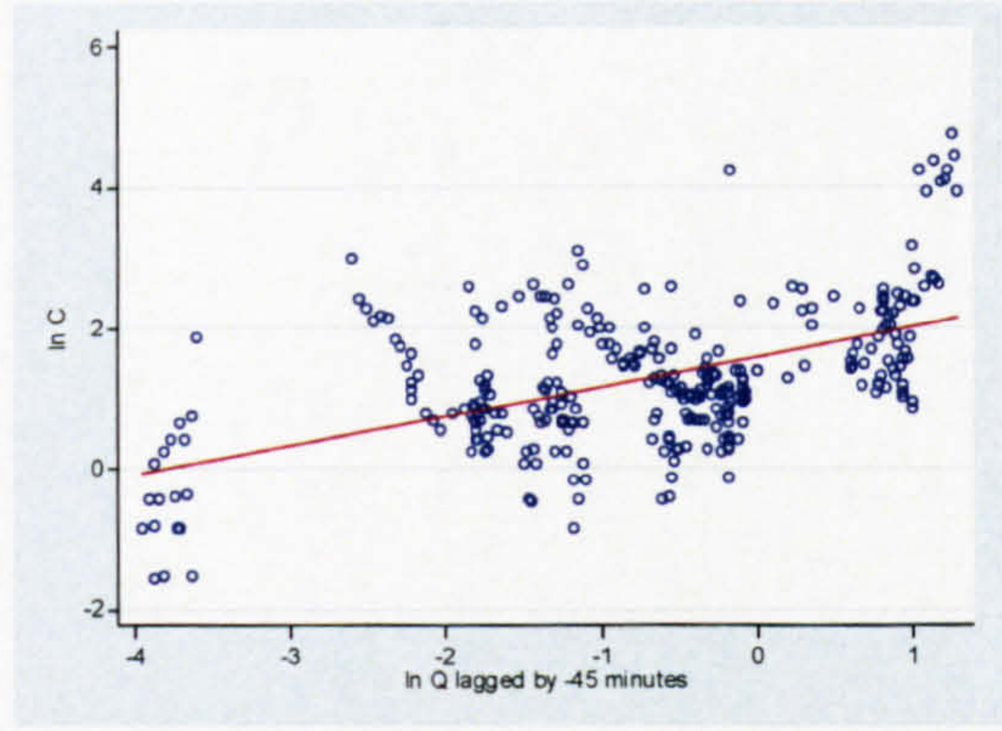

Figure 8.17. Linear regression models for Candleseaves. (A) All data; (B) data divided into rising and falling limb; (C) data divided into summer and winter; (D) data divided into spring, summer, autumn and winter; (E) data divided into summer-rising, summer-falling, winter-rising, winter-falling; (F) *Q* class method; and (G) *Q* lagged by minus 45 minutes.

A difference in the distribution of rising and falling limb data is evident (Figure 8.17) and this is reflected in the different model forms (Table 8.10). The rising limb regression line plots higher than the falling limb: ln C tends to be higher on the rising limb for any given discharge (Figure 8.17). The gradient of the falling limb regression line is steeper but is caused by one group of data points close to the origin from the same storm (Figure 8.17). The fit of the falling limb model is superior in terms of R^2 and RMSE (Table 8.10). The sampled period load estimate derived from these models is less accurate than that derived from the all data model (Table 8.10).

With regard to the split-year model, the winter regression line is steeper than the summer regression line (Figure 8.17). This suggests that for a given change in ln Q there is a greater change in ln C indicating that there is a more constant sediment supply during the winter. The fit of the summer regression line is better in terms of R^2 and RMSE (Table 8.10), and both the summer and winter models are superior to the all data model with respect to R^2 and RMSE (Table 8.10). The load estimate derived from these two regression equations is 10% more accurate than the all data model estimate (Table 8.10).

Given the poor temporal spread of the data (Figure 8.15), there is an argument that the seasonal model should not be developed. However, to allow comparison between sites, and the effect of limited data sets to be investigated, the model has been developed. The gradient of the winter regression line is negative which suggests that as ln Q increases ln C decreases (Figure 8.17), which may be attributable to sediment supply. The gradients of the spring and autumn regression lines are very similar with the autumn regression line plotting above the spring regression line (Figure 8.17). Therefore, the rate of change in ln C given a change in ln Q is the same in spring and autumn, but more sediment is transported at each given ln Q in the autumn. The gradient of the summer regression line is slightly steeper than those for the spring and autumn (Figure 8.17) and suggests that as ln Q increases there is a greater increase in ln C. The summer regression line plots between the spring and autumn regressions (Figure 8.17). RMSE and R^2 are variable for the four models with the spring and winter models being the poorest fit (Table 8.10). The sampled period load estimate derived from these seasonal curves is 5% more accurate than the load estimate derived from the all data model (Table 8.10).

Table 8.10. Adapted linear regression rating curve equations for Candleseaves, associated R^2 and RMSE values, predicted annual loads, monitored period predicted loads and percentage difference between actual and predicted load for the monitored period. Annual loads were calculated from 1st May 2003 to 30th April 2004. The R^2 and RMSE values for linear regression relate to ln C not C. None of the load estimates are corrected for back-transformation bias.

Model	Equation	R^2	RMSE	n	Annual load, kg	Monitored period Load, kg	Monitored period % difference
All data	$\ln C = 0.25 \ln Q + 1.54$	0.10	0.96	300	33.6	0.40	–53.6
Limb:							
Rising	$\ln C = 0.19 \ln Q + 1.68$	0.05	0.96	215	53.3	0.39	–59.4
Falling	$\ln C = 0.40 \ln Q + 1.13$	0.45	0.70	85			
Season (4):							
Spring	$\ln C = 0.48 \ln Q + 1.10$	0.06	0.71	48			
Summer	$\ln C = 0.62 \ln Q + 1.48$	0.19	0.99	90	67.9	0.45	–48.2
Autumn	$\ln C = 0.56 \ln Q + 2.04$	0.45	0.80	66			
Winter	$\ln C = -0.03 \ln Q + 1.43$	0.00	0.84	96			
Split–year:							
Summer	$\ln C = 0.70 \ln Q + 1.41$	0.30	0.90	138	62.2	0.49	–43.0
Winter	$\ln C = 0.27 \ln Q + 1.76$	0.10	0.91	162			
Limb & split–year:							
Summer – rising	$\ln C = 0.84 \ln Q + 1.68$	0.27	0.99	84			
Summer – falling	$\ln C = 0.68 \ln Q + 1.05$	0.56	0.60	54	49.5	0.47	–45.6
Winter – rising	$\ln C = 0.15 \ln Q + 1.74$	0.03	0.85	131			
Winter – falling	$\ln C = 0.35 \ln Q + 1.19$	0.34	0.74	31			
Lag	$\ln C = 0.42 \ln Q + 1.60$	0.26	0.87	300	55.9	0.48	–45.1
ΔQ	$\ln C = 0.20 \ln Q + 8.71\ \Delta Q + 1.33$	0.19	0.90	300	21.4	0.45	–48.1
Time of year	$\ln C = 0.40 \ln Q - 0.08 \sin [2\pi \text{FOY}] + 0.35 \cos [2\pi \text{FOY}] + 1.67$	0.15	0.94	300	67.0	0.47	–46.1
***Q* class**	$\ln C = 0.34 \ln Q + 1.99$	0.30	0.85	22	95.8	0.66	–23.7
					Actual:	**0.87**	

The same trends are evident on the split-year and limb graph as on the separate split-year and limb graphs (Figure 8.17): the falling limb regressions are steeper than the rising limb regressions and below them; the summer regressions are steeper than the winter regressions and plot below them at low ln Q and above them at high ln Q (Figure 8.17). With the exception of the winter-rising model the R^2 are reasonably good in comparison with the all data model (Table 8.10). The summer-falling model is an exceptionally good fit in terms of R^2 and RMSE (Table 8.10). An 8% improvement is achieved by developing these four models compared with the all data model (Table 8.10).

Analysis of lags indicated that the best model fit, in terms of accuracy of the sampling period load estimation, is obtained at a lag of -45 minutes. This increases the R^2 and decreases the RMSE compared with the basic linear regression model (Table 8.10) and appears to increase the clustering on the graph (Figure 8.17). However, the sampled period load estimate accuracy is only increased by 5% (Table 8.10). Adding change in Q or the sine and cosine variables as additional explanatory variables slightly improves model fit and increases the accuracy of the sampled period load estimate by 5.5% and 7.5% respectively (Table 8.10). The rating curve developed by the Q class method is very similar to the model developed using all the data (Figure 8.17 & Table 8.10). However, the load estimate is discernibly different, a 30% improvement, and R^2 and RMSE indicate a better model fit (Table 8.10).

All the sample period load estimates substantially under-estimate the actual load (Table 8.10). This can be attributed to the under-estimation of 19th June storm load. It is clearly evident from Figure 8.16 that the rating curves will grossly under-predict this storm.

In summary, the Q class method is a better model in terms of R^2, RMSE and sampled period load estimate. To some extent this is inevitable as it fits the finer structure in the data better. Notable improvements in load estimates were also achieved by the split-year model, the lagged model and the split-year and limb model. Only two of the adapted models showed a worse fit than the all data model in terms of RMSE and five were deemed worse by R^2 (Table 8.10).

8.3.3 Langtae

8.3.3.1 Data characteristics and distributions

Fixed-interval sampling was undertaken at Langtae from 12th July 2000 to 25th December 2000. No storm sampling was undertaken. This will allow comparison of the effect of sampling regime on load estimates. Less than 20% of suspended sediment were taken on the rising limb (Table 8.11) but this is fairly representative of the continuous record, as 25% of the Q measurements were on the rising limb. Despite the fixed-interval sampling, some high SSC were recorded. The highest Q for which a suspended sediment sample was taken was 0.87 $m^3 s^{-1}$, which is only 0.03 $m^3 s^{-1}$ less than the maximum Q for the continuous record (Table 8.11 & Figure 8.9), and the mean discharges are very similar for the sampled and population suspended sediment series (Table 8.11). The coefficients of variation indicate that the SSC is more variable than the sampled Q series (Table 8.11). The SSC series is much more skewed and tail weighted than the sampled Q series (Table 8.11). The standard deviation, coefficient of variation, skew and kurtosis are fairly comparable between the sampled and 8 month Q series (curtailed due to foot and mouth).

Table 8.11. Summary statistics of the sampled SSC (mg l^{-1}) and Q ($m^3 s^{-1}$) series and the 8 month Q series for Langtae.

Measure	SSC sampled period SSC	SSC sampled period Q	8 month record Q
Number of samples:			
Total	458		22853
Rising	79		5542
Falling	379		18549
Range	0.3 - 125.1	0.00 - 0.87	0.00 - 0.90
Mean	5.50	0.21	0.22
Standard deviation	10.24	0.18	0.16
Coefficient of variation, %	186.0	85.6	72.5
Skew	7.51	0.83	1.11
Kurtosis	72.36	3.28	3.99

Graphical examination of the distributions of SSC and Q clearly illustrate that SSC is more variable: most SSC are low (< 25 mg l^{-1}) with a few very high (~100 mg l^{-1}) SSCs whereas the distribution of the sampled Q series is more continuous (Figure 8.18). The distribution of the 8 month Q series is smoother than that for the sampled Q series (Figure 8.18). In theory the distributions should be fairly similar due to the fixed-interval sampling. The difference could be due to seasonal differences in the Q regime:

the discharges associated with suspended sediment samples were taken from July to December and Q was quasi-continuously monitored from July to March.

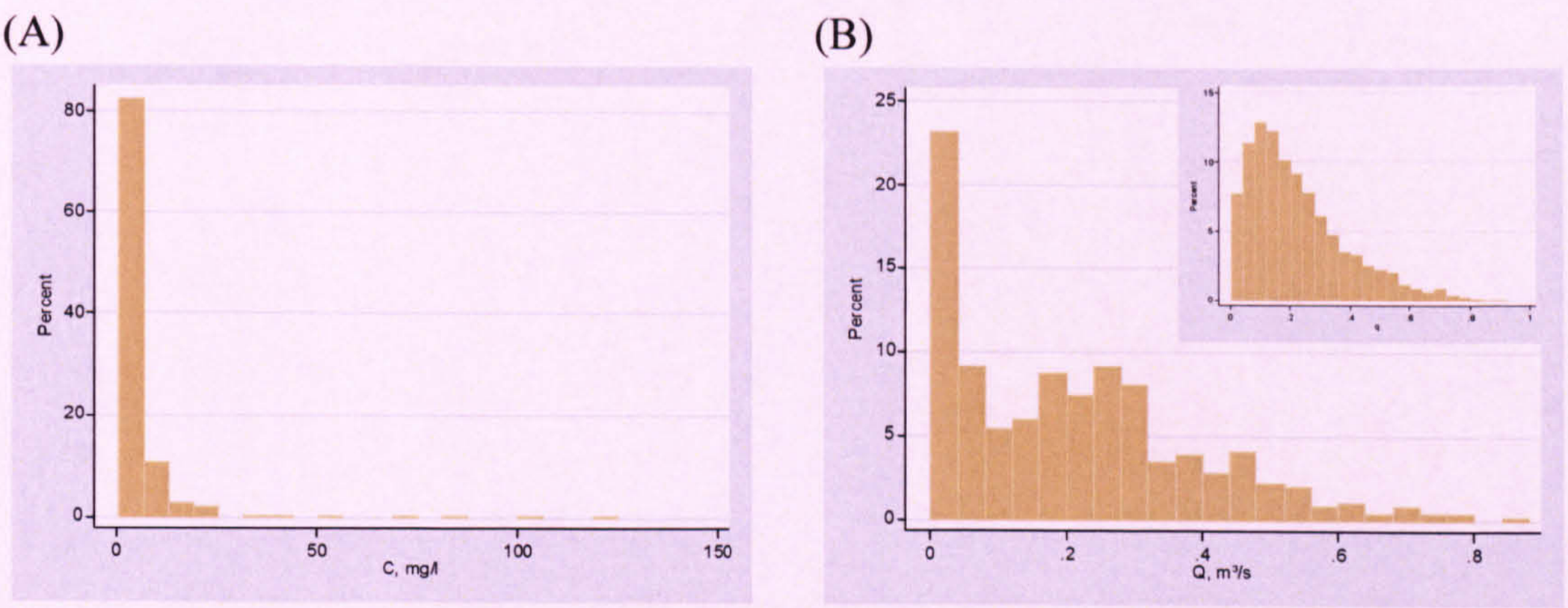

Figure 8.18. The distribution of (A) sampled SSC and (B) sampled Q with an inset of the distribution of the 8 month Q record for Langtae.

The boxplots of SSC by month show a seasonal signal in the variability in SSC (Figure 8.19). This is not an artefact of the number of sample taken in each month: 78 samples were taken in July, 84 in August, 113 in September, 114 in November and 69 in December. The magnitude and variability of Q increases from July to December (Figure 8.19). As only fixed-interval sampling was undertaken this is a genuine seasonal signal, not a result of the sampling regime.

In summary, a smaller percentage of samples were sampled on the rising limb than is representative of the 8 month Q series. Therefore, if sediment exhaustion is an influential factor in the catchment, sediment loads may be under-predicted. In terms of the Q range and distribution the sampled series is representative of the 8 month series. However, as no storm sampling was undertaken and there are very few high Q samples. Therefore, if the few samples that were taken are not representative, then errors could result. In addition the full annual range of SSC-Q relations may not have been captured as samples were only taken from July to December.

8.3.3.2 Basic rating curves

The R^2 values are very low for all of the models (Table 8.12), and are a result of a limited number of outliers (Figure 8.20). Examination of the R^2 values suggests that out of the ten basic models developed the linear regression model, gamma-log and Gaussian-log GLM models with ln Q as the explanatory variable are slightly superior (Table 8.12). In contrast, the RMSE suggests the linear regression model is the worst

(A)

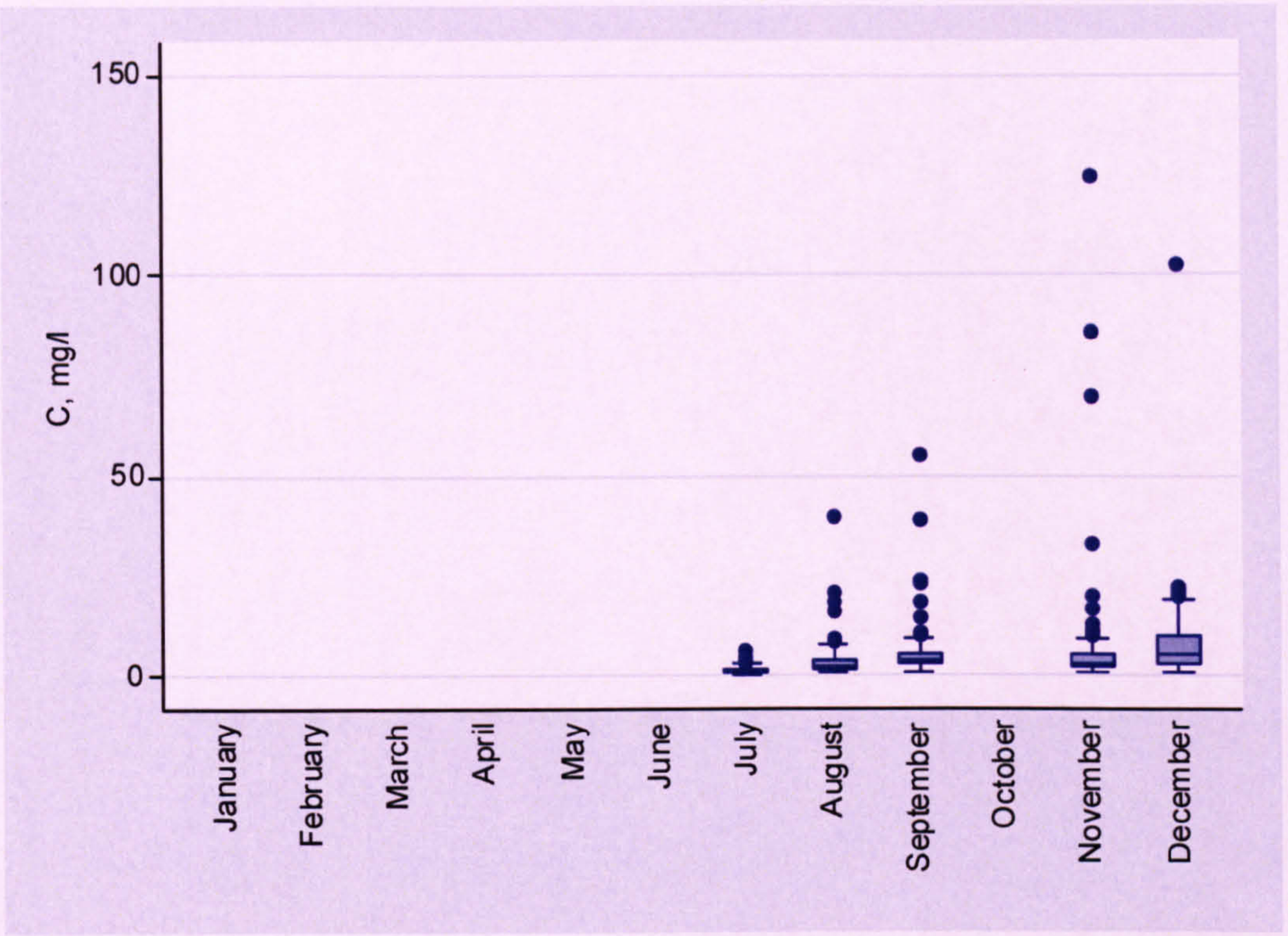

(B)

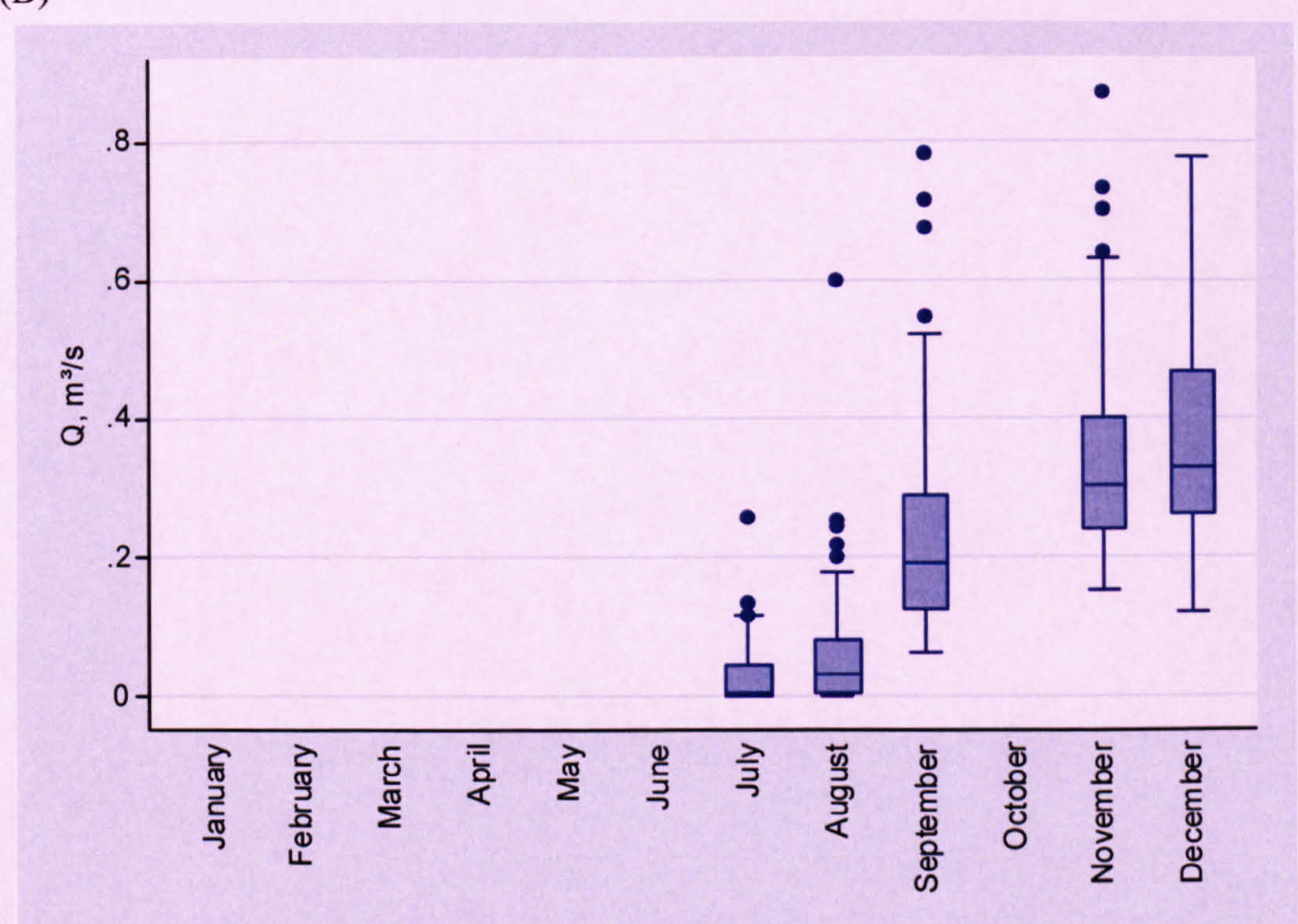

Figure 8.19. Boxplots illustrating the distribution of (A) SSC by month, and (B) Q by month for Langtae.

Table 8.12. Basic Langtae rating curve equations, associated R^2 and RMSE values and predicted 8 month loads. 8 month were calculated from 12th July 2000 to 20th March 2001. The R^2 and RMSE values for linear regression relate to C not ln C. UC = uncorrected, LNCF = corrected by the log-normal correction factor (1.29), SM = corrected by smearing (1.43), and BME = corrected by the Bradu-Mundlak estimator.

Model	Equation	R^2	RMSE	n	8 month load, t
Linear regression	$\ln C = 0.37 \ln Q + 2.07$	0.07	10.63	410	UC: 23.4 LNCF: 30.2 SM: 33.5 BME: 28.7
Gamma–identity, Q	$C = 17.72\,Q + 1.83$	0.10	9.71	458	35.9
Gamma–log, Q	$C = \exp(2.95\,Q + 0.94)$	0.13	9.59	458	37.4
Gaussian–log, Q	$C = \exp(2.97\,Q + 0.89)$	0.13	9.59	458	35.9
Gamma–identity, ln Q	Did not converge				
Gamma–log, ln Q	$C = \exp(0.39 \ln Q + 2.43)$	0.07	10.37	410	32.9
Gaussian–log, ln Q	$C = \exp(0.82 \ln Q + 2.96)$	0.08	10.30	410	35.7

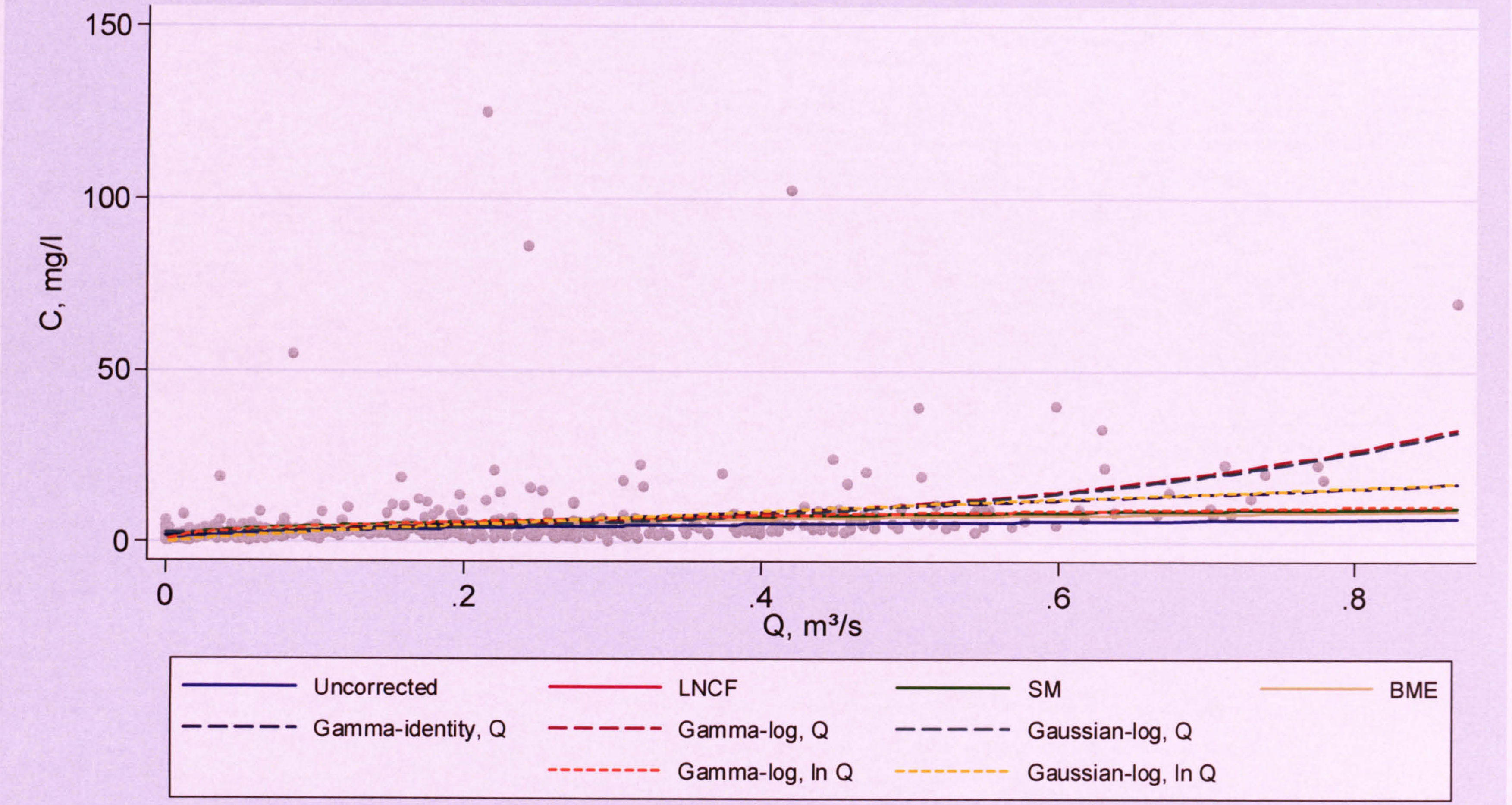

Figure 8.20. Comparison of the basic rating curves developed for Langtae.

and that the gamma-log and Gaussian-log models with Q as the explanatory variable are the best (Table 8.12). However, the difference in the highest and lowest RMSE is only 1.04 mg l^{-1}. Conversely, the diagnostic plots suggest that the linear regression model is preferred: the residuals are approximately homoscedastic and normally distributed, and there is no structure on the residual as a function of predicted and observed as a function of predicted plots. In comparison, the GLM diagnostic plots show non-normally distributed residuals with unequal variance but this is acceptable if a gamma distribution is assumed. There is evidence that the residuals generally decrease with an increase in the predicted SSC and some very large residuals at low values of predicted SSC.

As there is no storm data for Langtae no actual load estimates can be calculated as a reference for the predicted estimates.

Graphical analysis of the basic models indicates that the rating curves form three groups: (1) linear regression, including the various bias-corrected forms and the gamma-log GLM with ln Q as the explanatory variable; (2) gamma-identity with Q as the explanatory variable and Gaussian-log with ln Q as the explanatory variable; and (3) gamma-log and Gaussian-log, both with Q as the explanatory variable (Figure 8.20). From these plots it is evident that group (3) gives the highest load predictions due to the higher predicted SSC at the higher discharges. The group (2) models give similar loads and this can be attributed to the higher predictions of SSC at mid-ranges of Q. Group (1) models appear to under-predict at all ranges of Q (Figure 8.20).

On the basis of the higher R^2 and superior diagnostic plots linear regression is selected as the best model. The SM corrected version is chosen as although the residuals are approximately normally distributed and homoscedastic the difference in the correction factors is quite high (0.14).

8.3.3.3 Adapted rating curves

There is very little difference in the rating curve parameters for the rising and falling limb data: the gradient is 0.03 higher and the intercept 0.07 higher for the rising limb (Table 8.13). There is no clear distinction between the rising and falling limb data clouds (Figure 8.21), although the rising limb data appear slightly less variable, but this could reflect the difference in the number of rising and falling limb data points (Table 8.13). R^2 and RMSE indicate the models are similar and comparable with the all data

Table 8.13. Adapted linear regression rating curve equations for Langtae, associated R^2 and RMSE values, predicted 8 month loads. 8 month loads were calculated from 12th July 2000 to 20th March 2001. The R^2 and RMSE values for linear regression relate to ln C not C. None of the load estimates are corrected for back-transformation bias.

Model	Equation	R^2	RMSE	N	8 month load, t
All data	$\ln C = 0.37 \ln Q + 2.07$	0.28	0.71	410	23.4
Limb:					
Rising	$\ln C = 0.38 \ln Q + 2.22$	0.28	0.74	78	22.8
Falling	$\ln C = 0.35 \ln Q + 1.95$	0.27	0.70	332	
Season (4):					
Spring					
Summer	$\ln C = 0.34 \ln Q + 1.97$	0.26	0.71	114	22.1
Autumn	$\ln C = 0.46 \ln Q + 2.08$	0.13	0.68	227	
Winter	$\ln C = 0.46 \ln Q + 2.26$	0.05	0.81	69	
Split–year:					
Summer	$\ln C = 0.40 \ln Q + 2.16$	0.39	0.64	227	21.8
Winter	$\ln C = 0.74 \ln Q + 2.35$	0.13	0.77	183	
Limb & split–year:					
Summer – rising	$\ln C = 0.44 \ln Q + 2.54$	0.46	0.72	33	
Summer – falling	$\ln C = 0.38 \ln Q + 2.07$	0.38	0.62	194	22.0
Winter – rising	$\ln C = 0.74 \ln Q + 2.46$	0.17	0.72	45	
Winter – falling	$\ln C = 0.70 \ln Q + 2.27$	0.10	0.79	133	
Lag	No storm samples from which to determine the best lag				
ΔQ	$\ln C = 0.37 \ln Q + 5.68\, \Delta Q + 2.02$	0.28	0.71	410	22.4
Time of year	$\ln C = 0.38 \ln Q - 0.16 \sin [2\pi \text{FOY}] - 0.06 \cos [2\pi \text{FOY}] + 1.95$	0.28	0.71	410	21.1
***Q* class**	$\ln C = 0.41 \ln Q + 2.25$	0.76	0.41	19	26.8

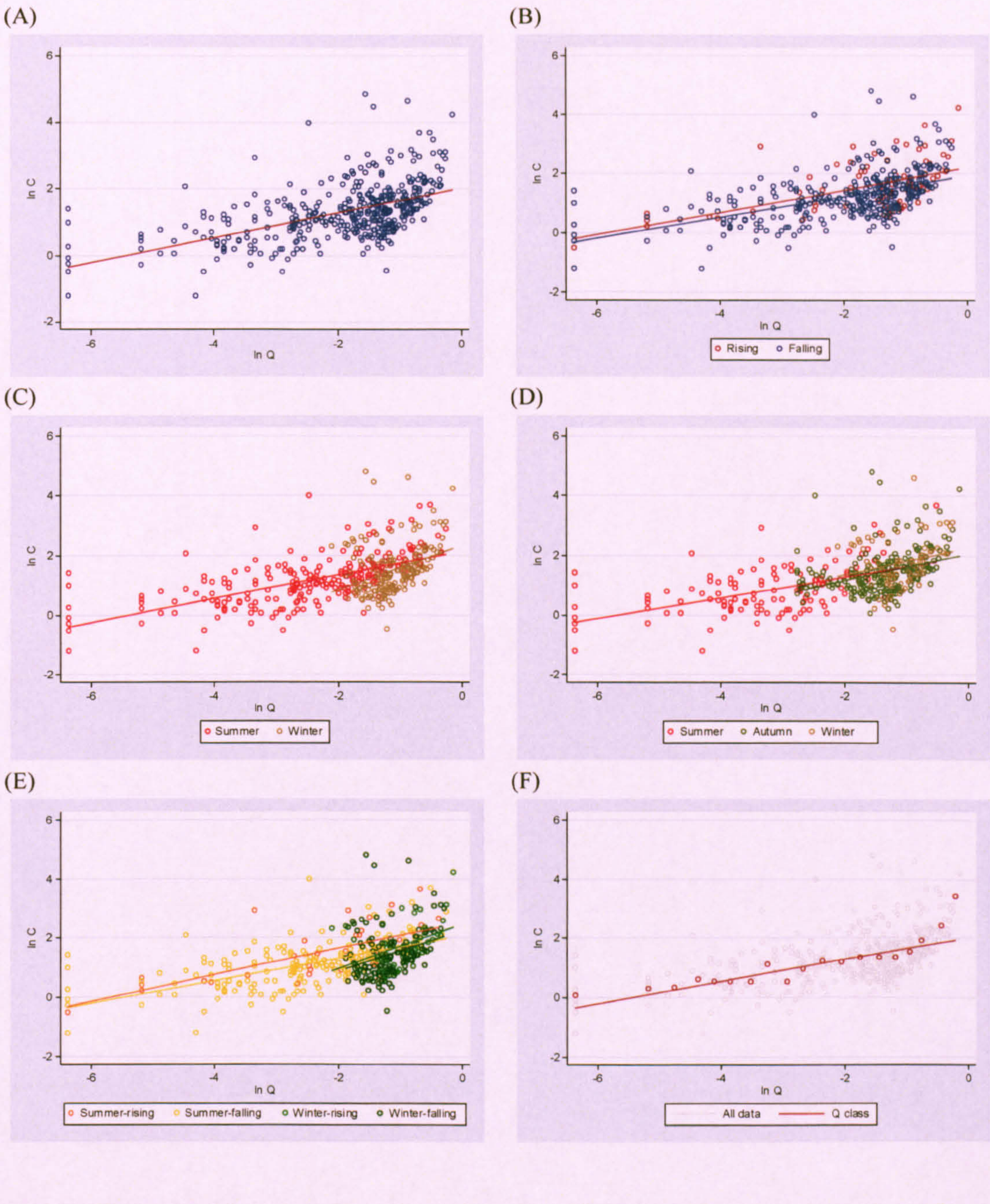

Figure 8.21. Linear regression models for Langtae. (A) All data; (B) data divided into rising and falling limb; (C) data divided into summer and winter; (D) data divided into spring, summer, autumn and winter; (E) data divided into summer-rising, summer-falling, winter-rising, winter-falling; and (F) *Q* class method.

model in terms of their fit. The similarity in the rising and falling limb models is affirmed by only a 0.6 t improvement on the load estimate obtained by the all data model (Table 8.13).

With reference to the four season models, the data clouds are indistinct, except there are no autumn or winter data points at values of ln Q less than –3.0 (Figure 8.21). There is no spring model, as no samples were collected during the spring. The forms of the rating curves for autumn and winter are almost identical (Table 8.13) and the data clouds are inseparable (Figure 8.21). In comparison, the rating curve for summer has a gentler gradient and a slightly lower intercept (Table 8.13). This suggests that for a given change in ln Q there is a greater change in ln C in the summer than in the autumn or winter. The fit of the summer rating curve is best in terms of R^2 and intermediate in terms of RMSE (Table 8.13). The winter rating curve is the worst fit in terms of R^2 and RMSE (Table 8.13).

With reference to the split-year model there is a substantial difference in the gradient of the summer and winter curves: the winter curve is almost twice as steep (Table 8.13 & Figure 8.21). This suggests SSC increases by a greater amount in winter than in summer for a given increase in Q. The model fit is notably worse for the winter curve compared with the summer and all data curves (Table 8.13).

The rating curves derived from the data sub-sets defined by split-year and limb reflect the patterns in the split-year model: summer-rising and summer-falling are very similar to each other and the split-year summer curve (Table 8.13 & Figure 8.21). Similarly, the winter-rising and winter-falling curves resemble the split-year winter curve (Table 8.13 & Figure 8.21). This is explained by the similarity in the rising and falling limb curves (Figure 8.21).

The model with change in Q as an additional explanatory variable has the same R^2 and RMSE as the basic linear regression model based on all data (Table 8.13). Therefore, no more of the variation in ln C is explained. The same is true for the model with sine and cosine variables incorporated as extra explanatory variables (Table 8.13). The Q class model has a considerably higher R^2 and lower RMSE than any of the other adapted models. The R^2 suggests that 76% of the variation in ln C is explained by ln Q. The

substantially improved fit suggests that unequal numbers of data points throughout the range of Q bias the model form.

The worth of lagging the data was assessed by comparing the storm period load estimates with the actual storm period loads at the other sites. As no storm sampling was undertaken at Langtae the worth of lagging can not be assessed. R^2 and RMSE are not appropriate measures as they have indicated models with less accurate storm period load estimates are superior and the diagnostic plots for the lagged models are indistinguishable.

All the load estimates, with the exception of the Q class model, give lower predictions than the basic linear regression developed from all data (Table 8.13). Statistical and graphical measures of fit are the only criteria in this case as there are no storm data from which load estimate can be calculated. The form of the basic regression curves in comparison with the actual data (Figure 8.20), suggests that the actual load is likely to be higher. Also the Q class model results in a higher load estimate and has higher R^2 and lower RMSE values.

8.3.4 Rough Sike

8.3.4.1 Data characteristics and distributions

Fourteen storms, the majority of which comprised 48 samples, were sampled at Rough Sike (Table 8.14). The storm samples were taken throughout the year (Table 8.14). No fixed-interval sampling was undertaken.

Approximately two thirds of the samples were taken on the falling limb, which is very similar to the proportions of rising and falling limb recordings in the annual record (Table 8.15). Only one third of the annual Q range was sampled (Table 8.15 & Figure 8.9), but the mean Q of the sampled period was higher than that of the annual record (Table 8.15). The coefficient of variation indicates that the sample SSC series is more variable than the sampled Q series (Table 8.15). The annual Q series is more variable than either of the sampled series (Table 8.15) and this suggests that the annual SSC series is even more variable. The skew and kurtosis values indicated that the sampled SSC series is more skewed and tail weighted that the sampled Q series (Table 8.15). The annual Q series is more skewed and tail weighted (Table 8.15) and therefore the annual SSC series is potentially even more skewed and tail weighted.

Table 8.14. Type, number and dates of samples taken in the Rough Sike catchment.

Sample type	Number	Details
Fixed-interval	0	
Storm		
Total:	522	
Per storm:	48	29th August 1997
	48	16th October 1997
	34	10th November 1997
	48	16th November 1997
	35	19th November 1997
	48	23rd December 1997
	37	6th February 1998
	48	11th February 1998
	48	26th March 1998
	48	5th May 1998
	48	2nd June 1998
	32	24th June 1998

Table 8.15. Summary statistics of the sampled SSC (mg l^{-1}) and Q (m^3 s^{-1}) series and the annual Q series for Rough Sike.

Measure	SSC sampled period SSC	SSC sampled period Q	Annual record Q
Number of samples:			
Total	522		26,718
Rising	177		10,119
Falling	345		16,599
Range	0.6 - 126.0	0.01 - 0.67	0.00 - 1.87
Mean	12.0	0.17	0.06
Standard deviation	12.14	0.12	0.13
Coefficient of variation, %	101.0	69.9	209.7
Skew	3.10	1.26	4.82
Kurtosis	20.08	5.34	37.98

Graphical examination of the distribution of the sampled SSC and Q series shows the distributions are quite different: SSC is more skewed and peaked (Figure 8.22). The distributions of the sampled and annual Q series are quite different and the biasing of sampling towards higher discharges is clearly evident (Figure 8.22).

The boxplots of SSC and Q by storm show that there are more outliers in the SSC series (Figure 8.23). Although not a strong trend, storms with a more variable Q series generally exhibit a more variable SSC series (Figure 8.23). The monthly boxplots of SSC and Q illustrate that although no samples were taken in January, April, July or September samples were collected throughout the year (Figure 8.23). Once again there are more outliers in the SSC boxplots than Q boxplots (Figure 8.23). A seasonal signal

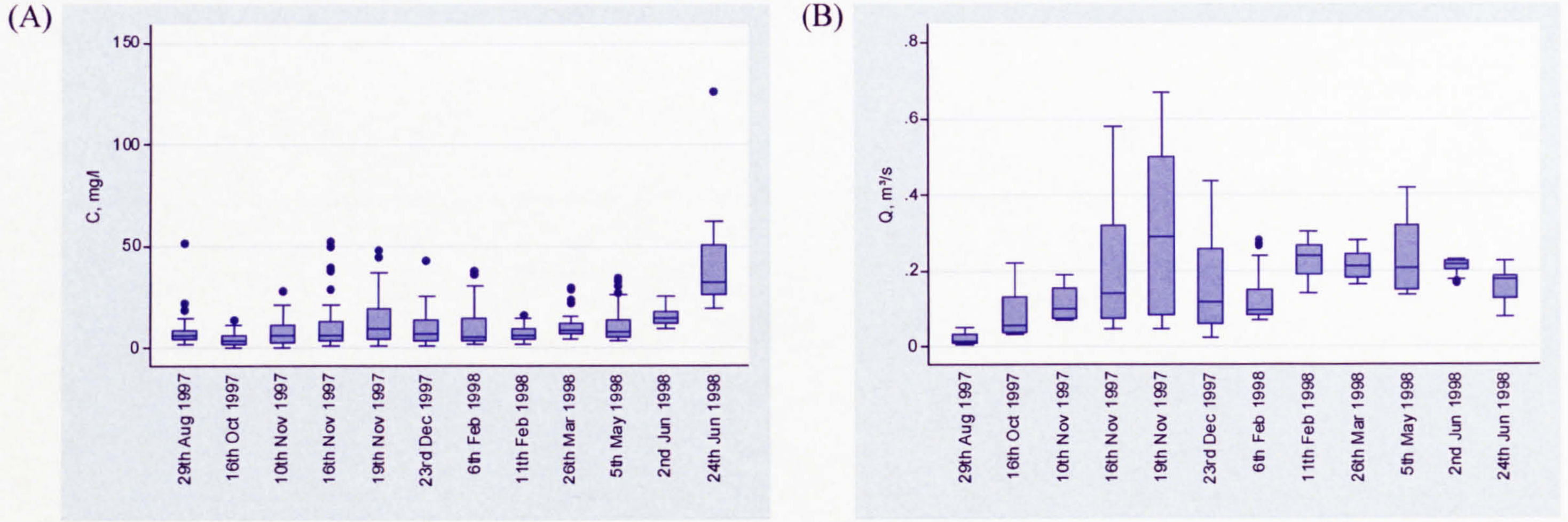

Figure 8.23. Boxplots illustrating the distribution of (A) SSC by storm, (B) Q by storm, (C) SSC by month, and (D) Q by month for Rough Sike.

is evident in the Q boxplots: peak in May, trough in August and rising again (Figure 8.23). However, as only storm sampling was undertaken this may reflect the sampling regime, i.e. the height at which the level switch was set, rather than a trend in the Q regime.

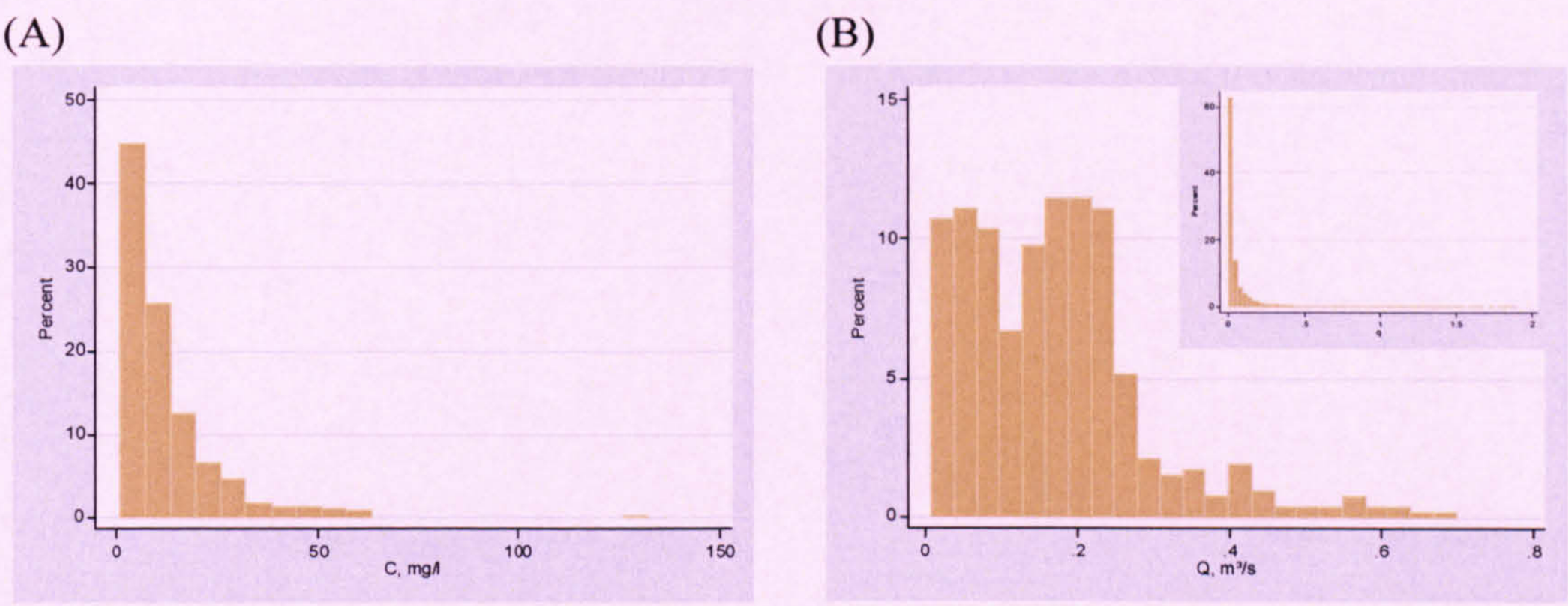

Figure 8.22. Distributions of (A) the sampled SSC, (B) sampled Q series with an inset of the distribution of the population Q series for Rough Sike.

In summary, the sampled series is representative of the annual series with regard to the percentage of samples taken on the rising and falling limb. However, only one third of the annual Q range was sampled and therefore extrapolation of the rating curves may result in errors. The distributions of sampled and annual Q series are also very different. Samples were taken throughout the year, so the full range of SSC-Q relations should have been captured, although there are limited baseflow samples given the storm sampling.

8.3.4.2 Basic rating curves

All of the models are very similar in terms of R^2 and RMSE (Table 8.16) and therefore it is not possible to select any which are markedly better than any of the others on this basis. The residual plots of the linear regression model indicate a fairly good fit: residuals are approximately normally distributed with equal variance; there is no structure in the residual as a function of predicted and observed as a function of predicted plots, except a tendency to under-predict at very low values of ln Q; and the quantile plots are gently sloping with slight tails. In comparison the diagnostic plots of the GLM models indicate a poorer model fit: residuals are non-normally distributed with unequal variance, structure is present in the residuals versus predicted and observed versus predicted plots, and the quantile plots have a steeper gradient and have

Table 8.16. Basic Rough Sike rating curve equations, associated R^2 and RMSE values, predicted annual loads, monitored period predicted loads and percentage difference between actual and predicted load for the monitored period. Annual loads were calculated from 1st August 1997 to 31st July 1998. The R^2 and RMSE values for linear regression relate to C not ln C. UC = uncorrected, LNCF = corrected by the log-normal correction factor (1.34), SM = corrected by smearing (1.35), and BME = corrected by the Bradu-Mundlak estimator.

Model	Equation	R^2	RMSE	n	Annual load, t	Monitored period Load, t	Monitored period % difference
Linear regression	$\ln C = 0.46 \ln Q + 3.06$	0.15	11.73	522			
UC:					17.4	0.81	–24.5
LNCF:					23.2	1.08	0.8
SM:					23.5	1.09	2.1
BME:					21.3	1.08	0.7
Gamma–identity, Q	$C = 43.13 Q + 4.67$	0.16	11.17	522	28.8	1.16	8.0
Gamma–log, Q	$C = \exp(3.39 Q + 1.83)$	0.12	11.74	522	96.5	1.26	17.7
Gaussian–log, Q	$C = \exp(2.29 Q + 2.06)$	0.14	11.30	522	40.3	1.11	4.0
Gamma–identity, ln Q	$C = 3.02 \ln Q + 18.01$	0.13	11.48	522	20.0	0.99	–7.7
Gamma–log, ln Q	$C = \exp(0.41 \ln Q + 3.27)$	0.15	11.24	522	22.7	1.06	–1.0
Gaussian–log, ln Q	$C = \exp(0.57 \ln Q + 3.55)$	0.16	11.16	522	25.1	1.13	5.4
					Actual:	**1.07**	

large tails in the upper fraction of the data. However, unequal variance and non-normal distribution of residuals is acceptable if a gamma distribution is assumed.

Examination of the form of the rating curve produced by each model shows that all models except the gamma-log GLM with Q as an explanatory variable are similar within the range of sampled Q (Figure 8.24). The rate of increase in SSC for a given increase in Q is much greater for the gamma-log with Q as the explanatory variable model (Figure 8.24). As a result the load estimates from Q above 0.4 $m^3 s^{-1}$ will become progressively larger than those predicted by the other models. The Gaussian-log model with Q as the explanatory variable also exhibits this behaviour, although to a lesser degree, and only starts to deviate from the other model forms at approximately 0.6 $m^3 s^{-1}$ (Figure 8.24).

The observed and predicted loads of the sampled storm period are very similar: the lowest estimate is 0.81 t and the highest estimate is 1.26 t (Table 8.16). The most accurate load estimation was obtained by the linear regression model corrected for back-transformation bias by the BME (Table 8.16), although the linear regression model corrected for bias using the LNCF and the gamma-log GLM with ln Q as the explanatory variable give very similar load estimates (Table 8.16). The largest error is associated with the uncorrected linear regression model and the second largest error with the gamma-log GLM with Q as the explanatory variable (Table 8.16). The gamma-log GLM with Q as the explanatory variable gives an over-prediction (Table 8.16) which is the result of the steep rise of the rating curve (Figure 8.24).

Linear regression bias-corrected using the LNCF is selected as the best model on the basis that the R^2 and RMSE are similar for all models, the diagnostic plots are superior for the linear regression model, this model gives the second most accurate storm period load estimate, and visually the rating curve fits the data well. LNCF was selected over SM as there was only a 0.01 difference and the diagnostic plots indicated that the residuals were approximately normally distributed with equal variance.

8.3.4.3 Adapted rating curves

There is not a distinct difference in the form of the rising and falling limb data clouds except with one exception, rising limb samples were not taken at ln Q of less than –3.2 (Figure 8.25), but this could be an artefact of the sampling regime. However, the rating

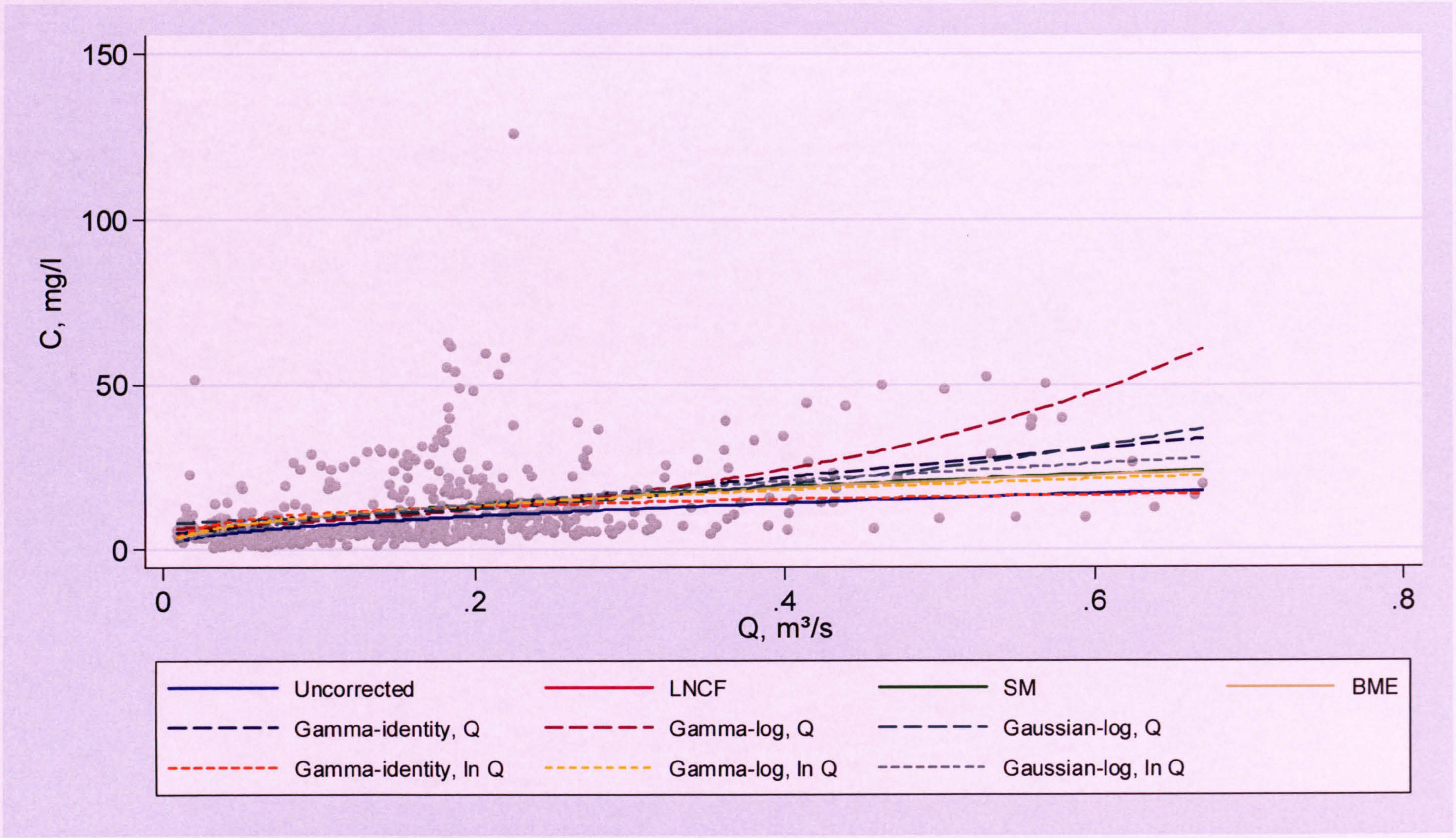

Figure 8.24. Comparison of the basic rating curves developed for Rough Sike.

(A)

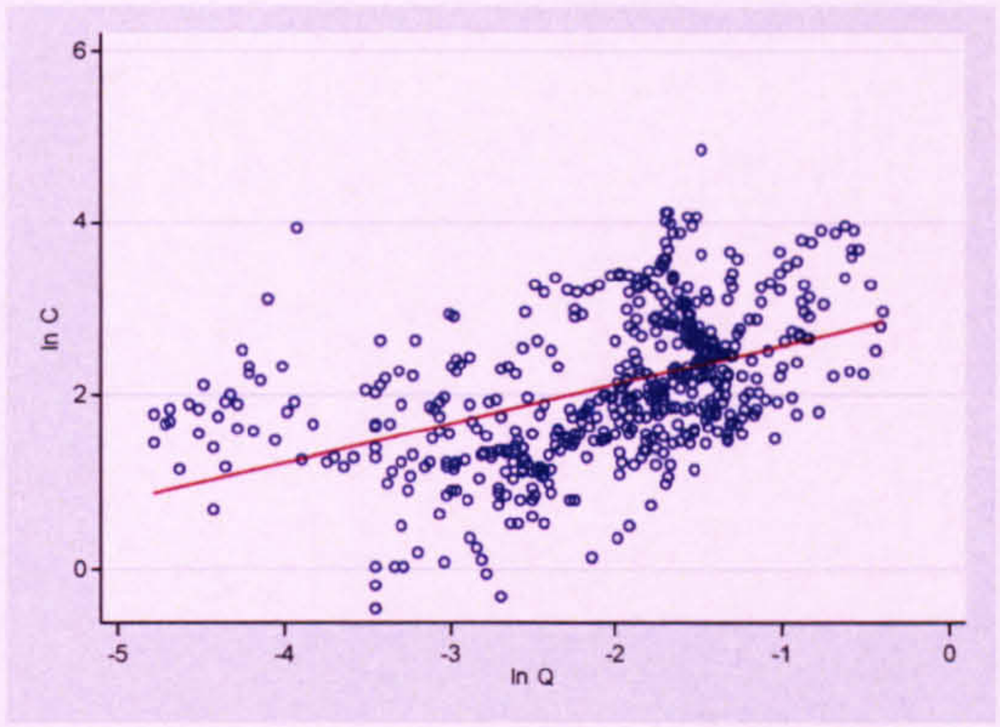

(B)

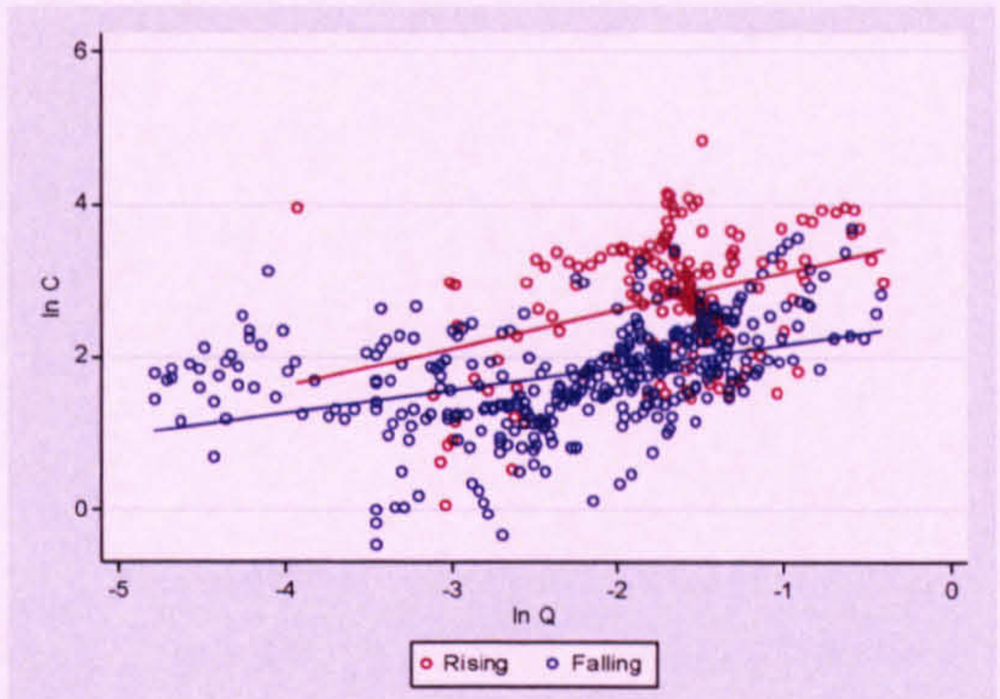

(C)

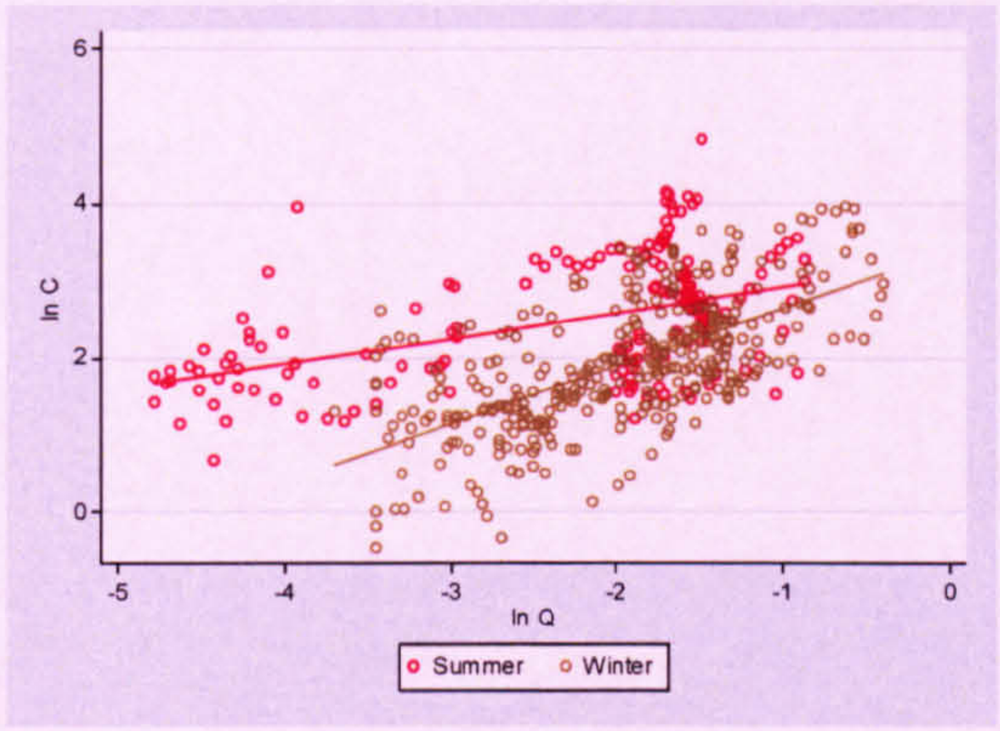

(D)

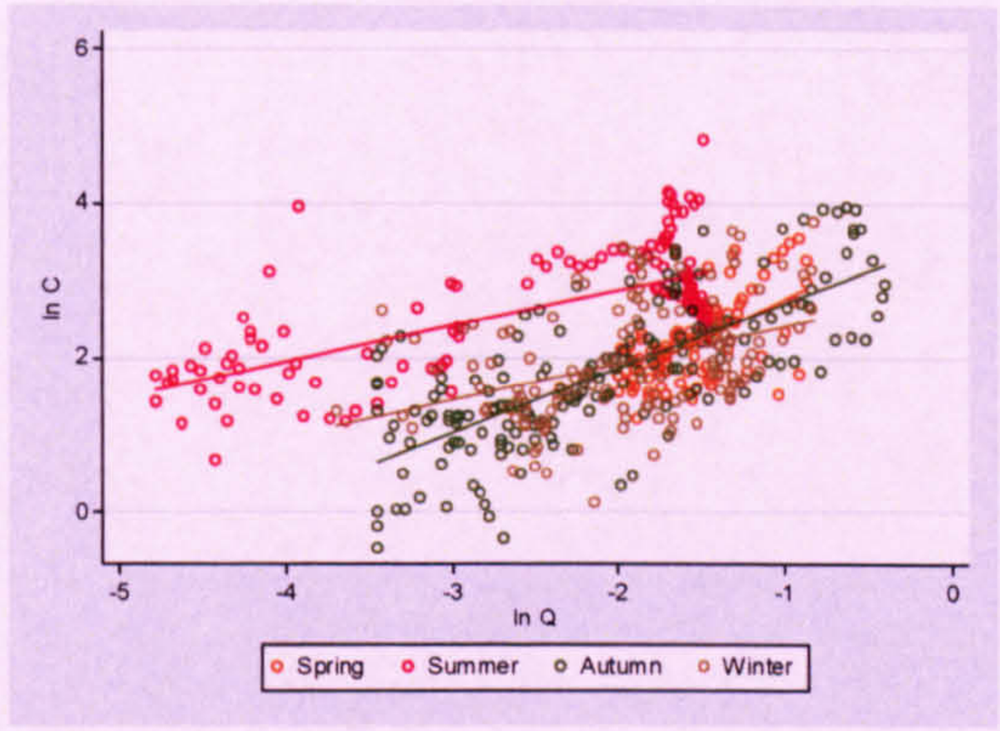

(E)

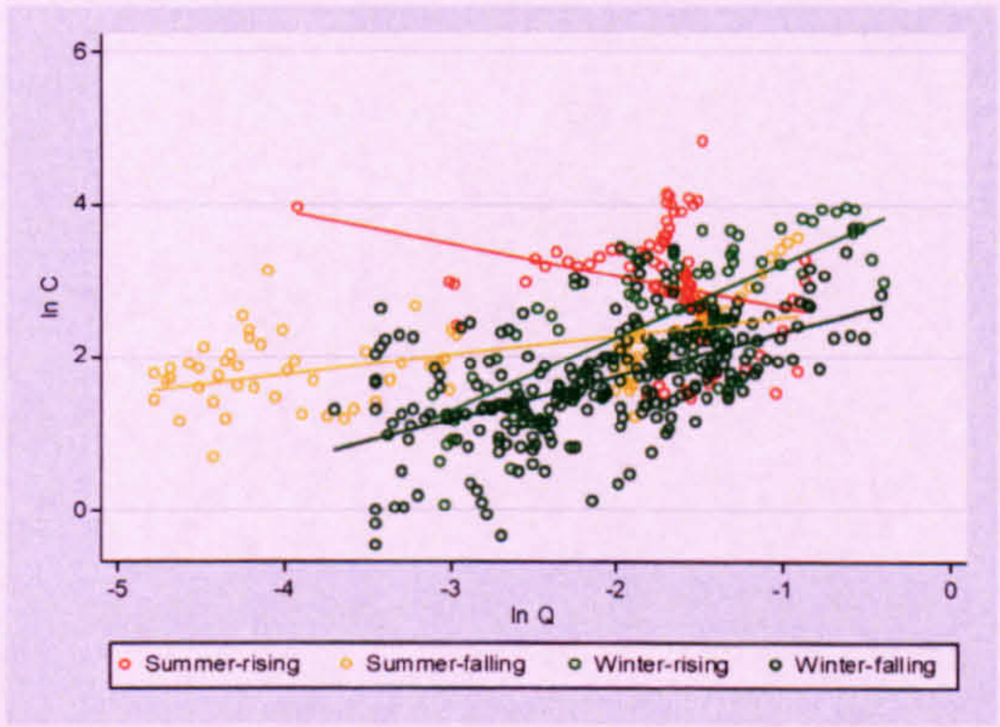

(F)

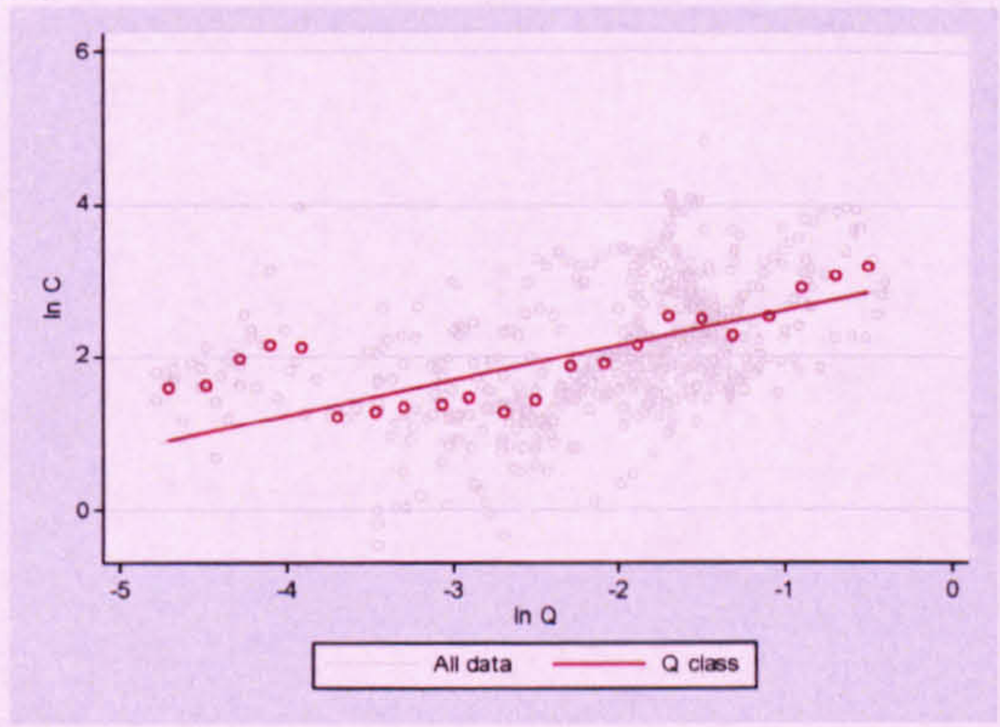

Figure 8.25. Linear regression models for Rough Sike. (A) All data; (B) data divided into rising and falling limb; (C) data divided into summer and winter; (D) data divided into spring, summer, autumn and winter; (E) data divided into summer-rising, summer-falling, winter-rising, winter-falling; and (F) *Q* class method.

curves developed from the rising and falling limb data sub-sets differ with respect to the gradient and intercept: the rising limb curve is steeper, indicating a greater increase in SSC for a given increase in ln Q compared with the falling limb, and has a higher intercept (Figure 8.25 & Table 8.17). According to R^2 the rising and falling limb models are a poorer fit than the model developed from all data (Table 8.17). RMSE suggests that the falling limb model is a slightly better fit than the rising and all data models (Table 8.17). Despite the lower R^2, the rising and falling limb models produce a load estimate which is 5% more accurate than that obtained from the all data model (Table 8.17).

There is a marked difference in the data cloud distributions of the split-year models and this is reflected in the form of the rating curves (Figure 8.25 & Table 8.17). The winter rating curve is much steeper: 0.74 in comparison with 0.33 (Table 8.17). This suggests that during the winter there is a greater increase in ln C for a given increase in ln Q. The summer and winter models are considered better fits, in terms of R^2 and RMSE, compared with the rating curve developed from all data (Table 8.17). The load estimate derived from the summer and winter rating curves is 7.3% more accurate (Table 8.17).

In the season model the summer data cloud is distinct from the spring, autumn and winter data clouds: it is elevated (Figure 8.25). There are no distinct differences in the spring, autumn and winter clouds except in their extent (Figure 8.25). The rating curves developed from the spring, summer, autumn and winter data sub-sets are superior, in terms of R^2 and RMSE, compared with the rating curve developed from all data with the exception of the winter curve which has a lower R^2. The gradients of the summer and winter regressions are very similar, but the intercepts are different: the summer curve has a higher intercept (Figure 8.25 & Table 8.17). The spring curve is the steepest and therefore suggests that there is a greater increase in ln C for a given increase in ln Q in the spring than any other season (Figure 8.25 & Table 8.17). The gradient of the autumn curve is between that of the spring and summer/winter (Figure 8.25 & Table 8.17). The intercepts of the spring, summer and autumn curves are very similar and greater than that of the winter curve which suggests there is less sediment available for transport at any given ln Q during the winter (Figure 8.25 & Table 8.17). The load estimate derived from the four season regression models gives a sampled period load estimate which is 3.4% more accurate than that calculated from the all data model (Table 8.17).

Table 8.17. Adapted linear regression rating curve equations for Rough Sike, associated R^2 and RMSE values, predicted annual loads, monitored period predicted loads and percentage difference between actual and predicted load for the monitored period. Annual loads were calculated from 1st August 1997 to 31st July 1998. The R^2 and RMSE values for linear regression relate to ln C not C. None of the load estimates are corrected for back-transformation bias.

Model	Equation	R^2	RMSE	n	Annual load, t	Monitored period Load, t	Monitored period % difference
All data	$\ln C = 0.46 \ln Q + 3.06$	0.22	0.76	522	17.4	0.81	–24.5
Limb:							
Rising	$\ln C = 0.49 \ln Q + 3.59$	0.13	0.76	177	18.3	0.87	–19.1
Falling	$\ln C = 0.30 \ln Q + 2.45$	0.17	0.63	345			
Season (4):							
Spring	$\ln C = 1.05 \ln Q + 3.83$	0.36	0.42	96			
Summer	$\ln C = 0.46 \ln Q + 3.79$	0.47	0.58	128	20.4	0.85	–21.1
Autumn	$\ln C = 0.83 \ln Q + 3.54$	0.54	0.65	165			
Winter	$\ln C = 0.48 \ln Q + 2.90$	0.16	0.69	133			
Split–year:							
Summer	$\ln C = 0.33 \ln Q + 3.25$	0.23	0.68	176	20.7	0.88	–18.2
Winter	$\ln C = 0.74 \ln Q + 3.37$	0.41	0.64	346			
Limb & split–year:							
Summer – rising	$\ln C = -0.42 \ln Q + 2.21$	0.08	0.66	93			
Summer – falling	$\ln C = 0.25 \ln Q + 2.77$	0.33	0.46	83	23.4	0.93	–12.9
Winter – rising	$\ln C = 0.96 \ln Q + 4.20$	0.54	0.61	84			
Winter – falling	$\ln C = 0.57 \ln Q + 2.87$	0.33	0.57	262			
Lag	Lag did not improve load estimate						
ΔQ	$\ln C = 0.43 \ln Q + 2.7 \Delta Q + 2.99$	0.29	0.73	522	17.3	0.86	–19.3
Time of year	$\ln C = 0.55 \ln Q - 0.15 \sin [2 \pi \text{FOY}] - 0.53 \cos [2 \pi \text{FOY}] + 3.34$	0.38	0.68	522	18.6	0.83	–22.4
***Q* class**	$\ln C = 0.34 \ln Q + 2.87$	0.52	0.43	22	16.6	0.79	–26.3
					Actual:	**1.07**	

There is no clear distinction in the data clouds as defined split-year and limb (Figure 8.25), although the regression equations are different (Table 8.17). The summer-rising regression has a negative gradient (Figure 8.25 & Table 8.17) which indicates that ln C decreases as ln Q increases. On closer inspection (Figure 8.25) it looks as though one data point (–3.8, 3.9) levers the rating curve to a negative gradient but even with this point removed the regression line remains in almost exactly the same place (Figure 8.26). If the data is colour-coded by storm event the reason for the negative gradient is identified (Figure 8.27): it is a result of increased sediment supplies as summer progresses. At the beginning of the summer it is likely that sediment sources would have been depleted given the higher baseflows and increased storm events during the winter. Then, during summer, sediment supplies build up as baseflow falls and storm events are less frequent.

The winter-rising rating curve is the steepest which indicates that ln C increases more for a given increase in ln Q on the rising limb during the winter (Figure 8.25 & Table 8.17). The intercept of the winter-rising limb curve is also the greatest which suggests that there is generally more sediment available for transport under these conditions (Figure 8.25 & Table 8.17). In terms of R^2 and RMSE, the regressions as defined by split-year and limb are superior to that developed from all data (Table 8.17), with the exception of the R^2 of the summer-rising curve (Table 8.17). The sampled period load estimate is the most accurate out of all the adapted models and more accurate than the all data model estimate: it gives a 13% under-estimation (Table 8.17).

A lagged model was not developed as the monitored period load estimates indicated that a zero lag model was the most appropriate. Adding change in Q as an additional explanatory variable results in a slight improvement in R^2 and RMSE and a 5.2% increase in the accuracy of the sample period load estimate compared with the all data model (Table 8.17). Adding sine and cosine variables as extra explanatory variables improved the fit of the model: R^2 increased to 0.38 and RMSE decreased to 0.68 (Table 8.17). However, the effect on sampled period load estimate was minimal: accuracy increased by just 2% (Table 8.17). The best model fit, in terms of R^2 and RMSE, was obtained by the Q class method. The RMSE was only 0.43 and ln Q explained 52% of the variance in ln C as indicated by R^2 (Table 8.17). However, the resulting regression equation is very similar to that derived from all data (Figure 8.25 & Table 8.17) and the sampled period load estimate is less accurate (Table 8.17).

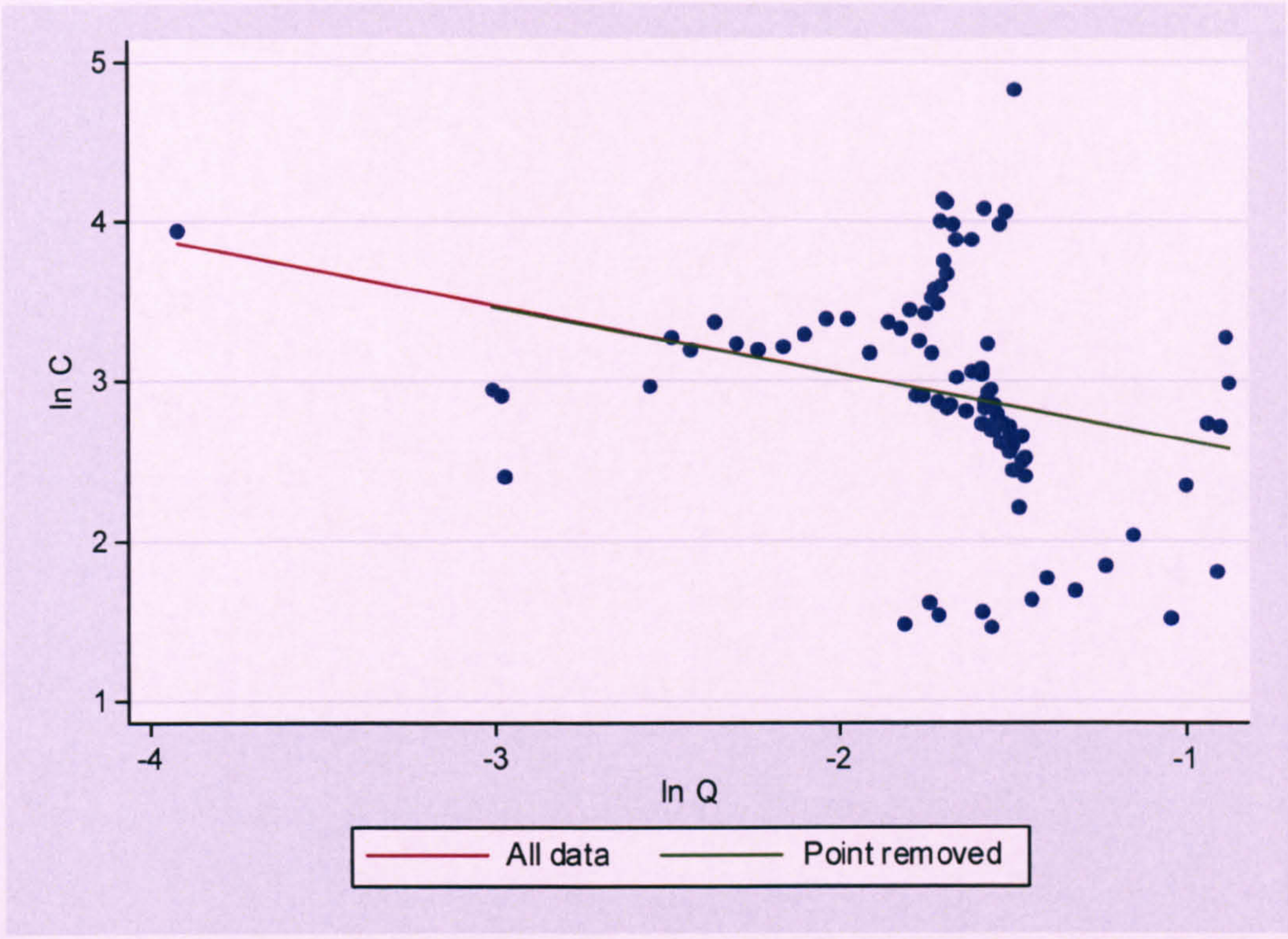

Figure 8.26. Comparison of summer-rising rating curve for Rough Sike with all data and with an obvious outlier removed.

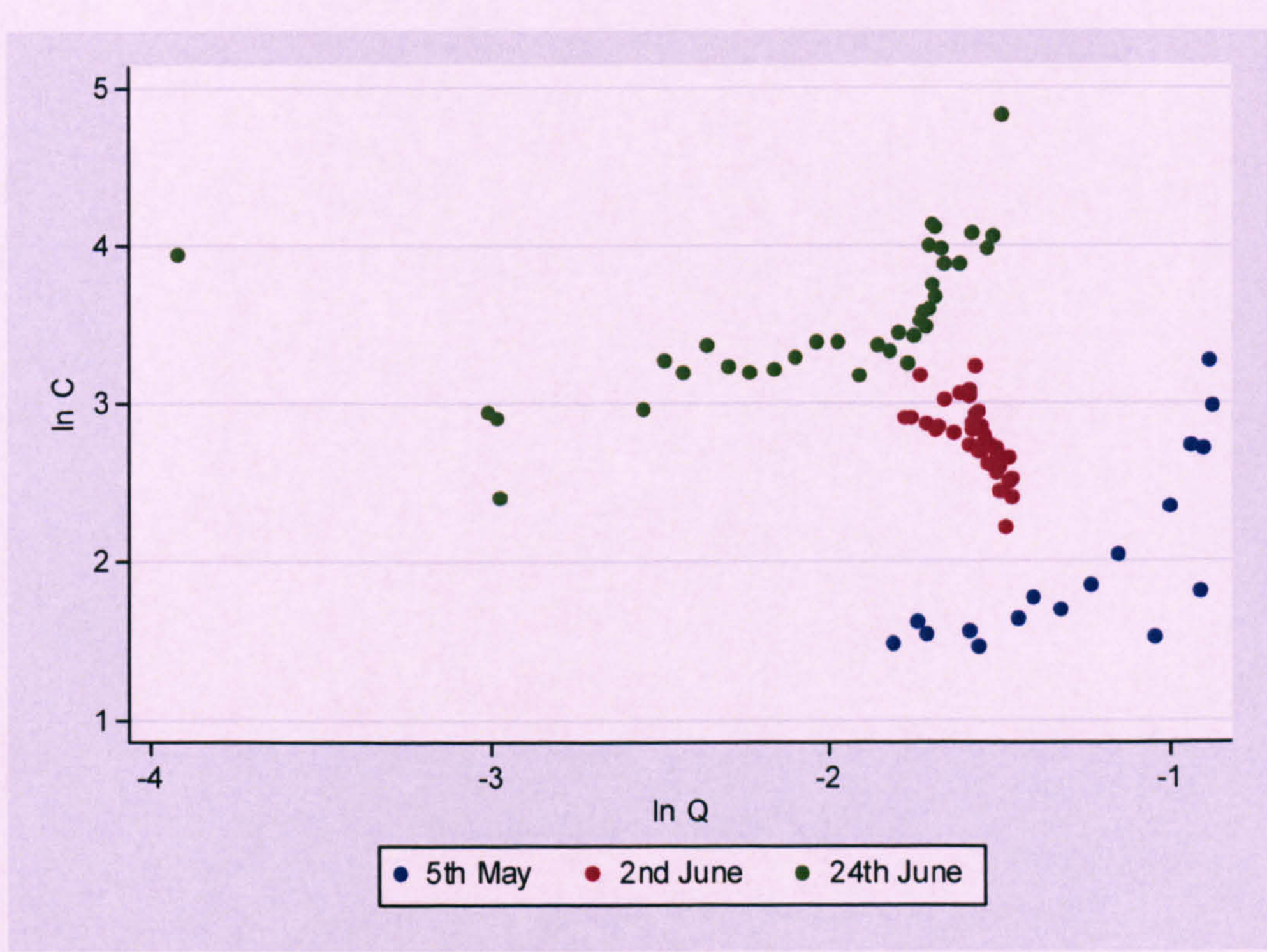

Figure 8.27. Comparison of summer-rising data points for Rough Sike colour-coded by storm event.

In summary, only the load estimate calculated from the models developed from data sub-sets as defined by limb and split-year produce a noteworthy improvement over the model developed from all data. The RMSE of the adapted models are equal to or less than the RMSE of the all data model and R^2 are higher for eleven out of the fifteen models.

8.3.5 Swinhope

It was not possible to calculate annual load estimates for Swinhope given the calibration problem with the stage-Q relationship at higher Q values. However, it was possible to calculate sampled period storm estimates.

8.3.5.1 Data characteristics and distributions

Fifteen storms were sampled at Swinhope and no fixed-interval samples were taken (Table 8.18). Storms were sampled over a two year period and throughout the year (Table 8.18).

Table 8.18. Type, number and dates of samples taken in the Swinhope catchment.

Sample type	Number	Details
Fixed-interval	0	
Storm		
Total:	572	
Per storm:	46	29th April 2002
	46	5th July 2002
	45	30th July 2002
	48	12th October 2002
	40	2nd November 2002
	45	8th November 2002
	13	14th November 2002
	48	1st March 2003
	48	1st April 2003
	12	1st May 2003
	29	9th October 2003
	48	19th November 2003
	48	20th December 2003
	42	6th January 2004
	14	29th March 2004

Approximately one third of the samples were taken on the rising limb and two thirds on the falling limb (Table 8.19). This is comparable to the proportion of rising and falling limb samples over the monitoring period: 28% and 72% respectively (the stage record can be used to define the number of rising and falling limb recordings). A wide range of

SSC were recorded and Q up to 4.5 m^3 s^{-1}, the approximate bankfull Q (Warburton, pers comm.). The distribution of the SSC series is more variable, more skewed and tail weighted than that of the Q series (Table 8.19). As the annual Q record is not available due to calibration problems no comparison can be made between the distribution of sampled and annual Q series.

Table 8.19. Summary statistics of sampled SSC (mg l^{-1}) and Q (m^3 s^{-1}) series at Swinhope.

Measure	SSC sampled period	
	SSC	Q
Number of samples:		
Total	572	
Rising	195	
Falling	377	
Range	0 - 393.7	0.04 - 4.09
Mean	30.3	0.42
Standard deviation	52.5	0.51
Coefficient of variation, %	169.8	123.3
Skew	3.34	3.16
Kurtosis	16.47	15.53

Graphical analysis of the distributions of sampled SSC and Q illustrates that the form of the two series are broadly similar, although SSC is more skewed and peaked (Figure 8.28).

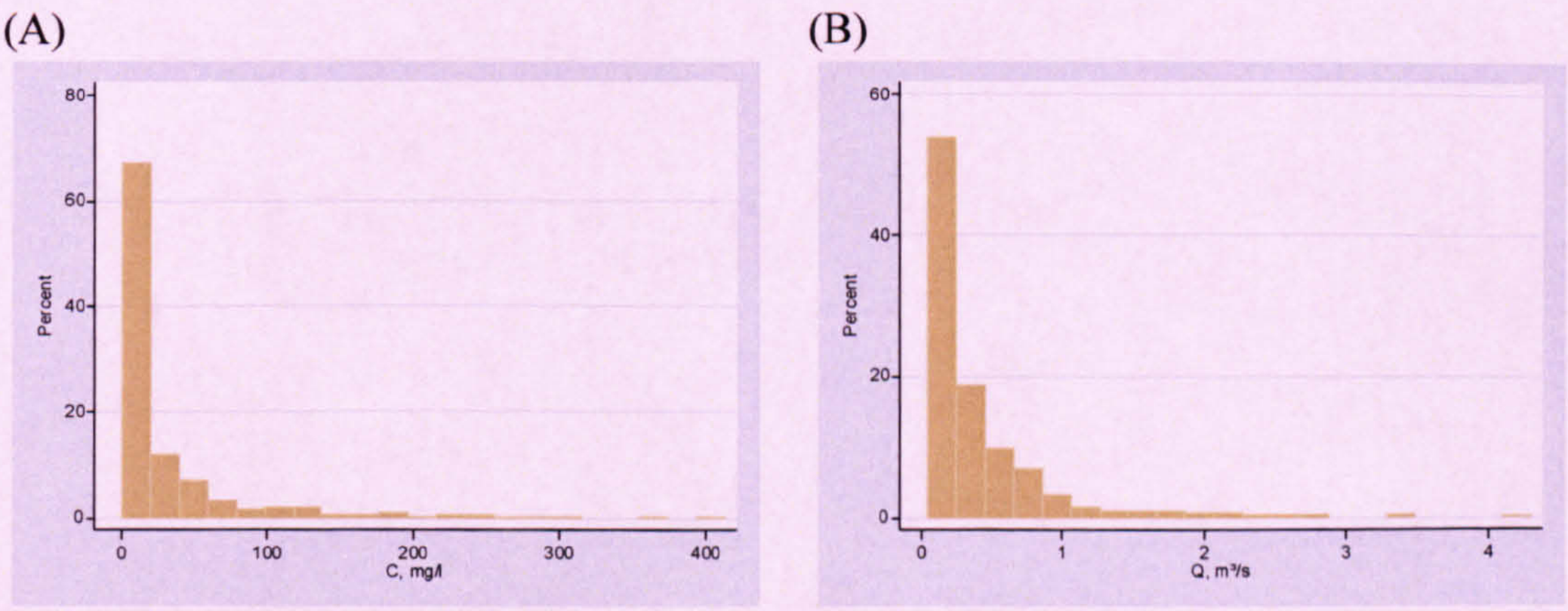

Figure 8.28. The distribution of (A) sampled SSC and (B) sampled Q for Swinhope.

Boxplots of the SSC and Q for each storm show there are more outliers in the SSC series (Figure 8.29). Generally the storms with the greater variability in SSC have a more variable Q distribution (Figure 8.29).

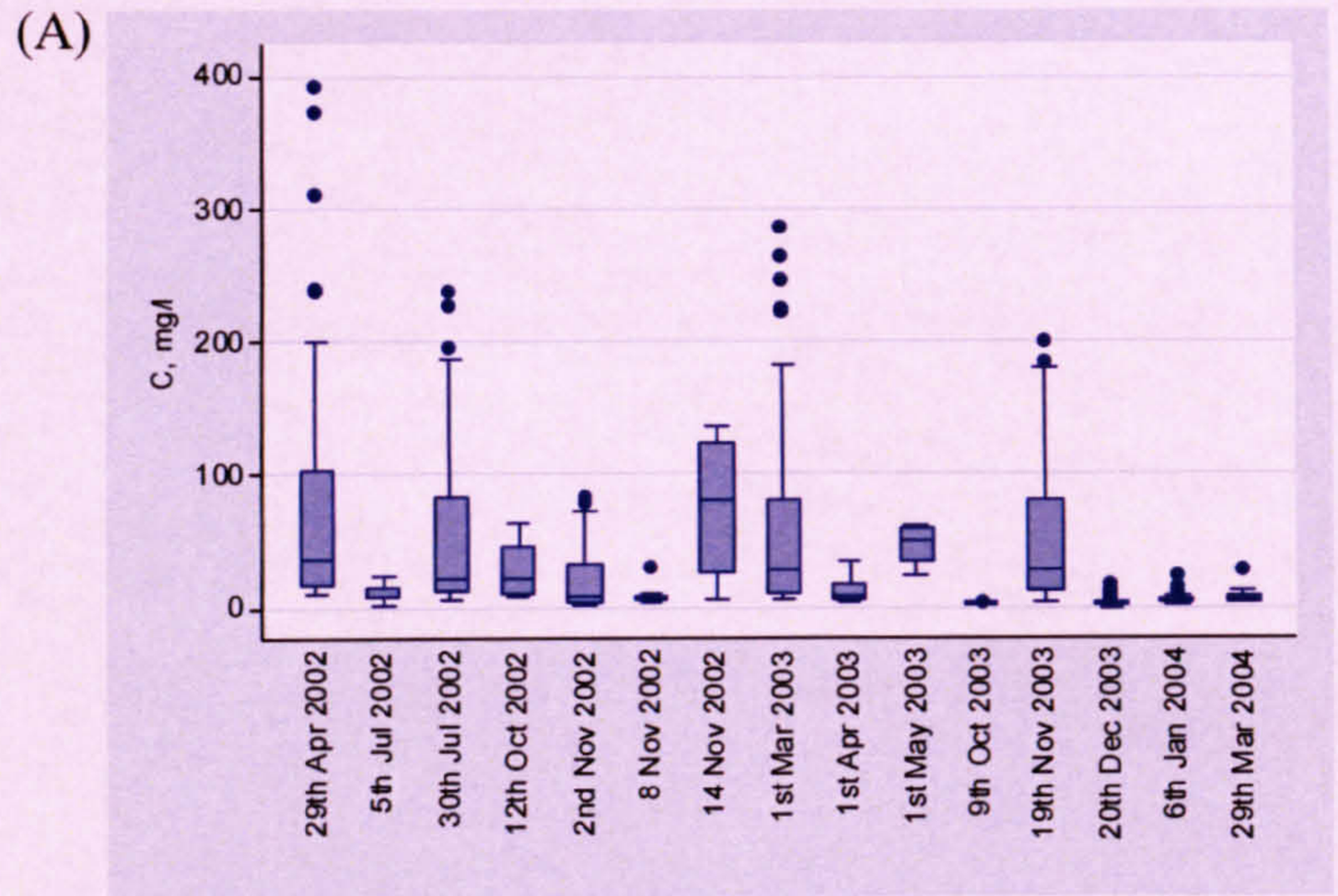

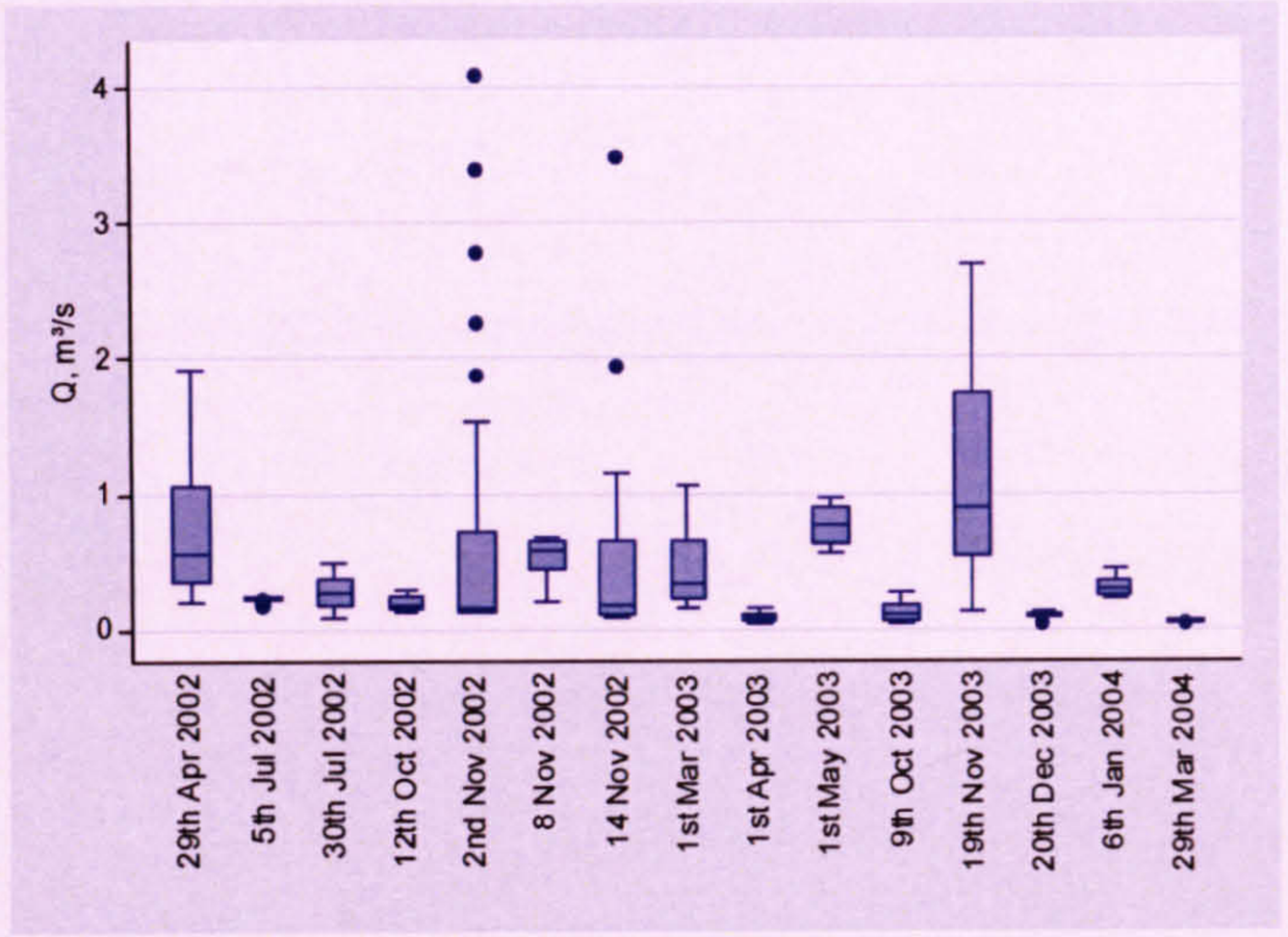

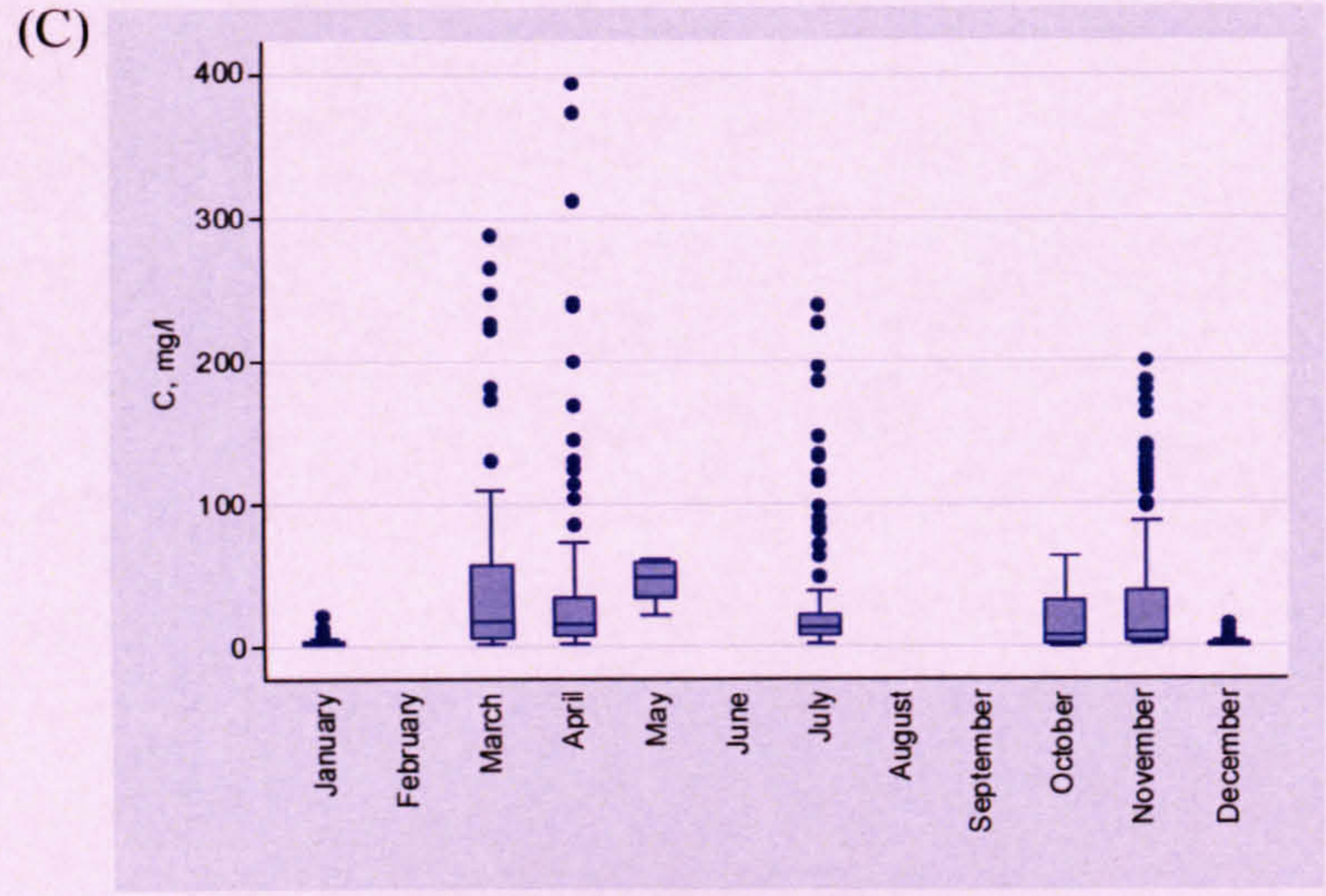

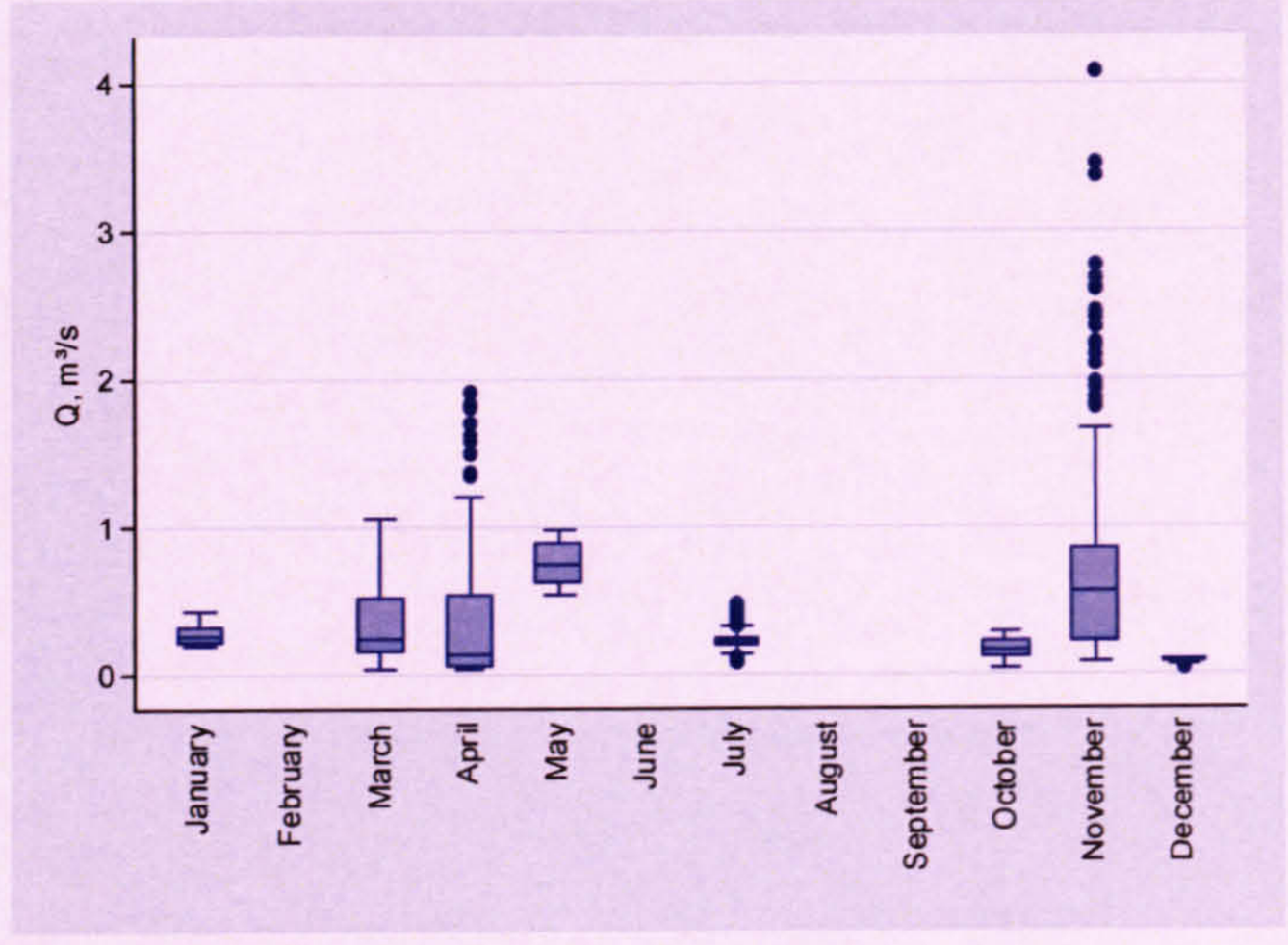

Figure 8.29. Boxplots illustrating the distribution of (A) SSC by storm, (B) Q by storm, (C) SSC by month, and (D) Q by month for Swinhope.

No samples (given low flows and technical problems with the auto-samplers) were taken in February, June, August or September but the coverage of samples is generally good; there were no seasons within which no samples were taken (Figure 8.29). No systematic variation of the variability in SSC or Q is evident by month (Figure 8.29). The variability is unlikely to be a function of the number of samples taken as the number of samples is approximately equal, with the exception of May, within which only twelve samples were taken, and November, within which 146 samples were taken.

In summary, the sampled series is representative of the annual series with regard to the number of samples taken on the rising and falling limb. Given the problem regarding the stage-Q calibration no inferences can be made regarding the representativeness of the sampled series, except that the full range of discharges was not sampled. The annual coverage of SSC samples is fairly good which suggests that the full range of SSC-Q relations will have been captured.

8.3.5.2 Basic rating curves

The R^2 values suggest the Gaussian-log model with ln Q as the explanatory variable is the best model, closely followed by the gamma-log model with ln Q as the explanatory variable, linear regression and the gamma-identity with Q as the explanatory variable (Table 8.20). The RMSEs confirm that the same models are the best fit (Table 8.20). The diagnostic plots indicate that the linear regression model is a fairly good fit: the residuals are approximately normally distributed, exhibit equal variance throughout the range of ln Q, the quantile plots are almost horizontal with small tails and there is no structure in the observed versus predicted and residuals versus predicted plots. The diagnostic plots for the GLMs are variable and the Gaussian distribution model plots all indicate a poorer model fit than the linear regression model. The residuals are non-normally distributed and their variances increase with increasing Q/ln Q, the quantile plots generally have a long tail at the upper fraction of the data and there is form on the observed versus predicted and residuals versus predicted plots. In terms of the predicted storm period loads the same models as indicated by R^2 and RMSE are the best fit, although the linear regression model estimate is poor, unless corrected for back-transformation bias (Table 8.20). The loads predicted by these models are very good; the error is less than 7% (Table 8.20).

Table 8.20. Basic Swinhope rating curve equations, associated R^2 and RMSE values, monitored period predicted loads and percentage difference between actual and predicted load for the monitored period. The R^2 and RMSE values for linear regression relate to C not ln C. UC = uncorrected, LNCF = corrected by the log-normal correction factor (1.73), SM = corrected by smearing (1.66), and BME = corrected by the Bradu-Mundlak estimator.

Model	Equation	R^2	RMSE	n	Monitored period	
					Load, t	% difference
Linear regression	$\ln C = 0.91 \ln Q + 3.72$	0.35	44.9	570		
UC:					5.58	–39.7
LNCF:					9.65	4.3
SM:					9.28	0.2
BME:					9.29	0.4
Gamma–identity, Q	$C = 69.79 Q + 1.34$	0.34	42.32	572	9.89	6.8
Gamma–log, Q	$C = \exp(1.76 Q + 2.35)$	0.02	646.18	572	48.62	425.3
Gaussian–log, Q	$C = \exp(0.58 Q + 4.26)$	0.20	46.36	572	7.08	–23.5
Gamma–identity, ln Q	$C = 6.94 \ln Q + 21.40$	0.31	51.56	570	2.59	–72.0
Gamma–log, ln Q	$C = \exp(0.93 \ln Q + 3.20)$	0.35	41.82	570	9.60	3.7
Gaussian–log, ln Q	$C = \exp(0.78 \ln Q + 4.24)$	0.36	41.31	570	9.09	–1.8
				Actual:	**9.26**	

Graphical analysis of the rating curves indicates that the gamma-log model with Q as the explanatory variable results in gross over-estimations at the upper ranges of Q (Figure 8.30) which results in large over-estimations in load. The other models, with the exception of the Gaussian-log model with Q as the explanatory variable, are approximately linear, but differ in terms of gradient and intercepts (Figure 8.30). There is most variation in the models at higher values of Q (Figure 8.30). The Gaussian-log model with Q as the explanatory variable is discounted as the model fit is obviously very poor. The poor fit is a result of the distribution of data points: the log link and the positive coefficient indicate that an exponential curve is being fitted and the data at lower values of Q promote the fitting of such a curve. However, the data at higher values of Q do not and as a result physically implausible values of SSC are predicted at high values of Q.

On the basis of R^2, RMSE, diagnostic plots, graphical analysis and storm period load estimates the linear regression model with back-transformation bias corrected by smearing is selected as the superior model. Smearing is selected over LNCF on the basis of the residual plots.

8.3.5.3 Adapted rating curves

Fifteen adaptations of the basic linear regression rating curve were developed and combined to produce seven load estimates (Table 8.21). A lagged model was not produced as the monitored period load estimate indicated that a zero lag was most appropriate.

There is no distinct difference in the distribution of the rising and falling limb data clouds (Figure 8.31). The model forms are fairly similar (Figure 8.31 & Table 8.21) with the rising limb curve having a steeper gradient, which indicates that the rate of increase in ln C for a given unit increase in ln Q is greater on the rising limb. Serial autocorrelation is evident in the plot (Figure 8.31). The fit of the falling limb model is superior in terms of RMSE, but inferior in terms of R^2. The measures of fit are similar to those obtained for the regression model based on all data but the load estimate obtained from the rising and falling limb regression models is more accurate by 10% (Table 8.21).

(A)

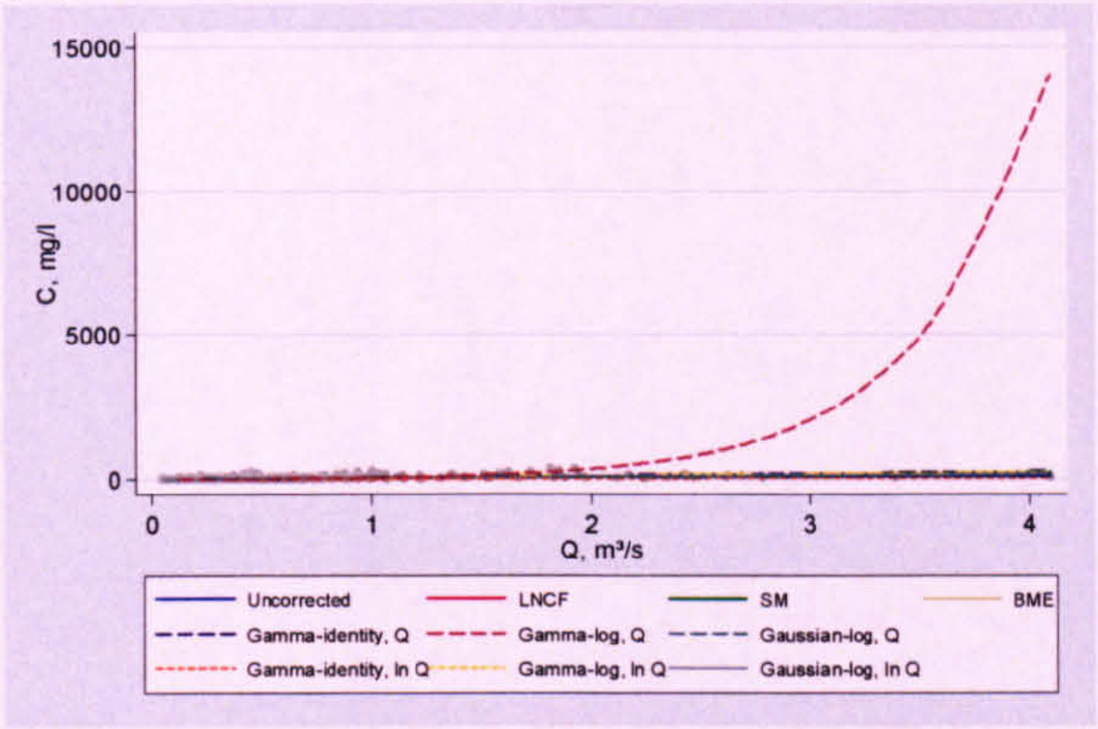

(B)

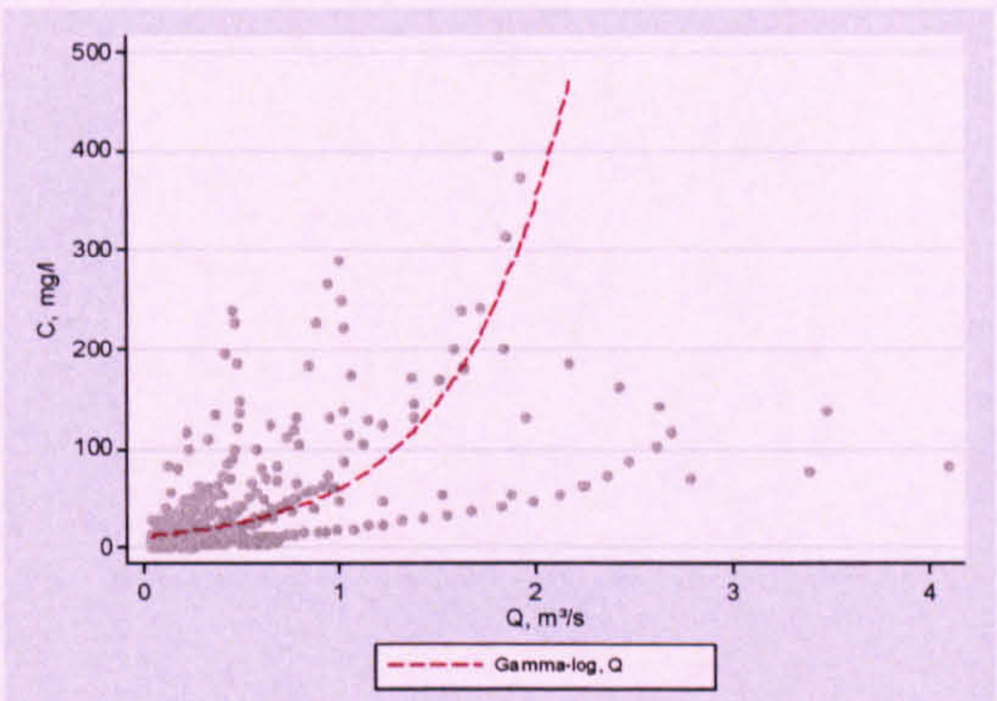

(C)

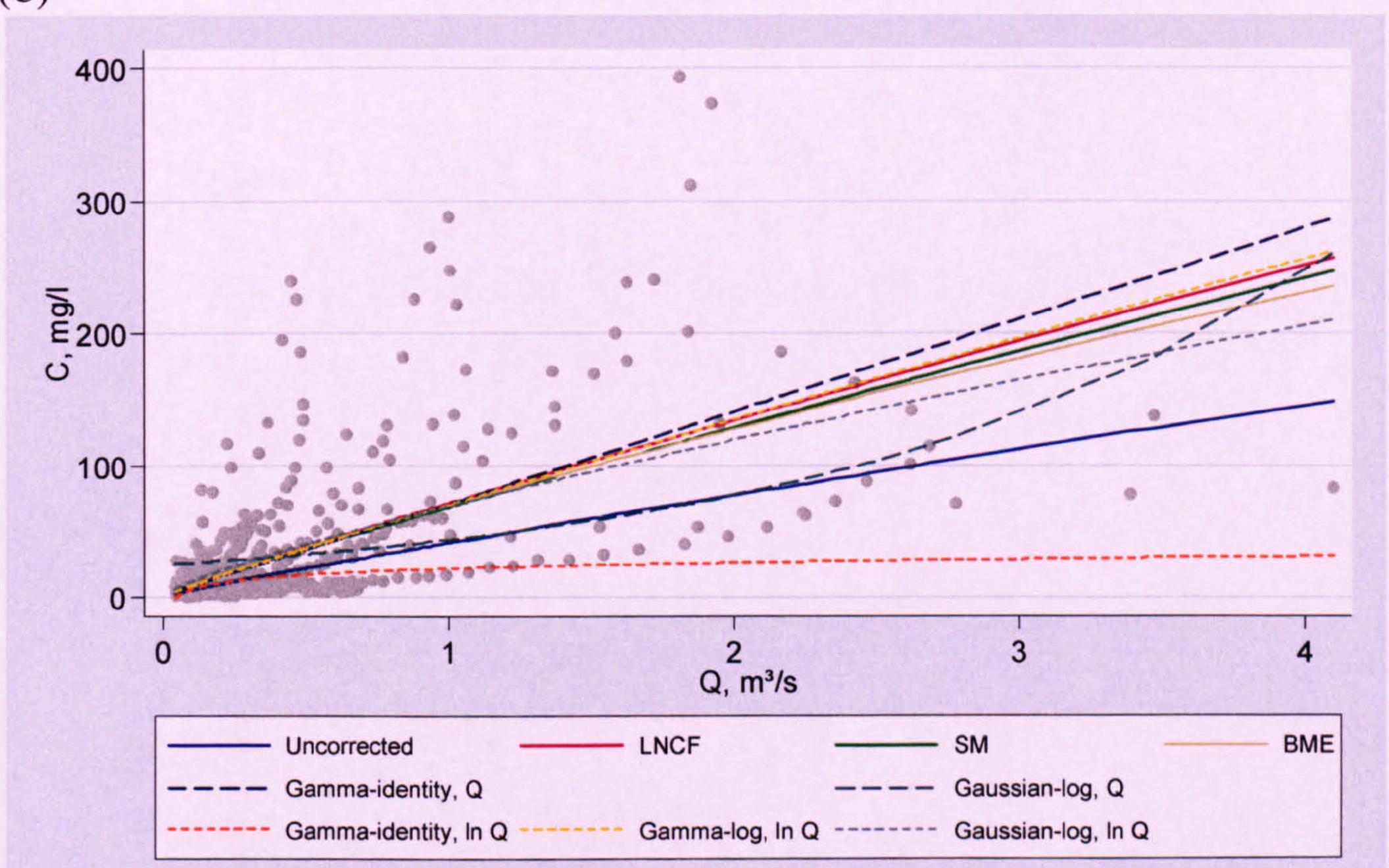

Figure 8.30. Comparison of the basic rating curves developed for Swinhope. (A) All models showing the deviance of the Gamma-log GLM with Q as the explanatory variable, (B) the Gamma-log GLM with Q as the explanatory variable only, and (C) all models except the Gamma-log GLM with Q as the explanatory variable.

Table 8.21. Adapted linear regression rating curve equations for Swinhope, associated R^2 and RMSE values, and monitored period predicted loads and percentage difference between actual and predicted load for the monitored period. The R^2 and RMSE values for linear regression relate to ln C not C. None of the load estimates are corrected for back-transformation bias.

Model	Equation	R^2	RMSE	n	Monitored period Load, t	Monitored period % difference
All data	$\ln C = 0.91 \ln Q + 3.72$	0.40	1.05	570	5.58	–39.7
Limb:						
Rising	$\ln C = 1.04 \ln Q + 4.10$	0.45	1.13	195	6.53	–29.5
Falling	$\ln C = 0.81 \ln Q + 3.47$	0.37	0.97	375		
Season (4):						
Spring	$\ln C = 0.93 \ln Q + 4.42$	0.76	0.59	168		
Summer	$\ln C = 2.17 \ln Q + 5.95$	0.49	0.75	91	5.75	–37.9
Autumn	$\ln C = 0.76 \ln Q + 3.32$	0.35	1.07	223		
Winter	$\ln C = 0.89 \ln Q + 2.63$	0.35	0.67	88		
Split–year:						
Summer	$\ln C = 0.96 \ln Q + 4.34$	0.60	0.69	197	5.65	–39.0
Winter	$\ln C = 0.92 \ln Q + 3.45$	0.40	1.09	373		
Limb & split–year:						
Summer – rising	$\ln C = 1.12 \ln Q + 4.84$	0.56	0.78	58		
Summer – falling	$\ln C = 0.89 \ln Q + 4.12$	0.65	0.61	139	6.53	–29.5
Winter – rising	$\ln C = 1.03 \ln Q + 3.83$	0.48	1.16	137		
Winter – falling	$\ln C = 0.81 \ln Q + 3.16$	0.34	1.01	236		
Lag	Lag did not improve load estimate					
ΔQ	$\ln C = 0.90 \ln Q + 0.89 \Delta Q + 3.67$	0.42	1.04	556	6.25	–32.5
Time of year	$\ln C = 0.96 \ln Q + 0.34 \sin [2 \pi \text{FOY}] - 0.59 \cos [2 \pi \text{FOY}] + 3.93$	0.53	0.92	570	5.79	–37.4
***Q* class**	$\ln C = 0.87 \ln Q + 3.76$	0.39	0.91	19	5.73	–38.1
				Actual:	**9.26**	

(A)

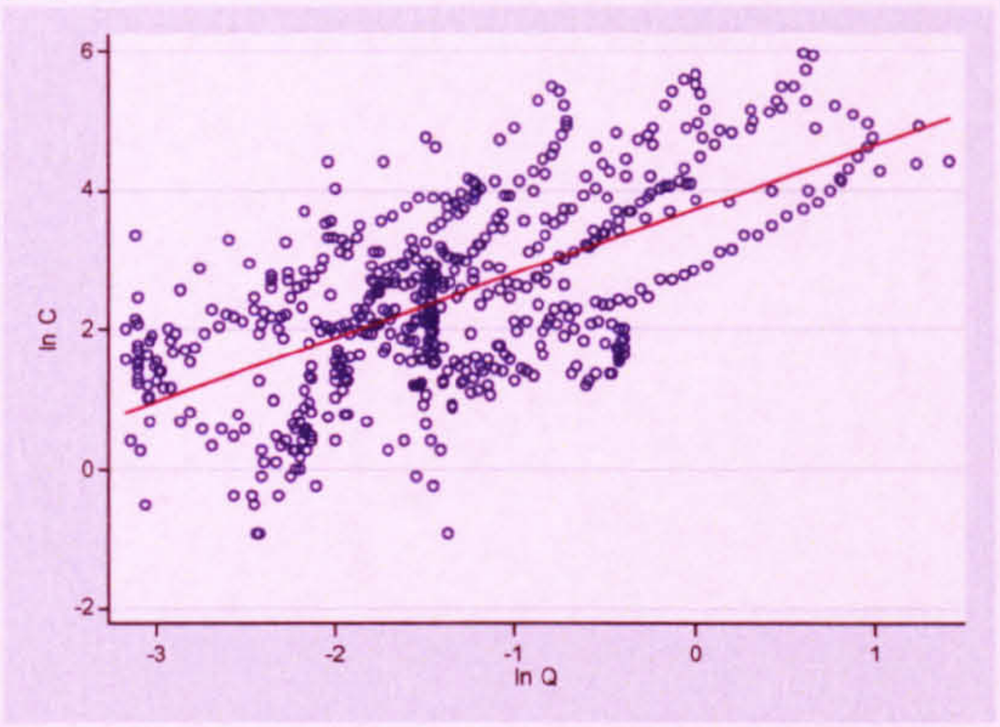

(B)

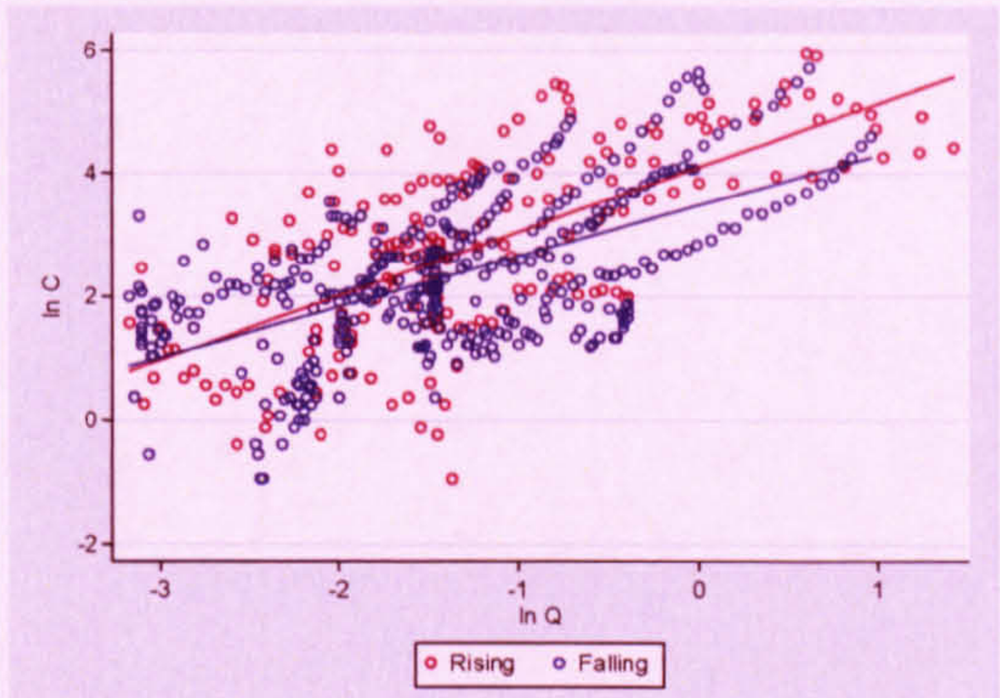

(C)

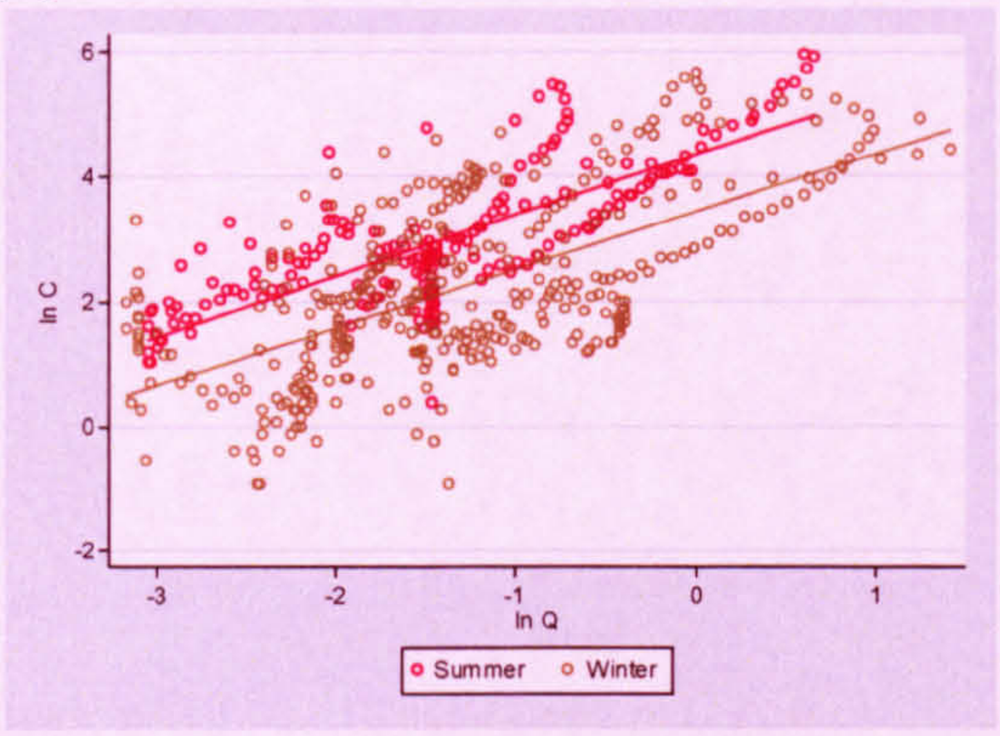

(D)

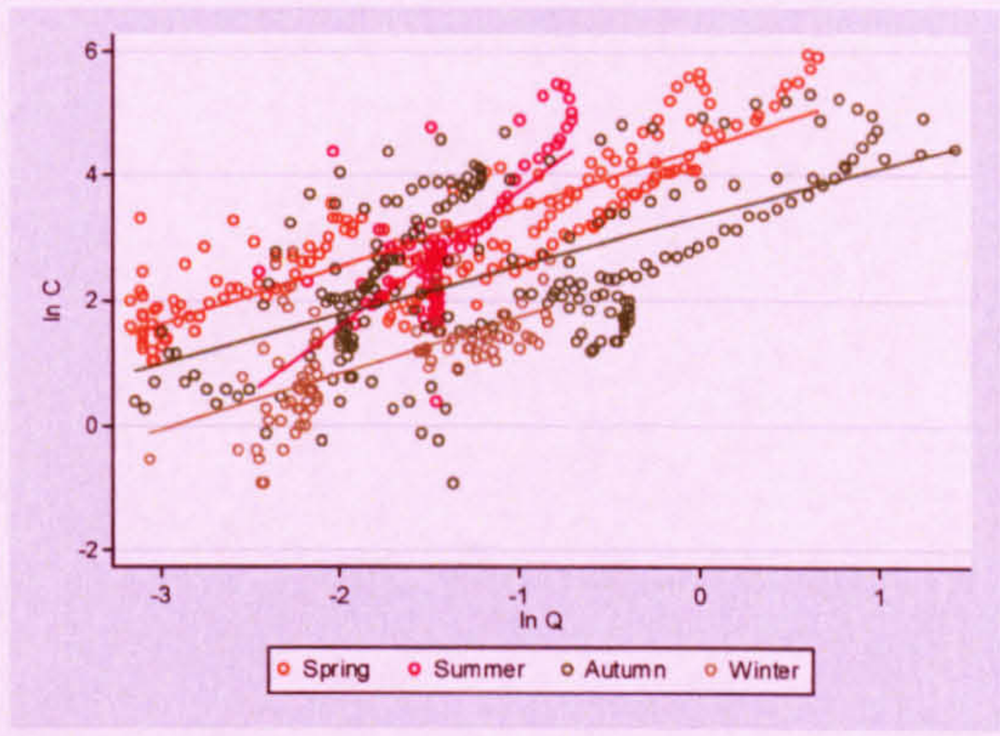

(E)

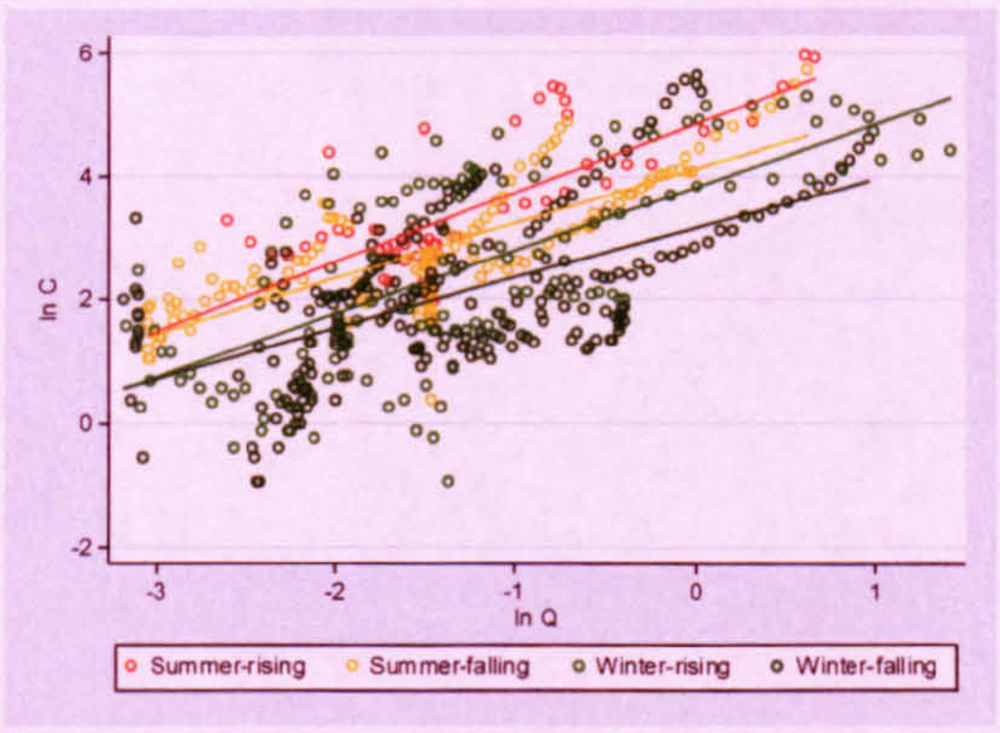

(F)

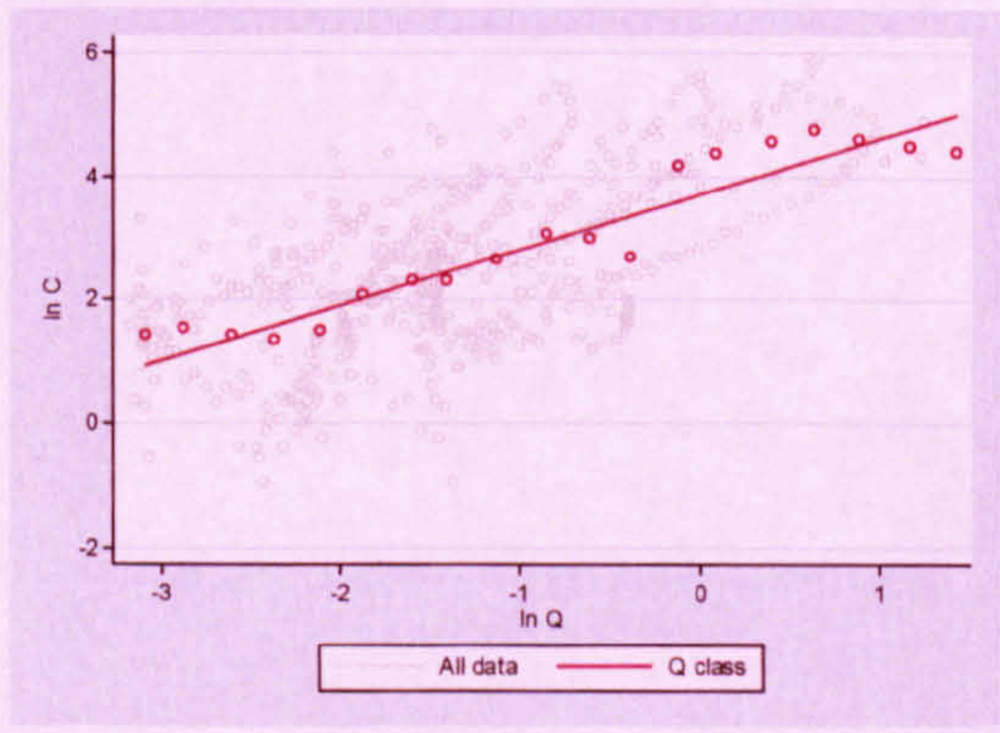

Figure 8.31. Linear regression models for Swinhope. (A) All data; (B) data divided into rising and falling limb; (C) data divided into summer and winter; (D) data divided into spring, summer, autumn and winter; (E) data divided into summer-rising, summer-falling, winter-rising, winter-falling; and (F) *Q* class method.

The models obtained from the split-year data sub-sets suggests that for any given ln Q there is a greater amount of sediment available in the summer months. The summer and winter curves have almost identical gradients but the intercept of the summer regression is higher than that of the winter regression (Figure 8.31 & Table 8.21). Serial autocorrelation is evident in the plot (Figure 8.31). Overall the R^2 and RMSE are improved by sub-dividing the data into summer and winter, but the resultant load estimate is almost identical (Table 8.21).

In the seasonal model, the spring, summer, autumn and winter data clouds all overlap and the only clear distinction is that the spring data points predominantly plot above the winter data points (Figure 8.31). The spring, autumn and winter rating curves are similar in terms of gradient although the intercepts differ (Figure 8.31 & Table 8.21). The intercept of the winter rating curve is lowest, indicating there is less sediment for transport for any given ln Q and highest for the summer curve, indicating there is most sediment for transport for any given ln Q (Figure 8.31 & Table 8.21). In contrast to the spring, autumn and winter rating curves, the gradient of the summer curve is much steeper (Figure 8.31 & Table 8.21), which indicates that for a given increase in ln Q there is a greater increase in ln C. With the exception of the RMSE for the autumn curve all the R^2 and RMSE are better for the seasonal models than for the model based on all data (Table 8.21). However, the resultant load estimate is only 2% more accurate than that obtained from the regression based on all data (Table 8.21).

There is no clear distinction between data clouds defined by split-year and limb (Figure 8.31). The summer- and winter-rising curves have approximately the same gradient, as do the summer- and winter-falling curves: the former are steeper (Figure 8.31 & Table 8.21). This indicates that for a given increase in ln Q there is a greater increase in ln C on the rising limb, regardless of the season. The intercepts are higher for the summer curves than for the winter curves and the rising limb intercepts are higher than the falling limb intercepts (Figure 8.31 & Table 8.21). This indicates that at any given Q, ln C is generally higher in the summer than in the winter and on the rising limb than on the falling limb. Serial autocorrelation is evident in the plot (Figure 8.31). The R^2 and RMSE are, for the most part, better for models developed from sub-sets of the data as defined by season and limb and the resultant load estimate is approximately 10% more accurate than that obtained by the model based on all data (Table 8.21).

Adding change in Q as a second explanatory variable did not result in a noteworthy improvement in the R^2 or RMSEs but the load estimate was 7% more accurate (Table 8.21). Adding sine and cosine variables to account for seasonality results in small improvements in the R^2 and RMSE but the load estimate is only improved by 3% (Table 8.21). Finally, the Q class method results in a very similar model in terms of the R^2 gradient, intercept and therefore load estimate (Figure 8.31 & Table 8.21).

To summarise, although most of the adapted models had higher R^2 values and lower RMSEs, in terms of improving the monitored period load estimate, the only adapted models worthy of development are those defined by limb, limb and split-year and with change in Q as an additional explanatory variable.

8.3.6 Trout Beck

8.3.6.1 Data characteristics and distributions

Fixed-interval and storm sampling were undertaken at Trout Beck (Table 8.22). Storms were primarily sampled in the winter months and fixed-interval sampling during the summer months (Table 8.22).

Table 8.22. Type, number and dates of samples taken in the Trout Beck catchment.

Sample type	Number	Details
Fixed-interval	126	20th March 2002 – 30th August 2002
Storm		
Total:	224	
Per storm:	23	10th October 2001
	24	1st April 2002
	9	26th October 2001
	24	7th November 2001
	24	3rd October 2001
	48	20th January 2002
	24	17th January 2002
	24	29th November 2002
	24	21st November 2001

Approximately one third of the sampled SSC were taken on the rising limb (Table 8.23). In comparison approximately one fifth of the discharges of the annual record are categorised as rising limb (Table 8.23). SSC ranged from zero to 60 mg l^{-1} (Table 8.23). A very small proportion of the annual discharge range was sampled in the sampled Q series: the highest Q in the annual record was over 40 m^3 s^{-1} in comparison to just 6.5 m^3 s^{-1} in the sampled period (Figure 8.9). In contrast the mean Q of the sampled period is higher than that of the annual record by a factor of three (Table 8.23). This is because

there was one very large flood in the catchment which increased the Q range and because the sampling strategy by which the majority of the samples were collected was biased towards high flows (storm sampling). The coefficient of variation is higher for the sampled SSC than for the sampled Q and the annual record Q has a higher coefficient of variation that the sampled Q record (Table 8.23). The sampled SSC series is more skewed and tail weighted than the sampled Q series (Table 8.23). The annual Q series is even more skewed and tail weighted (Table 8.23), an artefact of the very large storm.

Table 8.23. Summary statistics of the sampled SSC (mg l^{-1}) and Q (m^3 s^{-1}) series and the annual Q series for Trout Beck.

Measure	SSC sampled period SSC	SSC sampled period *Q*	Annual record *Q*
Number of samples:			
Total	350		35,040
Rising	103		7741
Falling	247		27,299
Range	0.0 - 59.3	0.03 – 6.53	0.01 - 44.68
Mean	9.03	1.91	0.62
Standard deviation	12.17	1.84	1.35
Coefficient of variation, %	134.7	96.3	217.6
Skew	2.24	0.88	10.6
Kurtosis	7.93	2.68	252.3

Graphical examination of the sampled SSC and Q series indicates that the distributions are broadly similar, although the SSC is more peaked (Figure 8.32). The distribution of the sampled and annual Q series are very different (Figure 8.32), although the distribution of the majority of the annual Q series is hidden due to one very large storm.

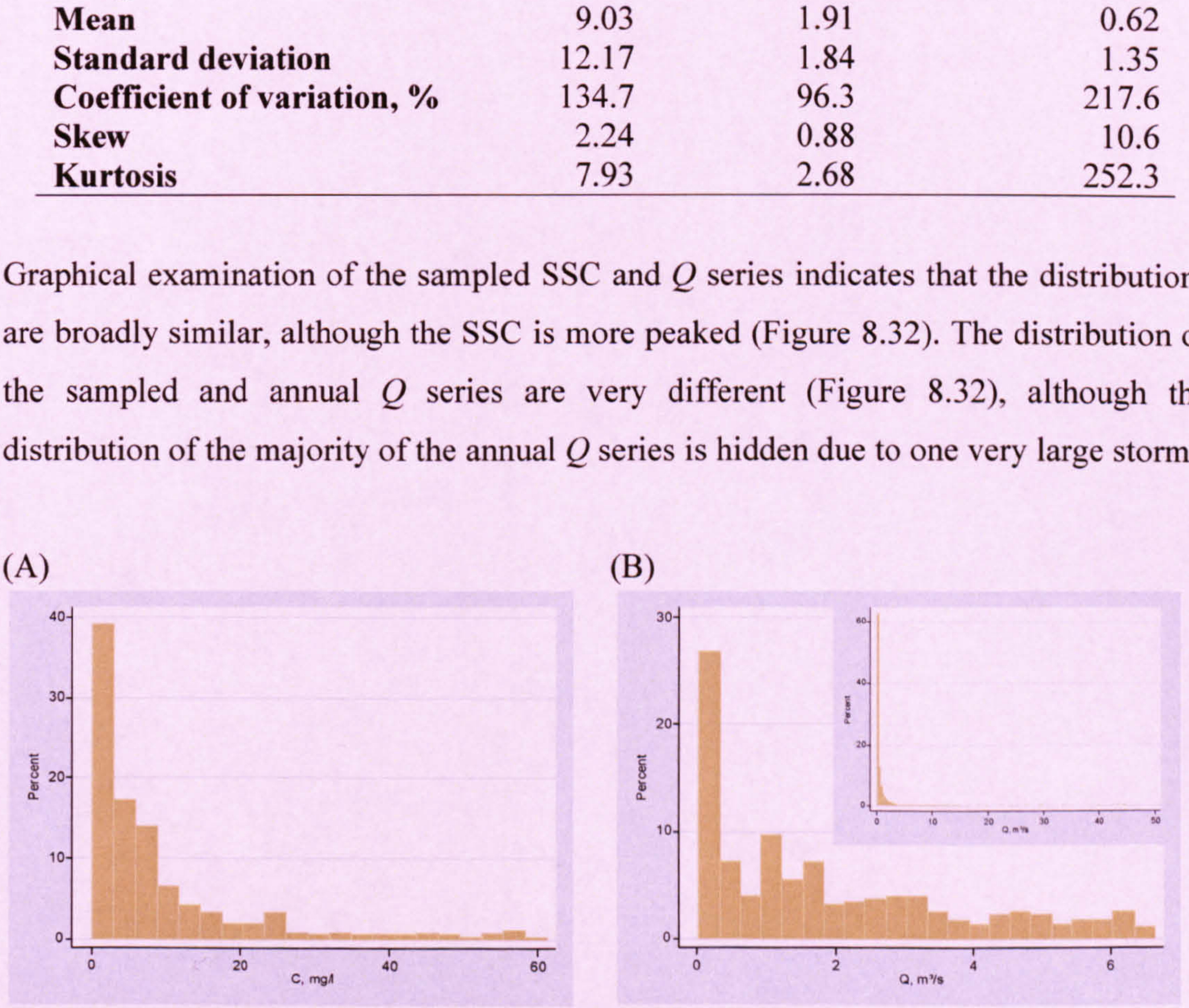

Figure 8.32. The distribution of (A) sampled SSC and (B) sampled Q with an inset of the distribution of the annual Q record for Trout Beck.

Examination of boxplots of SSC and Q for each of the storm events shows that generally higher variability in storm SSC distribution is associated with higher variability in storm Q distribution (Figure 8.33). The boxplots of SSC and Q by month indicate that samples were taken throughout the year with the exception of February, September and December (Figure 8.33). Generally months with higher variability in SSC are associated with higher variability in Q (Figure 8.33). However, it can not be determined if the variability is due to processes operating within the system or a result of different numbers of samples: broadly the months with more variable distributions are those when more samples were taken (Figure 8.33 & Table 8.24).

Table 8.24. Number of samples taken in each month for Trout Beck.

Month	Number of samples
January	72
February	0
March	27
April	53
May	1
June	48
July	20
August	1
September	0
October	56
November	72
December	0

In summary, a higher percentage of samples were taken on the rising limb than is representative of the annual record. As a result, over-estimations may occur if sediment exhaustion is a marked influence in the catchment. Only a fraction of the annual Q range was sampled which could lead to large errors in load estimations. This was primarily due to one very large event and casts doubt on the sampled period load estimate as an indicator of model fit. The distributions of sampled Q and annual Q are different and may affect load estimates. Samples were taken throughout the year which suggests the full range of SSC-Q relations were captured. However, storm samples were only taken from October to April.

8.3.6.2 Basic rating curves

Both R^2 and RMSE suggest the Gaussian-log GLM with Q as the explanatory variable is the best model. The poorest model, as suggested by both R^2 and RMSE is linear regression (Table 8.25). The diagnostic plots suggest that linear regression is the best

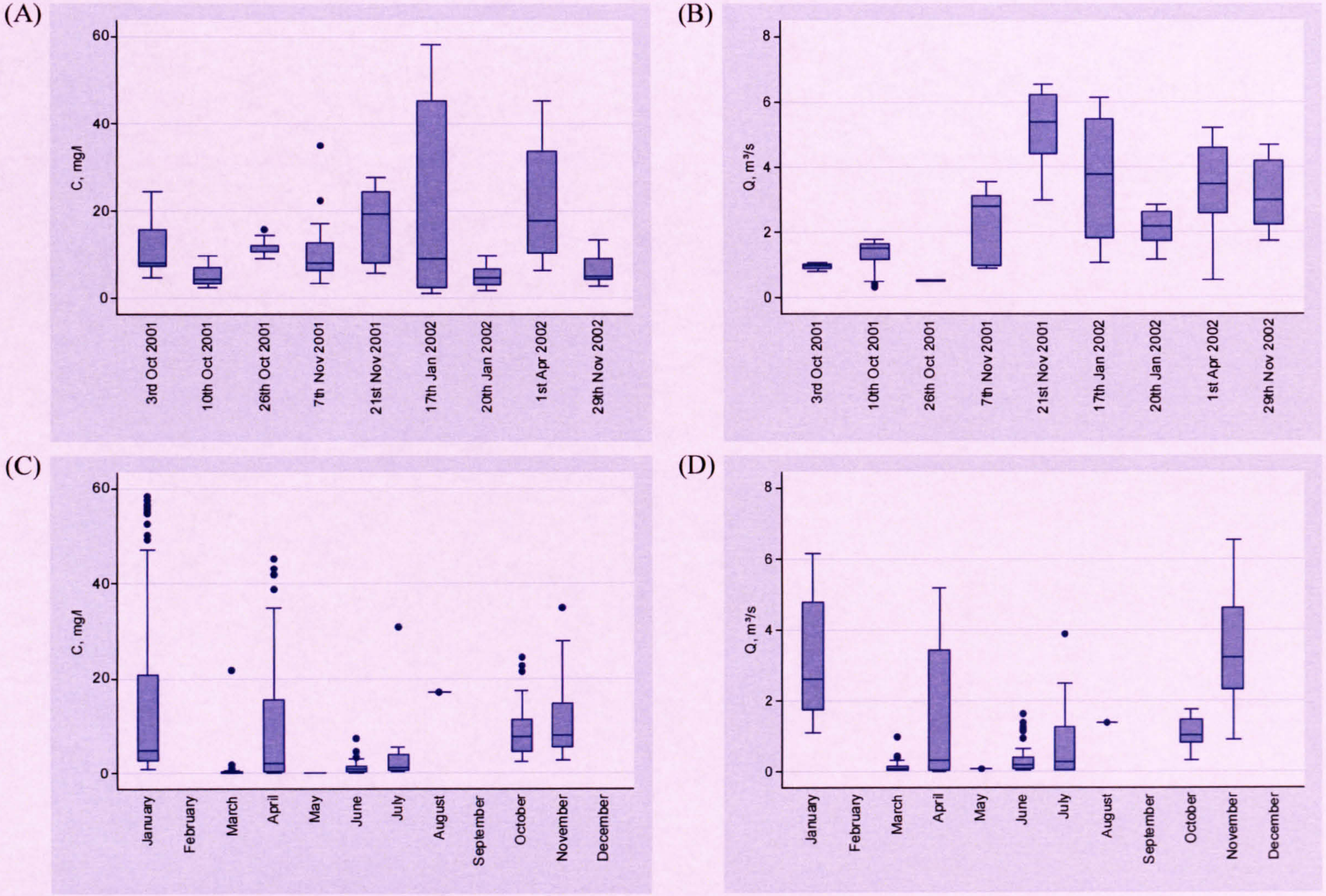

Figure 8.33. Boxplots illustrating the distribution of (A) SSC by storm, (B) Q by storm, (C) SSC by month, and (D) Q by month for Trout Beck.

Table 8.25. Basic Trout Beck rating curve equations, associated R^2 and RMSE values, predicted annual loads, monitored period predicted loads and percentage difference between actual and predicted load for the monitored period. Annual loads were calculated from 1st October 2001 to 30th September 2002. The R^2 and RMSE values for linear regression relate to C not ln C. UC = uncorrected, LNCF = corrected by the log-normal correction factor (1.48), SM = corrected by smearing (1.53), and BME = corrected by the Bradu-Mundlak estimator.

Model	Equation	R^2	RMSE	n	Annual load, t	Monitored period Load, t	% difference
Linear regression	$\ln C = 0.73 \ln Q + 1.46$	0.47	10.82	337			
UC:					184.4	6.16	–38.6
LNCF:					272.8	9.12	–9.1
SM:					282.5	9.44	–5.9
BME:					271.4	9.05	–9.8
Gamma–identity, Q	$C = 4.57 Q + 0.69$	0.52	8.49	350	1,439,329.1	10.03	0.0
Gamma–log, Q	$C = \exp(0.48 Q + 0.89)$	0.55	8.48	350	33,342,415.5	11.26	12.3
Gaussian–log, Q	$C = \exp(0.40 Q + 1.14)$	0.56	8.11	350	877,124,138.7	9.93	–1.0
Gamma–identity, ln Q	Model did not converge						
Gamma–log, ln Q	$C = \exp(0.68 \ln Q + 1.84)$	0.47	9.05	350	249.6	8.39	–16.4
Gaussian–log, ln Q	$C = \exp(1.44 \ln Q + 0.89)$	0.55	8.28	350	453.1	10.03	0.0
					Actual:	**10.03**	

model as the residuals are approximately normally distributed with equal variance, there is no structure on the observed versus predicted plot or residuals versus predicted plot and the quantile plots show straight, near horizontal lines. In contrast the residual plots for the GLM show non-normally distributed residuals within increasing variance with increasing Q/ln Q and the quantile plots are steeper and have a longer tail at the upper quantiles. However, this is acceptable if a gamma distribution is assumed. Nevertheless, there is structure in the observed versus predicted plot.

Graphical examination of the rating curves shows the forms differ substantially (Figure 8.34). The effect of bias correction of the linear regression rating is clear: the corrected rating lie well above the uncorrected ratings (Figure 8.34). The gamma-log and Gaussian-log curves with Q as the explanatory variable and the Gaussian-log model with ln Q as the explanatory variable appear visually to fit the data best (Figure 8.34). However, due to the steep rise in these curves they are likely to give gross over-predictions at high discharges and therefore should not be extrapolated. The gamma-identity model with ln Q as an explanatory variable over-predicts at low discharges and under-predicts at high discharges (Figure 8.34). Finally the gamma-identity with Q as the explanatory variable and gamma-log with ln Q as the explanatory variable appear to fit well at the lowest discharges, over-predict at intermediate discharges and under-predict at high discharges (Figure 8.34). Due to the difference in the form of these curves the accuracy with which each predicts suspended sediment loads is likely to be dependent on the differences in the distribution of the discharges that the curves are developed from and the distribution of the discharges they are being used to predict load from.

The estimated loads obtained for the sampled period by the gamma-identity with Q as the explanatory variable and Gaussian-log with ln Q as the explanatory variable are the same as the actual loads (Table 8.25). All the models, with the exception of the uncorrected linear regression model, give load predictions within 15% of the true load (Table 8.25). The smearing correction results in a more accurate load estimation than the parametric correction factors (Table 8.25).

The Gaussian-log GLM with ln Q as the explanatory variable was chosen as the best model. This choice was based primarily on the analysis of the rating curve model graph. The Gausian-log ln Q model visually fits the data best. Also, the predicted SSC at the

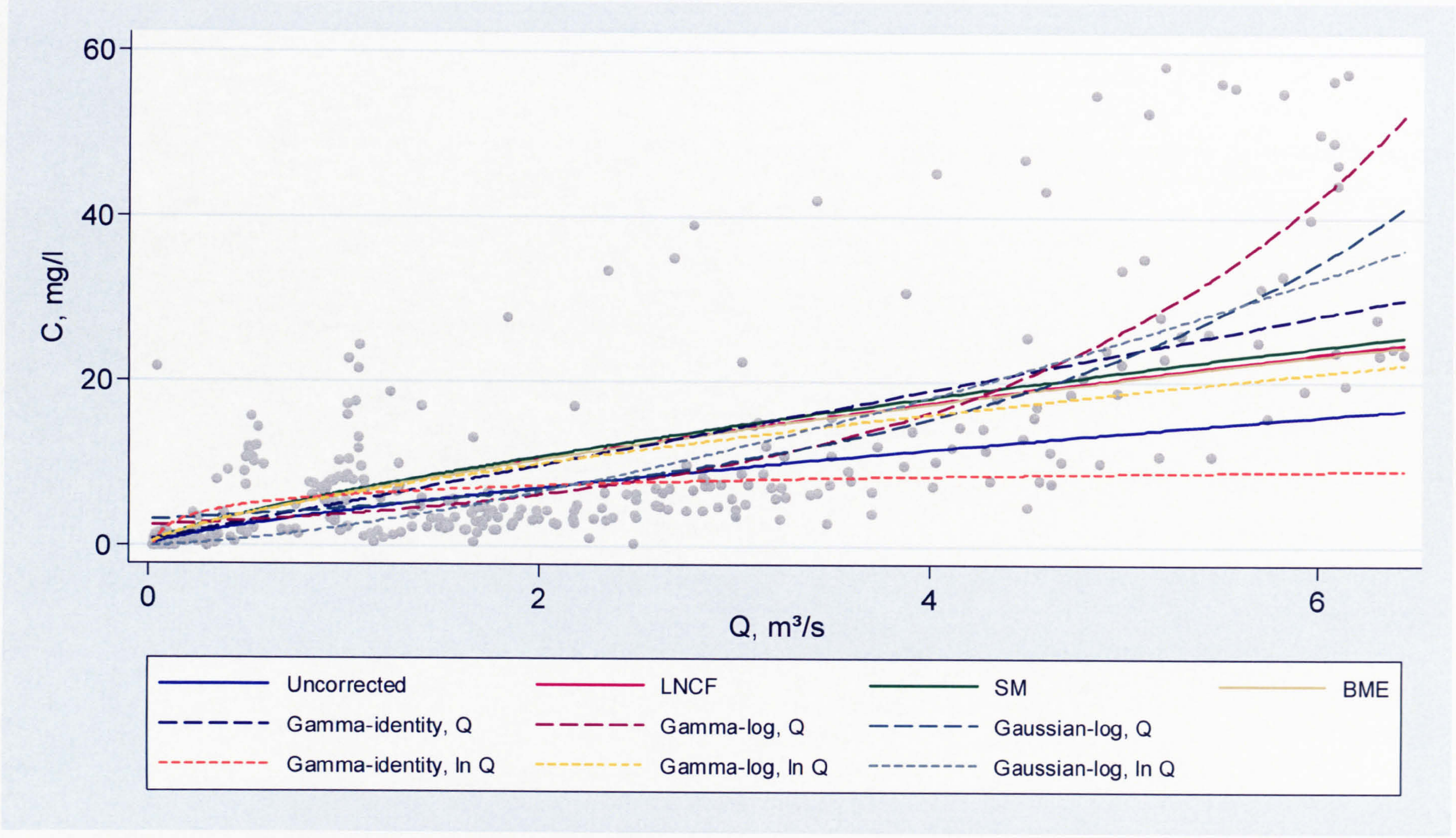

Figure 8.34. Comparison of the basic rating curves developed for Trout Beck.

peak Q which occurred during the study year (44 m^3 s^{-1}) is reasonable at 577 mg l^{-1}. This is important given that the majority of suspended sediment tends to be transported during storm events. In contrast the linear regression model predicts a SSC of 69 mg l^{-1} which is too low. Also, although the distributions of the sampled and annual Q series are very different the monitored period load estimate is exact, which indicates the model fits well at lower discharges. Furthermore, the R^2 is the second highest and the RMSE is the second lowest.

8.3.6.3 Adapted rating curves

There is no clear difference in the data clouds for the rising and falling limb data (Figure 8.35). However, the regression lines are notably different: the rising limb has a slightly lower intercept and a steeper gradient (Figure 8.35 & Table 8.26). R^2 indicates that the rising limb regression is a slightly better fit and RMSE suggests the falling limb regression is a better fit (Table 8.26). Combined they are a similar fit to the model developed from all data (Table 8.26). The sampled period load estimate is very similar to that obtained from the basic linear regression model (Table 8.26).

The regression lines for the split-year model are almost identical (Table 8.26 & Figure 8.35). The extent of the summer and winter data clouds are approximately the same, although the winter data is concentrated more at higher values of ln Q (Figure 8.35), but this may be a product of the sampling regime. The summer curve is a better fit as indicated by R^2 and the winter curve is a better fit as indicated by RMSE (Table 8.26). Overall, as indicated by R^2 and RMSE, the two models are a worse fit than the all data model (Table 8.26). The sampled period load estimate is almost identical to that derived from the basic linear regression model (Table 8.26).

In contrast to the split-year model, the seasonal model produces markedly different rating curves (Figure 8.35 & Table 8.26) and therefore indicates a strong seasonal trend. However, with the exception of no autumn or winter data points at lower values of ln Q there are no distinct differences in the data clouds (Figure 8.35). The winter curve is the steepest, indicating that there is a greater increase in ln C for any given increase in ln Q during the winter (Figure 8.35 & Table 8.26). The R^2 is very high for the winter curve and the RMSE very low, indicating a good model fit. The spring curve is the next steepest and a good fit in terms of R^2 but a poor fit in terms of RMSE (Figure 8.35 & Table 8.26). The autumn curve is the least steep; a given increase in ln Q results in a

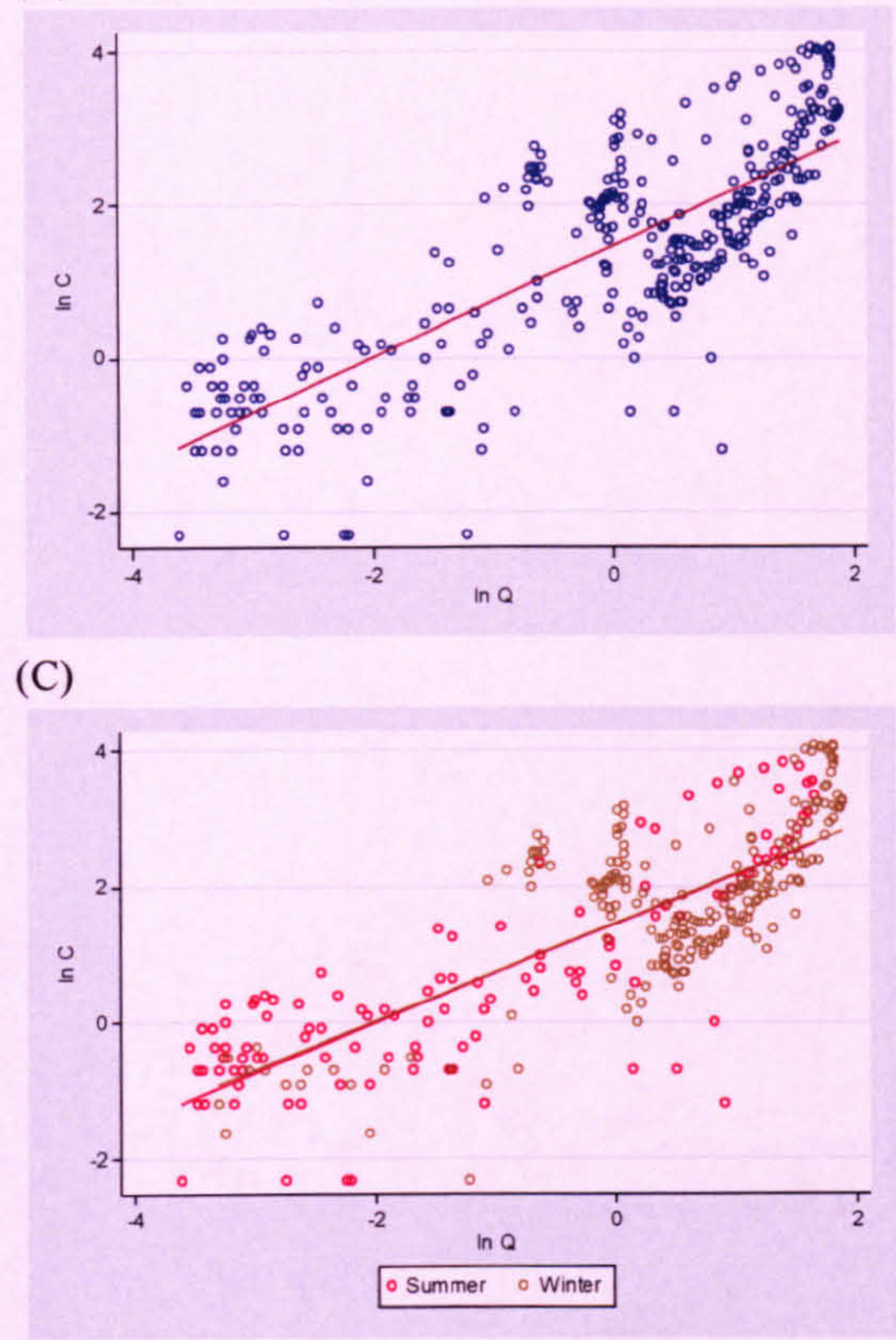

Figure 8.35. Linear regression models for Trout Beck. (A) All data; (B) data divided into rising and falling limb; (C) data divided into summer and winter; (D) data divided into spring, summer, autumn and winter; (E) data divided into summer-rising, summer-falling, winter-rising, winter-falling; (F) *Q* class method; and (G) *Q* lagged by minus 45 minutes.

Table 8.26. Adapted linear regression rating curve equations for Trout Beck, associated R^2 and RMSE values, predicted annual loads, monitored period predicted loads and percentage difference between actual and predicted load for the monitored period. Annual loads were calculated from 1st October 2001 to 30th September 2002. The R^2 and RMSE values for linear regression relate to ln C not C. None of the load estimates are corrected for back-transformation bias.

Model	Equation	R^2	RMSE	n	Annual load, t	Monitored period Load, t	Monitored period % difference
All data	$\ln C = 0.73 \ln Q + 1.46$	0.62	0.88	337	184.4	6.16	–38.6
Limb:							
Rising	$\ln C = 0.87 \ln Q + 1.82$	0.63	0.93	98	222.3	6.51	–35.2
Falling	$\ln C = 0.67 \ln Q + 1.32$	0.64	0.83	215			
Season (4):							
Spring	$\ln C = 0.82 \ln Q + 1.61$	0.71	1.01	70			
Summer	$\ln C = 0.43 \ln Q + 0.80$	0.32	0.83	67	247.5	7.70	–23.2
Autumn	$\ln C = 0.19 \ln Q + 2.02$	0.05	0.60	128			
Winter	$\ln C = 2.15 \ln Q - 0.21$	0.86	0.46	72			
Split–year:							
Summer	$\ln C = 0.73 \ln Q + 1.44$	0.65	0.91	116	182.8	6.15	–38.7
Winter	$\ln C = 0.72 \ln Q + 1.47$	0.46	0.88	221			
Limb & split–year:							
Summer – rising	$\ln C = 0.87 \ln Q + 1.82$	0.65	1.17	27			
Summer – falling	$\ln C = 0.65 \ln Q + 1.26$	0.66	0.78	89	220.0	6.52	–35.0
Winter – rising	$\ln C = 0.86 \ln Q + 1.82$	0.53	0.84	71			
Winter – falling	$\ln C = 0.68 \ln Q + 1.34$	0.48	0.88	126			
Lag	$\ln C = 0.74 \ln Q + 1.47$	0.64	0.87	334	189.3	6.19	–38.3
ΔQ	$\ln C = 0.75 \ln Q + 1.43\ \Delta Q + 1.50$	0.66	0.87	313	195,727.8	6.20	–38.2
Time of year	$\ln C = 0.69 \ln Q - 0.26 \sin [2\pi \text{FOY}] + 0.01 \cos [2\pi \text{FOY}] + 1.45$	0.64	0.87	337	173.6	6.01	–40.1
***Q* class**	$\ln C = 0.74 \ln Q + 1.37$	0.85	0.54	19	171.3	5.73	–42.9
					Actual:	**10.03**	

very slight increase in ln *C*. R^2 suggests the autumn rating curve is a very poor fit but RMSE indicates that it is a good fit (Table 8.26). The load estimate derived from these four regressions for the sampling period is 15% more accurate than the basic linear regression model and is the most accurate out of all of the rating curve adaptations (Table 8.26).

The models derived by categorising the data by split-year and limb produce rating curves very similar to those produced by categorising the data as rising or falling (Table 8.26 & Figure 8.35). This is due to the similarity in the split-year rating curves, as previously mentioned.

The model developed using lagged data is almost identical to the basic linear regression model in form, but the R^2 and RMSE indicate a better model fit (Table 8.26). In terms of R^2 and RMSE adding sine and cosine variables as extra explanatory variables does not improve the model fit and the predicted sampled period load estimate is less accurate than that predicted from the basic linear regression model (Table 8.26). The Q class method results in a regression very similar in form to the basic linear regression model. The R^2 and RMSE values are distinctly better, which is a result of the limited number of data points in comparison, but the load estimate is 4% less accurate (Table 8.26).

The annual load estimate derived from the model with change in Q as an additional explanatory variable is a large over-prediction (Table 8.26). This can be attributed to the effect of extrapolating the rating curve: the mean change in Q of the sampled period is –0.002, the minimum is –0.339 and the maximum 1.104 and in contrast is 0.285, –10.395 and 9999.022 respectively for the annual record.

The monitored period load estimate indicates that the four season model is the only model worth developing. Five of the adapted models were poorer fits as indicated by R^2 and four were poorer as indicated by RMSE.

8.4 Chapter summary

In summary, while annual sediment loads were not calculated by all possible model forms and input data sub-sets, enough models (resulting in up to 17 load estimates, 10 basic and up to 7 adapted) were developed to allow the resulting variability in annual

loads to be examined. The appropriateness of the different models was assessed by R^2, RMSE, diagnostic plots, graphical examination of rating curve fit to the raw data and by comparison of the actual suspended sediment load during the SSC monitoring period and the model predictions for that period. These indicators of model fit rarely suggest the same model is the most appropriate. For example, for Candleseaves R^2 suggested that the Gaussian-log and gamma-log models with Q as the explanatory variable were the best fit, RMSE suggested the Gaussian-log with ln Q as the explanatory variable model was the best fit, the diagnostic plots indicated linear regression was superior and the sampled period load estimate indicated that the gamma-identity model with Q as the explanatory variable was the best model. The most appropriate model was selected on reflection of all the indicators of model fit (Table 8.27). The rating curve adaptations give some illustration of the value of increasing the model complexity in terms of load predictions and gave insight into the processes controlling suspended sediment dynamics, although this is furthered in the next chapter. This chapter has focussed on the development of statistically sound rating curves and includes limited interpretation in light of the physical systems and no synthesis or discussion of the results from all six studies sites has been given as this is the focus of the next chapter.

Table 8.27. Summary of the optimal basic rating curve models. *Annual load for Candleseaves is in kg, it is a 10 month load for Burnhope and an 8 month load for Langtae.

Catchment	Optimal model	Model form	Correction	n	R^2	RMSE	Annual load, t*	Sampled period error, %
Burnhope	Gamma-identity, Q	$C = 25.26\,Q - 3.21$	-	1203	0.32	39.95	287.7	–6.8
Candleseaves	Linear regression, SM	$\ln C = 0.25 \ln Q + 1.54$	SM = 1.74	300	0.27	12.95	53.4	–19.4
Langtae	Linear regression, SM	$\ln C = 0.37 \ln Q + 2.07$	SM = 1.43	410	0.07	10.63	33.5	-
Rough Sike	Linear regression, LNCF	$\ln C = 0.46 \ln Q + 3.06$	LNCF = 1.34	522	0.15	11.73	23.2	0.8
Swinhope	Linear regression, SM	$\ln C = 0.91 \ln Q + 3.72$	SM = 1.66	570	0.35	44.90	-	0.4
Trout Beck	Gaussian-log, $\ln Q$	$C = \exp(1.44 \ln Q + 0.89)$	-	350	0.55	8.28	453.1	0.0

Chapter Nine: DISCUSSION OF SUSPENDED SEDIMENT RATING CURVES

9.1 Overview

This chapter discusses issues and outcomes of the rating curve chapter (Chapter 8). Some general methodological concerns related to sampling and indicators of model fit are outlined initially as they have some implications for the following sections and should be taken into consideration. The rating curves developed are discussed, the results from all sites synthesised, generalisations regarding model choice made and the effect on load estimates assessed. Differences in sediment dynamics between the catchments, based on the optimal load estimates derived from the rating curves, are then discussed by evaluating the sediment to water index, volumetric loss of sediment, effective discharge interval, and the magnitude and frequency of sediment delivery for each catchment. The suspended sediment loads and specific sediment loads are placed in the context of other British studies, and to a limited extent other upland catchments throughout the world, and related to catchment characteristics.

9.2 Methodological concerns

9.2.1 Sampling

In addition to establishing load estimates for each of the catchments the development of the different types of rating curves, in terms of model form and data sub-sets, has indicated some methodological issues which should be noted and the implications for resulting load calculations considered. The concerns include:

(1) Consideration of the number of falling and rising limb samples in the sampled period discharge series and annual discharge series.

(2) The range of discharges for which suspended sediment samples were taken compared with the range of discharges in the annual record.

(3) The distribution of the sampled discharge series in comparison with the annual discharge record.

9.2.1.1 Proportions of rising and falling limb samples

Consideration should be given to the proportion of suspended sediment samples taken on the rising and falling limb in relation to the numbers in the annual record. It was initially thought that if the relative proportions of rising and falling limb samples in the sampled and annual series were substantially different, bias would be introduced to the load estimates. The physical reasoning behind this is that if the study catchments are supply-limited, and hysteresis analysis (Chapter 10) indicated this, then the SSC for any given discharge on the rising limb would be higher than the SSC on the falling limb. Therefore, if a rating curve was developed from a substantially greater number of samples taken on the rising limb than was representative of the system then the suspended sediment load estimate would be anomalously high. Conversely, if a rating curve was developed from a data set with a higher proportion of falling limb samples, then a lower than actual suspended sediment load estimate would result. However, this proved unfounded, especially in terms of the annual load estimates. For example, the greatest disparity between the number of rising and falling limb samples between the sampled and annual series was at Candleseaves: two-thirds of the sampled series were taken on the rising limb, but only one-third were on the rising limb in the annual series (Table 8.8). If sediment exhaustion was a noteworthy factor, which hysteresis analysis (Chapter 10) and field observations suggest, it was expected that load estimates derived from the all data rating curve would be higher than the estimate derived from separate regressions for the rising and falling limbs. However, the annual load estimate from the rising and falling limb regressions was 1.6 times higher than that derived from the single regression (Table 8.10). This also occurred for Trout Beck: one-third of the sampled series was classified as rising limb compared with one-fifth of measurements in the population series (Table 8.23), but the load estimate derived from the rising and falling models was 1.2 times higher than that derived from the all data model (Table 8.26). However, this phenomenon may be illustrated at Burnhope, at which one-third of samples were taken on the rising limb as opposed to 15% in the annual record (Table 8.3). The difference in the load estimates was only 0.4 t (171.3 t derived from single

regression, 170.9 derived from rising and falling limb regressions). The possible reason for this disparity is explained in the following section.

9.2.1.2 Difference in the discharge series distributions

The rating curve models developed are a summary of the sampled data and the assumption is that the sampled data are representative of the population, but SSC sampling at all sites except Langtae was actively biased towards high flows (storm samples). Despite this, samples taken are assumed to be representative as long as sufficient samples are taken throughout the range of discharge.

It is fundamentally important that SSC samples are taken throughout the range of discharge in the population series. Not sampling at higher values of discharge is a particular problem as low discharges are less important in terms of load estimates and gaps at intermediate discharges are generally constrained by samples taken at lower and higher discharges. Extrapolation of rating curves towards high discharges can cause large errors in load estimates. For example, during the monitoring period at Trout Beck there was a flood with a peak discharge of 44.7 $m^3 s^{-1}$ and the maximum discharge for which a SSC sample was taken was 6.5 $m^3 s^{-1}$. Therefore, the rating curve was unconstrained between 6.5 $m^3 s^{-1}$ and 44.7 $m^3 s^{-1}$, and consequently the annual load estimates varied by six orders of magnitude (Table 9.1). The same problem is evident for Candleseaves and Rough Sike, although to a lesser degree (Table 9.1). The smallest differences between maximum sampled and annual discharge occur in the Langtae and Burnhope catchments and the ratio between the maximum and minimum load estimates is the least for these catchments (Table 9.1).

There is no difference, to one decimal place, between the maximum discharge in the sampled and part-annual records for Langtae. Therefore the errors in load estimates can be attributed to the different model forms as opposed to extrapolation error. However, only one sample was taken at a discharge above 0.8 $m^3 s^{-1}$: therefore if it is not representative, e.g. it was taken when sediment supplies were exhausted, bias will be introduced.

9.2.2 Indicators of model fit

The following section outlines the relative merits and problems associated with R^2, RMSE, diagnostic plots, graphical analysis of the rating curve form and sampled period

load estimate as indicators of model fit, and explains why different models apply in different contexts.

Table 9.1. Unconstrained Q range, the minimum and maximum load estimates and the ratio between them. *Q is in l s^{-1} and load in kg for Candleseaves. Swinhope was not included as the annual Q record is incomplete.

Site	Unconstrained Q range, $m^3 s^{-1}$	Minimum load, t	Maximum load, t	Ratio of maximum/minimum
Trout Beck	6.5 – 44.7	184.4	877,124,138.7	4756638.5
Rough Sike	0.7 – 1.9	16.1	94.0	5.8
Langtae	0.9 – 0.9	23.4	37.9	0.6
Burnhope	2.7 – 2.9	125.9	437.7	3.5
Candleseaves*	3.7 – 10.5	33.6	275.6	8.2

9.2.2.1 Coefficient of determination

The coefficient of determination (R^2) is commonly used, across many disciplines, to assess the goodness of fit of models by comparing observed and predicted data series. However, with regard to its application to suspended sediment rating curves there are two main problems. The first, and the most important, is the effect of the scale of the explanatory, or to be specific to sediment rating curves, the scale of discharge. R^2 is calculated from the differences between the actual and predicted values with no regard to the scale of the explanatory variable. As SSC is multiplied by discharge to estimate load, differences at higher values of discharge are more important (Figure 9.1).

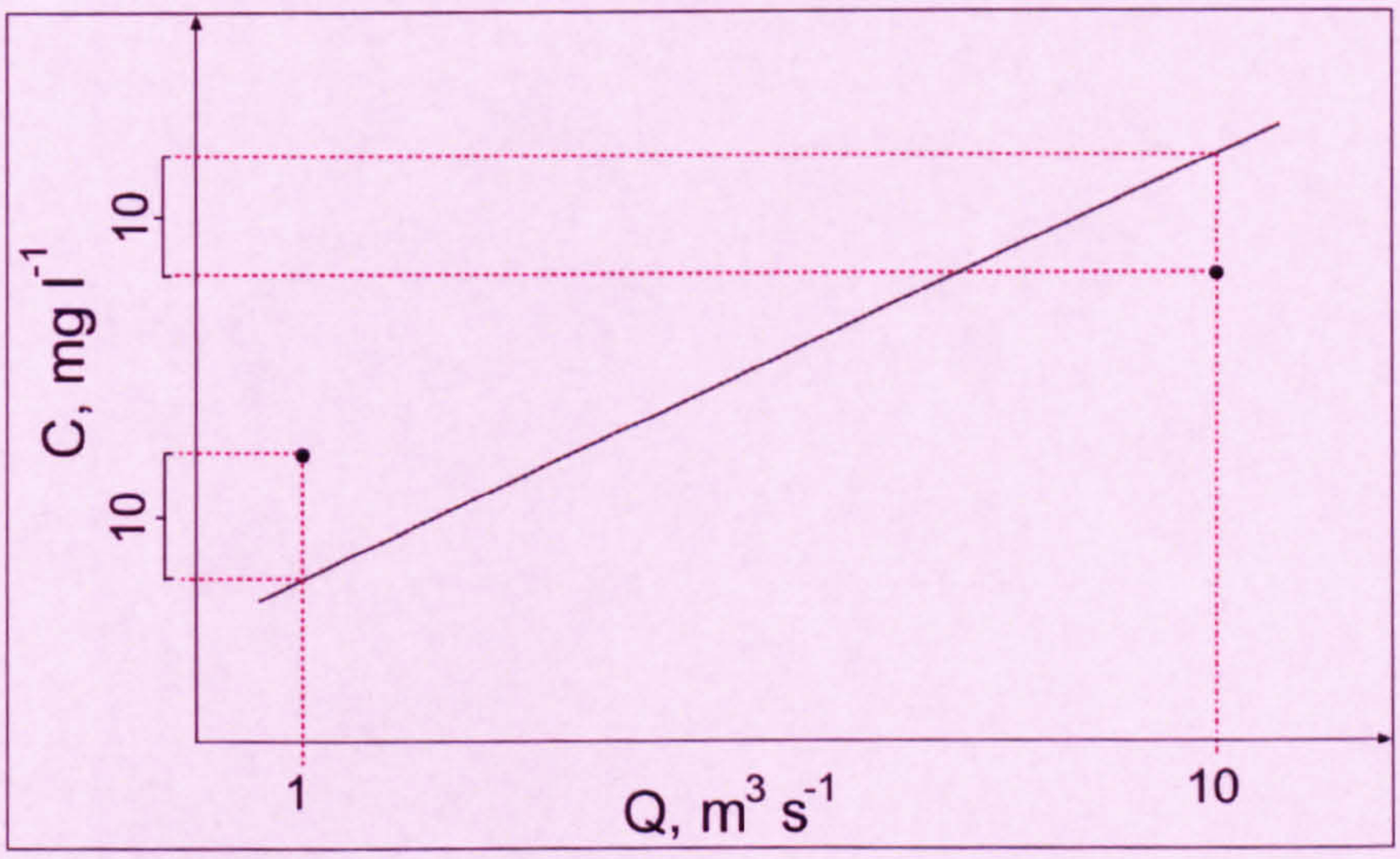

Figure 9.1. Schematic of the effect of the scale of the explanatory variable on R^2.

This is complicated further by the proportion of measurements at each discharge: is poor model fit a result of frequently occurring low discharges or intermediately occurring intermediate discharges or infrequently occurring high discharges? This is

illustrated by the linear regression rating curve for Rough Sike. It has an R^2 at least 0.14 lower than any of the GLM models, but has the second most accurate sampled period load estimate (Table 8.16).

Second, in investigations of this kind there are errors associated with the measured variables: for example, stage measurement error, stage-discharge calibration error and SSC determination error. Some of these errors are approximately constant. For example, the absolute error associated with the analytical determination of SSC is constant regardless of whether the concentration is 2 mg l^{-1} or 200 mg l^{-1}. Therefore the relative magnitude of these errors is more important at lower values. For example, if the SSC measurement error is 1 mg l^{-1} then this is a 50% error if the determined SSC is 2 mg l^{-1} and a 0.5% error if the determined SSC is 200 mg l^{-1}. Therefore, rating curves developed for sites with generally lower SSCs are likely to have lower R^2 values than sites with higher SSCs. This is difficult to assess with such noisy data sets. However, with respect to mean sampled SSC, the rank order of the catchments, starting with the highest mean SSC, is: Swinhope, Burnhope, Rough Sike, Trout Beck, Candleseaves and Langtae. With reference to the basic linear regression model the R^2 follows this pattern with the exception of Trout Beck, which has the highest R^2, and Rough Sike, which has the lowest R^2.

Other drawbacks of R^2 include that it summarises the fit in a single figure and does not take into account the effect of the distribution of the data (a high R^2 may be an artefact of one outlier). Additionally, if developing a rating curve from transformed series, statistical packages commonly give the R^2 of the model fit in terms of the transformed series and not the raw data series. This can give misleading results if misinterpreted. Despite these drawbacks R^2 is advantageous, as it can be compared across models, even if units differ.

9.2.2.2 Root mean square error

The root mean square error (RMSE) is advantageous over R^2 as a measure of model fit as it gives more weight to the errors at higher values of the explanatory variable. RMSE also returns an error in the same units as the response variable. The magnitude of the RMSE varies from <1 to 8 mg l^{-1} with an average of 3.1 mg l^{-1} for the basic rating curve models. These differences are within the range of other errors involved, e.g. SSC

determination, stage-discharge calibration etc. and therefore limit the importance of using RMSE as a means of choosing the most superior model.

9.2.2.3 Model diagnostic plots

Diagnostic plots are very important in assessing model fit as they are the only means of identifying anomalous data points which may be causing a deceptively good or poor model fit as measured by R^2 or RMSE. Diagnostic plots also suggest whether the assumptions of the model have been met and therefore indicate if the model is reliable. In addition, they allow insight into differences in the model fit at different scales of the explanatory variable. For example, the residuals versus predicted plots indicate if the model fit is better at any given range of discharge. However, comparison of diagnostic plots between models is subjective.

9.2.2.4 Graphical analysis of rating curve form

Graphical analysis of rating curve form is a very subjective measure of model fit. However, it highlights ranges of discharge over which the model is a poor, fair or good fit. This then gives some indication of the likely accuracy of the model fit, especially when considered in relation to the distribution of the discharge series.

9.2.2.5 Sampled period load estimates

As continuous or quasi-continuous records of SSC do no exist for any of the study sites there was no way of independently assessing the accuracy of the models. To gain some insight into the success of each model in determining sediment loads the loads of each of the monitored storms were predicted using each model, compared with the actual load estimates and the percentage differences calculated. Care must be taken when interpreting these, as they are an indication of the accuracy of each model in calculating those storm estimates, not annual loads. The Trout Beck results illustrate this point well. The sampled period load estimates derived from the gamma-identity and Gaussian-log GLMs with discharge as the explanatory variable were among the most accurate; percentage differences of 0.0 and –1.0 respectively (Table 8.25). However, the annual load estimates calculated by the same model were gross over-estimations: 1.5 and 877 million t yr^{-1} respectively. The correlation between the precision of the sampled period load estimates and the annual load estimates is dependent on the distribution between the sampled discharge series and annual discharge series. Study sites which have a similar distribution, in terms of the range of the annual discharge which was sampled

and the frequency of each discharge, will have similar accuracies with regard to the sampled period and annual load estimations. If the distributions are different, as they invariably are, then the percentage difference in sampled period load can not be assumed to be applicable to the annual load estimates. However, as most sediment is transported during storm events this is a justifiable indicator of model fit. Also, when assessing the worth of the different rating curve models the sampled period load estimates are useful in determining if the extra time and increased number of parameters are justifiable. Although the percentage errors may differ in the annual series it indicates if the processes which the adaptations are trying to simulate are discernible, especially as such processes are less likely to be noticeable in the annual series, given increased noise.

9.3 Synthesis of rating curve results

9.3.1 Comparison of basic models

The most appropriate model for each catchment was chosen on the basis of R^2, RMSE, sampled period load estimation and graphical analysis of the rating curves and diagnostic plots. The suitability of the models for extrapolation was checked by calculating the predicted SSC for the highest discharge in the annual record (Table 9.2). Some models proved physically implausible on this basis. For example, the gamma-log model with Q as the explanatory variable for Trout Beck predicted SSC to be 5 t l^{-1}.

Linear regression corrected for back-transformation bias by smearing proves to be the most widely applicable model (Table 9.2). There are some connections between catchment characteristics and the optimal model. Linear regression was optimal for all study sites except Burnhope and Trout Beck (Table 9.2). Burnhope and Trout Beck are the largest catchments, have the lowest average channel slopes, are the highest order (although Swinhope is the same order as Burnhope) and have the highest mean annual flows (Table 5.1). Therefore, it can be generalised that linear regression is optimal for the smaller, steeper, higher order, catchments with lower discharges. There is no relation between catchment geology and soil type and optimal model for the range of catchments studied in this investigation.

In terms of choosing a generic model for all catchments the linear regression model corrected by smearing produces reasonable load estimates for all catchments. The only sizeable difference in load estimate between the chosen model and smearing-corrected

Table 9.2. Selected models for each catchment, the maximum Q in the sampled and annual records, the maximum observed and predicted SSCs and the annual/part-annual load estimates. *For Candleseaves Q is in l s^{-1} and load in kg.

Catchment	Chosen model	Maximum Q, m^3 s^{-1}		Maximum SSC, mg l^{-1}		Load estimate, t
		Sampled	Annual	Observed	Predicted	
Burnhope	Gamma-identity, Q	2.72	2.86	389.1	69.0	287.7
Candleseaves*	Linear regression with SM	3.69	10.45	113.6	14.6	58.4
Langtae	Linear regression with SM	0.87	0.90	125.1	10.9	33.5
Rough Sike	Linear regression with LNCF	0.67	1.87	126.0	38.1	23.2
Swinhope	Linear regression with SM	4.09	-	393.7	-	-
Trout Beck	Gaussian-log, ln Q	6.53	44.68	59.3	579.0	453.1

linear regression model was for Trout Beck: the smearing estimate was 282.5 t compared with 453.1 t derived from the assumed optimal model. However, this smearing-corrected linear regression produces the nearest load estimate to that derived from the optimal model (Table 8.25). On this basis it can be stated that if a generic model is required, linear regression corrected for bias by smearing is the most robust. However, this generalisation is based on a selection of relatively small upland catchments in northern England and should be applied to rivers in different settings with caution.

The most prominent, and in many ways the most obvious, outcome of the development of ten different basic rating curves using different model forms, but the same data set, is the variability in load estimates (Figure 9.2). No load estimates were made for Swinhope given the uncertainty in the stage-discharge calibration. The gamma-identity models with ln Q as the explanatory variable for Langtae and Trout Beck are missing as the models did not converge. The Langtae load estimates are visually the least variable (Figure 9.2), the ratio between the minimum and maximum load estimate is the lowest and the coefficient of variation is the least (Table 9.3). Burnhope, which is the adjacent

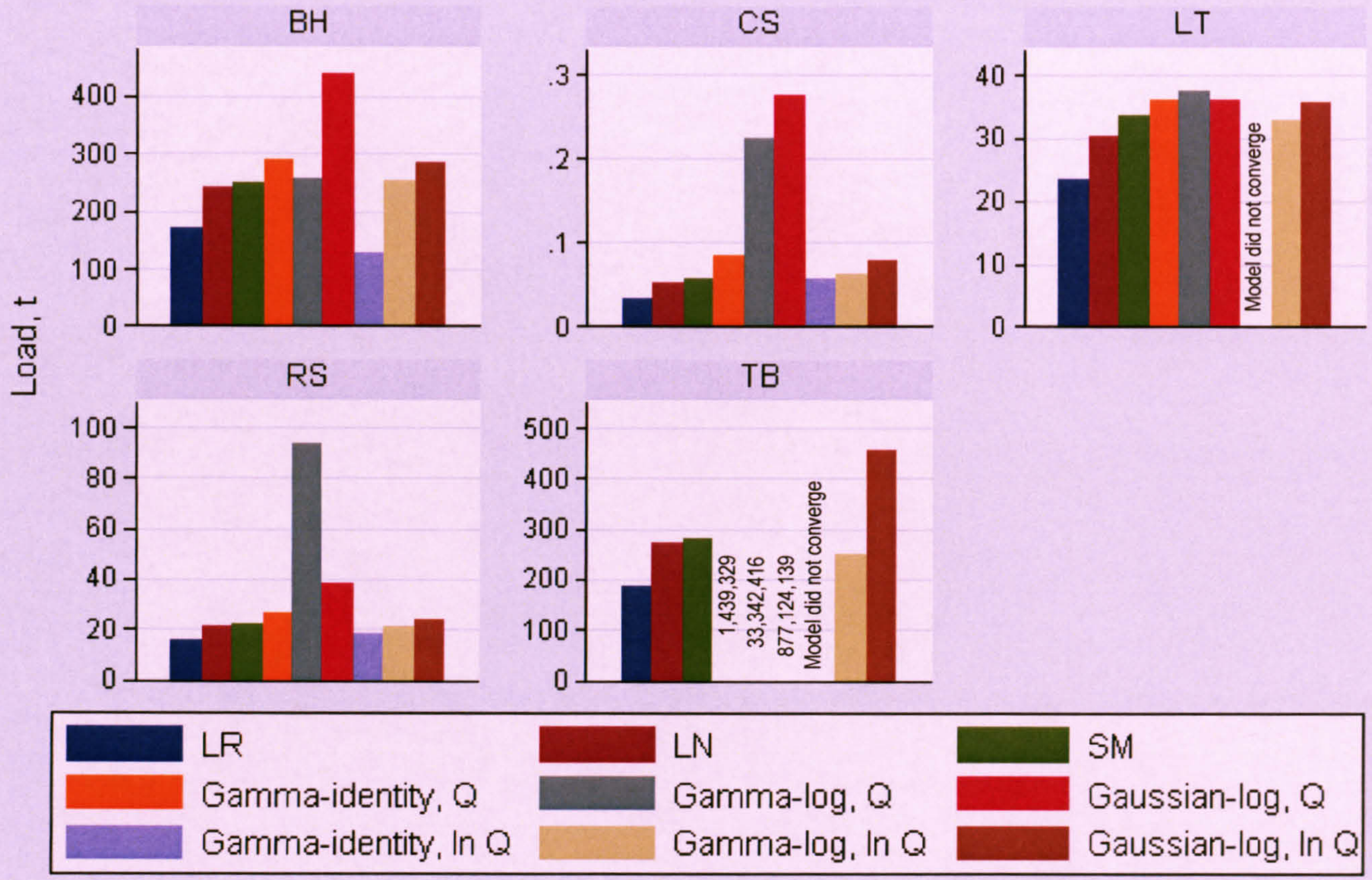

Figure 9.2. Load estimates generated by each of the basic models for the study sites. All load estimates are annual except Langtae (12th July 2000 – 20th March 2001) and Burnhope (16th May 2000 – 20th March 2001).

catchment to Langtae, has the second least variable load estimates (Figure 9.2 & Table 9.3). The lower variability in load estimates in these catchments can not be easily attributed to any of the catchment characteristics (Table 9.3 & 5.1). However, the discharge record is noticeably different for these catchments: the part-annual discharge records of Langtae and Burnhope have substantially lower coefficients of variation, skew and kurtosis compared with Rough Sike, Trout Beck and Candleseaves (Table 9.4). This may be a product of the shorter discharge record: 0.65 and 0.85 of the year for Langtae and Burnhope respectively (sampling was curtailed due to foot and mouth). The trend for the variability in load estimations to increase with increased variability in the discharge regime also applies to the remaining three catchments: Trout Beck has the most variable load estimates (Table 9.3) and also the most variable discharge record (Table 9.4); Candleseaves has the next most variable load estimates and the next most variable discharge record; and Rough Sike the third most (Table 9.3 & Table 9.4). Therefore, it can be stated that channels with a more variable discharge regime are more sensitive to the model chosen for rating curve development.

On the basis of the Trout Beck analysis it can be shown that catchments which experience a very large flood during the monitored period are very sensitive to model choice. This is clearly evident on comparison of the load estimates obtained by the different models: 184.4 to 877,124,139 t (Figure 9.2). This results from limited data to constrain the rating curve at the high discharges. This is especially bad for Trout Beck as the largest Q for which SSC samples were obtained was 6.54 $m^3 s^{-1}$ and the greatest Q on record was 44.68 $m^3 s^{-1}$. The gradients of the rating curves developed using gamma-identity, gamma-log and Gaussian-log GLMs with discharge as the explanatory variable become progressively steeper as discharge increases (Figure 8.34); therefore a small change in discharge at high values of discharge is associated with a substantially higher value of SSC and therefore results in high load estimates.

Table 9.3. The mean, standard deviation, maximum:minimum load estimate ratio and coefficient of variation of annual load estimates. All loads in t except for Candleseaves which is in kg.

Site	Mean	Median	Max/min estimate	St. Dev.	CV%
Burnhope	256.3	251.5	3.5	86.1	33.6
Candleseaves	103.6	62.9	8.2	85.6	82.7
Langtae	33.1	34.6	1.6	4.5	13.7
Rough Sike	31.3	21.8	5.8	24.4	78.0
Trout Beck	113,988,415.7	367.8	4,756,638	308,571,286.4	270.7

Table 9.4. Characteristics of the annual/part-annual discharge record. All discharges in $m^3 s^{-1}$ except for Candleseaves which is in $l s^{-1}$.

Measure	Burnhope	Candleseaves	Langtae	Rough Sike	Trout Beck
Number of samples:					
Total	29552	35136	22853	26718	35040
Rising	5069	12330	5542	10119	7741
Falling	24483	19809	18549	16599	27299
Range	0.00 - 2.86	0.00 - 10.45	0.00 - 0.90	0.00 - 1.87	0.01 - 44.68
Mean	0.51	0.23	0.22	0.06	0.62
Median	0.39	0.04	0.18	0.02	0.18
Standard deviation	0.37	0.71	0.16	0.13	1.35
CV%	72.2	310.50	72.5	209.7	217.6
Skew	1.96	6.74	1.11	4.82	10.6
Kurtosis	7.57	61.65	3.99	37.98	252.3

9.3.2 Rating curve adaptations

Eight load estimates (seven if the lag model was not applicable) based on adapted linear regression rating curve models were developed for each site. The effect of these different models on sampled period load estimates was investigated. The sampled period load estimate was used as the principal indicator of model fit as it provides the only comparable quantifiable measure. Most rating curve adaptations have more than one regression and hence more than one R^2, RMSE, and set of diagnostic plots and no accurate annual load estimate is available for any of the catchments.

The difference between the data sub-set regression gradient and intercepts within the same model (e.g. rising and falling limb) were tested by a Wald test, with results reported as a chi-square statistic, to established if the differences were statistically significant (at a 5% probability level). The gradient, or *a*, is the power in the back-transformed equation (eq. 4.3 & 4.4) and the intercept, or *b*, is in mg l^{-1}. The rationale for this was to assess if it was considered statistically worthwhile developing the limb, season, split-year, split-year and season, discharge class and lag adapted models. If the differences between regression gradients/intercepts are significant it suggests that they did not occur by chance, i.e. there is a physical reason. For example, a significantly higher rising limb gradient could be attributed to higher sediment availability on the rising limb and a significantly higher summer intercept could be attributed to more sediment ready for transport compared with the winter.

There were significant differences in the gradients of the data sub-sets of all models at Burnhope, all models except discharge class at Candleseaves, all models except limb at

Rough Sike and all models except split-year and discharge class at Swinhope and Trout Beck (Figure B.1). At Langtae there was only a significant difference between the split-year data sub-sets (Figure B.1). The matrices on Figure B.1 show which data sub-sets gradients were statistically significant when the data were divided by season and split-year and limb.

None of the intercepts were found to be significantly different at Langtae (Figure B.2). The differences between the limb, season and split-year and limb data sub-set intercepts were significant at all sites except Langtae (Figure B.2). The split-year intercepts were significantly different for Burnhope, Candleseaves and Swinhope (Figure B.2). The difference between the discharge class and all data regression intercepts was only significantly different at Candleseaves (Figure B.2). Trout Beck and Candleseaves were the only sites for which a lagged model was appropriate and the difference between the lagged and all data model intercepts was only significant at Candleseaves (Figure B.2). The matrices on Figure B.2 indicate which data sub-sets intercepts were statistically significant when the data were divided by season and split-year and limb.

The difference in intercepts between the different data sub-sets is, to some degree, dependent on the gradients as high gradients promote high (either negative or positive) intercepts, although there are several differences between the analyses (Figures B.1 & B.2). Also, large data sets, as in this study, promote significant differences as the *P*-value of a test is dependent on the sample size; even a small difference can be statistically significant (Freedman *et al.*, 1998). Given these methodological considerations, especially the effect of large sample sizes, the results of the significance testing will not be used to interpret the rating curve adaptations.

9.3.2.1 Value of adaptations for all sites

Figure 9.3 indicates the percentage difference of the sampled period load estimates obtained from the adapted rating curves from the all-data model. Therefore, negative values show that the adapted model produced a less accurate load estimate than the all-data model and positive values show an improved load estimate. Figure 9.4 shows the percentage deviation from the actual load and as all adapted model estimates are under-predictions all values are negative.

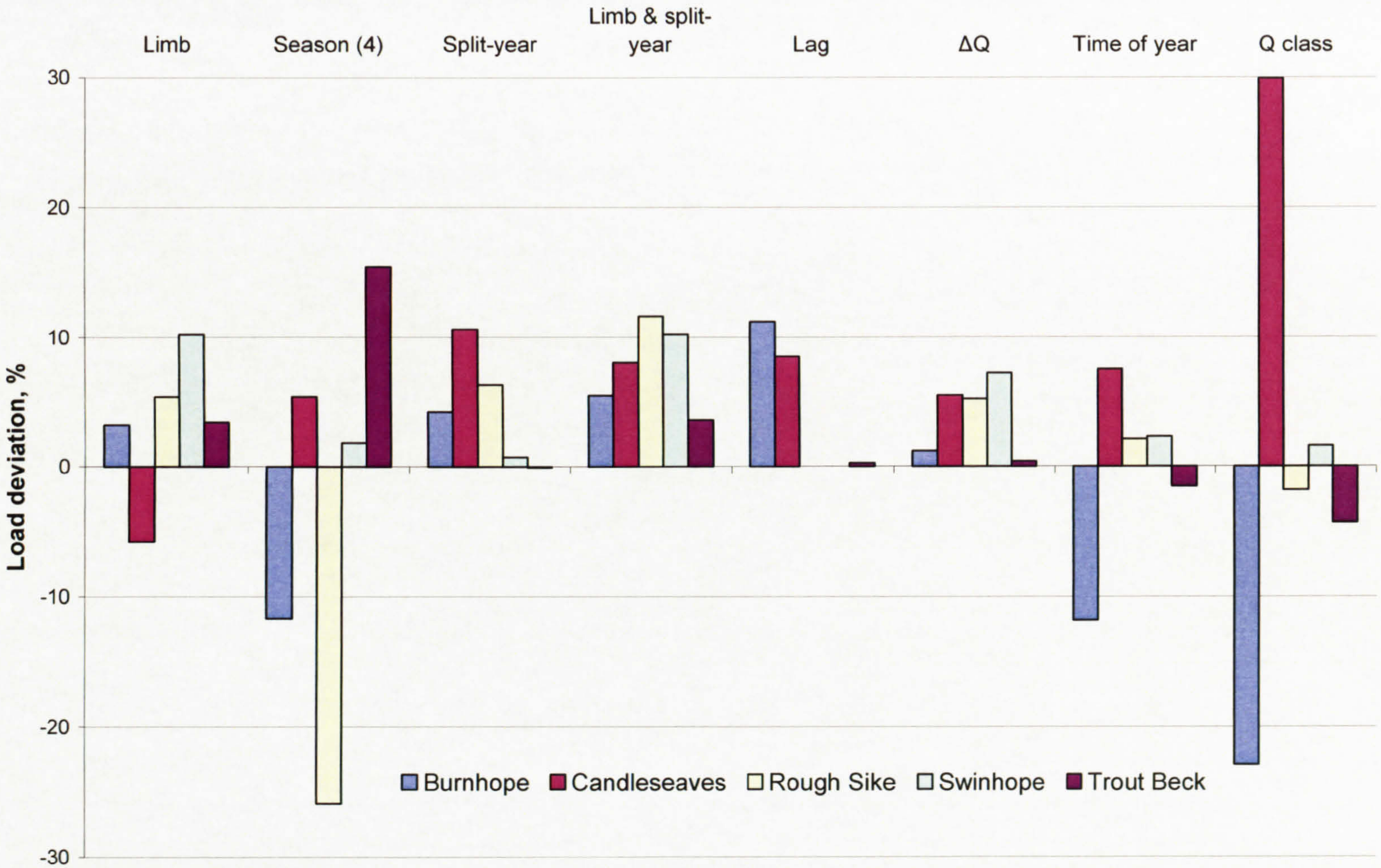

Figure 9.3. Percentage deviation of the adapted rating curve sampled period loads estimates from the all-data sampled period load estimate. Negative deviations indicate that the adapted rating curves produced a less accurate load estimate than the all-data model and positive values indicate a more accurate load estimate.

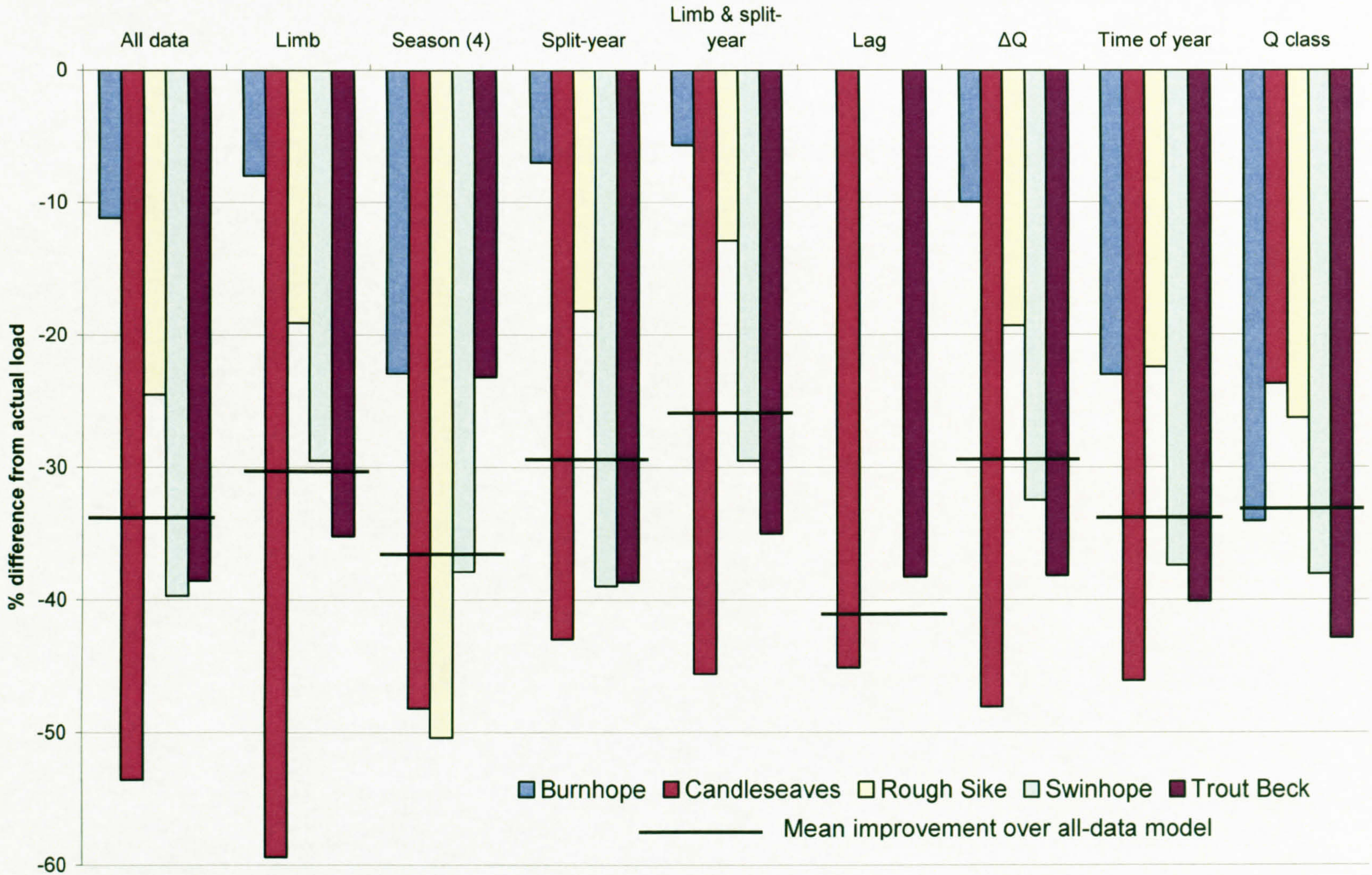

Figure 9.4. Comparison of the effect of rating curve adaptations on sampled period load estimates. Zero represents the actual load.

The accuracy of nine load estimates was decreased by the adapted models (Figure 9.3). The only models which did not cause a decrease in load accuracy at any of the sites were: (1) regressions developed from data sub-sets defined by limb and split-year; and (2) a regression with change in Q as a second explanatory variable (Figure 9.3).

All the adapted rating curve load estimates under-predict the true load (Figure 9.4). The mean precision indicates that, on average, calculating load from four separate regressions as defined by season (spring, summer, autumn and winter) and by lagging the data, produces less accurate load estimations compared with the basic all-data model (Figure 9.4). Adding time of year and using the discharge class method, on average, produces a similar mean error compared with loads estimated from the all-data rating curve (Figure 9.4). Dividing the data by limb, split-year, or adding change in discharge as a second explanatory variable caused an average increase in accuracy of ~4% (Figure 9.4) and dividing the data by limb and split-year resulted in the largest increase in accuracy: 8% on average (Figure 9.4).

9.3.2.2 Limb

Dividing the data by limb resulted in improved sampled period load estimates for every catchment except Candleseaves (Figure 9.3). The improvements varied from 3% to 10% with a mean of 3.3%. The smallest improvements in load estimates were for the largest catchments (Burnhope and Trout Beck) (Figure 9.3).

The data were separated into rising and falling limb to incorporate the effect of sediment exhaustion and timing of sediment delivery on SSC. *A priori* reasoning suggests (1) if less sediment is available on the falling limb, due to sediment exhaustion, the rising limb rating curve should plot above the falling limb curve. Alternatively, if the travel times are longer and the distant sources contribute more sediment than local sources the falling limb may plot above the rising limb curve. The gradient of the rising or falling limb rating curve may be steeper dependent on the characteristics of sources (i.e. continuity in supply, discharge at which sources are accessed and rate of supply) and travel distances. The magnitude of the gradient will partially control the magnitude of the intercept.

The rising limb rating curves have higher intercepts than the falling limb rating curves at all sites (Table 9.5). This affirms that sediment exhaustion is an important process in

the study catchments and suggests sediment sources are local to the channel. Out of the limited studies of suspended sediment in the British uplands Wilkinson (1971), Oxley (1974), Crisp & Robson (1979) and Evans & Burt (1998) also categorised SSC-discharge pairs into rising and falling limb and generated regression equations for each. Crisp & Robson (1979) and Evans & Burt (1998) examined Rough Sike and found the same trend as in this investigation: the rising limb intercept was greater than the falling limb intercept (Table 9.6). Wilkinson (1971) also found the intercept of the rising limb was higher, for Langden Brook, central Pennines. Oxley (1974) studied two small catchments in Montgomeryshire (Powys) and found the opposite trend: the intercept of the rising limb was less than that of the falling limb (Table 9.6). However, the relationship was derived from untransformed data and the gradients were very high and as intercepts, to some degree, are an artefact of the gradient as a slight increase in the gradient would have had a substantial effect on intercept.

The gradients of the rising limb rating curves are greater than those of the falling limb curves at all sites except Candleseaves (Table 9.5). Therefore ln C increases more for a given increase in ln Q on the rising limb than it decreases for a decrease in ln Q of the same magnitude on the falling limb. The majority of the hydrographs and sedigraphs (Figures 10.2, 10.5, 10.7, 10.9 & 10.12) exhibit a steeper rising limb than falling limb and the steeper rising limb rating curves are partially a result of this. The steep rise of ln C can be explained by the entrainment of readily available sediment, i.e. the sediment is entrained as opposed to eroded and entrained, at the beginning of an event. As ln Q increases the stage rises and more sediment sources are accessed which allows this trend to continue throughout the rising limb. This sediment is most likely sourced from the channel bed, banks and near channel sources, such as floodplains. Rising limb SSC may be less supply-restricted than the falling limb and therefore the rate of change in SSC is higher and more in line with theoretical transport thresholds. Also, higher velocities are required to entrain and erode sediment than required to retain it in suspension (Hjulström, 1935). As a result the rate of decrease in SSC is prone to be less than the rate of increase, especially with regard to finer particles. The rising limb of Rough Sike, as studied by Crisp & Robson (1979) and Evans & Burt (1998), and of Ebyr North and South (Oxley, 1974) also had higher gradients on the rising limb than on the falling limb (Table 9.6). In contrast, the falling limb gradient of Langden Brook was steeper (Table 9.6). This could be attributed to the limited number of samples.

Table 9.6. Regression parameters associated with SSC data sub-sets defined by limb and season for other British upland studies.

Reference	River	Region	Area, km^2	Response variable	Explanatory variable	Data sub-set	*a*	*b*	R^2
Wilkinson (1971)	Langden Brook	Central Pennines	15.34	Log C, mg l^{-1}	Log Q, l s^{-1}	Rising	–2.20	1.14	0.70
						Falling	–3.82	1.59	0.65
						Summer	–2.24	1.15	0.70
						Winter	–2.62	1.25	0.66
Oxley (1974)	Ebyr North	Powys	0.07	SSC, mg l^{-1}	Q, l s^{-1}	Rising	0.79	2.00	0.79
						Falling	1.79	0.74	0.66
	Ebyr South		0.09	SSC, mg l^{-1}	Q, l s^{-1}	Rising	7.15	5.81	0.69
						Falling	2.89	1.03	0.76
Stott *et al.* (1986)	Kirkton	West Scotland	6.85	$\log_{10} L$	$\log_{10} Q$	Autumn – rising		3.12	0.70
						Autumn – falling		3.85	0.74
						Winter		0.25	0.00
						Spring		1.95	0.41
						Summer		2.67	0.41
	Monachyle		7.70	$\log_{10} L$	$\log_{10} Q$	Autumn – rising		1.72	0.35
						Autumn – falling		1.12	0.23
						Winter		1.78	0.69
						Spring		1.33	0.32
						Summer		1.14	0.25
Evans & Burt (1998)	Rough Sike	North Pennines	0.83	log C	log Q	All	1.2	0.35	0.21
						Rising	1.7	0.68	0.48
						Falling	1.0	0.20	0.10

Table 9.5. Intercepts and gradients of rising and falling limb linear regression models. The numbers in brackets are the standard errors.

Site	Intercept			Gradient		
	Rising	Falling	Difference	Rising	Falling	Difference
Trout Beck	1.79 (0.09)	1.32 (0.05)	0.47	0.87 (0.07)	0.67 (0.03)	0.20
Rough Sike	3.59 (0.18)	2.45 (0.09)	1.14	0.49 (0.10)	0.30 (0.04)	0.19
Swinhope	4.10 (0.13)	3.47 (0.09)	0.63	1.04 (0.08)	0.81 (0.06)	0.23
Burnhope	3.02 (0.04)	2.42 (0.03)	0.60	1.88 (0.08)	1.63 (0.04)	0.25
Langtae	2.22 (0.14)	1.95 (0.07)	0.27	0.38 (0.07)	0.35 (0.03)	0.03
Candleseaves	1.68 (0.09)	1.13 (0.09)	0.55	0.19 (0.06)	0.40 (0.05)	–0.21

Only Candleseaves has a lower gradient on the rising limb than on the falling limb (Table 9.5). The gradient is low at 0.19 (Table 9.5). Examination of the scatter plot suggests that this may be a function of the data fitting procedure (Figure 9.5). The regression line is influenced by a cluster of points (from three storms) from –1.0 to 0 ln Q (Figure 9.5). A line fitted visually, using the upper and lower limits of the data cloud as a guide, would be steeper (Figure 9.5). The cluster of data points in this region may be caused by limited sediment supply as a result of previous storms depleting sediment supplies as found by Evans & Yang (in prep) (Figure 2.15). The gradient of the rising limb rating curve is much lower than for the other catchments (Table 9.5). The Candleseaves catchment is very small and is covered with dense heath vegetation. As a result the dominant sediment sources are the channel bed and channel banks. At the beginning of storms there is a sharp peak in SSC as sediment is entrained from the bed (Figure 10.5). As the storm progresses there is limited sediment for transport and therefore SSC can not increase as much per increase in ln Q. In addition, as the dominant sediment type is peat, which has a low density (dry density of 0.15 t m^3 (Warburton, pers comm.)); therefore, a larger volume of peat has to be transported to increase the SSC compared with mineral sediment (dry density 1.20 t m^3 (Warburton, pers comm.)) and this also promotes a less steep regression line. Furthermore, once entrained the peat will settle out very slowly; peat is very easily entrained and very hard to deposit.

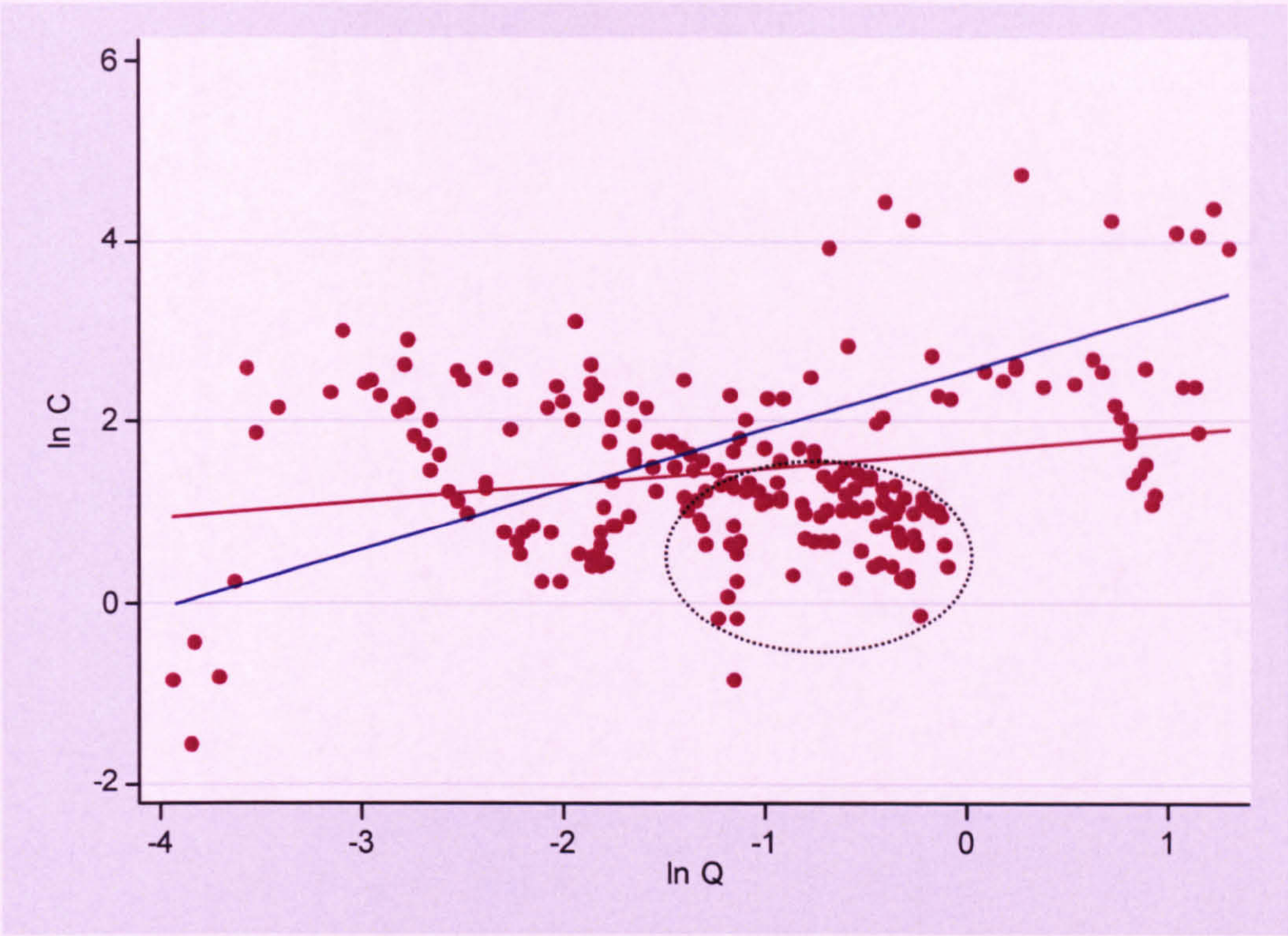

Figure 9.5. Effect of a cluster of data points, highlighted by ellipse on the rising limb rating curve for Candleseaves. The maroon line is the linear fit (gradient = 0.19) and the blue line is positioned by eye (gradient = 0.65).

Some of the interpretation of intercepts and gradients in the literature are confirmed by the rising and falling limb regression models developed in this study. Peters-Kummerly (1973) suggested that higher intercepts were indicative of more sediment available for transport. In the context of rising and falling limbs, in the sediment supply-limited systems of this investigation, this holds true: there is more available sediment on the rising limb and the intercepts are generally higher. Peters-Kummerly (1973) also suggested that higher gradients indicate more erosive power. In this case it is more the availability of sediment to erode than a difference in erosive power between the rising and falling limbs.

Asselman (2000) suggested that there was more variation in SSC for a given discharge if the gradient was higher, although this was based on a much larger range of catchment sizes. There appears to be more variation in SSC on the falling limb for Langtae (Figure 8.21), on the rising limb for Candleseaves (Figure 8.17): the variability is approximately equal at the other sites (Figures 8.13, 8.25, 8.30 & 8.35). Doubt is cast on the relative variability of the rising and falling limbs of Langtae and Candleseaves given the disproportionate number of samples taken on each limb (Table 9.4). Therefore, it is not

possible to confirm this proposal based on the data of this study, but it is suspected that there is not more variation in ln C with higher rating curve gradients.

Rannie (1977) suggested that higher rating curve gradients were indicative of more sensitive systems. In the context of rising and falling limb regressions this suggests that the systems, with the exception of Candleseaves, are more sensitive on the rising limb than on the falling limb. Once again this sensitivity is related to sediment supply: sediment supply is less sensitive on the falling limb as there is generally less available. Rannie (1977) also suggested the intercept reflects processes operating within a catchment reflective of the catchment characteristics. This is not reinforced by the results of this study, as there is no systematic variation between any characteristics such as area, mean annual flow, drainage density etc. (see Table 5.1 for complete list) and magnitude of the intercept of the rising or falling limb rating curves.

For Trout Beck, Swinhope, Burnhope and Rough Sike, the difference between the gradients of the rising limb and falling limb regression lines is 0.22 ± 0.03; the rising limb has a greater gradient than the falling limb (Table 9.5 and Figure 9.6). Candleseaves may not fit this trend due to the effect of a cluster of points, as demonstrated by Figure 9.5. If the rating curve gradient fitted by eye (Figure 9.5) is used then Candleseaves does fit the trend. However, fitting rating curves by eye is very subjective (Walling, 1977a). Therefore a unit increase in ln Q results in a rate of change in ln C which is 0.22 greater on the rising limb than on the falling limb. The gradients of the rising and falling limb regression lines are different between the catchments (Figure 9.7). Figure 9.7 also illustrates the differences in rate of response to changes in ln Q between the catchments.

This 0.22 difference between the gradients of the rising and falling limb regression equations is a curious observation and perhaps indicates some form of larger scale control on the relative SSCs between the rising and falling limbs in upland systems. There is no evidence of this trend in the British upland literature, but its form may depend on the model development procedure. This pattern must reflect sediment supply and transport processes common to all the catchments, especially considering the difference in the magnitude of the gradients. A possible explanation is that discharge is driving it. The hydrographs will generally be roughly the same shape between catchments, with an asymmetric form reflecting the greater change in discharge on the

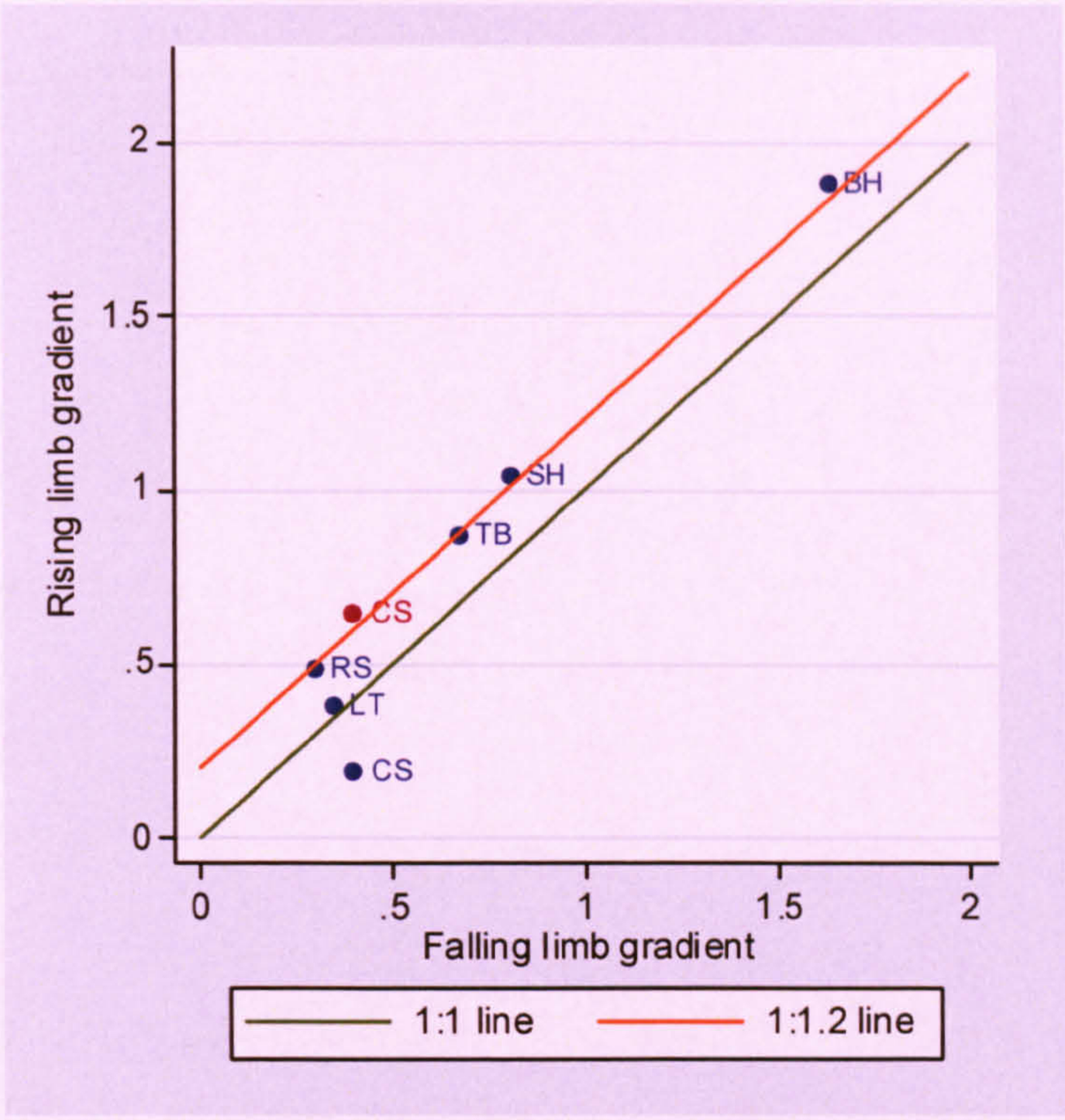

Figure 9.6. Scatter plot of the relationship between the rising and falling limb regression equation gradients. BH = Burnhope, CS = Candleseaves, LT = Langtae, RS = Rough Sike, SH = Swinhope, TB = Trout Beck. The blue Candleseaves point is the gradients from all data and the red point is the gradient with the cluster of points removed.

rising limb than on the falling limb. Given that higher SSC are associated with quicker changes in discharge (Bogen, 1987; section 26.2.1), and the strong control of discharge over SSC this pattern will be replicated, to some extent, in the SSC record. Given that these factors are likely to be consistent between each of the catchments it could explain the 0.22 difference. The difference in gradients indicates more sediment available in general. If this is the case then it is perhaps not surprising given the similar nature of the catchments. Candleseaves only fits the pattern if the cluster of data points is removed. However, Candleseaves, to some degree, may not be expected to fit the pattern as it is a grip and therefore is artificial in terms of morphology and sediment sources. The fixed-interval sampling may obscure the pattern at Langtae.

In summary, it can be postulated that higher intercepts and higher gradients on the rising limb are a feature of most upland UK catchments due to sediment availability: there is generally more sediment available for transport on the rising limb which gives a higher intercept and sediment ready for transport is entrained on the rising limb which results in a steeper gradient.

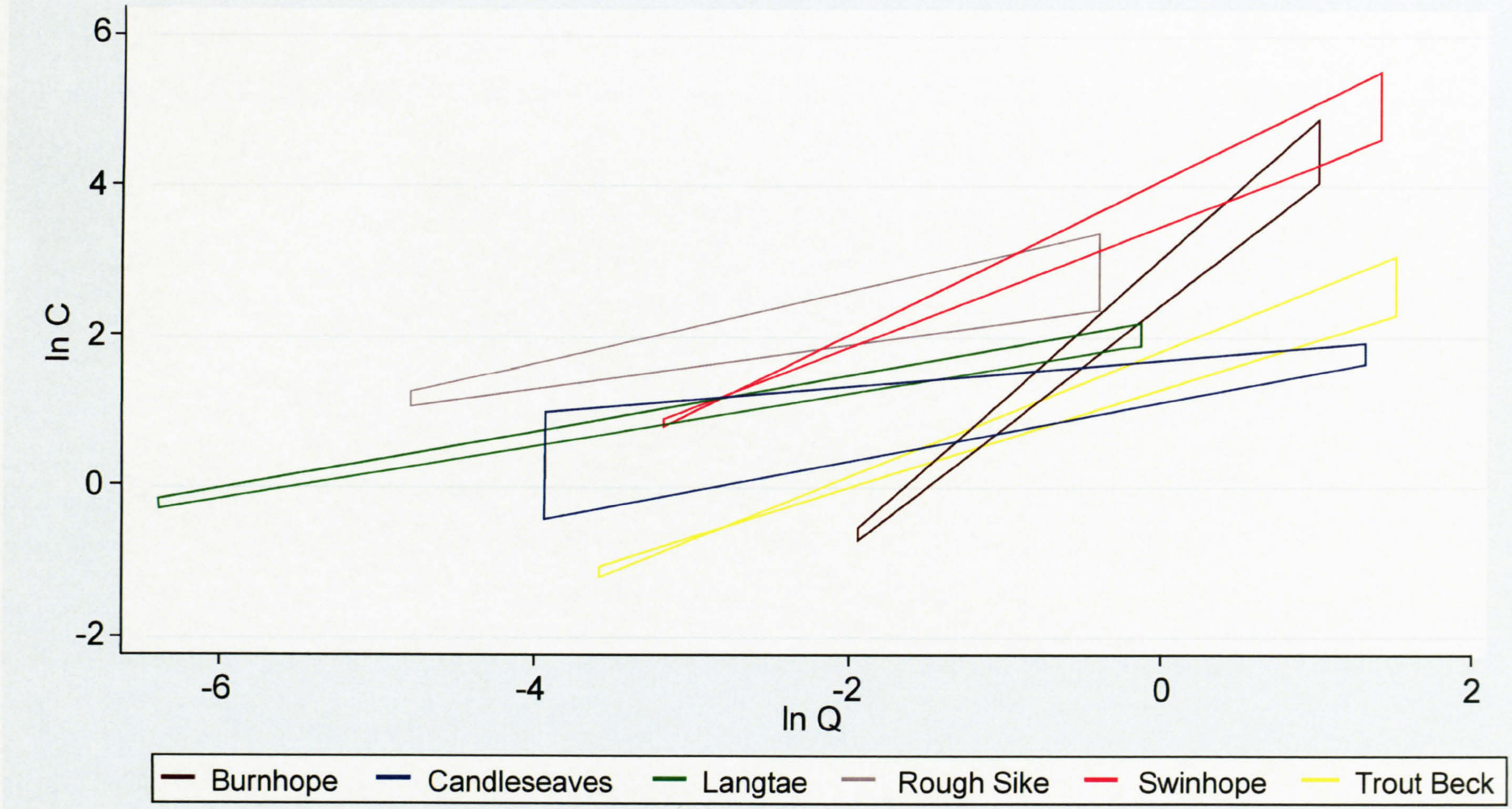

Figure 9.7. The relationship between the rising and falling limb regression equations for each site. The shaded areas area bounded by the rising limb and falling limb regression lines.

9.3.2.3 Season

Season was investigated by categorising the data into summer and winter (split-year); spring, summer, autumn and winter; and by adding sine and cosine variables to account for time of year. Each approach is discussed in turn and then summarised at the end of the section.

9.3.2.3.1 Four seasons

Dividing the data into four seasons produced less accurate sampled period load estimates for Burnhope and Rough Sike (Figure 9.3), and the average change in sampled period load estimate is 3% less accurate (Figure 9.4). There is no consistent pattern in the magnitude of the intercept or gradient with respect to season between study sites (Table 9.7). Some of the variations are within the standard errors indicating limited difference (Table 9.7). Stott *et al.* (1986) categorised data for two paired catchments (Kirkton and Monachyle, west Scotland) into spring, summer, winter, autumn-rising and autumn-falling and there was no consistency between the steepness of the curves (Table 9.6). However, the gradients of the rating curves for Kirkton were steeper than Monachlye for all seasons except winter (Table 9.6). This was attributed to land use: Kirkton was forested and Monachlye was moorland. There is no pattern in the gradient between the sites of this investigation (Table 9.7) which is perhaps indicative of the broadly similar catchment characteristics.

Table 9.7. Intercepts and gradients of the spring, summer, autumn and winter linear regression rating curve models for each study catchment. No SSC samples taken during the spring in Langtae as a result of foot and mouth. The numbers in brackets are the standard errors.

Site	Intercept				Gradient			
	Spring	Summer	Autumn	Winter	Spring	Summer	Autumn	Winter
Trout Beck	1.61	0.80	2.02	–0.21	0.82	0.43	0.19	2.15
	(0.14)	(0.15)	(0.07)	(0.12)	(0.06)	(0.08)	(0.07)	(0.10)
Rough Sike	3.83	3.79	3.54	2.90	1.05	0.46	0.83	0.48
	(0.22)	(0.12)	(0.14)	(0.20)	(0.14)	(0.04)	(0.06)	(0.10)
Swinhope	4.42	5.95	3.32	2.63	0.93	2.17	0.76	0.89
	(0.07)	(0.35)	(0.11)	(0.24)	(0.04)	(0.24)	(0.07)	(0.13)
Burnhope	2.49	1.31	2.34	3.17	2.34	0.73	1.50	1.91
	(0.09)	(0.24)	(0.03)	(0.04)	(0.15)	(0.20)	(0.04)	(0.08)
Langtae		1.97	2.08	2.26		0.34	0.46	0.46
	-	(0.19)	(0.12)	(0.27)	-	(0.05)	(0.08)	(0.24)
Candleseaves	1.10	1.48	2.04	1.43	0.48	0.62	0.56	–0.03
	(0.27)	(0.11)	(0.17)	(0.16)	(0.30)	(0.14)	(0.08)	(0.08)

9.3.2.3.2 Split-year

Dividing data into two seasons resulted in an improvement in the sampled period load estimates for all catchments except Trout Beck (Figure 9.3), but the decrease in load estimate for Trout Beck was only 0.1% (Figure 9.4). The sampled period load estimate is 4.3% more accurate on average. The greatest improvement in load estimate occurred in the smallest catchments (Candleseaves and Rough Sike) (Figure 9.4 & Table 5.1).

The intercept of the winter regression line is higher than the summer regression line for every catchment except Swinhope, although, the standard errors do not overlap for Trout Beck, Rough Sike and Langtae (Table 9.8). This suggests that there is generally more sediment available for transport in the winter than in the summer. However, the summer and winter regression lines often cross over as a result of the different gradients (e.g. Figure 8.17). Therefore in this case it can only be stated that there is more sediment for transport at the lower discharge in the winter compared with the summer. This does not make physical sense as sediment sources accessed by low flows should be more depleted in the winter, than in the summer, given the higher baseflows. It could reflect more runoff, and hence more suspended sediment transported to the channel, in the winter months, but this is not a convincing argument. Another possible cause is increased sediment supply from the banks released by frost action during the winter. Francis (1987) noted the importance of freeze-thaw as a sediment preparation processes in catchments in Mid Wales. Field observations, including the formation of needle ice, supports this hypothesis. This pattern could also be a reflection of bias in the sampling: the distribution of storm samples throughout the year is more concentrated during the winter (Tables 8.2, 8.7, 8.14, 8.18 & 8.22). This was not an intentional sampling strategy but reflects fewer large events during the summer months. Swinhope is the only catchment with a higher intercept in the summer and the difference between the summer and winter limb regression intercepts is reasonably large (Table 9.8). Some samples were taken during the summer but the sampling was concentrated in the winter months (Table 8.18), so sampling does not entirely explain this anomaly. It can not be attributed to catchment characteristics as none of the catchment characteristics are noticeably different from the other catchments (Table 5.1). The gradients are not particularly large and are very similar (Table 9.8), so the high intercept is not likely to be an artefact of this. The differences could be attributed to fewer freeze-thaw cycles, more favourable conditions for periphyton during the summer, which was flushed out during summer

storm events and thus increased the SSC. The importance of periphyton on SSC was noted by Gilvear & Petts (1992).

The intercepts are fairly consistent in magnitude between catchments in the summer and winter. The intercepts of the summer and winter rating curves are highest in Swinhope, the second highest is Rough Sike, third highest in Langtae/Burnope (summer/winter), fourth highest in Burnhope/Langtae (summer/winter), fifth highest in Trout Beck/Candleseaves (summer/winter) and sixth highest in Candleseaves/Trout Beck (summer/winter) (Table 9.8). From this it can be determined that the level of sediment transport in each catchment is Swinhope > Rough Sike > Burnhope/Langtae > Trout Beck/Candleseaves. Peters-Kummerly (1973) attributed higher intercepts to erosion severity, thus suggesting erosion is highest at Swinhope and lowest in Trout Beck/Candleseaves. Rannie (1977) attributed higher intercepts to the level of process, indicative of catchment character. However, the order cannot be related to quantified catchment characteristics. Therefore the theories of Peters-Kummerly (1973) and Rannie (1977) are not easily applied here.

The gradient of the summer rating curve is higher for Trout Beck, Swinhope and Candleseaves and the gradient of the winter curve is higher for Rough Sike, Burnhope and Langtae (although the differences in the gradients for Trout Beck and Swinhope are within the standard errors) (Table 9.8). Therefore according to Peters-Kummerly (1973) the erosive power is greatest during the summer in Trout Beck, Swinhope and Candleseaves and greatest during the winter in Rough Sike, Burnhope and Langtae. In accordance with Rannie (1977), Trout Beck, Swinhope and Candleseaves are more sensitive during the summer and Rough Sike, Burnhope and Langtae are more sensitive during the winter. These patterns can not be linked to catchment characteristics and so the theories of Peters-Kummerly (1973) and Rannie (1977) are not applicable and reflect the sediment supply limitations in the catchments. However, the most erosive events are likely to occur in the summer given the likelihood of intense convectional rainfall events. Therefore these patterns could reflect the number and intensity of convectional rainfall events during the summer in each of the catchments. Asselman (2000) suggested that high variability in SSC is associated with higher gradients. This holds true for all data sets of this investigation, although the difference in variability is not substantial (Figures 8.13, 8.17, 8.21, 8.25, 8.31 & 8.35).

Table 9.8. Intercepts and gradients of the summer and winter linear regression rating curve models for each study catchment. The numbers in brackets are the standard errors.

Site	Intercept			Gradient		
	Summer	Winter	Difference	Summer	Winter	Difference
Trout Beck	1.44 (0.10)	1.47 (0.06)	–0.03	0.73 (0.05)	0.72 (0.05)	0.01
Rough Sike	3.25 (0.11)	3.37 (0.10)	–0.12	0.33 (0.05)	0.74 (0.05)	–0.41
Swinhope	4.34 (0.09)	3.45 (0.10)	0.89	0.96 (0.06)	0.92 (0.06)	0.04
Burnhope	1.90 (0.10)	2.73 (0.03)	–0.83	1.18 (0.10)	1.79 (0.05)	–0.61
Langtae	2.16 (0.09)	2.35 (0.17)	–0.19	0.40 (0.03)	0.74 (0.14)	–0.34
Candleseaves	1.41 (0.08)	1.76 (0.13)	–0.35	0.70 (0.09)	0.27 (0.06)	0.43

9.3.2.3.3 Time of year

Time of year was used as a means of de-trending seasonality in the data series to improve model fit. Two variables based on sine and cosine were used to achieve this. The influence of the sine and cosine variables is inconsistent between catchments (Figure 9.3). The sampled period load estimate is less accurate for Burnhope and Trout Beck (Figure 9.3) and the average load estimate is 0.3% less accurate than the basic model based on all data (Figure 9.4).

The partial correlation coefficient was calculated to establish how much variability in ln C was explained if two of the explanatory variables (ln Q, sine and cosine) were held constant whilst the other was varied. This indicated that ln Q explains the most variation in ln C in every catchment as the partial correlation coefficient of ln Q is consistently larger than that of the sine and cosine variables (Table 9.9). The catchment with the most prominent seasonal signal is Burnhope (Table 9.9). This is not surprising given the continuity of sampling throughout the year and the large number of fixed-interval samples (Table 8.2). The lack of seasonal signal at Langtae (Table 9.9) is unexpected given the proximity to the Burnhope catchment and the fact that only fixed interval sampling was undertaken. Time of year is a weak influence in the Candleseaves and Trout Beck catchments (Table 9.9). This may be explained by the poor temporal coverage of samples for Candleseaves (Table 8.7), but this does not explain the lack of

influence at Trout Beck (Table 8.22). The most likely explanation is that the storm signals subsume any seasonal signal, especially given the dominance of storm sampling.

Table 9.9. Partial correlation coefficients for ln *Q*, sine and cosine variables. * indicates a significance level of >0.05, all others are significant.

Site	ln *Q*	Sine	Cosine
Burnhope	0.69	0.38	0.34
Candleseaves	0.39	-0.04*	0.24
Langtae	0.38	-0.05*	-0.03*
Rough Sike	0.52	-0.13	-0.35
Swinhope	0.70	0.25	-0.37
Trout Beck	0.67	-0.19	0.01*

9.3.2.3.4 Summary

In summary the inclusion of seasonality in rating curves, by either sub-dividing the data or adding extra variables which summarise time of the year, did not result in markedly improved sampled period load estimates. The split-year model was the most successful approach and resulted in increased sampled period load estimates of 4% on average.

The variability in the parameters of the regression models, regardless of whether the data are sub-divided and separate regressions developed or extra variables are added to simulate time of year, is almost entirely attributable to sediment supply factors. The factors controlling sediment supply are sediment preparation and connectivity to the channel. Sediment preparation within the study catchments is affected by meteorology (e.g. freeze-thaw cycles, wetting and drying) and impacts of flora and fauna (e.g. poaching and autochthonous sediment production). Increased transport efficiency to the channel will be promoted by: lower infiltration rates due to saturation or extreme desiccation (peat will not wet up immediately following drought), less dense vegetation, extent of runoff, rain-induced snowmelt and development of flow pathways on the hillslope. Using these factors it is possible to argue that the magnitude of the intercept and gradient should be greatest in any season given a combination of current hydrological and meteorological responses and the short-term hydrological and meteorological history of the catchment. Therefore, the lack of pattern in the magnitudes of the intercepts and gradients is perhaps a reflection of the arbitrary nature of the seasonal classifications/time of year and the potential differences in hydrological and meteorological characteristics, and therefore variable geomorphological responses. The relative success of the split-year model reinforces this as less specific

generalisations are made compared with dividing the data into four seasons or de-trending for time of year, although, in some respects de-trending for time of year is less arbitrary than imposing definite boundaries with discrete data sub-sets.

Time periods over which the sampling was undertaken differ for each catchment and the hydrological and meteorological characteristics would have been variable, including the short-term history which has an effect on the level of sediment supply, and therefore will have caused different responses in SSC. The complexity associated with different hydrological and meteorological characteristics and catchment history is likely to be greater in smaller catchments as the inter-annual differences have been shown to be more variable in smaller catchments (e.g. Wasson, 1994). Furthermore, it is likely that the sampling strategies had an influence on this analysis. As a storm sampling regime was employed at all sites except Langtae and the position of the level switch varied, to monitor storms of different magnitude, any seasonal influence may be obscured. Also, the seasonal signal may have been drowned out by sampling factors, such as timing of storm samples in relation to previous events and the size of storm sampled.

9.3.2.4 Limb and split-year

The summer-rising and winter-rising curves have higher intercepts and gradients than the summer-falling and winter-falling curves (Table 9.10). This trend was also found when the data was categorised by just limb (section 9.3.2.2). The highest intercepts occur in winter for Rough Sike, Burnhope and Candleseaves, in summer for Swinhope and Langtae and are equally high in summer and winter for Trout Beck (Table 9.10). The magnitude of the gradient is greater in winter at Rough Sike, Burnhope and Langtae and in the summer at Trout Beck, Swinhope and Candleseaves (Table 9.10). With the exception of the intercept of Langtae, the magnitudes of the intercepts and gradients with respect to summer and winter reflect the magnitudes of the intercepts and gradients when the data were categorised into just summer and winter (section 9.3.2.3.2). Therefore, the causes and interpretation of these are the same as for limb and season (two) (sections 9.3.2.2 & 9.3.2.3.2). However, these generalisations should be interpreted with care given the overlap in the standard errors (Table 9.10).

Categorising the data by limb and season gives the most accurate storm load estimates on average (Figure 9.4). This is inevitable, to some degree, given the increased number of parameters. Asselman (2000) also found sub-dividing the data by limb and split-year

Table 9.10. Intercepts and gradients of the summer-rising, summer-falling, winter-rising and winter-falling linear regression rating curve models for each study catchment. The numbers in brackets are the standard errors.

Site	Load improvement, %	Intercept				Gradient			
		summer-rising	summer-falling	winter-rising	winter-falling	summer-rising	summer-falling	winter-rising	winter-falling
Trout Beck	**3.6**	1.82 (0.24)	1.26 (0.11)	1.82 (0.11)	1.34 (0.07)	0.87 (0.13)	0.65 (0.05)	0.86 (0.10)	0.68 (0.06)
Rough Sike	**11.6**	2.21 (0.26)	2.77 (0.13)	4.20 (0.18)	2.87 (0.11)	–0.42 (0.15)	0.25 (0.04)	0.96 (0.10)	0.57 (0.03)
Swinhope	**10.2**	4.84 (0.20)	4.12 (0.10)	3.83 (0.15)	3.16 (0.12)	1.12 (0.13)	0.89 (0.06)	1.03 (0.09)	0.81 (0.07)
Burnhope	**5.5**	2.37 (0.25)	1.75 (0.11)	3.11 (0.05)	2.49 (0.03)	1.50 (0.27)	1.05 (0.11)	1.73 (0.09)	1.62 (0.05)
Langtae	**-**	2.54 (0.24)	2.07 (0.10)	2.46 (0.27)	2.27 (0.21)	0.44 (0.09)	0.38 (0.04)	0.74 (0.25)	0.70 (0.18)
Candlesaves	**8.0**	1.68 (0.12)	1.05 (0.08)	1.74 (0.14)	1.19 (0.23)	0.84 (0.15)	0.68 (0.08)	0.15 (0.07)	0.35 (0.09)

was preferable for the Rhine, although not as many adaptations were developed as in this study. The improvements in sampled period load estimate range from 3.6% to 11.6% with an average of 7.8% (Figure 9.4). The smallest improvements in load are associated with the largest catchments (Figure 9.4 & Table 5.1). This suggests that the effects of season and limb are more evident in smaller catchments. This was also the case when the data was divided by limb (section 9.3.2.2) and split-year (section 9.3.2.3.2).

Categorising the data by limb and split-year is recommended: it did not cause a decrease in sampled period load accuracy for any site, so therefore is robust, and resulted in an improvement in sampled period load estimate of 8%, on average.

9.3.2.5 Lag

Possible criteria for selecting the most appropriate lag were R^2, RMSE, diagnostic plots, examination of the resulting rating curves and the accuracy of the sampled period load estimate. The diagnostic plots and rating curves were very similar and could not be used as selection criteria. R^2, RMSE and sampled period load estimate were limited by the reasons outlined in section 9.2.2. Sampled period load estimate was chosen as the sole section criterion on the basis that R^2 and RMSE suggested some physically implausible

lags. For example, RMSE and R^2 both suggest that lagging ln Q by –90 minutes produces the best model for Rough Sike. This implies that ln Q is best matched with the ln C which occurred 90 minutes before but examination of storm hydrographs and sedigraphs does not confirm this (Figure 10.7). Discharge was lagged from –105 minutes to +105 minutes, the sampled period load estimates calculated and the lag associated with the most accurate sampled period load estimate selected.

Lagging the Q series only improved storm period load estimates for Trout Beck and Candleseaves. The most appropriate lags were minus 45 minutes, i.e. ln Q is best matched with ln C that occurred 45 minutes prior, for both catchments. The monitored period load estimate was improved by 0.3% for Trout Beck and 8.5% for Candleseaves. Candleseaves is the only grip catchment studied and possibly the most supply-constrained system. Therefore, most sediment is derived from within the channel and as a result the peak SSC occurs at the very beginning of an event (Figure 10.5). Consequently, there is potential for the peak SSC to precede the peak Q by a fairly long time period. The minus 45 minute lag for Trout Beck is harder to explain, and may have occurred by chance, especially given the very slight improvement in sampled period load estimate. The reasoning for lagging the Trout Beck data to improve the sampled period load estimate is that the system is large enough for a noticeable delay between the flood wave and sediment wave to develop. The reasoning against lag improving the load estimate is that the system has more spatially distributed sediment source areas; consequently the timings of sediment delivery to the gauging site will be variable and therefore a clear sediment wave will not develop. Whether a sediment wave develops may vary between events dependent on the amount and accessibility of sediment available.

The principle of lagging is to improve the correlation between the SSC and Q series. Lag times for individual storm events vary, for example from –56 to 186 minutes (not in multiples of the sampling interval as were derived from the hydrographs and sedigraphs) for Burnhope (Table 10.1). Therefore lagging may increase the correlation for one storm and decrease it for another. Insufficient storm sets were available to fully study the variation in lags and to investigate if there were dominant lags for each catchment, but the variability in the lags of the storm sets available suggests that lagging does not make physical sense. The form of the hysteresis plots (Figures 10.3, 10.6, 10.8,

10.10 & 10.13) clearly illustrate the inconsistencies in the timing of water and sediment delivery and therefore the variation in lags between storms.

On the basis of these results and the fact the most accurate monitored period load estimate was obtained with zero lag for Rough Sike, Swinhope and Burnhope it can be stated that lagging the Q series is not worthwhile for such responsive systems. It is likely that larger systems, larger than any of the catchments examined in this investigation, are characterised by a strong and more consistent lag between peak SSC and peak Q as there will be more time for a greater distance between the flood and sediment wave to develop and the SSC signal is likely to be less flashy.

9.3.2.6 Change in discharge

Adding change in Q (ΔQ) consistently resulted in an improved sampled period load estimate (Figure 9.3), although the improvement in load was 7% at the most and 3.9% on average (Figure 9.4). The ln Q regression coefficients varied from the basic linear regression model based on all data by no more than 0.03 and the ΔQ coefficients varied from 0.89 to 8.71 (Tables 8.6, 8.10, 8.13, 8.17, 8.21 & 8.26). The positive values of the ΔQ coefficients indicate that SSC is higher on the rising limb than on the falling limb for each of the study sites. The partial correlation coefficients indicate the correlation between ln $Q/\Delta Q$ if the variability in ln C if ΔQ/ln Q is held constant. ln Q is more important than ΔQ in all catchments except Candleseaves where they are of equal importance (Table 9.11). ΔQ does not explain much additional variability in ln C at Swinhope or Langtae but explains a notable amount at Trout Beck, Burnhope and Rough Sike (Table 9.11).

Richards (1984) ascribed the difference in the relative magnitude of the ln Q and ΔQ partial correlation coefficients between regressions for a proglacial stream to periods of dry weather with storms and the influence of snowmelt runoff. To derive some process meaning the partial correlation coefficients were calculated by month for each of the study sites in this investigation. The ΔQ partial correlation coefficients were not greater than the ln Q partial coefficients for any month in Langtae or Swinhope. The ΔQ partial correlation coefficients were greater than the ln Q partial correlation coefficients in January in Candleseaves, March in Burnhope, Rough Sike and Trout Beck, June in Burnhope and Rough Sike, July in Candleseaves, and August and December in Rough Sike (Table 9.12). This indicates that ΔQ is more important than ln Q in these months.

This may be related to the effect of snowmelt runoff in the December, January and March. While there is no snow measurements for the study sites a weekly photo archive for Moor House and Upper Teesdale NNR indicate that there was snow in Rough Sike in December and March and in March in Trout Beck. The effect of thunderstorms, with high rainfall intensities and consequently high erosion potentials, may explain the greater of importance of ΔQ during the summer months.

As no storm sampling was undertaken at Langtae, it is not surprising that ΔQ is not a highly influential factor. The large percentage of fixed-interval sampling at Burnhope may also have masked the ΔQ signal in comparison with the other catchments.

Table 9.11. Partial correlation coefficients of ln Q and ΔQ and the improvements in sampled period load estimates for each of the study sites. * significant at 5% level.

Site	Partial correlation coefficient of ln Q	Partial correlation coefficient of ΔQ	Estimate improvement, %
Burnhope	0.84	0.17*	1
Candleseaves	0.24	0.24*	5
Langtae	0.53	0.06	-
Rough Sike	0.46	0.29*	5
Swinhope	0.62	0.09*	7
Trout Beck	0.80	0.25*	0.5

Table 9.12. The relative importance of ln Q and ΔQ as indicated by the partial correlation coefficients. Shaded boxes indicate that ΔQ was of greater importance.

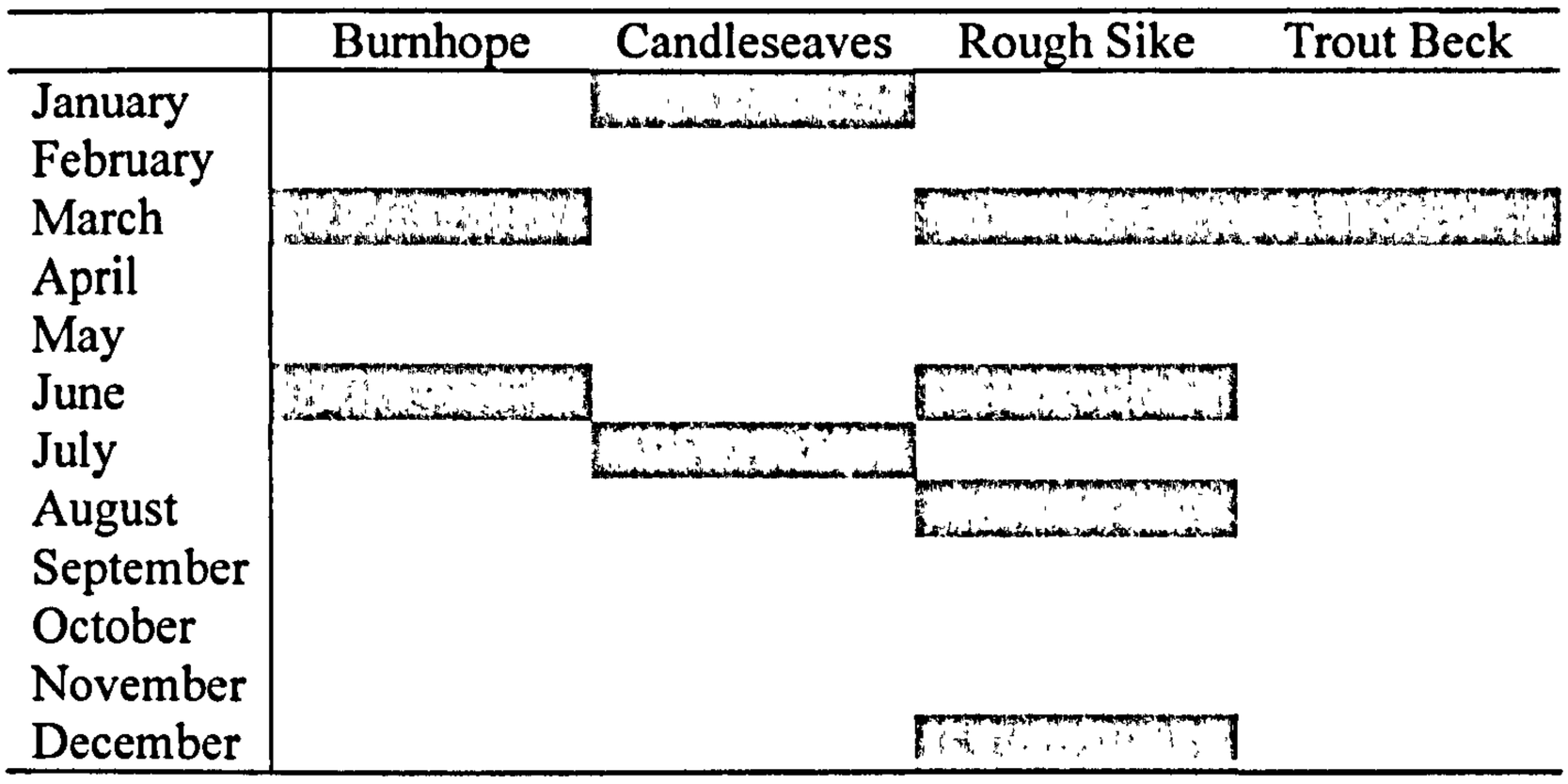

In summary, ΔQ did not substantially improve the sampled period load estimates and it is not worth developing on that basis. However, it may give some insight into the relative importance ln Q and ΔQ during snowmelt events and summer thunderstorms.

9.3.2.7 Discharge class

The Q class method differs from the other adaptations as it is used to improve the robustness of the rating curve model, not to include any measure of process (Jansson, 1996). Rating curves derived by the Q class method were very similar to the basic linear regression rating curves (Figure 9.8). This is encouraging as it suggests the sampling strategy used produced data from which robust models were developed. The largest differences between the basic and Q class curves occur at higher and lower values of ln Q (Figure 9.8). The difference in sampled period load estimate calculated using the two methods is under 5% for Trout Beck, Rough Sike, Swinhope, Burnhope and Langtae (Figure 9.4). The Q class method increased the accuracy of the sampled period load estimate by 30% for Candleseaves (Figure 9.4). The difference in the regression lines for Candleseaves is related to the distribution of the samples taken. There is a cluster of data points between –1 ln Q and 0 ln Q and another smaller cluster around ln Q = 1 (Figure 9.5). These clusters are responsible for decreasing the gradient of the regression line when it was developed from all the data. When the data was divided into Q classes the general effect of these clusters was removed which yielded a more representative regression line and consequently more accurate load estimation. On this basis it appears advantageous to use the Q class method if there are clear clusters evident in the data, especially if they are positioned such that they will lever the regression line.

In summary the Q class method illustrates the effect that clusters of data points can have on load estimates. It also indicates that the sampling procedures were not biased, except at Candleseaves.

9.3.3 Rating curve analysis summary

The rating curve analysis of this investigation has compared a range of different models from a variety of sites. This has highlighted several important considerations in the development of rating curve models:

(1) The importance of the sampling strategy has been outlined and the potential effects on models and resultant load estimates demonstrated.

(2) The short-falls and advantages of different indicators of model fit have been summarised and the reliance on the data characteristics outlined.

(3) The magnitude of variation in load estimates derived from the ten basic rating curve models has been characterised and related to the variability of the discharge series.

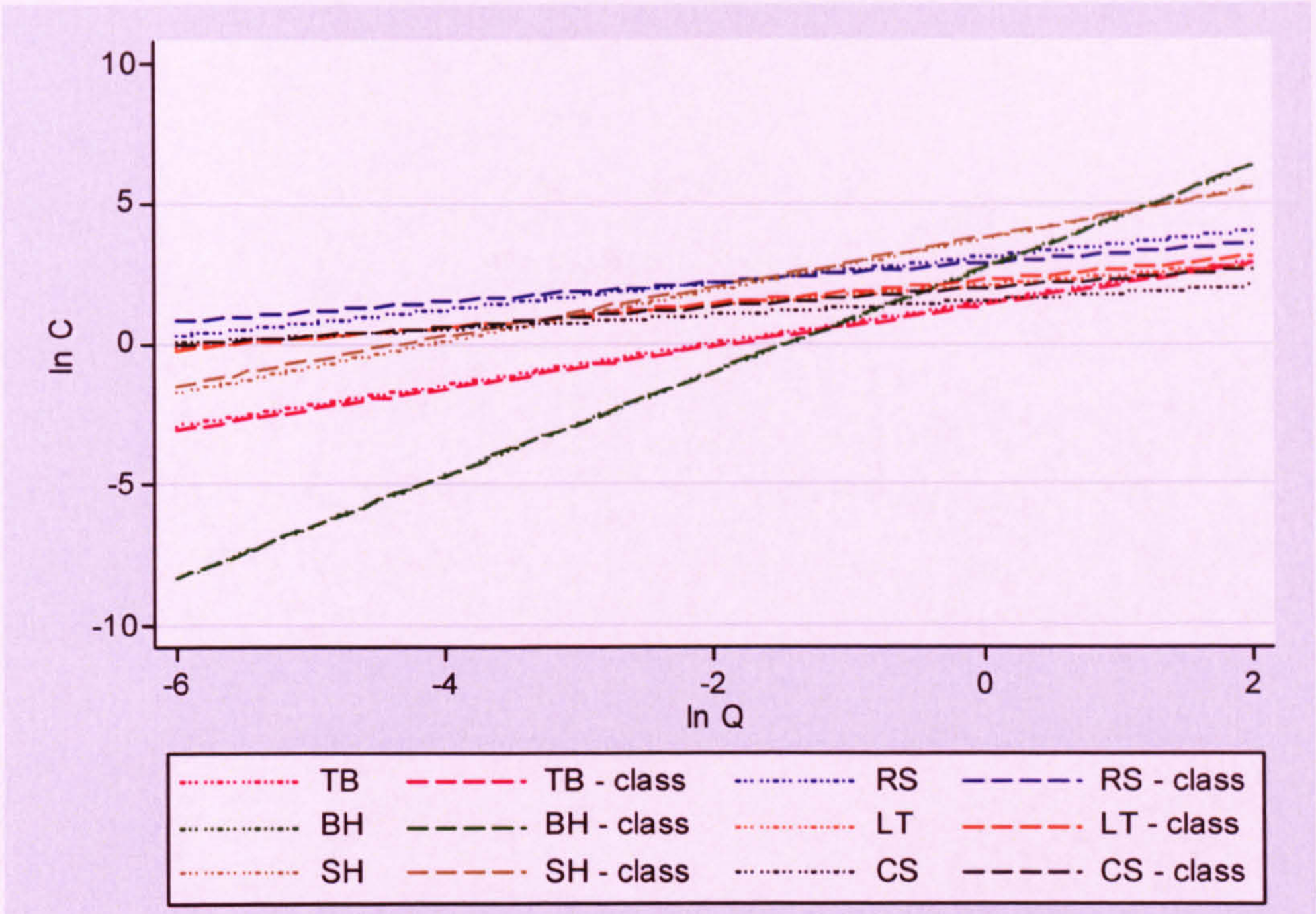

Figure 9.8. Rating curves as obtained by the basic linear regression method (dotted line) and the *Q* class method (dashed line).

(4) Linear regression corrected for bias by smearing has been shown to be the optimal model for several sites and is generally the most robust procedure. However, it was suggested this generalisation is transferred to other settings with caution as it is based on six broadly similar British upland catchments.

(5) Many of the rating curve adaptations do not result in marked improvements in load estimation or give insight into influential processes within the systems studied. The exceptions to this are categorising the data by limb, split-year, limb and split-year, and adding change in *Q* as an extra explanatory variable.

(6) The *Q* class method was shown useful for removing artefacts of sampling, although this was only relevant for one study site.

(7) No clear patterns between the rating curve parameters and catchment characteristics were found.

9.4 Characterisation of suspended sediment dynamics

The following sections use the load estimates derived from the optimal rating curve models to characterise sediment dynamics at each site. Volumetric sediment losses are determined, the effective discharge intervals established and magnitude and frequency

relations examined for each catchment. The suspended sediment loads and specific sediment yields are then discussed in relation to other upland studies.

Only ten and eight month discharge records were available for Burnhope and Langtae respectively. To allow comparison with the other sites they were up-scaled to annual loads. As no discharge record exists for prior or successive years for Burnhope or Langtae, the percentage of sediment transported in Candleseaves, Rough Sike and Trout Beck during the missing periods were calculated and averaged (Table 9.13). This resulted in a correction factor of 1.153 for Langtae and 1.094 for Burnhope and annual load estimates of 38.6 t for Langtae and 314.7 t for Burnhope.

Table 9.13. Percentage of sediment transported from the 21st March to 15th May (Burnhope) and 21st March to 11th July (Langtae) in Candleseaves, Rough Sike and Trout Beck and the mean. Swinhope was not included given the incomplete discharge record.

	Missing period for Langtae	Missing period for Burnhope
Candleseaves	17.9	13.7
Rough Sike	21.7	12.8
Trout Beck	6.2	1.5
Mean	**15.3**	**9.4**

9.4.1 Volume of sediment removed

Most studies investigate suspended sediment in terms of weight, not volume, removed from the catchment. Quantifying the volume of sediment removed gives a clearer indication of the effect on the physical landscape, e.g. channel and gully development.

The balance of organic and mineral sediment is extremely important in calculating the volume of sediment given their very different dry densities. Consequently, sediment volumes were only calculated for Trout Beck, Rough Sike and Candleseaves: the volume of sediment removed from Swinhope could not be calculated as the annual load is unknown given the problem with the stage-discharge calibration and the Burnhope and Langtae loads could not be converted into volumes as no time-integrated mass samplers (TIMS) were deployed and therefore the organic-mineral balance of the suspended sediment is not known.

The annual loads were converted into annual volume by determining the mineral-organic balance of the suspended sediment from the TIMS sediment (using loss-on-

ignition) and assuming a dry bulk density of 0.15 t m^{-3} for organic sediment and 1.2 t m^{-3} for mineral sediment (Table 9.14). These density values are representative of upland northern England sites (Warburton, pers comm). Not surprisingly this analysis suggests the largest volume of sediment is removed from the Trout Beck system, the second largest volume from Rough Sike and the least from Candleseaves (Table 9.14). In terms of specific volumetric sediment yield most sediment is removed from Candleseaves and the volumetric yields contrast to the gravimetric suspended sediment yields in their relative magnitude (Table 9.14). This illustrates that, in terms of visual impact on the physical landscape, specific suspended sediment yield is not a good measure and that the volume of suspended sediment transported out of the system should be calculated.

Table 9.14. Organic-mineral balance of suspended sediment; total, organic and mineral annual loads and volumes; and volumetric and gravimetric specific suspended sediment yields. 4 d.p. are given for Candleseaves given the lower sediment load.

Site	Organic:mineral	Load, t	Volume, m^3	Specific sediment yield Gravimetric, t km^2 yr^{-1}	Volumetric, m^3 km^2 yr^{-1}
Candleseaves:					
Total	0.75:0.25	0.0534	0.2784	17.8	91.6
Organic		0.0401	0.2673		
Mineral		0.0133	0.0111		
Rough Sike:					
Total	0.14:0.86	23.2	38.0	30.5	50.0
Organic		3.2	21.3		
Mineral		20.0	16.7		
Trout Beck:					
Total	0.16:0.84	453.1	800.5	38.3	67.6
Organic		72.5	483.3		
Mineral		380.6	317.2		

Very few authors calculate the volumetric loss of sediment. However, Francis (1987) reports total and organic suspended sediment yields for The Upper Severn, Nant Ysguthon and Ceunant Ddu, Mid-Wales (the yields prior to catchment disturbance are used). The volumetric yields were calculated assuming the same mineral and organic sediment densities (Table 9.15). The total and organic volumetric losses from the Severn are much higher than those of the other Mid-Wales catchments and the catchments of this investigation (Table 9.15). However, the mineral volumetric losses are in the same region as those from Trout Beck and Rough Sike (Table 9.15). This indicates that the peat cover of the Severn catchment was more actively eroding at the time of monitoring. This is reaffirmed by Francis' (1987) site description of the Severn:

dissected and actively eroding. The organic, mineral and total volumetric losses from Nant Ysguthon and Ceunant Ddu are lower than those of Trout Beck, Rough Sike and Candleseaves (Table 9.15). This may reflect true differences between the catchments: Walling & Webb (1987) noted that catchments in Mid-Wales and the Mendip Hills had lower suspended sediment yields compared with British upland and lowland catchments (section 2.9). Also, Francis (1987) noted an increase in organic matter content with discharge, which is contrary to other studies (Walling & Kane, 1987; Carling, 1983; and Hillier, 2000), and the interpretation of the organic matter content of the TIMS sediment in this study (section 7.5). Alternatively, it could be attributed to the differences in sampling methods, Francis (1987) used a combination of fixed-interval and storm samples; or difference in the determination or organic matter content, Francis (1987) determined the organic matter content by placing the SSC filter papers in a furnace at 500°C for one hour.

Table 9.15. Total, organic and mineral sediment volumetric losses of sediment from three Mid-Wales catchments (prior to catchment disturbance) and Trout Beck, Rough Sike and Candleseaves. Gravimetric yield data sourced from Francis (1987).

Site	Volumetric organic:mineral	Volumetric yield, $m^3\ km^{-2}\ yr^{-1}$		
		Organic	Mineral	Total
Trout Beck	0.61:0.39	40.9	26.8	67.6
Rough Sike	0.56:0.44	28.0	22.0	50.0
Candleseaves	0.97:0.03	89.1	2.5	91.6
Upper Severn	0.90:0.10	229.6	26.4	256.1
Nant Ysguthon	0.97:0.03	3.2	0.1	3.3
Ceunant Ddu	0.97:0.03	19.7	0.6	20.3

The volumetric ratio of organic to mineral sediment illustrates the importance of the organic fraction in terms of impact on the landscape. The volumetric ratio for Candleseaves is similar to those established by Francis (1987) (Table 9.15). A much larger proportion of mineral sediment makes up the volumetric yield in Trout Beck and Rough Sike (Table 9.15). This indicates the relative importance of mineral sediment in these catchments. Organic sediment constitutes a higher proportion of the volumetric load in Trout Beck in comparison with Rough Sike. This is unexpected as field observations indicate that organic sources are more dominant in Rough Sike. However, organic sediment transported in Rough Sike is likely to be larger (including peds and blocks) which could not be sampled by the TIMS. As these larger particles are transported they will abrade to sizes which the TIMS can sample.

9.4.2 Effective discharge interval

To establish the effective discharge interval, in terms of sediment transport, the discharges were classified, the frequency of each discharge established and the load contribution of each discharge class calculated by multiplying the total duration of that class by the SSC predicted by the optimal rating curve for the mean discharge of that class. A graph with the sediment rating, flow frequency and load curves was drawn and the effective discharge interval defined by observation as the peak in the load curve (Figure 9.9). Two effective discharge interval graphs were drawn for Trout Beck, including and excluding the exceptional flood of 30th July 2002 (Figure 9.9). Comparison of these graphs clearly illustrates the importance of high flow events in the transport of suspended sediment. The following discussion applies to the graph with the exceptional flood excluded.

The load curves of Candleseaves and Rough Sike indicate that lower discharges are important in terms of suspended sediment transfer. In Candleseaves the effective discharge is between 3% and 53% of the maximum discharge and in Rough Sike is 4% to 39% (Figure 9.9). In comparison it is the mid-range discharges which are more effective at transporting sediment in Burnhope, Langtae, and Trout Beck (Figure 9.9). The effective discharge is 12% to 71% of the maximum discharge in Burnhope, 12% to 65% in Langtae, and 10% to 63% in Trout Beck (Figure 9.9). This pattern can be related to the form of the annual discharge series graphs: Rough Sike and Candleseaves have a more peaked discharge distribution (Figure 9.10). Trout Beck also has a peaked discharge distribution but this is an artefact of the large flood that occurred within the study period.

These effective discharge classes could be used to assess the fit of the sediment rating curves as it is more important that the rating curve is a good fit at the discharges at which the majority of sediment is transported. However, the graphs from which the effective discharge intervals were derived are heavily reliant on the rating curves used to produce them and therefore are not a valuable measure of model fit in this study but could suggest an improved sampling strategy.

9.4.3 Magnitude and frequency of sediment delivery

The sediment transport regimes of the different catchments can also be examined by comparing the percentage of sediment transported in a given percent of the time (Figure

Burnhope

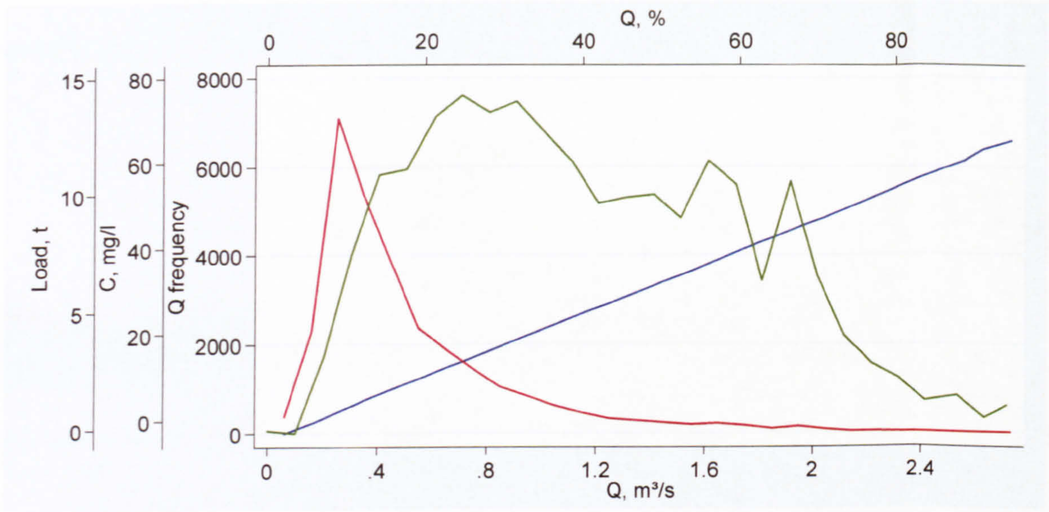

Rough Sike

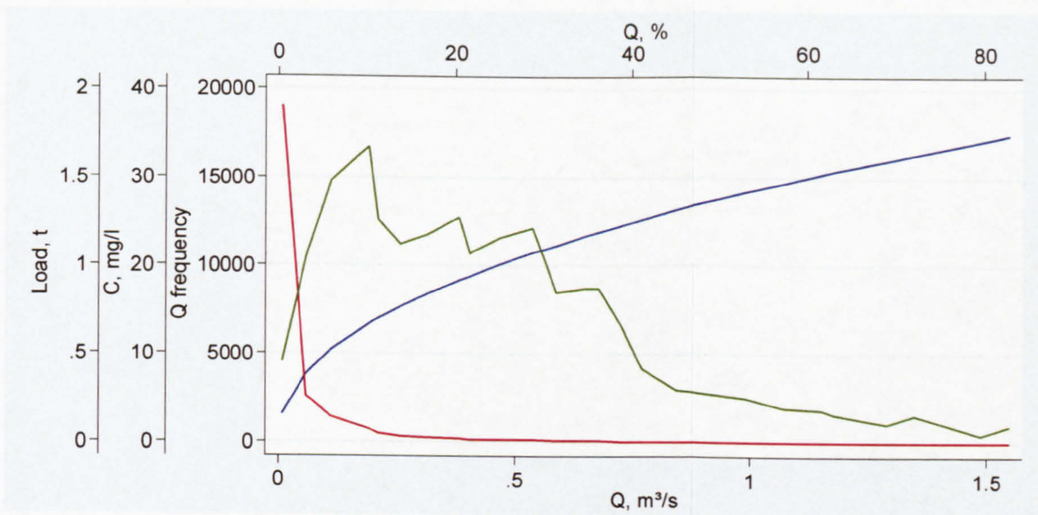

Candleseaves

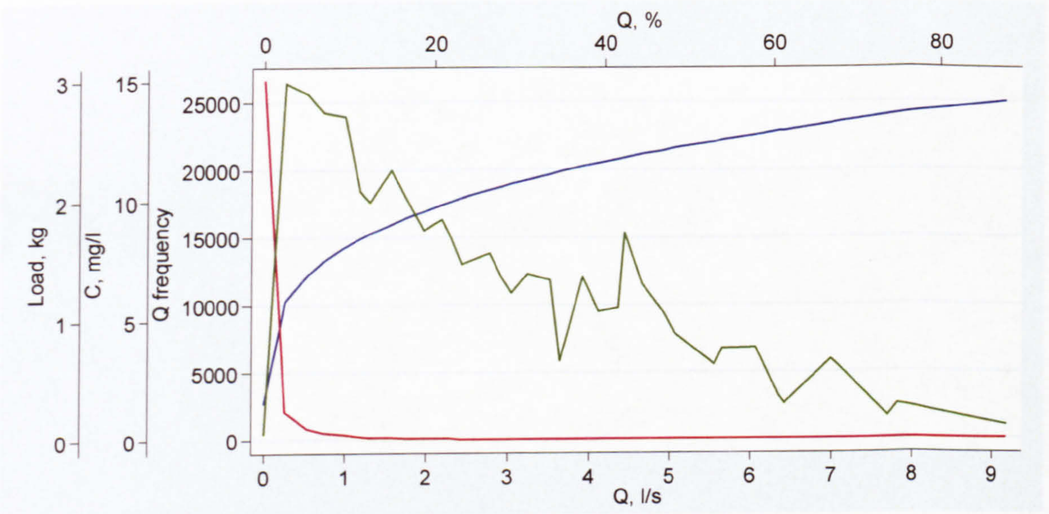

Trout Beck with large storm

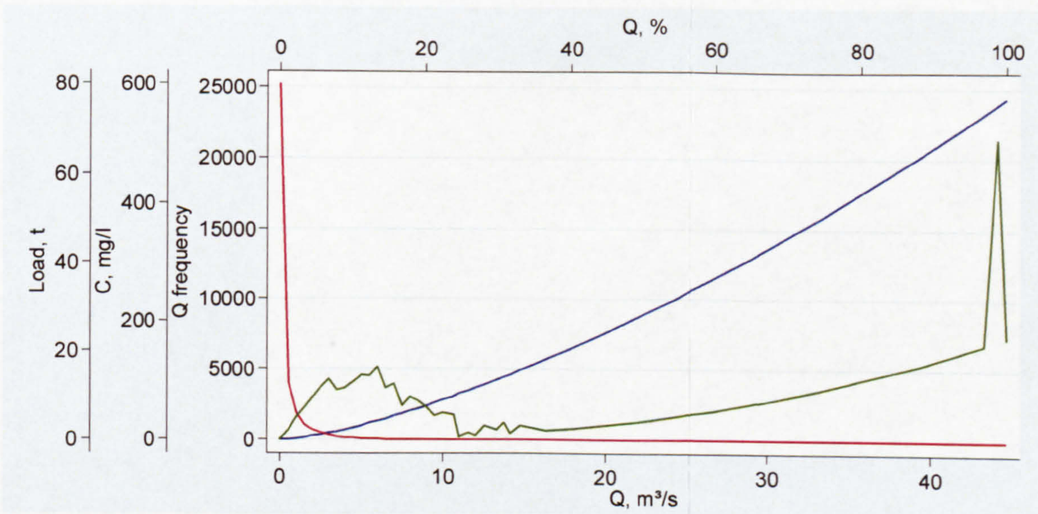

Langtae

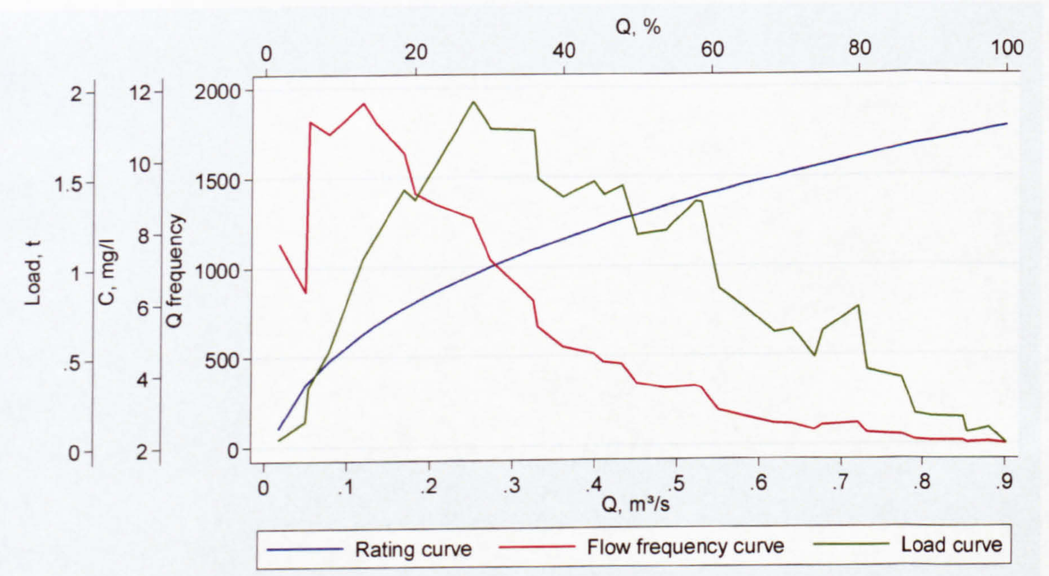

Trout Beck without large storm

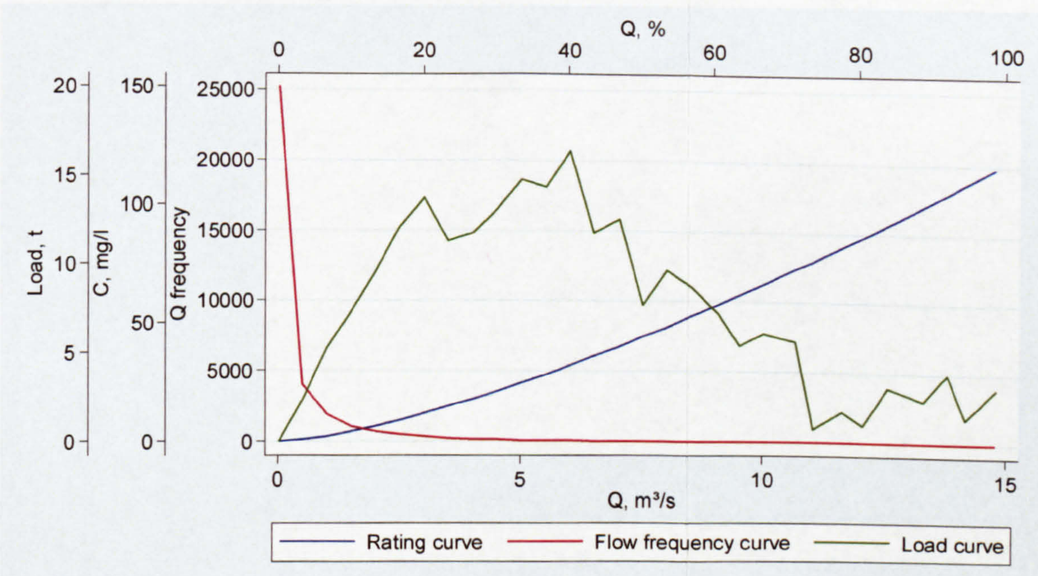

Figure 9.9. Flow frequency, rating and load curves used to establish the effective discharge interval. Discharge classes varied between catchments: Burnhope = 0.1 $m^3 s^{-1}$, Candleseaves = 0.2 $l s^{-1}$, Langtae = 0.025 $m^3 s^{-1}$, Rough Sike = 0.05 $m^3 s^{-1}$, Trout Beck with storm = 0.5 $m^3 s^{-1}$ and Trout Beck without storm = 0.4 $m^3 s^{-1}$.

Burnhope:

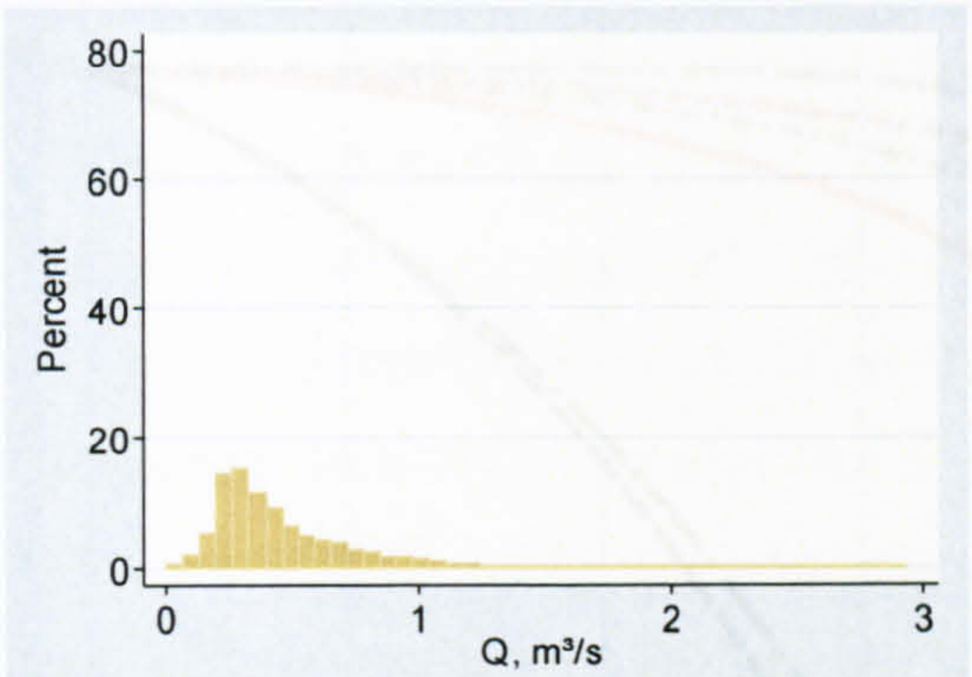

Candleseaves:

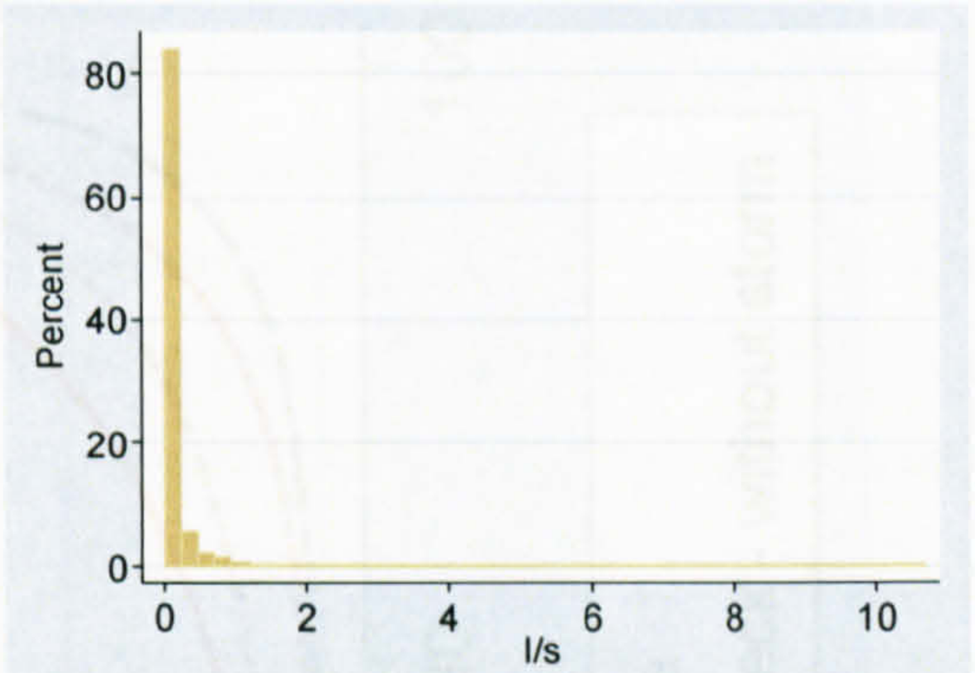

Langtae:

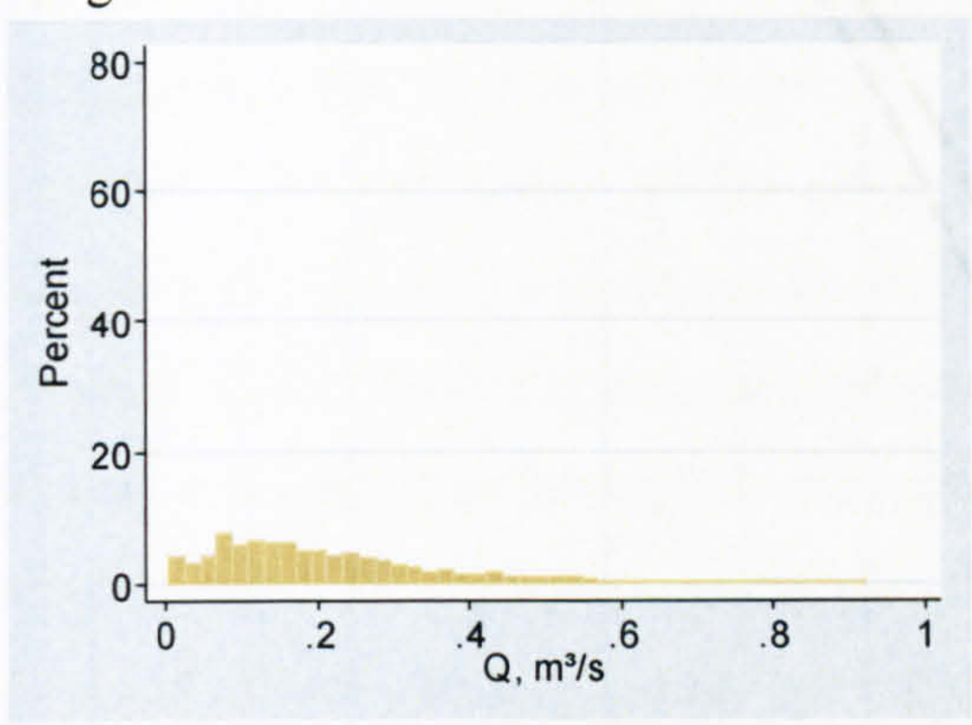

Rough Sike:

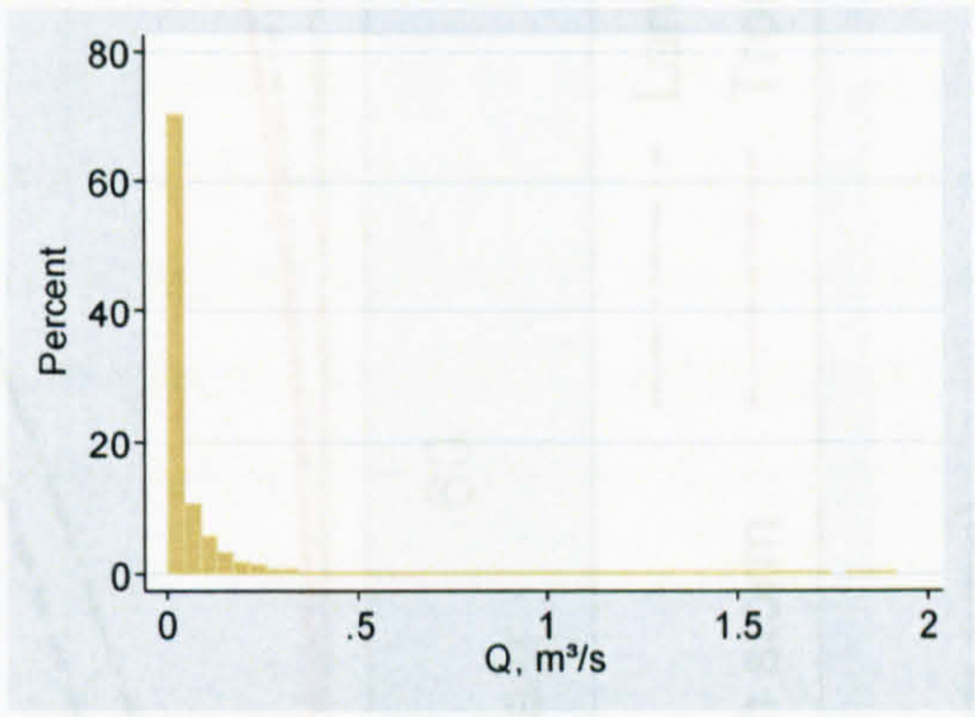

Trout Beck:

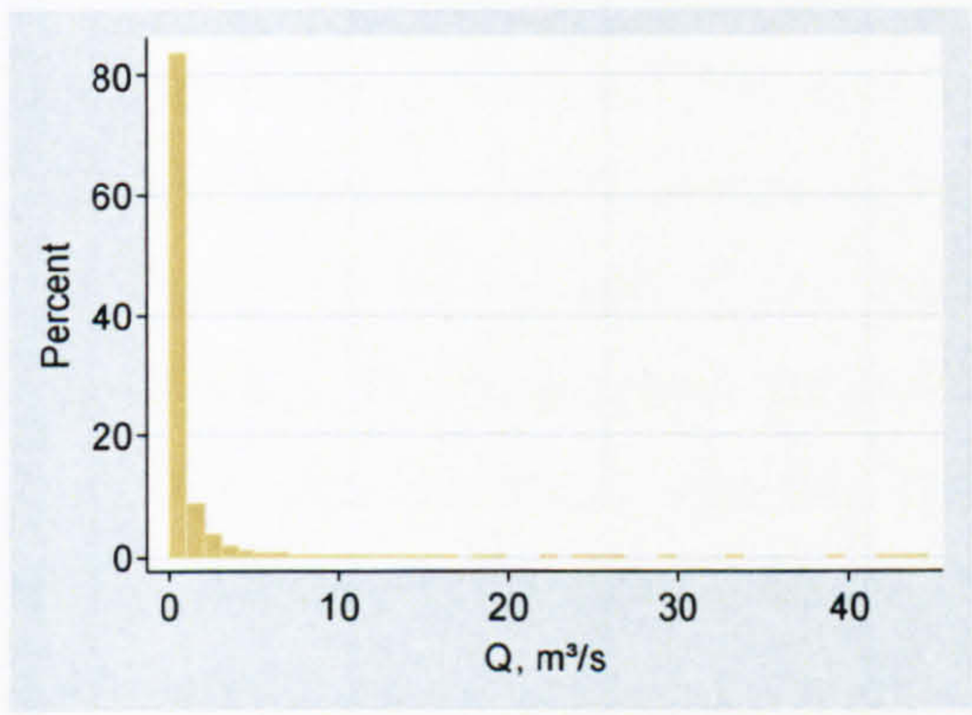

Figure 9.10. Discharge distributions for the annual (part-annual for Burnhope and Langtae) discharge record for each of the study sites.

9.11). This was achieved by calculating the load of sediment in each 15 minute period (as defined by the frequency of the discharge recordings), sorting them by magnitude and calculating the cumulative percent. The cumulative percentage of time was then calculated. This analysis indicates that Burnhope and Langtae have noticeably different sediment transport regimes from Candleseaves, Trout Beck and Rough Sike (Figure 9.11 & Table 9.16). Sediment transport in Burnhope and Langtae is more constant through time (Figure 9.11 & Table 9.16), suggesting that these catchments are not as flashy or responsive as Candleseaves, Trout Beck and Rough Sike. Based on catchment

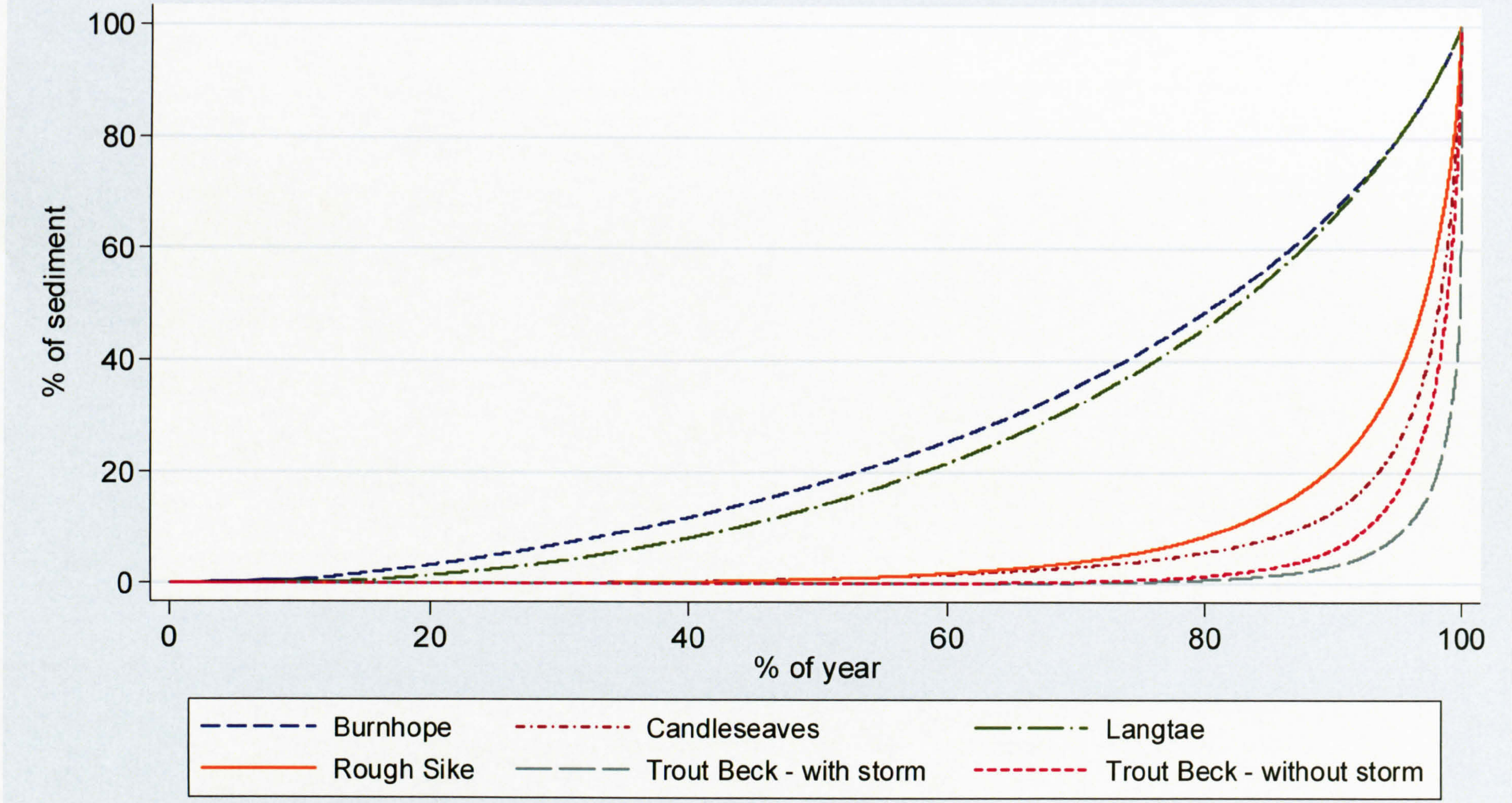

Figure 9.11. Percentage of sediment transported in a given percentage of time (Lorenz curve).

characteristics it would be expected that Trout Beck and Burnhope would be the least flashy as they have the greatest catchment areas (Table 5.1). The less responsive nature of Langtae and Burnhope is likely to be a reflection of the lower variability in their discharge series compared with the other catchments (Figure 8.9 & Table 9.4). This may be a characteristic of the hydrological regime in that particular year, a reflection of the incomplete annual discharge record giving a biased flow duration curve, or a result of the variation in peat cover: the peat cover of Candleseaves, Rough Sike and Trout Beck is fairly continuous whereas peat is only present in upper catchment in Burnhope, Langtae and Swinhope. As peat cover promotes flashy discharge regimes (Holden & Burt, 2003) this may explain the less variable discharge records for Burnhope and Langtae. The variability of the discharge records of Rough Sike is the third most variable (Table 9.4) and the sediment transport regime is the third least responsive (Figure 9.11). However, the most responsive catchment is Trout Beck (Figure 9.11), despite Candleseaves having the most variable discharge record (Table 9.4). It would be expected that Trout Beck would be one of the least responsive catchments given its size. Trout Beck was the only catchment to experience an exceptional flood in the study year. The flood had a peak discharge of 44.7 $m^3 s^{-1}$, and transported 49% of the sediment in less than 0.5% of the time. The effectiveness of this event in transporting suspended sediment was also clearly illustrated by the effective discharge interval graph (Figure 9.9). Even with the removal of this flood Trout Beck is still the most responsive system (Figure 9.11). This may reflect the difference in organic and mineral sediment sources: more mineral sediment is available for transport, given the broader floodplains and higher proportions of mineral banks, during flood events compared with the other catchments.

Table 9.16. The percentage of time taken to transported in 50%, 75%, 90% and 95% of the sediment, as determined by the selecting rating curve model.

Catchment	% sediment				
	50	75	80	90	95
Burnhope	19.2	40.7	47.1	63.6	75.3
Candleseaves	1.8	5.1	6.5	12.7	21.9
Langtae	17.6	36.5	41.9	56.5	67.5
Rough Sike	3.1	8.4	10.6	18.1	26.8
Trout Beck with storm	0.1	1.3	1.9	4.4	7.7
Trout Beck without storm	1.2	3.3	4.2	7.4	11.4

Storm events are considered dominant in sediment transport (e.g. Webb & Walling, 1998; Wass & Leeks, 1999; Walling & Webb, 1987). Existing studies generally found

that the majority of sediment is transported during a small percentage of the time (Table 2.7) and therefore hypothesised that storm events were the dominant cause of sediment transfer. This study confirms this and the magnitude-frequency relations are comparable with the exception of Burnhope and Langtae. For example, 90% of sediment was transported in between 7% and 25% of the time in Devon Rivers (Webb & Walling, 1998 and Wass & Leeks, 1999) (Table 2.7). CEH (2004) stated that 80% of sediment was transported in 5% of the time in the Plynlimon catchments (no specific reference to any of the catchments). Wilkinson (1971) also examined the magnitude and frequency of suspended sediment transport in British upland catchments (Table 2.7). On average, 50% of the sediment was transported in 0.1% of the time in West Grain and Langden Brook (Wilkinson, 1971). These figures are comparable to those of Rough Sike, Candleseaves and Trout Beck (Table 9.16), which is not surprising given West Grain and Langden Brook are also in northern England and have broadly similar catchment characteristics (Table 2.7 & 5.1). Less time was required to transport 90% of the sediment in West Grain and Langden Brook (1.1% and 0.9%, on average, respectively (Wilkinson, 1971)) than any of the study catchments of this investigation. This suggests that the study sites of this investigation are not as responsive. However, the differences are likely to be a result of inter-annual difference in the magnitude and frequency of storm events in the study years as opposed to difference in sediment transport regimes between the systems.

In summary, the study catchments are all responsive systems with respect to suspended sediment transfer. Burnhope and Langtae are noticeably less responsive than Candleseaves, Rough Sike and Trout Beck, but this can be attributed to the differences in the variability in the discharge series. The results support the hypothesis of other studies that the majority of sediment is transported during storm events and highlights the substantial role of exceptional flood events in suspended sediment transport. It is evident that the catchments are generally comparable with other British catchments.

9.5 Comparison with British upland studies

The following section compares loads, as estimated by the optimal rating curve model for each catchment, and specific sediment yields to those established for existing upland Britain studies and, to a limited extent, other upland catchments worldwide. As section 9.3.1 has indicated different models can lead to very variable estimates of suspended sediment loads. This study has attempted to select the optimal model, based on a range

of criteria, to ensure the most accurate load estimate is made. Knowledge of the accuracy of the load estimates is rarely known. Most report R^2 as the indicator of model fit which, as shown by this study, does not guarantee the most accurate load estimate. Another consideration when comparing the suspended sediment load estimates and specific sediment yields is the effect of inter-annual variability (section 2.7.4). Only initial generalisations can be made regarding annual suspended sediment loads or specific sediment yields of upland catchments based on a single year of data.

9.5.1 Suspended sediment loads

The suspended sediment loads of the study catchments are broadly comparable to those of existing upland UK studies which were undisturbed (Figure 9.12). The loads of Trout Beck and Burnhope are generally larger than those of similar sized catchments, for example Great Egglestone Beck, Northern Pennines, with a catchment area of 11.7 km^2 (Carling, 1983). The notable difference in load estimates could be attributed to the different sampling and modelling techniques. This study used rating curves, while Carling (1983) used Beale's ratio estimator. It cannot be stated which approach is superior, or how much bias each is likely to introduce, as this study has shown the variable effect of different models in different catchments. Regional variation in geology and soil type, may explain the variations as may different meteorological conditions during the study periods. For example, Trout Beck and Burnhope may have been monitored during years with meteorological conditions conducive to sediment preparation (freeze-thaw cycles, desiccation, intense precipitation) and transport (overland flow, intense rainfall) in comparison with the monitoring periods of Great Egglestone Beck and River Barle. The loads of Candleseaves, Rough Sike and Langtae are very comparable with catchments less than 5 km^2 (Figure 9.12).

It is difficult to identify any overall trend on the plot of load versus catchment area (Figure 9.12). However, when the loads and areas are logarithmically transformed there is a clearer trend. On this plot load (ln) increases linearly with increases in area (ln) (Figure 9.12). R^2 indicates that 85% of the variation in load (ln) is explained by the variation in area (ln). The diagnostic plots also indicate the model is a good fit. The scatter about the regression line can be explained by variability in models used, variability in meteorological characteristics of the study years and variable catchment characteristics such as lithology and catchment morphology. The most obvious outlier is Nant Ysguthon which was monitored by Francis (1987). The load is substantially over-

(A)

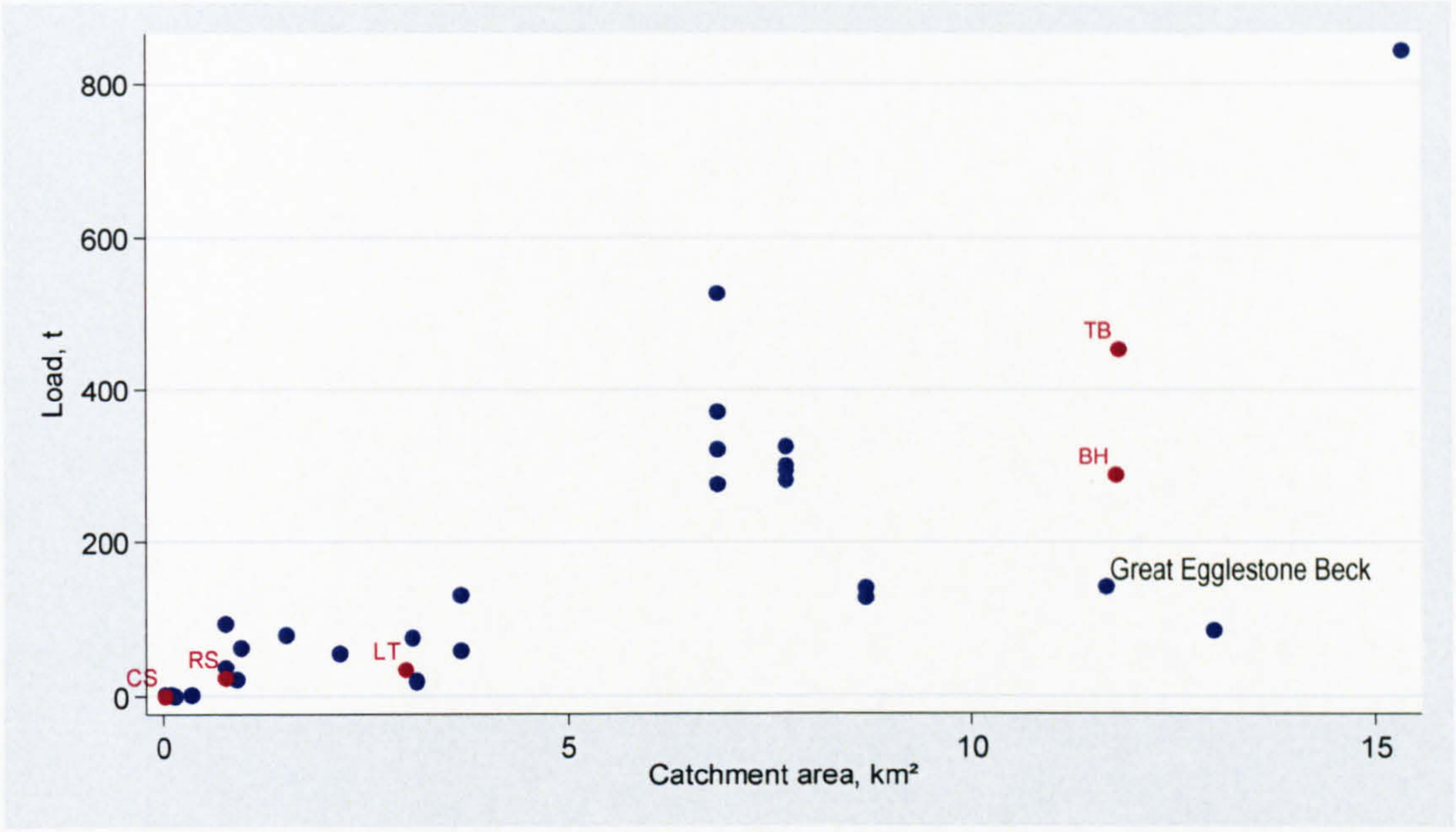

(B)

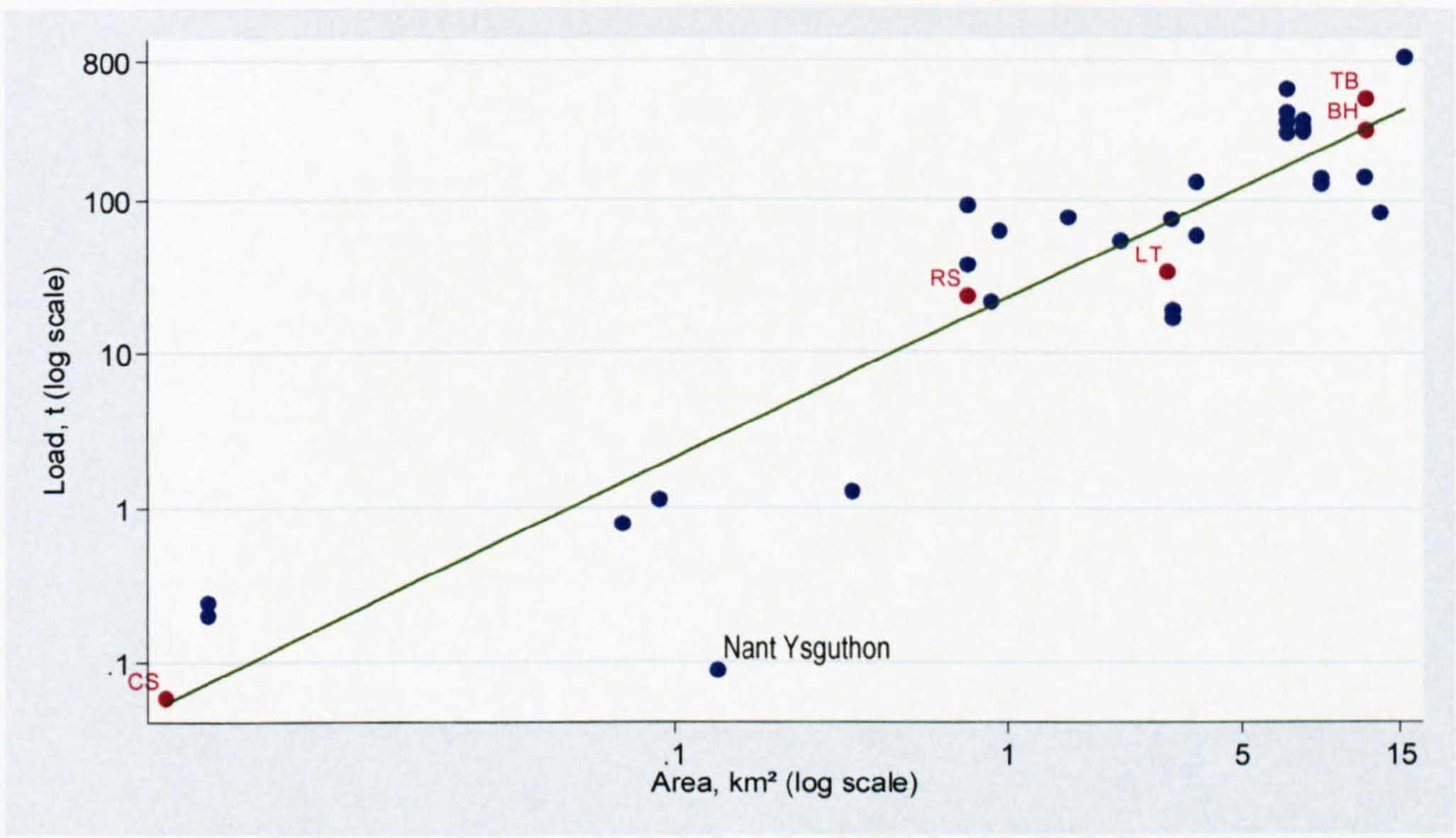

Figure 9.12. (A) Comparison of annual suspended sediment loads and catchment areas of the study sites of this investigation in comparison to those of other undisturbed British upland sites. The large loads and variations of the catchments with an area of 6.8 km^2 and 7.7 km^2 (Kirkton and Monachlye respectively) indicate the potential inter-annual variability in load estimates. (B) Relationship between ln load and ln area. ln load = 1.04 ln area + 3.13 with an R^2 of 0.85 and a RMSE of 1.04 and can be rearranged to load = 22.8 $area^{1.04}$.

predicted and can be explained by the extensive vegetation cover and dominance of peat in the catchments. The trend between load (ln) and area (ln) is sufficiently strong to allow the loads of ungauged small British upland catchments to be estimated from catchment area and results in an estimated annual load of 88.89 t for Swinhope. Given the similarity in the catchment sizes of Langtae and Swinhope this suggests that the annual load estimate of Langtae may be a large under-estimate as a result of the sampling regime (solely fixed-interval).

The relationship between load (ln) and area (ln) of the British upland sites was compared with the relationship between load (ln) and area (ln) of worldwide upland rivers compiled by Milliman & Syvitski (1992) (Figure 9.13). Unfortunately there are limited larger catchments in Milliman & Syvitski's database. The rationale for this analysis was to investigate if large-scale controls, such as lithology, relief and climate, exert an influence over the relationship between load and catchment area. A steeper relationship exists between the British upland study sites which suggests that large-scale controls are influential. The results indicate that loads are more sensitive to changes in catchment area in British rivers than in rivers in the rest of the world. However, it may be a continuous trend between upland Britain and the rest of the world (Figure 9.13). To test this either, smaller British upland catchments or more larger rest of world catchments would have to be studied. Alternatively, the rest of world data cloud may consist of groups of data points from different lithological and climatic regions. Unfortunately there is insufficient data to do this for all world regions. However, estimates from fourteen New Zealand rivers are included in Milliman & Syvitski's study. This indicates that the data cloud may be comprised of several distinct data clouds from different regions (Figure 9.13).

Several other equations relating suspended sediment load to catchment area have been established (Table 9.17). This British uplands equation developed by this study (Figure 9.13) has a very similar gradient but higher intercept in comparison with the relation established by Collins (1981) for lowland British rivers (Figure 9.14). This implies while the rate of increase in suspended sediment load is the same between British catchments and British upland catchments, there is generally more sediment available for transport in the uplands. This links with observations by Walling & Webb (1987) that there is generally higher suspended sediment loads in upland catchments (section 2.9). The British upland curve has a higher intercept and gradient than the curve derived

(A)

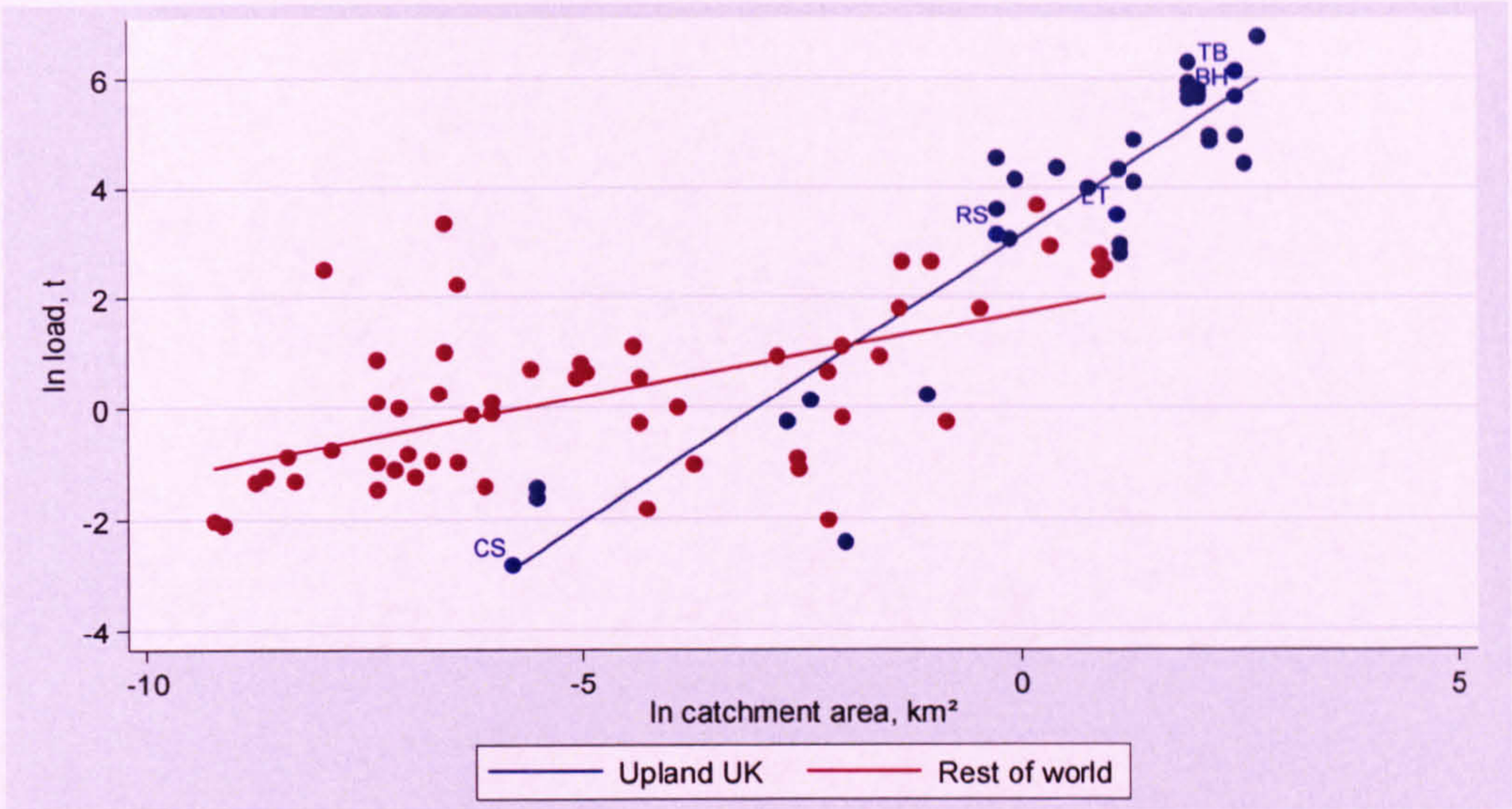

(B)

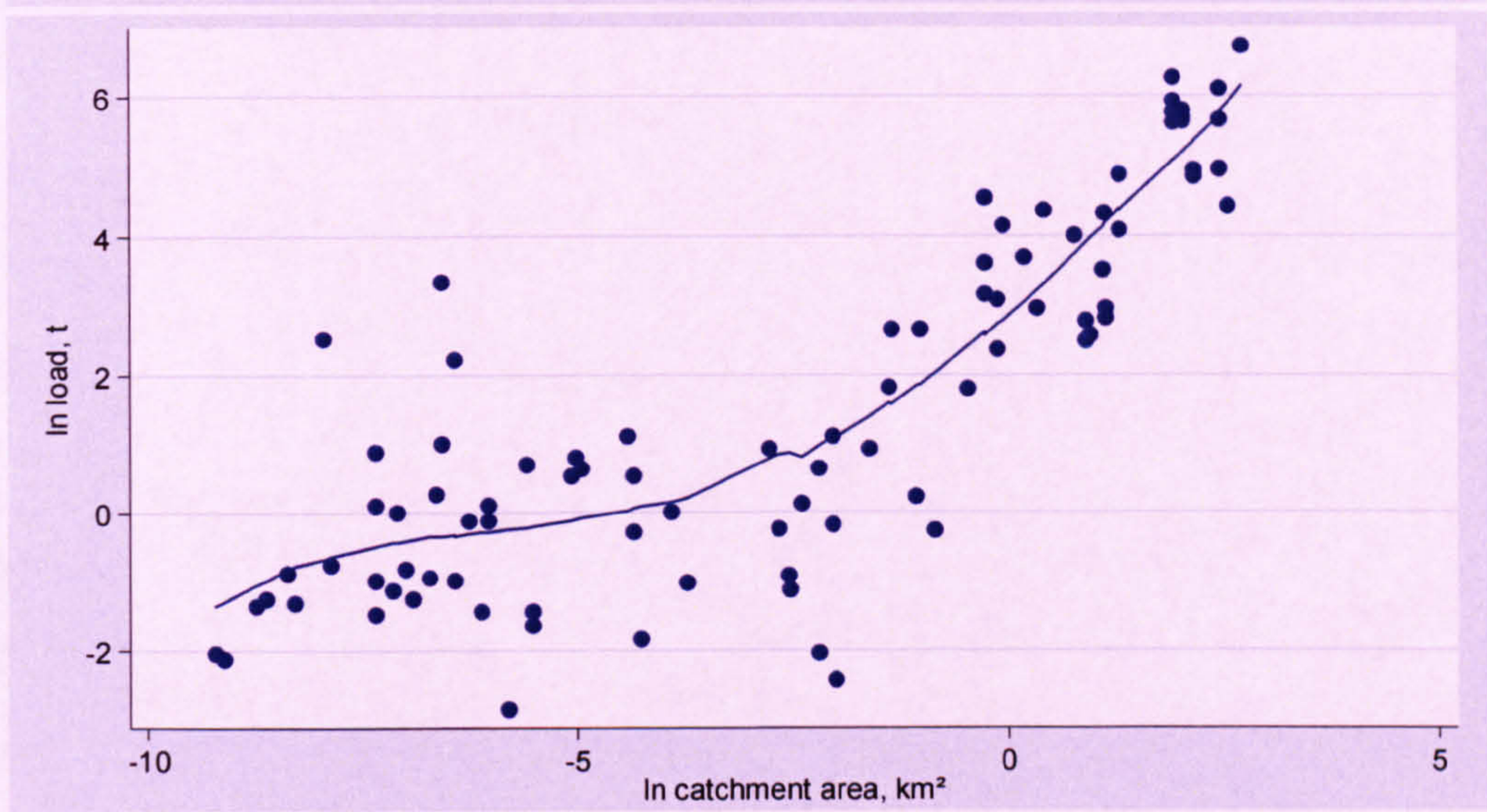

(C)

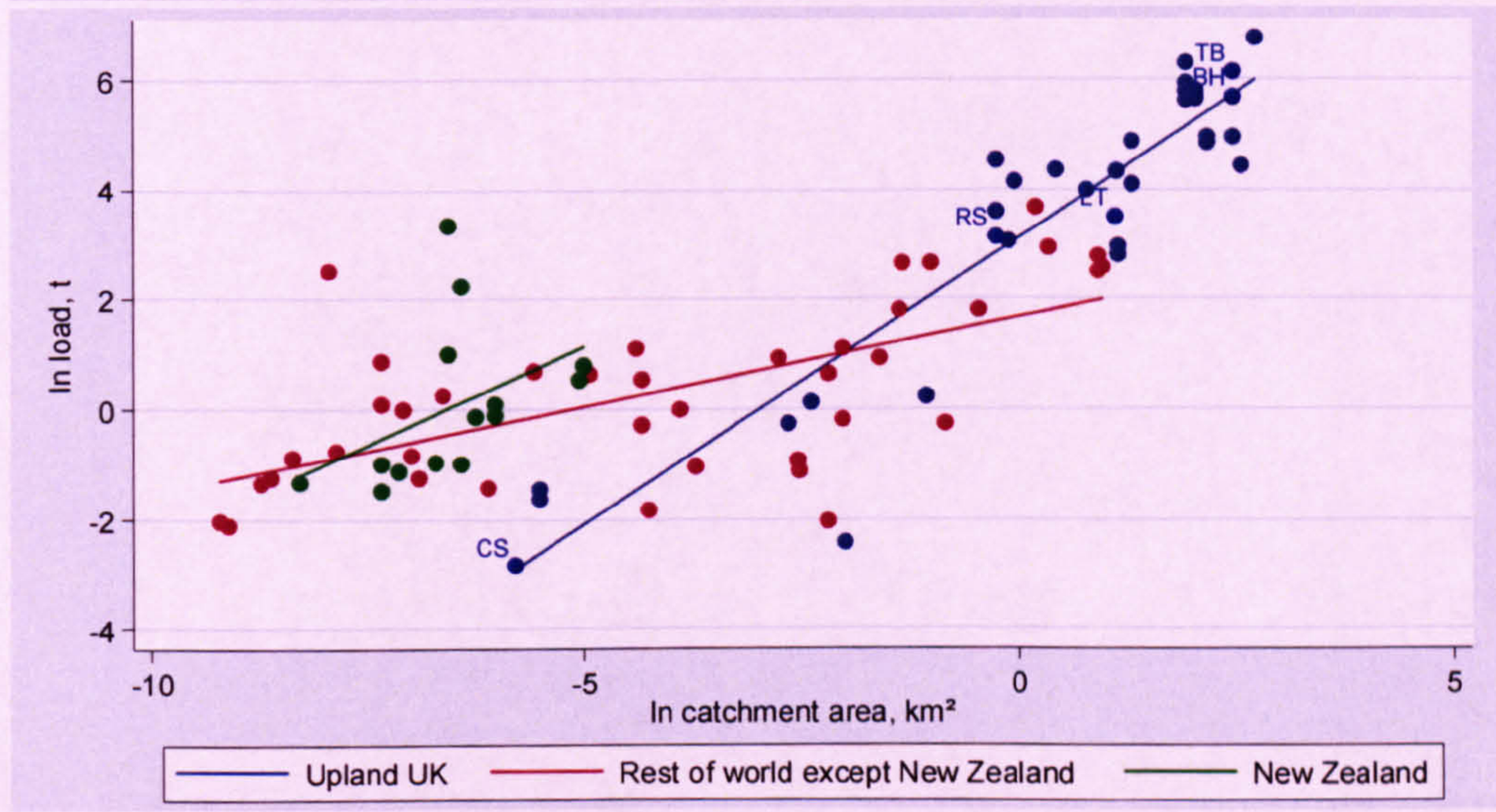

Figure 9.13. (A) Comparison of the relationship between ln load and ln area between upland UK site and upland world sites as sourced from Milliman & Syvitski (1992). (B) Continuous relationship between all upland sites with a LOWESS smooth fitted. (C) Comparison of the relationship between ln load and ln area for British, New Zealand and rest of world upland rivers. Upland UK ln load = 1.04 ln area + 3.13 with an R^2 of 0.85 and a RMSE of 1.04 rearranges to load = 22.8 area$^{1.04}$. Upland world: ln load = 0.30 ln area + 1.71 with an R^2 of 0.34 and a RMSE of 1.27 and rearranges to load = 5.5 area$^{0.30}$.

by Newson (1986) for small British rivers (Figure 9.14). This reaffirms that there is more sediment available in upland areas. The steeper gradient suggests that as catchment area increases, the rate of increase in suspended sediment load is greater. This may indicate better connectivity between hillslopes and the channel in upland catchments given the generally higher drainage densities, and limited anthropogenic influence.

Table 9.17. Equations relating annual suspended sediment load (L, in t) to catchment area (A, in km^2).

Reference	River type	Equation
Newson (1986)	Small (<100 km^2) British catchments	$L = 9.65\ A^{1.03}$
Collins (1981)	Lowland British	$L = 12.9\ A^{1.21}$
Walling (1982)	World's highest river loads	$L = 3487.8\ A^{0.92}$
This study	British uplands	$L = 22.8\ A^{1.04}$
This study	World uplands	$L = 5.5\ A^{0.30}$

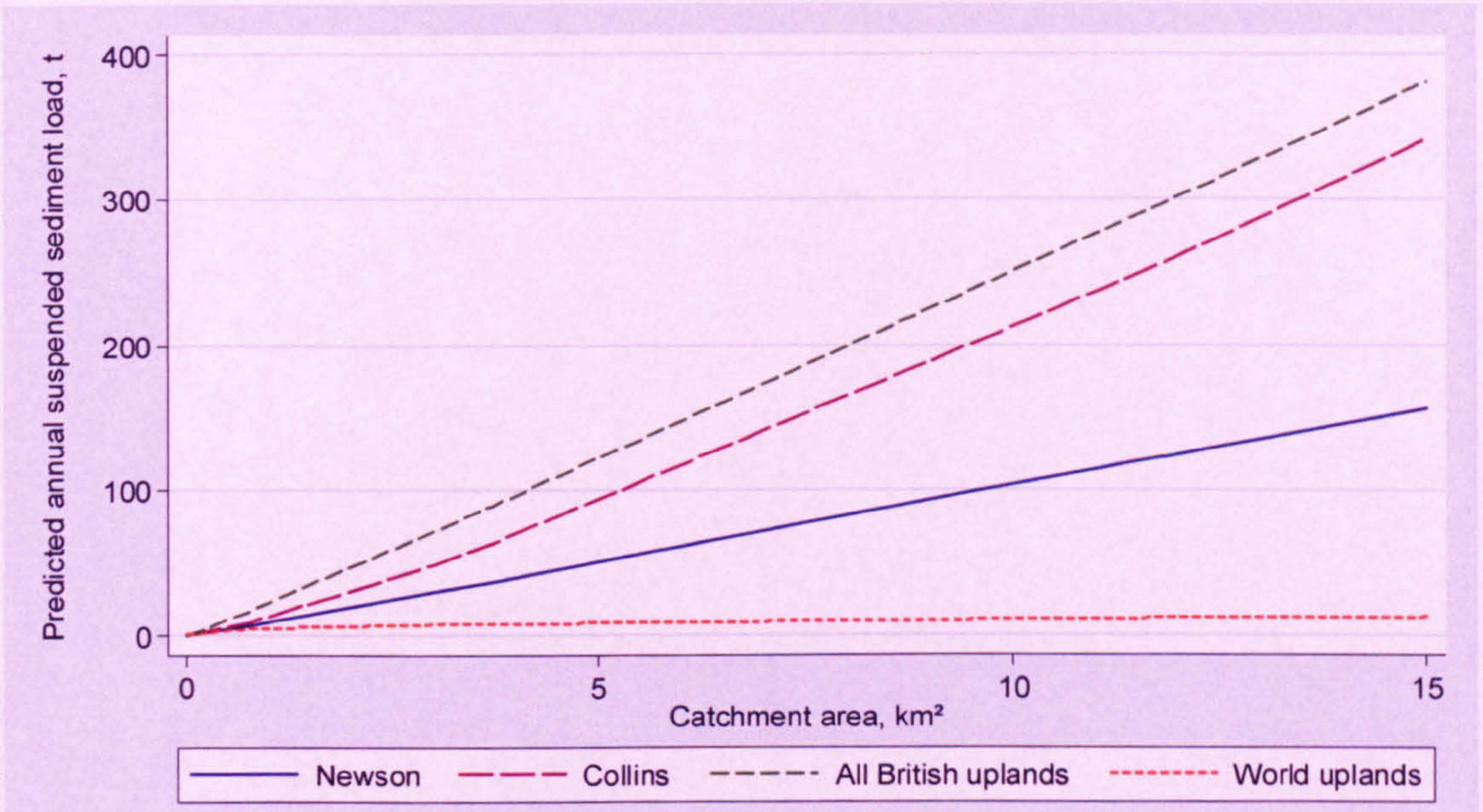

Figure 9.14. Suspended sediment loads predicted by published equations (see Table 9.17) and those established in this study (Figure 9.13).

Other studies have shown that there is more variability in the suspended sediment loads of smaller catchments (e.g. Wasson, 1994). Although this is not apparent graphically, statistically there is more variability in the smaller British upland catchment loads as indicated by comparison of the mean, standard deviation and coefficient of variation of load estimates when divided into four classes: catchments smaller than 2 km^2, catchments between 2 km^2 and 5 km^2, catchments between 5 km^2 and 10 km^2, and catchments greater than 10 km^2 (Table 9.18). The variability in catchments greater than

10 km^2 is greater than that of the middle two catchment classes. This is the result of the Langden Brook catchment (Wilkinson, 1971), which has a very high load compared with other catchments in the >10 km^2 class. There are very few catchments in each of the size classes. This illustrates the value of this study in terms of increasing the number of British upland catchments investigated.

Table 9.18. Mean, standard deviation and coefficient of variation of the load estimations of British upland catchments less than 2 km^2, between 2 km^2 and 5 km^2, between 5 km^2 and 10 km^2 and greater than 10 km^2 in area.

Area, km^2	N	Mean	St. Dev.	CV%
<2	13	24.5	33.1	135.1
>2 & <5	7	55.4	39.3	76.4
>5 & <10	10	295.7	112.6	38.1
>10	5	361.6	304.9	84.3

Examination of correlation coefficients (Table 9.19) and graphs indicate that the relationships between catchment length, relief range, minimum elevation, drainage density, precipitation, peak flow, mean temperature, minimum temperature or maximum temperature and the optimal load estimate for the study catchments are weak (a correlation coefficient of 0.85 was chosen as a threshold). There is a clear positive relationship between sediment load and catchment area (Table 9.19 & Figure 9.15). Positive relationships also exist between maximum elevation, stream order, total channel length and mean flow and sediment load estimate (Table 9.19 & Figure 9.15). The only negative relationship is between channel slope and load estimate (Table 9.19 & Figure 9.15). This suggests catchment area, maximum elevation, stream order, total channel length, mean flow and channel slope may control suspended sediment delivery. However, stream order, total channel length, mean flow and channel slope may be spurious correlations as will, to some degree, be related to catchment area.

The relationships between catchment characteristics and annual loads are weaker when all undisturbed British upland catchments are included (Table 9.19). This could be a result of the increased number of data points, the different methodologies used in the different studies (Figure A.1) or true differences between the catchments. The only catchment characteristics which correlate with load at > 0.75 are catchment area, total channel length and mean annual flow (Table 9.19). These are also the only characteristics which graphically show a good relationship with annual load (Figure 9.16)

Table 9.19. Correlation coefficients between suspended sediment loads for study catchments of this investigation and all undisturbed upland Britain catchments, and catchment characteristics.

Catchment characteristic	Correlation coefficient This study	All
Area	0.95	0.83
Catchment length	0.51	0.25
Average channel slope	-0.92	0.27
Relief range	0.73	0.58
Minimum elevation	0.03	-0.61
Maximum elevation	0.85	0.33
Stream order	0.95	0.70
Drainage density	-0.44	-0.25
Total channel length	0.99	0.81
Mean flow	0.96	0.76
Peak flow	0.84	0.30
Precipitation	0.24	0.32

There are numerous articles in the literature discussing the relationship between suspended sediment load and catchment area. Most exhibit a positive trend and the rate of increase in load often decreases with increasing catchment area (e.g. Milliman & Syvitski, 1992 and Wass & Leeks, 1992). This pattern was found for the study sites of this investigation (Figure 9.15), and is likely to be an indication of the decreasing proportion of contributing catchment area as the size of the catchment increases, i.e. as catchment area increases a smaller and smaller proportion of the catchment contributes to the suspended load of the channel as the travel distances between the hillslope and channel increases. This pattern is also evident on the plot of loads of all undisturbed catchments versus catchment area (Figure 9.16). Therefore, the control of catchment area over suspended sediment load is important (regardless of other catchment characteristics and is evident regardless of methods used).

It is interesting that there is a positive relationship between maximum elevation and suspended sediment load as elevation was defined as an influential factor in studies examining trends between catchment characteristics and specific sediment yield at a global scale (Dedkov & Moszherin, 1992; Milliman & Syvitski, 1992). There is limited evidence of the control of maximum elevation at a regional scale. Although, this is not surprising given the limited number of studies that compare more than one catchment within the same region. Also, the influence of topography may be easily subsumed by other factors, especially in larger basins with more anthropogenic activity. The maximum elevation is unlikely to be the causal factor. Dedkov & Moszherin (1992)

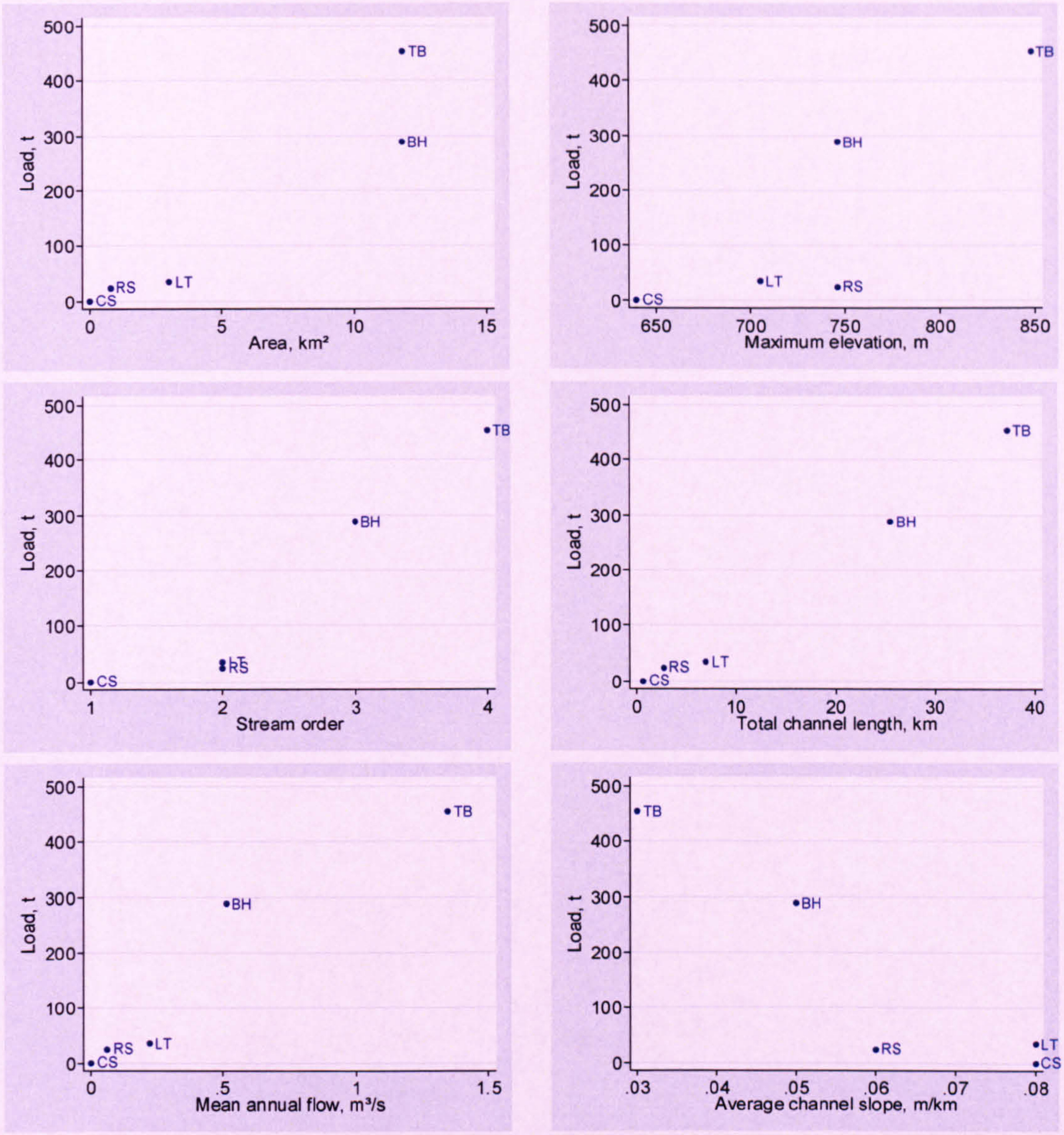

Figure 9.15. The relationship between various catchment characteristics and annual suspended sediment load as calculated by the optimum model for Burnhope, Candleseaves, Langtae, Rough Sike and Trout Beck.

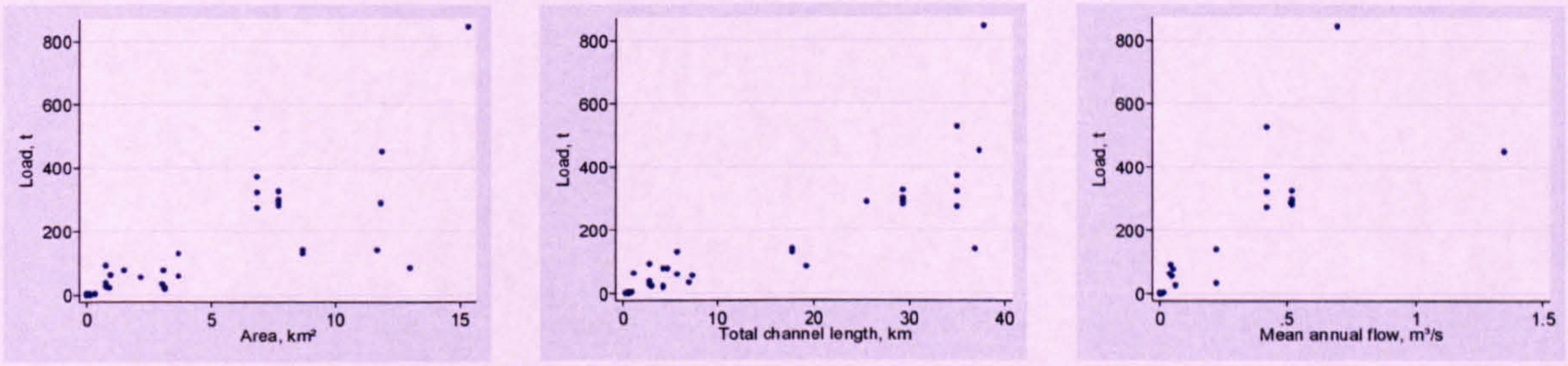

Figure 9.16. The relationship between suspended sediment load and catchment area, total channel length and mean annual flow for all undisturbed British upland catchments.

stated that erosion intensity was found to be directly related to the amplitude of the relief but was drowned out in many areas by the influence of anthropogenic activity. Millliman & Syvitski (1992) suggested that measure of topography may not be the causal factor but a proxy for tectonic activity. With reference to this study tectonic activity can be assumed to be constant for all the study areas. It is more likely that relief, especially as only maximum elevation (not minimum elevation or the range in relief) exhibited a positive relationship with sediment load, is a proxy for variables (i.e. precipitation, type and extent of vegetation, grazing impact, temperature), which are important for sediment delivery and vary with altitude.

The positive relationship between suspended sediment load and stream order (Figure 9.15) is likely to be a spurious correlation as stream order, especially with regard to the study sites of this investigation, is a good proxy for catchment area. Several studies detail this through the use of nested sampling stations.

Total channel length could also be a proxy for catchment area and hence explain the positive relationship between total channel length and suspended sediment load (Figure 9.15). However, channel length could be the causal variable. In fact, there may be an argument that catchment area is a good proxy for total channel length, which is actually the causal variable. This is suggested on the basis of several considerations. First, if the channel bed and channel banks are important sediment sources, (which the hysteresis analysis suggests this, especially for Candleseaves), then the greater the channel length the greater the amount of available sediment. Second, catchment area may exhibit a poor relationship with sediment load in some catchments as some of the catchment may be disconnected from the channel and therefore not contributing to the sediment load. Therefore, on this basis, stream length may be a better predictor. Limited studies compare total channel length and suspended sediment load. This is likely a result of the time-consuming nature of calculating total channel length for several catchments (although this is now quicker and more accurately done using GIS) and because it is not a catchment characteristic which is reported in many publications: hence those papers which compile databases from existing studies will not have the information. Total channel length of undisturbed British upland catchments also exhibited a positive relationship with annual suspended sediment load (Figure 9.16 & Table 9.19). Therefore, total channel length must be a important control as variation in other catchment characteristics and different methodologies do not obscure the pattern.

Dividing total channel length by catchment area provides an estimate of drainage density. Catchment drainage density has been related to suspended sediment loads successfully by Ludwig & Probst (1996) for 60 world rivers but no relationship was found for the study sites of this investigation (Table 9.19).

Mean flow also exhibits a positive relationship with suspended sediment load (Figure 9.15). Ludwig & Probst (1996) concluded that discharge was the strongest control over suspended sediment yield and it was also recognised as an influence by Dedkov & Moszherin (1992) and Milliman & Syvitski (1992). Once again these authors were assessing the controls over suspended sediment load operating at a global scale. Discharge is also generally the dominant control over SSC at a catchment scale (Lenzi & Marchi, 2001; Asselman, 2000 etc.). Therefore, it is not surprising that there is a positive relationship between mean flow and suspended sediment load. Discharge is an influential forcing on suspended sediment dynamics regardless of scale. There are exceptions to this, for example, snowmelt events (Stott & Grove, 2001) and bank collapse on the falling limb (Carling, 1983). As discharge is such an influential factor in this study, it is suggested that while sediment is not transported at transport capacity due to sediment supply constraints, sediment supply is not restricted enough to substantially distort the relationship between suspended sediment dynamics and discharge. The positive relationship between mean annual flow and suspended sediment load is also evident on the undisturbed British uplands plot (Figure 9.16). Therefore, discharge is important in suspended sediment dynamics at a range of scales: catchment, northern England upland catchments, British upland catchments and worldwide (Dedkov & Moszherin, 1992 and Milliman & Syvitski, 1992).

Channel slope exhibits a negative relationship with sediment load which means that as channel slope increases sediment load decreases (Figure 9.15). On initial examination this is illogical as a steeper channel slope means that the stream power, and therefore the erosion and entrainment potential, should be higher. However, there is less chance of sediment storage in steeper channels and therefore sediment has to be derived from stores which require more energy to be accessed, i.e. erosion from banks and hillslope sources. Related to this is the nature of the channel bed. Given the higher stream power the channel bed is likely to have a more developed armour layer which affords more protection, or the channel may have cut into more resistant material or could be bedrock controlled. Also, conceptual models of catchments suggest steeper channels are

generally those in the upper catchment (Beschta, 1987) and therefore have a smaller contributing area which means there is potentially less sediment available. However, this may be countered by improved connectivity between the hillslope and channel in steeper catchments. The author has found no published studies which identified a relationship between channel slope and suspended sediment load although some studies (Phillips, 1990 and Ludwig & Probst, 1996) established basin slope as an influential variable.

9.5.2 Specific suspended sediment yield

In terms of specific sediment yields the study sites are comparable to published undisturbed British upland studies (Figure 9.17). Many of the sites with higher specific sediment yields are those which underwent some form of land use change, mostly forestry, e.g. Monachlye and Kirkton (Johnson, 1988) (Table A.1).

Suspended sediment yields generally decline as catchment area increases, (Wass & Leeks, 1999, Labadz *et al.*, 1991; and Dedkov & Moszherin, 1992), but the specific sediment yield of Trout Beck is greater than that of Rough Sike (38.3 t km^{-2} yr^{-1} and 30.5 t km^{-2} yr^{-1} respectively). Catchments which experience an increase in specific sediment yield with an increase in catchment area may be characterised by a large number of first order streams (McManus & Duck, 1996), be dominated by channel sediment sources (Dedkov & Moszherin, 1992) or still be responding to the last glaciation (Church & Slaymaker, 1989). Church & Slaymaker (1989) found that specific sediment yield increased with increasing catchment areas for small (up to 3×10^4 km^2), undisturbed streams in British Columbia, Canada. This trend was attributed to the greater influence of remobilisation of Quaternary sediments over denudation of the land surface. Therefore, it is possible that the remobilisation of sediments delivered to the catchments during the last glaciation is exerting more control over suspended sediment dynamics than sediment derived from the current landscape. Potentially any of these explanations may apply to the Rough Sike-Trout Beck system. First, there are some first order channels which drain directly into Trout Beck, which is a fourth order stream (Figure 5.3) and there are also gully networks, some of which are sporadically connected to the Trout Beck system. Second, there are a lower percentage of peat banks in the Trout Beck catchment than the Rough Sike catchment. As peat is fairly resistant to erosion due to its fibrous nature (Evans and Burt, 1998), more sediment may be supplied by channel banks in the Trout Beck catchment. Third, the catchments were

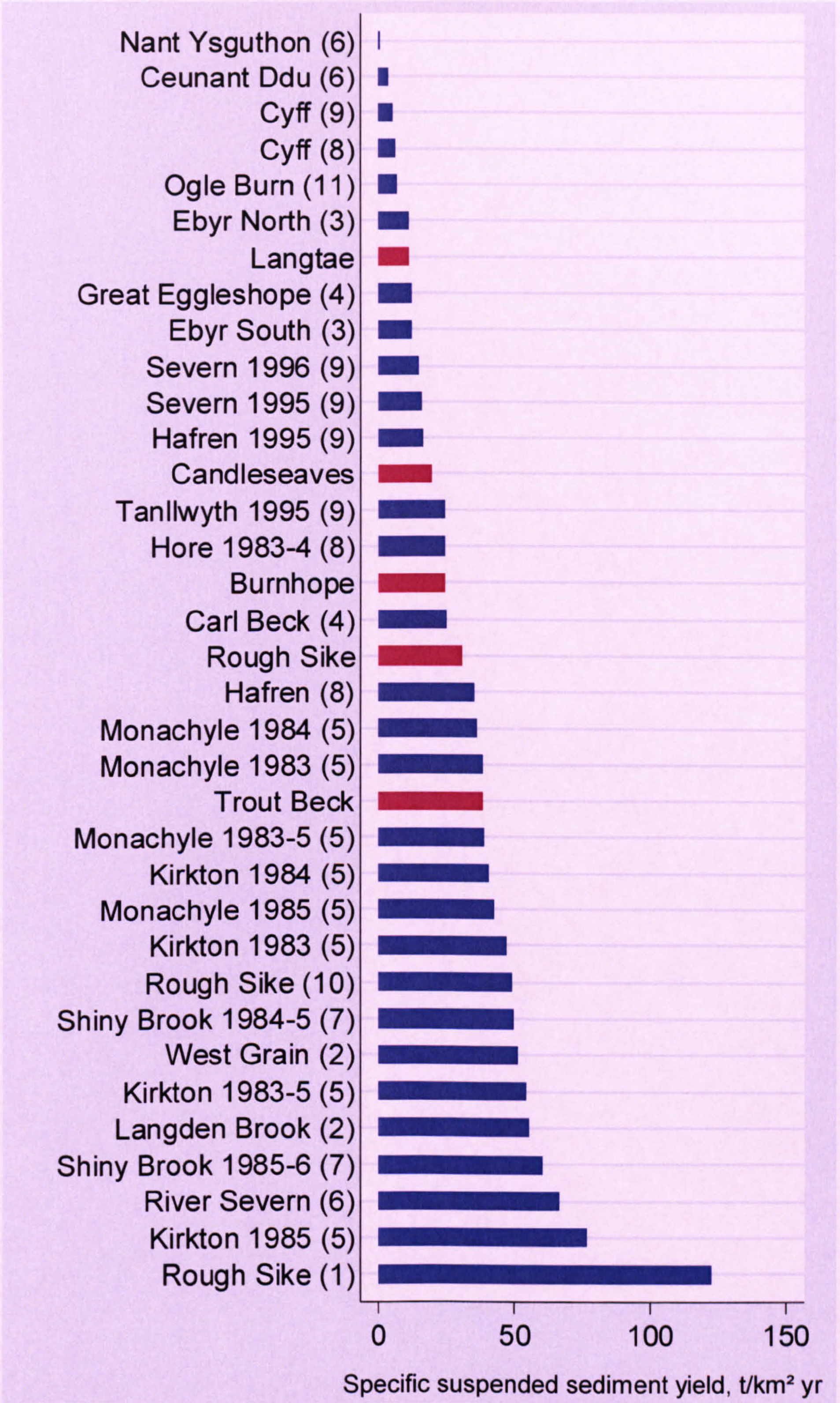

Figure 9.17. Comparison of upland UK specific suspended sediment yields. (1) Crisp, 1966; (2) Wilkinson, 1971; (3) Oxley, 1974; (4) Carling, 1983); (5) Johnson, 1995; (6) Francis, 1987; (7) Labadz *et al.*, 1991; (8) Kirby *et al.*, 1991(9) Leeks & Marks, 1997; (10) Evans & Warburton (in press); and (11) Duck, 1985. See Table A.1 for more information.

affected by the last glaciation and may still be responding. A fourth possible explanation is the relative percentages of mineral and organic sediment sources within the catchments. Analysis of the simultaneous SSC from Rough Sike and Trout Beck (section 7.3.1.2) suggested there was more mineral sediment available in the lower order catchments at Moor House. Therefore, the suspended sediment yield may be higher due to the greater gravimetric contribution of mineral sediment. However, this is contradicted by the organic matter contents of the TIMS sediment, which suggest that there is 2% less organic sediment in Rough Sike than Trout Beck. Although, the organic matter content of the TIMS sediment closest to the Rough Sike gauging site is higher than that of the TIMS sediment closest to the Trout Beck gauging site. Also, organic material transported in Rough Sike may be too large to be sampled by the TIMS. During transport the larger peds/blocks will be abraded and therefore a smaller fraction will be too large for sampling by the time it reaches Trout Beck. Finally, the difference in specific suspended sediment yields could be a result of the inter-annual variability in suspended sediment loads, which can be very variable for small catchments (Wasson, 1994).

The specific sediment yield of Burnhope is greater than that of Langtae (26.7 t km^{-2} yr^{-1} and 9.5 t km^{-2} yr^{-1} respectively). However, given the potential under-estimation of the Langtae suspended sediment load as a result of the sampling regime (solely fixed-interval) it is not possible to state, with confidence, if it is a real difference.

The specific sediment yield of Burnhope is very similar to that of Carl Beck (Carling, 1983) (Figure 9.17). This may be explained by their similar lithologies, as they are in the same region. However, in terms of other catchment characteristics Carl Beck and Burnhope are quite different. Burnhope is over five times as large as Carl Beck, has a mean flow over ten times as high, precipitation is substantially less (1900 mm yr^{-1} and 1100 mm yr^{-1} respectively) and Burnhope is higher in altitude (Table 5.1 & A.1). These similarities suggest that regional controls, i.e. lithology, are more influential than catchment-specific controls. It is not possible to make a definitive statement regarding this as while the specific sediment yields of Trout Beck, Rough Sike, Carl Beck and Burnhope are similar and they are all in the same region, while the yields of Langtae and Great Egglestone Beck are much lower (Figure 9.17). The low specific suspended sediment yield at Langtae could be explained by the proportion of bedrock-confined channels and sampling regime: only fixed-interval samples were taken which tends to

result in load under-estimations. However, this does not explain the low yield associated with Great Egglestone Beck. The difference between Great Egglestone Beck and Carl Beck could be explained by the lack of peat deposits in Carl Beck and extensive coverage in Great Egglestone Beck (Carling, 1983).

A broad regional signal is apparent in the specific sediment yields (Figure 9.18). Catchments in Scotland (Johnson, 1995) generally exhibit the highest yields, the Welsh catchments generally have the lowest yields (Oxley, 1974; Kirby *et al.*, 1991; Francis, 1987; and Leeks & Marks, 1987) and the Pennine catchments are dispersed throughout (Crisp, 1966; Evans & Warburton, in press; Labadz *et al.*, 1991; Wilkinson, 1971; Carling, 1983; and this study). This regional signal suggests that large-scale controls, lithology and the relationship between rainfall and runoff, must be an important forcing on suspended sediment dynamics.

The three specific suspended sediment yields estimated for Rough Sike (this study; Evans & Warburton, in press; and Crisp, 1966) are very different (Figure 9.17) and there was no land use change in the catchments. This is a clear illustration of the problems associated with comparing yields from different time periods and those derived by different methods.

The specific suspended sediment yields of the catchments of this study and all undisturbed British upland catchments were correlated with catchment area, catchment length, average channel slope, relief range, minimum elevation, maximum elevation, stream order, drainage density, total channel length, mean annual discharge, peak annual discharge and annual precipitation. Given that specific suspended sediment yield is in t km^2 yr^{-1} some of the relationships may be spurious. However, examining specific suspended sediment yield eliminates the effect of scale as a control. None of the correlations were > 0.85 except average channel slope for study sites of this investigation (Table 9.20). Precipitation and maximum elevation correlated with specific yield > 0.80 for the study sites of this investigation (Table 9.20). The correlations based on all undisturbed British upland sites are noticeably lower. This suggests that specific suspended sediment yields are more sensitive to changes in catchment characteristics than suspended sediment load (section 9.5.1), which may indicate the dominance of catchment area over suspended sediment dynamics.

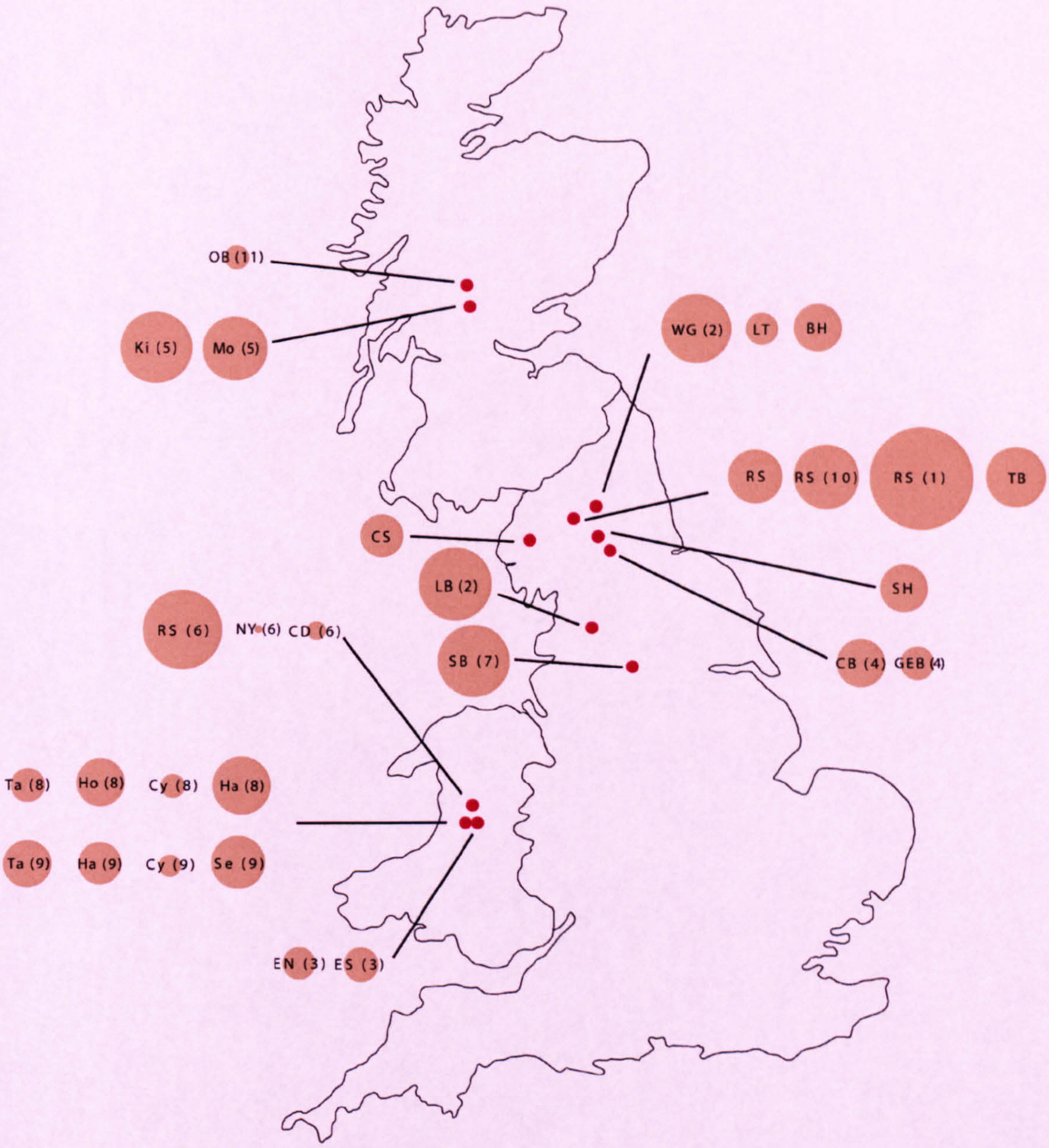

Figure 9.18. Spatial variation in specific suspended sediment yields of undisturbed catchments in Britain. OB = Ogle Burn; CS = Candleseaves; LB = Langden Brook; SB = Shiny Brook; RS = River Severn; NY = Nant Yusguthon; Ceunant Ddu; Ta = Tanllwyth; Ho = Hore; Cy = Cyff; Ha = Hafren; Se = Severn; EN = Ebyr North; ES = Ebyr South; WG = West Grain; LT = Langtae; BH = Burnhope; RS = Rough Sike; TB = Trout Beck; SH = Swinhope; CB = Carl Beck; and GEB = Great Eggleshope Beck. (1) Crisp, 1966; (2) Wilkinson, 1971; (3) Oxley, 1974; (4) Carling, 1983; (5) Johnson, 1995; (6) Francis, 1987; (7) Labadz *et al.*, 1991; (8) Kirby *et al.*, 1991; (9) Leeks & Marks, 1997; (10) Evans & Warburton (in press); and (11) Duck, 1985. See Table A.1 for more information.

Table 9.20. Correlation coefficients between specific suspended sediment yields for study catchments of this investigation and all undisturbed upland Britain catchments, and various catchment characteristics.

Catchment characteristic	Correlation coefficient	
	This study	All
Catchment area	0.48	0.08
Average channel slope	-0.89	0.21
Catchment length	-0.09	-0.11
Relief range	0.06	0.30
Minimum elevation	0.73	-0.06
Maximum elevation	0.80	0.37
Stream order	0.67	0.23
Drainage density	-0.28	-0.15
Total channel length	0.62	0.25
Mean flow	0.67	0.14
Peak flow	0.75	0.01
Precipitation	0.83	0.20

The relationship between yield and average channel slope is negative (Figure 9.19) which suggests that as channel slope increases the sediment yield decreases. *A priori* reasoning may suggest that the relationship should be positive: higher slopes results in higher stream powers and hillslopes are likely to be steeper and therefore hillslope-channel connectivity stronger. However, in common with the relationship between annual suspended sediment load and channel slope (section 9.5.1), this can be attributed to less in-channel storage, more developed bed armour, higher proportions of bedrock controlled channel and a smaller contributing area in catchments with steeper gradients.

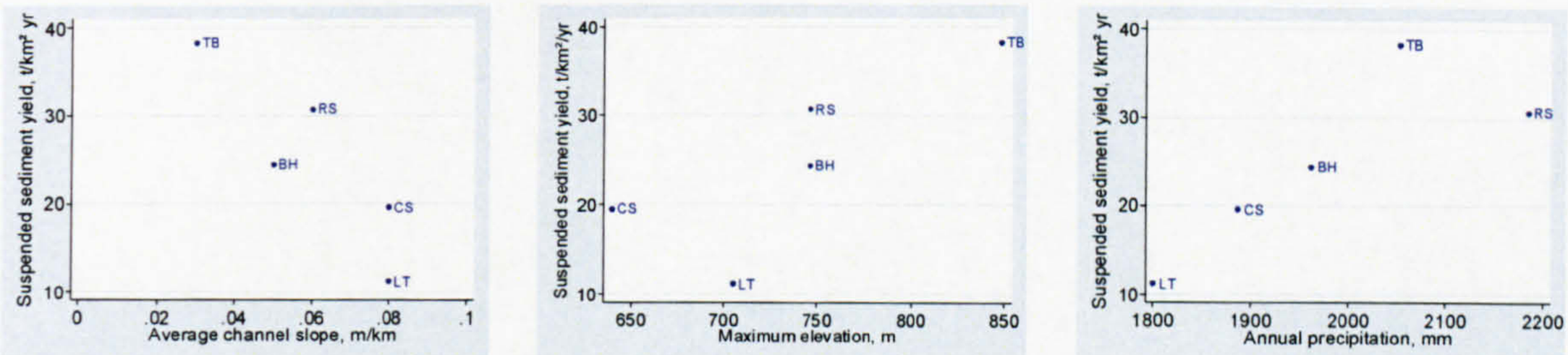

Figure 9.19. The relationship between specific suspended sediment yield and average channel slope, maximum elevation and annual precipitation for study sites of this investigation.

The relationship between sediment yield and maximum elevation is positive (Figure 9.19), suggesting that higher catchments have higher sediment yields. As in section 9.5.1 relating annual load to maximum elevation, this may be explained by maximum elevation acting as a proxy for the effect of precipitation (especially given its correlation

with yield), vegetation type and cover, grazing impact, temperature and other such characteristics which vary with altitude.

The positive relationship between precipitation and sediment yield (Figure 9.19) suggests that higher yields are associated with higher precipitation. This may be related to the role of precipitation in eroding and transporting sediment. It is interesting that annual precipitation shows this pattern because often it is precipitation intensity which is related to erosion and the likelihood of overland flow and hence transport of sediment to the channel (Evans, 1980). However, Francis (1987) found that precipitation totals were more important than precipitation intensities when investigating suspended sediment dynamics in three catchments in Mid-Wales.

9.6 Chapter summary

This chapter has discussed suspended sediment rating curve development and the resultant load estimates. It has highlighted the need to consider the number of rising and falling limb samples, the range of discharge and the distribution of discharge in the sampled discharge series and the annual discharge series, as differences that may cause bias. The limitations of indicators of model fit have been outlined which, if not considered, could lead to the development of poorly fitting models and therefore inaccurate load estimations.

One of the principal outcomes of this chapter is the demonstration of variability in the load estimates developed for different models for the same site, which is associated with the degree of variability in the annual discharge records. Consideration of each model for each site in light of the indicators of model fit suggest that linear regression corrected for back-transformation bias by smearing is the most applicable model for small British upland catchments. The most common method in the literature is linear regression back-transformed by the log-normal correction factor, so suggests most published load estimates should be reasonable given the similarity between smearing and log-normal corrected load estimates in this study (Tables 8.5, 8.9, 8.12, 8.16, 8.20 & 8.25). Published load estimates may not be so accurate for larger catchments as GLM models were found more suitable for Burnhope and Trout Beck, the largest study sites in this investigation.

The rating curve adaptations gave variable increases and decreases in accuracy. The main outcomes of this analysis for small British upland catchments are:

(1) Developing models from different data sub-sets allows little inferences to process operating within the catchment, with the exception of dividing the data into rising and falling limb data sub-sets.

(2) With the exception of categorising the data into summer-rising, summer-falling, winter-rising and winter-falling the adaptations do not result in a notable increase in load estimate accuracy across all sites.

(3) The discharge class method increases the accuracy of the load estimates if clusters exist in the SSC-discharge plot.

Differences in suspended sediment dynamics between catchments are illustrated by examining the sediment:water index, volume of sediment removed, effective discharge interval and the magnitude and frequency of sediment delivery. These sections show that while the catchments are broadly similar their responses may be quite different. However, there are enough critical methodological issues to cast doubt on these conclusions: the sample size is only 5; the sediment:water index will be altered dramatically by inaccuracies in the suspended sediment load estimates; and the effective discharge interval analysis has been influenced by the variability in the discharge series. The main outcomes of this section are:

(1) Between 7.32×10^{-6} and 2.32×10^{-5} t of sediment, on average, are transported by 1 m^3 of water in the study catchments, with Candleseaves and Langtae being the most sediment-restricted systems. Weak relationships exist between the sediment:water index and catchment characteristics.

(2) There is a difference in the relative magnitude of gravimetric and volumetric suspended sediment yields: Candleseaves has the highest volumetric suspended sediment yield but smallest gravimetric yield (out of Trout Beck and Rough Sike). This indicates the importance of using volumetric yields to assess the impact on landscape change.

(3) The effective discharge intervals of Rough Sike and Candleseaves indicate that lower discharges are more important in terms of sediment transfer in comparison with Burnhope, Langtae and Trout Beck. The mid-range discharges are most effective at transporting sediment in Burnhope, Langtae and Trout Beck, although an exceptionally large event was also very important in Trout Beck.

(4) The magnitude and frequency of sediment delivery is markedly different for Langtae and Burnhope; they are less responsive, compared with Rough Sike, Trout Beck and Candleseaves.

(5) The magnitude and frequency of sediment delivery is broadly comparable with other British upland sites: storm events transport the majority of sediment within all the catchments.

(6) The impact of one large flood in Trout Beck is substantial.

Comparison of the suspended sediment load and yield estimates of this investigation to published studies has had several outcomes:

(1) The annual suspended sediment loads of this study are comparable to those of other British upland sites with respect to catchment area.

(2) There is a strong relationship between annual load ($t\ yr^{-1}$) and catchment area (km^2) of British upland sites: load ≈ 22.8 area$^{1.04}$. This could be used to predict the suspended sediment loads of small, ungauged upland UK catchments, probably within the bounds of inter-annual variability.

(3) Variability in suspended sediment loads decreases with increase in catchment area.

(4) Annual suspended sediment load is positively correlated with catchment area, maximum elevation, stream order, total channel length and mean flow for the study sites of this investigation and area, total channel length and mean flow for all British upland catchments. There is a negative correlation between average channel slope and load for the study sites of this investigation.

(5) A broad regional signal in specific suspended sediment yield is evident in published studies and the results of this investigation strengthen this.

(6) There is no clear relation between specific suspended sediment yield and catchment area for the study sites of this investigation or all British upland catchments. This may be a result of inter-annual variability, sampling methods, modelling methods or a combination. Nor do strong correlations exist between specific suspended sediment yield and other catchment characteristics except maximum elevation, precipitation and channel slope for the study sites of this investigation.

Chapter Ten: WITHIN-STORM SUSPENDED SEDIMENT DYNAMICS

10.1 Overview

This chapter examines the temporal variability in suspended sediment concentration and sediment supply at the storm-scale by analysis of suspended sediment transport hysteresis loops. The forms of the hysteresis loops are related to antecedent catchment conditions, storm characteristics and potential sediment sources. This was undertaken for all study sites except Langtae, as no storm sampling was undertaken at this site. Inter-catchment variation in the frequencies of the hysteresis classes is examined and related to standardised, where appropriate, storm characteristics and antecedent catchment conditions (to account for catchment scale).

10.2 Quantification of antecedent conditions and storm characteristics

A range of variables reflecting antecedent catchment conditions and storm characteristics were quantified (Figure 10.1). These were chosen by reference to the literature and consideration of the study catchments. The variables chosen to represent antecedent catchment conditions were: total precipitation (mm) over the three and seven days before the event, total flow (m^3 in all catchments except Candleseaves in which it is l given the large difference in magnitude) over the three and seven days before the event, the number of hours since a storm with an equal or greater peak discharge, average surface wetness (percentage of the time the surface was classified as wet) over the three and seven days before the event (for Rough Sike and Trout Beck only) and soil moisture (%) over the three and seven days before the event (for Rough Sike only) (section 6.2.3) (Figure 10.1).

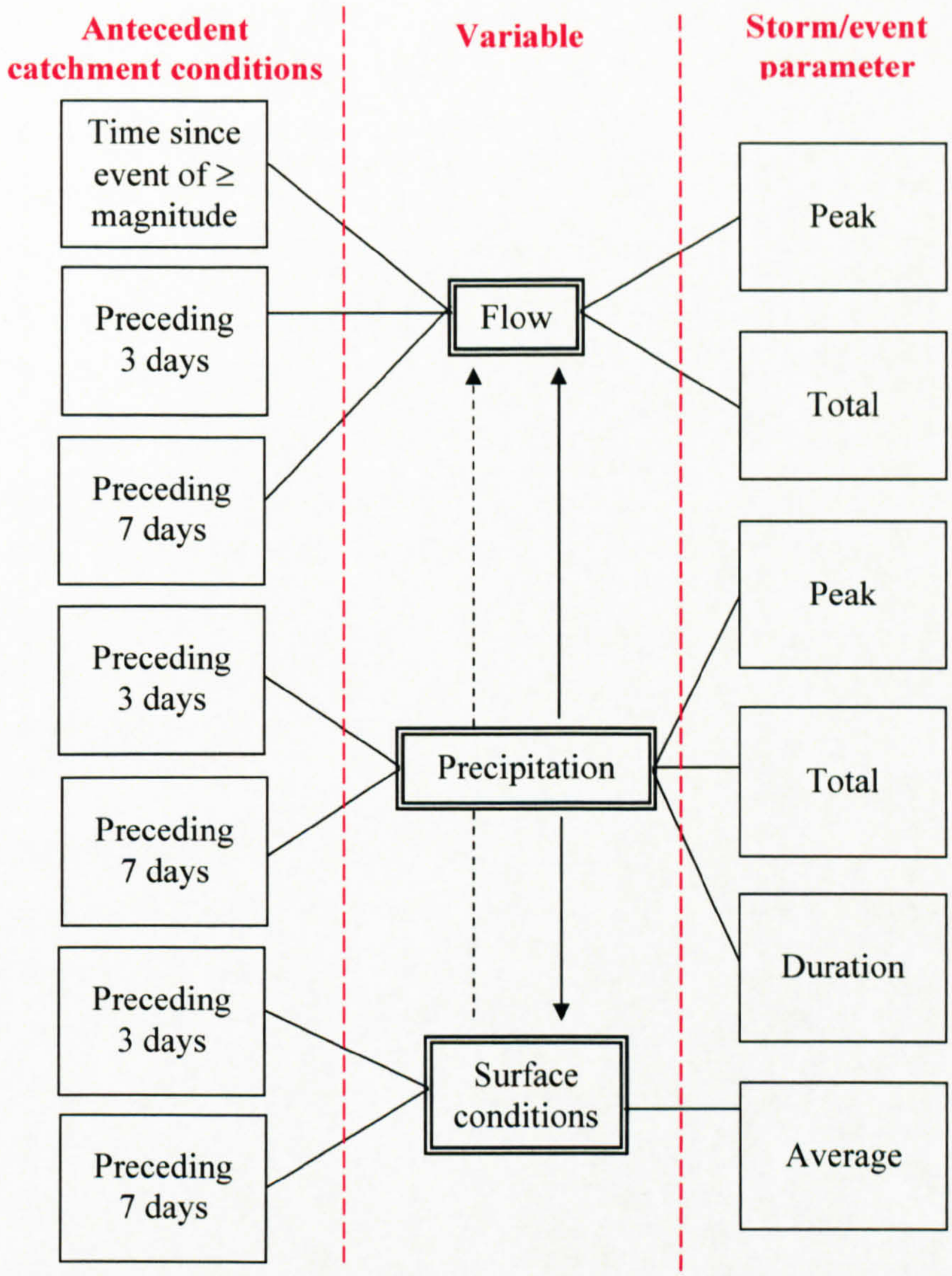

Figure 10.1. Diagram of variables quantifying antecedent catchment conditions and storm parameters used in assess the causes of hysteresis loops and sediment sources. Surface conditions refers to surface moisture and surface wetness.

The three and seven day intervals were used for all sites to allow direct comparison of the results and because the hydrological regimes are broadly similar. Precipitation, flow, surface wetness and soil moisture in the previous three days were selected as indicators of the current conditions within the catchment and because a three day interval was successful in discriminating hysteresis types in Arnás, a small, quickly responding, headwater catchment in the Pyrenees (Seeger *et al.*, 2004). Precipitation, flow, surface wetness and soil moisture in the preceding seven days were selected to capture the slightly longer-term history of the catchment, which may affect the response of the catchment in terms of likelihood of runoff and sediment available. For example, if rainfall and flow was high in the preceding three days a catchment is likely to respond

rapidly and to a greater extent. If there had been limited rainfall and flow in the preceding three days, but a notable amount in the four days before (which would be captured in the previous 7 days measurement), then the catchment is likely to respond fairly quickly but to a lesser extent. If there had been limited flow and rainfall in the preceding seven and three days then the catchment is likely to respond slower and to a lesser degree, unless the catchment had been dry long enough for a surface soil crust to form. The rainfall, surface moisture and surface wetness parameters were chosen to quantify the wetness of the catchments and therefore the likeliness of overland flow. The flow parameters were chosen to indicate the amount of sediment likely to be available for transport within the channel zone. The time since the maximum storm discharge was last attained also gives an indication of the amount of sediment available for transport within the channel, and on the floodplain if the peak discharge was greater than bankfull discharge.

The variables selected to characterise the storm events were total storm precipitation (mm), peak storm precipitation intensity (mm per 15 minutes), total storm flow (m^3 s^{-1} in all catchments except Candleseaves in which it is l s^{-1}), maximum storm discharge (m^3 s^{-1} in all catchments except Candleseaves in which it is l s^{-1}), storm duration (hours), mean surface wetness (% of time the surface was classified as wet), for Rough Sike and Trout Beck only, and mean soil moisture (%), for Rough Sike only (Figure 10.1). Total storm precipitation, peak storm precipitation intensity, surface wetness and soil moisture were chosen to quantify the likelihood of overland flow and also the potential for raindrop erosion. Total storm flow was selected to quantify the size of the storm. Maximum storm discharge was included in order to capture the extent of channel bank/floodplain sediment source areas accessed. Storm duration was included to allow inferences to be made regarding potential for sediment exhaustion.

Care must be taken when examining the variability of the selected parameters between sites as they are characteristics and conditions associated with sampled events and the sampling strategies were biased. This is clearly demonstrated by the antecedent conditions and storm characteristics of Rough Sike and Trout Beck properties which, with the exception of flow, were derived from the same weather station: larger events with wetter antecedent catchment conditions were sampled in Trout Beck (Table 10.1). There is much variability in the properties for the same catchment (Table 10.1). This is also partially attributable to the sampling strategy and time of year the samples were

Table 10.1. Antecedent catchment conditions and storm characteristics for each storm set suitable for hysteresis analysis in the study catchments. * Flow is in l per 3 or 7 day period and ** discharge is in l s^{-1} for Candleseaves. 'Simultaneous' lag indicates that SSC and *Q* peaked together.

	Storm	Hysteresis class	Precipitation: 3 days, mm	Precipitation: 7 days, mm	Flow*: 3 days, m^3	Flow*: 7 days, m^3	Average surface wetness: 3 days, %	Average surface wetness: 7 days, %	Average soil moisture: 3 days, %	Average soil moisture: 7 days, %	Flow*: storm, m^3	Peak precipitation intensity, mm per hour	Storm precipitation, mm	Storm duration, hrs	Q peak**, $m^3 s^{-1}$	Time since peak Q last reached, hrs	Average storm surface wetness, %	Average storm soil moisture, %	Lag			SSC range, mg l^{-1}
																			First to peak	Hrs	Min	
Burnhope	25th October	3	45.8	59.4	182918.8	328776.6					134164.2	1.8	33.2	31.8	2.12	58.5			*Q*		45	12-84
	2nd November	5	38.4	119.8	254947.3	560650.3					112686.0	1.6	24.4	26.3	2.18	1667.1			SSC	1	45	6-87
	12th November	2	24.8	142.2	149264.2	592900.3					121281.6	2.2	34.6	28.8	1.86	85.8			SSC		30	3-35
	28th November	3	43.0	65.2	231442.9	429899.5					155452.0	2.4	30.6	40.2	2.55	579.8			*Q*	1	15	9-245
	8th December	2	32.2	80.0	185795.1	498395.6					52585.3	1.4	25.6	15.2	1.69	371.8			SSC		45	7-47
	23rd January	3	17.8	18.4	99136.4	142955.7					164537.5	1.8	33.8	38.7	2.02	1345.8			*Q*		50	31-389
	10th February	2	19.6	114.0	118791.2	432827.5					147984.2	1.8	44.2	32.5	2.14	88.2			SSC	1	30	29-106
	7th March	2	0.2	0.2	76325.7	160623.6					138287.7	0.2	0.4	40.8	1.75	579.8			SSC	3	10	18-163
Candleseaves	17th May	3	19.8	47.0	14211.7	65386.4					8961.3	1.2	11.4	14.2	0.3	88.8			*Q*		20	0-3
	19th June	2	26.0	26.0	2563.3	7596.1					47491.6	8.6	21.8	23.3	3.7	1093.8			SSC		25	3-134
	21st July	2	26.6	38.2	12919.2	12919.3					20015.8	1.0	6.2	22.5	0.7	459.2			SSC		45	1-5
	28th July	2	15.8	50.4	18272.0	127518.5					67734.7	2.2	15.0	16.0	2.5	651.2			SSC	1	15	3-13
	23rd January	2	18.0	71.2	63382.5	304110.8					52671.1	1.8	12.8	18.7	3.2	61.2			SSC	2	10	2-18
	7th February	6	23.2	140.0	107471.1	858594.1					8857.3	0.6	4.6	15.7	0.2	54.5			SSC	1	40	1-10
Rough Sike	29th August	2	12.0	21.8	1272.6	6009.7	13.0	13.0	0.25	0.25	2493.6	2.6	3.6	28.0	0.05	7.4	35.1	0.25	SSC	1	00	2-51
	16th October	2	12.0	37.6	5584.7	32067.7	32.0	30.3	0.28	0.27	7458.7	1.4	6.2	23.2	0.22	5.5	39.4	0.27	SSC		30	1-14
	16th November	2	9.6	16.6	4204.1	24528.5	52.1	37.3	0.28	0.28	10041.0	5.2	9.4	19.5	0.58	70.9	32.9	0.27	SSC		30	1-52
	19th November	2	33.8	35.8	33797.8	40708.3	22.5	29.3	0.27	0.28	11705.3	4.4	13.2	15.5	0.67	73.6	53.3	0.28	SSC		45	1-48
	23rd December	2	-	-	4745.0	27368.3	62.4	70.1	0.31	0.30	7186.9	-	-	12.2	0.44	5.1	40.2	0.30	Simultaneous			1-43
	11th February	5	-	-	18077.3	39090.1	51.1	47.1	0.31	0.31	11622.7	-	-	20.8	0.30	4.6	14.9	0.30	SSC	1	45	2-17
	26th March	5	16.4	16.6	14683.3	19576.8	31.4	24.3	0.31	0.33	12329.9	2.4	10.4	20.9	0.28	14.7	23.1	0.30	SSC	1	00	5-30
	5th May	3	15.0	23.2	3100.0	12185.7	31.2	28.9	0.30	0.30	9031.1	2.4	11.0	12.3	0.42	12.7	67.3	0.29	*Q*		30	3-34
Swinhope	28th April	2	21.8	28.0	12971.1	21634.6					24650.5	1.0	5.2	9.8	1.94				SSC		10	10-394
	30th July	2	15.8	16.2	7113.4	17249.4					12309.7	1.4	17.8	16.5	0.49	1091.5			SSC		30	5-293
	12th October	2	21.4	21.8	6041.8	13113.3					9568.9	1.2	15.6	16.7	0.30	775.3			SSC		30	7-64
	8th November	2	14.4	48.2	40919.7						28423.5	0.4	8.6	19.7	0.68	54.8			SSC		50	4-29
	1st March	5	16.6	17.2	10987.5	22150					20681	3.2	13.8	20.3	1.06	520.2			*Q*		30	5-288
	1st April	5	8.4	8.4	5420.5	12906.8					5239.2	1.6	12.8	20.8	0.15	477.0			*Q*		50	3-34
	19th November	2	4.2	13.0	17009.7	48618					40950.4	0.6	5.8	12.2	2.71	397.8			SSC		40	3-201
Trout Beck	10th October	2	62.6	91.0	585150.0	865592.9	33.5	33.2			69962.8	2.0	5.4	25.3	1.80	30.0	15.4		SSC	2	30	3-10
	26th October	3	19.4	56.8	208275.9	546279.9	25.0	20.6			84612.9	2.0	6.8	24.8	1.84	56.7	12.8		*Q*		15	9-16
	21st November	2	23.4	23.8	76167.0	117995.4	44.8	31.5			184100.4	4.0	20.4	22.8	6.55	1047.3	30.8		*Q*		45	6-28
	17th January	2	29.6	47.6	177447.6	364068.9	22.4	25.7			220815.0	3.6	22.6	29.8	6.15	493.8			SSC	1	15	1-58
	20th January	2	25.0	60.6	278604.0	513987.3	22.1	25.1			87911.1	2.2	11.0	23.0	2.87	65.5	19.1		SSC		30	2-10
	1st April	2	16.8	17.8	13836.6	35668.8	24.0	12.9			120046.5	3.8	13.8	23.5	5.19	526.5	18.1		SSC	1	00	6-45

taken. For example, the average precipitation in the preceding seven days is likely to be higher for Burnhope, as all storms occurred during the winter, in comparison with Candleseaves, for which only two events occurred in the winter (Table 10.1). Throughout the storm-by-storm analysis the antecedent catchment conditions and storm characteristics are discussed in relative terms specific to that catchment so no interpretation of Table 10.1 by the reader is required.

10.3 Framework for analysis

Previous published studies provide a framework for the interpretation of the hysteresis plots derived for the study sites (Table 10.2). A review of such studies was given in section 2.7.1. One possible influence not outlined is the effect of sediment released by bed disturbance. However, it is not possible to attribute hysteresis loop form to bed disturbance with certainty as bed disturbance could promote class 2 or class 3 hysteresis, depending on the timing of flows of sufficient magnitude to cause bed movement; the infrequency of bed movement in the study systems; and the lack of verifying field observations. A limited number of studies provide a quantified framework in terms of measures of antecedent catchment conditions and storm characteristics (e.g. Seeger *et al.*, 2004 and Brasington & Richards, 2000). While the quantified catchment conditions and storm characteristics can not be directly compared, given differences in the hydrological and sediment transfer regimes, the relative magnitudes associated with each hysteresis type can. Information to guide the interpretation and analysis of the hysteresis plots is also derived from studies which did not quantify catchment conditions and storm characteristics (e.g. Nistor & Church, 2004; Asselman, 2000 and Williams, 1989).

Although hysteresis patterns have been categorised into discrete classes caused by distinct discharge and SSC relations, in reality there is a continuum in the various discharge and SSC relations which result in hysteresis plots which may exhibit combinations of hysteresis classes.

In the following sections the hysteresis class of each storm in each catchment is analysed, attributed to antecedent catchment conditions and storm characteristics in conjunction with consideration of the documented associations and sources in Table 10.2 and field observations of sediment delivery.

10.4 Analysis of Burnhope hysteresis plots

Out of the ten storm events sampled at Burnhope, two (7th November and 22nd January) were removed from the hysteresis analysis as suspended sediment was only sampled for a portion of the storm hydrograph (Figure 10.2). Incomplete events are not analysed as the form of the SSC-discharge relation is affected. Four out of the eight storms exhibit class 2 hysteresis, three class 3 and one class 5 (Figure 10.3)

10.4.1 25th October 2000

The event on 25th October begins with two separate class 3 loops and changes into a straight line after sample 30 as SSC and discharge both decline (Figure 10.3). Class 3 loops are associated with collapsing banks on the falling limb or extended sediment travel times which may be due to the physical distance between source and gauging location or time taken to travel: sediment derived from hillslopes will take longer to reach the gauging site than sediment derived from the channel bed (Table 10.2). Precipitation in the preceding three days was high (highest out of the eight events) and the time since the storm discharge peak was last reached was the shortest (Table 10.1). This suggests that the catchment was wet and sediment supply from the bed and immediate hillslopes was limited due to previous events. This is supported by the low-intermediate SSC in comparison with other events with similar discharges (Figure 10.2). Therefore, the sediment is likely to have originated from distant (in time or space) sources. This is supported by discharge peaking 45 minutes before SSC. Also, as the SSC decreased in line with discharge towards the end of the event it suggests the sources were not exhausted, suggesting hillslopes as the dominant source (as opposed to bank collapse). Field observations suggest that large bluffs linked directly to the channel are the dominant sources (Figure 10.4). The two loops suggest two distinct inputs of sediment, perhaps two tributaries within the catchment. This theory is reinforced by a small peak in the hydrograph before the main peak (Figure 10.2).

10.4.2 2nd November 2000

The event on 2nd November produced a figure of eight loop (class 5): the loop started as a class 3 loop and twisted to become a class 2 loop (Figure 10.3). As for the event on 25th October, this suggests distant sources were dominant at the beginning of the event; bank collapse is unlikely to be the cause as the class 3 loop occurs before the falling limb. The fact that it turns into a class 2 loop is suggestive of sediment exhaustion or dilution of SSC by baseflow. Although precipitation and flow in the preceding seven

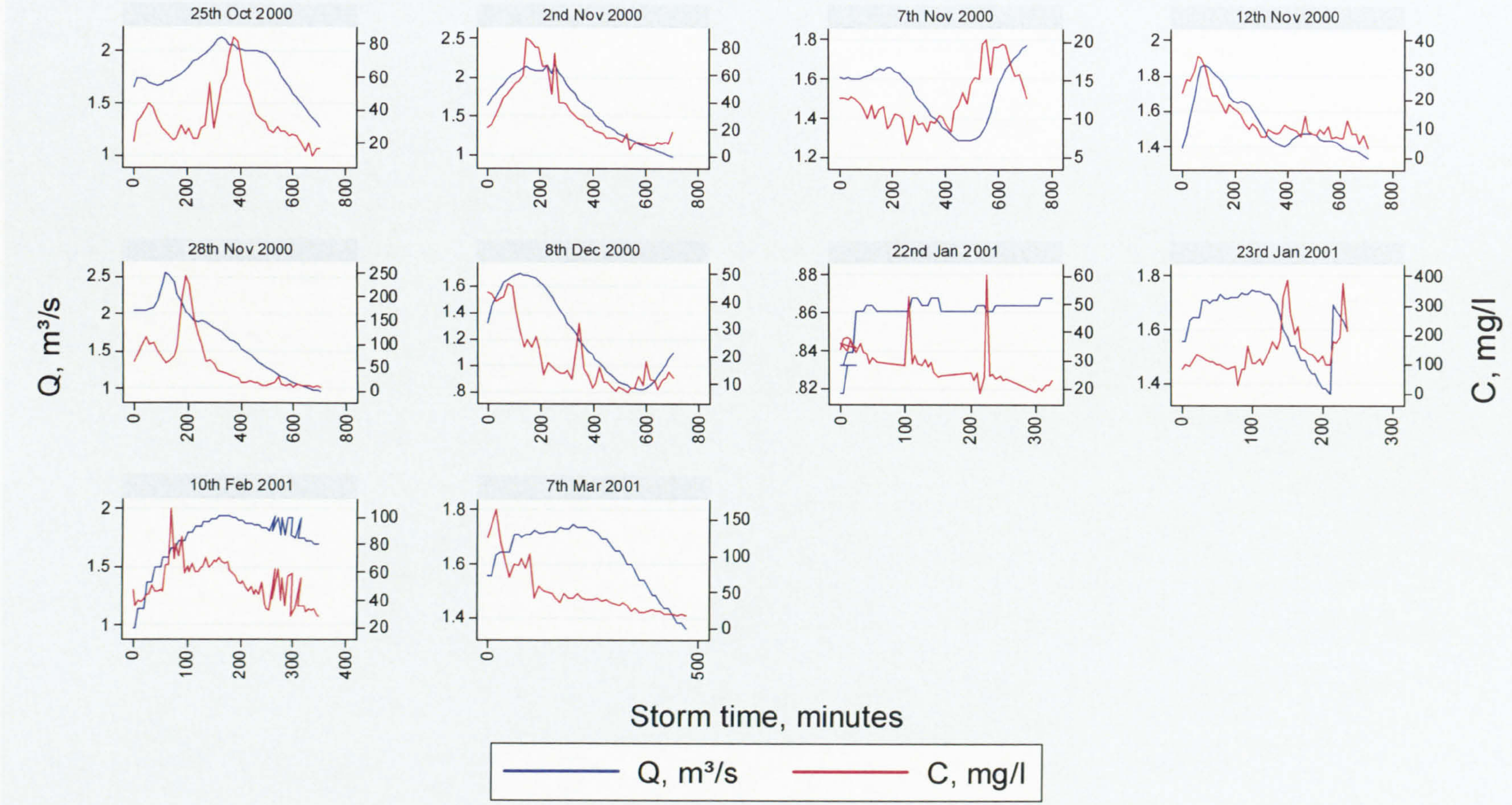

Figure 10.2. Hydrographs and sedigraphs for each storm at Burnhope. Note the different axis scales.

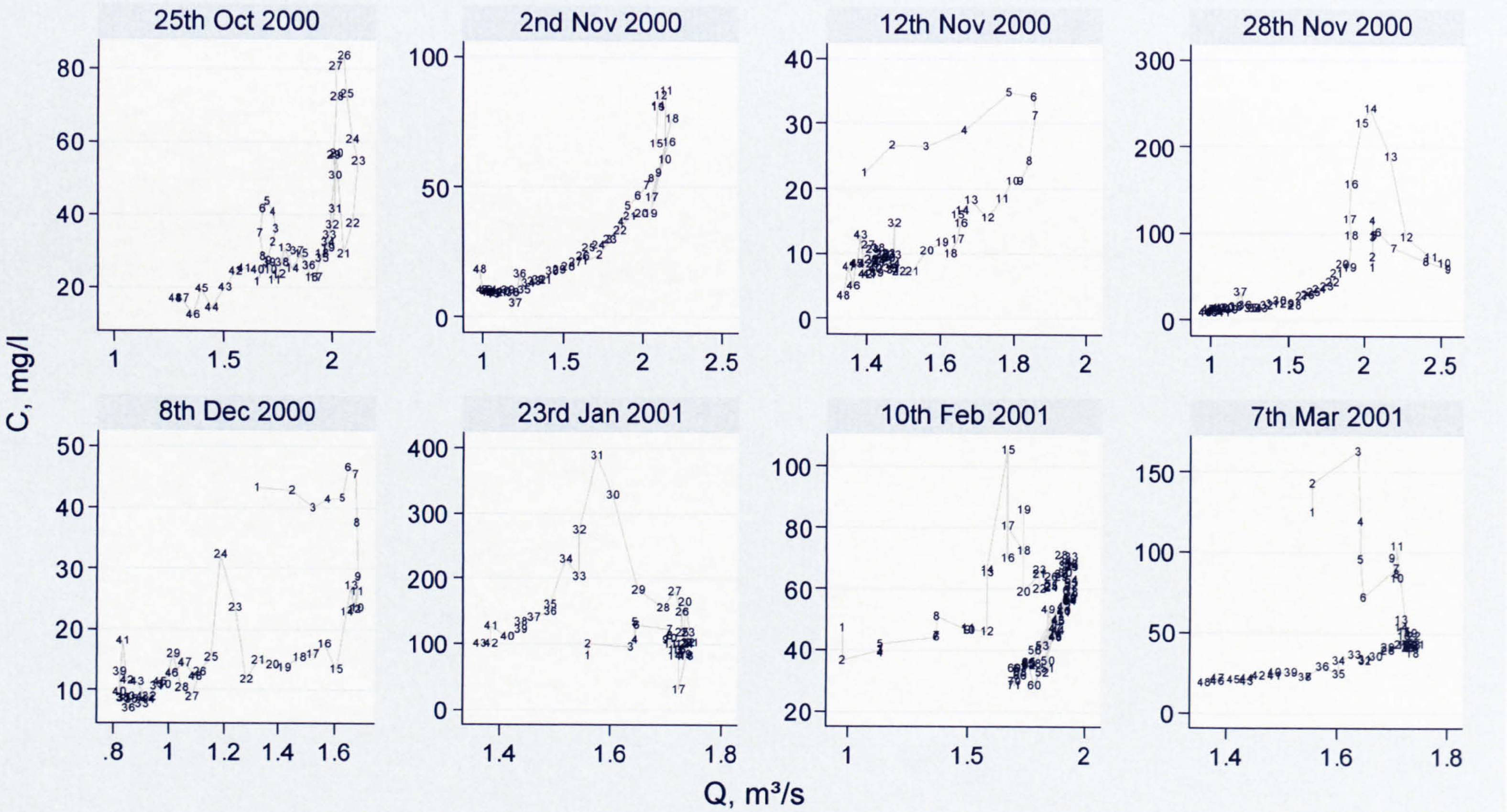

Figure 10.3. Hysteresis plots for each storm at Burnhope. The numbers represent the sample sequence, which were taken at 5 minute intervals for the storms on the 23rd January and 10th February; 10 minute intervals for the storm on the 10th February; and 15 minute intervals for the remainder of the storms. Note the different axis scales.

Figure 10.4. A large bluff in the Burnhope catchment.

days were higher than for the event on the 25th October, the precipitation in the preceding 3 days was lower (Table 10.1). Therefore, a substantial sediment source may have become uncoupled from the channel network, thus causing the class 2 loop. The loops are very narrow which suggests that the supply of sediment is fairly constant throughout the storm event; and overall the hysteresis is fairly weak. SSC peaks 1 hour 45 minutes before discharge but this could be misleading as the peak discharge is associated with a small peak superimposed on the general form of the hydrograph (Figure 10.2). This peak is indicative of a secondary input of flow, probably from an upstream tributary. The range of SSC is low-intermediate in comparison with events with similar discharges. This suggests that sediment sources were depleted which is supported by the flow in the preceding three and seven days (Table 10.1). However, there was ample time since an event of the same magnitude for sediment stores to recharge (Table 10.1). This suggests that sediment stores which are accessible during smaller events delivery the majority of the sediment to the channel.

10.4.3 12th November 2000

The event which occurred on 12th November exhibited class 2 hysteresis (Figure 10.3). There was limited flow and precipitation in the three days preceding the event but the flow and precipitation in the preceding seven days were very high (Table 10.1). The intensity of the precipitation and the total storm flow were both high (Table 10.1).

Based on these conditions the nature of the loop can be attributed to sediment exhaustion, as the higher flows in the first four days in the seven days before the event would have removed a proportion of the sediment and connected sediment sources to the channel. During the preceding three days before the event, some of the sources became unconnected, sediment was deposited in temporary storage and some sediment may have been prepared for transport. Therefore the onset of the storm was characterised by high SSCs which quickly decreased as sources diminished. The local nature of the sediment sources is also indicated by the lag: SSC peaked thirty minutes before discharge (Figure 10.2). The high event rainfall intensity would also have eroded and transported sediment. The SSC were low compared with events of a similar magnitude (Figure 10.2) which is indicative of the high flows preceding the event.

10.4.4 28th November 2000

The event on 28th November produced a class 3 hysteresis loop (Figure 10.3). A very steep increase in SSC is evident at the beginning of the event which is most likely due to the entrainment of sediment from the channel (Figure 10.2). The two sections of the loop (samples 4-12 and 12-19) are likely to be a result of two inputs of sediment which given the form of the hydrograph were probably delivered by tributaries (Figure 10.3). These sources are likely to be the same two sources as the 25th October event given the broad similarity in form: a small peak followed by larger peak. Most of the event characteristics are similar for this event and the 25th October event (Table 10.1) and discharge peaked before SSC. This, and the similar hysteresis plot forms, suggests the same sources and processes are responsible. The length of time between the two SSC peaks explains the two separate loops for the 25th October event compared with the different sections on the 28th November event (Figure 10.2). This difference in timing could be explained by the rainfall distribution over the catchment. The SSCs of this event were much larger than that of the other events and may be attributable to the high rainfall intensity and the length of time between this event and another of similar magnitude; sediment sources were accessed that had not been accessed in the last 24 days (Table 10.1).

10.4.5 8th December 2000

The event on 8th December was characterised by a class 2 hysteresis loop with a second class 2 loop which coincided with a second rise in discharge (Figures 10.2 & 10.3). The event was fairly small in terms of the duration, maximum discharge, storm rainfall and

rainfall intensity. The antecedent catchment characteristics were intermediate compared with the other events (Table 10.1). This suggests that sediment exhaustion from sources in close proximity to the channel supplied the sediment, as the catchment was not wet enough to connect more distant sources. SSC peaked before discharge by 45 minutes, which also suggests that local sediment sources were responsible (Figure 10.2). The SSC were low (Figure 10.2), indicative of exhaustion of the local sediment sources and the small scale of the storm.

10.4.6 23rd January 2001

The event on 23rd January was characterised by a class 3 hysteresis loop (Figure 10.3). The antecedent catchment conditions were dry (Table 10.1) and the storm was one of the largest in terms of storm flow, storm rainfall and peak storm rainfall. These factors suggest that the storm should have been characterised by class 2 hysteresis as a result of sediment exhaustion. However, it was a long time since an event of the same or greater magnitude (Table 10.1) which suggests sources will have recharged and the high storm precipitation may have connected distant sources during the event. There is no secondary rise in discharge as for the other class 3 events (Figure 10.2): however, the form of the hysteresis loop is comparable to the loop produced by the storm on 28th November (Figure 10.3). This implies two distinct sources were responsible, perhaps sediment delivered by two tributaries. However, the high SSC suggests a localised bank collapse as a possible cause, although the long time period (56 days) since a storm of the same magnitude or channel sediment sources may also explain this (Table 10.1). As for the other class 3 events discharge peaked prior to SSC (Figure 10.2), indicative of distant sources or bank collapse on the falling limb. Alternatively, this may have been a snowmelt event but unfortunately no snow cover data is available.

10.4.7 10th February 2001

Class 2 hysteresis characterised the storm event on 10th February (Figure 10.3). Although flow and precipitation in the preceding seven days were quite high compared with the other storm events the flow but precipitation in the preceding three days were fairly low (Table 10.1). The magnitude of the storm was intermediate, but it was only 3.5 days since a storm of a similar magnitude (Table 10.1). Based on these characteristics and the low-intermediate SSC compared with to events with similar discharges (Figure 10.2), the form of the hysteresis loop can be attributed to sediment exhaustion. Local sources are the likely origin of the sediment given the exhaustion and

because SSC peaked 1 hour 30 minutes before discharge (Figure 10.2). There is a section of high variability in both discharge and SSC on the falling limb of the event. Given the close correspondence between SSC and discharge it is probable that this is due to an episodic input of water and sediment to the channel, possibly from a hillslope source.

10.4.8 7th March 2001

The event on 7th March also exhibited class 2 hysteresis (Figure 10.3). The antecedent catchment characteristics were dry, although the low precipitation values in comparison with the high flows suggest it may have been a localised event and some areas of the catchment may have been wet (Table 10.1). The storm was intermediate in terms of total flow and peak flow and it was 24 days since an event of a similar magnitude (Table 10.1). The dry catchment conditions and SSC peak 3 hours and 10 minutes before the discharge peak suggest that only sources local to the channel, i.e. the channel bed and banks, were connected and the relative high SSC concentrations in association with an intermediate storm peak discharge (Figure 10.2) are explained by the long time period since a flow of a similar magnitude.

10.4.9 Comparison of events

The storms sampled indicate class 2 and class 3 events dominate the system. Interpretation of the form of the hysteresis loops and event statistics and consideration of likely sediment sources suggest that within the Burnhope catchment, class 3 events are characterised by wet antecedent catchment characteristics in the preceding three days and two distinct inputs of sediment are evident, possibly from tributaries. Class 3 events are similar with respect to storm characteristics, i.e. the peak precipitation, storm precipitation, storm flow, maximum storm flow and storm duration. The antecedent conditions are similar for the class 2 events, with the exception of the 7th March event, and are characterised by drier catchment conditions in the preceding three days (Table 10.1). The storm characteristics are variable for class 2 events (Table 10.2). Discharge peaks before SSC in all class 3 events and SSC peaks before discharge in all class 2 events and the class 5 event (Table 10.2). Also higher SSCs, with the exception of the 25th October event, are associated with class 3 events. This reinforces the idea that sediment is derived from more distant sources which are less likely to be exhausted during class 3 events and local channel sources during class 2 events. All the sampled events were in winter, so no inferences can be made regarding seasonal changes in

dominant sediment source. To confirm these patterns and to examine correlations between the event statistics and other hysteresis types more storms should be sampled and examined.

10.5 Analysis of Candleseaves hysteresis plots

At Candleseaves the form of hysteresis is strongly controlled by the section of the hydrograph (e.g. rising only) from which suspended sediment was sampled (Figures 10.5 & 10.6). Out of the fourteen storms sampled at Candleseaves, eight did not capture the complete storm cycle (Figure 10.5), thus leaving only six suitable storm series to examine hysteresis. Out of those six storms four exhibit class 2, one class 3, and one class 6 (Figure 10.6).

10.5.1 17th May 2003

The event on 17th May was initially characterised by a class 3 loop (samples 1-10) and then SSC declined in line with discharge producing class 1 hysteresis (Figure 10.6). Theoretically extended travel time seems the most likely explanation, especially as the loop (although early in the sample set) corresponds to the peak of the storm hydrograph which is the time when the catchment would be wettest, therefore connecting distant sources and allowing sufficient time for sediment to be transported from distant sources. However, field observations suggest that most of the sediment sources at Candleseaves are in-channel or adjacent to the channel and there are no distant sediment sources within the catchment due to its size and position in the grip network. It can not be attributed to bank collapse on the falling limb as discharge was not of sufficient magnitude (Table 10.1). A possible explanation is retention of sediment in the grip, perhaps behind vegetation and debris, which prevented transfer of sediment until discharge reached a threshold. Discharge peaked 20 minutes before SSC which supports the theory that the class 3 loop was a result of sediment retention. The SSC are low compared with the other events as are the discharges (Figure 10.5).

10.5.2 19th June 2003

The event on 19th June is characterised by a very clear class 2 hysteresis loop (Figure 10.6). The antecedent conditions in the catchment were relatively dry (with the exception of precipitation in the preceding three days), the peak storm rainfall intensity and total storm rainfall were high, and it was 46 days since a storm of a similar magnitude (Table 10.1). This suggests more easily exhausted sources were accessed and

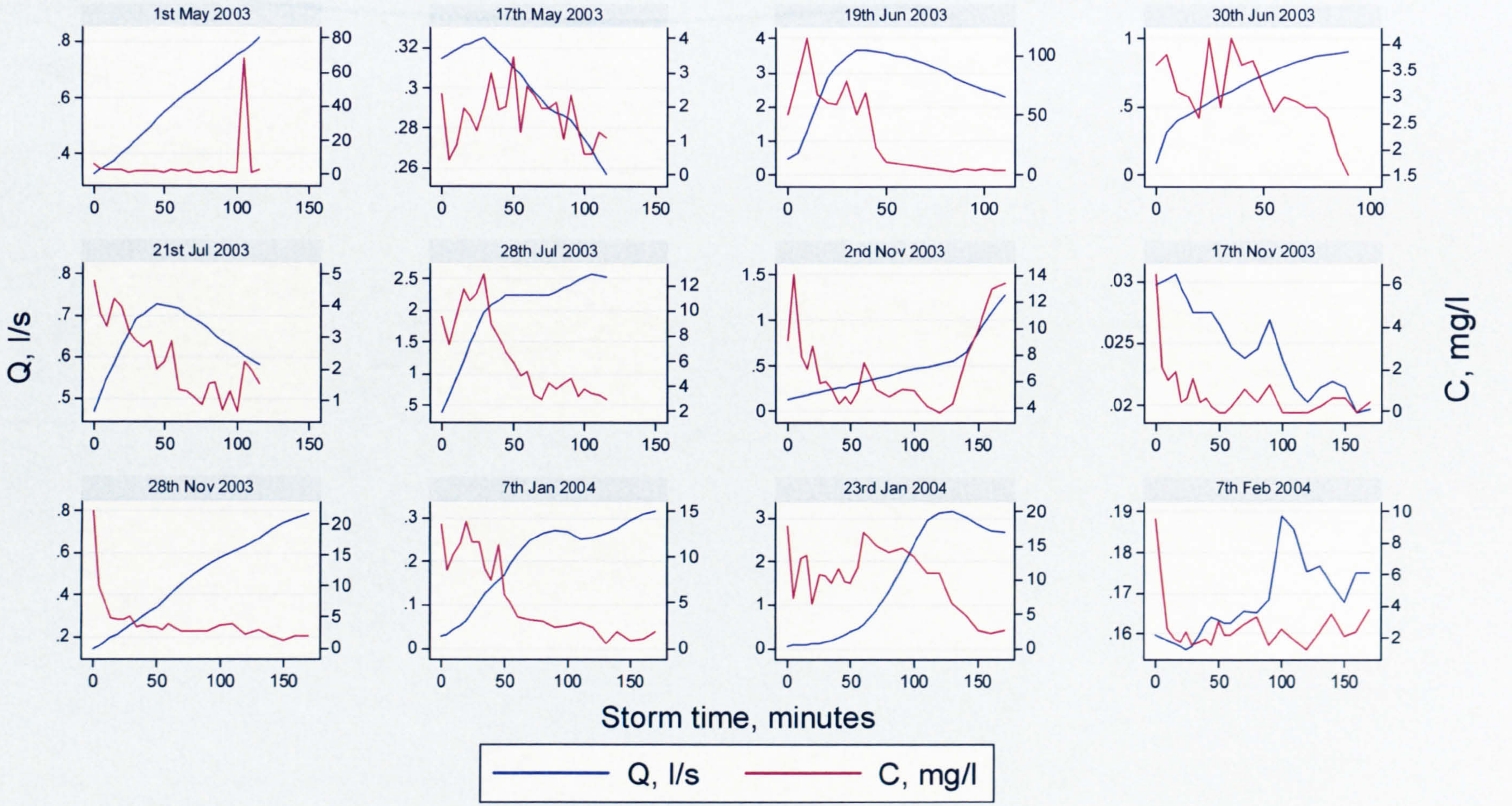

Figure 10.5. Hydrographs and sedigraphs for each storm at Candleseaves. Note the different axis scales.

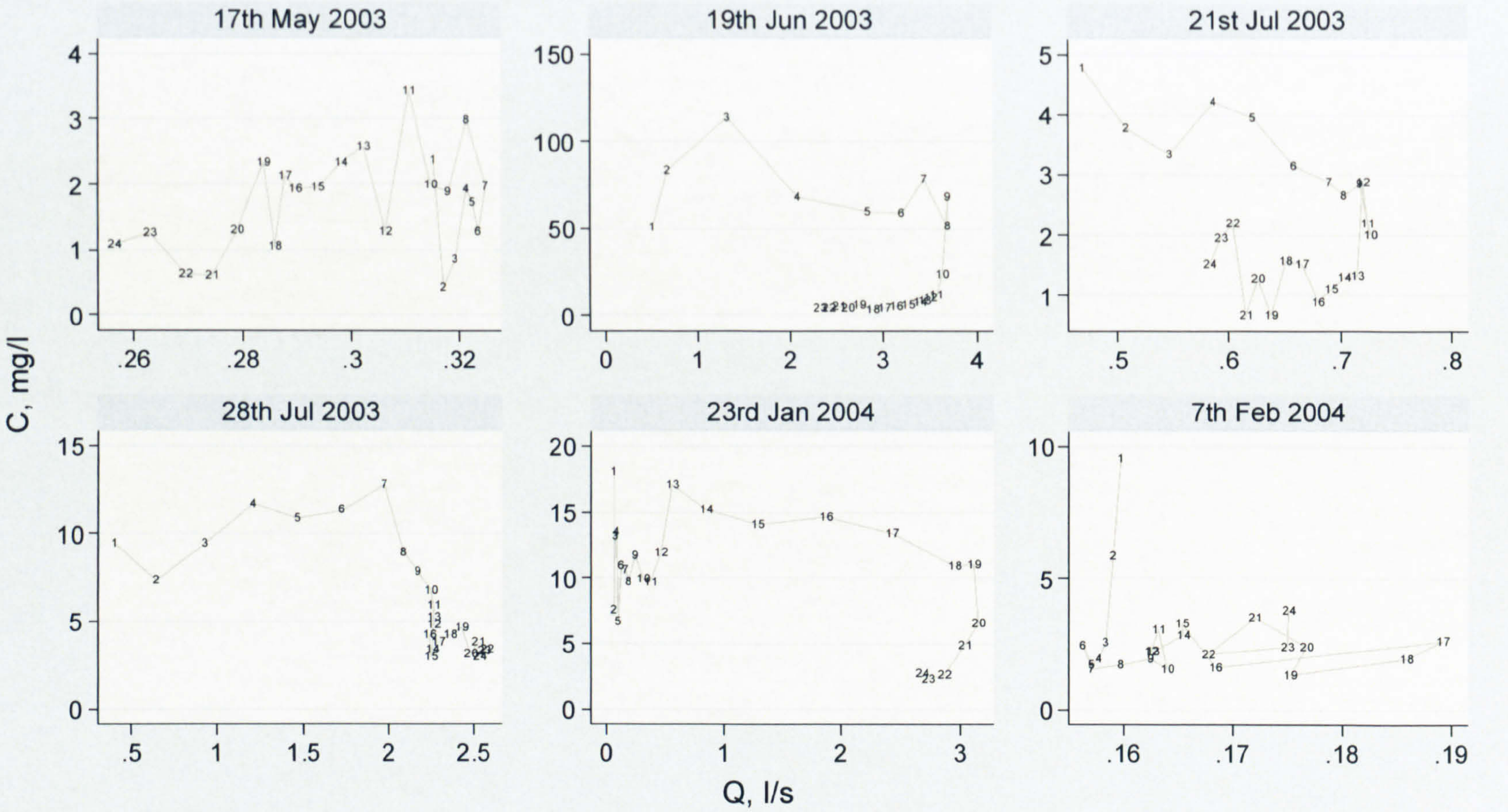

Figure 10.6. Hysteresis plots for each storm at Candleseaves. The numbers represent the sample sequence, which were taken at 5 minute intervals for storms up to and including the 28th July and at 5 minute intervals for bottles 1-13 and 10 minute intervals for bottles 14-24 for all storms after the 28th July. Note the different axis scales.

sediment exhaustion was responsible. SSC peaked 25 minutes before discharge which also indicates sediment exhaustion (Figure 10.5). Brasington & Richards (2000) also associated class 2 hysteresis with large events: the event on the 19th June was the largest sampled. The SSC were substantially larger than for any other storm (Figure 10.6), which are indicative of the long time since a storm of the same or greater magnitude and also could have resulted from dry grip walls supplying more sediment and the very high rainfall intensities (Table 10.1).

10.5.3 21st July 2003

A clear class 2 hysteresis loop characterised the event which occurred on 21st July (Figure 10.6). Precipitation in the preceding seven days and flow in the preceding three and seven days indicate the catchment was fairly dry, but precipitation in the preceding three days was higher than for any other event (Table 10.1). It had been only 19 days since a storm of a similar magnitude (Table 10.1) so there may not have been much sediment available for transport. Also, the storm rainfall intensity was very low (1 mm in 15 minutes) as was total storm rainfall (Table 10.1). SSC peaked 45 minutes prior to discharge (Figure 10.5). The SSCs were fairly low (Figure 10.5), which could be a result of the low discharges, and therefore low carrying capacity, or limited sediment available for transport. From these factors it is inferred that sediment exhaustion caused the class 2 hysteresis and most of the sediment was derived from within channel sources, which were limited due to previous events and this, coupled with low discharges, resulted in low SSC.

10.5.4 28th July 2003

The event on 28th July was also characterised by a class 2 hysteresis (Figure 10.6). Compared with the other events preceding flow (both three and seven days previous) and rainfall in the preceding seven days were intermediate (Table 10.1). This reinforces field observations which suggests hillslope sediment sources are of minor importance. Total storm rainfall and storm rainfall intensity were high and it was 23 days since the last storm of the same magnitude (Table 10.1). As with the event on the 19th June, sediment exhaustion is likely to be responsible for the form of the hysteresis loop, especially given that SSC peaked 1 hour 15 minutes before discharge (Figure 10.5). The loop is not as large and this can be explained by limited sediment availability: it was 46 days since the last storm and rainfall intensity was 25.6 mm hr^{-1} higher for the event on the 19th June.

10.5.5 23rd January 2004

The 23rd January event was characterised by a class 2 hysteresis loop (Figure 10.6). The loop is quite open but this can be attributed to the fact that samples were not taken on the throughout the falling limb (Figure 10.5). The flow in the preceding three and seven days and the rainfall in the preceding seven days were high (Table 10.1), which is generally indicative of a class 3 loop. However, the rainfall in the preceding three days was relatively low (Table 10.1). The last storm of similar magnitude was only two and a half days previously (Table 10.1) and SSC peaked 2 hours 10 minutes before discharge, which also promote the occurrence of class 2 hysteresis. These factors, combined with the low SSC (Figure 10.6) suggest the class 2 loop is likely to be caused by exhaustion of sediment derived from channel sources.

10.5.7 7th February 2004

The hysteresis plot for the 7th February event shows no clear hysteresis type and is therefore categorised as class 6 (Figure 10.6). This can be attributed to the jagged form of the hydrograph and the small range of discharge values (Figure 10.5), illustrating the sensitivity of the system to discharge. There is a very clear drop in SSC at the beginning of the event and SSC peaked 1 hour 40 minutes before discharge (Figure 10.5), which suggests entrainment of sediment stored on the bed which became rapidly exhausted. The antecedent conditions were very wet but the storm was small in terms of duration, flow, rainfall and rainfall intensity (Table 10.1). This means that there would have been very little sediment available for transport and very little water to transport what sediment there was available.

10.5.8 Comparison of events

Out of these six events four exhibited class 2 hysteresis, one class 3 and one class 6. The class 2 events possessed the highest maximum storm discharges, total storm flows, storm precipitation intensities and total storm precipitation (Table 10.1). Also, rainfall in the preceding three days was more indicative of the likelihood of a class 2 event occurring. This is demonstrated by events on the 28th July and 23rd January which had relatively high flow in the preceding three and seven days and relatively high rainfall in the preceding seven days but relatively low rainfall in the preceding three days and were characterised by class 2 hysteresis.

The antecedent conditions of class 2 events were not always dry, as suggested by Seeger *et al.* (2004), which reflects the limited importance of hillslope sources. The dominant sources of sediment are likely to be channel sources given that SSC generally peaked before discharge, the dominance of class 2 events, the steep sides of the grip (i.e. there are no floodplains) and low gradient, well-vegetated hillslopes. The storms were characterised by low SSCs which reflects the low discharges and high organic matter content of the sediment (on average 75% of the sediment retained in the time-integrated mass samplers was organic).

Although limited complete storm suspended series exist it can be concluded that few events in Candleseaves will be characterised by class 3 events as previous studies (Labadz *et al.*, 1991), suggest that small catchments promote class 2 hysteresis and there is limited supply from the hillslopes. However, class 3 hysteresis may occur as a result of bank collapse, especially given the steep channel sides.

10.6 Analysis of Rough Sike hysteresis plots

Out of the twelve storms sampled at Rough Sike four (10th November 1997, 6th February 1998, 2nd June 1998 and 24th June 1998) were discarded from hysteresis analysis as they did not capture the whole storm hydrograph (Figure 10.7). Five of the remaining eight storms exhibited class 2 hysteresis, one exhibited class 3 hysteresis and two exhibited class 5 hysteresis (Figure 10.8).

10.6.1 29th August 1997

The event on 29th August exhibited class 2 hysteresis, although the loop only extends from samples 1 to 11, after which the relation is a rough straight line (Figure 10.8). Sample 1 has a notably higher SSC (Figure 10.7) which may be spurious or due to the rapid entrainment of sediment stored on the channel bed. The antecedent conditions in the catchment were dry, and the storm was small, in terms of precipitation, flow, surface wetness and soil moisture parameters, but long in terms of duration (Table 10.1). It was a relatively short time since the last event of a similar magnitude (Table 10.1) and SSC peaked 1 hour before discharge (Figure 10.7). This suggests that the class 2 hysteresis was caused by sediment exhaustion and the lack of form in the loop after sample 11 (440 minutes) can be explained by limited sediment available for transport following a recent event of a similar magnitude. Due to the dry catchment, small storm size, and quick exhaustion of sediment the likely dominant source of sediment is the channel bed.

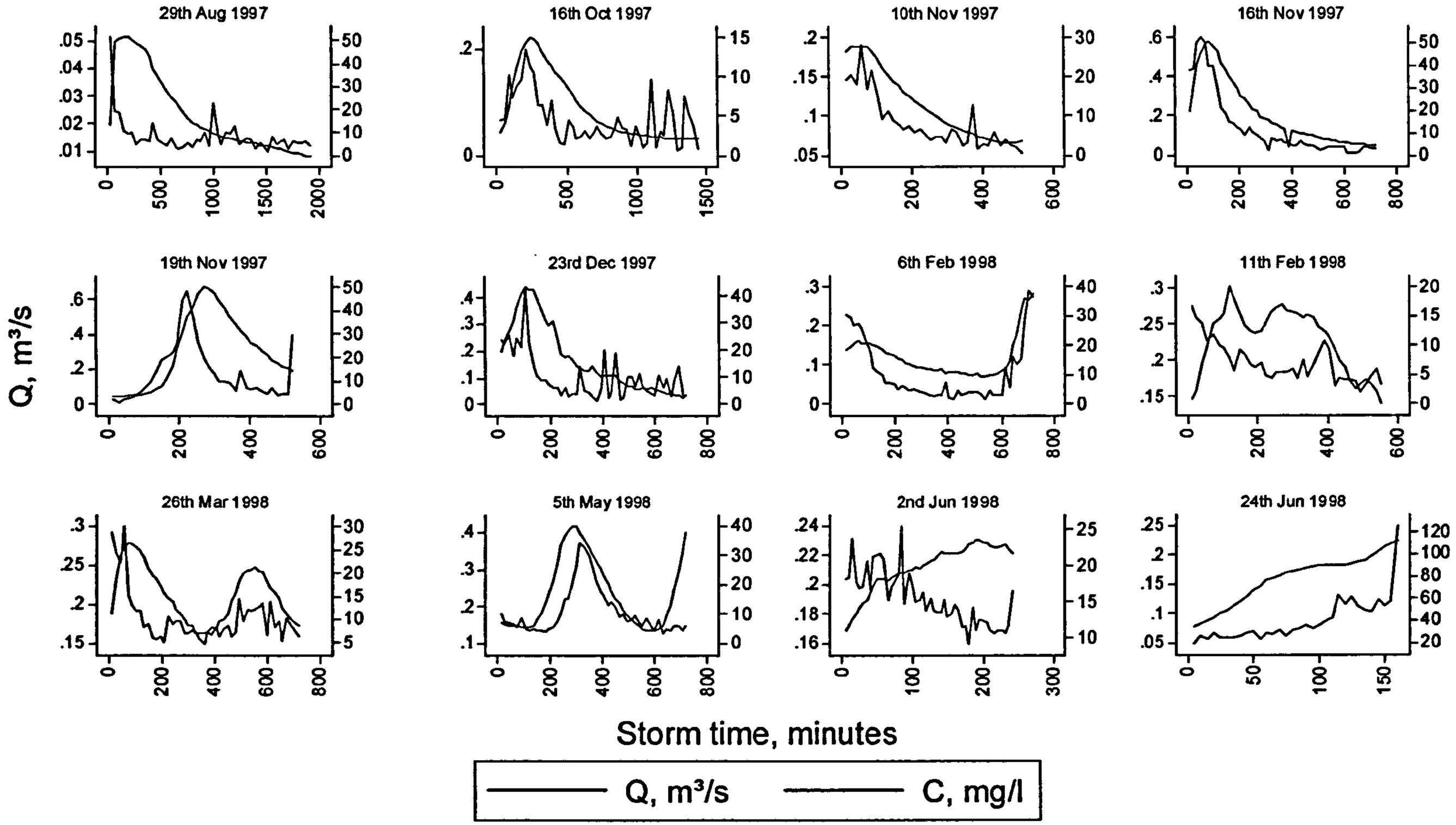

Figure 10.7. Hydrographs and sedigraphs for each storm at Rough Sike. Note the different axis scales.

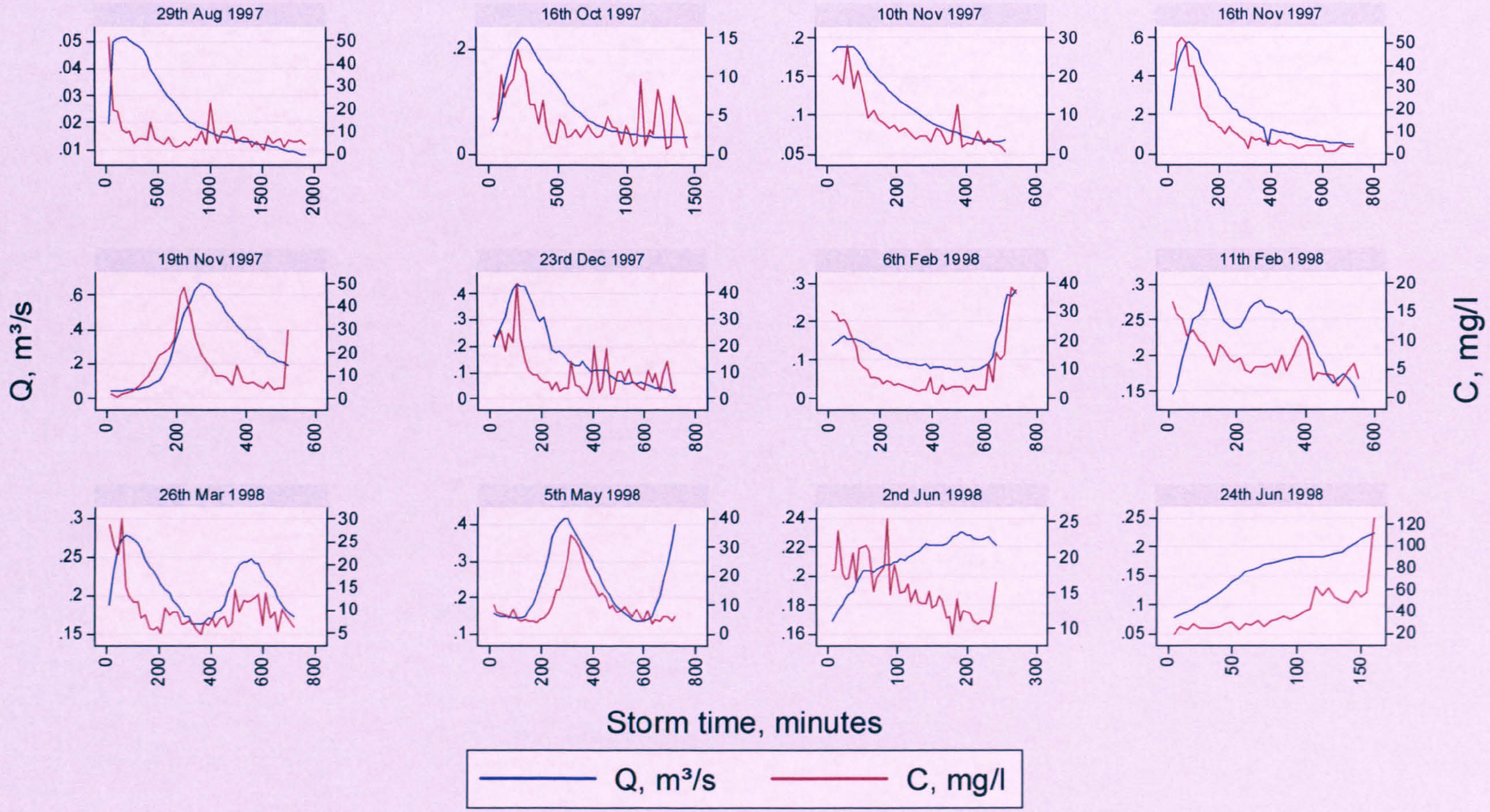

Figure 10.7. Hydrographs and sedigraphs for each storm at Rough Sike. Note the different axis scales.

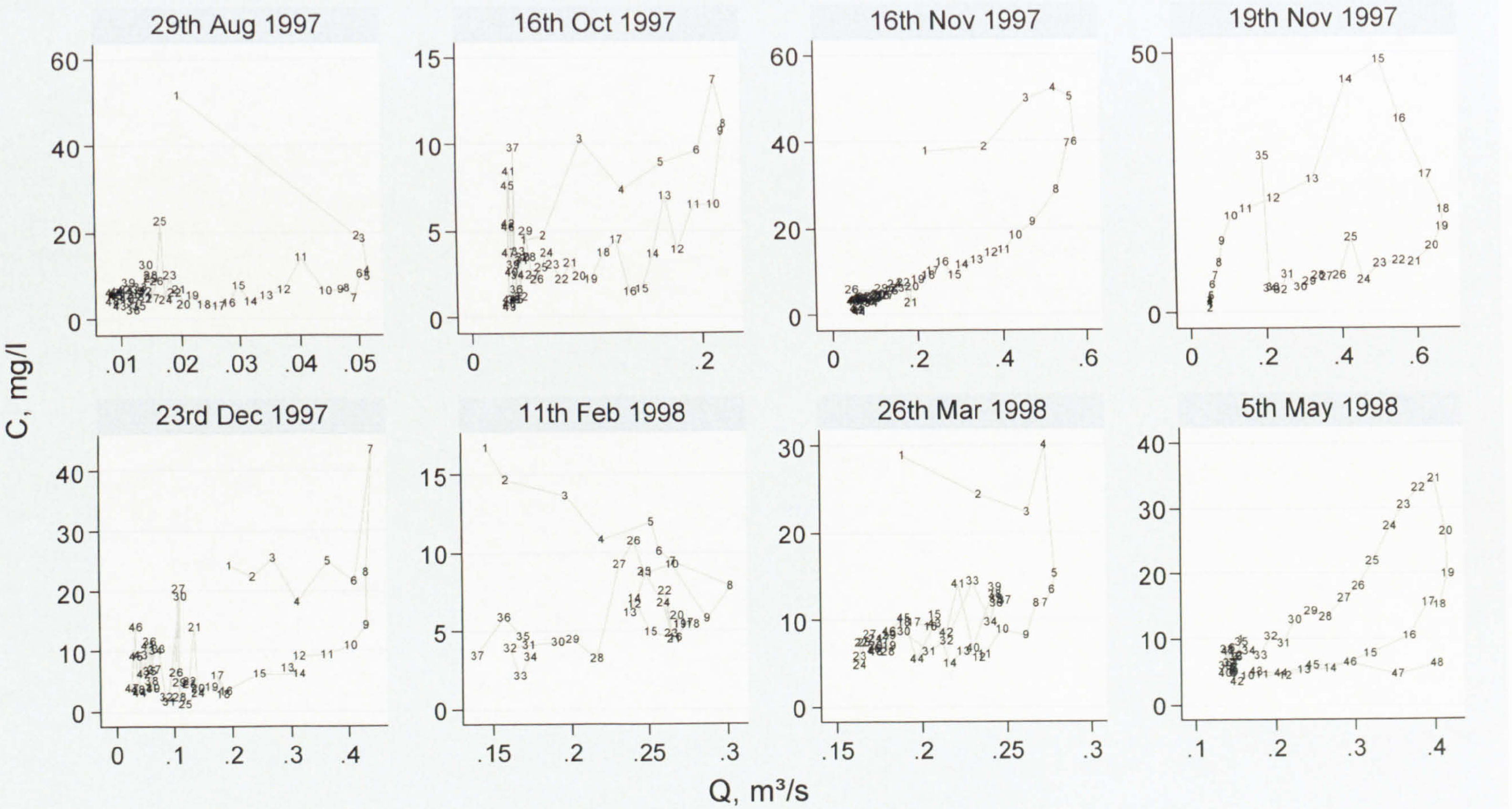

Figure 10.8. Hysteresis plots for each storm at Rough Sike. The numbers represent the sample sequence, which were taken at 40 minute intervals for the storm on the 29th August; 30 minute intervals for the storm on the 16th October; and 15 minute intervals for the remainder of the storms. Note the different axis scales.

10.6.2 16th October 1997

The event on 16th October produced a very clear, closed class 2 hysteresis loop (Figure 10.8). The antecedent conditions were intermediate, with the exception of precipitation in the preceding seven days which was high (Table 10.1). The storm characteristics were also intermediate, although it was long in duration and small in terms of peak flow (Table 10.1). SSC peaked 30 minutes before discharge (Figure 10.7), and this coupled with the low SSC (Table 10.1), suggest that the hysteresis may be attributed to sediment exhaustion, especially as the last event of the same magnitude was only five days previously (Table 10.1). The low SSC and quick exhaustion indicate that the sediment is likely to have originated primarily from the channel bed.

10.6.3 16th November 1997

Class 2 hysteresis also characterised the event on 16th November (Figure 10.8). The antecedent catchment conditions were intermediate (Table 10.1). The storm had the highest maximum precipitation intensity, the highest total flow, the second highest peak flow and the second longest duration since a storm of the same magnitude (71 days) (Table 10.1). The high flows and high precipitation intensity are the likely cause of the high SSC compared with the other events (Figure 10.8). The high flows would have enabled new, less depleted, sediment sources to be accessed and the high precipitation intensity would have promoted erosion of sediment. As the catchment was not particularly wet and as SSC peaked 30 minutes before discharge (Figure 10.7), it can be assumed that the sediment was derived from local sources and it is likely that a notable amount of sediment entrained originated from within the channel. This would also explain the rapid decline in SSC (Figure 10.7). Given these factors sediment exhaustion is the most likely explanation of the form of the hysteresis loop.

10.6.4 19th November 1997

The event on 19th November was classified as a class 2 hysteresis event (Figure 10.8). The antecedent conditions over the seven and three days before the event were wet (Table 10.1). However, the average soil moisture and the proportion of time the surface was classified as wet were relatively low (Table 10.1). The storm was fairly large in terms of flow, surface wetness and rainfall parameters, but soil moisture was low and it was 74 days since a storm of the same magnitude (Table 10.1). The high flows and precipitation in the catchment in the preceding days but low surface wetness and soil moisture suggest that before the seven days the catchment was fairly dry. The large

storm and long time since last event explain the high SSC (Figure 10.8). SSC peaked 45 minutes before discharge (Figure 10.7). Given these factors the class 2 form of the loop can be attributed to sediment exhaustion with the channel and local hillslope supplying the sediment.

10.6.5 23rd December 1997

Class 2 hysteresis characterised the event on 23rd December (Figure 10.8). The soil moisture and the percentage of time the surface was classified as wet indicate that antecedent conditions were wet, although flow was intermediate compared with the other sampled events (no precipitation data were available) (Table 10.1). The storm was small in duration and total flow, although peak flow was among the highest of the storms sampled (Table 10.1). It was only 5 days since a storm of the same magnitude (Table 10.1). The initial rapid decline in SSC and relatively low SSC after sample 8 (120 minutes) (Figure 10.7) suggests that most of the sediment was initially supplied by channel sources and indicates sediment exhaustion caused the class 2 hysteresis. Unusually for class 2 events SSC did not peak before discharge: SSC and discharge peaked simultaneously (Figure 10.7). The oscillations in SSC towards the end of the event may be attributed to hillslope inputs connected to the channel due to the high surface moisture conditions or minor bank collapses.

10.6.6 11th February 1998

The event on 11th February has the overall form of a class 2 loop, but also contains two class 3 loops within it, and therefore is classified as a class 5 loop (Figure 10.8). The proportion of time the surface was classified as wet, the soil moisture and flow indicate the antecedent conditions were wet in the preceding three and seven days (Table 10.1). The storm was long and the total flow high (Table 10.1). Other storm characteristics were intermediate (Table 10.1). The form of the hysteresis loop can be explained by an overall trend of sediment exhaustion, as suggested by the low SSC (Figure 10.8) and overall class 2 form, and the twin-peaked form of the storm hydrograph (Figure 10.7), causing the class 3 loops. Sediment probably originated from both channel sources given the preceding SSC peak (Figure 10.7) and the hillslopes given the wet catchment conditions.

10.6.7 26th March 1998

The event on 26th March also has the overall form of a class 2 hysteresis loop but twists

several times producing some smaller class 3 loops within it and is therefore classified as a class 5 loop (Figure 10.8). The catchment conditions before this event were fairly dry in the preceding seven days but precipitation and flow was among the highest in the previous three days (Table 10.1). The storm was intermediate in terms of precipitation but small with respect to total flow and peak flow (Table 10.1). It was a fairly long time since a storm of the same magnitude (Table 10.1). The event was classified by a twin-peaked storm hydrograph (Figure 10.7) which explains the class 5 loop form. Some degree of sediment exhaustion occurred as SSC peaked 1 hour before discharge and SSC were intermediate in comparison with other events with similar discharges (Figure 10.7). However, twin peaks are also apparent in the sedigraph (Figure 10.7). This suggests that sediment may have been restricted but was not exhausted or a second source, probably hillslope derived, was accessed during the second peak.

10.6.8 5th May 1998

A closed class 3 loop characterises the event on 5th May (Figure 10.8). Flow, the percentage of the time the surface was classified as wet and soil moisture all suggest the catchment was fairly dry (Table 10.1). However, precipitation in the preceding seven and three days were among the highest for the sampled storms (Table 10.1). All storm characteristics were intermediate except total storm precipitation, soil moisture and the proportion of time the surface was classified as wet, which were high (Table 10.1). The catchment and storm characteristics are not strikingly different from the other storms to the degree that class 2 hysteresis would have been expected. The sedigraph peak clearly lags behind the discharge peak (Figure 10.7). The class 3 hysteresis may have been caused by localised precipitation higher in the catchment and therefore sediment was transported from distant sources, with the sediment wave following the flood wave. There is no evidence to suggest this is due to bank collapse.

10.6.9 Comparison of events

The storms sampled indicate that class 2 hysteresis is undoubtedly the dominant hysteresis type for Rough Sike and even the two class 5 events were class 2 in overall form. The class 2 events are most likely to be caused by sediment exhaustion within the system and the dominant source is likely to be the channel bed with some sediment input from the banks and local hillslopes. It is not possible to make any firm generalisations regarding antecedent catchment conditions or storm characteristics which promote class 2 events as they varied substantially between the events. However,

SSC peaks prior to discharge for all class 2 events and the class 5 events and discharge peaks prior to SSC for the class 3 event (Table 10.1).

The class 5 events were associated with twin-peaked hydrographs; wet catchment conditions in terms of flow, rain and soil moisture in the preceding three days; and long storms. The class 5 events occurred within six weeks of each other, perhaps indicating a seasonal (late winter/early spring) influence. The dominant sediment sources of the class 5 events were likely to be the channel bed and banks, which became exhausted and produced the overall class 2 loop form and hillslope, and possibly gully, sources which produced the class 3 loops.

It is not possible to make any inferences regarding the catchment conditions and storm characteristics which promoted the class 3 loop as none of the statistics are distinct from those of the other events. However, the peak in SSC after the peak in discharge suggests that it may have been caused by rainfall in the upper catchment and differences in the flood and sediment wave velocities. It is unlikely to be bank collapse as the peak discharge was not that high and gullies within the catchment are generally weakly coupled to the channel.

10.7 Analysis of Swinhope hysteresis plots

Eight of the fifteen storm events sampled at Swinhope were discounted from hysteresis analysis due to incomplete capture of the event (Figure 10.9). The events on 29th April 2002, 30th July 2002, 12th October 2002, 8th November 2002, 1st March 2003, 1st April 2003, and 19th November 2003 were retained for analysis and fiver were characterised by class 2 hysteresis and 2 by class 5 hysteresis (Figure 10.10).

10.7.1 29th April 2002

The event on 29th April was categorised by a smooth and symmetrical sedigraph and hydrograph (Figure 10.9) which formed a tight class 2 hysteresis loop (Figure 10.10). The loop is so tight that it is almost a class 1 hysteresis loop; such loops are related to constant sediment supply. This is also reflected in the symmetry between the sedigraph and hydrograph (Figure 10.9). The SSCs are higher compared with other storms (Table 10.1), which may in part be due to the high discharges but also indicate plentiful sediment supply. The antecedent catchment conditions were among the wettest for the analysed storms (Table 10.1). The storm was large in terms of flow but storm

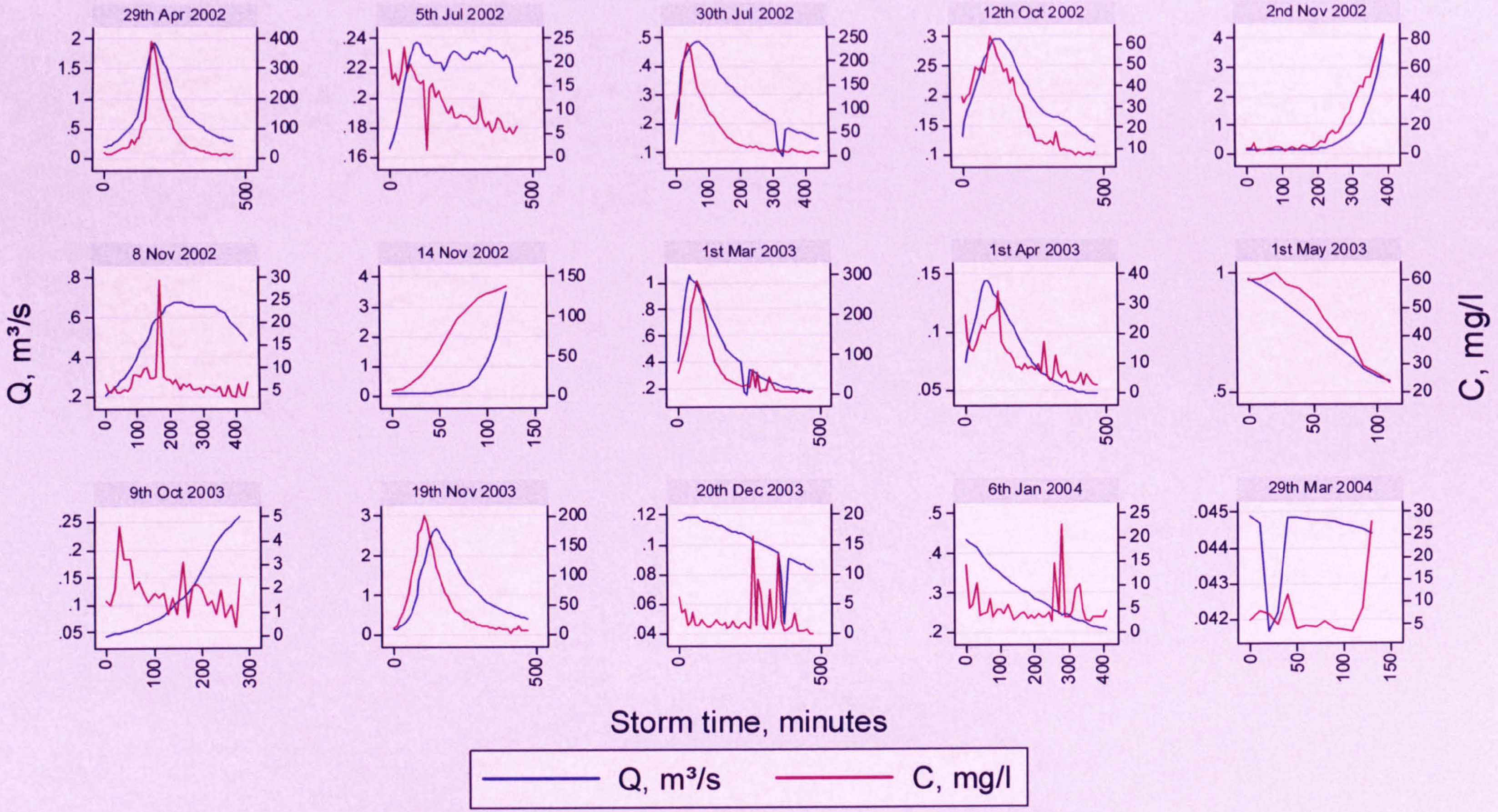

Figure 10.9. Hydrographs and sedigraphs for each storm at Swinhope. Note the different axis scales.

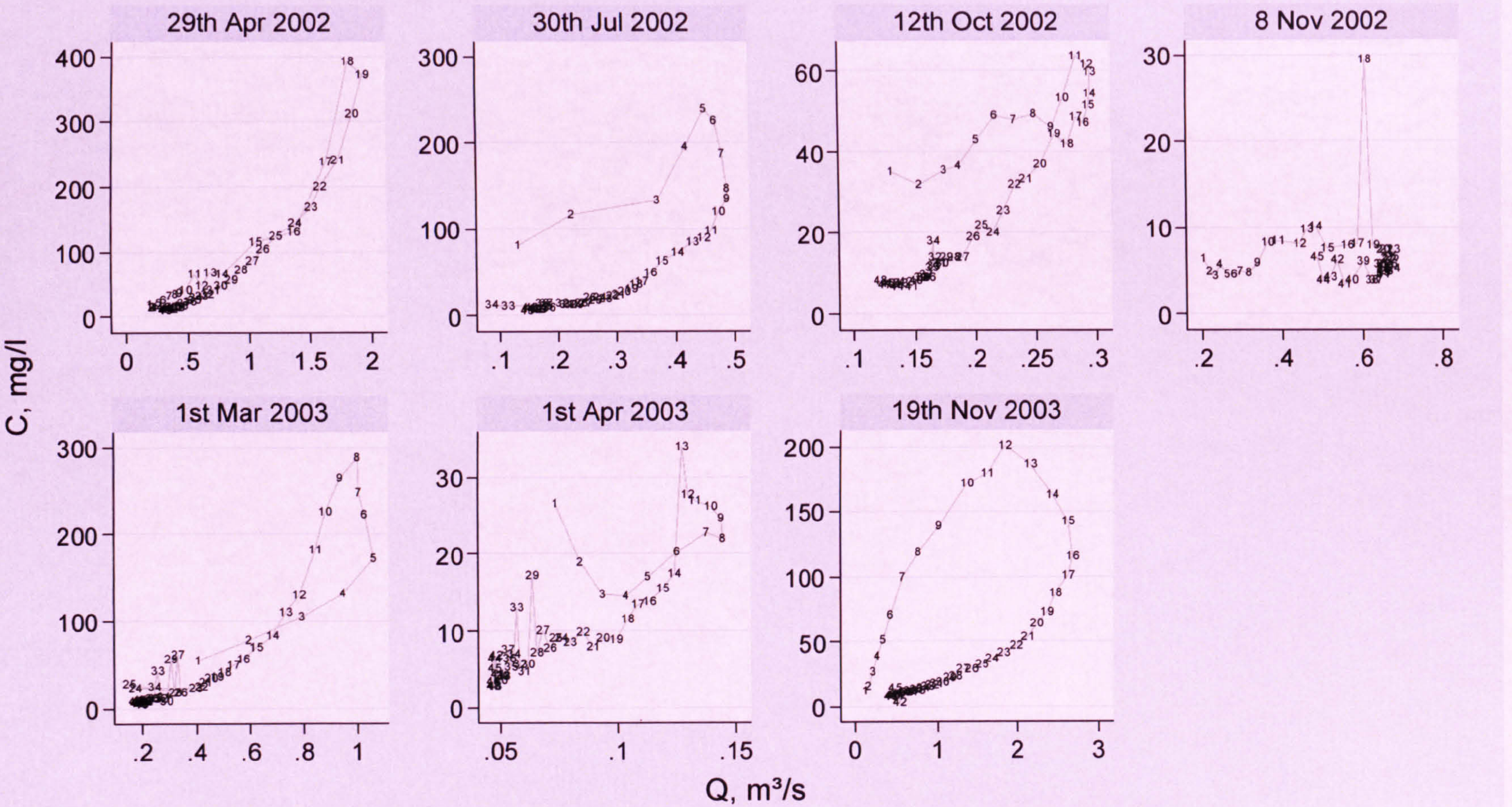

Figure 10.10. Hysteresis plots for each storm at Swinhope. The numbers represent the sample sequence, which were taken at 10 minute intervals for all storms. Note the different axis scales.

precipitation and intensity were relatively low (Table 10.1). New sediment sources may have been activated as a result of the size of the storm and transport pathways from the sources to the channel may have already been connected given the wet antecedent catchment conditions, thus reducing the likelihood of class 3 hysteresis.

10.7.2 30th July 2002

The event on 30th July is characterised by a class 2 hysteresis loop (Figure 10.10). The flow and precipitation in the preceding three and seven days were intermediate (Table 10.1). It was 45 days since an event of the same magnitude (Table 10.1), which explains the relatively high SSC given the relatively low discharges (Figure 10.10). The high intensity rainfall may have also contributed to the high SSCs (Table 10.1). SSC peaked 30 minutes before discharge (Figure 10.9). Therefore, sediment exhaustion is the likely cause of the class 2 loop.

10.7.3 12th October 2002

A class 2 hysteresis loop also categorises the event which occurred on 12th October (Figure 10.10). There is a 'pinch' near the top of the loop (samples 9 and 19) which is also apparent, to varying degrees, on other hysteresis loops: 29th April, samples 16 and 24; 30th July, samples 3 and 14; 1st March, samples 3 and 13; and 1st April, samples 6 and 14 (for the last two storms mentioned this is the point where the hysteresis loops twist into class 5 loops) (Figure 10.10). This pinch may be a result of inputs from two distinct sources, which are likely to be the two tributaries which join just upstream from the gauging site (Figure 4.3) due to the strength of this signal. The long time since a storm of the same magnitude (32 days) and the fact that SSC peaked 30 minutes before discharge (Figure 10.9), indicate that the class 2 form of the hysteresis loop was caused by sediment exhaustion. Given the wetness of the catchment in terms of flow and precipitation (Table 10.1), sediment was potentially derived from more distant sources in addition to local sources, which are commonly associated with class 2 hysteresis. The SSC are low compared with other events but the associated discharges are also comparatively low (Figure 10.10).

10.7.4 8th November 2002

The event on 8th November exhibited class 2 hysteresis but is very different from the other storms which are characterised by class 2 hysteresis (Figure 10.10). The difference is clearly evident by comparison of the sedigraphs. The event on the 8th November is

characterised by fairly low and steady SSC between 5 and 12 mg l^{-1} with one sharp peak of 30 mg l^{-1} (Figure 10.9). However, even without this peak there is still a weak class 2 loop (Figure 10.10). The antecedent catchment conditions were very wet (Table 10.1). However, the storm itself was small, except with respect to total storm flow, and it had only been two days since a storm of the same magnitude (Table 10.1). Therefore it is likely sediment supplies, including distant sources, were depleted, especially as a larger than bankfull storm must have occurred in the preceding seven days.

10.7.5 1st March 2003

The event on 1st March was characterised by a class 5 hysteresis loop (Figure 10.10). Given the lack of class 3 events in those sampled, despite variable catchment conditions and storm characteristics, and the pinch in most of the class 2 events, the class 5 form is most likely attributable to different sediment sources. Sediment delivered by the two tributaries just upstream of the gauging site is the probable cause, given the similar sediment sources throughout the catchment. The antecedent catchment characteristics of this event were intermediate with the exception of flow in the previous seven days which was high (Table 10.1). This coupled with the large storm (in all aspects apart from total flow) (Table 10.1), and the fact that discharge peaked 30 minutes before SSC (Figure 10.9) suggests that distant hillslope sources were connected to the channel.

10.7.6 1st April 2003

Class 5 hysteresis also characterised the event on 1st April (Figure 10.10). The antecedent catchment conditions were much drier than those for the class 5 event on the 1st March (Table 10.1). The storm rainfall characteristics are high and very similar to those of the 1st March event, storm duration and time since an event of the same magnitude are also similar (Table 10.1) and discharge peaked before SSC (Figure 10.9). However, the flow and peak discharge are much lower than the event on 1st March (Table 10.1). The form of the hysteresis loop can be attributed to sediment delivered by different tributaries for the same reasons as those outlined for the event on 1st March.

10.7.7 19th November 2003

The event on 19th November was classified as a class 2 hysteresis event (Figure 10.10). Precipitation in the preceding three and seven days was very low but flow was high (Table 10.1). This storm was the largest sampled in terms of peak discharge and total flow but was small in terms of precipitation and duration (Table 10.1). It had been 17

days since an event of a similar magnitude (Table 10.1) so there would have been sediment available for transport. SSC peaked 40 minutes before discharge (Figure 10.9) which suggests that local sediment sources were dominant. The SSC were high in comparison to other events but the associated discharges were also high (Figure 10.10). This, coupled with sediment exhaustion, suggests that large local sediment stores were accessed at higher discharges.

10.7.8 Comparison of events

The total storm precipitation of the class 5 events were very similar but intermediate in comparison with the other storm events; and class 5 hysteresis was associated with long duration storms (Table 10.1). Also, the class 5 events occurred within a month of each other, possibly indicating a seasonal influence promoting class 5 events in spring. The class 5 hysteresis can be attributed to sediment delivered from different sources, most likely the two tributaries just upstream from the gauging site. This signal is also evident on three of the five class 2 events (Figure 10.10). Discharge peaked before SSC for each of the class 5 events (Table 10.1) which suggests that the water from the tributary which reaches the gauging site first has the lower SSC. Gulp samples taken during a storm event from the TIMS locations suggest that the right tributary has lower SSCs than the left (Figure 10.11). Therefore, it can be deduced that the input from the right tributary reaches the gauging site before that of the left.

The class 2 hysteresis is attributable to sediment exhaustion within the system. SSC always peaked before discharge for the class 2 events (Table 10.1). The lack of class 3 events is unusual and indicates distant sources are at most weakly connected to the channel. Class 3 hysteresis is also produced by bank collapse; this suggests the banks were relatively stable during the period of monitoring. The range of SSC is very varied for the class 2 and 5 events and can be attributed in part to variation in discharge (Figure 10.9) but also to the effects of sediment supply.

10.8 Analysis of Trout Beck hysteresis plots

Three (3rd October 2001, 7th November 2001 and 29th November 2002) of the nine storms sampled on Trout Beck were discounted from hysteresis analysis due to incomplete sampling of the storm hydrograph (Figure 10.12). Five of the remaining six displayed class 2 hysteresis and the other displayed class 3 hysteresis (Figure 10.13).

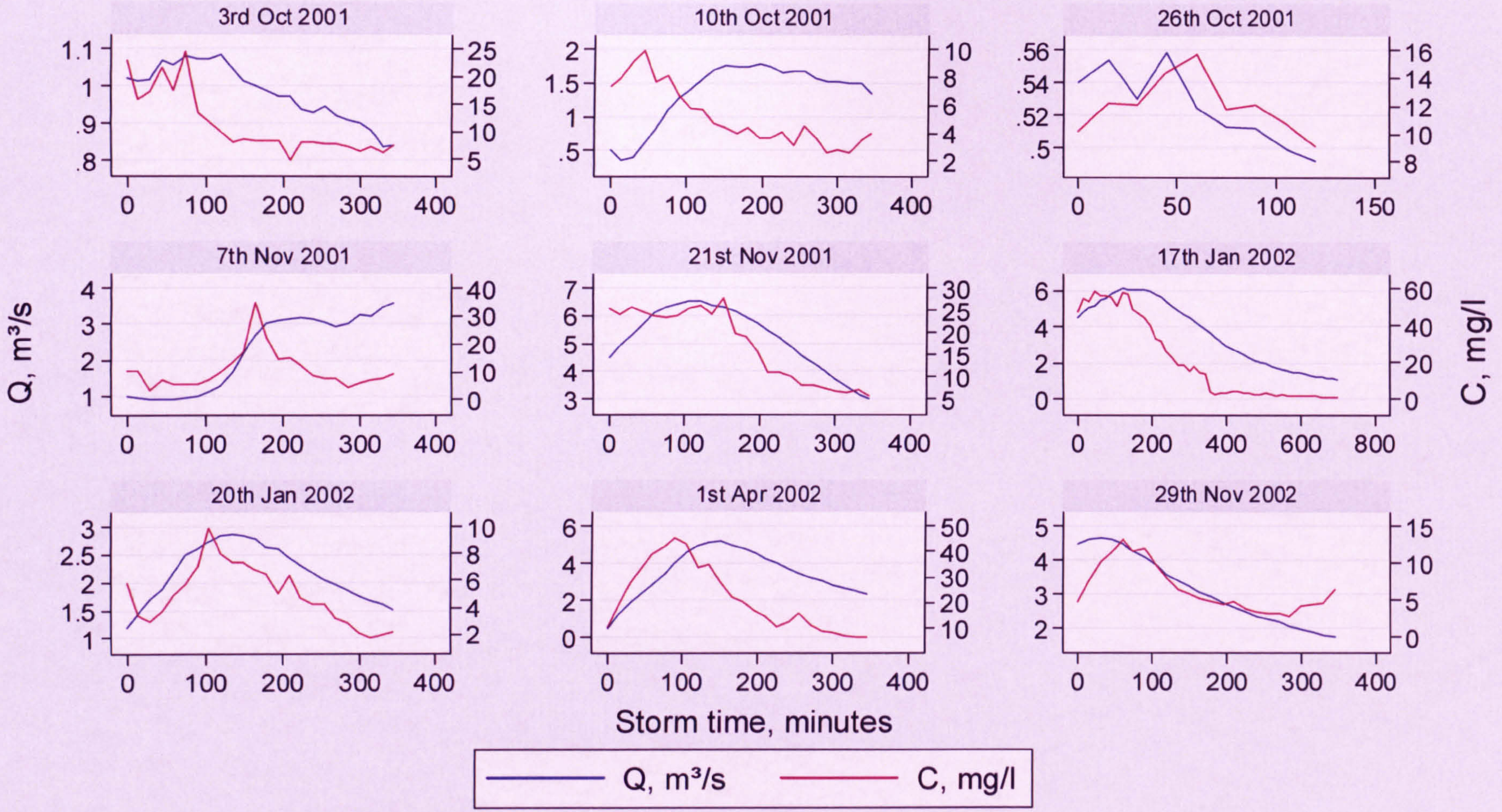

Figure 10.12. Hydrographs and sedigraphs for each storm at Trout Beck. Note the different axis scales.

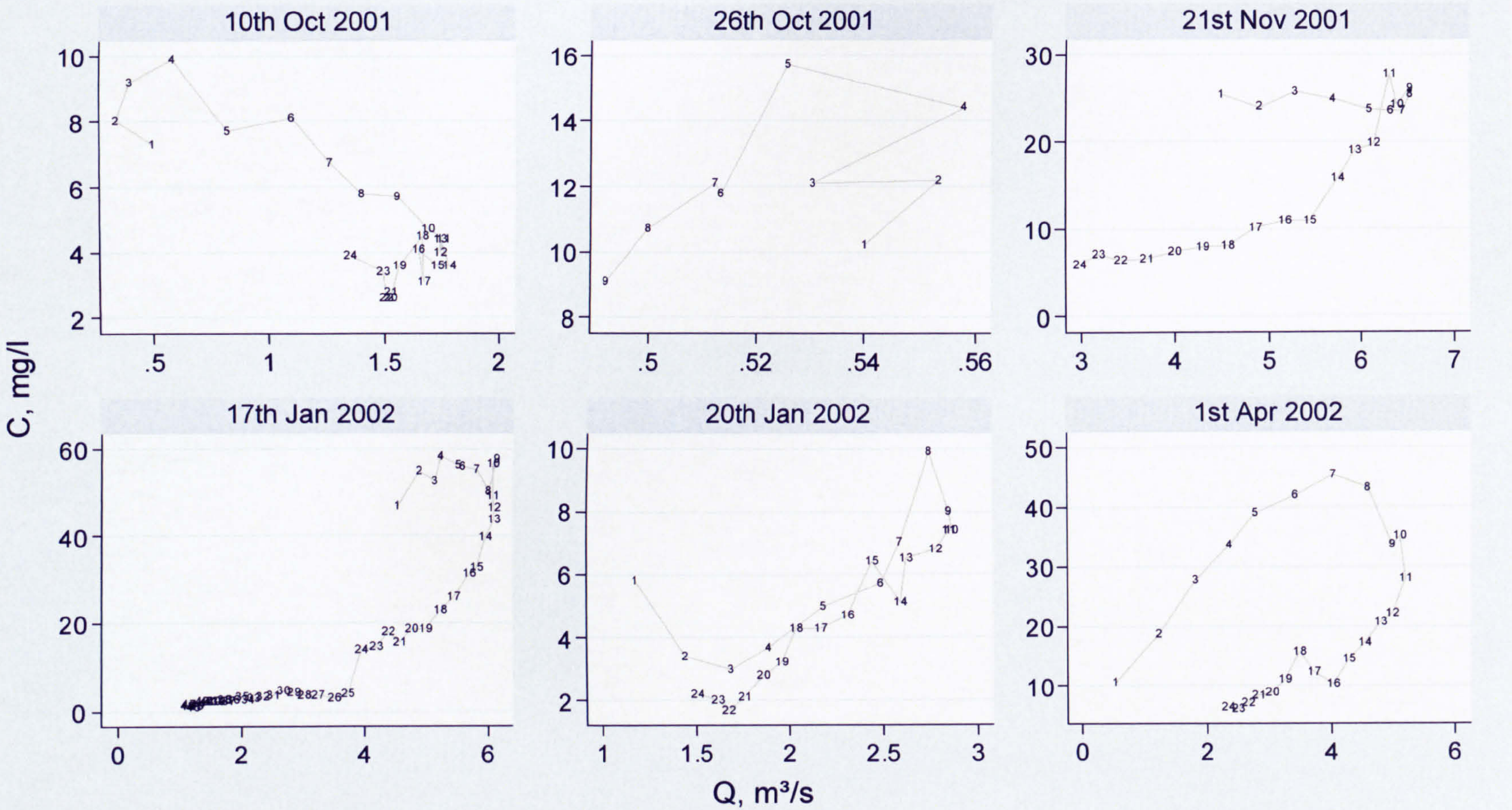

Figure 10.13. Hysteresis plots for each storm at Trout Beck. The numbers represent the sample sequence, which were taken at 15 minute intervals for all storms. Note the different axis scales.

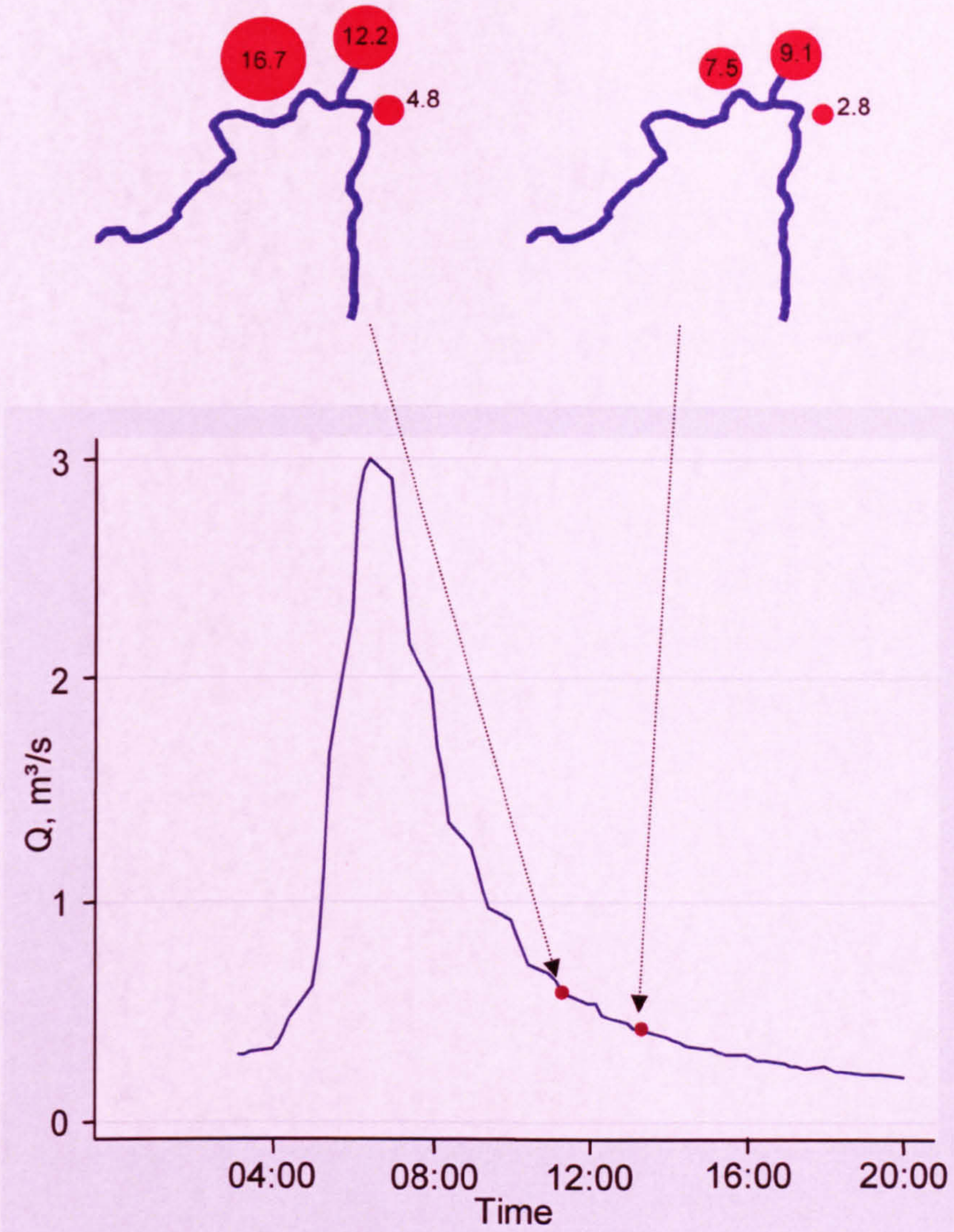

Figure 10.11. SSC, in mg l^{-1}, at the three spatial sample locations at Swinhope on the falling limb of a flood event on 6th January 2004.

10.8.1 10th October 2001

The 10th October event exhibited a class 2 hysteresis loop (Figure 10.13). SSC peaked before discharge (Figure 10.12) and indicates local sediment sources, although the antecedent catchment conditions were wetter than for any other event (Table 10.1). The storm was small in terms of total precipitation, peak precipitation, total flow and peak flow and it was only 30 hours since the peak discharge was last reached (Table 10.1). As a result it is unlikely that any new sources of sediment were accessed during the event. As the SSC are relatively low the class 2 hysteresis may have been a result of what little sediment there was available being exhausted or diluted by higher discharges. Alternatively, as the storm was part of a series of storms the sediment may have been

supplied by more distant sources which were activated by a previous and larger storm event, but had only just reached the channel.

10.8.2 26th October 2001

Only nine samples were taken during the event on 26th October and they exhibited class 3 hysteresis (Figure 10.13). The antecedent catchment conditions were intermediate and the storm was relatively small (Table 10.1). As it was only a short time period (56 hours) since an event of a similar or larger magnitude (Table 10.1), it is possible that the storm, although not large, was large enough to activate more distant sources which promoted the class 3 hysteresis. This is reinforced by the fact that the SSC peak occurs after the discharge peak: the sediment may have been derived from upstream/distant sources which were mobilised by the previous storm but did not reach the gauging site. The class 3 hysteresis is unlikely to be caused by bank collapse as the peak discharge was not particularly high (Table 10.1).

10.8.3 21st November 2001

The event on 21st November exhibited class 2 hysteresis (Figure 10.13). The relatively dry catchment conditions, as indicated by the precipitation and flow parameters, are indicative of a class 2 event, although surface wetness indicated the catchment was fairly wet (Table 10.1). The storm was one of the largest in terms of all the storm parameters except duration and it was just over two days since a storm of the same magnitude (Table 10.1). This would have promoted sediment exhaustion, especially as the catchment was not wet enough for more distant hillslope sources to be connected. The relatively high SSC, despite a recent event, are likely to be a result of the large and intense storm eroding and transporting sediment from local sources. Discharge peaked 45 minutes before SSC which is unusual for a class 2 event (Figure 10.12). However, the sedigraph (Figure 10.12) suggests that the complete event was not captured so the true sedigraph peak may have occurred before sampling commenced.

10.8.4 17th January 2002

The storm on 17th January was also categorised as a class 2 hysteresis event (Figure 10.13). The antecedent catchment conditions were intermediate, the storm was large and it was a long time since an event of equal or greater magnitude (Table 10.1). It is likely that the cause of the hysteresis was sediment exhaustion of local sources as for the event on the 21st November. SSC peaked 1 hour 15 minutes before discharge (Figure 10.12),

which suggests rapid entrainment of sediment from channel sources. Also, the SSC were fairly low given the magnitude of the associated discharges (Table 10.1).

10.8.5 20th January 2002

The event on 20th January was characterised by a very tight, class 2 hysteresis loop (Figure 10.13). The catchment was fairly wet with reference to flow and precipitation in the preceding three and seven days, although not in terms of the surface wetness (Table 10.1): therefore the likelihood of connected hillslopes is uncertain. The low SSC (Figure 10.12), can be explained by the short time since an event of the similar magnitude and the intermediate size of the storm (Table 10.1). These factors and the fact that SSC peaked 1 hour before discharge (Figure 10.12) suggest that sediment exhaustion was responsible and the sediment originated from fairly depleted sources in close proximity. However, the tightness of the loop suggests a fairly constant supply of sediment in relation to discharge.

10.8.6 1st April 2002

Class 2 hysteresis also categorised the event on 1st April (Figure 10.13). The antecedent catchment conditions were the driest as indicated by every parameter except surface wetness in the preceding three days (Table 10.1), and therefore it is unlikely hillslope sources were connected to the channel. The storm was intermediate in size and it had been 22 days since an event of a similar magnitude (Table 10.1). The openness of the loop and high SSC are indicative of the relatively long time since an event of the same magnitude. The hysteresis is likely to be caused by sediment exhaustion and the sediment is likely to have been derived from local sources as SSC peaked 1 hour prior to discharge (Figure 10.12).

10.8.7 Comparison of events

Generalisations can only be made regarding class 2 events given that only one event was not class 2. The cause of the dominance of class 2 hysteresis is likely to be sediment exhaustion. SSC peaked before discharge for all class 2 events except the event on the 21st November 2001 (Table 10.1). However, there is evidence the sedigraph was incompletely sampled. The limited number of class 3 events may be due to the poor connectivity between hillslope and channel local to the gauging site due to gentler hillslopes and broader floodplains.

The antecedent catchment conditions and storm characteristics of the one class 3 event were not distinct from the other events, which prevents the identification of causal factors. However, as the discharge peaked before SSC and Trout Beck is the largest study catchment, it is likely that the sediment was derived from a distant source. As the catchment was not especially wet and the relatively poor connectivity near the gauging site the distant source is likely to be an upstream source as opposed to local hillslopes, possibly activated by a localised rain storm.

10.9 Inter-catchment comparison of hysteresis

Class 2 hysteresis is the dominant form in each of the study catchments (Figure 10.14). Class 3, 5 and 6 hysteresis loops also occurred in some of the catchments and class 1 and class 4 hysteresis were not sampled (Figure 10.14).

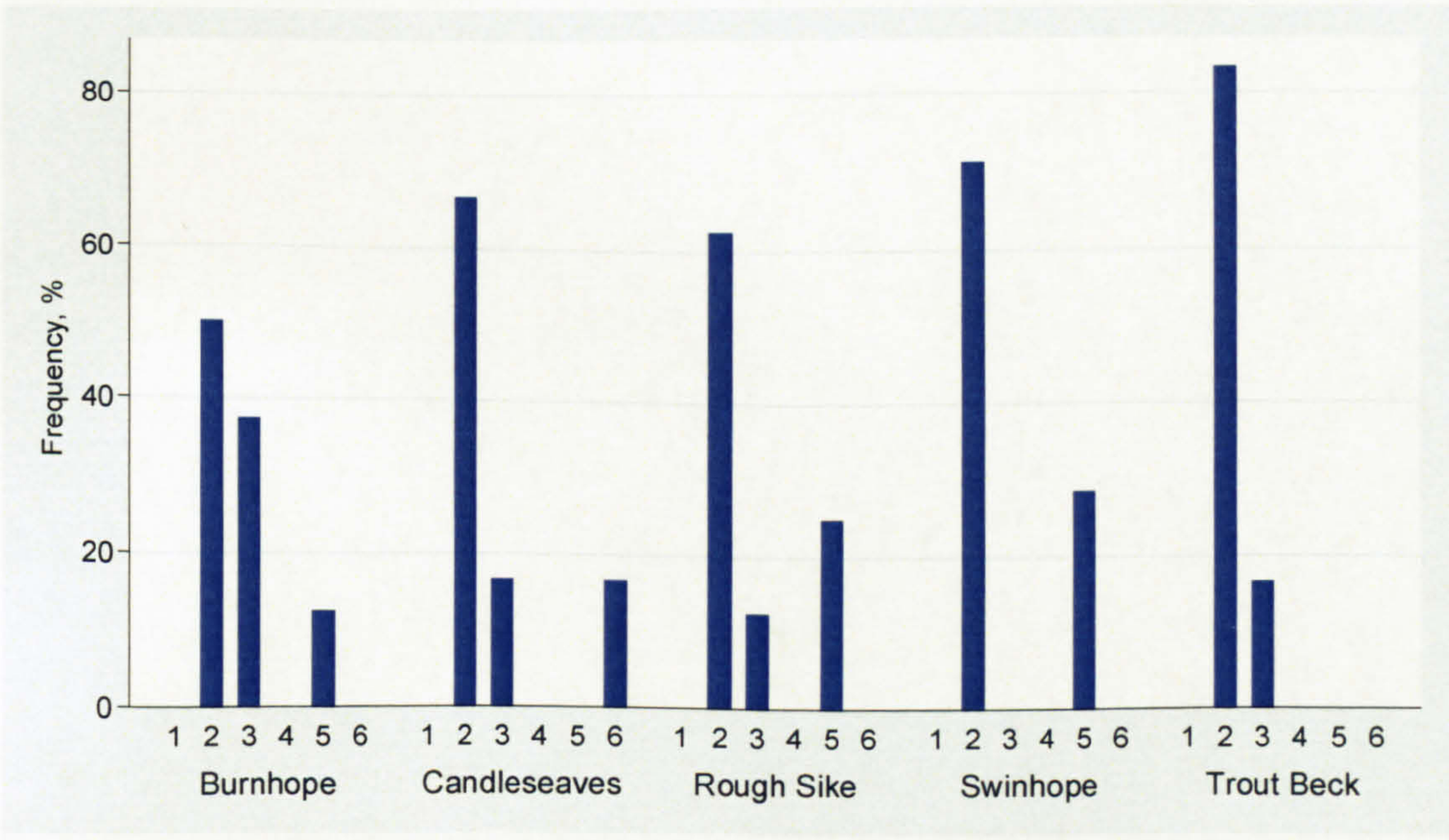

Figure 10.14. Percentage of each hysteresis class in each study catchment. n = 8 for Burnhope, 6 for Candleseaves, 8 for Rough Sike, 7 for Swinhope, and 6 for Trout Beck.

Class 2 hysteresis is reportedly dominant in catchments where sediment dynamics are controlled by supply as opposed to transport (Burt *et al.*, 1984). As the catchments are all supply-limited it is not surprising that class 2 hysteresis dominates (Table 10.14). Williams (1989) and Brasington & Richards (2000) linked class 2 hysteresis to sediment exhaustion caused by larger storms. This pattern is confirmed by the results of this investigation and the largest storms were exclusively associated with class 2 hysteresis at Candleseaves (Table 10.1). Burnhope had some of the larger storms, in terms of storm flow, precipitation, duration and peak discharge (Table 10.1), but the

smallest percentage of class 2 events. However, the size of the storm is relative to catchment size. Labadz *et al.* (1991) postulated that class 2 hysteresis is associated with smaller catchments. This investigation confirms this, as in the context of global rivers the study catchments are all small and all dominated by class 2 hysteresis. Seeger *et al.* (2004) found that class 2 hysteresis was encouraged by dry catchment conditions where sediment was derived from local sources. However, the study catchments were in a different environment, the Spanish Pyrenees. The antecedent catchment conditions and storm characteristics varied substantially for class 2 events within the same catchment and between catchments (Table 10.1). Class 2 events were associated with dry catchment conditions at Burnhope and to a lesser extent at Candleseaves, but no such generalisations could be made for the other catchments. The inter-catchment variation could be a function of catchment scale, although this is perhaps only applicable to flow parameters and generalisations should be made with care due to the bias in the sampling strategy. The dominant sediment sources during class 2 events were assumed to be the channel bed, channel banks and possibly some local hillslope sediment sources.

The class 3 events were attributed to connection of distant sources at Burnhope, Trout Beck and Rough Sike. Williams (1989) and Brasington & Richards (2000) reported that class 3 hysteresis could be caused by the difference in the relative speed of the flood and sediment waves. Class 3 hysteresis generated by this mechanism is probably fairly infrequent in the study sites of this investigation given the small catchment sizes. However, there was some evidence of this mechanism at Trout Beck and Rough Sike. Long travel times, as a result of physically distant sources or low transport efficiency, have also been reported as a cause of class 3 hysteresis by several authors (Walling, 1974; Asselman, 1999; and Brasington & Richards, 2000), and the input of sediment by bank collapse on the falling limb was reported to cause class 3 hysteresis by Ashbridge (1995). The class 3 event at Candleseaves suggest another mechanism may cause class 3 hysteresis: sediment retention by debris within the channel. Seeger *et al.* (2004) linked wet catchments, and therefore connectivity of more distant sources, with class 3 hysteresis. The antecedent catchment conditions indicated this at Burnhope but evidence was not as convincing in the other catchments.

Burnhope had a much higher percentage of class 3 events than the other catchments (Figure 10.14). This may be a result of catchment shape as Burnhope is a fairly rounded catchment (Figure 4.3), on the basis that hillslope sources are more distant from the

gauging site. However, this trend is not applicable to all the study sites. For example, Rough Sike has the second highest proportion of class 3 events (Figure 10.14) but is very elongated (Figure 4.3). However, given the small number of events it may be mis-representative of the catchment.

Class 5 events are produced by a combination of the factors which produce class 2 and class 3 hysteresis: sediment exhaustion, dilution by baseflow, distant sediment sources, bank collapse and the difference in the flood wave and sediment wave velocities (Williams, 1989 and Ashbridge, 1995). This investigation indicates that differences in timing of sediment from two distinct sources can also produce class 5 hysteresis. This was apparent at Swinhope and Burnhope. The class 5 events generally began with the form of a class 2 event and then twisted into a class 3 event. Therefore it can be reasoned that longer storms promote the likelihood of a class 2 event developing into a class 5 event due to the activation of another sediment source. The class 5 events at Rough Sike and Swinhope were associated with longer duration storms and in the late winter/early spring. However, the class 5 storm at Burnhope was in winter and short compared with the other Burnhope storms (Table 10.1). This may have been a snowmelt event. All other storm characteristics and antecedent catchment conditions of the class 5 events were not distinct from those of other events except precipitation, flow and average soil moisture in the preceding 3 days were relatively high at Rough Sike. At Swinhope the two sources are thought to be two tributaries just upstream of the gauging site, especially as these inputs are also evident on most of the class 2 loops. The class 5 events at Rough Sike were attributed to the twin-peaked hydrographs.

Hydrograph form for storms in all catchments were examined to investigate if symmetry, smoothness or number of peaks was related to hysteresis class. No relations between symmetry, smoothness and hysteresis class were found. Hydrographs with more than one peak were always associated with class 3 or class 5 hysteresis. However, there were also some class 3 and class 5 events associated with smooth single-peaked hydrographs, for example, the event on 1st April in Swinhope.

One of the limitations of this analysis is the limited number of storm events monitored in each catchment. However, given the broad similarity in the catchment conditions it is possible to combine the results and make inferences regarding catchment conditions and storm characteristics between catchments. Catchment scale is standardised according to

Table 10.2. The effect of season was also incorporated into this analysis to give insight to the representativeness of the events analysed.

Table 10.2. Standardisation of catchment conditions and storm characteristics.

Catchment condition/storm characteristic	Standardisation
Precipitation:	
3 days	Not required
7 days	
Storm	
Flow:	
3 days	Divide by total annual
7 days	
Storm	
Average surface wetness:	
3 days	Data for Rough Sike and Trout Beck only
7 days	
Storm	
Average soil moisture:	
3 days	Data for Rough Sike only
7 days	
Storm	
Total storm precipitation	Not required
Peak storm precipitation intensity	Not required
Storm duration	Divide by catchment area
Storm discharge peak	Divide by mean annual discharge
Time since peak discharge last reached	Not required

Generally, the storms sampled covered a broad range of antecedent catchment conditions and storm characteristics, although fewer events were sampled during the summer months, but this is symptomatic of the system. In addition, there was not good coverage of storm duration: only shorter storms were sampled in Swinhope, Candleseaves and Rough Sike, mid-length storms in Trout Beck and long storms in Burnhope.

Total storm flow did not exert a noteworthy control over hysteresis class. This can be explained by the fact that both discharge and storm length contribute to total flow. Therefore, a storm with a high discharge and short duration could have the same total flow as a storm with a low discharge and long duration but could be associated with very different sediment dynamics.

With reference to standardised peak discharge, Class 2 hysteresis events occured throughout the range of standardised peak discharge but the larger storms (standardised peak discharge of greater than seven), were all class 2 events (Figure 10.15). Class 3 events, with the exception of one event in Rough Sike, occurred at standardised peak discharge of less than five and class 5 events occurred between standardised peak discharge values of four and five (Figure 10.15). This suggests there may be ranges in peak discharge standardised by mean annual discharge within which class 3 and 5 hysteresis are more likely to occur. These boundaries of the standardised peak discharge between hysteresis types are fuzzy, which is expected given the influence of other factors on hysteresis class, e.g. time since storm of the same magnitude.

Class 2 events are more clustered at lower values of standardised flow in the preceding three days and class 3, 5 and 6 events are more dominant at higher values (Figure 10.16). This suggests that storms preceded by a smaller proportion of the total annual flow in the preceding three days, i.e. drier antecedent catchment conditions, were more likely to exhibit class 2 hysteresis. This is in agreement with the findings of Seeger *et al.* (2004). There are no class 3, 5 or 6 events from June to mid-October (Figure 10.16). This could be a symptom of the dry catchment conditions during these months or the heightened importance of autochthonous sediment which becomes quickly exhausted, therefore producing class 2 hysteresis. In contrast, there was no pattern with regard to hysteresis class and standardised flow in the preceding seven days, suggesting that flow in the preceding seven days is not a noteworthy control over hysteresis class and confirms the results of the individual catchment analysis.

Storms which had maximum precipitation intensities of less than 3 mm per 15 minutes were characterised by class 2, 3, 5 and 6 hysteresis (Figure 10.17). All storms with maximum precipitation intensities of greater than 3 mm per 15 minutes were characterised by class 2 hysteresis (Figure 10.17). Dominance of class 2 events during storms with high intensity rainfall may be attributed to the indirect effects, such as increased likelihood of overland flow and rapid increases in discharge, as opposed to the direct effects. This finding is in agreement with Williams (1989) and Brasington & Richards (2000), who associated class 2 hysteresis with large storms.

All hysteresis types occur across the range of total storm precipitation. However, storms characterised by less than 22 mm of precipitation between June and February are all class 2 with the exception of one class 3 event in Trout Beck (Figure 10.18). This may

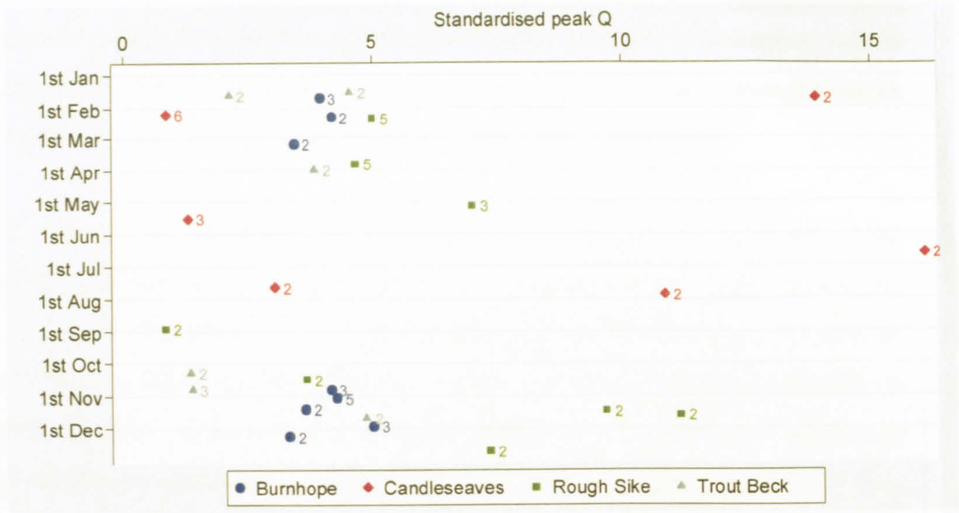

Figure 10.15. Associations between standardised peak storm discharge, hysteresis class, time of year and catchment. The colours correspond to the catchment and the numbers the hysteresis class.

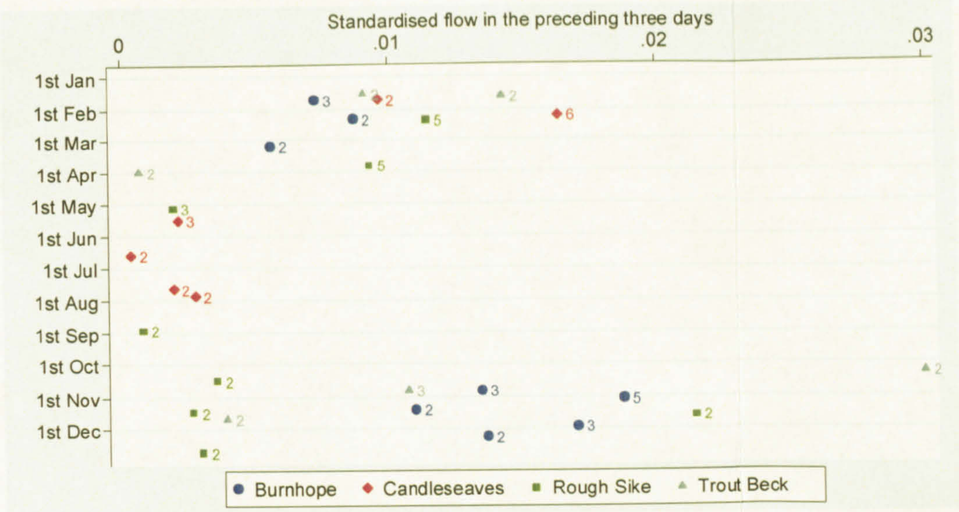

Figure 10.16. Associations between standardised flow in the three days preceding the event, hysteresis class, time of year and catchment. The colours correspond to the catchment and the numbers the hysteresis class.

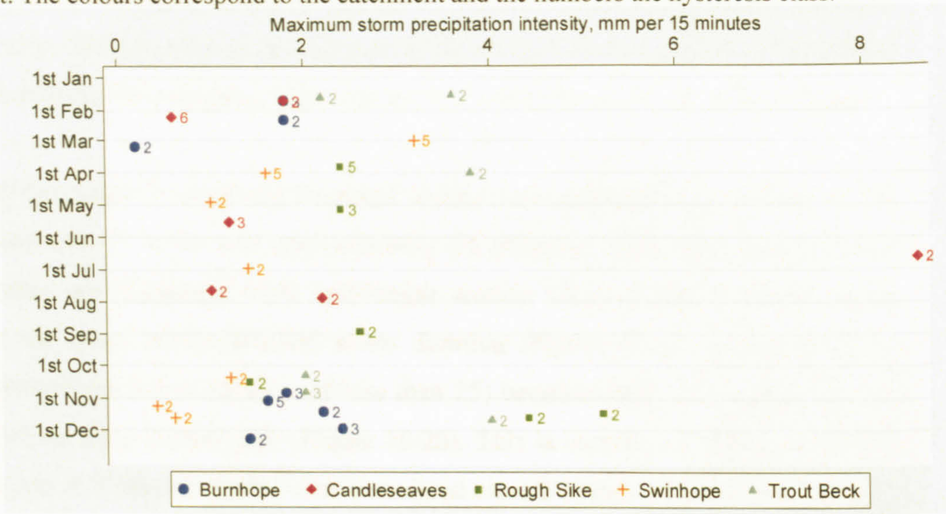

Figure 10.17. Associations between maximum precipitation intensity during the event, hysteresis class, time of year and catchment. The colours correspond to the catchment and the numbers the hysteresis class.

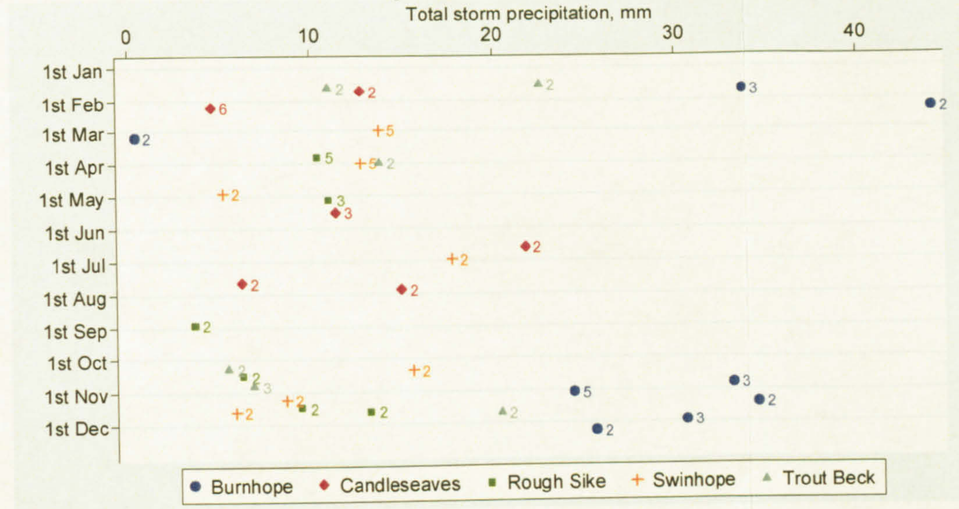

Figure 10.18. Associations between total precipitation during the event, hysteresis class, time of year and catchment. The colours correspond to the catchment and the numbers the hysteresis class.

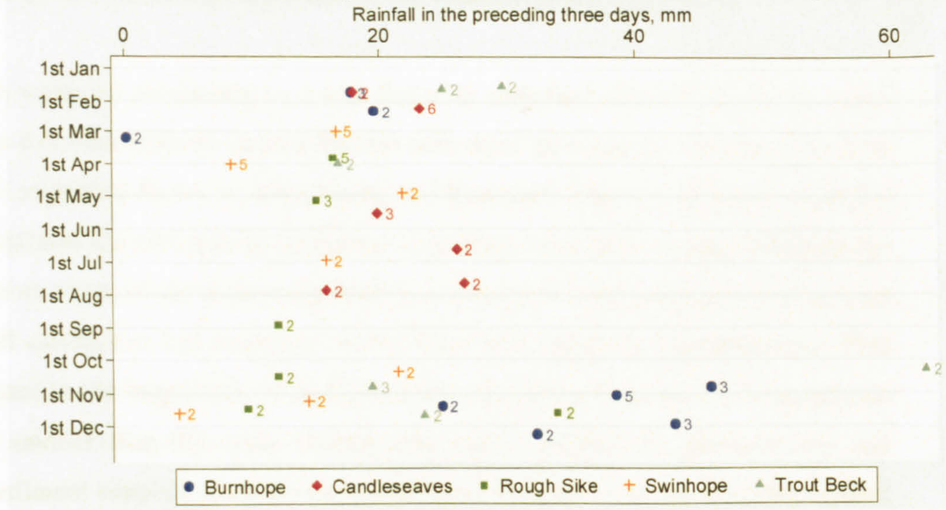

Figure 10.19. Associations between rainfall in the three days preceding the event, hysteresis class, time of year and catchment. The colours correspond to the catchment and the numbers the hysteresis class.

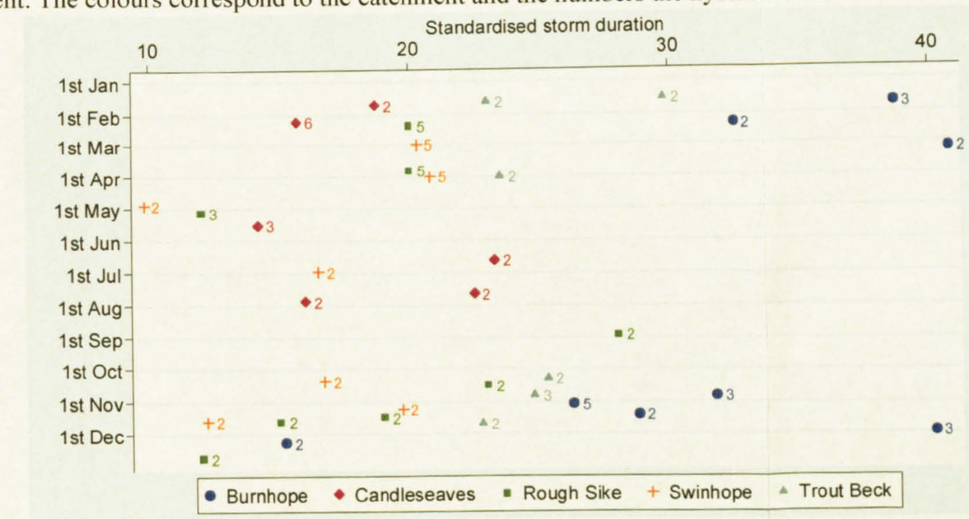

Figure 10.20. Associations between standardised storm duration, hysteresis class, time of year and catchment. The colours correspond to the catchment and the numbers the hysteresis class.

be indicative of enough precipitation to transport sediment from local sources, which become depleted. During storms with higher total precipitations more distant sources may be connected to the channel, thus producing class 3 and 5 hysteresis.

As with the total storm precipitation plot all events preceded by less than 30 mm in the previous three days between June and January were characterised by class 2 hysteresis with the exception of one event in Trout Beck (Figure 10.19). This can also be explained by the depletion of local sediment supplies and insufficient precipitation to connect more distance sources to the channel. Seeger *et al.* (2004) associated wet catchment conditions with class 3 hysteresis. Figure 10.19 does not confirm this although it was evident on a catchment by catchment basis. This may be explained by the difference in catchment response to a given amount of precipitation dependent on catchment size. Similar patterns are evident in the rainfall in the preceding seven days plot, which reflects the correlation between the two variables, especially at low values.

Four of the five class 5 events are clustered around a standardised storm length of 20 and the other class 5 event is at approximately 25 (Figure 10.20). This suggests that class 5 events are associated with mid-length storms. Class 2 and 3 storms occur throughout the range of standardised storm duration (Figure 10.20). However, short storms (standardised storm duration of less than 25) between June and January are all characterised by class 2 hysteresis (Figure 10.20). This is contrary to Williams (1989) and Brasington & Richards (2000) who associated class 2 hysteresis with large storms. However, the storms might be large by other measures (e.g. peak discharge) and may reflect the degree of sediment exhaustion in the systems during that period.

Given that sediment exhaustion is a key factor in sediment delivery in all the study catchments it is reasonable to assume that the time since an event of a similar magnitude may be an important factor in determining the hysteresis class of an event. Holliday (2003) illustrates the variation in hysteresis loop form over three events in Burnhope. Time since an event of the same magnitude was examined with reference to hysteresis class for all catchments but no pattern was evident with regard to hysteresis type. This can attributed to the magnitude of smaller events occurring between. For example, an event just smaller than the event studied may have occurred the previous day and depleted sediment supplies or no events could have occurred between the event studied

and the last event of that magnitude. To resolve this, a continuous or quasi-continuous SSC series is required.

SSC peaks prior to discharge in the overwhelming majority of class 2 events (Table 10.1). The only class 2 event for which discharge peaked before SSC was 21st November in Trout Beck (Figure 10.12, section 10.8.3). However, the form of the sedigraph suggests that SSC may have peaked before measurement commenced (Figure 10.12). The dominance of SSC peaking before discharge in class 2 events is indicative of sediment exhaustion. The class 3 events were all characterised by discharge peaking before SSC (Table 10.1) which suggests distant sediment sources, flood waves reaching the gauging site before the sediment wave or bank collapse on the falling limb (e.g. Asselman, 1999; Brasington & Richards, 2000; and Ashbridge, 1995). SSC generally peaks first during class 2 events and discharge first in class 3 events. However, both types can occur if SSC and Q peak simultaneously (Williams, 1989). SSC peaked before discharge in approximately 50% of class 5 events and SSC peaked before discharge in the only class 6 event examined.

10.10 Chapter summary

The main outcome of this analysis is that class 2 hysteresis is dominant in the upland catchments studied and is attributed to sediment exhaustion of local supplies. Analysis of the hysteresis class in relation to antecedent catchment conditions, storm characteristics and field observations of sediment delivery lead to the following generalisations:

(1) Class 3 hysteresis was attributed to the difference in water and sediment wave velocities, the supply of sediment from distant sources (hillslopes) and the difference in timing of sediment delivery from two sources.

(2) Class 5 hysteresis was attributed to two different supplies of sediment delivered sediment at different times and twin-peaked hydrographs. Also, class 5 events were associated with late winter and early spring, suggesting a seasonal influence, and longer storm durations.

(3) Flow in the preceding three days was important in determining hysteresis class.

(4) Class 2 hysteresis was associated with SSC peaking before discharge and class 3 hysteresis is associated with discharge peaking before SSC. This is generally the case but both class 2 and class 3 hysteresis can result if SSC and discharge peak simultaneously (Williams, 1989).

(5) Sediment retention in the channel by debris was identified as a possible cause of class 3 hysteresis in Candleseaves.

The hysteresis types of all the study catchments were examined and related to catchment characteristics and standardised, where necessary, measures of antecedent catchment conditions and storm character (to exclude the effect of scale). From this analysis several conclusions were made:

(1) Standardised flow in the preceding three days suggested that the events preceded by smaller proportions of the total annual flow are most likely to exhibit class 2 hysteresis, as sediment would have built up ready for transport. This confirms the results of the individual catchment analysis and the suggestion by Seeger *et al.* (2004) that class 2 hysteresis is promoted by dry catchment conditions.

(2) Class 5 events occurred during events with peak discharges between four and five times the mean annual discharge, class 3 events occurred during events with peak discharges less than seven times the mean annual discharge and class 2 events occurred throughout.

(3) Maximum storm precipitation intensities of greater than 3 mm per 15 minutes were associated with class 2 hysteresis. This pattern is partially explained by the indirect affects of precipitation intensity, e.g. overland flow and surface wash.

(4) From June to January events with lower rainfalls (in the preceding three and seven days and total storm precipitation) and smaller storm durations were characterised by class 2 hysteresis. With respect to precipitation this is explained by insufficient moisture to connect more distant sediment sources.

Chapter Eleven: CONCLUSIONS, SYNTHESIS, RECOMMENDATIONS AND APPLICATIONS

11.1 Overview

This chapter presents the main conclusions, specific to each objective; a synthesis of the results; recommendations; limitations and future research possibilities; and applications to other studies.

11.2 Main conclusions

The aim of this thesis was to monitor and model suspended sediment flux in six British upland catchments at event and annual time-scales in an attempt to elucidate both catchment-specific and larger-scale controls over suspended sediment dynamics. The conclusions, categorised into the specific objectives defined to fulfil the aim, are outlined below:

1a. Monitor suspended sediment in a range of catchments representative of the British uplands and produce a database of suspended sediment loads.

Suspended sediment concentration was monitored in three upland catchments (Swinhope, Trout Beck and Candleseaves) and existing records for three other catchments were incorporated (Langtae, Burnhope and Rough Sike) in the analysis. The monitoring, which led to the load estimates, was primarily derived from auto-sampler samples. The sampling regime was predominantly storm-sampling, with the exception of Langtae, which was fixed-interval sampling, and Burnhope which was approximately 60% fixed-interval sampling. Some supplementary gulp samples were taken when the

river was in flood. This resulted in a database of 3333 SSC and discharge pairs (Burnhope: 1204, Candleseaves: 306, Langtae: 379, Rough Sike: 522, Swinhope: 572 and Trout Beck: 350).

1b. Examine the spatial variation in suspended sediment dynamics and properties at the between and within catchment spatial scales.

The spatial variation in suspended sediment dynamics was primarily investigated at Moor House NNR given the infrastructure and background information associated with its ECN status. Some supplementary information from Swinhope was also incorporated. The spatial variation in SSC, variability in bed sediment storage and the organic-mineral balance and geochemistry of suspended sediment were examined at the within catchment scale and the variation in dynamics, volumetric yield and relationships between suspended sediment load and catchment characteristics were examined at the between catchment scale.

The spatial variation in SSC in fixed-interval samples taken simultaneously at two nested gauging sites (Rough Sike and Trout Beck) and in gulp samples taken in eight spatially distributed sampling locations during storm events was investigated. The results of this section indicated that more sediment is supplied by the smaller, lower order channels; SSC is more variable in higher order catchments given the more complex patterns of sediment supply and delivery; catchment geology and vegetation exert some control over the fixed-interval SSCs; the system is generally supply-limited; and discharge is the dominant control over suspended sediment load.

Eight bed sediment storage experiments were undertaken in the Moor House channel network and indicated contribution of sediment from the channel bed during storms in which there was no, slight and severe bed movement. The least sediment was supplied from the bed when there was no bed movement (50 to 1573 mg l^{-1}) and most when there was severe bed movement (2,306 to 19,854 mg l^{-1}). There was substantial spatial variation in the amount of sediment supplied by the bed at each stage of agitation and this was related to flow regime, particle size distribution of the bed sediment and existence of periphyton on the bed surface.

Investigation of the organic-mineral balance of suspended sediment involved the deployment of 21 time-integrated mass samplers (TIMS) in the Moor House channel

network and 3 in the Swinhope channel network. The sediment was analysed for organic matter content using loss-on-ignition. The main outcomes of this were that the organic matter contents of the Moor House TIMS sediment was different throughout the channel network, some statistically significant, and could be related to catchment soil cover. There were also links between the organic matter content and geology and vegetation cover. The organic matter contents of the Swinhope TIMS showed variability but differences were statistically insignificant and were explained by the close proximity of the TIMS. Organic matter generally decreased with catchment area and distance downstream. Decreases in organic matter content were attributed to increased contribution of mineral sediment.

Examination of the suspended sediment geochemistry was exploratory in nature. It involved analysing TIMS and source sediment for a suite of elements, conducting principal components analysis and investigating the patterns with reference to the spatial location of the TIMS sampling points. The main outcomes of this analysis were: catchment geology, soil and vegetation type influence sediment geochemistry; sediment geochemistry is variable at cross-section scale and was related to sediment and water mixing; there are relations between sediment geochemistry before and after confluences; and with the exception of peat sources all other source types have variable geochemistry.

Analysis of the optimal load estimates for each site indicated that: all the catchments are highly responsive, especially those with continuous peat cover (Candleseaves, Rough Sike and Trout Beck); the effective Candleseaves and Rough Sike have lower effective discharge intervals than Burnhope, Langtae and Trout Beck; and volumetric yields are importance when assessing landscape change.

Analysis of all undisturbed British upland catchment loads indicated that suspended sediment loads are positively correlated with indicators of catchment size (catchment area, maximum elevation, stream order, total channel length and mean flow) and negatively correlated with average channel slope. Correlations between specific sediment yields and catchment characteristics are weak, suggesting catchment scale is an important control over suspended sediment dynamics.

Consideration of the results of these four sections leads to the general conclusion that the quantity and character of suspended sediment vary from the cross-section scale to catchment scale. SSCs are higher in lower order channels, where the sediment is composed of more organic sediment

1c. Examine the temporal variation in suspended sediment dynamics at storm to sub-annual time-scales.

The temporal variation in suspended sediment was examined at the storm-scale and sub-annual scale. Storm-scale variation was investigated by analysing hysteresis plots for each storm in each catchment. The main conclusion of this section is that class 2 hysteresis dominates in small upland catchments and is attributed to sediment exhaustion. Class 3 and class 5 hysteresis also occurred. No class 1 events occurred as sediment supply has to be abundant and class 4 events are very rare (require equal supply of sediment on rising and falling limb and variable supply during the peak). Class 2 hysteresis was characterised by SSC peaking before discharge and class 3 hysteresis by discharge peaking before SSC.

Temporal variation in organic matter content of TIMS sediment was investigated at Swinhope and Moor House. At Moor House there was a pattern but no seasonal signal. In contrast, there was a clear seasonal signal at Swinhope, with the organic matter content peaking in the summer. This was attributed to autochthonous sediment production and limited storm events during the summer. The lack of seasonal signal at Moor House was attributed to the input of mineral sediment during summer storm events and the amount of allochthonous peat throughout the catchment.

1d. Infer sources of suspended sediment and controls over the delivery of sediment from those sources.

Sediment sources were inferred from analysis of the spatial and temporal variation in suspended sediment. The hysteresis analysis, coupled with quantification of the antecedent catchment conditions and storm characteristics, allowed potential sediment sources to be identified. The dominant sediment sources were in channel (bed and banks) and local hillslopes. Some of the class 5 events and some of the class 3 events indicated that there were two distinct sediment sources, which were identified as tributaries upstream for the gauging site at Burnhope and Swinhope and channel and hillslope or gully sources at Rough Sike. Twin-peaked hydrographs were also

associated with class 5 events. Retention of sediment by debris in the channel was identified as a control over sediment delivery at Candleseaves, and resulted in class 3 hysteresis; a cause not outlined by Williams' (1989) classification.

Combining the hysteresis results from all catchments and standardising for scale suggested that events preceded by smaller proportions of the total annual flow were most likely to exhibit class 2 hysteresis, as sediment would have built up ready for transport. Analysis of standardised peak storm discharge and hysteresis class showed class 5 events occurred during events with peak discharges between four and five times the mean annual discharge; class 3 events were associated with events with peak discharges less than seven times the mean annual discharge; and class 2 events occurred throughout. Total storm precipitation intensity, standardised precipitation in the preceding three and seven days and standardised storm duration all showed a similar pattern: from June to January events with lower rainfalls and smaller storm durations were characterised by class 2 hysteresis. With respect to precipitation this was explained by insufficient moisture to connect more distant sediment sources. Finally, maximum storm precipitation intensities of greater than 3 mm per 15 minutes were associated with class 2 hysteresis. This pattern was partially explained by the indirect effects of precipitation intensity, e.g. overland flow.

Analysis of the spatial variation in suspended sediment quantity and character also gave some insights into the sources of sediment. Examination of the spatial variation in SSC indicated that more sediment is derived from the upper catchments. The bed sediment storage experiments indicated the periphyton may be a noteworthy component of suspended sediment when the channel bed is not disturbed. Periphyton was also noted as an important component in Rough Sike and Trout Beck by Crisp (1966) and Crowe (2002) respectively.

2. Establish appropriate techniques and identify the optimum technique for modelling suspended sediment flux in British upland streams.

The most appropriate modelling technique for British upland streams was determined by examining the success of ten basic models (different model forms: GLMs and linear regression) and eight adapted models (different data sub-sets), based on linear regression, for the six study sites. The main conclusion of this section was that different models can result in load estimates which vary by several orders of magnitude. The load

estimates ranged from 126 to 438 t for Burnhope, 34 to 276 kg for Candleseaves, 23 to 37 t for Langtae, 17.4 to 96.5 t for Rough Sike, 6 to 49 t for Swinhope and 184 to 877,124,139 t for Trout Beck. The very large variation for Trout Beck was caused by one large event during the study year. This highlights the substantial impact of a generally unconsidered aspect of load estimation. The variability in load estimates derived from different models was related to the variability in the annual discharge series: the more variable the annual discharge series the more variable the annual load estimates from the different models. Therefore the discharge characteristics of the annual series can be used as a means of inferring some information regarding the precision of load estimates. The variability in the discharge series also affected the magnitude and frequency relations: catchments with less variable annual discharge records were less responsive in terms of sediment transfer. The variability in SSC cause by sediment supply and delivery also causes some of the variation in the load estimates.

Logarithmically transforming SSC and discharge, establishing a relationship using ordinary least squares regression and correcting for back-transformation bias using smearing was the best method for three of the six sites. This approach was robust because when applied to sites for which it was not the optimal model, the load estimates were reasonable. On the whole the majority of the rating curve adaptations were not considered worthwhile as some caused decreases in accuracy at some sites and average increases in precision were low (<5%). However, categorising the data by limb and split-year did not cause a decrease in accuracy at any site and the load estimate accuracy increased by 8% on average, and the discharge class method was beneficial if a strong structure existed on the SSC-discharge plots.

Development of numerous models for several sites indicated that there is not a single perfect measure of model fit. It highlighted that R^2, which is often used as the principal indicator of model fit, can not be relied on to indicate the most appropriate model. It also highlighted the potential bias introduced by the difference in the number of rising and falling limb samples, the range of discharge and the distribution of discharge, in the sampled and annual discharge series.

The load estimates derived from the optimal models for each site were combined with existing load estimates for undisturbed British upland sites. From this it was concluded that the suspended sediment loads and yields of the study sites are broadly comparable

to those of existing studies; suspended sediment load (L, t yr^{-1}) of British upland catchments is related to catchment area (A, km^2) by:

$$L = 22.8\ A^{1.04}. \qquad (11.1)$$

11.3 Synthesis of results

Relationships were established between SSC and discharge for each of the study sites using various models. Scatter around the rating curve was present in all of the models and therefore temporal variation in the SSC-discharge relationship was investigated at the storm scale. Within-storm variations in the SSC-discharge relationship were investigated through analysis of hysteresis plots. Some hysteresis loops are evident on SSC-discharge rating curves and may influence the form of rating curves if insufficient data are collected. Therefore analysis of hysteresis aids in the explanation of the scatter on SSC-discharge plots. The hysteresis analysis also allows sediment sources, arguably the main cause of the variation in the SSC-discharge relationship, to be inferred.

The spatial variation in suspended sediment during storms was examined by taking gulp samples at eight point locations in the Moor House channel network. This adds to the understanding of the scatter in suspended sediment rating curves as it demonstrates variation in SSC at different points in the catchment which combine before reaching the gauging station. Comparison of simultaneous SSC in the two nested catchments (Rough Sike and Trout Beck) examined the difference in SSC at different locations using more samples (70 in comparison with 9 obtained by the spatial gulp samples) and included samples from baseflow conditions. This also illustrates the difference in SSC at different locations and therefore supports the assumption that variability occurs in the SSC-discharge relationship at gauging sites due to the difference in sediment delivered by sub-catchments. This variability is attributable to sediment supply and factors which control suspended sediment transport to the channel. Bed sediment storage has been shown to be an important source, especially in channels with limited connected sediment sources outside the channel. The variation in bed sediment storage explains some of the spatial variability in SSC and therefore some of the variability in the SSC-discharge relationship. However, variability in bed sediment storage will only be of importance at the beginning of the event, unless there is deep bed disturbance, as these sources are rapidly exhausted. This was demonstrated in some of the storm sedigraphs (e.g. Figure 10.5).

Examination of sediment geochemistry and organic matter content gives an indication of the bulk properties of the suspended sediment. However, it also feedbacks into the explanation of the variability in the SSC-discharge relationship on the basis that the character of suspended sediment, especially the organic-mineral balance, will affect the SSC-discharge relationship and is related to its source (although some in-stream processing may occur). Differences in the organic matter and sediment geochemistry can be related to different sediment sources and different sediment sources are likely to be accessed and connected to the channel at different times during an event. Principal components analysis of sediment geochemistry gave insight into the effect of in-stream mixing of water and sediment from tributaries and the likely importance of sources local to the sampling sites.

All of the above factors were related to catchment characteristics to examine the effects on suspended sediment dynamics and delivery. This is rarely done at this scale and in as much detail. The controls elucidated within this study are not the only ones, and many of the patterns found between catchment characteristics and suspended sediment transport are tentative, as a result of the small number of sites. However, this is nevertheless an important contribution because it is unfeasible to study many more catchments in the detail presented here.

11.4 Recommendations

On the basis of this study, several recommendations can be made regarding the investigation of suspended sediment dynamics in British upland catchments. These recommendations are divided into three sections: monitoring methods for load determination, techniques for examination of spatial variability and data analysis.

11.4.1 Suspended sediment concentration for load determination

SSC should ideally be measured continuously or quasi-continuously. In some respects it is more important for SSC to be measured continuously or quasi-continuously in upland catchments than in lowland catchments given their flashy nature and variable response characteristics. However, suspended sediment characteristics (variable particle size, water colour, sediment density differences) associated with upland river systems limits the use of turbidity monitoring (the most common and proven method of quasi-continuously monitoring SSC). Some of the more experimental methods of suspended sediment measurement, e.g. video microscopy (Baier & Bechtler, 1996) and LISST-ST

(Thonon & Van Der Perk, 2003), may prove applicable to upland catchments, and should be tested in such environments.

If it is not possible to measure SSC continuously then auto-samplers should be used to establish a relationship between discharge and SSC. Although expensive to purchase and run, auto-samplers are advantageous over other methods as they do not require an operator to be on site during sampling and because of the flexibility in sampling programs (e.g. fixed-interval, stage triggered, turbidity triggered, logger controlled, etc.). If gulp samplers or depth-integrated samplers were used then sampling collection would be restricted to only when operators were on site. Given the flashy nature of upland streams and their remoteness this is likely to lead to limited samples of high flow events.

If auto-samplers are used then there are several issues which should be considered. First, the intake nozzle should be located in such a position that it does not pick up bed/bank material when water samples are taken. This can be avoided by locating the intake on a structure, such as a bridge, and by ensuring the bed under the intake nozzle is not covered in fine material. If using a level switch to trigger the sampler it should be placed in an area of calm water, for example in a stilling well or in the lee of a structure or natural bank formation, to prevent it being triggered by rough surface water. Given the flashy nature of upland streams and the frequency of out of bank flood events auto-samplers should be sited a sufficient distance from the channel. The cross-sectional variability in SSC should also be assessed at a range of discharges to ensure the representativeness of the intake nozzle. Locating the sampler after a section of turbulent water will mix the sediment throughout the water column and promote a uniform distribution. The interval between samples should be optimised to ensure whole events are sampled at the highest resolution and can be estimated from the discharge record. These are just some of the considerations highlighted by this study. Further discussion of operating considerations and types of auto-sampler is given by Edwards & Glysson (1999).

The sampling regime should be dominantly storm sampling, although it is also important to obtain baseflow samples. This could be done by installing two samplers, one programmed to sample at fixed intervals and the second to sample storm events. If only one auto-sampler is available a convenient way of obtaining baseflow samples

would be to take a sample at each field visit. This sample could even be taken using the auto-sampler to ensure all samples are from the same point in the channel cross-section. Assuming field visits are frequent this would ensure baseflow samples are taken throughout the year.

Attention should be given to the temporal spacing of samples at the storm and annual time-scales. Samples should be taken throughout the duration of storms by optimising the interval between bottles. Ensuring complete storms are sampled will also allow hysteresis to be examined. A disadvantage of basic auto-samplers is that after the sampler has been triggered a bottle set is taken and the sampler remains dormant until reset. Therefore, there may be a tendency for the beginning of multi-peaked flow events to be sampled and so imply higher than representative SSC. This could be tackled by installing a cascade of samplers but unless the samplers were interfaced the success would be variable. Alternatively, some auto-samplers can be integrated with stage loggers, e.g. they can be programmed to take a sample every 15 minutes if stage is above 20 cm and every 5 minutes if stage is above 30 cm or to take 5 samples 15 minutes apart each time stage rises above 20 cm if the effect of sediment exhaustion is being investigated. Auto-samplers can also be triggered by other conditions such as turbidity, pH or conductivity (American Sigma, 1998). In addition, the auto-sampler could be controlled by a data logger to take samples for a particular discharge value or change in discharge. This is the basis of probability sampling techniques (section 3.3.2.2). Samples should be taken throughout the year. Despite regular field visits the sample sets of this investigation are generally biased towards winter storms. However, this is partially a result of the higher frequency of storm events in the winter.

There is no ideal number of samples which should be taken as it depends on the storms captured. However, the results of this investigation indicate at least 350 samples should be taken. Only 306 samples were taken at Candleseaves and this was the only catchment for which the discharge class rating curve method, which alleviates bias introduced by clustering in the data, was recommended. Such few samples were taken at Candleseaves as it was part of a larger project examining the effect of grip blocking and timing of the grip blocking was pre-determined. The best way of determining if sufficient samples have been taken is to examine a plot of SSC versus discharge for obvious bottle sets traces which exert an influence on the form of the rating curve; sometimes bottle set traces are evident but do not affect the form of the rating curve. Bottle set traces are

clearly evident on the SSC-discharge plot for Candleseaves (Figure 11.1A) but none is evident on the SSC-discharge plot for Burnhope (Figure 11.1B).

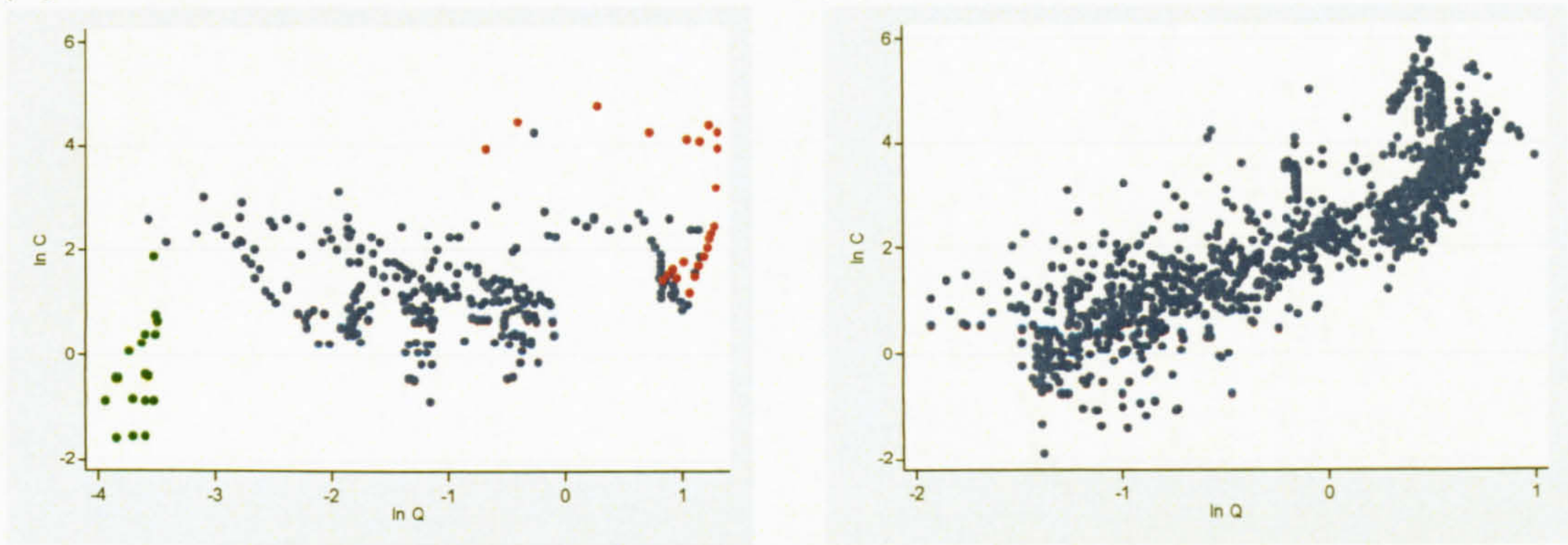

Figure 11.1. SSC-discharge plots with (A) bottle sets (highlighted in red and green) evident for Candleseaves and (B) no bottle sets evident for Burnhope.

It is not possible to suggest a specific sampling regime as it is so dependent on the meteorological conditions and hydrological characteristics of the study year (which are not known in advance), and to a lesser degree, the catchment characteristics. This is especially the case in upland catchments given the high temporal and inter-annual variability in hydrological and meteorological characteristics. Even if a good relationship can be established these are not easily transferred between years (Fenn, 1989).

The other main consideration in sampling is that sufficient samples should be taken on the rising and falling limbs. If this is not achieved then the resultant rating curve could be biased and produce over-estimates if samples were predominantly taken on the rising limb and under-estimates if predominantly on the falling limb. However, if the numbers of rising and falling limb samples are not representative of the annual record, separate rating curves can be developed for each data sub-set, assuming sufficient samples were taken.

11.4.2 Spatial monitoring of suspended sediment

Spatial sampling is recommended as it provides supplementary information regarding suspended sediment dynamics which may help explain the variability in the SSC-discharge relationship at a gauging site. Relating measures of spatial variation to catchment characteristics may also provide insight into sediment sources and delivery mechanisms.

When analysing spatial variation in suspended sediment it is important to take samples concurrently. Arguably the best way to do this is to program a range of auto-samplers to take samples at defined times. For example, an interval of eight hours is recommended if the auto-sampler bottle capacity is 24 and weekly field visits are made. However, although this would give a full week of data it is important to collect storm samples. To achieve this auto-samplers could be programmed to collect a sample at short time intervals if rainfall is forecast. Storm sampling is not recommended as the samplers will be triggered at different times, although this could be useful in assessing the flood wave passage. However, spatial gulp samples, which are inexpensive, can also give a good indication of the spatial variability in suspended sediment. If sufficient sediment is required for physical and/or chemical analysis, then TIMS are recommended as they are inexpensive: hence several can be deployed concurrently and provide bulk, time-integrated suspended sediment samples. TIMS are not recommended for estimating sediment loads or validating the loads estimated by other means as the inlet and channel velocities differ; their field efficiency is difficult to assess; they only sample from a small cross-section of the channel, which may not be representative; changing stage may affect the local flow regime; the inlet may become blocked; local sediment sources may dominant the sample, the organic fraction may be under-sampled (Appendix B).

11.4.3 Data analysis

Rating curves were studied in this investigation and are recommended as the most suitable choice when modelling data sets with limited, unequally spaced (in relation to each other and time of year) samples. If it is possible to ascertain a quasi-continuous record then transfer functions may well prove to be a superior modelling technique (e.g. Fenn, 1989). If the data set is continuous or quasi-continuous (high resolution) then there will be no need for a model, unless gaps exist. It is possible that artificial neural networks (ANN) would be a good modelling technique to establish the relationship between SSC-discharge given the limited assumptions and ability to model fragmented data sets. Existing studies (Abrahart & White, 2001 and Yitian & Gu, 2003) have shown the potential success of the application of ANN to sediment transfer. ANN were not applied in this investigation given the limited data sets: as there are limited applications of ANN to suspended sediment vigorous testing would be required. Also, ANN can not be summarised using a few parameters, like a and b for rating curves, so between site comparison would be subjective.

Analysis of the rating curve development section leads to the following recommendations, the first three of which are generic while the last two are specific to the British uplands:

(1) Several indicators of model fit should be used (R^2, RMSE, diagnostic plots, graphical analysis of rating curve fit and storm period load estimates) to select the most appropriate model. R^2 of the observed and predicted SSC should be calculated (not of SSC and discharge) and should not be used as the only measure of fit, as appears to be the case in many investigations, as it does not take into account the magnitude of discharge.

(2) A range of models should be developed and the optimal model selected, as suggested by the indicators of model fit. Although this requires more calculations, many of the procedures can be automated and in comparison with the time spent in the field and processing the samples in the laboratory the model development time is small. Developing a range of models also gives an indication of the potential errors in load estimates associated with the study site. However, if just one model is going to be developed for small British upland catchments linear regression back-transformed by smearing should be used.

(3) If clustering is evident in the data then the discharge class method should be employed (as recommended by Jansson, 1996).

(4) The limb, seasonal, lagged, time of year, split-year and change in discharge adaptations are not recommended as some lead to decreases in load estimations for some catchments, and the average improvement in load estimate is small (<5%).

(5) If enough data exist it should be divided into summer-rising, summer-falling, winter-rising, and winter-falling sub-sets, rating curves developed for each and load estimates calculated as the limb and split-year adaptation resulted in improved load estimates for each of the catchments and the average improvement was 8%.

11.5 Limitations of methods and future research

This section outlines some of the limitations identified within this study and suggests future research which could examine their influence or alternative methods to prevent them. The short time-frame is a limitation for the whole project as the conclusions made are specific to the study years and not necessarily generally indicative of the study

catchments. However, this is unavoidable given the research framework timescale and highlights the need for monitoring suspended sediment over longer timescales.

11.5.1 Rating curves

In this project a problem in using rating curves to estimate load was that no actual load estimates were available. It would be interesting to develop the same basic and adapted models for catchments with quasi-continuous turbidity records (although generally more successful in lowland catchments, turbidity does work well in some mountain streams (e.g. Nistor & Church, in press) from which actual loads can be determined.

Also, some of the post-load estimation analysis is potentially biased by the rating curve approach. For example, calculation of the effective discharge intervals and magnitude and frequency analysis use the modelled annual SSC series and therefore may be more characteristic of the discharge record rather than the actual SSC series. It would be interesting to examine the relationships between the effective discharge intervals and magnitude and frequency analysis calculated from a true (turbidity) SSC series and a rating curve-derived SSC series.

11.5.2 Hysteresis analysis

A limitation of the hysteresis analysis in this thesis (Chapter 10) is the limited number of storms sampled. To increase the robustness of the hysteresis analysis more storms in each catchment should be monitored. An ideal solution would be to monitor SSC continuously/quasi-continuously. Turbidity is the obvious method but is generally problematic in upland catchments given the water colour, and varying particle size, shape and density. However, there have been some successful applications of turbidity in upland channels (e.g. Nistor & Church, in press) and the problems of varying particle characteristics could potentially be overcome by investigating their change during storm events. Some of the more experimental methods outlined in section 3.3.1.8 could be investigated. For example, Thonon & Van Der Perk (2003) deployed a portable particle sizer and settling tube device (LISST-ST) which uses laser diffraction principles to measure grain size distribution, settling velocities and SSC. This techniques could provide continuous SSC series and information regarding the particle size distribution may help infer sediment sources and explain the variation in the SSC-discharge relationship. Alternatively, more frequent field visits could be made (although this can

be prohibited by weather conditions and access) and/or more auto-samplers deployed with the level sensors set at different heights.

11.5.3 Effect of particle characteristics on suspended sediment concentration

Although not investigated in this thesis it would be interesting to examine the relationship between SSC and the size, shape and density of the sediment. This analysis would provide estimates of the proportions of organic and mineral sediment, give insight into sediment delivery and sources and potentially explain some of the variation in the SSC-discharge relationship. It would also be useful when assessing sediment-associated nutrient and contaminant transfer. Characterising suspended sediment is difficult given the limited amount of material, the effect of sampling on the characteristics (Phillips & Walling, 1995), and available equipment. However, recent approaches, such as those used by Thonon & Van Der Perk (2003) have proved successful. Also, image analysis techniques are effective. For example, Droppo *et al.* (2005) used a computerised image analysis system to analyse particle size, shape and roughness.

11.5.4 Time-integrated mass samplers

In the context of this investigation the TIMS have been used to calculate the organic matter content of the suspended sediment. There are arguments that the organic fraction may be under- or over-sampled compared with the mineral fraction. The organic fraction may be under-sampled because the intake velocities are lower than the channel velocities and therefore coarser particles are less likely to enter the sampler; during high flow events large particles of peat may be transported nearer the channel surface and therefore not enter the sampler; and during high flow events the samplers may sample some of the bed load which is dominantly mineral sediment. Conversely, the organic fraction may be over-sampled because it is less dense and therefore requires less energy to transport; and organic particles are generally larger and therefore more likely to settle out in the main body of the TIMS. Phillips *et al.* (2000) and Russell *et al.* (2000) investigated the representativeness of total carbon (C) content of sediment retained in the TIMS and collected manually during times of high transport in two catchments: Lower Smisby and New Cliftonthorpe (at two gauging locations), Devon. Particulate riverine C is generally dominated by organic C and organic matter is approximately 50% organic C (Ball, 1964). The deviations of total C in TIMS sediment varies from –4.7% to +5.4% (Table 11.1). Ankers (2003) estimated the average discrepancy of

organic C content of TIMS sediment, from manually collected suspended sediment, was –7.1%. In other words, the organic C content of sediment retained in the TIMS was, on average, 7.1% less than that of the suspended sediment collected directly from the channel. Therefore, it is likely that the organic matter contents derived from the TIMS in this study are slightly under-estimated. The magnitude of the under-estimation could be assumed to be approximately 7% organic C or 14% organic matter. However, in peatland streams this could potentially be much greater. The bias in TIMS sediment could be investigated using field or flume approaches.

Table 11.1. Percentage deviation of carbon (C) retained in TIMS from sediment sampled manually during high transport events. The unspecified catchments studied by Ankers (2003) are local to Exeter.

Reference	Catchment	Property	Deviation, %
Phillips *et al.* (2000)	Lower Smisby		–1.8
	New Cliftonthorpe	Total C	+5.4
	New Cliftonthorpe		–1.6
Russell *et al.* (2000)	Lower Smisby		–4.7
	New Cliftonthorpe	Total C	+2.6
	New Cliftonthorpe		–3.4
Ankers (2003)	Unspecified	Organic C	–7.1

11.6 Application of results

This final section highlights the importance of some of the findings of this study in relation to their applicability to future research and how they can be combined to further knowledge of suspended sediment dynamics and delivery in British upland catchments.

11.6.1 Quantification of organic carbon fluxes

The global carbon (C) cycle is fundamentally important in many Earth surface processes, physical and biological (Bolin *et al.*, 1979). C is important and topical due to its feedback on climate change (Prentice *et al.*, 2001) and the introduction of policies promoting C neutrality. Fluvial transfer of organic C from land to ocean is an important pathway in the C cycle (Hope *et al.*, 1994) but limited data exist on fluxes, especially particulate organic C (POC). POC fluxes are generally poorly quantified because of inferior sampling strategies (e.g. Hope *et al.*, 1994) and quantification methods (Walling & Webb, 1981). Worrall *et al.* (2003b) indicated that fluvial POC is the largest export of C from Moor House NNR (excluding CO_2 as only net values were given). The TIMS deployed in this study provide evidence that suspended sediment, on average, is composed of 15.6% organic matter. This figure was calculated from the organic matter

contents of each TIMS deployed in Moor House NNR and Swinhope. The fact that the average organic matter contents were so close for both of the channel networks, 15.5% and 15.7% for Moor House and Swinhope respectively, suggest that approximately 16% is characteristic of small upland British catchments. From this it is possible to calculate the amount of particulate organic C discharged from Burnhope, Candleseaves, Langtae, Rough Sike and Trout Beck respectively (Table 11.2). These estimates are considered superior to others found in the literature for Britain (Hope *et al.*, 1997a & 1997b & Worrall *et al.*, 2003b) as they are based on a sound sampling regime, involved load estimates derived from the best of ten models, and organic matter content was established from sediment collected by a network of over 20 samplers at two sites.

Table 11.2. Particulate organic C loads and yields for the study sites of this investigation.

Catchment	Area, km^2	Load, t	Yield, t km^{-2} yr^{-1}
Burnhope	11.80	46	3.9
Candleseaves	0.003	0.0093	3.1
Langtae	3.00	5.4	1.8
Rough Sike	0.76	3.7	4.9
Trout Beck	11.83	72.5	6.1

11.6.2 Upland erosion

Upland erosion has been recognised as an environmental concern (Evans, 1990 and DETR/MAFF, 2001). One gross method of investigating contemporary upland erosion is to monitor suspended sediment, calculate the load and divide this by the catchment area to give an erosion rate in t km^{-2} yr^{-1}. However, this does not quantify the amount of sediment eroded and/or stored on the hillslopes. Some studies attempt to take this into account by adjusting the load by the sediment delivery ratio (SDR). However, even if the SDR was an accurate correction, the findings of this investigation indicate that quantifying upland erosion by monitoring suspended sediment does not provide information on the distribution or erosion and deposition within a catchment.

The hysteresis analysis indirectly illustrated that the six study systems of this investigation are generally sediment supply-limited and that the majority of sediment originates from local sources, predominantly channel, floodplain and possibly some local hillslope sources. Therefore, the majority of the sediment output of the catchment in suspension is a measure of channel erosion, not the general denudation of the landscape. This is reinforced by the lack or relationship between specific suspended

sediment yield and catchment area found for the study sites of this investigation (Figure 11.2). The importance of channel sources over hillslope sources is clearly illustrated by sediment budgets developed by Warburton *et al.* (2003) for Iron Crag, Lake District, and Rough Sike (Figure 11.3).

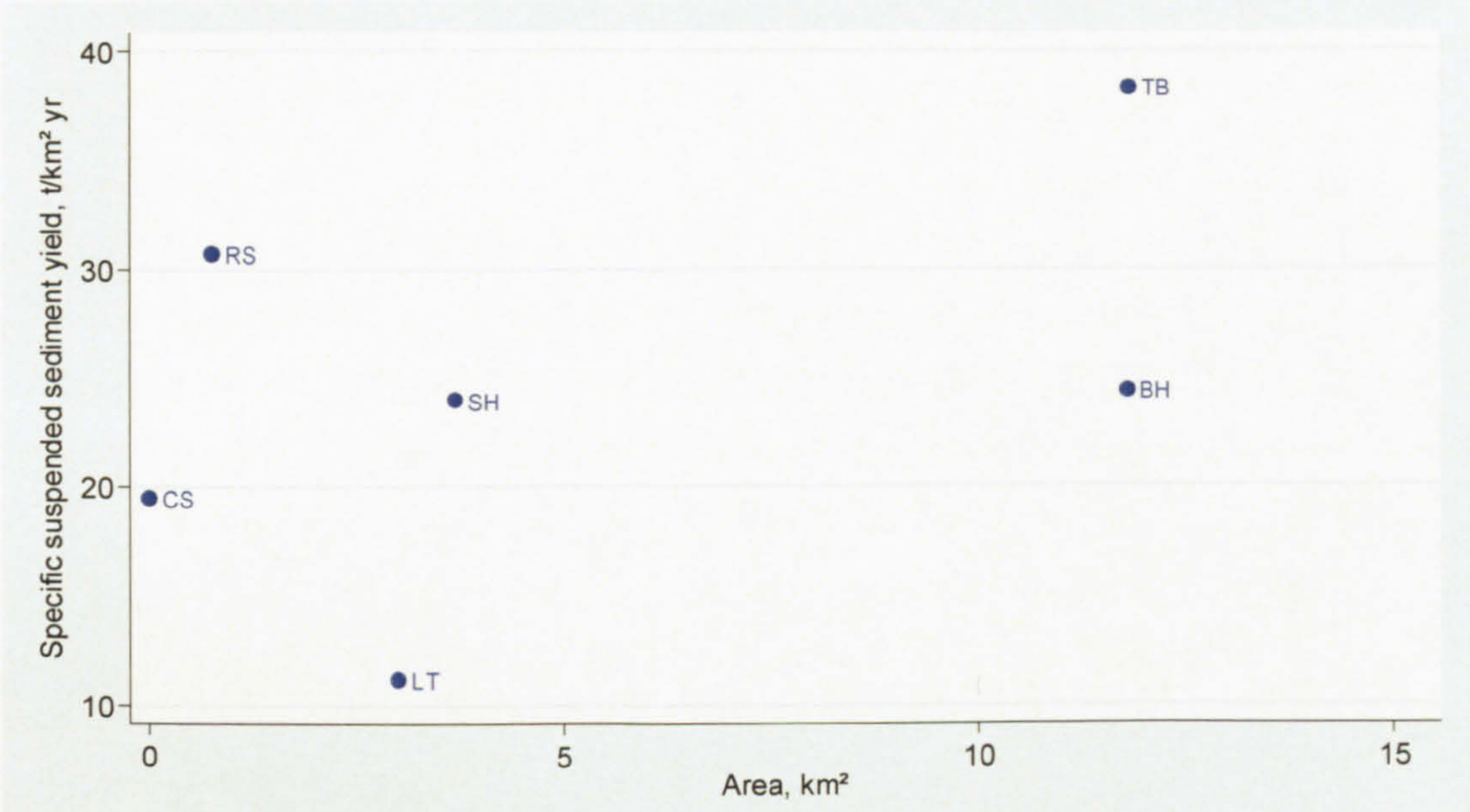

Figure 11.2 Relationship between specific suspended sediment yield and catchment area for the study sites of this investigation. Swinhope yield predicted from British upland relationship (Figure 9.12).

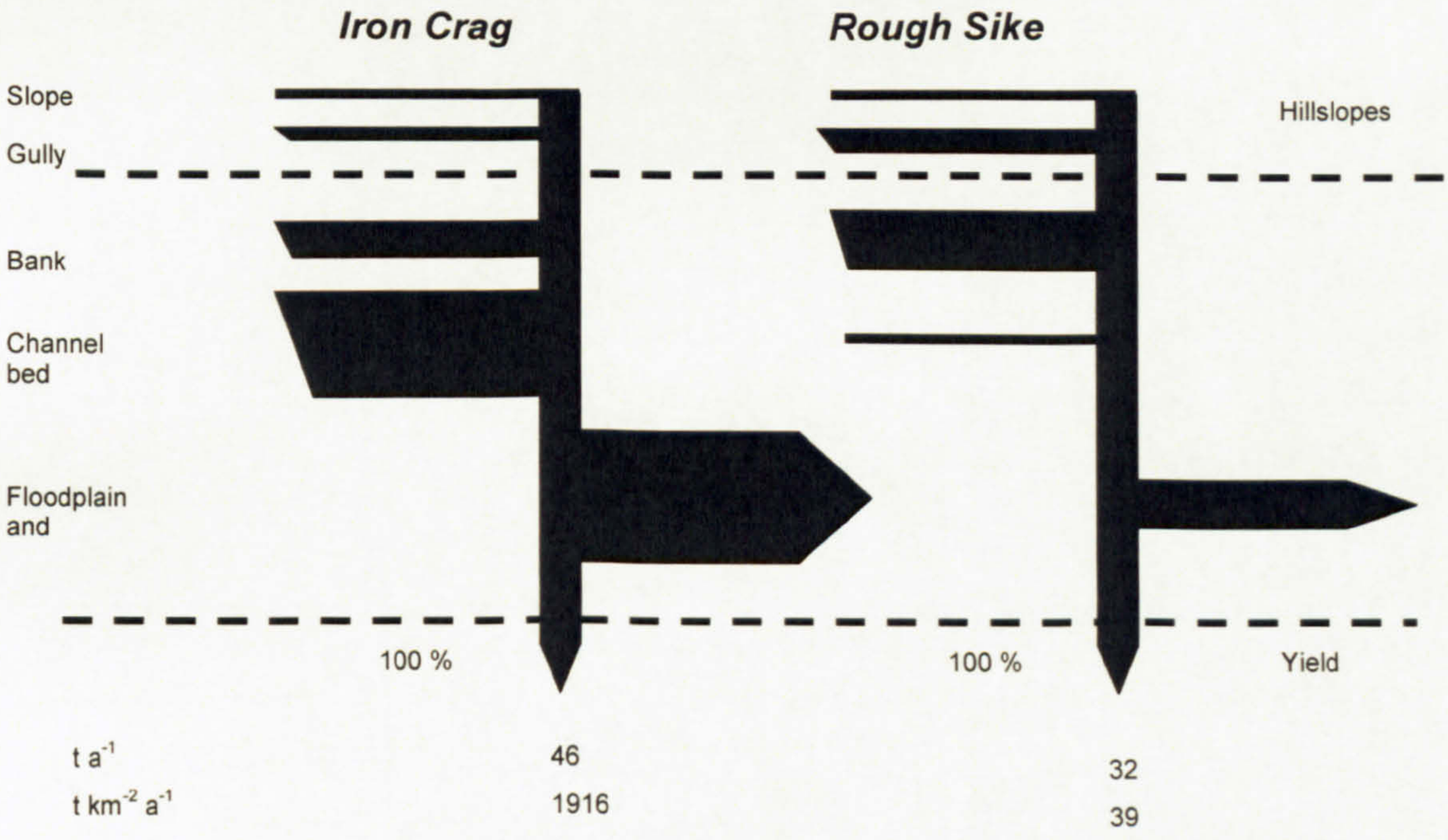

Figure 11.3. Annual sediment budgets for Iron Crag, Lake District, and Rough Sike, Northern Pennines (study site of this investigation). Lines are proportional to the magnitude of each sediment transfer process and storage. Source: Warburton *et al.* (2003).

However, this does not mean that hillslopes are not being eroded, simply that if they are being eroded only a limited amount of the sediment is transported to the channel. The growth of vegetation due to climate change and the reduced toxicities, which limited vegetation growth, around mining relicts will have slowed, and in some cases stopped, sediment transfer from the hillslopes and gullies to the channel making this approach of quantifying land denudation less accurate than in earlier years (Higgitt *et al.*, 2001).

In summary, this investigation hypothesises, using evidence from six upland field sites, that specific suspended sediment yield should not be used as a measure of land denudation as it is primarily a measure of channel erosion and that estimates derived in this way should be considered with caution. This has been demonstrated by Warburton *et al.* (2003) and Warburton & Evans (in press). Erosion rate estimates obtained by this method may be more indicative of channel erosion and changes in the rates over time may be indicative of increased numbers and intensity of storm events.

11.6.3 Sediment budgets

Sediment budgets quantify the inputs, outputs, stores and pathways of sediment in fluvial systems. However, it is difficult to develop a comprehensive sediment budget for a river system given the number and spatial and temporal variation in inputs, outputs, stores and sediment transfer (Dietrich *et al.*, 1982 and Phillips, 1991). There are two main types of errors in sediment budgets, those associated with measured variables and those of the unmeasured variables. Generally, it is possible to assign some level of error to the measured variables. The unmeasured variables are either discounted as negligible or calculated as the residual (i.e. assigned a value that ensures the outputs and stores balance the inputs).

If calculating a fluvial sediment budget, at a reach or catchment scale, then suspended sediment load is arguably the most important term against which inputs and stores are balanced (e.g. Evans & Warburton, in press). Suspended sediment loads are also of importance in reservoir sediment budgets if they are the dominant input (Holliday, 2003). Therefore the variability in suspended sediment load estimates as a function of the different modelling methods has important implications on sediment budget studies. For example, the minimum suspended sediment load of Rough Sike is 17.4 t yr^{-1} and the maximum is 96.5 t yr^{-1}. Evans & Warburton (in press) evaluated a sediment budget for Rough Sike using similar SSC and discharge records as used in this investigation. Evans

& Warburton (in press) used an estimated suspended sediment yield of 37 t and measured sediment inputs to be 32.5 t and storage to have increased by 18.8 t, thus leaving a deficit of 23.5 t. If the lowest estimated sediment load for Rough Sike generated by this study was used then the deficit would be 3.7 t and if the highest was used then the deficit would be 82.8 t. The greatest potential deficit associated with the highest load estimate is greater than any measured component in Evans & Warburtons' (in press) budget.

Poorly quantified suspended sediment loads can have significant impacts on sediment budgets in terms of the potential errors and estimates of unmeasured components. Therefore, it is important to establish the most appropriate model for the catchment. It is also essential that researchers are aware of the variability in suspended sediment load estimates and take them into consideration when developing sediment budgets. Variability in the suspended sediment load estimates found in this study are solely a result of modelling method; the variability introduced by sampling technique and regime is not quantified.

11.6.4 Suspended sediment load prediction

A relationship between catchment area and suspended sediment load was established from the existing British upland catchment data (Figure 9.12). This could potentially be used to predict the suspended sediment loads of un-gauged catchments. However, it should only be used to give an approximation and should not be relied on given the scatter. In order to test the accuracy of this the suspended sediment loads of the catchments from which the relationship was derived were predicted and the percentage differences between the predicted and observed loads calculated (Figure 11.4). The maximum percentage error was an over-estimate by 3178% for Nant Ysguthon (Francis, 1987). The minimum percentage error was an under-estimate of 2% for Hore (Kirby *et al.*, 1991) (Figure 11.4). The mean percentage error (calculated using the absolute percentage errors) was 152%. There is a marked asymmetry in Figure 11.4, which may reflect the number of annual load estimates for the same catchments (Monachyle and Kirkton) or difference between the sensitivity of the systems given their geographical location.

Walling & Webb (1987) compiled suspended sediment yields from British studies and summarised that catchments in Mid-Wales had low suspended sediment yields. This

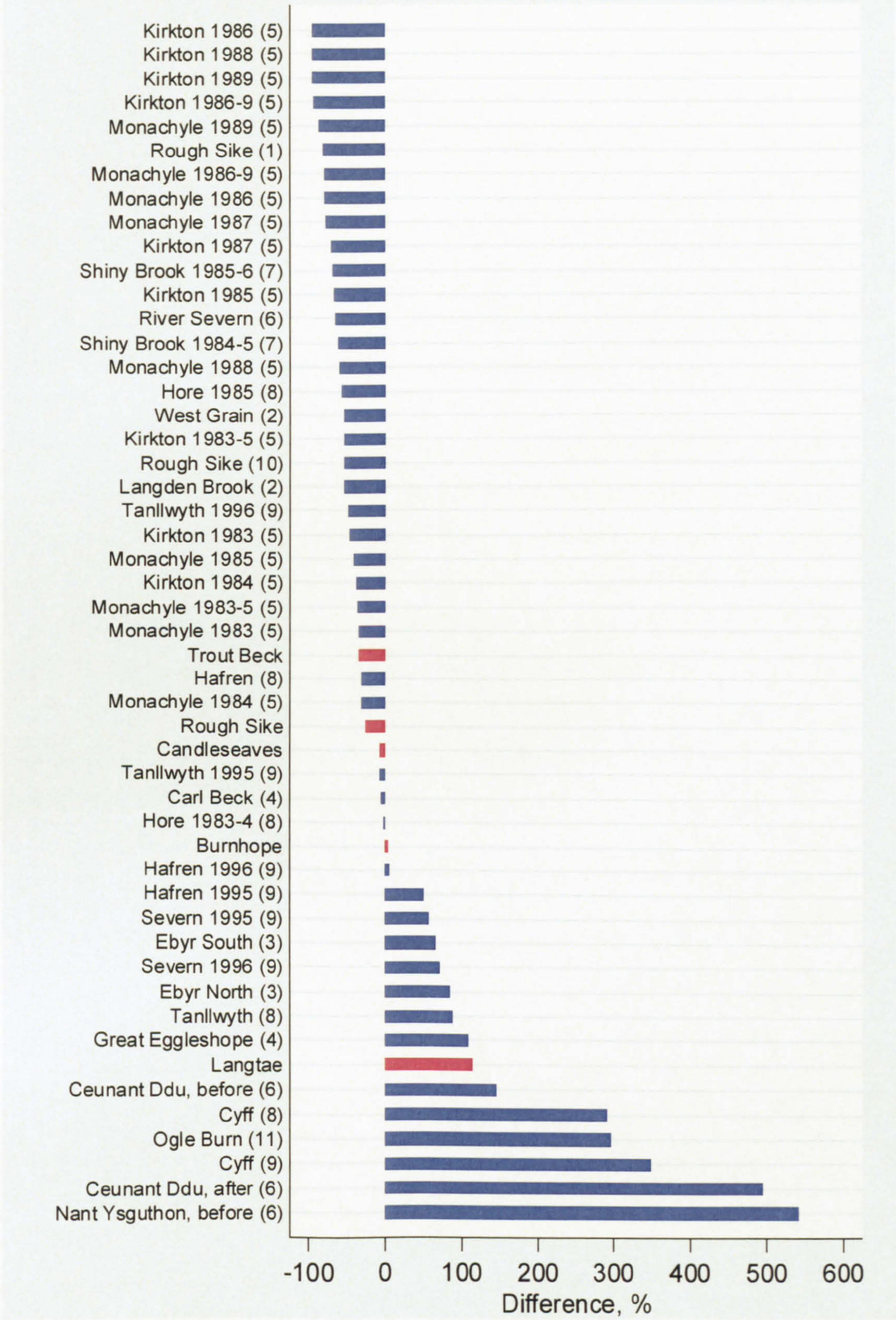

Figure 11.4. Percentage difference between actual and predicted (from the relationship between catchment area and load for British upland catchments) loads for each of the British upland catchments. Nant Ysguthon post land disturbance was removed given its scale: 3178% over-estimate. (1) Crisp, 1966; (2) Wilkinson, 1971; (3) Oxley, 1974; (4) Carling, 1983; (5) Johnson, 1995; (6) Francis, 1987; (7) Labadz *et al.*, 1991; (8) Kirby *et al.*, 1991(9) Leeks & Marks, 1997; (10) Evans & Warburton (in press); and (11) Duck, 1985. See Table A.1 for more information.

signal is weakly shown in the percentage differences between actual and predicted suspended sediment loads: most of the over-predictions are Welsh catchments, and many of them were substantial over-predictions (Figure 11.4). While the predictions for Monachyle and Kirkton (Johnson, 1988 and Stott *et al.*, 1986), were all under-estimated by the model, the percentage errors in the load estimates were higher after the land use changed in the catchments (1986 onwards) (Figure 11.4). The load estimate of Rough Sike, as determined by Crisp (1966), is the greatest under-estimation for an undisturbed catchment (Figure 11.4). This may be attributable to environmental change, difference in monitoring and modelling techniques or a combination of both.

There is no relationship between study year and the error (Figure 11.4), suggesting that the errors are not all attributable to short-term climatic change (although short-term climatic change may be subsumed by the magnitude of inter-annual variability). There is also no relationship between the difference between the actual and predicted load and catchment area (Figure 11.5) which demonstrates that the accuracy of the prediction is not scale dependent and the model is a good fit. The variability in model estimates appears higher in smaller catchments (Figure 11.5). This may be a result of the greater number of smaller catchments or the greater variability which is found in sediment load estimates in smaller catchments (Wasson, 1994).

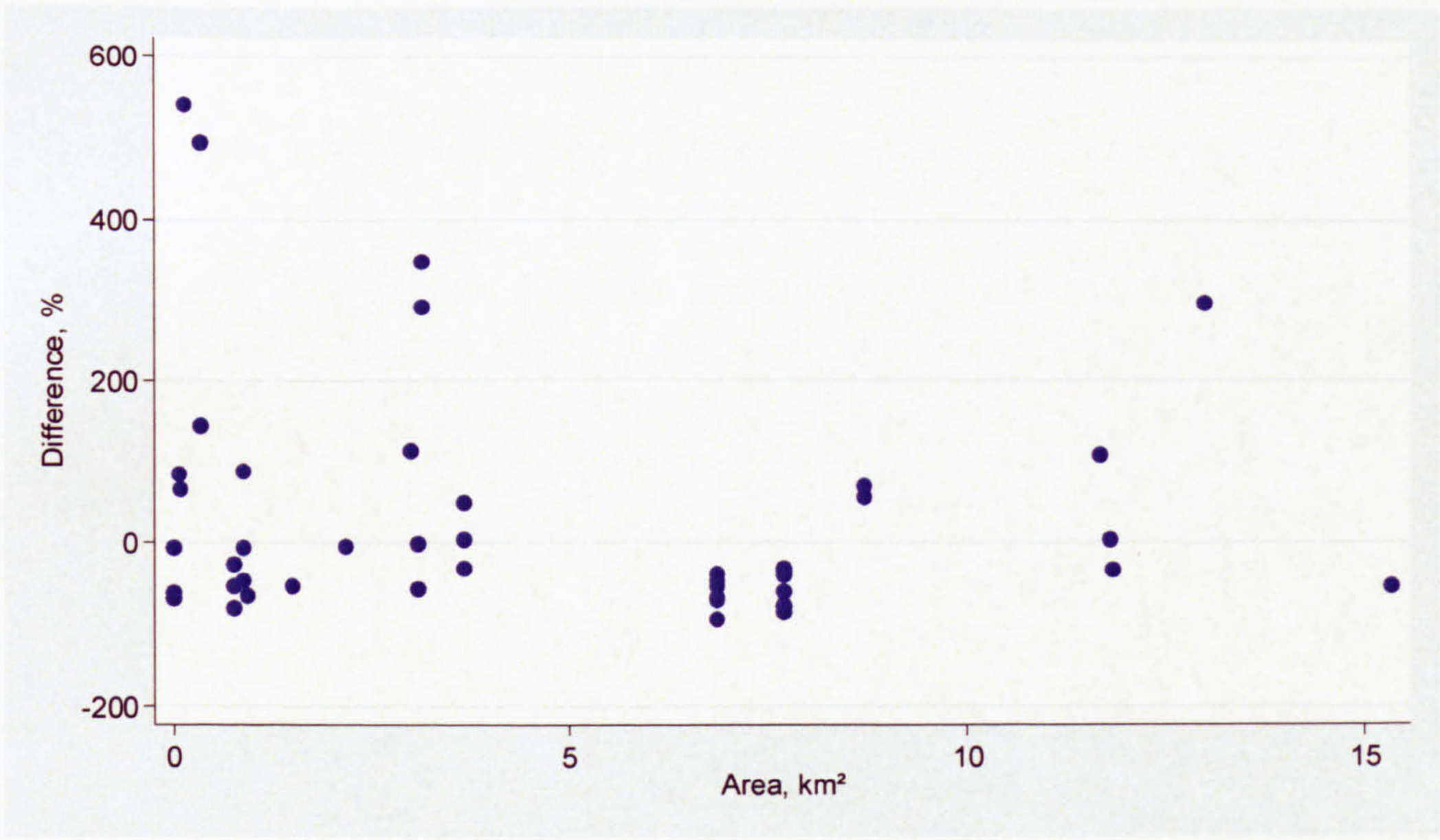

Figure 11.5. Percentage difference between the observed and predicted suspended sediment loads in relation to catchment area. Nant Ysguthon post land disturbance was removed given its scale: 3178% over-estimate.

In summary, it is possible to use the relation developed to predict suspended sediment load from catchment area to estimate the suspended sediment loads of ungauged catchments. However, the errors are potentially very high. The errors are lower if the catchments are undisturbed and not located in areas with noticeably lower suspended sediment yields (i.e. Mid Wales). The accuracies may be more accurate than expected in terms of average annual suspended sediment load given the magnitude of inter-annual variation in suspended sediment loads, especially in small catchments. The potential errors in estimated suspended sediment loads generated by using a generic model for British upland catchments indicates the problems associated with predicting suspended sediment loads from catchment characteristics and at a global scale as attempted by various authors (e.g. Langbein & Schumm, 1958).

11.6.5 Response to environmental change

The response of sediment dynamics to environmental change is dependent on the type and duration of change and the sensitivity of the river catchment. Predicting the effect of environmental change, including land use change and climate change, is important given the role of sediment in biogeochemical cycles, the relationship with erosion rates, the impacts on riverine flora and fauna, and implications for water treatment works, hydro-electric power and reservoir storage. Within the British uplands there are limited long-term suspended sediment records and limited sites for which there are historic suspended sediment load estimations. The exceptions to this are Kirkton and Monachyle, Scotland (Johnson, 1988), Plynlimon catchments (Leeks & Marks, 1997), and Rough Sike (Crisp, 1966; Evans & Warburton, in press; and this study).

The suspended sediment load for Rough Sike in 1962/3 was 93 t (Crisp, 1966) and in 1987/8 was 37 t as determined by Evans & Warburton (in press) and 23 t as determined by this study. The difference in sediment load estimates for the 1997/8 year is partly attributable to the different modelling techniques used. The difference between the 1997/8 and 1962/3 loads is substantially larger. This could be due to differences in the monitoring and modelling techniques but is more likely to reflect environmental change. As there has been no land disturbance in the catchment this is attributed to climate change which may have influenced temperature, precipitation amount, intensity and timing and vegetation growth. In addition vegetation growth may have increased as the toxicity as a result of mining decreased over time.

There is information detailing channel bank composition and catchment vegetation cover for the time period of Crisps' study and the present work (Crisp, unpub; ECN, 2004; and Warburton & Evans, unpub). The percentages of eroding peat are the same for both time periods (Table 11.3). This casts doubt on the validity of the data as photographic evidence form another sub-system of Moor House NNR indicates revegetation since 1958 (see Evans & Warburton (in press) for photographs). The higher percentage cover of grass and lower percentage of heather cover at the present day (Table 11.3) may partially explain the lower suspended sediment load in this study as grass is more effective at preventing or slower sediment transfer than heather (Clement, unpub). The percentage bank compositions were obtained by different methods. Crisp (unpub) measured the length of different bank types and then calculated the percentages. The peat bank types and mineral bank types were summed for this investigation. In contrast, Evans & Warburton (unpub) noted the bank composition every 100 metres from the source. This suggests that the percentage of mineral banks have increased. These differences may be a result of the different quantification methods or a result of change within the system e.g. channel incision into mineral substrate.

Table 11.3. Variation in Rough Sike vegetation cover and channel bank composition between 1960s and the present. Source: 1960s data from Crisp (unpub), present vegetation data from GIS (ECN, 2004) and present bank composition data from Warburton and Evans (unpub).

Type	1960	Present
Vegetation:		
Eroding peat, %	20	20
Heather, %	79	46
Grass, %	1	21
Recolonised, %		11
Bank composition:		
Mineral, %	17	80
Peat, %	83	20

REFERENCES

Abrahart, R. J. & See, L. 2000, Comparing neural network and autoregressive moving average techniques for the provision of continuous river flow forecasts in two contrasting catchments. *Hydrological Processes*, **14**, 2157-2172.

Abrahart, R. J. & White, S. M. 2001, Modelling sediment transfer in Malawi: comparing backpropagation neural network solutions against a multiple linear regression benchmark using small data sets. *Physics and Chemistry of the Earth. Part B - Hydrology, oceans and atmosphere*, **26**(1), 19-24.

Al-Ansari, N. A. & McManus, J. 1979, Fluvial sediments entering the Tay Estuary: sediment discharge from the River Earn. *Scottish Journal of Geology*, **15**(3), 203-216.

Al-Ansari, N. A., Asaad, N. M., Walling, D. E. & Hussan, S. A. 1988, The suspended sediment discharge of the River Euphrates at Haditha, Iraq: an assessment of the potential for establishing sediment rating curves. *Geografiska Annaler. Series A. Physical Geography*, **70**, 203-213.

American Sigma. 1998, *American Sigma 900MAX Portable Sampler Operating and Maintenance Manual*, American Sigma, Loveland. American Society of Agronomy, Inc, Wisconsin, pp. 961-1010.

Ankers, C. 2003, *An Investigation of the Influences of Catchment Characteristics and Source Materials on Suspended Sediment Properties*. Ph.D. Thesis, University of Exeter, Exeter.

Anon. 2003, The United Kingdom Parliament. Available: http://www.parliament.the-stationery-office.co.uk/pa/ld199900/ldhansrd/pdvn/lds03/text/30127w03.htm. Accessed: 31st January 2003.

Anon. 2004. Climateprediction.net. Last updated: 22 March 2004. Available: http://www.climateprediction.net/index.php. Accessed: 22nd March 2004

Arnett, R. R. 1978, Regional disparities in the denudation rate of organic sediment. *Zeitschrift für Geomorphologie*, **29**, 169-179.

Arnett, R. R. 1980, Soil erosion and heather burning on the North York Moors. In: Doornkamp, J. C., Gregory, K. J. & Burn, A. S. (Editors), *Atlas of Drought in Britain 1975-6*. Institute of British Geographers, London, pp. 82.

Ashbridge, D. 1995, Processes of river bank erosion and their contribution to the suspended sediment load of the River Culm, Devon. In: Foster, I. D. L., Gurnell, A. M. & Webb, B. W. (Editors), *Sediment and Water Quality in Catchments*. John Wiley & Sons, Chichester, pp. 229-245.

Asselman, N. E. M. 1999, Suspended sediment dynamics in a large drainage basin: the River Rhine. *Hydrological Processes*, **13**, 1437-1450.

Asselman, N. E. M. 2000, Fitting and interpretation of sediment rating curves. *Journal of Hydrology*, **234**(3-4), 228-248.

Atherden, M. 1992, *Upland Britain. A Natural History*. Manchester University Press, Manchester.

Baier, V. & Bechteler, W. 1996, An underwater videomicroscope to determine the size and shape of suspended particles by means of digital image processing, Proceedings of 6th International Offshore and Polar Engineering Conference, Los Angeles, pp. 138-144.

Ball, D. F. 1964, Loss-on-ignition as an estimate of organic matter and organic carbon in non-calcareous soils. *Journal of Soil Science*, **15**(1), 84-92.

Ballantyne, C. K. & Harris, C. 1994, *The Periglaciation of Great Britain*. Cambridge University Press, Cambridge.

Barrett, B. 2002, LOIS. Last updated: 15th March 2002. Available: http://www.pml.ac.uk/lois/. Accessed: 26th March 2004.

Beschta, R. L. 1978, Long-term patterns of sediment production following road construction in the Oregon Coast Range. *Water Resources Research*, **14**, 1011-1016.

Beschta, R. L. 1987, Conceptual models of sediment transport in streams. In: Thorne, C. R., Bathurst, J. C. & Hey, R. D. (Editors), *Sediment Transport in Gravel-bed Rivers*. Wiley & Sons, Chichester, pp. 387-419.

Bierkens, M. F. P., Knotters, M. & van Geer, F. C. 1999, Calibration of transfer function-noise models to sparsely or irregularly observed time series. *Water Resources Research*, **35**(6), 1741-1750.

Blacknell, C. 1981, River erosion in an upland catchment. *Area*, **13**, 39-44.

Bogardi, J. 1961, Some aspects of the application of the theory of sediment transportation to engineering problems. *Journal of Geophysical Research*, **66**, 3337-3346.

Bogen, J. 1980, The hysteresis effect of sediment transport systems. *Norsk Geologisk Tidsskrift*, **34**, 45-54.

Bogen, J. 1987, Discussion by J. Bogen on "Suspended load in gravel-bed rivers: UK experience". In: Thorne, C. R., Bathurst, J. C. & Hey, R. D. (Editors), *Sediment Transport in Gravel-Bed Rivers*. John Wiley & Sons, Chichester, pp. 725-727.

Bogen, J. 1992, Monitoring grain size of suspended sediment in rivers. In: Bogen, J., Walling, D. E. & Day, T. (Editors), *Erosion and Sediment Transport Monitoring Programmes in River Basins*. IAHS publication 210. International Association of Hydrological Sciences, Oslo, pp. 183-190.

Bolin, B. 1970, The carbon cycle. *Scientific American*, **223**(3), 124-132.

Brasington, J. & Richards, K. 2000, Turbidity and suspended sediment dynamics in small catchments in the Nepal Middle Hills. *Hydrological Processes*, **14**, 2559-2574.

Braune, E. & Looser, U. 1989, Cost impacts of sediments in South African rivers, *Sediment and the Environment*. International Association of Hydrological Sciences, pp. 131-143.

British Geological Survey. 1992, *Regional Geochemistry of the Lake District and Adjacent Areas*. NERC, Nottingham.

British Geological Survey. 1993a, Alston. England and Wales. Sheet 25. Solid and drift edition. 1:50,000. British Geological Survey.

British Geological Survey. 1993b, Cockermouth. England and Wales Series. Sheet 23. Solid geology. 1:50,000. British Geological Survey.

Bull, L. J. 1997, Magnitude and variation in the contribution of bank erosion to the suspended sediment load of the River Severn, UK. *Earth Surface Processes and Landforms*, **22**, 1109-1123.

Burt, T. P. & Gardiner, A. T. 1984, Runoff and sediment production in a small peat-covered catchment: some preliminary results. In: Burt, T. P. & Walling, D. E. (Editors), *Catchment Experiments in Fluvial Geomorphology*. Geo Books, Norwich, pp. 133-151.

Burt, T. P. & Oldman, J. 1986, *Sediment yields from peat covered catchments*. Paper presented at British Ecological Society Winter Meeting, University College, London. Quoted in: Francis, I. S., *Blanket peat erosion in Mid-Wales: two catchment studies*, Ph.D. 1987. University of Wales, Aberystwyth.

Burt, T. P. Unpublished. In: Soutar, R. G. (Editor), *Afforestation and sediment yields in British fresh waters. Soil Use and Management, 5, 82-86.*

Burt, T. P., Donohoe, M. A. & Vann, R. A. 1984, Changes in the yield of sediment from a small upland catchment following open ditching for forestry drainage. In: Schick, A. P. (Editor), *Channel Processes - Water, Sediment, Catchment Controls*. Catena Supplement 5. Catena Verlag, Cremlingen, pp. 63-74.

Cameron, D., Kneale, P. & See, L. 2002, An evaluation of a traditional and a neural net modelling approach to flood forecasting for an upland catchment. *Hydrological Processes*, **16**, 1033-1046.

Campolo, M., Andreussi, P. & Soldati, A. 1999, River flood forecasting with a neural network model. *Water Resources Research*, **35**(4), 1191-1197.

Carling, P. A. 1983, Particulate dynamics, dissolved and total load, in two small basins, Northern Pennines, UK. *Hydrological Sciences Journal*, **28**(3), 355-375.

Carling, P. A. 1984, Comparison of suspended sediment rating curves obtained using two sampling methods. In: Schick, A. P. (Editor), *Channel Processes - Water, Sediment, Catchment Controls*. Catena Supplement 5. Catena Verlag, Cremlingen, pp. 43-49.

Caroni, E., Singh, V. P. & Ubertini, L. 1984, Rainfall-runoff-sediment yield relation by stochastic modelling. *Hydrological Sciences*, **29**(2), 203-218.

CEH. 2004, Plynlimon Experimental catchments. Last updated: 9th August 2004. Available: http://www.bangor.ceh.ac.uk/plynlimon/About_Plynlimon/results.htm. Accessed: 24th November 2004

Chang, A. T. C. & Tsang, L. 1992, A neural network approach to inversion of snow water equivalent from passive microwave measurements. *Nordic Hydrology*, **23**(3), 173-182.

Chatfield, C. & Collins, A. J. 1980, *Introduction to Multivariate Analysis*. Chapman and Hall, London, 246 pp.

Church, M. & Slaymaker, O. 1989, Disequilibrium of Holocene sediment yield in glaciated British Columbia. *Nature*, **337**(6206), 452-454.

Cigizoglu, H. K. 2004, Estimation and forecasting of daily suspended sediment data by multi-layer perceptrons. *Advances in Water Resources*, **27**, 185-195.

Clement, S. in prep, *The Future Stability of Upland Blanket Peat Following Historical Erosion and Recent Re-vegetation.* Ph.D. Thesis, University of Durham, Durham.

Cohn, T. A., Caulder, D. L., Gilroy, E. J., Zynjuk, L. D. & Summers, R. M. 1992, The validity of a simple statistical model for estimating fluvial constituent loads: an empirical study involving nutrient loads entering Chespeake Bay. *Water Resources Research*, **28**(9), 2353-2363.

Cohn, T. A., DeLong, L. L., Gilroy, E. J., Hirsch, R. M. & Wells, D. K. 1989, Estimating constituent loads. *Water Resources Research*, **25**(5), 937-942.

Collins, A. L. & Walling, D. E. 2002, Selecting fingerprint properties for discriminating potential suspended sediment sources in river basins. *Journal of Hydrology*, **261**, 218-244.

Collins, M. B. 1973, *Transport of Sediment in Streams in Sussex, in Relation to Geological and Hydrological Characteristics of Catchments*. D.Phil. Thesis, University of Sussex, Brighton.

Collins, M. B. 1981, Sediment yield studies of headwater catchments in Sussex, S.E. England. *Earth Surface Processes and Landforms*, **6**, 517-539.

Cook, D. F. & Wolfe, M. L. 1991, A back-propagation neural network to predict average air temperature. *AI Applications*, **5**, 40-46.

Cox, N. J., Warburton, J., Armstrong, A., & Holliday, V. J. in review, Suspended sediment rating curves, generalised linear models and residual plots. *Earth Surface Processes and Landforms*.

Crawford, C. G. 1991, Estimation of suspended-sediment rating curves and mean suspended-sediment loads. *Journal of Hydrology*, **129**, 331-348.

Crisp, D. T. & Robson, S. 1979, Some effects of discharge upon the transport of animals and peat in a north Pennine headstream. *Journal of Applied Ecology*, **16**, 721-736.

Crisp, D. T. 1966, Input and output of minerals for an area of Pennine moorland: the importance of precipitation, drainage, peat erosion and animals. *Journal of Applied Ecology*, **3**, 327-347.

Crisp, D. T. Unpublished, *Rough Sike 1962-1964*, Environmental Change Network.

Crosby, G. & DeBoer, D. H. 1995, Suspended sediment characteristics and drainage basin scale on the Canadian Prairies. In: Osterkamp, W. R. (Editor), *Effects of scale on interpretation and management of sediment and water quality*. IAHS publication 226. International Association of Hydrological Sciences, Washington, D.C., pp. 65-72.

Crowe, S. 2002, *The Role of Large Peat Blocks on Sedimentation and Their Control on Invertebrate Ecosystem Dynamics: an Experimental Field Investigation*. M.Sc. Thesis, University of Durham, Durham.

Curr, R. H. 1984, *The Sediment Dynamics of Corston Brook*. Ph.D. Thesis, University of Exeter, Exeter.

Dedkov, A. P. & Moszherin, V. I. 1992, Erosion and sediment yield in mountain regions of the world. In: Walling, D. E., Davies, T. R. & Hasholt, B. (Editors), *Erosion, Debris Flows and Environment in Mountain Regions*. IAHS publication 209, International Association of Hydrological Sciences, Wallingford, pp. 29-36.

DETR/MAFF. 2001, *The draft soil strategy for England - a consultation paper*, Department of the Environment, Transport and the Regions.

Dietrich, W. E., Dunne, T., Humphrey, N. F. & Reid, L. M. 1982, Construction of sediment budgets for drainage basins, *Sediment Budget and Routing in Forested Drainage Basins*. US Forest Service Technical Report. PNW-141, pp. 5-23.

Diplas, P. & Parker, G. 1992, Deposition and removal of fines in gravel-bed streams. In: Billi, P., Hey, R. D., Thorne, C. R. & Tacconi, P. (Editors), *Dynamics of Gravel-Bed Rivers*. Wiley, Chichester, pp. 313-329.

DoE. 1995, *The Investigation and Management of Erosion, Deposition and Flooding in Great Britain*, Department of the Environment: HMSO, London.

Doherty, R., Kutzbach, J., Foley, J. & Pollard, D. 2000, Fully coupled climate/dynamical vegetation model simulations over Northern Africa during the mid-Holocene. *Climate Dynamics*, **16**, 561-573.

Dolan, D. M., Yui, A. K. & Geist, R. D. 1981, Evaluation of river load estimation methods for total phosphorus. *Journal of Great Lakes Research*, **7**(3), 207-214.

Doty, C. W. & Carter, C. E. 1965, Rates and particle-size distribution of soil erosion from unit source areas. *Transactions of American Society of Agricultural Engineers*, **8**, 309-311.

Droppo, I. G. 2001, Rethinking what constitutes suspended sediment. *Hydrological Processes*, **15**, 1551-1564.

Droppo, I. G., Nackaerts, K., Walling, D. E. & Williams, N. 2005, Can flocs and water stable soil aggregates be differentiated within fluvial systems? *Catena*, **60**, 1-18.

Droppo, I. G., Walling, D. E. & Ongley, E. D. 2002, *Suspended sediment structure: implications for sediment transport/yield modelling*. SC-2002/WS/48, UNESCO, Paris.

Duck, R. W. & McManus, J. 1990, Relationships between catchment characteristics, land use and sediment yield in the Midland Valley of Scotland. In: Boardman, J., Foster, I. D. L. & Dearing, J. A. (Editors), *Soil Erosion on Agricultural Land*. John Wiley & Sons, London.

Duck, R. W. 1985, The effect of road construction on sediment deposition in Loch Earn, Scotland. *Earth Surface Processes and Landforms*, **10**, 401-406.

ECN. 2004, The UK Environmental Change Network. Last updated: 17th November 2004. Available: http://www.ecn.ac.uk/. Accessed: 20th November 2004.

Edwards, T. K. & Glysson, G. D. 1999, Field methods for measurement of fluvial sediment, *Techniques of Water Resources Investigations of the US Geological Survey. Book 3 Applications of Hydraulics*. USGS, Virginia.

Evans, M. & Burt, T. P. 1998, Contemporary erosion in the Rough Sike catchment, Moor House National Nature Reserve, north Pennines. In: Warburton, J. (Editor), *Geomorphological Studies in the North Pennines: Field Guide*. pp. 37-45.

Evans, M. & Warburton, J. 2001, Transport and dispersal of organic debris (peat blocks) in upland fluvial systems. *Earth Surface Processes and Landforms*, **26**(10), 1087-1103.

Evans, M. & Warburton, J. in press, Sediment budget for an eroding peat-moorland catchment in Northern England. *Earth Surface Processes and Landforms*.

Evans, M. G. & Yang, J. in prep, Sediment production and sediment yield from eroding peatland catchments; controls on the export of particulate carbon.

Evans, R. 1990, Soils at risk of accelerated erosion in England and Wales. *Soil Use and Management*, **6**(3), 125-131.

Evans, R. 1997, Soil erosion in the UK initiated by grazing animals. A need for a national survey. *Applied Geography*, **17**(2), 127-141.

Everitt, B. S. 1993, *Cluster Analysis*. Edward Arnold, London.

Farr, I. S. & Clarke, R. T. 1984, Reliability of suspended load estimates in chalk streams. *Archiv für Hydrobiologie*, **101**, 1-19.

Farr, I. S. 1978. Quoted in: Walling, D. E., Webb, B. W. & 1987, Suspended load in gravel-bed rivers: UK experience. In: Thorne, C. R., Bathurst, J. C. & Hey, R. D. (Editors), *Sediment Transport in Gravel-Bed Rivers*. John Wiley & Sons, Chichester, pp. 691-732.

Fenn, C. R. 1989, Quantifying the errors involved in transferring suspended sediment rating equations across ablation seasons. *Annals of Glaciology*, **13**, 64-68.

Fenn, C. R., Gurnell, A. M. & Beecroft, I. R. 1985, An evaluation of the use of suspended sediment rating curves for the prediction of suspended sediment concentration in a proglacial stream. *Geografiska Annaler. Series A. Physical Geography*, **67**(1-2), 71-82.

Ferguson, R. I. & Church, M. 2004, A simple universal equation for grain settling velocity. *Journal of Sedimentary Research*, **74**(6), 933-937.

Ferguson, R. I. 1986, River loads underestimated by rating curves. *Water Resources Research*, **22**(1), 74-76.

Ferguson, R. I. 1988, River loads under-estimated by rating curves - reply. *Water Resources Research*, **24**(7), 1220.

Fielding, F. G. A. & Haworth, P. F. 1999, *Upland Habitats*. Routledge, London.

Finlayson, B. L. & McMahon, T. A. 1988, Australia v the World: a comparative analysis of streamflow characteristics. In: Warner, R. F. (Editor), *Fluvial Geomorphology of Australia*. Academic Press, Sydney, pp. 17-40.

Finlayson, B. L. 1978, Suspended solid transport in a small experimental catchment. *Zeitschrift für Geomorphologie*, **22**, 192-210.

Fleming, G. & Poodle, T. 1970, Particle size of river sediments. *Proceedings of the American Society of Civil Engineers, Hydraulic Division*, **96**, 431-439.

Fleming, G. 1969, *The Clyde Basin: Hydrology and Sediment Transport*. Ph.D. Thesis, University of Strathclyde, Strathclyde.

Foster, I. D. L. & Lees, J. A. 1999, Changes in the physical and geochemical properties of suspended sediment delivered to the headwaters of LOIS river basins over the last 100 years: a preliminary analysis of lake and reservoir bottom sediments. *Hydrological Processes*, **13**, 1067-1086.

Foster, I. D. L., Dearing, J. A., Simpson, A. & Carter, A. D. 1985, Lake catchment based studies of erosion and denudation in the Merevale catchment, Warwickshire, UK. *Earth Surface Processes and Landforms*, **10**, 45-68.

Foster, I. D. L., Millington, R. & Grew, R. G. 1992, The impact of particle size controls on stream turbidity measurement; some implications for suspended sediment yield estimation. In: Bogen, J., Walling, D. E. & Day, T. (Editors), *Erosion and Sediment Transport Monitoring Programmes in River Basins*. IAHS publication 210. International Association of Hydrological Sciences, Oslo, pp. 51-62.

Francis, I. S. & Taylor, J. A. 1989, The effect of forestry drainage operations on upland sediment yields: a study of two peat-covered catchments. *Earth Surface Processes and Landforms*, **14**, 73-83.

Francis, I. S. 1987, *Blanket Peat Erosion in Mid-Wales: Two Catchment Studies*. Ph.D. Thesis, University of Wales, Aberystwyth.

Francis, I. S. 1990, Blanket peat erosion in a Mid-Wales catchment during two drought years. *Earth Surface Processes and Landforms*, **15**, 445-456.

French, M. N., Krajewski, W. F. & Cuykendall, R. R. 1992, Rainfall forecasting in space and time using a neural network. *Journal of Hydrology*, **137**, 1-31.

Fukushima, Y. 1988, A model of river flow forecasting for a small forested mountain catchment. *Hydrological Processes*, **2**, 167-185.

Galay, V. 1987, *Erosion and Sedimentation in the Nepal Himalaya.*, Water and Energy Commission Secretariat, Kathmandu.

Gardiner, A. T. 1983, *Runoff and Erosional Processes in Blanket Peat Moorland.* M.Phil. Thesis, Huddersfield Polytechnic, Huddersfield.

Gellis, A. 1993, The effects of Hurricane Hugo on suspended sediment loads, Lago Loiza basin, Puerto Rico. *Earth Surface Processes and Landforms*, **18**, 505-517.

Geological Survey of Great Britain. 1973, Cockermouth drift edition. Sheet 23. Geological Survey of Great Britain.

Gibbs, R. J. 1965, The geochemistry of the Amazon River system: Part 1. The factors that control the salinity and the composition and concentration of the suspended solids. *Geological Society of America Bulletin*, **78**, 1203-1232.

Gilvear, D. J. & Petts, G. E. 1985, Turbidity and suspended solids variations downstream of a regulating reservoir. *Earth Surface Processes and Landforms*, **10**, 363-373.

Good, J. E. G. 1987, *Environmental Aspects of Plantation Forestry in Wales*, Institute of Terrestrial Ecology, Grange-over-Sands.

Graf, W. H. 1998, *Fluvial Hydraulics. Flow and Transport Processes in Channels of Simple Geometry*. John Wiley & Sons, Chichester, 681 pp.

Gurnell, A. M. & Fenn, C. R. 1984, Box-Jenkins transfer function models applied to suspended sediment concentration - discharge relationships in a proglacial stream. *Arctic and Alpine Research*, **16**(1), 93-106.

Gurnell, A. M. 1987, Suspended sediment. In: Gurnell, A. M. & Clark, M. J. (Editors), *Glacio-Fluvial Sediment Transfer*. John Wiley & Sons Ltd, pp. 305-354.

Gurtz, M. E., Webster, J. R. & Wallace, J. B. 1980, Seston dynamics in southern Appalachian streams: effects of clear-cutting. *Canadian Journal of Fisheries and Aquatic Sciences*, **37**(4), 624-631.

Haag, I. & Westrich, B. 2002, Processes governing river water quality identified by principal component analysis. *Hydrological Processes*, **16**, 3113-3130.

Hadley, R. F. & Shown, L. M. 1976, Relations of erosion to sediment yield, Third Federal Inter-Agency Sedimentation Conference. US Water Resources Council, Washington, D.C., pp. 1.132 - 1.139.

Halcrow. 2001, *Sedimentation in Storage Reservoirs*, Department of the Environment, Transport and the Regions, Swindon.

Hall, D. 1967, The pattern of sediment movement in the River Tyne. *International Association of Scientific Hydrology*, **75**, 117-142.

Hasegawa, K. 1989, Studies on qualitative and quantitative prediction of meander channel shift. In: Ikeda, S. & Parker, G. (Editors), *River Meandering*. Water Resources Monograph 12. AGU, Washington, DC.

Hecht-Nielsen, R. 1988, Neurocomputing. *IEEE Spectrum*, **25**(3), 36-41.

Helsel, D. R. & Hirsch, R. M. 1992, *Statistical Methods in Water Resources*. Studies in Environmental Science, 49. Elsevier, Amsterdam.

Herschy, R. W. 1995, *Streamflow Measurement*. E & FN Spon, London, 524 pp.

Herschy, R. W. 1998, Accuracy. In: Herschy, R. W. & Fairbridge, R. W. (Editors), *Encyclopedia of Hydrology and Water Resources*. Encyclopedia of Earth Sciences Series. Kluwer Academic Publishers, London, pp. 3-11.

Hicks, M. 1994, Land-use effects on magnitude-frequency characteristics of storm sediment yields: some New Zealand examples. In: Olive, L. J., Loughran, R. J. & Kesby, J. A. (Editors), *Variability in Stream Erosion and Sediment Transport*. IAHS publication 224. International Association of Hydrological Sciences, Washington D.C., pp. 395-402.

Higgitt, D. L., Warburton, J. & Evans, M. G. 2001, Sediment transfer in upland environments. In: Higgitt, D. L. & Lee, E. M. (Editors), *Geomorphological Processes and Landscape Change*. Blackwell, Oxford, pp. 190-214.

Hill, A. R. 1973, Erosion of river banks composed of glacial till near Belfast, Northern Ireland. *Zeitschrift fur Geomorphologie*, **17**, 428-442.

Hillier, S. 2001, Particulate composition and origin of suspended sediment in the R. Don, Aberdeenshire, UK. *The Science of the Total Environment*, **265**, 281-293.

Hjulström, F. 1935, Studies of the morphological activity or rivers as illustrated by the River Fyris. *Bulletin of the Geological Institute University of Uppsala*, **25**, 221-527.

Hodson, A. J. & Ferguson, R. I. 1999, Fluvial suspended sediment transport from cold and warm-based glaciers in Svalbard. *Earth Surface Processes and Landforms*, **24**, 957-974.

Holden, J. & Burt, T. P. 2003, Hydrological studies on blanket peat: the significance of the acrotelm-catotelm model. *Journal of Ecology*, **91**, 86-102.

Holliday, V. J. 2003, *Sediment Budget for a North Pennine Upland Reservoir Catchment, UK*. Ph.D. Thesis, University of Durham, Durham.

Hooke, J. M. 1980, Magnitude and distribution of rates of river bank erosion. *Earth Surface Processes and Landforms*, **5**, 143-157.

Hooke, J. M. 2000, Spatial variation in channel morphology and sediment dynamics: Gila River, Safford Valley, Arizona, *The Hydrology-Geomorphology Interface: Rainfall, Floods, Sedimentation, Land Use*. International Association of Hydrological Sciences, pp. 251-272.

Hope, D., Billet, M. F. & Cresser, M. S. 1994, A review of the export of carbon in river water: fluxes and processes. *Environmental Pollution*, **84**, 301-324.

Hope, D., Billet, M. F. & Cresser, M. S. 1997a, Exports of organic carbon in two river systems in NE Scotland. *Journal of Hydrology*, **193**, 61-82.

Hope, D., Billet, M. F., Milne, R. & Brown, T. A. W. 1997b, Exports of organic carbon in British rivers. *Hydrological Processes*, **11**, 325-344.

Hopfield, J. J. 1982, Neural networks and physical systems with emergent collective computational abilities. *Proceedings of the National Academy of Sciences*, **79**, 2554-2558.

Horowitz, A. J. & Elrick, K. 1987, The relation of stream sediment surface area, grain size, and composition to trace element chemistry. *Applied Geochemistry*, **2**, 437-451.

Horowitz, A. J. 2000, NASQAN*: the design and implementation of a large-river suspended sediment and trace element flux programme. In: Stone, M. (Editor), *The Role of Erosion and Sediment Transport in Nutrient and Contaminant Transfer*. IAHS publication 263. International Association of Hydrological Sciences, Oxford, pp. 3-17.

Horowitz, A. J., Elrick, K. A. & Smith, J. J. 2001, Annual suspended sediment and trace element fluxes in the Mississippi, Columbia, Colorado and Rio Grande drainage basins. *Hydrological Processes*, **15**, 1169-1207.

Horowitz, A. J., Rinella, F. A., Lamothe, P., Miller, T. L., Edwards, T. K., Roche, R. L. & Rickert, D. A. 1989, Cross-sectional variability in suspended sediment and associated trace element concentrations in selected rivers in the US, *Sediment and the Environment*. International Association of Hydrological Sciences, pp. 57-66.

House, W. A., Leach, D. & Warwick, M. S. 1997, Nutrient transport in the Humber rivers. *Science of the Total Environment*, **194/195**, 303-320.

Howard, P. J. A. & Howard, D. M. 1990, Use of organic carbon and loss-on-ignition to estimate soil organic matter in different soil types and horizons. *Biology and Fertility of Soils*, **9**, 306-310.

Hsu, K., Gupta, H. V. & Sorooshian, S. 1995, Artificial neural network modelling of the rainfall-runoff process. *Water Resources Research*, **31**(10), 2517-2530.

Hutchinson, S. M. 1995, Use of magnetic and radiometric measurements to investigate erosion and sedimentation in a British upland catchment. *Earth Surface Processes and Landforms*, **20**, 293-314.

Ichim, I., Surdeanu, V. & Radoane, N. 1984, Landsliding, slope development and sediment yield in a temperate environment: Northeast Romania. In: Burt, T. P. & Walling, D. E. (Editors), *Catchment Experiments in Fluvial Geomorphology*. Geo Books, Norwich, pp. 289-299.

Imeson, A. C., Vis, M. & Duysings, J. J. H. M. 1984, Surface and subsurface sources of suspended solids in forested drainage basins in the Keuper region of Luxembourg. In: Burt, T. P. & Walling, D. E. (Editors), *Catchment Experiments in Fluvial*

Geomorphology. Geo Books, Norwich, pp. 219-233.

Irvine, K. N. & Drake, J. J. 1987, Process-orientated estimation of suspended sediment concentration. *Water Resources Bulletin*, **23**(6), 1017-1025.

Jansson, M. B. 1985, Logarithmic regressions and power function regressions. *Geografiska Annaler. Series A. Physical Geography*, **67**, 61-70.

Jansson, M. B. 1988, A global survey of sediment yield. *Geografiska Annaler. Series A. Physical Geography*, **70A**(1-2), 81-98.

Jansson, M. B. 1996, Estimating a sediment rating curve of the Reventazon river at Palomo using logged mean loads within discharge classes. *Journal of Hydrology*, **183**, 227-241.

Johnson, R. C. 1988, Changes in the sediment output of two upland drainage basins during forestry land use changes. In: Bordas, M. P. & Walling, D. E. (Editors), *Sediment Budgets*. IAHS publication 174. International Association of Hydrological Sciences, Washington D.C., pp. 463-471.

Johnson, R. C. 1992, Towards the design of a strategy for sampling suspended sediments in small headwater catchments. In: Bogen, J., Walling, D. E. & Day, T. (Editors), *Erosion and Sediment Transport Monitoring Programmes in River Basins*. IAHS publication 210. International Association of Hydrological Sciences, Oslo, pp. 225-232.

Johnson, R. C. 1994, Suspended sediment from two small upland drainage basins: using variability as an indicator of change. In: Olive, L. J., Loughran, R. J. & Kesby, J. A. (Editors), *Variability in Stream Erosion and Sediment Transport*. IAHS publication 224. International Association of Hydrological Sciences, Washington D.C., pp. 403-410.

Johnson, R. C. 1995, *Effects of upland afforestation on water resources. The Balquhidder Experiment 1981-1991*, Institute of Hydrology, Wallingford.

Jones, J. A. A. 1997, *Global Hydrology. Processes, Resources and Environmental Management*. Longman, Harlow, 399 pp.

Kaufman, L. & Rousseeuw, P. J. 1990, *Finding Groups in Data*. John Wiley & Sons, New York.

Kirby, C., Newson, M. D. & Gilman, K. 1991, *Plynlimon Research: The First Two Decades*. 109, Institute of Hydrology, Wallingford.

Knighton, D. 1998, *Fluvial Forms and Processes*. Arnold, London, 383 pp.

Koch, R. W. & Smillie, G. M. 1986, Bias in hydrologic prediction using log-transformed regression models. *Water Resources Bulletin*, **22**(5), 717-723.

Kohonen, T. 1982, Self-organized formation of topologically correct feature maps. *Biological Cybernetics*, **43**, 59-69.

Krishnaswamy, J., Richter, D. D., Halpin, P. N. & Hofmockel, M. S. 2001, Spatial patterns of suspended sediment yields in a humid tropical watershed in Costa Rica. *Hydrological Processes*, **15**, 2237-2257.

Kronvang, B., Grant, R. & Laubel, A. L. 1997, Sediment and phosphorus export from a lowland catchment: quantification of sources. *Water, Air and Soil Pollution*, **99**, 465-476.

Kurashige, Y. 1994, Mechanisms of suspended sediment supply to headwater rivers. *Transactions, Japanese Geomorphological Union*, **15**(A), 109-129.

Kurashige, Y. 1996, Process-based model of grain lifting from river bed to estimate suspended-sediment concentration in a small headwater basin. *Earth Surface Processes and Landforms*, **21**(12), 1163-1173.

Labadz, J. C., Burt, T. P. & Potter, A. W. R. 1991, Sediment yield and delivery in the blanket peat moorlands of the Southern Pennines. *Earth Surface Processes and Landforms*, **16**, 255-271.

Lambert, C. P. & Walling, D. E. 1988, Measurement of channel storage of suspended sediment in a gravel-bed river. *Catena*, **15**, 65-80.

Lane, P. W. 2002, Generalized linear models in soil science. *European Journal of Soil Science*, **53**, 241-251.

Lane, S. N. 1998, Hydraulic modelling in hydrology and geomorphology: a review of high resolution approaches. *Hydrological Processes*, **12**, 1131-1150.

Langbein, W. B. & Schumm, S. A. 1958, Yield of sediment in relation to mean annual precipitation. *Transactions of the American Geophysical Union*, **39**, 1076-1084.

Lawler, D. M. 1986, River bank erosion and the influence of frost: a statistical examination. *Transactions of the Institute of British Geographers*, **11**, 227-242.

Lawler, D. M. 1987, Bank erosion and frost action: an example from South Wales. In: Gardiner, V. (Editor), *International Geomorphology 1986*, Chichester, pp. 575-590.

Lawler, D. M. 1994, Temporal variability in streambank response to individual flow events: the River Arrow, Warwickshire, UK. In: Olive, L. J., Loughran, R. J. & Kesby, J. A. (Editors), *Variability in Stream Erosion and Sediment Transport*. IAHS publication 224. International Association of Hydrological Sciences, Washington D.C., pp. 171-180.

Lawler, D. M. 1995a, The impact of scale on the processes of channel-side sediment supply: a conceptual model. In: Osterkamp, W. R. (Editor), *Effects of Scale on Interpretation and Management of Sediment and Water Quality*. IAHS publication 226. International Association of Hydrological Sciences, Washington, D.C., pp. 175-184.

Lawler, D. M. 1995b, Turbidimetry and nephelometry, *Encyclopedia of Analytical Science*. Academic Press Limited, pp. 5289-5297.

Ledger, D. C., Lovell, J. P. B. & McDonald, A. T. 1974, Sediment yield studies in

upland catchment areas in south-east Scotland. *Journal of Applied Ecology*, **11**, 201-206.

Leeks, G. J. L. 1992. Impact of plantation forestry on sediment transport processes. In: Billi, P., Hey, R. D., Thorne, C. R. & Tacconi, P. (Editors), *Dynamics of Gravel-bed Rivers*, John Wiley & Sons, Chichester, pp. 651-670.

Leeks, G. J. L. & Marks, S. 1997, Dynamics of river sediments in forested headwater streams: Plynlimon. *Hydrology and Earth System Sciences*, 1(3), 483-497.

Lemke, K. A. 1991, Transfer function models of suspended sediment concentration. *Water Resources Research*, **27**(3), 293-305.

Lenzi, M. A. & Marchi, L. 2000, Suspended sediment load during floods in a small stream of the Dolomites (northeastern Italy). *Catena*, **39**, 267-282.

Leopold, L. B. & Maddock, T. 1953, The Hydraulic Geometry of Stream Channels and Some Physiographic Implications. USGS Professional Paper 252.

Lewin, J. & Macklin, M. 1987, Metal mining and floodplain sedimentation in Britain. In: Gardiner, V. (Editor), *International Geomorphology 1986*. John Wiley & Sons, Chichester, pp. 1009-1027.

Lewin, J. 1974, Sources for sediments and solutes in mid-Wales. In: Gregory, K. J. & Walling, D. E. (Editors), *Fluvial Processes in Instrumented Watersheds: Studies of Small Watersheds in the British Isles; a Contribution to the International Hydrological Decade*. Special Publication. IBG, London, pp. 73-85.

Lewin, J. 1987, Discussion by J. Lewin on "Suspended load in gravel-bed rivers: UK experience". In: Thorne, C. R., Bathurst, J. C. & Hey, R. D. (Editors), *Sediment Transport in Gravel-Bed Rivers*. John Wiley & Sons, Chichester, pp. 727.

Lewis, A. J. & Rasmussen, T. C. 1996, *A new, passive techniques for the in situ measurement of total suspended solids concentrations in surface water*. ERC 08-96, Environmental Resources Center, Georgia Institute of Technology for U.S. Department of the Interior, Geological Survey.

Lewis, J. & Eads, R. 2001, Turbidity threshold sampling for suspended sediment load estimation, 7th Federal Interagency Sedimentation Conference, Reno, Nevada, pp. III.110-II.117.

Longfield, S. A. & Macklin, M. G. 1999, The influence of recent environmental change on flooding and sediment fluxes in the Yorkshire Ouse basin. *Hydrological Processes*, **13**, 1051-1066.

Loughran, R. J. 1976, The calculation of suspended-sediment transport from concentration v discharge curves: Chandler River, N.S.W. *Catena*, **3**, 45-61.

Ludwig, W. & Probst, J. L. 1996, A global modelling of the climatic, morphological, and lithological control of sediment discharges to the oceans. In: Walling, D. E. & Webb, B. W. (Editors), *Erosion and Sediment Yield: Global and Regional Perspectives*. IAHS publication 236. International Association of Hydrological Sciences,

Wallingford, pp. 21-28.

Maier, H. R. & Dandy, G. C. 1996, The use of artificial neural networks for the prediction of water quality parameters. *Water Resources Research*, **32**(4), 1013-1022.

Malmquist, B., Nilsson, L. & Svensson, B. 1987, Dynamics of detritus in a small stream in southern Sweden and its influence on the distribution of bottom communities. *Oikos*, **31**, 3-16.

Marron, D. C. 1989, The transport of mine tailings as suspended sediment in the Belle Fourche River, west-central South Dakota, USA, *Sediment and the Environment*. International Association of Hydrological Sciences, pp. 19-26.

Masters, T. 1993, *Practical Neural Network Recipes in C.* Academic Press, San Diego.

McCulloch, W. S. & Pitts, W. 1943, A logical calculus of the ideas immanent in nervous activity. *Bulletin of Mathematical Biophysics*, **5**, 115-133.

McManus, J. & Duck, R. W. 1985, Sediment yield estimated from reservoir siltation in the Ochil hills, Scotland. *Earth Surface Processes and Landforms*, **10**, 193-200.

McManus, J. & Duck, R. W. 1996, Regional variations of fluvial sediment yield in eastern Scotland. In: Walling, D. E. & Webb, B. W. (Editors), *Erosion and Sediment Yield: Global and Regional Perspectives*. IAHS publication 236. International Association of Hydrological Sciences, Wallingford, pp. 157-161.

Meade, R. H. & Parker, R. S. 1985, Sediment in rivers of the United States. National Water Summary 1984. US Geological Survey Water Supply Paper 2275, pp. 49-60.

Meade, R. H., Dunne, T., Richey, J. E., Santos, U. & Salati, E. 1985, Storage and remobilization of suspended sediments in the lower Amazon River of Brazil. *Science*, **228**, 488-490.

Meybeck, M. 1982, Carbon, nitrogen, and phosphorus transport by world rivers. *American Journal of Science*, **282**, 401-450.

Miller, T. K. 1988, Comment on "River loads underestimated by rating curves" by R. I. Ferguson. *Water Resources Research*, **24**(7), 1217-1219.

Milliman, J. D. & Syvitski, J. P. M. 1992, Geomorphic/tectonic control of sediment discharge to the ocean: the importance of small mountain rivers. *The Journal of Geology*, **100**, 525-544.

Moore, R. J. & Newson, M. D. 1986, Production, storage and output of coarse upland sediments: natural and artificial influences as revealed by research catchment studies. *Journal of the Geological Society*, **143**, 921-926.

Morris, G. L. & Fan, J. 1997, *Reservoir Sedimentation Handbook.* McGraw-Hill, London.

Mossa, J. 1989, Hysteresis and nonlinearity of discharge-sediment relationships in the Atchafalaya and lower Mississippi rivers, *Sediment and the Environment*. International

Association of Hydrological Sciences, volume 2, pp. 105-112.

Naiman, R. J. 1982, Characteristics of sediment and organic carbon export from pristine boreal forest watersheds. *Canadian Journal of Fisheries and Aquatic Sciences*, **39**, 1699-1718.

Neal, C., Robson, A. J., Harrow, M., Hill, L., Wickham, H., Bhardwaj, C. L., Tindall, C. I., Ryland, G. P., Leach, D. V., Johnson, R. C., Bronsdon, R. K. & Cranston, M. 1997, Major, minor, trace element and suspended sediment variations in the River Tweed: results from the LOIS core monitoring programme. *The Science of the Total Environment*, **194/195**, 193-205.

Nelder, J. A. & Wedderburn, R. W. M. 1972, Generalized linear models. *Journal of the Royal Statistical Society, Series A*, **135**, 370-384.

Nelson, D. W. & Sommers, L. E. 1996, Total carbon, organic carbon and organic matter. In: Sparks, D. L. (Editor), *Methods of Soil Analysis. Part 3: Chemical Methods.* Soil Science Society of America, Inc, Madison, WI.

Newson, M. D. 1986, River basin engineering - fluvial geomorphology. *Journal of the Institution of Water Engineers and Scientists*, **40**, 307-324.

Nistor, C. J. & Church, M. in press, Suspended sediment transport regime in a debris-flow gully on Vancouver Island, British Columbia. *Hydrological Processes*.

Norwick, N. X. 1969, *SALT (selection at list time) sampling: a new method and its application in forestry*. M.A. Thesis, University of California, Berkeley.

Odgaard, A. J. 1987, Streambank erosion along two rivers in Iowa. *Water Resources Research*, **23**, 1225-1236.

Okunishi, K., Walling, D. E. & Saito, T. 1990, Discharge of suspended sediment and solutes from a hilly drainage basin in Devon, UK, as analysed by a cascade tank model. *Bulletin of the Disaster Prevention Research Institute, Kyoto University*, **40**(4), 143-160.

Okunishi, K., Walling, D. E. & Saito, T. 2000, A hydrological model of the mobilisation of fine suspended sediment from slopes. *Transactions, Japanese Geomorphological Union*, **21**(3), 243-260.

Olive, L. J. & Rieger, W. A. 1988, An examination of the role of sampling strategies in the study of suspended sediment transport. In: Bordas, M. P. & Walling, D. E. (Editors), *Sediment Budgets*. IAHS publication 174. International Association of Hydrological Sciences, Washington D.C., pp. 259-267.

Olive, L. J. & Rieger, W. A. 1992, Stream suspended sediment transport monitoring - why, how and what is being measured? In: Bogen, J., Walling, D. E. & Day, T. (Editors), *Erosion and Sediment Transport Monitoring Programmes in River Basins.* IAHS publication 210. International Association of Hydrological Sciences, Oslo, pp. 245-254.

Openshaw, S. & Openshaw, C. 1997, *Artificial Intelligence in Geography*. Wiley, Chichester.

Oxley, N. C. 1974, Suspended sediment delivery rates and the solute concentration of stream discharge in two Welsh catchments. In: Gregory, K. J. & Walling, D. E. (Editors), *Fluvial Processes in Instrumented Watersheds: Studies of Small Watersheds in the British Isles; a Contribution to the International Hydrological Decade*. Special Publication. IBG, London, pp. 141-154.

Parzen, E. 1984, *Time series analysis of irregularly observed data.* Springer-Verlag, New York.

Peart, M. R. & Walling, D. E. 1982, Particle size characteristics of fluvial suspended sediment. In: Walling, D.E. (Editor), *Recent Developments in the Explanation and Prediction of Erosion and Sediment*. IAHS publication 137. International Association of Hydrological Sciences, Wallingford, pp. 397-407.

Peart, M. R. & Walling, D. E. 1986, Fingerprinting sediment source: The example of a drainage basin in Devon, UK. In: Hadley, R. F. (Editor), *Drainage Basin Sediment Delivery*. IAHS publication 159. International Association of Hydrological Sciences, Wallingford, pp. 41-55.

Peters-Kummerly, B. E. 1973, Examination of composition and transport of various suspended loads in several Swiss rivers. *Geographica Helvetica*, **28**(3), 137-151.

Phillips, J. D. 1990, Relative importance of factors influencing fluvial soil loss at the global scale. *American Journal of Science*, **290**, 547-568.

Phillips, J. D. 1991, Fluvial sediment budgets in the North Caroline Piedmont. *Geomorphology*, **4**, 231-241.

Phillips, J. M. & Walling, D. E. 1995, An assessment of the effects of sample collection, storage and resuspension on the representativeness of measurements of the effective particle size distribution of fluvial suspended sediment. *Water Research*, **29**(11), 2498-2508.

Phillips, J. M., Russell, M. A. & Walling, D. E. 2000, Time-integrated sampling of fluvial suspended sediment: a simple methodology for small catchments. *Hydrological Processes*, **14**, 2589-2602.

Phillips, J. M., Webb, B. W., Walling, D. E. & Leeks, G. J. L. 1999, Estimating the suspended sediment loads of rivers in the LOIS study area using infrequent samples. *Hydrological Processes*, **13**, 1035-1050.

Pickup, G. & Marks, A. 2000, Identifying large-scale erosion and deposition processes from airborne gamma radiometrics and digital elevation models in a weathered landscape. *Earth Surface Processes and Landforms*, **25**(5), 535-557.

Picouet, C., Hingray, B. & Olivry, J. C. 2001, Empirical and conceptual modelling of suspended sediment dynamics in a large tropical African river: the Upper Niger river basin. *Journal of Hydrology*, **250**, 19-39.

Poole, M. A. & O'Farrell, P. 1971, The assumptions of the linear regression model. *Transactions of the Institute of British Geographers*, **52**, 145-158.

Prentice, I. C. 2001, The carbon cycle and atmospheric carbon dioxide. In: IPCC (Editor), *Climate Change 2001: The Scientific Basis*. Cambridge University Press, New York, pp. 183-237.

Prestegaard, K. L. 1988, Morphological controls on sediment delivery pathways. In: Bordas, M. P. & Walling, D. E. (Editors), *Sediment Budgets*. IAHS publication 174. International Association of Hydrological Sciences, Wallingford, pp. 533-540.

Raman, H. & Sunilkumar, N. 1995, Multivariate modelling of water resources time series using artificial neural networks. *Hydrological Sciences Journal*, **40**(2), 145-163.

Ranjithan, S. J., Eheart, J. W. & Garrett, H. H. 1993, Neural-network-based screening for groundwater reclamation under uncertainty. *Water Resources Research*, **29**(3), 563-574.

Rannie, W. F. 1977, An approach to the prediction of suspended sediment rating curves. In: Davidson-Arnott, R. & Nickling, W. (Editors), *Research in Fluvial Geomorphology*. Geo Abstracts, Norwich, pp. 149-167.

Reid, I. & Frostick, L. E. 1987, Flow dynamics and suspended sediment properties in arid zone flash floods. *Hydrological Processes*, **1**, 239-253.

Richards, K. 1984, Some observations on suspended sediment dynamics in Storbregrova, Jotunheimen. *Earth Surface Processes and Landforms*, **9**, 101-112.

Riggs, H. C. 1985, *Streamflow Characteristics*. Developments in Water Science. Elsevier, New York, 249 pp.

Rinaldi, M., Casagli, N., Dapporto, S. & Gargini, A. 2004, Monitoring and modelling of pore water pressure changes and riverbank stability during flow events. *Earth Surface Processes and Landforms*, **29**(2), 237-254.

Ritchie, J. C. 1972, Sediment, fish, and fish habitat. *Journal of Soil and Water Conservation*, **27**, 124-125.

Robinson, M. 1979, *The effects of pre-afforestation ditching upon the water and sediment yields of a small upland catchment*, University of Leeds, School of Geography, Working Paper 252, Leeds.

Robinson, M. 1980, *The effect of pre-afforestation drainage on the streamflow and water quality of an upland catchment*, Institute of Hydrology, Wallingford.

Rondeau, B., Cossa, D., Gagnon, P. & Bilodeau, L. 2000, Budget and sources of suspended sediment transported in the St. Lawrence River, Canada. *Hydrological Processes*, **14**, 21-36.

Rumelhart, D. E., Hinton, G. E. & Williams, R. J. 1986, Learning internal representations by error propagation. In: Rumelhart, D. E. & McClelland, J. L. (Editors), *Parallel Distributed Processing: Explorations in the Microstructures of Cognition*. MIT Press, Cambridge, pp. 318-362.

Russell, M. A., Walling, D. E. & Hodgkinson, R. A. 2000, Appraisal of a simple

sampling device for collecting time-integrated fluvial suspended sediment samples. In: Stone, M. (Editor), *The Role of Erosion and Sediment Transport in Nutrient and Contaminant Transfer*. IAHS publication 263. International Association of Hydrological Sciences, Oxford, pp. 119-127.

Russell, M. A., Walling, D. E. & Hodgkinson, R. A. 2001, Suspended sediment sources in two small lowland agricultural catchments in the UK. *Journal of Hydrology*, **252**, 1-24.

Sarma, J. N. 1986, Sediment transport in the Burhi Dihing River, India. In: Hadley, R. F. (Editor), *Drainage Basin Sediment Delivery*. IAHS publication 159. International Association of Hydrological Sciences, Wallingford, pp. 199-215.

Schick, A. P. & Lekach, J. 1993, An evaluation of two ten-year sediment budgets, Nahal Yael, Israel. *Physical Geography*, **14**(3), 225-238.

Schumm, S. A. 1960, *The shape of alluvial channels in relation to sediment type. US Geological Survey Professional Paper*. 352-B.

Schumm, S. A., Mosley, M. P. & Weaver, W. E. 1987, *Experimental Fluvial Geomorphology*. John Wiley & Sons, Chichester, 413 pp.

Seeger, M., Errea, M. P., Begueria, S., Arnaez, J., Marti, C. & Garcia-Ruiz, J. M. 2004, Catchment soil moisture and rainfall characteristics as determinant factors for discharge/suspended sediment hysteretic loops in a small headwater catchment in the Spanish Pyrenees. *Journal of Hydrology*, **288**, 299-311.

Sekely, A. C., Mulla, D. J. & Bauer, D. W. 2002, Streambank slumping and its contribution to the phosphorus and suspended sediment loads of the Blue Earth River, Minnesota. *Journal of Soil and Water Conservation*, **57**(5), 243-250.

Shamseldin, A. Y. 1997, Application of a neural network technique to rainfall-runoff modelling. *Journal of Hydrology*, **199**, 272-294.

Simons, D. B. & Sentürk, F. 1992, *Sediment Transport Technology. Water and Sediment Dynamics*. Water Resource Publications, Colorado, 897 pp.

Singh, K. P. & Durgunoglu, A. 1989, Developing accurate and reliable stream sediment yields, *Sediment and the Environment*. International Association of Hydrological Sciences, pp. 193-199.

Skinner, J. V. 1989, Model-B sediment-concentration gage: Factors influencing its readings and a formula for correcting its errors, *A Study of Methods used in Measurement and Analysis of Sediment Loads in Streams*. U.S. Army Engineer District, St. Paul.

Smith, B. P. G., Naden, P. S., Leeks, G. J. L. & Wass, P. D. 2003, The influence of storm events on fine sediment transport, erosion and deposition within a reach of the River Swale, Yorkshire, UK. *The Science of the Total Environment*, **314-316**, 451-474.

Soil Survey of England and Wales. 1983, Soil map of England and Wales. Harpenden.

Sparks, B. W. 1986, *Geomorphology*. Longman, London.

StataCorp. 2003a, *Stata Base Reference Manual: Release 8. Volume 2, G-M*. Stata Press, Texas.

StataCorp. 2003b, *Stata Cluster Analysis Reference Manual: Release 8*. Stata Press, Texas.

Stone, P. M. & Walling, D. E. 1997, Particle size selectivity considerations in suspended sediment budget investigations. *Water, Air and Soil Pollution*, **99**, 63-70.

Storer, D. A. 1984, A simple high sample volume ashing procedure for determination of soil organic matter. *Communications in Soil Science and Plant Analysis*, **15**, 759-772.

Stott, A. P. 1985, *Reservoir Sedimentation and Land Use Change in N.W. England*. Ph.D. Thesis, University of Manchester, Manchester.
Stott, A. P. 1987a, Medium-term effects of afforestation on sediment dynamics in a water supply catchment: A mineral magnetic interpretation of reservoir deposits in the Macclesfield, N. W. England. *Earth Surface Processes and Landforms*, **12**, 619-630.

Stott, T. A. 1987b, *Forestry Effects on Sediment Sources and Yields in the Balquhidder catchments, Central Scotland*. Ph.D. Thesis, University of Stirling, Stirling.

Stott, T. A. & Grove, J. R. 2001, Short-term discharge and suspended sediment fluctuations in the proglacial Skeldal River, north-east Greenland. *Hydrological Processes*, **15**, 407-423.

Stott, T. A., Ferguson, R. I., Johnson, R. C. & Newson, M. D. 1986, Sediment budgets in forested and unforested basins in upland Scotland. In: Hadley, R. F. (Editor), *Drainage Basin Sediment Delivery*. IAHS publication 159. International Association of Hydrological Sciences, Albuquerque, pp. 57-68.

Sugawara, M. 1961, On the analysis of runoff structure about several Japanese rivers. *Japanese Journal of Geophysics*, **2**(4), 1-76.

Tallis, J. H., Meade, R. & Hulme, P. D. (Editors). 1997, *Blanket mire degradation: causes, consequences and challenges*. Macaulay Land Use Research Insitute, Aberdeen.

Ternan, J. L. & Murgatroyd, A. L. 1984, The role of vegetation in baseflow suspended sediment and specific conductance in granite catchments, S. W. England. In: Schick, A. P. (Editor), *Channel Processes - Water, Sediment, Catchment Controls*. Catena Supplement 5. Catena Verlag, Cremlingen, pp. 51-61.

Thomas, R. B. & Lewis, J. 1993, A comparison of selection at list time and time stratefied sampling for estimating suspended sediment load. *Water Resources Research*, **29**(4), 1247-1256.

Thomas, R. B. & Lewis, J. 1995, An evaluation of flow-stratified sampling for estimating suspended sediment loads. *Journal of Hydrology*, **170**, 27-45.

Thomas, R. B. 1985, Estimating total suspended sediment yield with probability sampling. *Water Resources Research*, **21**(9), 1381-1388.

Thomas, R. B. 1988a, Measuring sediment yields of storms using P-SALT, Sediment Budgets. IAHS publication 174. International Association of Hydrological Sciences, Wallingford, pp. 315

Thomas, R. B. 1988b, Monitoring baseline suspended sediment in forested basins: the effects of sampling on suspended sediment rating curves. *Hydrological Sciences*, **33**(5), 499-514.

Thomas, R. B. 1989, *Piecewise SALT sampling for estimating suspended sediment yield*. Gen. Tech. Rep., PSW-114. USDA Forest Service.

Thonon, I. & Van Der Perk, M. 2003, Measuring suspended sediment characteristics using a LISST-ST in an embanked flood plain of the River Rhine. In: Bogen, J., Fergus, T. & Walling, D. E. (Editors), *Erosion and Sediment Transport Measurement in Rivers: Technological and Methodological Advances*. IAHS publication 283. International Association of Hydrological Sciences, Wallingford, pp. 37-44.

Thorne, P. D., Vincent, C. E., Hardcastle, P. J., Rehman, S. & Pearson, N. 1991, Measuring suspended sediment concentrations using acoustic backscatter devices. *Marine Geology*, **98**, 7-16.

Tipping, E., Marker, A. F. H., Butterwick, C., Collett, G. D., Cranwell, P. A., Ingram, J. K. G., Leach, D. V., Lishman, J. P., Pinder, A. C., Rigg, E. & Simon, B. M. 1997, Organic carbon in the Humber rivers. *The Science of the Total Environment*, **194/195**, 345-355.

Tipping, E., Woof, C. & Clarke, K. 1993, Deposition and resuspension of fine particles in a riverine "dead zone". *Hydrological Processes*, **7**, 263-277.

University of Wales. 1977, *The Sedimentation of Aberystwyth Harbour, a report to Ceredigion District Council*, Departments of Geography and Geology, University College of Wales, Aberystwyth.

USGS. 2003, Suspended Sediment Database. Last updated: 24th November 2003. Available: http://webserver.cr.usgs.gov/sediment/. Accessed: 25th May 2004.

Van Rijn, L. C. & Schaafsma, A. S. 1986, Evaluation of measuring instruments for suspended sediment, International Conference on Measuring Techniques of Hydraulics Phenomena in Offshore, Coastal & Inland Waters. London, England, pp 401-423.

Van Sickle, J. & Beschta, R. L. 1983, Supply-based models of suspended sediment transport in streams. *Water Resources Research*, **19**(3), 768-778.

Verhoff, F. H., Melfi, D. A. & Yaksich, S. M. 1979, Storm travel distance calculations for total phosphorus and suspended materials in rivers. *Water Resources Research*, **15**(6), 1354-1360.

Vorosmarty, C. J., Meybeck, M., Fekete, B. & Sharma, K. 1997, The potential impact

of neo-Castorization on sediment transport by the global network of rivers. In: Walling, D. E. & Probst, J. L. (Editors), *Human Impact on Erosion and Sedimentation*. IAHS publication 245. International Association of Hydrological Sciences, Wallingford, pp. 261-173.

Walling, D. E. & Kane, P. 1982, Temporal variation of suspended sediment properties. In: Walling, D. E. (Editor), *Recent Developments in the Explanation and Prediction of Erosion and Sediment Yield*. IAHS publication 137. International Association of Hydrological Sciences, Wallingford.

Walling, D. E. & Webb, B. W. 1981, Water quality. In: Lewin, J. (Editor), *British Rivers*. George Allen & Unwin, London, pp. 126-169.

Walling, D. E. & Webb, B. W. 1983, Patterns of sediment yield. In: Gregory, K. J. (Editor), *Background to Paleohydrology*. John Wiley & Sons, Chichester, pp. 69-100.

Walling, D. E. & Webb, B. W. 1987, Suspended load in gravel-bed rivers: UK experience. In: Thorne, C. R., Bathurst, J. C. & Hey, R. D. (Editors), *Sediment Transport in Gravel-Bed Rivers*. John Wiley & Sons, Chichester, pp. 691-732.

Walling, D. E. & Webb, B. W. 1988, The reliability of rating curve estimates of suspended sediment yield: some further comments. In: Bordas, M. P. & Walling, D. E. (Editors), *Sediment Budgets*. IAHS publication 174. International Association of Hydrological Sciences, Washington D.C., pp. 337-350.

Walling, D. E. & Webb, B. W. 1996, Water quality I. Chemical characteristics. In: Petts, G. & Calow, P. (Editors), *River Flows and Channel Forms*. Blackwell Science, Oxford, pp. 77-101.

Walling, D. E. & Woodward, J. C. 2000, Effective particle size characteristics of fluvial suspended sediment transported by lowland British rivers. In: Stone, M. (Editor), *The Role of Erosion and Sediment Transport in Nutrient and Contaminant Transfer*. IAHS publication 263. International Association of Hydrological Sciences, Oxford, pp. 129-139.

Walling, D. E. 1974, Suspended sediment and solute yields from a small catchment prior to urbanisation. In: Gregory, K. J. & Walling, D. E. (Editors), *Fluvial Processes in Instrumented Watersheds*. Institute of British Geographers, pp. 169-190.

Walling, D. E. 1977a, Assessing the accuracy of suspended sediment rating curves for a small basin. *Water Resources Research*, **13**(3), 531-538.

Walling, D. E. 1977b, Limitations of the rating curve technique for estimating suspended sediment loads, with particular reference to British rivers, *Erosion and Solid Matter Transport in Inland Waters*. IAHS publication 122. International Association of Hydrological Sciences, Wallingford, pp. 34-48.

Walling, D. E. 1982, Physical hydrology. *Progress in Physical Geography*, **6**(1), 122-133.

Walling, D. E. 1994, Measuring sediment yield from river basins. In: Lal, R. (Editor), *Soil Erosion Research Methods*. St Lucie Press, Florida, pp. 39-80.

of neo-Castorization on sediment transport by the global network of rivers. In: Walling, D. E. & Probst, J. L. (Editors), *Human Impact on Erosion and Sedimentation*. IAHS publication 245. International Association of Hydrological Sciences, Wallingford, pp. 261-173.

Walling, D. E. & Kane, P. 1982, Temporal variation of suspended sediment properties. In: Walling, D. E. (Editor), *Recent Developments in the Explanation and Prediction of Erosion and Sediment Yield*. IAHS publication 137. International Association of Hydrological Sciences, Wallingford.

Walling, D. E. & Webb, B. W. 1981, Water quality. In: Lewin, J. (Editor), *British Rivers*. George Allen & Unwin, London, pp. 126-169.

Walling, D. E. & Webb, B. W. 1983, Patterns of sediment yield. In: Gregory, K. J. (Editor), *Background to Paleohydrology*. John Wiley & Sons, Chichester, pp. 69-100.

Walling, D. E. & Webb, B. W. 1987, Suspended load in gravel-bed rivers: UK experience. In: Thorne, C. R., Bathurst, J. C. & Hey, R. D. (Editors), *Sediment Transport in Gravel-Bed Rivers*. John Wiley & Sons, Chichester, pp. 691-732.

Walling, D. E. & Webb, B. W. 1988, The reliability of rating curve estimates of suspended sediment yield: some further comments. In: Bordas, M. P. & Walling, D. E. (Editors), *Sediment Budgets*. IAHS publication 174. International Association of Hydrological Sciences, Washington D.C., pp. 337-350.

Walling, D. E. & Webb, B. W. 1996, Water quality I. Chemical characteristics. In: Petts, G. & Calow, P. (Editors), *River Flows and Channel Forms*. Blackwell Science, Oxford, pp. 77-101.

Walling, D. E. & Woodward, J. C. 2000, Effective particle size characteristics of fluvial suspended sediment transported by lowland British rivers. In: Stone, M. (Editor), *The Role of Erosion and Sediment Transport in Nutrient and Contaminant Transfer*. IAHS publication 263. International Association of Hydrological Sciences, Oxford, pp. 129-139.

Walling, D. E. 1974, Suspended sediment and solute yields from a small catchment prior to urbanisation. In: Gregory, K. J. & Walling, D. E. (Editors), *Fluvial Processes in Instrumented Watersheds*. Institute of British Geographers, pp. 169-190.

Walling, D. E. 1977a, Assessing the accuracy of suspended sediment rating curves for a small basin. *Water Resources Research*, **13**(3), 531-538.

Walling, D. E. 1977b, Limitations of the rating curve technique for estimating suspended sediment loads, with particular reference to British rivers, *Erosion and Solid Matter Transport in Inland Waters*. IAHS publication 122. International Association of Hydrological Sciences, Wallingford, pp. 34-48.

Walling, D. E. 1982, Physical hydrology. *Progress in Physical Geography*, **6**(1), 122-133.

Walling, D. E. 1994, Measuring sediment yield from river basins. In: Lal, R. (Editor), *Soil Erosion Research Methods*. St Lucie Press, Florida, pp. 39-80.

Walling, D. E. 1999, Linking land use, erosion and sediment yields in river basins. *Hydrobiologia*, **410**, 223-240.

Walling, D. E., Owens, P. N. & Leeks, G. J. L. 1999, Fingerprinting suspended sediment sources in the catchment of the River Ouse, Yorkshire, UK. *Hydrological Processes*, **13**, 955-975.

Walling, D. E., Webb, B. W. & Russell, M. A. 1997, Sediment-associated nutrient transport in UK rivers. In: Webb, B. W. (Editor), *Freshwater contamination*. IAHS publication 245. International Association of Hydrological Sciences, Wallingford, pp. 69-81.

Walling, D. E., Webb, B. W. & Woodward, J. C. 1992, Some sampling considerations in the design of effective strategies for monitoring sediment-associated transport. In: Bogen, J., Walling, D. E. & Day, T. (Editors), *Erosion and Sediment Transport Monitoring Programmes in River Basins*. IAHS publication 210. International Association of Hydrological Sciences, Oslo, pp. 279-287.

Warburton, J., Evans, M. G. & Johnson, R. M. 2003, Discussion on 'The extent of soil erosion in upland England and Wales'. *Earth Surface Processes and Landforms*, **28**(2), 219-223.

Wass, P. D. & Leeks, G. J. L. 1999, Suspended sediment fluxes in the Humber catchment, UK. *Hydrological Processes*, **13**, 935-953.

Webb, B. W. & Walling, D. E. 1984, Magnitude and frequency characteristics of suspended sediment transport in Devon rivers. In: Burt, T. P. & Walling, D. E. (Editors), *Catchment Experiments in Fluvial Geomorphology*. Geo Books, Norwich, pp. 399-415.

Webb, B. W., Foster, I. D. L. & Gurnell, A. M. 1995, Hydrology, water quality and sediment behaviour. In: Foster, I. D. L., Gurnell, A. M. & Webb, B. W. (Editors), *Sediment and Water Quality in Catchments*. John Wiley & Sons, Chichester.

Welch, N. H. & Allen, P. B. 1973, Field calibration and evaluation of a nuclear sediment gage. *Water Resources Research*, **9**(1), 154-158.

White, P., Labadz, J. C. & Butcher, D. P. 1996, Sediment yield estimates from reservoir studies: an appraisal of variability in the southern Pennines of the UK. In: Walling, D. E. & Webb, B. W. (Editors), *Erosion and Sediment Yield: Global and Regional Perspectives*. IAHS publication 236. International Association of Hydrological Sciences, Wallingford, pp. 163-173.

Wilkin, D. C. & Hebel, S. J. 1982, Erosion, redeposition, and delivery of sediment to Midwestern streams. *Water Resources Research*, **18**, 1278-1282.

Wilkinson, T. P. 1971, *The Transport of Rock Debris in Upland Streams with Particular Reference to Northern England*. Ph.D. Thesis, University of Newcastle-upon-Tyne, Newcastle-upon-Tyne.

Williams, G. P. 1989, Sediment concentration versus water discharge during single hydrologic events in rivers. *Journal of Hydrology*, **111**, 89-106.

Winter, T. S. R. 1950, The silting of impounding reservoirs. *Journal of the Institution of Civil Engineers*, 65-88.

Wischmeier, W. H. & Smith, D. D. 1958, Rainfall energy and its relation to soil loss. *Transactions of the American Geophysical Union*, **39**, 285-291.

Wohl, E. 2000, *Mountain Rivers*. American Geophysical Union, Washington, 320 pp.

Wolman, M. G. 1959, Factors influencing erosion of a cohesive river bank. *American Journal of Science*, **257**, 204-216.

Wood, P. A. 1977, Controls of variation in the River Rother, West Sussex, England. *Sedimentology*, **24**, 437-445.

Worrall, F., Burt, T. P. & Adamson, J. K. 2003a, Controls on the chemistry of runoff from an upland peat catchment. *Hydrological Processes*, **17**, 2063-2083.

Worrall, F., Reed, M., Warburton, J. & Burt, T. P. 2003b, Carbon budget for a British upland peat catchment. *The Science of the Total Environment*, **312**(1-2), 133-146.

Wren, D. G., Barkdoll, B. D., Kuhnle, R. A. & Derrow, R. W. 2000, Field techniques for suspended-sediment measurement. *Journal of Hydraulic Engineering*, **126**(2), 97-103.

Xu, J. 2002, Implication of relationships among suspended sediment size, water discharge and suspended sediment concentration: the Yellow River basin, China. *Catena*, **49**, 289-307.

Yaksich, S. M. & Verhoff, F. H. 1983, Sampling strategy for river pollution transport. *Journal of Environmental Engineering*, **109**, 219-231.

Yang, C. T., Song, C. C. S. & Woldenberg, M. J. 1981, Hydraulic geometry and minimum rate of energy dissipation. *Water Resources Research*, **17**, 1014-1018.

Yitian, L. & Gu, R. R. 2003, Modelling flow and sediment transport in a river network systems using an artificial neural network. *Environmental Management*, **31**(1), 122-134.

Young, A. 1958, A record of the rate of erosion on Millstone Grit. *Proceedings of the Yorkshire Geological Society*, **31**(2), 149-156.

Appendix A:
DETAILED BRITISH UPLAND SUSPENDED SEDIMENT STUDY TABLE

Table A.1. Monitoring studies of British upland suspended sediment loads.

Reference	River	Region	Area, km^2	Altitude, m	Lithology	Vegetation	Annual load, t	Specific sediment yield, t km^{-2} yr^{-1}	Number of samples	Sampler type	Sampling regime	Load estimation method
Crisp (1966)	Rough Sike	North Pennines	0.83	563-686	Peat, glacial till, sandstone, limestone, shale	Moorland	93	112.0	NS	Siphon and filter	Continuous	Summed
Wilkinson (1971)	West Grain	North Pennines	1.51	411-640	Shale, sandstone, limestone, glacial till, peat	Moorland	77.4	51.1	18	Grab samples	Irregular	Rating curve
	Langden Brook	Central Pennines	15.34	168-518	Shale, sandstone, glacial till, peat	Moorland	843	55.0	43	Grab samples	Irregular	Rating curve
Oxley (1974)	Ebyr North	Montgomeryshire	0.07	500-900	Greywackes	Forested	0.779	11.1	<50	Depth-integrated	2 samples pre month	Rating curve
	Ebyr South		0.09	500-800		Moorland	1.125	12.5	<50			
Carling (1983)	Carl Beck	North Pennines	2.18	245-513	Shale, limestone, sandstone, glacial till	Moorland	54	24.8	531	Auto-sampler	Storm with additional baseflow samples	Beales ratio estimator
	Great Eggleshope Beck	North Pennines	11.68	343-653	Shale, limestone, sandstone, glacial till, peat	Moorland	141	12.1	362	Auto-sampler	Storm with additional baseflow samples	Beales ratio estimator
Burt *et al.* (1984)	Hades Clough	West Yorkshire	0.22	340-430	Sandstone, shale	Moorland, some ditching	No loads. Pre-ditching SSC 200 mg l^{-1}, post ditching frequently >1000 mg l^{-1}		NS	Auto-sampler	Fixed interval – 1 or 2 hrs unless storm imminent then 15 mins	N/A
Duck (1985)	Ogle Burn	Central Scotland	13.0	97-663	Dalradian series, glacial till, peat	Moorland	83	6.4	NS	Turbidity	Continuous	Rating curve
Francis (1987)	Ceunant Ddu	Mid-Wales	0.342	460-490	Grits, shales, peat	Moorland, ploughed	Pre-ploughing: 1.257	3.7	153	Auto-sampler	Fixed interval – 8 hrs	NS
							Post-ploughing: 3.048	8.9	276		Some storm	
	Nant Ysguthon	Mid-Wales	0.135	480-510	Grits, shales, peat	Moorland, ploughed	Pre-ploughing: 0.088	0.7	149	Auto-sampler	Fixed interval – 8 hrs	NS
							Post-ploughing: 0.443	3.3	88		Some storm	
	River Severn	Mid-Wales	0.94	550-610	Grits, shales, peat	Moorland	62.3 (32.4 organic)	66.3	276	Auto-sampler	Fixed interval – 8 hrs (196 samples) Storm (80 samples)	NS
Labadz *et al.* (1991)	Shiny Brook	West Yorkshire	0.004	485-520	Sandstone, clay, head, peat	Moorland	1984/5: 0.198	49.6	NS	Auto-sampler	Fixed interval – 1 hr	Calculated from hourly measurements. Gaps filled in using a rating curve.
							1985/6: 0.240	60.0				
Kirby *et al.* (1991)	Severn	Mid-Wales	8.70	320-700	Mudstone, sandstone, slate	Forest/moorland	-	-	NS	Turbidity	Quasi-continuous	Rating curve
	Tanllwyth	Mid-Wales	0.89	350-680		Forest	10.7	12.1	NS	Turbidity	Quasi-continuous	
	Hore	Mid-Wales	3.08	360-700		Forest	Pre-felling: 75.2	24.4	NS	Turbidity	Quasi-continuous	
							Felling year: 175.9	57.1	NS	Turbidity	Quasi-continuous	
	Hafren	Mid-Wales	3.67	350-650		Forest/moorland	130.0	35.3	NS	Turbidity	Quasi-continuous	
	Cyff	Mid-Wales	3.13	360-560		Moorland/pasture	19.1	6.1	NS	Turbidity	Quasi-continuous	
	Iago	Mid-Wales	1.02	390-700		Moorland/pasture	-	-	NS	Turbidity	Quasi-continuous	
	Gwy	Mid-Wales	3.98	390-700		Moorland	-	-	NS	Turbidity	Quasi-continuous	
Johnson (1995)	Kirkton	West Scotland	6.85	242-852	Mica-schist, glacial till, peat	Forest	Pre-felling 1983: 321	46.9	123	Auto-sampler and depth-integrated	Storm	Rating curve developed from mean SSC of Q groups
							Pre-felling 1984: 275	40.1	94			
							Pre-felling 1985: 526	76.8	116			
							Post-felling 1986: 4353	635.5	319			
							Post-felling 1987: 599	87.4	432			
							Post-felling 1988: 4044	590.4	1096			
							Post-felling 1989: 3610	527.0	876			
	Monachyle	West Scotland	7.70	292-906	Mica-schist, glacial till, peat	Moorland	Pre-ploughing 1983: 293	38.1	245	Auto-sampler and depth-integrated	Storm	Rating curve developed from mean SSC of Q groups
							Pre-ploughing 1984: 280	36.4	91			
							Pre-ploughing 1985: 326	42.3	71			
							Post-ploughing 1986: 934	121.3	179			
							Post-ploughing 1987: 909	118.1	438			
							Post-ploughing 1988: 493	64.0	741			
							Post-ploughing 1989: 1419	184.3	739			

Reference	River	Region	Area, km^2	Altitude, m	Lithology	Vegetation	Annual load, t	Specific sediment yield, t km^{-2} yr^{-1}	Number of samples	Sampler type	Sampling regime	Load estimation method
Leeks & Marks (1997)	Tanllwyth	Mid-Wales	0.89	350-680	Mudstone, sandstone, slate	Forest	Pre-felling 1995: 21.6	24.3	NS	Turbidity	Quasi-continuous	Rating curve
							Post felling 1996: 39.0	43.8	NS	Turbidity	Quasi-continuous	
	Hafren	Mid-Wales	3.67	350-650		Forest	1995: 59.1	16.1	NS	Turbidity	Quasi-continuous	
							1996: 84.7	23.1	NS	Turbidity	Quasi-continuous	
	Severn	Mid-Wales	8.70	320-700		Forest/moorland	1995: 138.4	15.9	NS	Turbidity	Quasi-continuous	
							1996: 127.0	14.6	NS	Turbidity	Quasi-continuous	
	Cyff	Mid-Wales	3.13	360-560		Moorland	1996: 16.7	5.3	NS	Turbidity	Quasi-continuous	
Evans & Warburton (in press)	Rough Sike	North Pennines	0.83	563-686	Peat, glacial till, sandstone, limestone, shale	Moorland	1998: 35.9	43.3	252	Auto-sampler	Storm	Rating curve
							*1999: 39.3	47.3				
							*2000: 36.8	44.3				
							*2001: 36.2	43.6				

Studies which use the same data sets as Johnson (1995) and Kirby *et al.* (1991) are not included. For example, Stott *et al.* (1986), Stott (1987b), Johnson (1988a, 1988b, 1994), Good (1986), Moore & Newson (1986), Francis & Taylor (1987) and Francis (1990). * Evans & Warburton (in press) annual suspended sediment loads for 1999-2001 were derived from the 1997/1998 suspended sediment data.

Appendix B: RESULTS OF SIGNIFICANCE TESTING OF RATING CURVE GRADIENTS INTERCEPTS

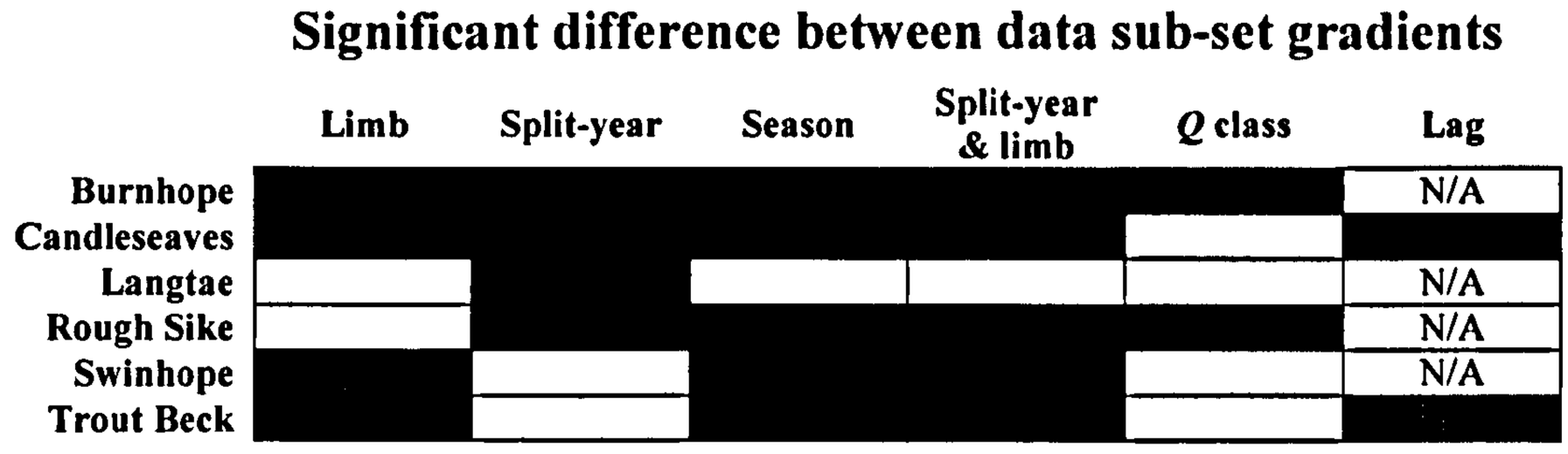

Figure A.1. Significant differences between the gradients of the adapted and the all-data models. The seasonal and split-year and limb matrices indicate which data sub-sets had significantly different gradients. Shaded boxes represent a significant difference at the 5% probability level.

Significant difference between data sub-set intercepts

	Limb	Split-year	Season	Split-year & limb	*Q* class	Lag
Burnhope	■	■	■	■		N/A
Candleseaves	■	■	■	■	■	■
Langtae						N/A
Rough Sike	■		■	■		N/A
Swinhope	■	■	■	■		N/A
Trout Beck	■		■	■		

Seasonal matrices

Burnhope

Spring	Summer	Autumn	Winter
	■	■	■

Candleseaves

Spring	Summer	Autumn	Winter
		■	

Rough Sike

Spring	Summer	Autumn	Winter
			■

Swinhope

Spring	Summer	Autumn	Winter
■	■	■	■

Trout Beck

Spring	Summer	Autumn	Winter
■	■	■	■

Limb & split-year matrices

Burnhope

Summer Rising	Summer Falling	Winter Rising	Winter Falling
■	■	■	

Candleseaves

Summer Rising	Summer Falling	Winter Rising	Winter Falling
■	■		■

Rough Sike

Summer Rising	Summer Falling	Winter Rising	Winter Falling
■	■	■	

Swinhope

Summer Rising	Summer Falling	Winter Rising	Winter Falling
	■	■	■

Trout Beck

Summer Rising	Summer Falling	Winter Rising	Winter Falling
■	■		■

Figure A.2. Significant differences between the intercepts of the adapted and the all-data models. The seasonal and split-year and limb matrices indicate which data sub-sets had significantly different intercepts. Shaded boxes represent a significant difference at the 5% probability level.

Appendix C:
FIELD CALIBRATION AND ASSESSMENT OF THE TIME-INTEGRATED MASS SAMPLERS

Phillips *et al.* (2000) documented three main short-comings of TIMS which may affect the representativeness of the sediment captured: (1) internal flow structure within the main body; (2) the sampling efficiency (which is related to internal flow structures); and (3) the effect of frictional resistance of the inlet tube. The flow structure within the main body was examined by inserting dye into a TIMS constructed of clear perspex. Two distinct dead zones, which encouraged the deposition of finer sediment, were identified immediately adjacent to the inlet and outlet tubes. This was reported to decrease the tendency of the TIMS to under-sample fine sediment.

Efficiency was measured using flume experiments in two ways: the total mass and the grain size distribution retained in the sampler compared with that of the stream water. The flume experiments showed between 31% and 71% of sediment was retained within the sampler, with higher sediment retention associated with higher velocities (Phillips *et al.*, 2000). Sediment from all particle size fractions was retained but higher proportions of the coarser fractions; this bias increased with greater velocities. The difference between the particle size distribution of inflowing water and that of the sediment retained in the TIMS was found to be statistically significantly except when flow velocities were low and suspended sediment relatively coarse (Phillips *et al.*, 2000). Phillips *et al.* (2000) report that improved results could be expected in field conditions as dispersed mineral sediment was used in the flume experiments whereas in the field aggregates will be inputted from sediment sources and flocs form due to the organic fraction, thus making sediment sizes larger and therefore increasing the chance of retention in the TIMS.

The reduction of velocity in the inlet tube compared with the channel flow is a result of the effect of frictional resistance of the inlet tube and inertia of water contained within the sampler. Phillips *et al.* (2000) measured the velocity of the inlet tube by placing a glass tube over the inlet with a water-tight seal, placing in a flume orientated with the flow (Figure C.1). A bubble was then inserted into the glass tube using a syringe and the time taken for the bubble to travel along the glass tube was timed (Figure C.1). The velocity in the glass tube was assumed to be controlled by the velocity within the smaller inlet tube and was corrected for the smaller diameter. Bias may result given the effect of resistance on the glass tube. The flume velocity was measured concurrently. This experiment was run at several velocities representative of field velocities.

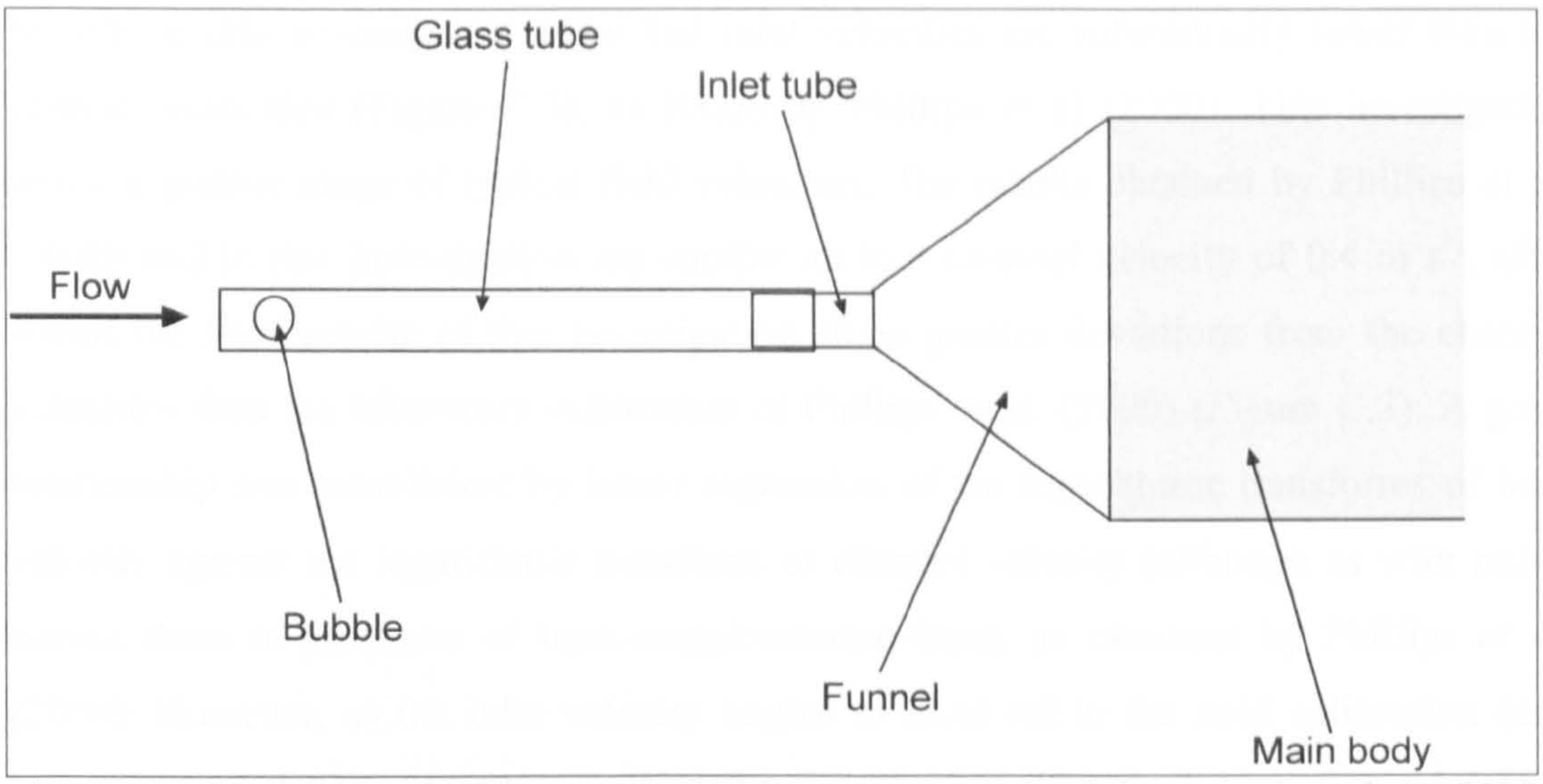

Figure C.1. Set up by Phillips *et al.* (2000) to measure the inlet velocity of the TIMS. Not to scale.

In this investigation the difference between inlet and channel velocity was determined in the field. A small turbine velocity meter (GEMS turbine flow rate sensor, FT-110 series) was mounted inside the funnel between two sections of the inlet pipe (Figure C.2). The velocity meter has a normal range of 30 to 300 cm s^{-1} with an accuracy of 3% and an extended range of 15 to 600 cm s^{-1}. The channel velocity was measured first using an electromagnetic flow meter, the flow meter was moved and the inlet of the TIMS placed in the same location. Measurements were completed within four minutes of each other.

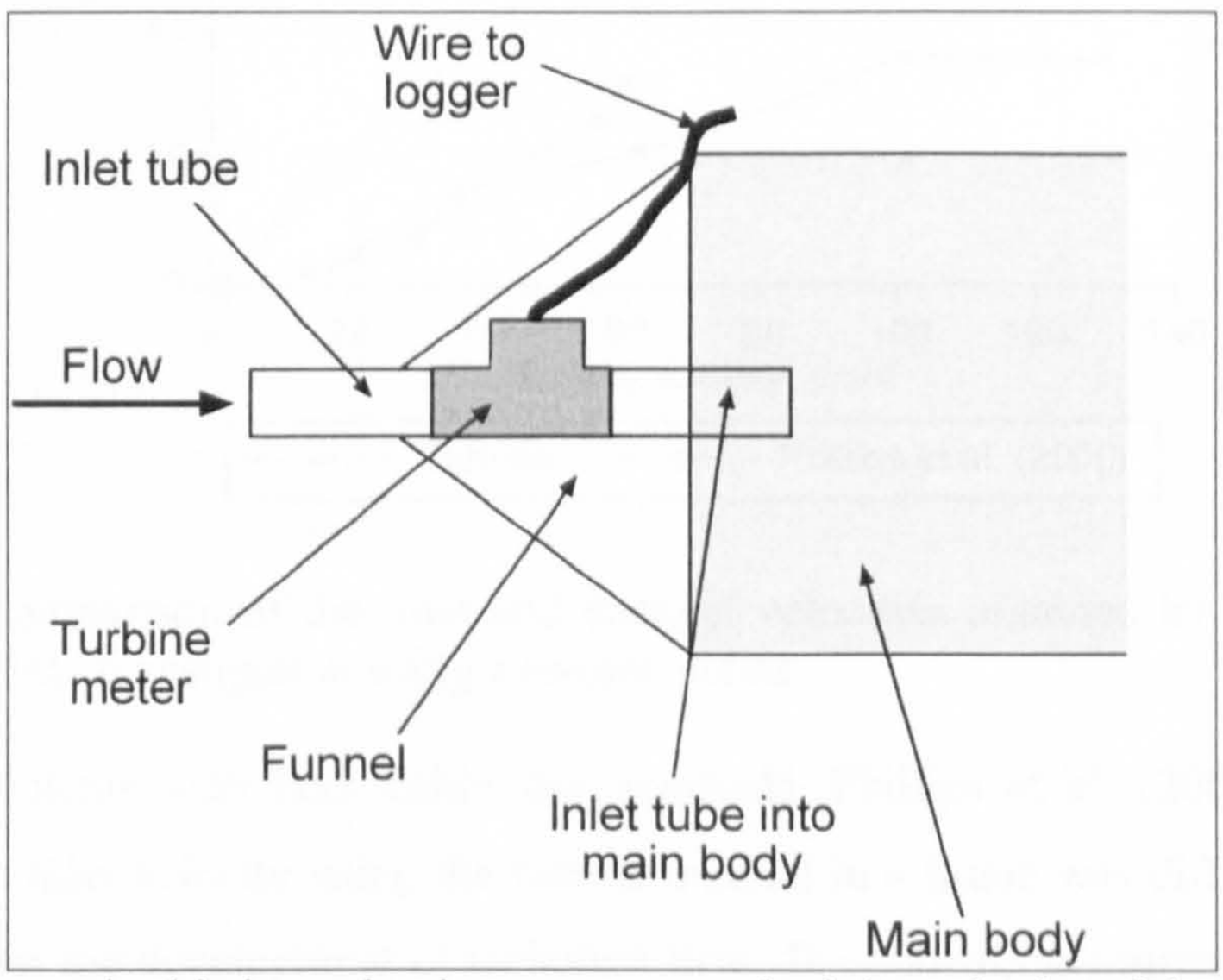

Figure C.2. Set up in this investigation to measure the inlet velocity of the TIMS. Not to scale.

Results of this investigation show that inlet velocities are substantially lower than the channel velocities (Figure C.3), as found by Phillips *et* al (2000). This investigation tested a greater range of typical field velocities. The results obtained by Phillips *et al.* (2000) and in this investigation are similar up to a channel velocity of 0.4 m s^{-1}, after which the field results of this investigation show greater deviations from the channel velocities than the laboratory calibration of Phillips *et al.* (2000) (Figure C.3). A good relationship was established by linear regression of the logarithmic transforms of inlet velocity against the logarithmic transform of channel velocity (although as with rating curves there is problems of back-transformation bias), as obtained by Phillips *et al.* (2000). However, as the inlet velocity begins to level off in the field calibration (this investigation) the linear regression line fitted to the logarithmically transformed data is a poor fit (Figure C.4). A superior relationship is obtained by fitting a quadratic to the raw data (Figure C.5).

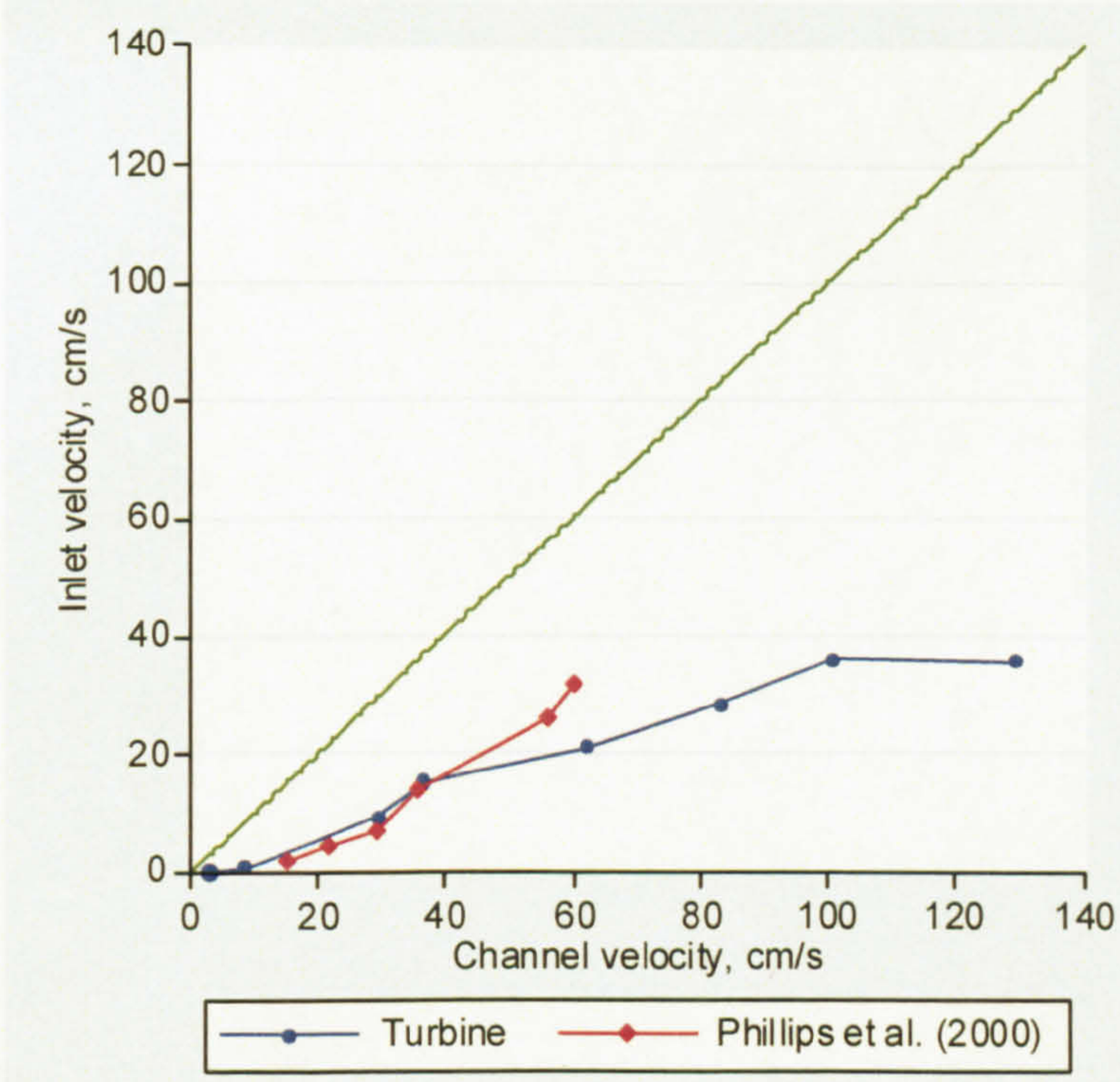

Figure C.3. Comparison of the inlet and channel velocities obtained by Phillips *et al.* (2000) and in this investigation using a turbine meter.

There are problems with both calibration methods. Phillips et al. (2000) noted that measuring the inlet velocity using the bubble method in a flume was difficult at higher velocities given the development of turbulent flow. In contrast, measurements could be taken at higher velocities in the field. Also, the inlet velocities were averaged over a period of 3 minutes in the field compared with triplicate measurements of the time it

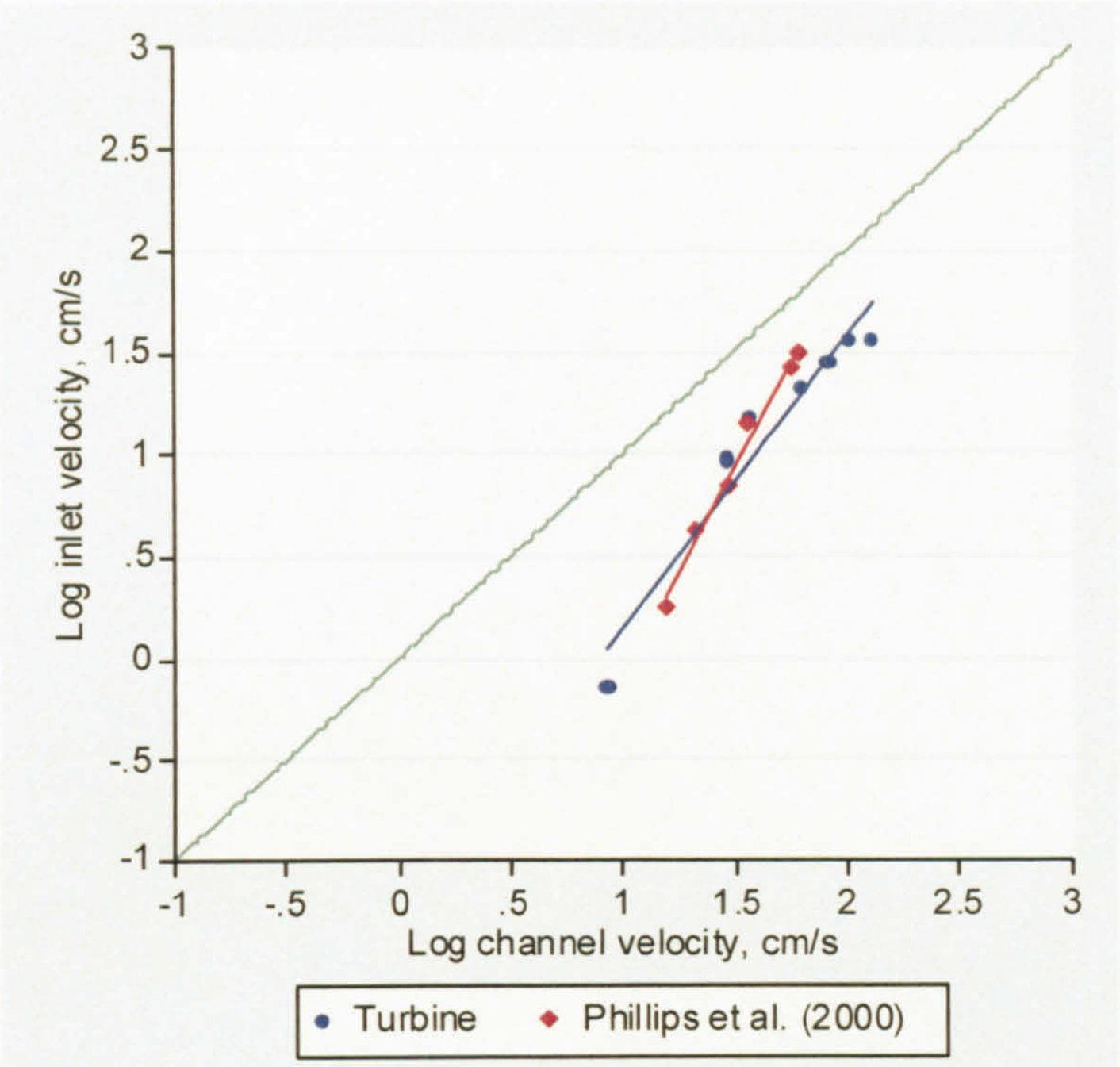

Figure C.4. Linear regression trend lines fitted to the logarithmically transformed channel and inlet velocities. Trend line for the Phillips *et al.* (2000) data is: log (inlet velocity) = 2.074 log (channel velocity) – 2.182. $R^2 = 0.99$. This investigation: log (inlet velocity) = 1.427 log (channel velocity) – 1.279. $R^2 = 0.93$.

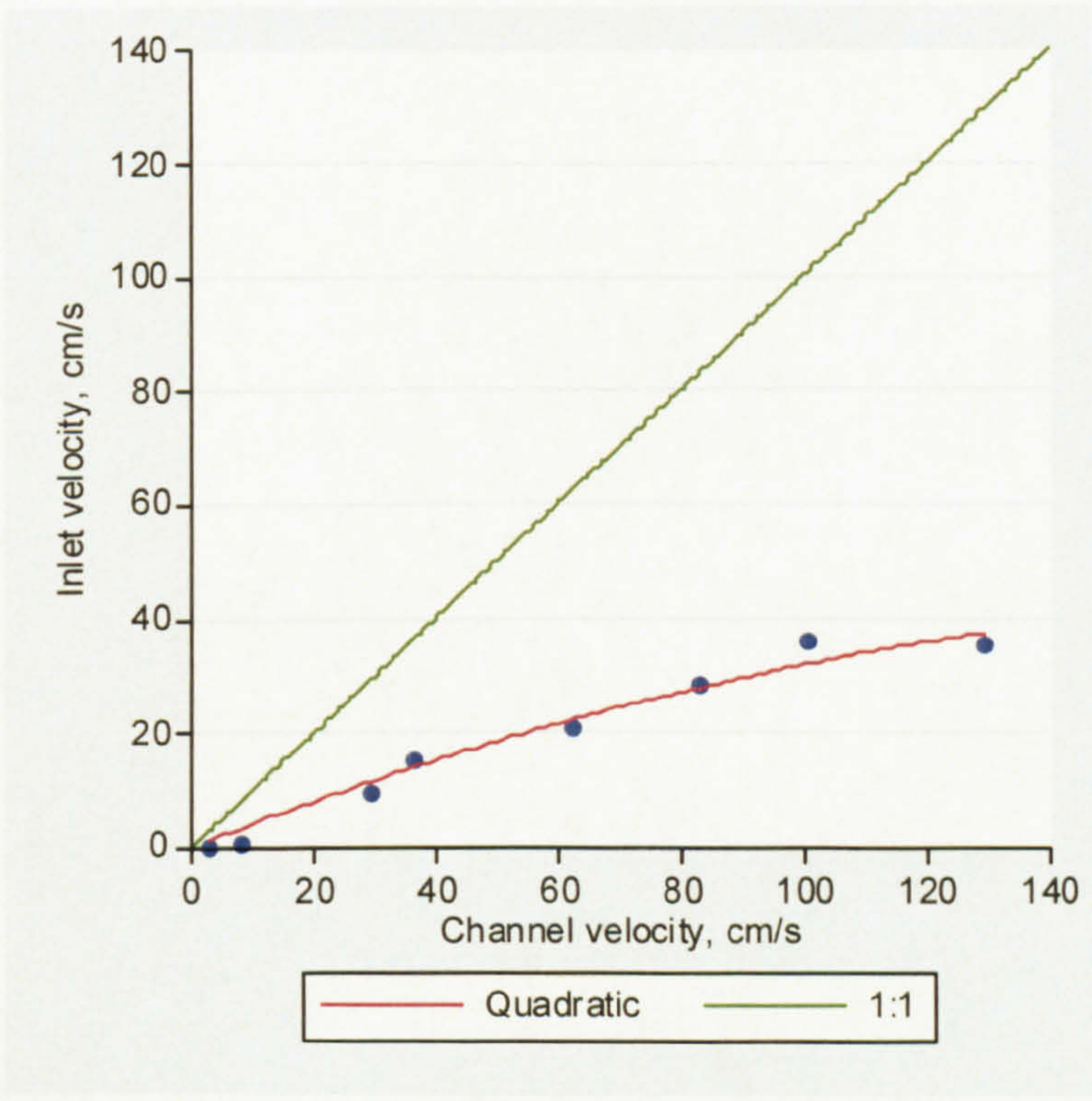

Figure C.5. Quadratic trend line fitted between the channel velocity and inlet velocity. Inlet velocity = -0.001 channel velocity^2 + 0.420 channel velocity. $R^2 = 0.99$

took the bubble to move 5 cm in the flume experiment by Phillips *et al.* (2000). However, the controlled flow in the laboratory is advantageous as it will be more constant than in the field. Regardless of the various advantages and shortcomings of the calibration methods both illustrate that the inlet velocity of the TIMS is much lower than the stream velocity. Phillips *et al.* (2000) suggest that the slower intake velocities will cause over-sampling of coarse (>62.5 μm) particles. However, given the peatland component of the study sites of this investigation, the coarser fraction is likely to be under-sampled as some peat particles transported in suspension are larger than the diameter of the inlet tube.

In addition to the differences to the problems documented by Phillips *et al.* (2000) this investigation has highlighted several other problems, some of which are more problematic in upland streams:

(1) Phillips *et al.* (2000) recommended that the samplers be fixed at 0.6 of the water depth. However, it was not possible to achieve this due to the large variation in river stage as a result of the flashy nature of upland streams. In order that results from different TIMS could be compared the TIMS were fixed at approximately 0.6 of water depth during low flow so they were continuously submerged. A consequence of this is that during periods of high flow they may tend to sample coarser suspended sediment given the vertical distribution of suspended sediment.

(2) Changes in stage affect the local flow regime of the TIMS, for example bed material could deflect flow away from the inlet. While care was taken not to site TIMS in such locations bed movement during high flow events meant that this did have some effect, obstructing clasts were removed when the TIMS were emptied.

(3) Large pieces of peat are easily transported in suspension and by rolling along the stream bed (Evans & Warburton, 2001) and as a result inlet tubes of the TIMS were occasionally blocked. This poses a particular problem: the remoteness of some of the TIMS means that no details are known as regards when blockages occurred.

(4) Local sediment sources may dominate the suspended sediment collected. This is likely to be especially problematic in sections of active bed movement and narrow sections of channels due to the influence of banks.

(5) The TIMS may under-sample the organic fraction relative to the mineral fraction due to the difference in flow pathways; peat is buoyant and therefore more is transported in the upper section of the water column. However, this may be countered by mixing caused by turbulence, especially given the shallow rough-bed nature of the channels. The buoyant nature of peat may also decrease the amount that settles out in the main body of the TIMS, as lower flows will be required to cause it to fall out of suspension.

(6) Flow pathways within the channel change with changing stage. Therefore, although the TIMS were orientated with flow on deployment the alignment changed for some with change in stage.

(7) The representativeness of the TIMS location is unknown. Cross-sectional variability in suspended bed sediment is commonplace and the TIMS only sample sediment from 64 mm^2 of the channel cross-section.